National Research Council Canada

Conseil national de recherches Canada

NRC · CNRC

Canadian Journal of Fisheries and Aquatic Sciences

Journal canadien des sciences halieutiques et aquatiques

http://cjfas.nrc.ca

http://jcsha.cnrc.ca

ISSN 0706-652X / CJFSDX 62(3) 483–724 (2005)

The *Canadian Journal of Fisheries and Aquatic Sciences*, previously published as *Contributions to Canadian Biology* 1901–1925, *Contributions to Canadian Biology and Fisheries* 1926–1934, *Journal of the Biological Board of Canada* 1934–1937, and *Journal of the Fisheries Research Board of Canada* 1938–1979, is issued monthly to form annual volumes of 12 numbers plus supplements.

Editorial policy. The Journal publishes original research articles, perspectives (syntheses, critiques, re-evaluations), discussions (comment and reply), and rapid communications. Manuscripts may concern cells, organisms, populations, communities, ecosystems, or processes that affect aquatic systems. They may cover a range of disciplines including biology and ecology of marine and freshwater organisms, limnology, oceanography, physiology, toxicology, genetics, economics, disease, and management. Preference will be given to manuscripts that emphasize understanding of observed phenomena and interpretation of experimental results. The Journal encourages papers that lead from clearly stated purpose or rationale and from testable hypotheses, concepts, or questions to identifiable conclusions or syntheses. Such papers may amplify, modify, question, or redirect accumulated knowledge embodied in contemporary perceptions of a particular state of aquatic sciences. The Journal discourages papers that are essentially descriptive, except in emerging disciplines; have only site-specific or local applications (a certain year, place, taxon, chemical compound, etc.); only confirm previously established principles; or apply standard techniques without breaking new methodological ground.

Manuscripts for publication should be submitted to the Senior Editor, *Canadian Journal of Fisheries and Aquatic Sciences*, Department of Integrative Biology, Building #006, Room 118, University of Guelph, Guelph, ON N1G 2W1, Canada (519-824-4120 ext. 52646; fax: 519-767-9798; e-mail: cjfas@uoguelph.ca).

Submissions in either English or French are acceptable. The information must be original, that is, not copyrighted, published, or submitted elsewhere except in abstract form or unless by written consent of the Editor.

Correspondence concerning accepted manuscripts and corrected proofs should be sent to NRC Research Press, National Research Council of Canada, Ottawa, ON K1A 0R6, Canada (fax: 613-952-7656; e-mail: pubs@nrc-cnrc.gc.ca).

Instructions to Authors are published once a year in the first issue of each volume. Copies are available from NRC Research Press or at http://cjfas.nrc.ca. The **Publication Policy** of NRC Research Press is available at http://pubs.nrc-cnrc.gc.ca.

Microfilm. Issues from 1934 through the current volume can be purchased on 16- or 35-mm microfilm. Photocopies of individual articles or issues can be purchased from University Microfilms International, 330 North Zeeb Road, Ann Arbor, MI 48106, USA.

US periodical postage paid at Champlain, NY 12919, USA, and at additional mailing offices. Attention US POSTMASTER: Send address changes to **Canadian Journal of Fisheries and Aquatic Sciences**, c/o USACAN Media Distribution Center, P.O. Box 2888, Plattsburgh, NY 12901, USA.

Publié sans interruption depuis 1901, le *Journal canadien des sciences halieutiques et aquatiques* a paru sous plusieurs titres : *Contributions to Canadian Biology* 1901–1925, *Contributions to Canadian Biology and Fisheries* 1926–1934, *Journal of the Biological Board of Canada* 1934–1937, et *Journal of the Fisheries Research Board of Canada* 1938–1979. Le Journal paraît tous les mois, formant ainsi un volume de 12 numéros, et offre en plus jusqu'à deux suppléments par année.

Politique éditoriale. On publie, dans le Journal, des articles rendant compte de recherche originale, des perspectives (synthèses, critiques et réévaluations), des discussions (commentaires et réponses) et des communications rapides. Les documents peuvent porter sur les cellules, organismes, populations, communautés, écosystèmes ou processus qui affectent les systèmes aquatiques. Ils peuvent relever de divers domaines y compris la biologie et l'écologie des organismes marins et d'eau douce, la limnologie, l'océanographie, la physiologie, la toxicologie, la génétique, l'économie, la pathologie et la gestion. On accorde la préséance aux articles qui contribuent à la compréhension de phénomènes observés et à l'interprétation de résultats expérimentaux. On invite les auteurs à soumettre des articles ayant des objectifs précis ou relevant d'hypothèses, de concepts ou de questions vérifiables et se terminant par de solides conclusions ou d'utiles synthèses. Ces articles enrichissent, changent, mettent en question ou réorientent les connaissances acquises sur divers aspects des sciences aquatiques. On décourage toutefois la soumission d'articles simplement descriptifs (à moins qu'il ne s'agisse de nouvelles disciplines), d'application très limitée (applicables à une seule année, une seule région ou un seul taxon, portant sur un unique composé chimique, etc.); d'articles qui ne font que reprendre les principes énoncés dans des articles précédents; et d'articles rendant compte de l'application de normes sans gain de méthodologie.

Les auteurs voudront adresser leurs **manuscrits** à la directrice scientifique principale, *Journal canadien des sciences halieutiques et aquatiques*, Département de biologie intégrative, édifice 006, bureau 118, University of Guelph, Guelph, ON N1G 2W1, Canada (519-824-4120 poste 52646; télécopieur : 519-767-9798; courriel : cjfas@uoguelph.ca).

Les contributions peuvent être en anglais ou en français. Elles doivent être originales, c.-à.-d. qu'elles ne doivent pas avoir fait l'objet d'un copyright, avoir été publiées ou soumises ailleurs, sauf sous forme abrégée ou avec le consentement du rédacteur. Le CNRC ne se tient en aucune façon responsable des opinions exprimées par un collaborateur ou des déclarations qui pourrait faire ce dernier.

La correspondance ayant trait aux manuscrits acceptés et les **épreuves corrigées** doivent être envoyées aux Presses scientifiques du CNRC, Conseil national de recherches du Canada, Ottawa, ON K1A 0R6, Canada (télécopieur : 613-952-7656; courriel : pubs@nrc-cnrc.gc.ca).

Les Recommandations aux auteurs sont publiées une fois par année dans le premier numéro de chaque volume. Des copies sont disponibles auprès du Bureau de la rédaction aux Presses scientifiques du CNRC ou au http://jcsha.cnrc.ca. **La Politique de publication** est disponible auprès des Presses scientifiques du CNRC ou au http://pubs.nrc-cnrc.gc.ca.

Microfilms. On peut acheter sur microfilms de 16 ou 35 mm tous les numéros depuis 1934. Des photocopies d'articles ou de numéros individuels sont aussi en vente auprès de University Microfilms International, 330 North Zeeb Road, Ann Arbor, MI 48106, É.-U.

This Journal is indexed or abstracted in / Cette revue est signalée ou résumée dans
ABSEARCH, Applied Science and Technology Index and Abstracts, Aquatic Sciences and Fisheries Abstracts, Biological Abstracts, Biological and Agricultural Abstracts, CAB Abstracts, Chemical Abstracts, Current Contents, Elsevier BIOBASE, Environmental Abstracts, ETDE Energy Database, General Science Index and Abstracts, GEOBASE, GeoRef, Life Sciences Collection, Meteorological and Geoastrophysical Abstracts, Oceanic Abstracts, PASCAL Database, and Science Citation Index.

Volume 62, Number 3, March 2005

Canadian Journal of Fisheries and Aquatic Sciences

Published by the National Research Council of Canada

Volume 62, numéro 3, mars 2005

Journal canadien des sciences halieutiques et aquatiques

Publié par le Conseil national de recherches du Canada

Senior Editor / Directrice scientifique principale **Moira M. Ferguson**

Editors / Directeurs

Jeffrey A. Hutchings, *Dalhousie University, Halifax*
Pierre Pepin, *Northwest Atlantic Fisheries Centre, DFO/MPO, St. John's, Newfoundland*
W. Gary Sprules, *University of Toronto at Mississauga*
Assistant to the Editors / Adjointe aux directeurs scientifiques **Holly Foster**

Associate Editors / Directeurs scientifiques associés

D. Boisclair, *Université de Montréal*
U. Borgmann, *Environment Canada, Burlington*
M.J. Bradford, *DFO/MPO and Simon Fraser University*
S.E. Campana, *DFO/MPO, Dartmouth*
R. Carignan, *Université de Montréal*
J.J. Dodson, *Université Laval*
G.T. Evans, *DFO/MPO, St. John's, Newfoundland*
K.T. Frank, *DFO/MPO, Dartmouth*
J.W.A. Grant, *Concordia University*
M.M. Hansen, *Danish Institute for Fisheries Research, Silkeborg, Denmark*
R. Hilborn, *University of Washington*
A. Hontela, *Université du Québec à Montréal*
D.F. Houlihan, *University of Aberdeen*
F.A. Huntingford, *University of Glasgow*
G.S. Jamieson, *DFO/MPO, Nanaimo*
J.M. Jech, *NFSC/NOAA, Woods Hole, Mass.*
B. Jonsson, *Norwegian Institute for Nature Research, Oslo, Norway*
D.L. MacLatchy, *University of New Brunswick, Saint John*
P. Magnan, *Université du Québec à Trois Rivières*
C.T. Marshall, *University of Aberdeen*
R.B. Millar, *University of Auckland, New Zealand*
W.P. Patterson, *University of Saskatchewan*
Y.T. Prairie, *Université du Québec à Montréal*
T.J. Quinn II, *University of Alaska–Fairbanks, Juneau, Alaska*
T.P. Quinn, *University of Washington*
C.W. Ramcharan, *Laurentian University*
R.D. Roberts, *Environment Canada, Saskatoon*
B. Sainte-Marie, *DFO/MPO, Mont-Joli*
D.W. Schindler, *University of Alberta*
R.E.H. Smith, *University of Waterloo*
S.J. Smith, *DFO/MPO, Dartmouth*
W.F. Vincent, *Université Laval*
R.D. Vinebrooke, *University of Alberta*
C.J. Walters, *University of British Columbia*
R.D. Ward, *CSIRO Marine Research, Australia*
B. de Young, *Memorial University of Newfoundland*

NRC Research Press / Presses scientifiques du CNRC

Editor-in-Chief / Directeur scientifique en chef **Bruce P. Dancik**
Assistant Editor-in-Chief / Adjoint au directeur scientifique en chef **Iain E.P. Taylor**

Journals Program / Programme des revues

Fax / Télécopieur : 613-952-7656; e-mail / courriel : pubs@nrc-cnrc.gc.ca; URL / URL : pubs.nrc-cnrc.gc.ca
Director / Directeur **Cameron D. Macdonald**
Business Manager / Gestionnaire des affaires **Jason Charron**
Manager, Journals Program / Gestionnaire, Programme des revues **Carolyn Brown**
Managing Editor / Rédactrice administrative **Cecily M. Pearson** (613-993-9099)
Publication Officers / Agents de publication **Jennifer McColl, Thad Costigan**
Advertising and reprints / Annonces publicitaires et tirés à part **Roxanne Landriault** (613-990-2254)
Subscriptions / Abonnements **Eileen Evans-Nantais** (613-990-7873)

The National Research Council of Canada accepts no responsibility for statements or opinions expressed by a contributor. Acceptance of an advertisement, announcement, or other material does not imply endorsement by either the Journal's Senior Editor or the National Research Council.

© National Research Council of Canada 2005. All rights reserved.

No part of this publication may be reproduced, stored, or transmitted in any form or by any means, without the written permission of the publisher, except as stated below.

The National Research Council of Canada grants **permission*** to individuals to make single copies of articles for personal use. Any person may reproduce short excerpts from articles in the journal for any purpose that respects the moral rights of authors, provided that the source is fully acknowledged. As a courtesy, the consent of authors of such material should be obtained directly from the author.

Authorization to reproduce items for other than personal use, as stated above, is granted by the National Research Council of Canada provided that the copyright fee of $7.00 per copy is paid directly to CANCOPY, One Yonge Street, Suite 1900, Toronto, ON M5E 1E5, Canada.

*The above permission does not extend to other kinds of copying, such as copying for general distribution, for advertising, or promotional purposes, for creating new collective works, or for resale. For such copying, arrangements must be made with the publisher, National Research Council of Canada, Ottawa, ON K1A 0R6, Canada.

Subscription information

The *Canadian Journal of Fisheries and Aquatic Sciences* (ISSN 0706-652X) is published monthly by the National Research Council of Canada. The 2005 annual subscription rates (second class postage) for Canada are $892CAN institutional and $276CAN personal, for US & foreign $892US institutional and $276US personal. For air mail add $175US to foreign rate. Canadian customers please include 7% GST (business no. 12149 1807 RT 0275). Subscriptions are entered for the calendar year. Remittances should be made payable to the Receiver General for Canada, credit NRC. Price for regular single issues: institutional, $110.00; personal, $35.00. Supplements will be priced separately. Special rates apply to members of Canadian scientific and engineering societies if they subscribe through their respective societies.

There are no refunds on cancelled subscriptions once delivery has begun. Claims for missing issues should be made within four months (N. America) or six months (outside N. America) following the date of publication. The publisher expects to supply missing issues only when losses have occurred in transit and when the reserve stock will permit. For change of address and subscription enquiries: Subscription Office, NRC Research Press, National Research Council of Canada, Ottawa, ON K1A 0R6, Canada; tel.: 613-993-9064; fax: 613-952-7656; e-mail: pubs@nrc-cnrc.gc.ca.

Microform backfiles are available from UMI, P.O. Box 1346, Ann Arbor, MI 48106-1346, USA, and Micromedia Ltd., 20 Victoria St., Toronto, ON M5C 2N8, Canada.

All issues of the *Canadian Journal of Fisheries and Aquatic Sciences* since 1996 are available on the Web. Pricing information can be found at http://pubs.nrc-cnrc.gc.ca.

Le Conseil national de recherches du Canada ne se tient en aucune façon responsable des opinions exprimées par un collaborateur ou des déclarations que pourrait faire ce dernier. La publication d'annonces publicitaires, d'avis et autres n'implique pas l'endossement de leur contenu par la directrice principale de la Revue ou le CNRC.

© Conseil national de recherches du Canada 2005. Tous droits réservés.

Il est interdit de reproduire, de sauvegarder ou de transmettre quelque partie de la présente publication dans quelque format ou de quelque façon sans le consentement écrit de l'éditeur, à l'exception des conditions suivantes.

Le Conseil national de recherches du Canada accorde aux particuliers le droit de faire des copies individuelles pour leur usage personnel. Toute personne peut reproduire de courts extraits des articles de la Revue pour autant que les droits moraux de l'auteur soient respectés et que la mention de provenance soit clairement indiquée. Il est de convenance de demander le consentement de l'auteur avant de faire mention de son travail.

On obtiendra l'autorisation de reproduire des articles à d'autres fins que l'usage personnel (tel qu'on l'a décrit ci-dessus) auprès du Conseil national de recherches du Canada pour autant que des redevances de droits d'auteurs de 7,00 $/copie soient versées au CANCOPY, 1, rue Yonge, bureau 1900, Toronto, ON M5E 1E5, Canada.

*La permission ci-dessus ne s'applique pas à la reproduction à grande échelle, telle que la reproduction aux fins de distribution générale, publicitaire ou promotionnelle, de compilation de nouveaux ouvrages collectifs ou de revente. Dans de tels cas, il faudra ratifier une entente particulière avec l'éditeur, le Conseil national de recherches du Canada, Ottawa, ON K1A 0R6, Canada.

Renseignements sur l'abonnement

Journal canadien des sciences halieutiques et aquatiques (ISSN 0706-652X) est une publication mensuelle du Conseil national de recherches du Canada. Le prix de l'abonnement annuel en 2005 au Canada (courrier de deuxième classe) est de 892 $CAN pour les organismes et de 276 $CAN pour les particuliers. À l'étranger (y compris les É.-U.), le prix de l'abonnement est de 892 $US pour les organismes et de 276 $US pour les particuliers. L'expédition par avion exige des frais de 175 $US en sus du prix d'abonnement à l'étranger. Les clients du Canada doivent ajouter la TPS de 7 % (numéro d'entreprise 12149 1807 RT 0275). Les abonnements sont pour l'année civile. Tout paiement doit être adressé au Receveur général du Canada, crédit du CNRC. Le prix par numéro est de 110 $ pour les organismes et de 35 $ pour les particuliers. Le prix des hors-série varie. Les membres des sociétés canadiennes de sciences et de génie bénéficient de taux préférentiels en s'abonnant via leurs sociétés respectives.

Aucun remboursement ne sera accordé ni aucune annulation acceptée une fois que les livraisons auront commencé. Les réclamations de numéros manquants devront être soumises dans les quatre mois (Amérique du Nord) ou dans les six mois (à l'extérieur de l'Amérique du Nord) suivant la date de publication. L'éditeur ne fournira de numéros manquants que si le document a été perdu pendant l'expédition et que si le stock le permet. Adressez tout changement d'adresse ou toute question quant à l'abonnement au : Bureau des abonnements, Presses scientifiques du CNRC, Conseil national de recherches Canada, Ottawa, ON K1A 0R6, Canada; téléphone : 613-993-9064; télécopieur : 613-952-7656; courriel : pubs@nrc-cnrc.gc.ca.

On peut obtenir les fichiers rétrospectifs sur **microforme** auprès de UMI, P.O. Box 1346, Ann Arbor, MI 48106-1346, É.-U., et auprès de Micromedia Ltée, 20, rue Victoria, Toronto, ON M5C 2N8, Canada.

À partir de 1996, tous les numéros de *Journal canadien des sciences halieutiques et aquatiques* sont accessibles sur le Web. On trouvera des renseignements sur les tarifs à http://pubs.nrc-cnrc.gc.ca.

Developmental differences and a test for reciprocity in the tolerance of *Chaoborus punctipennis* larvae to ultraviolet radiation

A.D. Persaud and N.D. Yan

Abstract: We estimated the ultraviolet radiation (UVR) tolerance of *Chaoborus punctipennis* in five 2- to 4-day in situ experiments conducted with third and fourth instar larvae at 0.25, 1.25, 3.0, and 5.0 m in Ruth Roy Lake, a lake with low dissolved organic carbon levels (0.2 mg·L^{-1}). UVR tolerance increased with larval age. Third and late fourth instar LD_{50} (median lethal dose) ranged from 52.3 to 62.2 J·cm^{-2} and from 82.4 to 119.6 J·cm^{-2}, respectively, among the four depths. Reciprocity held for UVR exposure down to 5.0 m, i.e., toxicity was independent of dose rate. At any given depth, the LT_{50} (median lethal time) increased with larval stage, but even at 5.0 m, third and late fourth instars died in less than 10 and 20 h, respectively, under sunny skies. These results suggest that *Chaoborus* abundance and distribution might be affected by UVR, especially in clear lakes. If UVR levels continue to increase in some lakes because of stratospheric ozone loss and climate change, we predict that UVR damage to *Chaoborus* will increase in the future, thereby affecting trophic interactions in temperate freshwater food webs.

Résumé : Nous avons estimé la tolérance à la radiation ultraviolette (UVR) chez *Chaoborus punctipennis* dans cinq expériences in situ de 2–4 jours, en utilisant des larves de troisième et quatrième stades aux profondeurs de 0,25, 1,25, 3,0 et 5,0 m dans le lac Ruth Roy, un lac à faible teneur en carbone organique dissous (0,2 mg·L^{-1}). La tolérance à l'UVR augmente en fonction de l'âge des larves. Les LD_{50} (doses létales médianes) des larves de troisième stade et de fin de quatrième stade varient respectivement de 52,3–62,2 J·cm^{-2} et de 82,4–119,6 J·cm^{-2} aux quatre profondeurs. La loi de la réciprocité s'applique aux expositions à l'UVR jusqu'à une profondeur de 5,0 m, c'est-à-dire que la toxicité est indépendante du taux de la dose. À toutes les profondeurs, LT_{50} (temps létal moyen) augmente en fonction des stades larvaires, mais même à 5,0 m les larves de troisième et de fin de quatrième stades meurent respectivement en moins de 10 et 20 h, sous un ciel ensoleillé. Ces résultats indiquent que l'abondance et la répartition de *Chaoborus* peuvent être affectées par l'UVR, particulièrement dans les lacs clairs. Si les niveaux d'UVR continuent à augmenter dans certains lacs à cause de la perte d'ozone dans la stratosphère et le changement climatique, nous prédisons que les dommages causés par l'UVR à *Chaoborus* croîtront dans le futur, affectant ainsi les interactions trophiques dans les réseaux alimentaires des eaux douces tempérées.

[Traduit par la Rédaction]

Introduction

With the depletion of stratospheric ozone, ultraviolet (UV) irradiation of the earth's surface has increased (Caldwell 1979; Schindler 1998), especially at mid- and upper latitudes (e.g., Kerr and McElroy 1993). However, underwater UV levels are largely a function of depth and chromophoric dissolved organic carbon (DOC) concentrations (Scully and Lean 1994). The 1% depth of UV radiation (UVR) increases dramatically at DOC levels <2 mg·L^{-1}; therefore, any decreases in DOC concentrations in low-DOC lakes can significantly increase UVR penetration (Scully and Lean 1994; Williamson et al. 1996). The interaction of acid rain, stratospheric ozone depletion, and climate change may be leading to such declines in DOC (Gunn et al. 2001). As drought frequency increases in the temperate region, DOC falls in response to reduced DOC export from catchments and increased in-lake photolysis given longer hydraulic retention times (Schindler et al. 1996; Schindler 1998). Droughts that lead to reacidification events may also elevate aluminum levels, further reducing DOC levels via metal complexation and precipitation (Yan et al. 1996) or increased rates of photolysis at low pH (Gennings et al. 2001).

UVR is damaging to aquatic organisms (Zagarese and Williamson 2000). It alters DNA (Jeffrey et al. 1996; Malloy et al. 1997) and proteins (Sinha et al. 1996), carbon allocation (Arts and Rai 1997), and the formation rate of highly reactive oxygen species (Vincent and Neale 2000). Hence,

Received 19 December 2003. Accepted 12 November 2004. Published on the NRC Research Press Web site at http://cjfas.nrc.ca on 30 March 2005.
J17885

A.D. Persaud.[1,2] Department of Biology, York University, 4700 Keele Street, Toronto, ON M3J 1P3, Canada.
N.D. Yan. Dorset Environmental Science Centre, Ontario Ministry of the Environment, P.O. Box 39, Dorset, ON P0A 1E0, Canada, and Department of Biology, York University, 4700 Keele Street, Toronto, ON M3J 1P3, Canada.

[1]Corresponding author (e-mail: anuranipersaud@trentu.ca).

 doi: 10.1139/F04-204 © 2005 NRC Canada

we should quantify the impacts of UVR exposure, especially on those biota that are ecologically important and UV sensitive. One such organism is the larval phantom midge *Chaoborus* spp.

Chaoborus are an important energy transfer point between zooplankton and fish (Moore et al. 1994; Ramcharan et al. 2001); however, they appear to be highly susceptible to UVR (Williamson et al. 1999; Persaud and Yan 2003). Our first objective was to determine whether there are developmental differences in UVR sensitivity of larval *Chaoborus punctipennis*, the most common *Chaoborus* species in temperate lakes (Yan et al. 1985). To do this, we developed survival versus UVR dose–response and time–response models comparing LD_{50} (median lethal dose) and LT_{50} (median lethal time) for different larval stages.

The term reciprocity has a unique meaning in photobiology. Where reciprocity holds, damage is a function of cumulative UV dose instead of dose rate (Norins 1969; Zagarese and Williamson 2000). Reciprocity has been found to hold for copepods (Zagarese et al. 1998*a*; Browman et al. 2000) and eggs of Atlantic cod (*Gadus morhua*) (Kouwenberg et al. 1999*a*) exposed to UVR. In contrast, reciprocity does not hold for some crustaceans (Damkaer and Dey 1983; Grad et al. 2001) and larval northern anchovy (*Engraulis mordax*) (Hunter et al. 1981). Béland et al. (1999) and Kouwenberg et al. (1999*b*) stressed the importance of testing for reciprocity in UV damage studies. Such tests are required to model UVR-induced damage from biological weighting functions and action spectra (de Gruijl et al. 1986; Coohill 1991). However, we have few tests of reciprocity (Browman et al. 2000; Grad et al. 2001) and none for *Chaoborus*. Our second objective was to test whether reciprocity holds for the exposure of *C. punctipennis* to UVR down to 5.0 m in a low-DOC lake. Dose rates were varied naturally by exposing larvae to natural radiation at different depths.

Methods

Incubation and source lakes

Dose–response models and time–response models were developed using UVR doses and larval *C. punctipennis* survival data from in situ experiments conducted in Ruth-Roy Lake, Killarney Park, Ontario, Canada. Ruth-Roy Lake is an acidic (pH = 4.8), low-DOC (0.2 mg·L^{-1}) lake. As a result of the low DOC, light penetrates deeply in the water column (Perez-Fuentetaja et al. 1999). The Secchi depth transparency is high, ranging from 13 to 18 m (bottom of the lake = 18 m). Given this great light penetration, thermal stratification does not occur (Yan 1983). The 1% depths of photosynthetically active radiation (PAR) (400–700 nm), UVA (320–400 nm), and UVB (280–320 nm) were calculated to be 37.0, 10.3, and 8.9 m, respectively (Gunn et al. 2001).

The biodiversity of Ruth-Roy Lake is limited by its acidity. There are no fish and the zooplankton community consists of a few acid-tolerant species (Holt and Yan 2003). Despite the large populations of *Chaoborus* species in nearby Johnnie Lake (71.1 larvae·m^{-3}; Yan et al. 1985), none were found at six stations in Ruth-Roy Lake in the early 1980s (Yan et al. 1985). In August 2001, 14 stations were sampled in the lake after dark, and only a few third and fourth instar *C. punctipennis* were found at one station in the north basin. When the abundance was corrected by the 70% net tow efficiency, density was estimated to be 0.13 larva·m^{-3}. This density is considerably low for fishless Ontario lakes of similar size and nutrient status (Wissel et al. 2003). Kirk (1993) reported a median density of 21 larvae·m^{-3} for *C. punctipennis* in 21 Sudbury lakes, and Persaud and Yan (2001) reported a median density of 33.2 larvae·m^{-3} in 47 Dorset, Ontario, lakes. The low abundance of *Chaoborus* larvae in acidic lakes with low DOC concentrations is not caused by acidity per se because *Chaoborus* are extremely acid tolerant (Price and Swift 1985). Consequently, the rarity of *C. punctipennis* in Ruth-Roy Lake led to the hypothesis that the water clarity and high UVR are important factors affecting this species.

As a result of the low density of *C. punctipennis* in Ruth-Roy Lake, all larvae were collected from Johnnie Lake (pH = 5.9 and DOC = 4.2 mg·L^{-1}). Larvae from a different source lake were used, since the UV sensitivity of *Chaoborus* appears to be the same regardless of their origin (Williamson et al. 1999; Persaud et al. 2003). The larvae were collected after dark by hauling a 46-cm-diameter, 150-µm-mesh conical net vertically through the water column. At the same time, small zooplankton were collected using a 12.5-cm-diameter, 55-µm-mesh net. All larvae were kept in source lake water and stored in glass jars at room temperature (21 °C). The following day, larvae were sorted according to size and fed excess zooplankton.

UVR tolerance experiments

Chaoborus punctipennis larvae were held in polystyrene culture flasks (210 mL) that were suspended horizontally. The upper surface of the polystyrene culture flasks had been replaced with quartz and a window covered with 40-µm mesh was inserted in a sidewall to facilitate circulation and exchange of lake water (details in Persaud and Yan 2003). These experimental flasks were tested for toxicity to eliminate any possibility of a flask effect on *Chaoborus* survival. We found that all larvae survived in the flasks after being submerged in lake water for approximately 8 h in the laboratory (Persaud and Yan 2003).

Chaoborus were exposed to full-spectrum light (UVR plus PAR) at four depths (0.25, 1.25, 3.0, and 5.0 m) in Ruth-Roy Lake between 0900 and 1800 local time. The full-spectrum treatment can be used to quantify UVR doses, since Persaud and Yan (2003) demonstrated that it is UVR, not PAR, that is responsible for the mortality observed under natural light. Dark controls, i.e., flasks wrapped in aluminum foil and black duct tape, were also incubated at each depth. We selected the four depths that gave us a wide range in dose rate without changes in spectral composition. The 9-h time period accounted for >90% of the daily UVR dose (M.T. Arts, National Water Research Institute, 867 Lakeshore Road, Burlington, ON L7R 4A6, personal communication).

We believe that these 9-h fixed incubation experiments can accurately predict UVR effects on *Chaoborus* larvae for several reasons. It is usual for early instar *Chaoborus* larvae to be at shallow depths during the day, and all instars can occupy the selected depths in lakes without fish, such as Ruth-Roy (Federenko and Swift 1972; McQueen et al. 1999). Once the larvae select a depth, it is common for them to stay

© 2005 NRC Canada

at depth all day (McQueen et al. 1999). Furthermore, Zagarese et al. (1998*a*) reported that static or fixed incubation systems could accurately predict mortality for vertically migrating species such as *Chaoborus* larvae.

At the end of the daily exposure period, the larvae were removed from the experimental flasks, dead larvae were separated, and the live larvae were fed excess small zooplankton collected from Johnnie Lake. Dead larvae were identified based on the integrity of their outer integument and immobility. In both treatments, survival was recorded at the end of each day as well as the following morning before the daily exposure. Each replicate consisted of 6–10 larvae, except for one replicate (fourth instar, dark control) that consisted of three larvae. Experiments were repeated over 2- to 4-day periods for third, early fourth, and late fourth instars.

At the end of the experiments, all larvae were preserved in ethanol. They were subsequently identified according to Saether (1972) and Borkent (1979) and aged. Distinctions between third instar and late and early fourth instars were based on head capsule length, overall size, and pupation.

Five separate experiments were run between 19 July and 19 August 2001. Two of these experiments were run using late fourth instars and one each with early fourth instars only, third instars only, and a mixture of third and early fourth instars. The average percent survival was calculated from three replicates ($n = 3$) at each depth for each exposure experiment, except for the 5.0-m exposure with the mixture of third and fourth instars ($n = 2$). We did not correct percent survival for mortality in dark controls, since control mortality was random and rare (overall weighted average = 3%).

Optical measurements

Throughout the experimental periods, we used a LI-COR LI-1400 photometer equipped with a LI-190S flat quantum sensor (LI-COR, Lincoln, Nebraska) to measure PAR fluxes and thereby estimate exposure irradiance. Instantaneous PAR values (micromoles per square metre per second) obtained from the LI-COR quantum sensor at regular intervals (8–10 min) daily were converted to radiometric units (milliwatts per square centimetre, irradiance) using the LI-COR conversion coefficient for daylight source (Biggs 1984). This Biggs (1984) conversion is extensively applied by LI-COR users; however, it only gives an approximation of the exposure irradiance.

For a 2-day sunny interval, we had access to an Optronics OL 754 UV-Visible scanning spectroradiometer equipped with a spherical OL IS-470-WP underwater sensor and an OL IS-670 (6-in.-diameter) integrating sphere (Optronics, Orlando, Florida). We employed this instrument to calculate underwater attenuation coefficients and model surface irradiance fluxes for the UVB and UVA wavebands. Since the OL IS-470-WP underwater sensor was calibrated in air, immersion correction factors were applied to the unweighted measurement of each scan to account for the response differences of the instrument's acrylic dome in air and water. The Optronics OL 754 UV-Visible scanning spectroradiometer was calibrated in July 2001 prior to use for our measurements in Ruth-Roy Lake.

On average, PAR fluxes were approximately 13% (SD = 8.4%) higher with the LI-COR than with the Optronics instrument. Since the Optronics spectroradiometer is a more robust, reliable, and accurate system, all LI-COR PAR values were adjusted (by reducing the values by 13%).

Attenuation coefficients

Immersion-corrected irradiance measurements were used to calculate the integrated downwelling irradiances for the PAR, UVA, and UVB wavebands at the 13 depths. The diffuse attenuation coefficients (K_d) were subsequently calculated for the PAR, UVA, and UVB wavebands for Ruth-Roy Lake according to Kirk (1994) as follows:

$$(1) \qquad K_d = -(\ln I_Z - I_0)/Z$$

where I_0 and I_Z are the irradiances at the surface and depth (Z), respectively.

The K_d values were initially calculated separately from morning and afternoon profiles. However, since the regression coefficients of the morning and afternoon profiles did not differ (paired t test, $p = 0.225$), they were pooled and a single combined K_d value was calculated and employed. The combined (i.e., morning and afternoon) K_d values for UVB, UVA, and PAR were 0.35, 0.13, and 0.09·m^{-1}, respectively ($r^2 \geq 0.90$ and $p < 0.0001$ for all regressions). As expected, short UVB wavelengths were more rapidly attenuated in the water column compared with UVA and PAR.

Modeling of UVB and UVA

PAR fluxes collected with the LI-COR sensor were used to reconstruct UVB and UVA levels through the use of regression models because a UV-Visible spectroradiometer was not available for use throughout the exposure periods. Gennings et al. (2001) have also successfully used this method to model UVA and UVB data. Linear regressions were developed using LI-COR PAR and Optronics UVA and UVB irradiances.

Surface UVA and UVB irradiance fluxes were determined from corrected LI-COR PAR irradiance flux (milliwatts per square centimetre) using the following regression models:

$$(2) \qquad \text{UVA} = 0.109\text{PAR} + 0.419 \quad (r^2 = 0.961,\ n = 41,\ \text{SE slope} = 0.004,\ p < 0.0001)$$

$$(3) \qquad \text{UVB} = 0.005\text{PAR} - 0.0112 \quad (r^2 = 0.8561,\ n = 41,\ \text{SE slope} < 0.001,\ p < 0.0001)$$

To obtain the cumulative doses (joules per square centimetre) at different depths, we corrected the UVA and UVB irradiance fluxes by the respective K_d and then integrated the irradiance fluxes (milliwatts per square centimetre) over different exposure time periods (seconds).

Estimation of LD_{50} and LT_{50}

UVR dose–response models were developed from linear regressions of percent survival and cumulative UVR (UVA and UVB) dose (joules per square centimetre) for the different instars at different depths. Regressions were performed using untransformed survival and UVR data. Because the larvae died rapidly, some regressions were based on only a few data points. Linear regressions were also run using

© 2005 NRC Canada

Fig. 1. Relative irradiance versus wavelengths (280–320 nm) for the four experimental depths (0.25 m (◆), 1.25 m (■), 3.0 m (▲), and 5.0 m (○)) on 23 July 2001 between (*a*) 1107 and 1133 and (*b*) 1505 and 1550 local time. Points represent the irradiance at each wavelength relative to that at 320 nm. Similarity of the different spectra indicates that spectral composition did not change with depth. Variations among spectra were due to changes in irradiance, which occurred over the time period when the spectral scans were obtained.

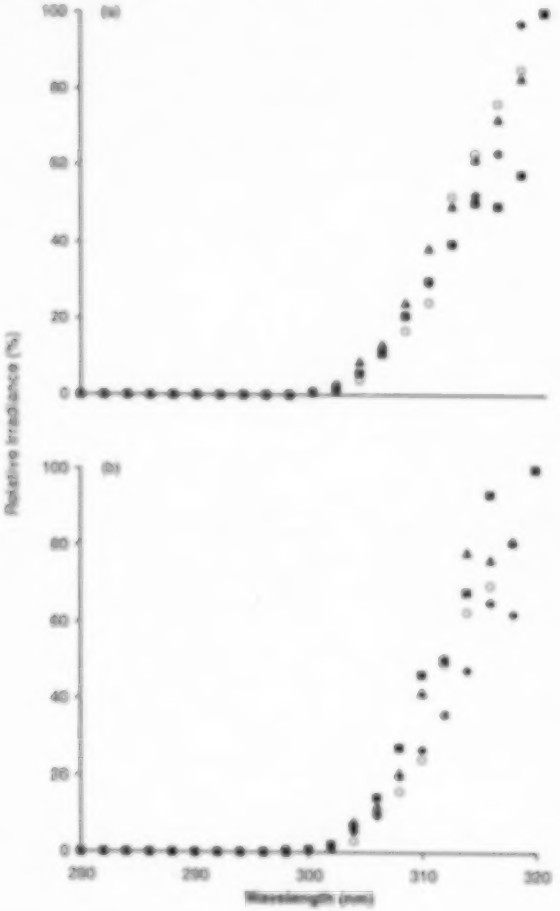

probit transformed data for the larger data sets and the r^2 and p values were compared.

To determine if rates of mortality differed among depths for each larval stage, we compared the survival versus cumulative UVR dose regressions using the methods outlined in Zar (1999). We found significant differences ($p < 0.001$ among the depths for all instars) between the regression coefficients. Consequently, LD_{50}s were calculated for each exposure depth for all instars from the linear dose–response models using the inverse prediction method (Zar 1999), that is, survival (the dependent variable) was used to obtain LD_{50} estimates (the independent variable).

To test for differences in UVR tolerance between developmental stages, we used only late fourth and third instar lethal doses, since only these values could be reported with confidence limits (Draper and Smith 1998). Small sample size prevented us from calculating confidence limits for some lethal doses. Two-way analysis of variance (ANOVA) was employed to test for differences in UVR tolerance between larval stages.

Table 1. UVB and UVA dose rates at different experimental depths.

	Dose rate ($mW \cdot cm^{-2}$)	
Depth (m)	UVB	UVA
0.25	0.135	3.233
1.25	0.093	2.874
3	0.054	2.451
5	0.032	1.800

Note: Spectral scans were done with the Optronics OL-754 between 1105 and 1149 on 23 July 2001; 1 W = 1 $J \cdot s^{-1}$.

For estimation of LT_{50}, we developed survival time–response models using untransformed percent survival data and duration of the exposures for the different instars at different depths. As with LD_{50}, LT_{50}s were calculated by applying the inverse prediction method (Zar 1999).

Reciprocity

When testing reciprocity under natural light conditions in a lake, the issue of maintaining similar spectral conditions among the treatments becomes especially important. Usually, reciprocity is tested in the laboratory under a stable light source and using a series of filters to achieve different dose rates. However, for this study, we used natural full-spectrum light and varied dose rates by incubating at different depths. We therefore carefully selected our incubation lake and depths. By choosing a study lake with a very low DOC concentration (0.2 $mg \cdot L^{-1}$), we were able to maintain similar spectral composition among the four experimental depths (see Fig. 1), since there was little selective absorption of different wavelengths with depth.

We tested for reciprocity using a one-way ANOVA to determine whether LD_{50} differed among the four depths, i.e., among the different dose rates, for all instars. As UVR irradiance was attenuated with depth, dose rate declined with depth in all experiments. At 0.25 m, the UVB and UVA dose rates were approximately five times and two times greater, respectively, than that at 5.0 m (Table 1). If reciprocity holds, LD_{50} will not differ among the depths. On the contrary, if physiological repair retards mortality at depth, reciprocity may not hold, and LD_{50} will increase with depth.

Results

Highly significant linear relationships were generally found between the untransformed percent survival data and UVR doses (Table 2; Fig. 2). Probit transformation did not improve the regressions for the larger data sets; hence, we used the linear regressions of untransformed data to develop the dose–response models.

UVR tolerance increased with age of larvae. The fourth instar *Chaoborus* were more tolerant than third instars (two-way ANOVA, $p = 0.022$). For third, early fourth, and late fourth instar LD_{50} ranged from 52.3 to 62.2 $J \cdot cm^{-2}$, from

© 2005 NRC Canada

Table 2. Dose–response models, calculated LD_{50} (median lethal doses), and 95% confidence intervals (CI) for the different *Chaoborus* instars at four depths.

Instar	Date	Depth (m)	Dose–response model	r^2	p	LD_{50} (J·cm^{-2})	CI
Late fourth	19–21 July	0.25	$y = -0.59x + 110.99$	0.82	0.035	102.3	52.8
		1.25	$y = -0.43x + 105.16$	0.97	0.013	127.1	37.9
		3.00	$y = -0.56x + 104.48$	0.98	0.008	96.9	22.6
		5.00	$y = -0.46x + 104.66$	0.88	0.057	119.6	49.7
	14–17 Aug.	0.25	$y = -0.55x + 99.24$	0.99	0.0003	88.8	6.9
		1.25	$y = -0.54x + 100.20$	0.99	0.0001	93.8	8.5
		3.00	$y = -0.70x + 113.42$	0.91	0.011	90.2	46.6
		5.00	$y = -0.76x + 112.93$	0.89	0.015	82.4	35.3
Early fourth	6–8 Aug.	0.25	$y = -0.86x + 109.43$	0.88	0.22	69.4	—
		1.25	$y = -0.70x + 114.61$	0.59	0.23	91.8	—
		3.00	$y = -0.94x + 114.65$	0.91	0.047	68.5	—
		5.00	$y = -1.01x + 111.46$	0.95	0.005	60.7	—
Third and early fourth	31 July – 1 Aug.	0.25	$y = -0.83x + 98.81$	0.99	0.049	58.6	—
		1.25	$y = -0.86x + 103.79$	0.95	0.144	62.2	—
		3.00	$y = -0.97x + 104.86$	0.95	0.138	56.3	—
		5.00	$y = -1.01x + 114.57$	0.87	0.069	63.7	—
Third	4–5 Aug.	0.25	$y = -0.94x + 99.35$	0.99	0.054	52.3	—
		1.25	$y = -0.68x + 97.97$	0.99	0.004	70.1	10.6
		3.00	$y = -0.89x + 98.91$	0.99	0.003	54.5	12.0
		5.00	$y = -0.93x + 107.68$	0.95	0.005	62.2	35.8

Note: All dose–response models were derived from linear regressions (such as Fig. 2) where y is the % survival of *Chaoborus* and x is the UVR dose.

Fig. 2. Dose–response models for experiments run 14–17 August 2001 with late fourth instar *Chaoborus punctipennis*. Points represent the untransformed mean survival ± SE (n = 3) at different doses for the four depths: 0.25 m (◆), 1.25 m (■), 3.00 m (▲), and 5.00 m (○). See Table 2 for the regression equations used as dose–response models.

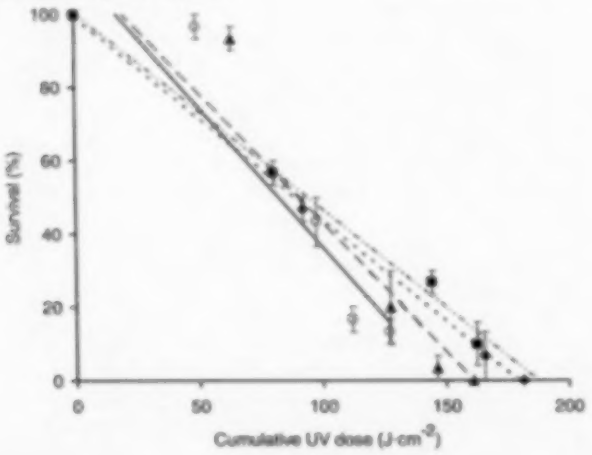

Fig. 3. Time–response models for experiments run 14–17 August 2001 with late fourth instar *Chaoborus punctipennis*. Points represent the untransformed mean survival ± SE (n = 3) at different exposure time periods for the four depths: 0.25 m (◆), 1.25 m (■), 3.00 m (▲), and 5.00 m (○).

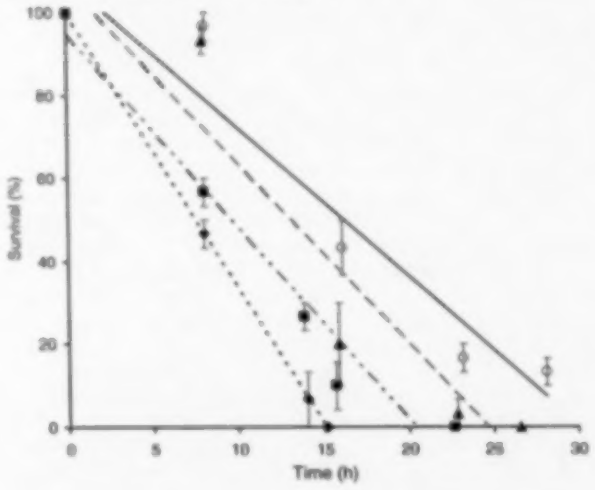

60.7 to 91.8 J·cm^{-2}, and from 82.4 to 127.1 J·cm^{-2}, respectively, among the four depths (Table 2). LD_{50} varied among depths, but there was no consistent relationship between the LD_{50} and incubation depth for any instar stage (two-way ANOVA, p = 0.719).

With the exception of early fourth instars, LT_{50} increased with depth and larval stage (Figs. 3 and 4). At 5.0 m, third, early fourth, and late fourth instars died in less than 10 (n = 3), 12 (n = 3), and 30 h (n = 6), respectively (Fig. 4). All third instars died at all depths within 2 clear (i.e., cloudless) exposure days. The early fourth instars died within 3 clear days. The mixture of third and early fourth instars died within 3 clear days. Four days of exposure killed all late fourth instars held down to 3.0 m deep in the water column.

© 2005 NRC Canada

Fig. 4. Calculated LT_{50} (median lethal time) for the different *Chaoborus punctipennis* instars at different depths (0.25 m (shaded bars), 1.25 m (hatched bars), 3.00 m (open bars), and 5.00 m (solid bars)) in Ruth-Roy Lake. All LT_{50}s were calculated from time–response models derived from linear regressions.

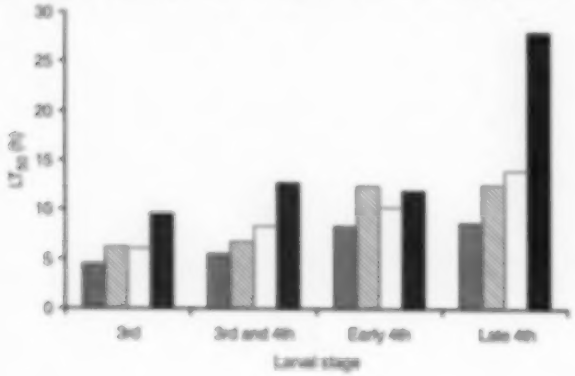

At 5.0 m, 13.3% of the late instars were still alive after 4 exposure days.

Dose rate did not affect LD_{50}; instead, survival was directly related to dose (e.g., Fig. 2). Reciprocity therefore held down to 5.0 m. Lethal doses for the four dose rates (depths) were not significantly different ($p = 0.689$).

Discussion

Developmental changes in UVR tolerance

Our results indicate that UVR tolerance increases with age for larval *C. punctipennis*. It is common for older life stages and larger organisms to be more tolerant of UVR. Karanas et al. (1979) found a direct positive relationship between age of the copepod *Acartia clausii* and UVR tolerance. Naupliar *A. clausii* died at much lower doses compared with copepodites under an artificial UVR source (Karanas et al. 1979). Lacuna and Uye (2000, 2001) reported higher lethal doses for older life stages of *Sinocalanus tenellus* and *Acartia omorii* compared with early life stages (eggs and nauplii). Leech and Williamson (2000) found that adult *Diaptomus minutus* were more tolerant to UVR than naupliar *D. minutus* in laboratory exposures. Of direct relevance to our work, Leech and Williamson (2000) also reported that young *Chaoborus* (first and second instar size-class) were less tolerant than older instars (third and fourth instar size-class). For young *Chaoborus* instars, this lower UVR tolerance combined with a diurnal epilimnetic habit strongly suggests that the survival of *Chaoborus* may be limited by UVR in low-DOC lakes such as Ruth-Roy Lake.

We can only speculate about the causes of developmental changes in UVR tolerance of *Chaoborus*. The stage-specific tolerances may be attributed to differences in integument protection and gene expression among instars (Naganuma et al. 1997; Lacuna and Uye 2000). Gene expression is more active in early life stages; consequently, UVR-induced damage is greater in these instars (Karanas et al. 1979; Naganuma et al. 1997; Zagarese and Williamson 2000). In general, the outer protective integument develops as organisms age; this renders early life stages least protected from UVR damage (Lacuna and Uye 2000). While it is not known whether the integument of *C. punctipennis* is photoprotective, it is possible that differences in integument resistance to damage could explain the differences in tolerance observed.

To minimize UVR-induced damage, aquatic invertebrates can employ three basic mechanisms: adaptation strategies (production of photoprotective pigments), behavioural strategies (diel vertical migration), and repair mechanisms (photoenzymatic repair). Several species reduce their UVR exposure by producing photoprotective compounds (Siebeck 1978; Ringelberg 1984). These pigments either reflect UVR or absorb and dissipate its energy, thereby protecting cellular components such as DNA (Vincent and Roy 1993). For example, Siebeck (1978) found that pigmented *Daphnia pulex obtusa* could tolerate higher UVR doses than transparent *Daphnia galeata gracilis* species. Hairston (1978) found the highest concentration of carotenoid pigments in *Diaptomus nevadensis* and *Diaptomus sicilis* near the lake surface, enabling these species to feed in the algal-rich layer despite UV exposure. Hessen (1994) found significantly greater survival time for a melanic clone of *Daphnia pulex* ($LT_{50} = 41.5 \pm 2.1$ h) compared with two different nonmelanic clones ($LT_{50} = 34.4 \pm 0.9$ and 35.0 ± 0.3 h) in laboratory experiments. Like transparent species, juvenile stages such as *C. punctipennis* larvae often lack any visible photoprotective pigments to protect their internal structures and are therefore highly vulnerable to UVR-induced damage (Williamson et al. 1997).

Upon detection of UVR, aquatic biota may respond by moving to more protected locations, thereby minimizing damage by these wavelengths (Barcelo and Calkins 1980; Pennington and Emlet 1986). Barcelo and Calkins (1980) found that the crustacean *Cyclops* moved away from a UVR source to a protected location, the rate of movement being dose dependent. Diel vertical migration is normally thought of as a predator avoidance strategy but also offers a behavioural means by which zooplankton and other aquatic biota can avoid photodamage by UVR (Hessen 1994; Siebeck et al. 1994). Even though older instar *Chaoborus* larvae normally migrate to the bottom, in shallow, low-DOC lakes where UVR penetrates to the bottom, our results suggest that UVR will still affect survival if the animals do not burrow into the sediments. Additionally, when visual predators are absent (as in fishless lakes), older instars tend to stay higher in the water column (Northcote et al. 1978; McQueen et al. 1999), exposing themselves to UVR. In deep, low-DOC lakes where very little UVR reaches the substrate, the UVR effect may be negligible for older instars, but young instars that dwell in the surface waters may still be affected.

DNA repair mechanisms may increase the tolerance of some species to UVR exposure (Zagarese et al. 1997); however, not all organisms possess such repair mechanisms. UVA and PAR are widely considered triggers for photorepair mechanisms that are vital for recovery from UVR-induced damage (Siebeck and Böhm 1994). The rapid mortality rates that we observed and the presence of reciprocity (discussed below) suggest that photorepair mechanisms may be absent in larval *Chaoborus* or inadequate in repairing UVR-induced damage under the natural UVA and PAR irradiances of our experiments. Instead, the combined results from Persaud and Yan (2003) and work done by Williamson et al. (1999) sug-

© 2005 NRC Canada

gests that UVA is just as effective as UVB in inducing photodamage in *Chaoborus*. Williamson et al. (1999) found high mortality with UVB (quartz treatment: UVB plus UVA plus PAR) and without UVB (mylar treatment: UVA plus PAR), while Persaud and Yan (2003) found very low mortality under PAR only (OP3). Setlow (1974) reported that UVA is ineffective in altering DNA molecules; however, other studies (Zagarese et al. 1997; Zellmer 1998) have reported that UVA is involved in incurring damage. It is unknown whether PAR can trigger photorepair mechanisms in *Chaoborus*, but it is clear from our experiments that PAR-mediated and dark repair mechanisms are ineffective in alleviating UVR-induced damage.

Reciprocity

The UVR-induced mortality observed for *C. punctipennis* in Ruth-Roy Lake was not dose rate dependent; it was dose dependent. In other words, for UVR exposure of *C. punctipennis*, reciprocity holds.

Reciprocity often fails when a broad range of exposure conditions is examined; in contrast, under a narrow range of conditions, reciprocity will most likely hold (Zagarese and Williamson 2000). The natural UVR attenuation capacity of DOC and water enabled us to administer a wide range of dose rates during these experiments; however, the DOC content was low enough that we did not have changes in spectral composition at the experimental depths. At 5.0 m, the UVB and UVA dose rates are reduced to approximately 20% and 55%, respectively, of those administered at 0.25 m, yet reciprocity held over the four different dose rates administered. Even though the dose rates administered under natural conditions cannot be kept constant, ultimately, UVR effects and reciprocity must be tested under natural conditions to account for natural spatial and temporal variability of the solar spectrum and changes in the spectral intensity of light with depth in aquatic environments. To our knowledge, this is only the second demonstration of reciprocity in a freshwater invertebrate exposed to UVR under natural light conditions and intensities. Zagarese et al. (1998*a*, 1998*b*) reported that reciprocity held under natural conditions in the freshwater copepod *Boeckella gracilipes*, a species with no photoreactivation capabilities. Under the same natural conditions, Zagarese et al. (1998*b*) found failure of reciprocity in *Ceriodaphnia dubia*, which they attributed to photorepair mechanisms. Siebeck and Böhm (1994) tested for reciprocity under natural light levels, but reciprocity failed in the *Daphnia* species that they studied.

Reciprocity has been found to hold in copepods (Browman et al. 2000) and ichthyoplankton (Kouwenberg et al. 1999*a*) exposed to UVR. Browman et al. (2000) reported that reciprocity held for both *Calanus finmarchicus* and Atlantic cod eggs when incubated under a solar simulator. Like Browman et al. (2000), Kouwenberg et al. (1999*a*) found that reciprocity held for Atlantic cod eggs under similar laboratory conditions. In contrast, failure of reciprocity has been found in cladocerans (Grad et al. 2001), other ichthyoplankton (Hunter et al. 1981), and larval shrimp (Damkaer and Dey 1983; Wubben 2000). Grad et al. (2001) found that reciprocity did not hold for *Daphnia pulicaria* in experiments run under laboratory conditions. Damkaer and Dey (1983) reported that reciprocity failed in the larval shrimp *Pandalus platyceros* under laboratory conditions. Hunter et al. (1981) found that reciprocity failed when survival of juvenile northern anchovy was examined under laboratory conditions. Wubben (2000) reported that reciprocity held for larvae of the brown shrimp *Crangon crangon* under a sunshine simulator.

It is clear that *Chaoborus* are highly sensitive to current UVR levels in shallow, low-DOC Canadian Shield lakes. Even though older *Chaoborus* instars are not found in the surface waters during the day, in shallow, fishless, low-DOC lakes where there is UVR penetration to the sediments, their survival will be affected by UVR. In contrast, survival of young instars will always be at risk from UVR, since they are present in the surface waters during daylight hours. Furthermore, the presence of reciprocity suggests that *C. punctipennis* do not possess the mechanisms essential for repairing any UV-induced damage. Consequently, UVR may negatively affect *Chaoborus* abundance and restrict their distribution. As *Chaoborus* are integral in freshwater food web function (Moore et al. 1994) but more sensitive than higher trophic levels to UVR (Williamson et al. 1999), it is possible that UVR will indirectly affect the trophic dynamics of Canadian Shield lakes. UVR may also hinder the recovery of aquatic biota from historical acidification damage whenever DOC levels are low or in decline.

UV irradiance of surface waters has and will probably continue to increase because of the two global stressors: stratospheric ozone depletion and climate change. Industrial atmospheric pollution has led to the acidification and clarification of many Ontario lakes. Neary et al. (1990) reported that 7% of Ontario lakes have a DOC concentration <2 mg·L^{-1}. While recovery from acidification is associated with a rise in DOC levels, climate change promotes a decline in DOC (Williamson et al. 1996; Yan et al. 1996; Gunn et al. 2001). Additionally, stratospheric ozone depletion is forecasted to continue for several decades (Shindell et al. 1998), leading to higher UVR levels and a shift in the UVB:UVA and UVB:PAR ratios reaching the earth's surface (Madronich et al. 1995; Whitehead et al. 2000). Hence, many lakes with DOC close to 2 mg·L^{-1} will experience further declines in DOC, placing them in the same category as Ruth-Roy Lake. Consequently, UVR penetration into freshwater environments will increase, and *Chaoborus*, may have more difficulty employing their typical "avoidance strategy" (Siebeck and Böhm 1994) to reduce their UVR exposure. It is therefore possible that UVR damage to *Chaoborus* will become more common in the future.

Acknowledgements

We thank the staff of the Co-operative Freshwater Ecology Unit at Laurentian University in Sudbury, Ontario, and Killarney Provincial Park staff for their assistance. Kevin Shaughnessy assisted in all data collection in the field. Vijay Tumber and Michael Arts, National Water Research Institute, Saskatoon, Saskatchewan, assisted with collection of light data. We also thank Dr. Grabriella Dee at Lehigh University for her helpful comments. This project was supported by a Natural Sciences and Engineering Research Council of Canada postgraduate scholarship awarded to Anurani Persaud and a Natural Sciences and Engineering Research

© 2005 NRC Canada

Council of Canada industrial-oriented research grant to N.D. Yan and J. Gunn.

References

Arts, M.T., and Rai, H. 1997. Effects of ultraviolet-B radiation on the production of lipid, polysaccharide and protein in three freshwater algal species. Freshw. Biol. **38**: 597–610.

Barcelo, J.A., and Calkins, J. 1980. The kinetics of avoidance of simulated solar UV radiation by two arthropods. Biophys. J. **32**: 921–930.

Béland, F., Browman, H.I., Rodriguez, C.A., and St-Pierre, J.-F. 1999. Effect of solar ultraviolet radiation (280–400 nm) on the eggs and larvae of Atlantic cod (*Gadus morhua*). Can. J. Fish. Aquat. Sci. **56**: 1058–1067.

Biggs, W.W. 1984. Radiation measurement. *In* Advanced agricultural instrumentation: design and use. Proceedings of the NATO Advanced Study Institute on "Advanced Agricultural Instrumentation". *Edited by* W.G. Gensler. Martinus Nijhoff Publishers, Dordrecht, Holland. pp. 20–24.

Borkent, A. 1979. Systematics and bionomics of the species of the subgenus *Schadonophasma* Dyar and Shannon (*Chaoborus*, Chaoboridae, Diptera). Quaest. Entomol. **15**: 123–255.

Browman, H.I., Rodriguez, C.A., Béland, F., Cullen, J.J., Davis, R.F., Kouwenberg, J.H.M., Kuhn, P.S., McArthur, B., Runge, J.A., St-Pierre, J.-F., and Vetter, R.D. 2000. Impact of ultraviolet radiation on marine crustacean zooplankton and ichthyoplankton: a synthesis of results from the estuary and Gulf of St. Lawrence, Canada. Mar. Ecol. Prog. Ser. **199**: 293–311.

Caldwell, M.M. 1979. Plant life and ultraviolet radiation: some perspective in the history of the earth's UV climate. BioScience, **29**: 520–525.

Coohill, T.P. 1991. Action spectra again? Photochem. Photobiol. **54**: 859–870.

Damkaer, D.M., and Dey, D.B. 1983. UV damage and photoreactivation potentials of larval shrimp, *Pandalus platyceros*, and adult euphausiids, *Thysanoessa raschii*. Oecologia, **60**: 169–175.

de Gruijl, F.R., Sterenoborg, H.J.C.M., Slaper, H., and Van der Leun, J.C. 1986. Dose and dose rate responses to UV-B radiation: implications for reciprocity. *In* Stratospheric ozone reduction, solar ultraviolet radiation and plant life. *Edited by* R.C. Worrest and M.M. Caldwell. Springer-Verlag, New York. pp. 119–126.

Draper, N.R., and Smith, H. 1998. Applied regression analysis. Wiley-Interscience, New York.

Federenko, A.Y., and Swift, M.C. 1972. Comparative biology of *Chaoborus americanus* and *Chaoborus trivittatus* in Eunice Lake, British Columbia. Limnol. Oceanogr. **17**: 721–730.

Gennings, C., Molot, L.A., and Dillon, P.J. 2001. Enhanced photochemical loss of organic carbon in acidic waters. Biogeochemistry, **52**: 339–354.

Graf, G., Williamson, C.E., and Karapelou, D.M. 2001. Zooplankton survival and reproduction responses to damaging UV radiation: a test of reciprocity and photoenzymatic repair. Limnol. Oceanogr. **46**: 584–591.

Gunn, J.M., Snucins, E., Yan, N.D., and Arts, M.T. 2001. Use of water clarity to monitor the effects of climate change and other stressors on oligotrophic lakes. Environ. Monit. Assess. **67**: 69–88.

Hairston, H.G. 1978. Carotenoid photoprotection in *Diaptomus kenai*. Int. Ver. Theor. Angew. Limnol. Verh. **20**: 2541–2545.

Hessen, D.O. 1994. *Daphnia* responses to UV-light. Arch. Hydrobiol. Beih. Ergebn. Limnol. **43**: 185–195.

Holt, C., and Yan, N.D. 2003. Recovery of zooplankton communities from acidification in Killarney Park, Ontario, 1971–2000: pH 6 as a recovery goal. Ambio, **32**: 219–224.

Hunter, J.R., Taylor, J.H., and Moser, H.G. 1981. Effects of solar and artificial ultraviolet-B radiation on larval northern anchovy, *Engraulis mordax*. Photochem. Photobiol. **34**: 477–486.

Jeffrey, W.H., Aas, P., Lyons, M.M., Coffin, R.B., Pledger, R.J., and Mitchell, D.L. 1996. Ambient solar radiation-induced photodamage in marine bacterioplankton. Photochem. Photobiol. **64**: 419–427.

Karanas, J.J., Van Dyke, H., and Worrest, R.C. 1979. Midultraviolet (UV-B) sensitivity of *Acartia clausii* Giesbrecht (Copepoda). Limnol. Oceanogr. **24**: 1104–1116.

Kerr, J.B., and McElroy, C.T. 1993. Evidence for large upward trends of ultraviolet-B radiation linked to ozone depletion. Science (Wash., D.C.), **262**: 1032–1034.

Kirk, J.T.O. 1994. Light and photosynthesis in aquatic ecosystems. 2nd ed. Cambridge University Press, New York.

Kirk, R.J. 1993. Distribution of *Chaoborus* spp. in Sudbury area lakes. Report for the Ministry of Natural Resources/Laurentian University Cooperative Freshwater Ecology Unit, Laurentian University, Sudbury, Ont.

Kouwenberg, J.H.M., Browman, H.I., Cullen, J.J., Davis, R.F., St-Pierre, J.-F., and Runge, J.A. 1999*a*. Biological weighting of ultraviolet (280–400 nm) induced mortality in marine zooplankton and fish. I. Atlantic cod (*Gadus morhua*) eggs. Mar. Biol. **134**: 269–284.

Kouwenberg, J.H.M., Browman, H.I., Runge, J.A., Cullen, J.J., Davis, R.F., and St-Pierre, J.-F. 1999*b*. Biological weighting of ultraviolet (280–400 nm) induced mortality in marine zooplankton and fish. II. *Calanus finmarchicus* (Copepoda) eggs. Mar. Biol. **134**: 285–293.

Lacuna, D.L., and Uye, S.-I. 2000. Effect of UVB radiation on the survival, feeding and egg production of the brackish-water copepod, *Sinocalanus tenellus*, with notes on photoreactivation. Hydrobiologia, **434**: 73–79.

Lacuna, D.L., and Uye, S.-I. 2001. Influence of mid-ultraviolet (UVB) radiation on the physiology of the marine planktonic copepod *Acartia omorii* and the potential role of photoreactivation. J. Plankton Res. **23**: 143–155.

Leech, D.M., and Williamson, C.E. 2000. Is tolerance to UV radiation in zooplankton related to body size, taxon, or lake transparency? Ecol. Appl. **10**: 1530–1540.

Madronich, S., McKenzie, R.L., Caldwell, M.M., and Bjorn, L.O. 1995. Changes in ultraviolet radiation reaching the earth's surface. Ambio, **24**: 143–152.

Malloy, K.D., Hollman, M.A., Mitchell, D., and Detrich, H.W., III. 1997. Solar UVB-induced DNA damage and photoenzymatic DNA repair in Antarctic zooplankton. Proc. Natl. Acad. Sci. U.S.A. **94**: 1258–1263.

McQueen, D.J., Ramcharan, C.W., Demers, E., Yan, N.D., Conforti, L.M., and Perez-Fuentetaja, A. 1999. *Chaoborus* behavioural responses to changes in fish density. Arch. Hydrobiol. **145**: 165–179.

Moore, M.V., Yan, N.D., and Pawson, T. 1994. Omnivory of the larval phantom midge (*Chaoborus* spp.) and its potential significance for freshwater planktonic food-webs. Can. J. Zool. **72**: 2055- 2065.

Naganuma, T., Inoyue, T., and Uye, S. 1997. Photoreactivation of UV-induced damage to embryos of a planktonic copepod. J. Plankton Res. **19**: 783–787.

Neary, B.P., Dillon, P.J., Munro, J.R., and Clark, B.J. 1990. The acidification of Ontario lakes: an assessment of their sensitivity and current status with respect to biological damage. Ontario Ministry of the Environment, Dorset, Ont.

Norins, A.L. 1969. Immediate effects of light. *In* Biologic effects of ultraviolet radiation. *Edited by* F. Urbach. Pergamon Press, Oxford, UK.

© 2005 NRC Canada

Northcote, T.G., Walters, C.J., and Hume, J.M. 1978. Initial impacts of the experimental fish introduction on the macrozooplankton of small oligotrophic lakes. Verh. Int. Ver. Limnol. **20**: 2003–2012.

Pennington, J.T., and Emlet, R.B. 1986. Ontogenetic and diel vertical migration of a planktonic echinoid larva, *Dendraster excentricus* (Eschscholtz): occurrence, causes and probable consequences. J. Exp. Mar. Biol. Ecol. **104**: 69–95.

Perez-Fuentetaja, A., Dillon, P.J., Yan, N.D., and McQueen, D.J. 1999. Significance of dissolved organic carbon in the prediction of thermocline depth in small Canadian Shield lakes. Aquat. Ecol. **33**: 127–133.

Persaud, A.D., and Yan, N.D. 2001. Accounting for spatial variability in the design of sampling programmes for *Chaoborus* larvae. J. Plankton Res. **23**: 279–285.

Persaud, A.D., and Yan, N.D. 2003. UVR sensitivity of *Chaoborus* larvae. Ambio, **32**: 219–224.

Persaud, A.D., Arts, M.T., and Yan, N.D. 2003. Photoresponses of late instar *Chaoborus punctipennis* larvae to UVR. Aquat. Ecol. **37**: 257–265.

Price, E.E., and Swift, M.C. 1985. Inter- and intra-specific variability in the response of zooplankton to acid stress. Can. J. Fish. Aquat. Sci. **42**: 1749–1754.

Ramcharan, C., McQueen, D.J., Perez-Fuentetaja, A., Yan, N.D., Demers, E., and Rusak, J. 2001. Analyses of lake foodwebs using individual-based models to estimate *Chaoborus* production and consumption. Arch. Hydrobiol. Spec. Issues Adv. Limnol. **56**: 101–126.

Ringleberg, J., Keyser, A.L., and Flik, B.J.G. 1984. The mortality effect of ultraviolet radiation in a translucent and in a red morph of *Acanthodiaptomus denticornis* (Crustacea, Copepoda) and its possible ecological relevance. Hydrobiologia, **112**: 217–222.

Saether, O.A. 1972. Chaoboridae. *In* Die Binnengewasser Bd 26. *Edited by* H.-J. Elser and W. Ohle. E. Schweizerbart'sche Verlagsbuchhandlung, Stuttgart. pp. 257–280.

Schindler, D.W. 1998. A dim future for boreal waters and landscapes. BioScience, **48**: 157–164.

Schindler, D.W., Curtis, P.J., Parker, B.R., and Stainton, N.P. 1996. Consequences of climatic warming and lake acidification for UV-B penetration in North American boreal lakes. Nature (Lond.), **379**: 705–708.

Scully, N.M., and Lean, D.R.S. 1994. The attenuation of ultraviolet radiation in temperate lakes. Arch. Hydrobiol. Beih. Ergebn. Limnol. **43**: 135–144.

Setlow, R.B. 1974. The wavelengths in sunlight effective in producing skin cancer: a theoretical analysis. Proc. Natl. Acad. Sci. U.S.A. **71**: 3363–3366.

Shindell, D.T., Rind, D., and Lonergan, P. 1998. Increased polar stratospheric ozone losses and delayed eventual recovery owing to increasing greenhouse-gas concentrations. Nature (Lond.), **392**: 589–592.

Siebeck, O. 1978. Ultraviolet tolerance of planktonic crustaceans. Verh. Int. Ver. Limnol. **20**: 2469–2473.

Siebeck, O., and Böhm, U. 1994. Challenges for an appraisal of UV-B effects upon planktonic crustaceans under natural radiation conditions with a non-migrating (*Daphnia pulex obtusa*) and a migrating cladoceran (*Daphnia galeata*). Arch. Hydrobiol. Beih. Ergebn. Limnol. **43**: 197–206.

Siebeck, O., Vail, T.L., Williamson, C.E., Vetter, R., Hessen, D., Zagarese, H., Little, E., Balseiro, E., Modenutti, B., Seva, J., and Shumate, A. 1994. Impact of UV-B radiation on zooplankton and fish in pelagic freshwater ecosystems. Arch. Hydrobiol. Beih. Ergebn. Limnol. **43**: 101–114.

Sinha, R.P., Singh, N., Kumar, H.D., Häder, H.D., Häder, M., and Häder, D.-P. 1996. Effects of UV radiation on certain physiological and biochemical processes in cyanobacteria. Photochem. Photobiol. **32**: 107–113.

Vincent, W.E., and Neale, P.J. 2000. Mechanisms of UV damage to aquatic organisms. *In* The effects of UV radiation in the marine environment. *Edited by* S. de Mora, S. Demers, and M. Vernet. Cambridge University Press, New York. pp. 149–176.

Vincent, W.E., and Roy, S. 1993. Solar ultraviolet-B radiation and aquatic primary production: damage, protection and recovery. Environ. Rev. **1**: 1–11.

Whitehead, R.R., de Mora, S.J., and Demers, S. 2000. Enhanced UV radiation — a new problem for the marine environment. *In* The effects of UV radiation in the marine environment. *Edited by* S. de Mora, S. Demers, and M. Vernet. Cambridge University Press, New York. pp. 1–34.

Williamson, C.E., Stemberger, R.S., Morris, D.P., Frost, T.M., and Paulsen, S.G. 1996. Ultraviolet radiation in North American lakes: attenuation estimates from DOC measurements and implications for plankton communities. Limnol. Oceanogr. **41**: 1024–1034.

Williamson, C.E., Metzgar, S.L., Lovera, P.A., and Moeller, R.E. 1997. Solar ultraviolet radiation and the spawning habitat of yellow perch, *Perca flavescens*. Ecol. Appl. **7**: 1017–1023.

Williamson, C.E., Hargreaves, B.R., Orr, P.S., and Lovera, P.A. 1999. Does UV play a role in changes in predation and zooplankton community structure in acidified lakes? Limnol. Oceanogr. **44**: 774–783.

Wissel, B., Yan, N.D., and Ramcharan, C. 2003. Predation and refugia: implications for *Chaoborus* abundance and species composition. Freshw. Biol. **48**: 1421–1431.

Wubben, D.L. 2000. UV-induced mortality of zoea I larvae of brown shrimp *Crangon crangon* (Linnaeus, 1758). J. Plankton Res. **22**: 2095–2104.

Yan, N.D. 1983. The effects of changes in pH on transparency and on thermal regimes of Lohi Lake, near Sudbury, Ontario. Can. J. Fish. Aquat. Sci. **40**: 621–626.

Yan, N.D., Nero, R.W., Keller, W., and Lasenby, D.C. 1985. Are *Chaoborus* larvae more abundant in acidified than in non-acidified lakes in Central Canada? Holarct. Ecol. **8**: 93–199.

Yan, N.D., Keller, W., Scully, N.M., Lean, D.R.S., and Dillon, P.J. 1996. Increased UV-B penetration in a lake owing to drought induced acidification. Nature (Lond.), **381**: 141–143.

Zagarese, H.E., and Williamson, C.E. 2000. Impact of solar UV radiation on zooplankton and fish. *In* The effects of UV radiation in the marine environment. *Edited by* S. de Mora, S. Demers, and M. Vernet. Cambridge University Press, New York. pp. 279–309.

Zagarese, H.E., Feldman, M., and Williamson, C.E. 1997. UV-B induced damage and photoreactivation in three species of *Boeckella* (Copepoda, Calanoida). J. Plankton Res. **19**: 357–367.

Zagarese, H.E., Cavero, W., Gonzalez, P., and Pedrozo, F. 1998*a*. Copepod mortality induced by fluctuating levels of natural ultraviolet radiation simulating vertical water mixing. Limnol. Oceanogr. **43**: 169–174.

Zagarese, H.E., Tartarotti, B., Cavero, W., and Gonzalez, P. 1998*b*. UV damage in shallow lakes: the implications of water mixing. J. Plankton Res. **20**: 1423–1433.

Zar, J.H. 1999. Biostatistical analysis. Prentice Hall, Englewood Cliffs, N.J.

Zellmer, I.D. 1998. The effect of solar UVA and UVB on subarctic *Daphnia pulicaria* in its natural habitat. Hydrobiologia, **379**: 55–62.

© 2005 NRC Canada

Empirical model for predicting a catchment-scale metric of surface water transit time in streams

Erwin E. Van Nieuwenhuyse

Abstract: Estimates of average water velocity (v_w) extracted from tracer dye studies (v_{dye}) or calculated from velocity–discharge relationships at continuous-flow gauges (v_{gage}) were combined with catchment area (A) and other readily available data for 111 streams throughout the conterminous United States. The resulting data set (n = 305) represented broad ranges of A (65 – 62 419 km^2), mainstem length (L_{main}, 15.6–867 km), slope (S, 0.14–11.5 m·km^{-1}), and daily average discharge (Q, 0.09–634 m^3·s^{-1}). A catchment-scale metric of surface water transit time (T_w, $L_{main}v_{dye}^{-1}$) ranged from 0.3 to 40 days, averaging 7.2 days. A bivariate regression model using $\log_{10} A$ and $\log_{10} Q$ explained 83% of the variation in $\log_{10} T_w$ and predicted T_w with an average precision of ±49%. By contrast, a previously published model based on hydraulic geometry relationships overestimated T_w by 100%. Application of my model to five streams nested in a ninth-order (ω = 9) catchment indicated that under dry (September) and wet (March), long-term (1954–2001) median flow conditions, v_w increased with Q ($v_w \propto Q^{0.3}$) as far downstream as ω = 8 and then remained constant or declined. The slope of this longitudinal v_w–Q relationship was three times greater than the expected value. Longitudinal velocity gradients in many streams may thus be much steeper than commonly assumed.

Résumé : Des estimations de la vitesse moyenne du courant (v_w) obtenues d'études faites avec des colorants traceurs (v_{dye}) ou calculées à partir des relations vitesse–débit à des stations de jaugeage continu (v_{gage}) ont été combinées à la surface du bassin versant (A) et à d'autres données généralement disponibles dans 111 cours d'eau des États-Unis continentaux. La banque de données obtenue (n = 305) représente une gamme étendue de surfaces (A, 65 – 62 419 km^2), de longueurs du cours principal (L_{main}, 15,6–867 km), de pentes (S, 0,14–11,5 m·km^{-1}) et de débits journaliers moyens (Q, 0,09–634 m^3·s^{-1}). Une métrique du temps de passage de l'eau en surface à l'échelle du bassin versant (T_w, $L_{main}v_{dye}^{-1}$) varie de 0,3–40 jours, avec une moyenne de 7,2 jour. Un modèle de régression bidimensionnel qui relie $\log_{10} A$ et $\log_{10} Q$ explique 83 % de la variation de $\log_{10} T_w$ et prédit T_w avec une précision moyenne de ±49 %. Par comparaison, un modèle publié antérieurement basé sur des relations de « géométrie hydraulique » surestime T_w de 100 %. L'application du présent modèle à cinq cours d'eau appartenant à un bassin versant d'ordre 9 (ω = 9) montre que, dans des conditions de débit moyen à long terme (1954–2001) en périodes de sécheresse (septembre) et d'humidité (mars), v_w augmente en fonction de Q ($v_w \propto Q^{0.3}$) vers l'aval jusqu'à ω = 8, pour ensuite demeurer constant ou décliner. La pente de cette relation longitudinale v_w–Q est trois fois plus importante que prévu. Les gradients longitudinaux de vitesses du courant dans plusieurs cours d'eau peuvent ainsi être beaucoup plus prononcés qu'on le croit généralement.

[Traduit par la Rédaction]

Introduction

How long on average surface water takes to travel from source to mouth within a stream channel network has long been of interest to fluvial ecologists, hydrologists, and geomorphologists. Studying how surface water transit time (T_w) varies among systems or how T_w varies longitudinally within a stream has often led to useful (and occasionally even unexpected) findings that have furthered the understanding of how lotic ecosystems function. For example, prior to field studies documenting the positive relationship between average mainstem transit time and sestonic algal abundance (e.g., Talling and Rzoska 1967), most researchers believed that all suspended algae in lotic ecosystems originated from washout of phytoplankton produced in floodplain lakes (Des Cilleuls 1928) or from dislodged benthic production (Butcher 1932). By studying longitudinal variation in sestonic algal abundance and T_w within a stream, Eddy (1934) was even able to estimate a threshold value (20 days) below which an appreciable potamoplankton community was unlikely to develop. The geographic position of this threshold T_w, moreover, moved upstream or downstream as flow within the network decreased or increased, respectively. Similarly, Leopold and Maddock's (1953) finding that mainstem velocity (as measured at a flow gauge) either remained constant or even increased slightly with longitudinal distance within a network ($v_w \propto Q_{ave}^{0.1}$) was unexpected and initially quite controversial. Prior to this discovery, most experts agreed that surface water flow grew more sluggish as streams coalesced into rivers (Carlston 1969).

Such findings are important because, in addition to plankton production, transit time affects the rate and outcome of a

Received 1 August 2003. Accepted 12 November 2004. Published on the NRC Research Press Web site at http://cjfas.nrc.ca on 30 March 2005.
J17685

E.E. Van Nieuwenhuyse. Bureau of Reclamation, Division of Environmental Affairs, 2800 Cottage Way, MP-150, Sacramento, CA 95825, USA (e-mail: evannieuwenhuyse@mp.usbr.gov).

 doi: 10.1139/F04-202 © 2005 NRC Canada

wide variety of lotic ecosystem processes, including reaeration and other forms of gas exchange with the atmosphere (O'Connor and Dobbins 1956), erosion or deposition of bed and bank materials (Leopold et al. 1964), the spiraling of nutrients or contaminants, and other biogeochemical exchanges between the water column and the benthos (Newbold 1992) and the washout of invertebrates and fish larvae (Waters 1961). Given the difficulty and high cost of measuring transit time with dye-tracking experiments, the ability to reliably predict T_w using data that are comparatively easy to obtain would thus be of some practical value.

Soballe and Kimmel (1987) developed such a model to compare average hydraulic conditions among streams, lakes, and reservoirs representing broad ranges of fertility and algal productivity. They needed for streams a bulk hydraulic variable similar to the theoretical hydraulic residence time (volume divided by outflow) of lakes. And they needed a simple empirical model for quantifying this variable for a large sample of streams. The theoretical variable that they defined (implicitly) for this purpose was in effect a catchment-scale metric of surface water transit time:

$$(1) \qquad \tau_w = \Lambda v_w^{-1}$$

where τ_w is the average transit time from source to outlet, Λ is the average path length of surface flow from source to outlet, and v_w is the average velocity of surface flow along the way. In their operational version of this equation, Soballe and Kimmel (1987) used an estimate of mainstem length (L_{max}) as a surrogate for Λ and substituted an estimate of average cross-sectional velocity at the outlet's flow gauge (v_{gage}) for v_w. They estimated L_{max} on the basis of catchment area (A) using Hack's (1957) L_{max}–A relationship for Virginia and Maryland streams ($L_{max} \propto A^{0.6}$), whereas gauge velocity was calculated using a regional velocity–discharge relationship ($v_{gage} \propto Q_{ave}^{0.1}$) for streams in the Midwest United States (see table 7-5 in Leopold et al. 1964). Thus, their empirical model for estimating the transit time of whole streams was

$$(2) \qquad T_{w(ave)} = 0.08\ A^{0.6}\ Q_{ave}^{-0.1}$$

where $T_{w(ave)}$ is the annual average transit time (days), A is the catchment area upstream of the gauge (square kilometres), and Q_{ave} is the mean annual discharge at the gauge (cubic metres per second).

Soballe and Kimmel's (1987) metric of long-term average transit time (which they called water residence time) has proved useful for making coarse-scale comparisons of the effect of T_w on plankton abundance in streams (Basu and Pick 1996), but a tool that could also quantify how T_w differs between dry and wet years or varies seasonally within a year would be even more useful. The goal of this study was to provide stream ecologists with just such a tool. The principal objectives of this study were to (*i*) compile estimates of A, L_{max}, Q, v_{gage}, v_{dye}, and other variables for a large sample of streams, (*ii*) use these data to calibrate and validate an empirical model for predicting T_w, (*iii*) examine how T_w varies longitudinally within a network by applying the model to a group of streams nested in a ninth-order catchment, and (*iv*) compare my model's $T_{w(ave)}$ predictions with values calculated using eq. 2.

Methods

The random variable that I used to represent τ_w in developing my empirical model was defined as

$$(3) \qquad T_w = L_{max}\ v_{dye}^{-1}$$

where T_w is the surface water transit time metric for the entire length of a stream's mainstem, L_{max} is mainstem length (drainage divide to outlet), and v_{dye} is the average velocity of surface water flow as estimated by the travel time of a tracer dye cloud. I used L_{max} as a surrogate for Λ because L_{max} data are readily available or can be calculated with reasonable precision from L_{max}–A relationships (Mueller 1973). Moreover, there is some evidence to suggest that the relationship between L_{max} and Λ may (like the L_{max}–A relationship) be a conservative property of streams. Over a broad range of A (1 – 23 569 km^2), the ratio Λ:L_{max} apparently varies within a narrow range (0.49–0.68), averaging perhaps 0.6 ± 0.06 (Thomas and Benson 1970; Robinson et al. 1995). I used v_{dye} as a surrogate for v_w because dye tracking is still the most accurate way to measure the actual surface water velocity of a stream channel (Jobson 1996). I hypothesized that most of the variation in T_w should be accounted for by variation in catchment area (because of its tight relationship with L_{max}), discharge (because of its relationship with velocity), and mainstem slope, assuming that at a given Q, velocity should increase with S (Leopold et al. 1964).

All of the data for this study were compiled from the literature and existing databases. Data extracted from time-of-travel reports presenting the results of tracer dye experiments were used to estimate v_{dye}, whereas estimates of A, L_{max}, and S were obtained from catchment characteristics files maintained by the US Geological Survey (Don Dolnack, Data Base Administrator/WATSTORE, 12201 Sunrise Valley Drive, Reston, VA 20192, USA). Similarly, daily average discharge data (http://waterdata.usgs.gov/nwis/sw) and field measurements of average cross-sectional width, depth, and velocity at the reference gauge (http://nwis.waterdata.usgs.gov/nwis/measurements) were downloaded from the web.

I was able to obtain hard copies of some 130 dye time-of-travel reports for hundreds of streams throughout the United States. The results of many studies, however, could not be included in this analysis because (*i*) the stream did not have a continuous-flow gauge, (*ii*) the stream had a flow gauge but was not represented in the catchment characteristics or field measurements databases, or (*iii*) the study reach included a reservoir, lock-and-dam system, or some major irrigation or other diversion structure or was located in a losing stream. Thus ultimately, the data used to calculate estimates of v_{dye} for this study were drawn from 34 sources (Table S1[1]).

A continuous US Geological Survey flow gauging station marked the location of each stream's outlet and served as the reference gauge for the entire mainstem. Flow data for this

[1] Supplementary data for this article are available on the Web site or may be purchased from the Depository of Unpublished Data, Document Delivery, CISTI, National Research Council Canada, Ottawa, ON K1A 0S2, Canada. DUD 3648. For more information on obtaining material refer to http://cisti-icist.nrc-cnrc.gc.ca/irm/unpub_e.shtml.

© 2005 NRC Canada

station were used to quantify prevailing flow conditions during a tracer dye experiment conducted upstream of the gauge. Prevailing flow conditions were defined as the arithmetic mean of Q over the duration of the experiment. An experiment required from one to several days to complete (depending on the size of the stream, the number of dye releases required, and the discharge). This average Q typically had a low coefficient of variation (<10%), however, because most tracer dye experiments were purposely conducted under relatively stable low, moderate, or high flow conditions rather than under rapidly changing flow conditions (Kilpatrick and Wilson 1989).

A dimensionless variable, relative discharge (Q_{rel}), provided another measure of prevailing flow conditions. The Q_{rel} was defined as Q divided by Q_{ave}, where Q_{ave} is the long-term arithmetic mean value of Q calculated for the entire period of record for the outlet gauge (Jobson 1996). This period of record ranged from 19 to 111 years but averaged 63 years for all of the gauges represented in the data set. The Q_{rel} provided a convenient way to compare flow conditions among catchments of widely differing size.

A typical dye study consisted of a series of dye injection experiments. Most (82%) were conducted during May–October. Each experiment involved the release of a fluorescent dye (usually some form of Rhodamine) at the upstream end of a subreach and the subsequent monitoring of dye concentration at two or more transects downstream (Kilpatrick and Wilson 1989). Dividing the thalweg length of the subreach (l_i) by the time required for the most concentrated portion of the dye cloud to pass from one transect to the next (t_i) defined the dye's modal velocity for that subreach (v_i). Most experiments required several contiguous subreaches (five on average) and an equal number of dye releases to cover the entire study reach at a given Q. The sum of these subreach lengths thus defined the total length of the study reach (L_r). The L_r for the studies included in my data set ranged from 1.5 to 390 km, averaging 54 km overall. Most (80%) were between 18 and 95 km long.

The ratio L_r:L_{max} ranged from 0.02 to 2.0 (values >1 occurred when the dye cloud was tracked well downstream of the reference gauge), but for 80% of the observations, this ratio was between 0.10 and 0.82. The mean value of L_r:L_{max} for the entire data set was 0.38. Thus, the portion of a stream's mainstem upon which I based my estimate of v_{dye} was on average about 54 km long and accounted for some 38% of the mainstem's total length.

The average dye velocity for L_r at a given discharge (v_{dye}) was defined as the length-weighted mean of the modal dye velocity in all of the subreaches of a study reach:

$$(4) \qquad v_{dye} = (\Sigma v_i l_i)(\Sigma l_i)^{-1}$$

where v_i is the velocity of the peak dye concentration for subreach i, l_i is subreach length, and $\Sigma l_i = L_r$. Given that Soballe and Kimmel's (1987) model was based on a velocity–Q relationship developed from data collected at stream gauge transects, I compared v_{dye} with estimates of v_w based on the velocity–Q relationship at each flow gauge. For each gauge, $\log_{10}$ of average cross-sectional velocity (v_{gage}) was regressed against $\log_{10}$ of instantaneous discharge. Most stations required the development of two v_{gage}–Q rating curves, one for low-flow conditions (based on wading measurements) and the other for high-flow conditions (based on bridge-crane or boat measurements).

Collectively, the 34 reports selected for this analysis provided data on dye studies conducted in 111 streams scattered among 18 states (Fig. 1). Most studies performed their series of experiments under at least two flow conditions, usually low and moderately high. Thus, the number of observations with concurrent estimates of v_{dye}, v_{gage}, L_{max}, A, Q, and S ultimately totaled 305. For purposes of this analysis, I assumed that any two observations, even if made in the same stream reach, could nevertheless be treated as statistically "independent" because they were made at different dates, by different investigators, or under different flow conditions.

To develop and evaluate an empirical model for predicting T_w, I split the full data set (n = 305) into a calibration data set and a validation data set. The split was made using a random integer generator (specifically, the function "= between(0,1)" in Excel). Each observation in the full data set was thus randomly assigned a value of either 0 or 1. Values equal to 1 (n = 136) were used for model calibration; the rest (n = 169) were used for model validation. I used regression analysis to quantify the relationship between variation in T_w and variation in the three independent variables A, Q, and S. All variables were $\log_{10}$ transformed to normalize and stabilize variance (Sokal and Rohlf 2003). I used the Shapiro–Wilk statistic (W) to test for normality (Sokal and Rohlf 2003). To verify the stability of the computed estimates of regression coefficients, I calculated the variance inflation factor for each variable in the model. A variance inflation factor value >10 signals the possibility of collinearity and thus the need to consider ridge regression or other alternatives to simple linear regression (Sokal and Rohlf 2003). The coefficient of determination (R^2) and F ratio were used as indices of the goodness of fit. The standard error of regression in $\log_{10}$ units (s) provided a biased measure of the model's average precision. Average precision was also expressed as a percentage (s') by taking the antilog of $\pm s$, subtracting 1 from either result, and then multiplying it by 100 (Riggs 1973). Thus, for example, an s of 0.20 in $\log_{10}$ units became ($10^{0.20} - 1$) or +58% and ($10^{-0.20} - 1$) or –37% in arithmetic units. Antilogs calculated from any regression equation were corrected for transformation bias by multiplying the antilogs by e^c, where $c = 2.65s^2$ (Ferguson 1986).

To evaluate the performance of the regression model, I used the validation data set to calculate T_w and subtracted these predicted T_w values from the corresponding observed T_w values. I summed the squares of these differences, took the square root of the sum, and divided by the square root of $n - p$, where p is the number of variables used in the regression model. This standard error estimate and the strength of the Pearson's correlation coefficient (r) between predicted and observed values of T_w provided two unbiased measures of the model's accuracy and precision.

To study longitudinal variation in v_w within a stream network, I used the validated model to predict T_w among streams of increasing size within the White River, a large mostly agricultural stream draining central Indiana in the Midwest United States (Table 1). I chose this catchment because it in-

© 2005 NRC Canada

Fig. 1. Map of the conterminous United States showing the locations of reference flow gauges (n = 111).

Table 1. Summary statistics for five nested streams in the White River catchment, Indiana, and for the Moisie River near Sept-Îles, Quebec.

Stream	USGS gauge No.	Order	A (km^2)	Elevation (m)	L_{max} (km)	S (m·km^{-1})	Q_{ave} (m^3·s^{-1})	% L	% A_ω	% V
Buck Creek near Muncie	03347500	5	92	288	20	1.93	1.1	3.3	8	11
White River at Muncie	03347000	6	624	280	79	0.89	6.2	1.5	8	13
White River at Noblesville	03349000	7	2 222	261	164	0.74	24.0	1.1	19	18
White River at Newberry	03360500	8	12 090	142	407	0.45	142	0.9	25	33
White River at Petersburg[a]	03374000	9	28 813	122	507	0.36	349	0.2	9	10
Moisie River near Sept-Îles[b]	—	9	19 871	20	434	1.6	466	0.2	9	10

Note: Order, nominal Strahler stream order; A, catchment area at the US Geological Survey (USGS) flow gauge; elevation, elevation above mean sea level of gauge datum; L_{max}, mainstem length from gauge to drainage divide; S, mainstem slope; Q_{ave}, arithmetic mean of daily mean discharge for the period of record (1 October 1954 – 30 September 2001) (the period of record is identical for all five gauges (n = 16 801)); percentage of total network length (L), wetted channel surface area (A_ω), and volume (V) occupied by channels of specified order.

[a]72 km upstream of confluence with the Wabash River.

[b]Data from Naiman and Sedell (1981) and Naiman et al. (1987).

cluded five continuous-flow gauges (representing Strahler stream orders 5–9), each of which had a relatively long (1954–2001) and complete (no missing values) record of daily mean discharge and because the White River at Petersburg (A = 28 813 km^2) is about the same size as the Moisie River near Sept-Îles (A = 19 871 km^2), a pristine ninth-order (ω = 9) stream in northeastern Quebec. To my knowledge, the Moisie is the only stream for which previously published data (Naiman and Sedell 1981; Naiman et al. 1987) allow one to estimate the network's total channel length (ΣL), wetted surface area (ΣA_ω), and volume (ΣV) and to subdivide each total by ω. I assumed that fifth-, sixth-, seventh-, eighth-, or ninth-order channels in the White River occupied the same relative percentages of ΣL, ΣA_ω, or ΣV as channels of equal order in the Moisie River. This assumption allowed me to calculate L-, A_ω-, or V-weighted mean values of any property for the White River network as a whole. For example, the arithmetic average elevation for all five stations in Table 1 is 219 m, whereas a V-weighted average would be $(11 \times 288 + 13 \times 280 + 18 \times 261 + 33 \times 142 + 10 \times 122)/(11 + 13 + 18 + 33 + 10)$, i.e., 205 m.

To determine if any longitudinal patterns differed between low- and high-flow conditions, I used the discharge records for each station to calculate median monthly Q for the driest (September) and wettest (March) months of the year and used the empirical model to calculate corresponding esti-

© 2005 NRC Canada

Table 2. Summary statistics for variables describing catchment characteristics (n = 111).

Variable	Mean ± SE	Min.–max.	Percentile				
			10th	25th	50th	75th	90th
Catchment area, A (km^2)	6392±905	65 – 62 419	368	919	2303	7229	18 855
Mainstem length, L_{max} (km)	192±15.5	15.6–867	49.7	78.0	140	248	422
Mainstem slope, S (m·km^{-1})	2.17±0.26	0.14–11.5	0.34	0.47	0.91	2.7	6.7
Mean annual discharge, Q_{ave} (m^3·s^{-1})	84.1±13.2	0.9–969	5.1	10.9	32.5	94	219
Mean annual runoff, R_{ave} (cm·year^{-1})	47.4±3.0	4.9–178	25.0	30.3	37.6	54	88

Note: A, catchment area for reference flow gauge at or near downstream end of dye study reach; L_{max}, longest stream length from gauge to catchment divide; $S = (h_{0.85} - h_{0.15})(0.70L_{max})^{-1}$, where $h_{0.85}$ and $h_{0.15}$ are elevations (m) at $0.85L_{max}$ and $0.15L_{max}$ upstream from the gauge (Thomas and Benson 1970); Q_{ave}, arithmetic mean of daily mean discharge for period of record; $R_{ave} = Q_{ave}A^{-1}$.

mates of T_w. Using median monthly values for the entire period of record allowed me to compare T_w among nested systems flowing at discharges of equal recurrence interval, which is a key assumption of the velocity–Q relationship used in Soballe and Kimmel's (1987) formulation (Leopold et al. 1964).

Results

Catchment characteristics

The catchments included in this study (n = 111) represented a broad range of physiographic and climatological conditions, from the Trinity Alps of northern California to the Glacial Drift Plains of southern Illinois and from hot and semi-arid to cool and humid (Fig. 1). Annual mean runoff ranged from 4.9 to 178 cm·year^{-1}, averaging 47 cm·year^{-1} (Table 2). Nearly half the catchments (n = 49 or 44%), however, were in Midwest states (Ohio, Indiana, Illinois, and Nebraska) and most (80%) runoff values were between 25 and 88 cm·year^{-1}.

Catchment area (A) ranged over three orders of magnitude from 65 to 62 419 km^2, averaging 6392 km^2 overall. The smallest stream in the data set was Jones Falls at Sorrento, Maryland; the largest was the Susquehanna River at Harrisburg (Table S2[1]). Most systems (80%), however, were mid-sized, with A ranging between 368 and 18 855 km^2 (Table 2).

Mainstem length (L_{max}) ranged from 15.6 to 867 km and bore a tight $\log_{10}$-linear relationship with catchment area (Fig. 2*a*). In its exponential form ($L_{max} = 1.8A^{0.554}$), the L_{max}–A relationship was essentially identical to Mueller's (1973) global-scale model ($L_{max} = 1.6A^{0.554}$ for A = 0.03 – 7 770 000 km^2) and indicated that any 10-fold increase in A was accompanied by a 3.6-fold increase in L_{max}. Mean annual discharge (Q_{ave}) among streams ranged from 0.9 to 969 m^3·s^{-1}, averaging some 84 m^3·s^{-1} overall (Table 2). Like L_{max}, Q_{ave} was strongly correlated with A (Fig. 2*b*). Average mainstem slope (S) ranged from 0.14 to 11.5 m·km^{-1}, averaging 2.17 m·km^{-1} (Table 2). $\log_{10} S$ and $\log_{10} A$ were negatively correlated ($p < 0.0001$), indicating that smaller streams tended to have steeper slopes ($S = A^{-0.41}$), but this tendency was not strong (r = –0.55, n = 111). $\log_{10} S$ was even less strongly correlated with $\log_{10} Q_{ave}$ (r = –0.32, p = 0.0007).

Mainstem discharge, velocity, and transit time

Average daily discharge at the reference gauge during a dye release experiment (Q) ranged from 0.09 to 634 m^3·s^{-1}, averaging 55.9 m^3·s^{-1} overall (n = 305). Corresponding values of relative discharge (Q_{rel}) ranged from 0.02 to 7.8, averaging 0.70. Most Q_{rel} values, however, were between 0.11 and 1.8 (Table 3). Thus, most dye studies were conducted under low- to moderately high-flow conditions.

Average dye velocity (v_{dye}) ranged from 1.9 to 193 km·day^{-1} and was positively correlated with Q (r = 0.83, $p < 0.0001$). Most values were between 9.7 and 74 km·day^{-1}, with an overall average of 37 km·day^{-1} (Table 3). On aver-

Fig. 2. Relationship between catchment area (A) and (*a*) mainstem length (L_{max}), $\log_{10} L_{max} = 0.26\ (\pm 0.05) + 0.55\ (\pm 0.01) \times \log_{10} A$ (s = 0.098, R^2 = 0.93, n = 111), and (*b*) mean annual discharge at the reference gauge for entire period of record (Q_{ave}), $\log_{10} Q_{ave} = -1.63\ (\pm 0.14) + 0.920\ (\pm 0.04) \times \log_{10} A$ (s = 0.27, R^2 = 0.82, n = 111). The ± value in parentheses after each regression coefficient is the coefficient's standard error. Solid lines are the least squares regression lines.

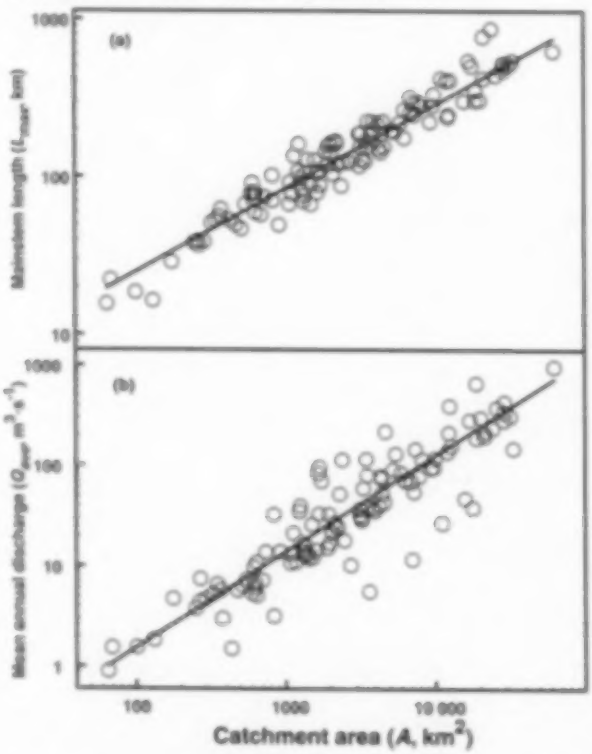

© 2005 NRC Canada

Table 3. Summary statistics for variables describing hydraulic conditions during dye study experiments (n = 305).

Variable	Mean ± SE	Min.–max.	Percentile				
			10th	25th	50th	75th	90th
Discharge, Q ($m^3 \cdot s^{-1}$)	55.9±5.8	0.09–634	1.4	3.8	13.7	61.7	150
Relative discharge, Q_{rel} (unitless)	0.70±0.05	0.02–7.8	0.11	0.23	0.45	0.93	1.8
Dye velocity, v_{dye} ($km \cdot day^{-1}$)	37±1.6	1.9–193	9.7	17	30	50	74
v_{gage}:v_{dye} (unitless)	1.6±0.05	0.4–6.0	0.8	1.0	1.3	1.9	2.9
Transit time metric, T_w (days)	7.2±0.3	0.3–40	1.5	3.0	5.5	10	15

Note: Q, discharge at the reference gauge; $Q_{rel} = QQ_{ave}^{-1}$, where Q_{ave} is the arithmetic mean of daily mean discharge for period of record; v_{dye}, average dye velocity for the entire study reach (eq. 4); v_{gage}, average cross-sectional velocity calculated from velocity–discharge rating curves for the reference gauge; $T_w = L_{mss}v_{dye}^{-1}$, where L_{mss} is the mainstem length from the drainage divide to the reference gauge.

age, v_{dye} increased with Q as $v_{dye} \propto Q^{0.4}$ (Fig. 3). Estimates of mean cross-sectional velocity at each reference gauge (v_{gage}) also ranged over three orders of magnitude and like v_{dye} were positively correlated with Q (r = 0.69, $p < 0.0001$). The slope of the v_{gage}–Q relationship ($v_{gage} \propto Q^{0.2}$) was significantly lower than the slope of the v_{dye}–Q relationship ($v_{dye} \propto Q^{0.4}$), whereas the intercept of the v_{gage}–Q relationship was higher (Fig. 3). Consequently, v_{gage} often exceeded v_{dye} under low-flow conditions but equaled or was slightly less than v_{dye} at high flows. The v_{gage}:v_{dye} ratio ranged widely (0.4–6) among streams, however (Table 3), and there was a marked tendency for v_{dye} and v_{gage} to converge as Q increased at a given gauging station, especially if the stream was small or midsized ($A \leq 10\,000$ km^2, n = 246). For example, v_{gage} was 4.3-fold faster than v_{dye} in the Molalla River near Canby, Oregon (A = 837 km^2, Q_{ave} = 33 $m^3 \cdot s^{-1}$) at low flow (Q_{rel} = 0.04) but equal to v_{dye} under high-flow conditions (Q_{rel} = 2.1). Similarly, in the Embarras River at Sainte Marie, Illinois (A = 3926 km^2, Q_{ave} = 35 $m^3 \cdot s^{-1}$), v_{gage}:v_{dye} decreased from 2.6 at Q_{rel} = 0.07 to 1.2 at Q_{rel} = 0.94. Overall, v_{gage} exceeded v_{dye} for 198 (80%) of the values observed among small- to mid-sized streams. By contrast, among large streams ($A > 10\,000$ km^2, n = 59), v_{gage} (n = 36 or 61%) was often less than v_{dye} and this disparity increased slightly under high-flow conditions as, for example, in the Wabash River at Terre Haute (A = 31 766 km^2, Q_{ave} = 313 $m^3 \cdot s^{-1}$) where v_{gage}:v_{dye} was 0.9 at Q_{rel} = 0.23 decreasing to 0.7 at Q_{rel} = 1.85.

Dividing v_{dye} into mainstem length yielded the observed transit time metric T_w. The T_w ranged from 0.3 to 40 days with an overall average of about 1 week. Most (80%) of the 305 observations, however, were between 1.5 and 15 days (Table 3). $\log_{10} T_w$ bore a weak (r = 0.52) but highly significant ($p < 0.0001$) positive correlation with $\log_{10} A$ (Fig. 4*a*) and a negative correlation with $\log_{10} S$ (r = –0.49) (Fig. 4*b*). There was no significant correlation, however, between $\log_{10} T_w$ and $\log_{10} Q$ (Fig. 4*c*).

Predicting transit time

Model calibration

Among the observations in the randomly generated calibration data set (n = 136), T_w ranged from 0.3 to 40 days, with an overall mean of 6.7 days and a median of 4.7 days. These values were similar to those characterizing the full data set (Table 3). The distributions of A, S, and Q in the calibration and full data sets were also similar. Neither T_w nor any of the potential independent variables was normally distributed prior to transformation ($W < 0.84$, $p < 0.0001$, n = 136). $\log_{10}$-transformed values of T_w, A, and Q were, however, normally distributed ($W > 0.98$, p = 0.12), whereas $\log_{10} S$ and its interaction terms with $\log_{10} A$ and $\log_{10} Q$ were not ($W < 0.89$, $p < 0.0001$).

Of the six candidate variables (i.e., A, Q, S, and their interaction terms), no single variable explained more than 29% of the variation in $\log_{10} T_w$. The best-fitting bivariate model was

$$\log_{10} T_w = -1.59\ (\pm 0.10) + 0.85\ (\pm 0.03) \times \log_{10} A - 0.55\ (\pm 0.03) \times \log_{10} Q \quad (5)$$

Fig. 3. Relationship between daily average discharge during the tracer dye experiment (Q) and average mainstem surface water velocity (v) as estimated by the transit time of the most concentrated portion of a dye cloud (v_{dye}, circles) and by the average cross-sectional velocity at the reference gauge (v_{gage}, triangles). The slope and intercept of the two v–Q relationships are significantly different ($p < 0.0001$) as evidenced by the following regression model (analysis of covariance): $\log_{10} v$ = 1.42 (±0.01) – 1.18 (±0.04) × $I_{1,0}$ + 0.15 (±0.008) × $\log_{10} Q$ + 0.72 (±0.03) × $I_{1,0}$ × $\log_{10} Q$, where v is v_{dye} or v_{gage} and $I_{1,0}$ is a dummy variable equaling 1 if $v = v_{dye}$ or 0 if $v = v_{gage}$ (s = 0.12, R^2 = 0.82, n = 610). The ± value in parentheses after each regression coefficient is the coefficient's standard error. Solid and broken lines are the least squares regression lines for the v_{dye}–Q and v_{gage}–Q relationships, respectively.

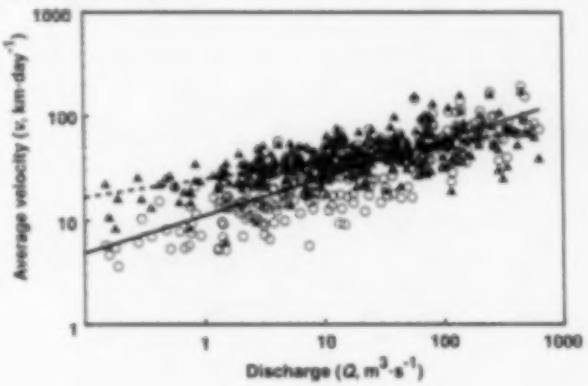

© 2005 NRC Canada

Fig. 4. Mainstem transit time metric (T_w) plotted as a function of (*a*) catchment area (*A*), (*b*) mainstem slope (*S*), and (*c*) average discharge (*Q*) during a dye experiment. The lines are least squares regression lines used to indicate overall trends.

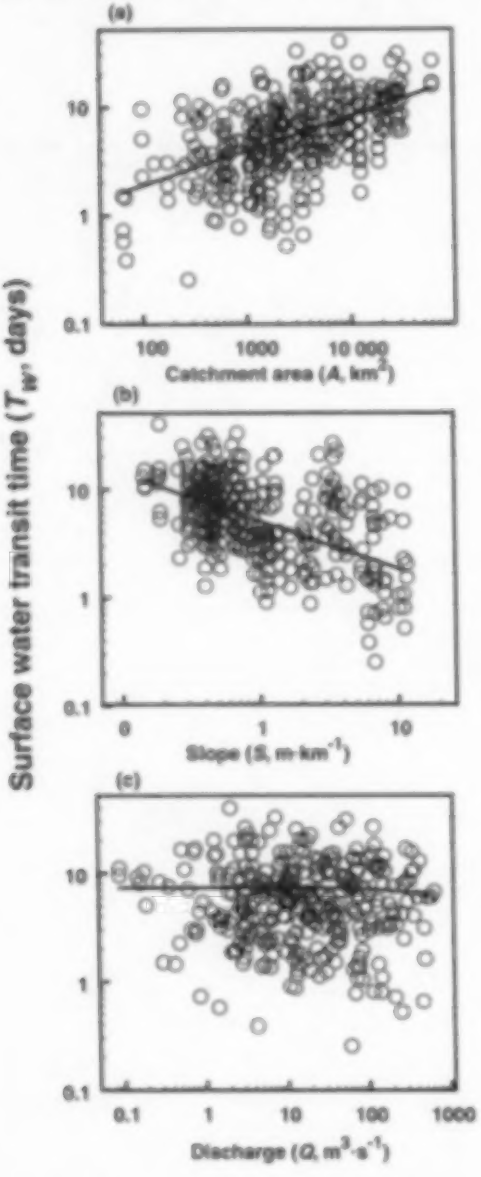

Fig. 5. Residual values (the difference between observed and predicted values) of the transit time metric (T_w, $\log_{10}$ transformed) plotted as a function of: $\log_{10}$-transformed values of (*a*) catchment area (*A*), (*b*) mean discharge (*Q*) during a dye release experiment, and (*c*) the observed values of $\log_{10} T_w$. Predicted values of $\log_{10} T_w$ were calculated using eq. 5 in the text. Observed T_w values are from the calibration data set (data set "1" in Table S1[1], n = 136).

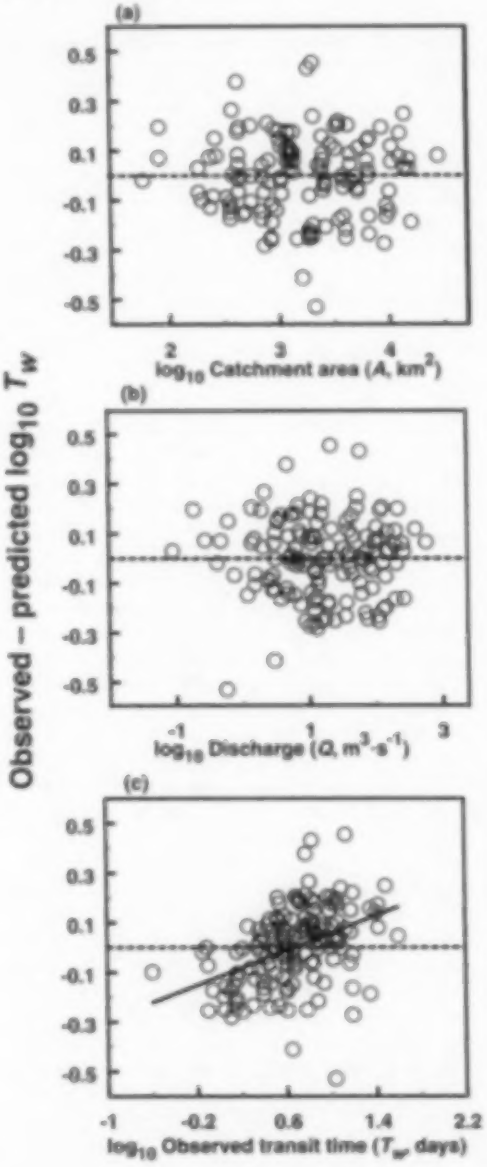

This model explained 83% of the variation in $\log_{10} T_w$ (F = 314, R^2 = 0.83, s = 0.16) and indicated that T_w increased with A and decreased with Q. The best-fitting trivariate model included $\log_{10} A$, $\log_{10} Q$, and the $\log_{10} Q - \log_{10} S$ interaction term. Although this model explained slightly more variation in $\log_{10} T_w$ (R^2 = 0.85) than eq. 5, it did not predict T_w with better accuracy or precision than the simpler bivariate model (see Model validation section).

Residual plots for eq. 5 indicated no systematic error with $\log_{10} A$ or $\log_{10} Q$ (Figs. 5*a* and 5*b*). Similarly, the low variance inflation factor (2.1) for both variables signaled that all of the model parameters exerted independent effects on T_w. In these respects, the model was statistically "well behaved". Plotting the residual values of $\log_{10} T_w$ as a function of observed values, however, indicated that eq. 5 might tend to

© 2005 NRC Canada

Fig. 6. Scatterplot of predicted transit time (T_w) (calculated using eq. 5 in text) versus observed T_w from the validation data set ($r = 0.78$, $p < 0.0001$, $n = 169$) (data set "0" in Table S1[1]). The line is the 1:1 line.

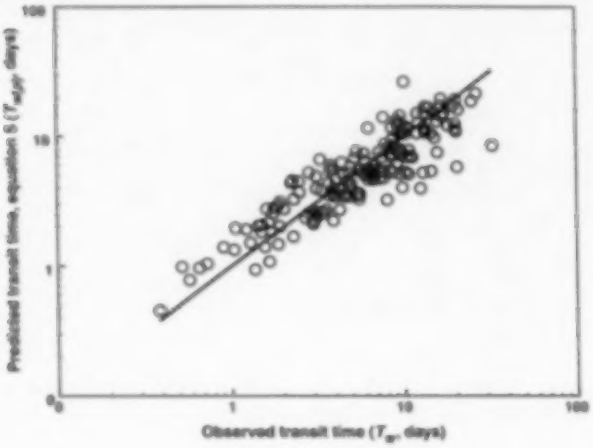

overestimate T_w at very low values and underestimate T_w at very high values (Fig. 5*c*).

Model validation

Estimates of observed T_w in the validation data set (n = 169) ranged from 0.4 to 33 days, with an overall mean of 7.5 days and a median of 6.3 days. These summary statistics for T_w and those for the independent variables A, S, and Q were similar to the summary statistics for these variables in the full data set (Table 3) and in the calibration data set.

Predicted values of T_w calculated using eq. 5 were positively correlated with the observed T_w values in the validation data set ($r = 0.78$, $p < 0.0001$) (Fig. 6). Residual plots indicated no systematic error with A or Q (Figs. 7*a* and 7*b*), but as expected (Fig. 5*c*), the model did tend to underpredict T_w for T_w values exceeding 10 days (Fig. 7*c*). The standard error of the model overall was 3.7 daays or ±49% of the mean observed T_w. Adding the $\log_{10} Q$–$\log_{10} S$ interaction term to the bivariate model did not significantly increase the correlation between observed and predicted T_w ($r = 0.77$) nor did it decrease the model's standard error (s = 3.7 days). Thus, of all possible multiple linear regression models, a simple bivariate model (eq. 5) turned out to be the most apt for predicting T_w.

Model application

Applying eq. 5 to catchment area and flow data for five streams nested in the White River catchment (Table 1) first revealed how hydraulic conditions varied longitudinally within a river under low- and high-flow conditions and second provided still another way to test the model's validity.

First, the long-term (1954–2001) flow records indicated that median discharge during the height of the dry season (September) or the wet season (March) increased with stream order (Table 4). Median Q for the month of September (n = 1380) increased from 0.4 $m^3 \cdot s^{-1}$ at Buck Creek near Muncie ($\omega = 5$) to 70.5 $m^3 \cdot s^{-1}$ for the most downstream station at Petersburg ($\omega = 9$). During March, the median Q (n = 1426) increased from 1.1 $m^3 \cdot s^{-1}$ at $\omega = 5$ to 522.5 $m^3 \cdot s^{-1}$ at $\omega = 9$. The volume-weighted mean Q_{ref} for the whole system was 0.21 for September and 1.22 for March.

Fig. 7. Residual plots for the empirical model (eq. 5 in the text) as applied to the validation data set (data set "0" in Table S1[1]). Plots depict residual value (observed minus predicted transit time (T_w)) versus (*a*) catchment area (A), (*b*) mean discharge (Q) during dye experiment, and (*c*) observed T_w.

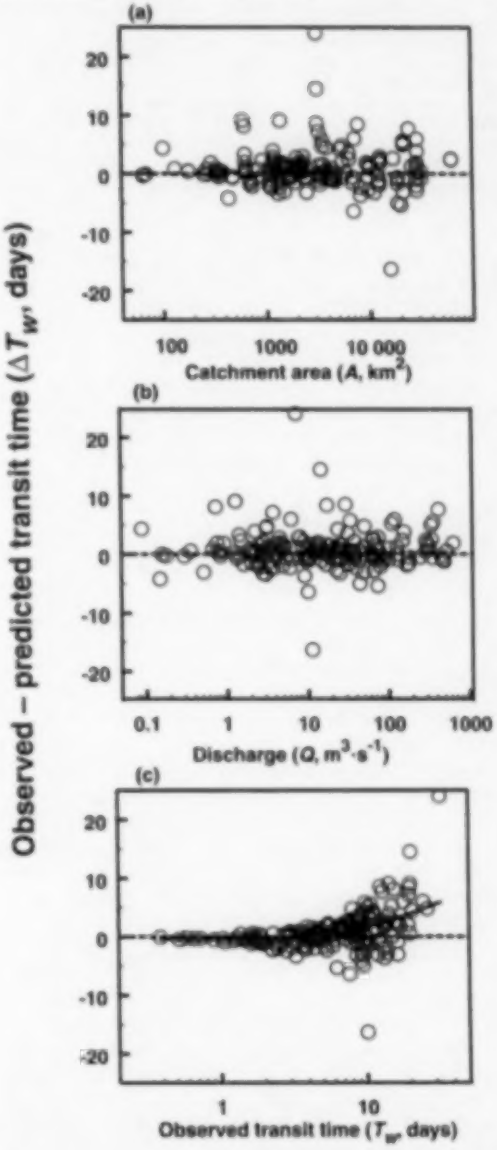

Under these hydrologic circumstances, eq. 5 indicated that average hydraulic conditions changed systematically with increasing ω. Under low-flow conditions (September), T_w increased from 2.1 days for the fifth-order stream to 16.4 days for the ninth-order station (Table 4). Corresponding estimates of average mainstem velocity ($v_w = L_{mainstem} T_w^{-1}$) increased threefold to nearly sixfold (depending on the month)

© 2005 NRC Canada

Table 4. Summary of hydraulic conditions in five nested streams of the White River catchment, Indiana.

Stream	Order	Q ($m^3 \cdot s^{-1}$)		Q_{rel}		T_w (days)		v_w ($km \cdot day^{-1}$)		z (m)	
		Sept.	Mar.	Sept.	Mar.	Sept.	Mar.	Sept.	Mar.	Sept.	Mar.
Buck Creek near Muncie	5	0.4	1.1	0.39	1.00	2.1	1.2	10	16	—	—
White River at Muncie	6	0.6	6.0	0.10[a]	0.96	8.5	2.5	9	33	0.16	0.69
White River at Noblesville	7	4.9	26.6	0.20	1.11	8.1	3.2	20	52	0.36	0.85
White River at Newberry	8	28.1	196.0	0.20	1.38	13.0	4.5	31	91	0.75	2.01
White River at Petersburg	9	70.5	522.5	0.20	1.50	16.4	5.4	31	93	2.08	3.55

Note: *Order*, nominal Strahler stream order; Q, median of daily mean discharge values measured during September (driest month) and March (wettest month) for the 1954–2001 period of record; $Q_{rel} = QQ_{ave}^{-1}$, where Q_{ave} is arithmetic mean of daily mean discharge for the period of record; T_w, transit time metric calculated for Q using eq. 5 in the text; v_w, mainstem velocity calculated as mainstem length (L_{mas}) divided by T_w; z, mean cross-sectional depth at the flow gauge calculated using the z–Q rating curve (data not available for Buck Creek near Muncie).

[a]This relatively low Q_{rel} value probably resulted from diversions by the city of Muncie (to supply water to some 87 000 residential customers).

as ω increased from 5 to 9. A plot of v_w against ω indicated that streamflow indeed accelerated with increasing ω ($v_w \propto \omega^{0.2}$) as far downstream as Newberry (ω = 8) and then remained constant as the stream approached its confluence with the Wabash River some 72 km downstream (Fig. 8*a*). The v_{gage}–ω curve followed a similar trajectory up to ω = 8 (although its slope did not differ significantly from zero) but indicated a substantial reduction in velocity (rather than just a leveling off) further downstream, especially during March (Fig. 8*a*). Plots of v_w (and to a lesser extent v_{gage}) versus the median Q during September or March also indicated longitudinal acceleration of streamflow ($v_w \propto Q^{0.3}$) up to a threshold beyond which velocity either remained constant or declined (Fig. 8*b*). Thus, the v_w–Q relationship within the White River system resembled the v_{dye}–Q relationship among systems ($v_{dye} \propto Q^{0.4}$) (Fig. 3) in that its scaling exponent (0.3) was much greater than the expected value of 0.1 (eq. 2) but differed from the among-system relationship in that the latter offered no evidence of any downstream threshold effect.

Second, multiplying the March transit time metric T_w for Newberry (4.5 days) by the March median outflow at Newberry (196 $m^3 \cdot s^{-1}$) provided an estimate of the system's total volume under moderately high-flow conditions (Q_{rel} = 1.38), i.e., 76 × 10^6 m^3. Dividing this volume estimate by the volume-weighted mean depth of the network (1.43 m) (data in Tables 1 and 4) resulted in a total wetted channel area A_w estimate of 53 km^2. This estimate of A_w based on my predicted value of T_w agreed remarkably well with the 67-km^2 value calculated for the White River at Newberry (A = 12 090 km^2) using an empirical model (A_w (m^2) = $294A^{1.315}$) developed for Iowa streams of comparable size (A = 1 – 13 000 km^2) operating under slightly higher flow conditions (Q_{rel} = 1.6) but draining a region of similar geology, climate, topography, and land use as for central Indiana (Swanson and Bachmann 1976). This result instilled further confidence in the accuracy of eq. 5's predictions.

Model comparison

Estimates of the long-term average T_w ($T_{w(ave)}$) for all 111 streams calculated using eq. 5 and Soballe and Kimmel's (1987) model (eq. 2) ranged from 0.8 to 30 days. The Soballe and Kimmel (1987) predictions were on average double the $T_{w(ave)}$ values calculated using my model (Fig. 9*a*). Consequently, estimates of average mainstem velocity (L_{mas} $T_{w(ave)}^{-1}$) using their model averaged about half the velocity estimates calculated using my model (Fig. 9*b*). Given the relatively high-flow conditions under which these streams were assumed to be operating (Q_{rel} = 1), the Soballe and Kimmel (1987) velocities (0.13–0.51 $m \cdot s^{-1}$) seemed unrealistically slow, especially for Q_{ave} > 10 $m^3 \cdot s^{-1}$ (Fig. 9*b*). These results indicated that the Soballe and Kimmel (1987) model probably overestimated the true surface water transit time of streams.

Discussion

This study led to two principal findings, one expected and the other somewhat surprising. Not unexpectedly, the regression analysis results confirmed that a property that is difficult and costly to measure (T_w) can be reliably (±49%) predicted on the basis of two catchment-scale variables (A and Q) for which data are often readily available. This result was not surprising because I had already used this approach to develop a T_w model for a much smaller sample of Midwest streams (Van Nieuwenhuyse 1993). Also, Boning (1974) and later Jobson (1996) had succeeded in developing empirical models for predicting dye velocity at the scale of individual subreaches using A, Q, or Q_{rel} and local slope. In contrast with a variable like reach velocity, however, precisely what the T_w metric is measuring may not be immediately obvious.

When dye is injected into a stream channel, it immediately starts to disperse into a cloud that elongates and becomes more dilute as it moves downstream with the current. The leading edge of the cloud arrives, on average, about 1.12 times sooner than the cloud's most concentrated portion (Jobson 1996) so that if the cloud's modal travel time from source to outlet were predicted to be, say 7 days, one could expect to begin detecting dye at the outlet after 6 days. If the experiment were repeated at a lower or higher discharge, arrival times would lengthen or shorten in accordance with the stream's v_w–Q relationship. The T_w metric divides an estimate of a dye cloud's modal velocity (which is an accurate measure of true modal water velocity) into a stream's mainstem length. Thus, a T_w estimate for a given reference gauge is dividing a quantity that varies (v_{dye}) into a quantity that is assumed to remain constant (L_{mas}). In this sense, T_w is similar to the theoretical flushing time of a lake, which likewise divides a variable quantity (discharge at the lake's outlet Q) into something assumed to remain constant (lake volume V).

© 2005 NRC Canada

Fig. 8. (*a*) Longitudinal variation in average water velocity of the mainstem (circles) and elevation of the reference flow gauge datum (triangles) as a function of Strahler stream order in the White River at Petersburg drainage network. Solid circles describe median high-flow (March) conditions and open circles depict median low-flow (September) conditions for the entire period of overlapping flow record at all five stations (1954–2001). Solid lines connect velocity estimates calculated as $L_{main}T_w^{-1}$, where L_{main} is mainstem length (km) upstream of the reference gauge and T_w is the predicted transit time (days) of the most concentrated portion of a dye cloud calculated using eq. 5 in the text. Broken lines connect estimates of the average cross-sectional velocity at the reference gauge (v_{gage}) calculated from the gauge's v_{gage}–discharge rating curve. No rating curve data were available for the fifth-order station (Buck Creek near Muncie). (*b*) Same as Fig. 8*a* except velocities are plotted as a function of median discharge at each reference gauge instead of stream order.

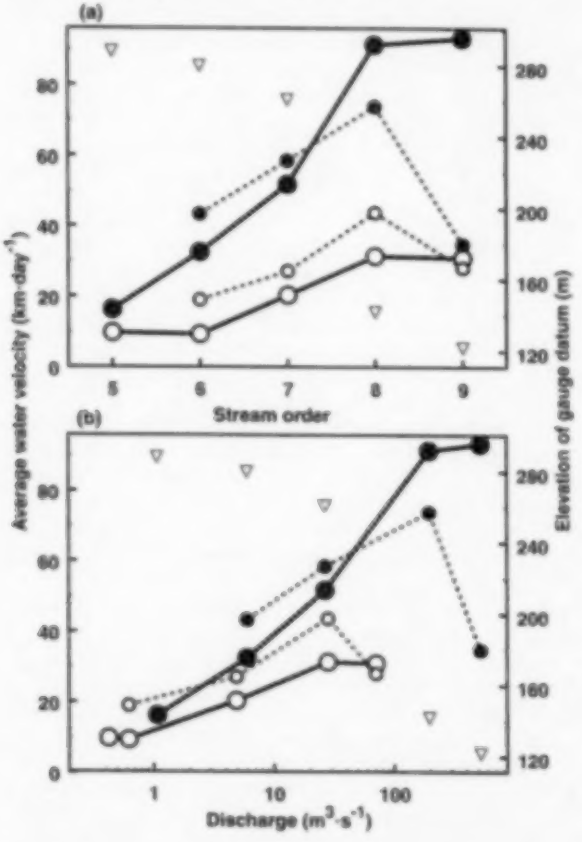

Fig. 9. (*a*) Comparison of predicted values of long-term average surface water transit time ($T_{w(obs)}$) calculated for study streams (n = 111) using eq. 2 (Soballe and Kimmel 1987) and eq. 5 in the text. The line is the 1:1 line (perfect agreement). (*b*) Predicted values of long-term average surface water velocity (i.e., $L_{main}T^{-1}_{w(obs)}$, where L_{main} is mainstem length (km)) calculated for study streams (n = 111) using eq. 2 (Soballe and Kimmel 1987) (solid circles) and eq. 5 (open circles) plotted against long-term mean annual discharge at each reference gauge. Note that velocity units have been converted to metres per second.

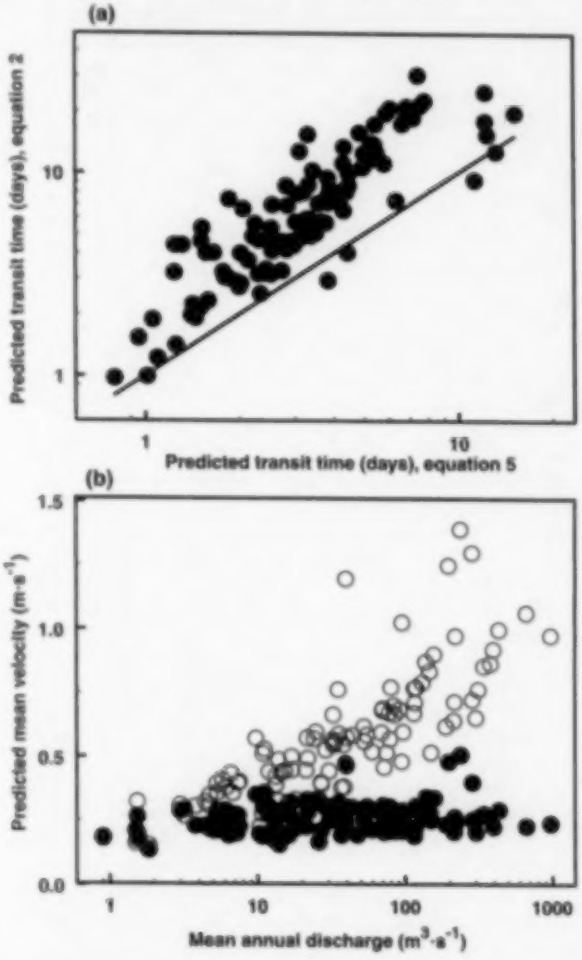

But just as VQ^{-1} does not really represent the true water retention time of a lake (Monsen et al. 2002), T_w would equal the true average residence time of water in a stream only if all of the water flowing past the outlet had entered the network at the head of each first-order channel (ω = 1) and none had succumbed to evaporation, seepage, or any other loss process on its way to the outlet (ω = Ω). In this idealized system, T_w would be equivalent not only to the water's transit time but also its flushing time, residence time, retention time, turnover time, exposure time, and "age" (Monsen et al. 2002). In a real stream, however, water enters the network by a limited number of processes (e.g., spring flow, interflow, overland flow, and direct precipitation) but from a nearly infinite number of possible locations (picture a patch of permafrost melting in the remotest corner of a catchment's divide or a raindrop splashing directly onto the stream surface just upstream of the outlet gauge). Consequently, in real streams, the population of surface water molecules flowing past a gauge may include individuals ranging in exposure time from the neophyte (<1 s) to the downright jaded (>30 days). Thus, T_w may provide a good first-cut estimate of how soon a permanently entrained particle could be washed out of a stream network, but it provides

© 2005 NRC Canada

no information about the average age of the water molecules supporting the particle's immersed weight.

Fortunately, knowing how fast an entrained particle or organism is likely to be flushed from a system often matters more than knowing how old the water imposing this loss rate might be. For example, to calculate a first-cut estimate of the loss rate that a stream network exerts on any process that supplies a constituent to the system, one need only divide the concentration of the constituent by the T_w at the outlet. The use of nested T_w values to calculate L-, A_w-, or V-weighted mean T_w values for the catchment as a whole would presumably provide an even more accurate estimate. Which weighted mean to use would depend on the constituent and thus process under consideration. For example, assuming that most of the suspended sediment flowing past the White River at Petersburg originates from entrainment in furrows, ditches, gullies, and other low-order systems (as opposed to, say, bed or bank erosion along the lower mainstem), the L-weighted mean T_w would be of greatest interest because the tens of thousands of $\omega < 5$ channels throughout the White River network probably account for >90% of the network's total length. Thus, dividing the average suspended sediment concentration during the March high-flow season at Petersburg (say, 100 mg·m^{-3}) by the corresponding L-weighted mean of T_w (2.3 days) may provide a more accurate operational estimate of the sediment loading rate required to maintain that concentration (i.e., 43 mg·m^{-3}·day^{-1}) than the unadjusted T_w would (19 mg·m^{-3}·day^{-1}). Similarly, dividing September chlorophyll concentration by the V-weighted mean T_w may provide a useful catchment-scale estimate of the network's sestonic algal biomass loss rate. In systems where washout dwarfs grazing and all other loss processes (e.g., Sivko et al. 1972), this washout rate estimate would approximate the net algal production rate (Swanson and Bachmann 1976). In other systems, grazing and other losses would have to be estimated independently and added to the washout rate to estimate production rate. This approach to quantifying a catchment's lotic algal production rate could complement or replace methods that extrapolate bioassay-scale (<1 m^2) indices of algal production rate (e.g., ^{14}C assimilation rate in a scintillation vile or photosynthetic oxygen production rate in a plexiglass chamber or a borosilicate flask) to ecosystems that occupy >100 km^2 (e.g., Naiman et al. 1987).

In contrast with the regression results, however, the finding that the longitudinal velocity gradient in streams may be as steep as $v_w \propto Q^{0.4}$ was not expected. Numerous studies of stream hydraulic geometry based on width–, depth–, and velocity–discharge relationships at stream gauges throughout the United States had indicated that small- to midsized streams accommodate downstream increases in Q principally by increasing their width rather than their velocity (Leopold and Maddock 1953; Leopold et al. 1964; Carlston 1969). Similarly, dye studies encompassing hundreds of miles of mainstem flow in the Mississippi, Missouri, Susquehanna, and Potomac rivers had led to the conclusion that very large rivers accommodate downriver increases in Q principally by increasing their depth with essentially no increase in velocity (Carlston 1969). And even though Pilgrim (1976) had also found that v_{dye} increased with Q as $v_{dye} \propto Q^{0.4}$ (instead of as $v_{dye} \propto Q^{0.1}$), it was easy to dismiss this result as some artifact of the tiny size (0.4 km^2) of his catchment (e.g., see p. 333 in Rodriguez-Iturbe and Rinaldo 2001). So why, as my results suggest, would the v_{gage}–Q relationship be so flat compared with the v_{dye}–Q relationship among streams and why would velocity increase with ω and then level off (or even decrease substantially) at some downstream threshold within a given stream?

Why the v_{gage}–Q and v_{dye}–Q relationships differ may be an artifact of where stream gauges tend to be situated. Stream gauges (which monitor stage) are usually placed where there is some kind of stable hydraulic control (e.g., a bedrock outcrop) not too far downstream. Gauge transects (where the discharge is actually measured) are thus located upstream of miniweirs that create local hydraulic conditions suitable for quantifying the relationship between stage and Q but not necessarily for characterizing the average water velocity of the entire network upstream. Moreover, under low-flow conditions, the cross-sectional depth and velocity measurements needed to calculate Q are usually made while wading in the thalweg, whereas high flows are often measured at a different location by suspending a velocity meter from a bridge (Leopold et al. 1964). Thus, under low flows, when much of the network's volume and surface area consist of near stagnant pools connected by short glides and lazy runs (whose velocity would be impossible to measure accurately without performing a dye experiment), velocity at the flow gauge is fast enough to measure with a velocity meter. By contrast, under high-flow conditions, the distinction between riffles, pools, and runs becomes blurred (riffles are drowned out) so v_{gage} and v_{dye} tend to converge. At even higher Q, v_{gage} may be slower than v_{dye} because of the backwater effect imposed by the gauge's downstream hydraulic control or by the pylons supporting the bridge. This line of reasoning leads to the conclusion that the real v_w–Q relationship is $v_w \propto Q^{0.4}$, not $v_w \propto Q^{0.1}$, and therefore that previous analyses may have grossly underestimated the scaling exponent because they depended on velocity data collected at stream gauges instead of velocity estimates based on tracer dye experiments.

The question of why velocity would, as in the White River, accelerate longitudinally remains unclear. This effect is observed under low- and high-flow conditions but is particularly marked under high flows. If eq. 5 overpredicts T_w at low T_w (low ω) and underpredicts T_w at high T_w (high ω), it would lead to underprediction of velocity at low ω and overprediction of velocity at high ω. Either tendency could certainly amplify the observed longitudinal pattern especially for low-flow conditions, but the high-flow value of T_w for the White River at Petersburg (5.4 days) is well within the range for which eq. 5 likely provides its most accurate predictions. So again, it would seem that longitudinal acceleration of streamflow is not the result of model bias but is instead a real phenomenon.

Even so, it is also possible that the observed longitudinal acceleration may be artificially created or exaggerated among the streams in my sample because so many of them, especially those in Indiana and other Midwest states, are so highly altered from their natural geomorphological configuration (Emerson 1971). For example, a heavily channelized,

© 2005 NRC Canada

extensively leveed network (common in the Midwest) would tend to accommodate longitudinal increases in Q first by increasing mainstem depth (because the levees would have prevented much widening) and then by increasing its velocity (because bedrock or a consolidated layer of bed material would have eventually prevented further deepening). By contrast, a pristine system like the Moisie River in Quebec would be free to meander and widen itself in response to increased Q. Perhaps this difference explains why my estimate of A_ω for the White River (based on predicted T_ω) agrees so well with Swanson and Bachmann's (1976) A_ω–A relationship for nearby Iowa streams, whereas the Swanson and Bachmann (1976) model underestimates A_ω for the Moisie by a factor of 2. Similarly, why else would the White River at Petersburg flowing at $Q_{rel} = 1$ be 1.3-fold narrower (158 versus 209 m) but 1.2-fold deeper (3.1 versus 2.5 m) than the Moisie at $Q_{rel} = 1$ (even though the Moisie conveys 1.3-fold more flow at $Q_{rel} = 1$)? Dye studies in large undisturbed systems are needed to determine whether longitudinal acceleration is a natural phenomenon or one induced by human activities.

Why flow in the White River should eventually decelerate at some point downstream, especially under high-flow conditions, may also be due to a backwater effect. This effect presumably originates near the confluence of the White and Wabash rivers. Under high flows, White River water may in effect "pile up" and thus slow down as it approaches the mouth. In theory, this backwater effect could reduce current velocity at Newberry some 72 km upstream, especially in an artificially straightened channel like the lower White River. I have no data to test this hypothesis directly, however.

If it turns out to be a natural (rather than human-induced) phenomenon, the observed downstream acceleration of flow helps solve one of the oldest puzzles in fluvial geomorphology, namely why catchments elongate with increasing size (Hack 1957; Mueller 1973; Rodriguez-Iturbe and Rinaldo 2001). If streams really do speed up (as well as widen and deepen) with increasing size, their ability to entrain and transport debris (their competence) must also increase longitudinally (Leopold et al. 1964). If so, a nascent drainage network would lengthen faster than it would widen and so wind up embedded in a pear-shaped (rather than circular) catchment.

Finally, if the results of this study are true (or nearly so) for streams, they may also apply in some analogous way to other branched networks that convey matter, energy, or information from a multitude of possible beginnings ($\omega = 1$) to some uniquely, improbable end (Ω).

In summary, regression analysis of a data set compiled from the literature and the World Wide Web indicated that a catchment-scale metric of surface water transit time (defined as mainstem length divided by average dye velocity) varied predictably (±49%) with catchment area and mean daily discharge. Application of this empirical model to five streams nested in a ninth-order catchment indicated that under dry (September) and wet (March), long-term (1954–2001) median flow conditions, mainstem velocity v_ω increased with Q as $v_\omega \propto Q^{0.3}$ (instead of $v_\omega \propto Q^{0.1}$, as expected from previous studies). Longitudinal velocity gradients in many streams may thus be much steeper than is commonly assumed.

Acknowledgements

The Interagency Ecological Program for the San Francisco Estuary (Bureau of Reclamation) and the Anadromous Fish Restoration Program (US Fish and Wildlife Service) provided funding for this research. Many thanks go to all of the US Geological Survey district personnel who kindly provided copies of time-of-travel reports and to Randy Dahlgren, Stephen Jones, and Nicolas Sakata for their assistance in compiling the data set. Thanks also to Barbara Simpson for help in preparing Fig. 1. This analysis benefited substantially from the comments of two anonymous reviewers to whom I express my sincere gratitude. I dedicate this paper to my mentor, Professor Jacqueline D. LaPerriere (1942–1999).

References

Basu, B.K., and Pick, F.R. 1996. Factors regulating phytoplankton and zooplankton biomass in temperate rivers. Limnol. Oceanogr. **41**: 1572–1577.

Boning, C.W. 1974. Generalization of stream travel rates and dispersion characteristics from time-of-travel measurements. U.S. Geol. Surv. J. Res. **2**: 495–499.

Butcher, R.W. 1932. Studies in the ecology of rivers. II. The microflora of rivers with special reference to the algae on the river-bed. Ann. Bot. **46**: 813–861

Carlston, C.W. 1969. Downstream variations in the hydraulic geometry of streams: special emphasis on mean velocity. Am. J. Sci. **64**: 241–256.

Des Cilleuls, J. 1928. Revue générale des études sur le plankton des grandes fleuves ou rivières. Int. Rev. Hydrobiol. Hydrogr. **20**: 174–206.

Eddy, S. 1934. A study of fresh-water plankton communities. Ill. Biol. Monogr. **12**: 1–93.

Emerson, J.W. 1971. Channelization: a case study. Science (Wash., D.C.), **173**: 325–326.

Ferguson, R.I. 1986. River loads underestimated by rating curves. Water Resour. Res. **22**: 74–76.

Hack, J.T. 1957. Studies of longitudinal profiles in Virginia and Maryland. U.S. Geol. Surv. Prof. Pap. 294-B.

Jobson, H.E. 1996. Prediction of traveltime and longitudinal dispersion in rivers and streams. U.S. Geol. Surv. Water Resour. Invest. Rep. 96-4013.

Kilpatrick, F.A., and Wilson, J.F., Jr. 1989. Measurement of time of travel and dispersion in streams by dye tracing. U.S. Geol. Surv. Tech. Water Resour. Invest. Book 3. Chap. A9.

Leopold, L.B., and Maddock, T. 1953. The hydraulic geometry of stream channels and some physiographic implications. U.S. Geol. Surv. Prof. Pap. 252.

Leopold, L.B., Wolman, M.G., and Miller, J.P. 1964. Fluvial processes in geomorphology. W.H. Freeman and Co., San Francisco, Calif.

Monsen, N.E., Cloern, J.E., Lucas, L.V., and Monismith, S.G. 2002. A comment on the use of flushing time, residence time, and age as transport time scales. Limnol. Oceangr. **47**: 1545–1553.

Mueller, J.E. 1973. Re-evaluation of the relationship of master streams and drainage basins: reply. Geol. Soc. Am. Bull. **84**: 3127–3130.

Naiman, R.J., and Sedell, J.R. 1981. Stream ecosystem research in a watershed perspective. Verh. Int. Ver. Limnol. **21**: 804–811.

© 2005 NRC Canada

Naiman, R.J., Melillo, J.M., Lock, M.A., Ford, T.E., and Reice, S.R. 1987. Longitudinal patterns of ecosystem processes and community structure in a subarctic river continuum. Ecology, **68**: 1139–1156.

Newbold, J.D. 1992. Cycles and spirals of nutrients. *In* The rivers handbook. I. Hydrological and ecological principles. *Edited by* P. Calow and G.E. Petts. Blackwell Scientific Publications, Oxford, UK. pp. 379–408.

O'Connor, D.J., and Dobbins, W. 1956. The mechanism of reaeration in natural streams. J. Sanit. Eng. Div. Proc. Am. Soc. Civ. Eng. **82**(SA6): 1115(1)–1115(30).

Pilgrim, D.H. 1976. Travel times and nonlinearity of flood runoff from tracer measurements on a small watershed. Water Resour. Res. **12**: 487–496.

Riggs, H.C. 1973. Regional analyses of streamflow characteristics. U.S. Geol. Surv. Tech. Water Resour. Invest. Book 4. Chap. B3.

Robinson, J.S., Sivapalan, M., and Snell, J.D. 1995. On the relative roles of hillslope processes, channel routing and network geomorphology in the hydrologic response of natural catchments. Water Resour. Res. **31**: 3089–3101.

Rodriguez-Iturbe, I., and Rinaldo, A. 2001. Fractal river basins: chance and self-organization. Cambridge University Press, Cambridge, UK.

Sivko, T.N., Kovalevskaja, R.Z., Mikheeva, T.M., and Ostapenia, A.P. 1972. Biological transformation of organic matter in a river. Verh. Int. Ver. Limnol. **18**: 756–760.

Soballe, D.M., and Kimmel, B.L. 1987. A large-scale comparison of factors influencing phytoplankton abundance in rivers, lakes, and impoundments. Ecology, **68**:1943–1954.

Sokal, R.R., and Rohlf, F.J. 2003. Biometry: the principles and practice of statistics in biological research. 3rd ed. 8th printing. W.H. Freeman and Company, New York.

Swanson, C.D., and Bachmann, R.W. 1976. A model of algal exports in some Iowa streams. Ecology, **57**: 1076–1080.

Talling, J.F., and Rzoska, J. 1967. The development of plankton in relation to hydrological regime in the Blue Nile. J. Ecol. **55**: 637–662.

Thomas, D.M., and Benson, M.A. 1970. Generalization of streamflow characteristics from drainage basin characteristics. U.S. Geol. Surv. Water Supply Pap. 1975.

Van Nieuwenhuyse, E.E. 1993. The phosphorus–chlorophyll relation in streams and some comparisons with lakes. Ph.D. dissertation, University of Missouri, Columbia, Mo.

Waters, F.F. 1961. Standing crop and drift of stream bottom organisms. Ecology, **42**: 352–357.

© 2005 NRC Canada

The "Crustacean Seas" — an evolutionary perspective on the Ponto–Caspian peracarids

Melania E.A. Cristescu and Paul D.N. Hebert

Abstract: A spectacular adaptive radiation of crustaceans has occurred in the Black, Caspian, and Aral seas. This study tests several evolutionary scenarios based on the extent of genetic differentiation and the phylogenetic relationships among endemic mysids and gammarid amphipods from the Black and Caspian seas. Molecular phylogenies for these taxa were based on two mitochondrial genes: cytochrome *c* oxidase subunit I and the large ribosomal RNA subunit (16S), and one nuclear gene, the large ribosomal RNA subunit (28S). The results support the monophyly of the Ponto–Caspian gammarids (genera *Dikerogammarus*, *Echinogammarus*, *Obesogammarus*, and *Pontogammarus*), suggesting their origin from one colonization event. By contrast, several colonization events preceded the radiation of the Ponto–Caspian mysids (genera *Limnomysis* and *Paramysis*). Levels of intraspecific divergence were variable, with mysids showing either no geographic structure or deep genetic splits reflecting a long history of reproductive isolation between populations in marine settings and those in fresh waters. These findings suggest that the diversity of the Ponto–Caspian crustaceans has been underestimated and that species regarded as euryhaline are often composed of distinct evolutionary groups whose taxonomic status should be reevaluated.

Résumé : Il s'est produit une extraordinaire radiation des crustacés dans la mer Noire, la mer Caspienne et la mer d'Aral. Nous évaluons plusieurs scénarios évolutifs basés sur l'étendue de la différentiation génétique et les relations phylogénétiques chez les mysidés et les amphipodes gammaridés endémiques des mers Noire et Caspienne. Les phylogénies moléculaires de ces taxons se basent sur deux gènes mitochondriaux, la sous-unité I de la cytochrome *c* oxydase et la grande sous-unité d'ARN ribosomique (16S), ainsi qu'un gène nucléaire, la grande sous-unité d'ARN ribosomique (28S). Nos résultats appuient l'hypothèse de la monophylie des gammaridés Ponto–Caspiens (genres *Dikerogammarus*, *Echinogammarus*, *Obesogammarus* et *Pontogammarus*), ce qui laisse croire qu'ils sont issus d'un même épisode de colonisation. En revanche, plusieurs épisodes de colonisation ont précédé la radiation des mysidés Ponto–Caspiens (genres *Limnomysis* et *Paramysis*). Les niveaux de divergence interspécifique sont variables : chez les mysidés, ou bien il n'y a pas de structure géographique, ou alors il y a d'importantes divergences génétiques qui reflètent une longue période d'isolement génétique entre les populations des milieux marins et celles d'eau douce. Ces résultats indiquent que la diversité des crustacés ponto-caspiens a été sous-estimée et que les espèces considérées comme euryhalines sont souvent composées de groupes évolutifs distincts dont le statut taxonomique a besoin d'être réévalué.

[Traduit par la Rédaction]

Introduction

Many groups of organisms including fishes, mollusks, turbellarians, and crustaceans have radiated in the Ponto–Caspian biogeographic region, which includes the Black, Azov, Caspian, and Aral seas. However, the endemism in varied crustacean lineages (e.g., cladocerans, copepods, cumaceans, decapods, amphipods, and mysids) is significantly higher than in most other animal groups. For example, more than 70 endemic amphipods and approximately 28 mysid species have been described from the Ponto–Caspian region (Cărăuşu 1943; Băcescu 1954; Barnard and Barnard 1983). In fact, the Ponto–Capian mysid fauna is the most diverse fresh–brackish water mysid fauna in the world (Băcescu 1954; Mauchline 1980). Since most of these endemics are confined to the Caspian Sea, this region has been considered the center for their radiation (Zenkevitch 1963). As a result of this diversity, the Caspian Sea has been nicknamed the "Crustacean Sea". However, its sibling seas, the Black and Azov seas, also support a substantial number of endemics in their less saline estuaries, peripheral lakes, and rivers. In fact, almost 50% of Ponto–Caspian taxa are shared between these basins and their evolutionary origin is particularly ambiguous.

The four basins in the Ponto–Caspian region formed some 6 million years (Mys) ago following disintegration of the Paratethys Sea, an arm of the more extensive Tethys Sea (Dumont 1998). The shared occurrence of species in the Black and Caspian seas could be explained by either these late Miocene – early Pliocene vicariance events that sepa-

Received 19 April 2004. Accepted 25 October 2004. Published on the NRC Research Press Web site at http://cjfas.nrc.ca on 31 March 2005.
J18075

M.E.A. Cristescu[1,2] and P.D.N. Hebert. Department of Zoology, University of Guelph, Guelph, ON N1G 2W1, Canada.

[1]Corresponding author (e-mail: mcristes@bio.indiana.edu).
[2]Present address: Department of Biology, Indiana University, 1001 East Third Street, Bloomington, IN 47405, USA.

 doi: 10.1139/F04-210 © 2005 NRC Canada

rated the basins or more recent (late Pleistocene) dispersal from the Caspian Sea into the Black Sea. This matter is unresolved. Several authors have suggested that most Ponto–Caspian lineages originated long before the present basin configuration, possibly during the late Miocene (Băcescu 1940; Barnard and Barnard 1983; Dumont 2000), while others argued for a more recent Pliocene or Pleistocene origin (Mordukhai-Boltovskoi 1964; Grigorovich et al. 2003).

The Ponto-Caspian mysids have been partitioned into nine genera: *Acanthomysis*, *Caspiomysis*, *Diamysis*, *Heteromysis*, *Katamysis*, *Limnomysis*, *Mysis*, *Paramysis*, and *Schistomysis* (Băcescu 1940, 1954). Väinölä (1995) showed that the pelagic flock of Caspian *Mysis* (*Mysis microphthalma*, *Mysis amblyops*, and *Mysis caspia*) reflects a recent intralacustrine radiation, but their relationships with the other endemic mysid genera have not been investigated. The present study addresses this gap in knowledge by examining the genera *Paramysis* and *Limnomysis*. Not only is *Paramysis* the most speciose of the nine Ponto-Caspian mysid genera, but it also contains species such as *Paramysis kroyeri*, which occurs in salinities ranging from fresh–brackish coastal lakes (salinity < 4‰) to the intertidal and subtidal zones of the Black Sea (salinity = 18‰).

The Ponto–Caspian amphipods belong largely to the families Gammaridae, Pontogammaridae, and Corophiidae, which are each represented by several speciose genera (Cărăuşu 1943; Barnard and Barnard 1983; Martin and Davis 2001). The morphological radiation of Ponto–Caspian amphipods has been linked to their fossorial adaptations because most species are burrowers. Although a general evolutionary trend towards increased specialization for burrowing is evident, the phylogenetic affinities among Ponto–Caspian gammarids are unclear. It has been suggested that the nonfossorial genus *Echinogammarus* is primitive because its gnathopods resemble those of the *Gammarus* group (Barnard and Barnard 1983). *Dikerogammarus* is thought to be derived from the Ponto–Caspian *Echinogammarus* lineage, since its first gnathopod lacks the palmar spination typical of *Echinogammarus* while retaining the *Gammarus* type of first antenna (Barnard and Barnard 1983). Other genera such as *Obesogammarus* and *Pontogammarus* share additional derived characters such as setae on the bases of periopods 5–7 and setae on the posterior margins of periopods 3 and 4. While *Obesogammarus* has the primitive condition of setal tufts, *Pontogammarus* has a single row of coalesced setae. Within *Pontogammarus*, a further subdivision has been proposed by Karaman and Barnard (1997), who suggested the removal of *Pontogammarus maeoticus* from the genus because of the presence of a plesiomorphic longer inner ramus on uropod 3 establishing the genus *Euxinia*. We employ the original nomenclature. Although generally accepted, the morphological phylogeny for this group is based on shared derived states (synapomorphies). It seems likely that the assemblage of primitive features and shared derived characters has been altered by convergent evolution. Furthermore, most diagnosable characters are affected by phenotypic plasticity.

Despite more than a century of taxonomic investigations, the mechanisms of speciation along with the factors responsible for the speciation of the Ponto–Caspian crustaceans remain controversial. There is, for example, no information on whether species flocks descended from a single ancestor or arose through the recurrent colonization of each basin. Similarly, the timing of speciation events is poorly understood.

The present study examines the extent of genetic differentiation and phylogenetic relationship among six species of mysids and eight species of gammarid amphipods from the Black and Caspian seas. Additionally, taking these crustaceans as an example, this study explores the tempo and the mode of speciation responsible for the high species richness in the Ponto–Caspian area.

Materials and methods

Taxon sampling

Fourteen Ponto–Caspian crustacean species, including six mysids and eight amphipods, were analyzed in this study (Table 1). Samples were collected in 1999–2001 from brackish lagoons and estuaries, brackish inland seas, and freshwater ponds and lakes along the northwestern Black Sea coast and in the Caspian Sea (Fig. 1). The samples were sorted and preserved in 90% ethanol shortly after collection. The amphipod *Gammarus lacustris* and the mysids *Tenagomysis australis* and *Mysis relicta* were used as outgroups in the first phase of phylogenetic analyses. To test the monophyly of the Ponto–Caspian gammaroids, we included 16 additional taxa belonging to four gammaridean families (Acanthogammaridae, Gammaridae, Hyalellidae, and Crangonyctidae). These more inclusive phylogenies were rooted using the isopod *Glyptidotea lichtensteini*. Most amphipod taxa were represented by several populations in the phylogenetic analyses of the cytochrome *c* oxidase subunit I (COI) gene, with samples from both the Black and Caspian seas. A phylogeographic survey was also conducted for the mysids *Limnomysis benedeni* and *Paramysis kroyeri* at sites within the Black Sea region.

DNA extraction, amplification, and sequencing

Phylogenies were constructed using two mitochondrial genes: COI and 16S ribosomal RNA (rRNA), and one nuclear gene, 28S rRNA. The primer pairs LCO1490 (5′-GGTCAACAAATCATAAAGATATTGG-3′) and HCO2198 (5′-TAAACTTCAGGGTGACCAAAAAATCA-3′) (Folmer et al. 1994), 16Sar (5′-CGCCTGTTTATCAAAAACAT-3′) and 16Sbr (5′-CCGGTCTGAACTCAGATCACGT-3′) (Palumbi 1996), and 28Sa (5′-TTGGCGACCCGCAATTTAAGCAT-3′) and 28Sb (5′-CCTGAGGGAAACTTCGGAGGGAAC-3′) (Taylor et al. 1999) were used to amplify a 658-base pair (bp) fragment of the COI gene, an approximately 500-bp fragment of the 16S gene, and a 1400-bp fragment of the 28S gene. Total DNA was extracted by grinding one or several appendages in 50–100 µL of a proteinase K extraction buffer (Schwenk et al. 1998).

Each polymerase chain reaction (PCR) had a total volume of 50 µL and contained 1–2 µL of DNA template, 5 µL of 10× PCR buffer, 2.0 mmol/L $MgCl_2$, 0.2 mmol/L each dNTP, 5 pmol of each primer, and 1 unit of *Taq* DNA polymerase. The PCR conditions for COI consisted of one cycle of 94 °C (60 s) followed by five cycles of 94 °C (60 s), 45 °C (90 s), and 72 °C (60 s), 35 cycles of 94 °C (60 s), 51 °C (90 s), 72 °C (60 s), and 72 °C (3 min). The PCR conditions for 16S involved two cycles of 94 °C (30 s), 60 °C (45 s), and 72 °C (45 s) and five cycles of 93 °C (30 s),

© 2005 NRC Canada

Table 1. Species included in the molecular analyses, their geographic distribution, site code, site description, collection date, and GenBank accession Nos.

Taxon[a]	Geographic distribution	Site code[b]	Site description	Collection date	GenBank accession No. COI	GenBank accession No. 16S/28S[c]
Order Mysidacea						
Family Mysidae						
Subfamily Mysinae						
Tribe Mysini						
Limnomysis benedeni	Black and Caspian seas	B5	Agighiol, Danube Delta, Romania	July 1999	AY529017[d]	
		B9	Burnas Lake, Ukraine	July 1999	AY529018[d]	
					AY529019[d]	
		B8	Pokrov Lake, Ukraine	July 1999	AY529020[d]	
		B3	Leahova Mica, Danube Delta, Romania	Aug. 2001	AY529021[d]	
		B2	Golovita Lake, Danube Delta, Romania	Aug. 2001	AY529022[d]	
		BA	Ditch De Gyster, Netherlands	June 2001	AY529023[d]	
					AY529024[d]	
		BA	River Ktoine, Netherlands	June 1999	AY529025[d]	
Mesopodopsis slabberi	B, eastern Atlantic Ocean, (41°N–58°N) and Baltic and Mediterranean seas	B04	Sf. Gheorghe, Black Sea, Romania	Aug. 2001	AY529026[d]	AY529054[d]
Mysis relicta	Circumarctic and Baltic and North seas	NA			AY529027[d]	AY529055[d]
Neomysis integer	Eastern North Atlantic Ocean (44°N–71°N) and Baltic and Mediterranean seas	NE	River Rhine, Netherlands	June 1999	AY529028[d]	
					AY529029[d]	
Paramysis baeri	Black and Caspian seas	C5	North Caspian Sea, Russia	Aug. 2000	AY529030[d]	AY529056[d]
Paramysis intermedia	Black and Caspian seas	B2	Golovita, Danube Delta, Romania	Aug. 2001	AY529031[d]	AY529057[d]
					AY529032[d]	
Paramysis kessleri	Black and Caspian seas	B2	Golovita, Danube Delta, Romania	Aug. 2001	AY529033[d]	AY529058[d]
					AY529034[d]	
Paramysis kroyeri	Black Sea	B11	Dniestr Liman, Ukraine	July 1999	AY529035[d]	AY529059[d]
					AY529036[d]	
		B4	Sf. Gheorghe, Black Sea, Romania	Aug. 2001	AY529037[d]	AY529060[d]
Paramesopodopsis rufa	Pacific and Indian oceans		Jarman et al., unpublished data		AF052393[e]	
Tribe Leptomysini						
Tenagomysis australis	Pacific and Indian oceans		Jarman et al., unpublished data		AF052394[e]	
Order Amphipoda						
Suborder Gammaridea						
Family Pontogammaridae						
Obesogammarus crassus	Black and Caspian seas	B5	Agighiol, Razim Lake, Romania	Sept. 2001	AY189478[f]	
		B7	Kahul Lake, Ukraine	Aug. 1999	AY189481[f]	
		C8	Bandar-e Anzali, Iran	Aug. 2000	AY189482[f]	AY529061[d]

© 2005 NRC Canada

Table 1 (*continued*).

Taxon[a]	Geographic distribution	Site code[b]	Site description	Collection date	GenBank accession No. COI	GenBank accession No. 16S/28S[c]
Pontogammarus (Euxinia) maeoticus	Black and Caspian seas	B11	Dniester Liman, Black Sea, Ukraine	Aug. 1999	AY189490[d]	AY529061[d]
		B13	Chernomorka, Ukraine	Sept. 2001	AY529038[d]	
		B10	Lebedivca, Black Sea, Ukraine	Aug. 1999	AY189483[d]	
		B6	Sulina, Black Sea, Romania	Aug. 1999	AY189494[d]	AY529062[d]
		C6	Baku, Azerbaijan	Aug. 2000	AY189500[d]	AY529063[d]
		C7	Lankaran, Azerbaijan	Aug. 2000	AY189504[d]	
		C8	Bandar-e Anzali, Iran	Aug. 2000	AY189503[d]	
Pontogammarus obesus	Black and Caspian seas	B1	Istria, Sinoie Lake, Romania	Aug. 1999	AY529039[d]	AY529064[d]
		C1	Volgograd Reservoir, Russia	Aug. 2000	AY529040[d] AY529041[d]	AY529065[d]
Pontogammarus robustoides	Black and Caspian seas	B5	Agighiol, Razim Lake, Romania	Aug. 1999	AY529042[d]	
		B7	Kahul Lake, Ukraine	Aug. 1999	AY529043[d]	
		B16	Krasnaya, Dnieper River	Sept. 2001	AY529044[d]	AY529066[d]
		BA	Pregora River, Baltic Sea	Feb. 2001	AY529045[d]	
		C3	Volga Delta, Astrakhan, Russia	Aug. 2000	AY529046[d]	
		C1	Volgograd Reservoir, Russia	Aug. 2000	AY529047[d]	AY529067[d]
Dikerogammarus villosus	Black Sea	B4	Sf. Gheorghe, Danube River, Romania	Aug. 2001	AY529048[d]	
		B5	Agighiol, Razim Lake, Romania	Aug. 1999	AY529048[d]	
		B6	Sulina, Danube River, Romania	Aug. 1999	AY529048[d]	AY529068[d]
Dikerogammarus haemobaphes	Black and Caspian seas	C2	Volga River, Astrakhan, Russia	Aug. 2000	AY529049[d]	AY529069[d]
		C4	North Caspian Sea, Russia	Aug. 2000	AY529049[d]	
Family Gammaridae						
Echinogammarus ischnus	Black and Caspian seas	B5	Agighiol, Razim Lake, Romania	Aug. 1999	AY326120[e]	AY529070[d]
		B15	Kozarovichi, Irpen River	Feb. 1999	AY326122[e]	
		B14	Novodniestrovsk, Middle Dniestr River	Sept. 2001	AY326124[e]	
		C3	Stream Bystraya, Volga River Delta	Sept. 2000	AY326125[e]	AY529071[d]
		C3	Priamaya Bolda, Volga River Delta	Aug. 2000	AY326126[e]	
Echinogammarus trichiatus	Black and Caspian seas	B12	Krasnaya Kosa, Dniestr Liman, Ukraine	Aug. 2001	AY529050[d]	
		B5	Agighiol, Razim Lake, Romania	Aug. 2001		AY529072[d]
		B1	Istria, Sinoie Lake, Romania	Aug. 1999	AY529051[d]	
Gammarus lacustris		NA	Blue Pond, Manitoba, Canada	Sept. 2000	AY529052[d]	AY529073[d]
Gammarus duebeni	Northeast Atlantic Ocean		Ironside et al., unpublished data		AF448520[h]	
Family Acanthogammaridae						
Acanthogammarus maculosus	Lake Baikal	BL	Lake Baikal (Väinölä et al. 2001)		AY061799[f]	
Acanthogammarus flavus	Lake Baikal	BL	Lake Baikal (Väinölä et al. 2001)		AY061800[f]	
Eulimnogammarus cyaneus	Lake Baikal	BL	Lake Baikal (Väinölä et al. 2001)		AY061801[f]	

© 2005 NRC Canada

Table 1 (*concluded*).

Taxon[a]	Geographic distribution	Site code[b]	Site description	Collection date	GenBank accession No. COI	GenBank accession No. 16S/28S[c]
Family Gammaracanthidae						
Gammaracanthus lacustris	Boreal	NE	Finnish Lakes (Väinölä et al. 2001)		AY061796[j]	
Gammaracanthus caspius	Caspian Sea	C	Central Caspian Sea (Väinölä et al. 2001)		AY061797[j]	
Gammaracanthus aestuariarum	Circumarctic	NE	Western White Sea (Väinölä et al. 2001)		AY061798[j]	
Family Hyalellidae						
Hyalella montezuma	North America	NA	Witt et al. 2003		AY152807[k]	
Hyalella sp.	North America	NA	Witt et al. 2003		AY152783[k]	
Hyalella sp.	North America	NA	Witt et al. 2003		AY152752[k]	
Family Crangonyctidae						
Crangonyx sp.	North America	NA			AY529053[d]	
Order Isopoda						
Suborder Valvifera						
Family Idoteidae						
Glyptidotea lichtensteini			Wetzer 2001		AF255781[l]	

[a]Classification after Bousfield (1977), Mauchline (1980), and Martin and Davis (2001).
[b]B, Black Sea; BA, Baltic Sea; C, Caspian Sea; BL, Baikal Lake; NE, north Europe; NA, North America.
[c]16S for mysids and 28S for amphipods.
[d]GenBank accession Nos. AY529017–AY529073 represent taxa sequenced during this project.
[e]GenBank accession Nos. AF052393–AF052394 correspond to specimens to S. Jarman, S. Nicol, N. Elliott, and A. McMinn (Institute of Antarctic and Southern Ocean Studies, University of Tasmania, G.P.O. Box 252-77, Hobard, TAS 7001, Australia, unpublished data).
[f]Genbank accession Nos. AY189478–AY189504 correspond to specimens in Cristescu et al. (2003).
[g]Genbank accession Nos. AY326120–AY326126 correspond to specimens in Cristescu et al. (2004).
[h]GenBank accession No. AF448520 corresponds to specimen in J.E. Ironside, A.M. Dunn, D. Rollinson, and J.E. Smith (Biological Sciences, University of Leeds, Miall Building, Leeds, West Yorkshire LS2 9JT, UK, unpublished data).
[j]GenBank accession Nos. AY061796–AY061801 correspond to specimens in Väinölä et al. (2001).
[k]Genbank accession Nos. AY152752–AY152807 correspond to specimens in Witt et al. (2003).
[l]Genbank accession No. AF255781 corresponds to specimen in Wetzer (2001).

© 2005 NRC Canada

Fig. 1. Collection sites for mysids (solid circles) and amphipods (open circles) examined in this study.

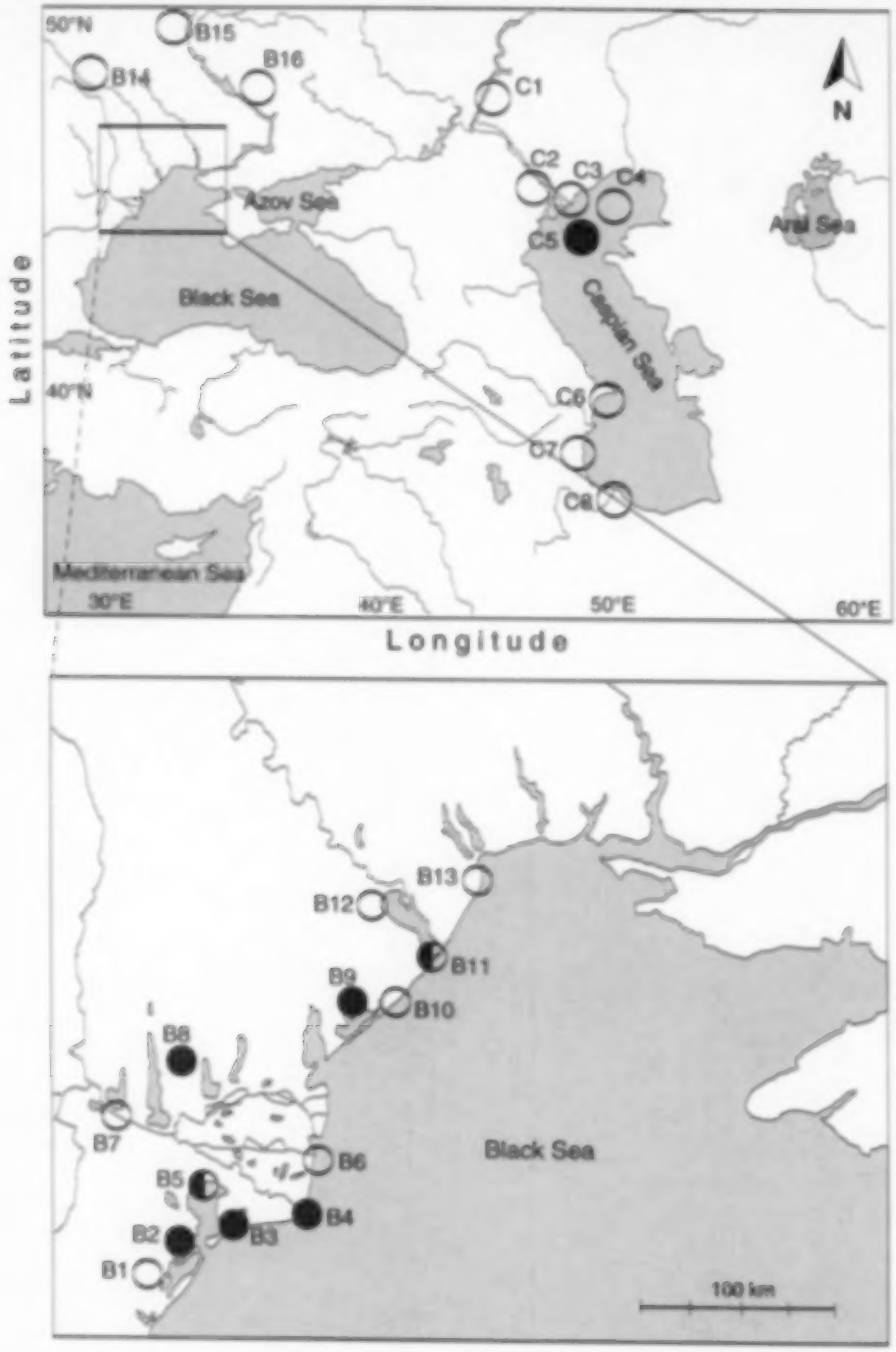

55 °C (45 s), and 72 °C (45 s) followed by 29 cycles of 93 °C (30 s), 50 °C (1 min), and 72 °C (3 min). The temperature profiles for 28S consisted of 35 cycles at 93 °C (30 s), 50 °C (30 s), and 72 °C (1 min). Amplified PCR products were gel purified (2% agarose) using the Qiaex kit (QIAGEN Inc., Valencia, Calif.) and sequenced in one or both directions (for the 28S fragment, both strands were sequenced) using an ABI 377 automated sequencer (ABI, Foster City, California) and the Big Dye terminator 3 sequencing kit (ABI). All sequences obtained during this study

© 2005 NRC Canada

Table 2. Number of sites available (TS), variable sites (VS), cladistically informative sites (IS), base frequencies, transition to transversion ratio (Ti/Tv), and χ^2 test of homogeneity of base frequencies across ingroup taxa for each data set and each partition.

					Base composition (%)					
Data set	Best fit model	TS	VS	IS	A	C	G	T	Ti/Tv	χ^2
Amphipoda										
COI	TVM + I + G	643	297	284	25	21	18	36	1.3	64.36, df = 108, p = 0.99
COI + 28S	GTR + I + G	2034	451	294	24	23	27	26	1.5	6.20, df = 36, p = 0.99
Mysidacea										
COI	TVM + I + G	633	354	291	22	18	24	36	1.1	235.66, df = 81, p < 0.01
COI + 16S	HKI + I + G	1121	527	339	25	17	23	35	1.1	85.34, df = 30, p < 0.01

Note: COI, cytochrome *c* oxidase subunit I; 28S and 16S, ribosomal RNA subunits; TMV, transversional model; I, invariable sites; G, gamma; GTR, general time-reversible model; HKY, Hasegawa–Kishino–Yano model.

have been deposited in GenBank under accession Nos. AY529017–AY529073 (Table 1).

Phylogenetic analyses

Sequences were aligned using the SeqApp 1.9 sequence editor and Sequencher (Gene Codes Corporation, Ann Arbor, Michigan). The estimates of sequence divergence in the amphipod data set were corrected using Tamura and Nei's (1993) method. LogDet distances (Lake 1994; Gu and Li 1996) were used to correct for inequalities of base composition in the mysid data set. COI amino acid distances were estimated using a Poisson correction. Molecular phylogenies were based on nucleotide data. Since most trees had congruent topologies regardless of the inclusion or exclusion of the third codon position of the COI gene, we only present trees based on the complete data set while discussing the few cases of incongruence. Phylogenies were inferred in PAUP* 4.0b.10 (Swofford 2001) and MRBAYES 3.0 (Huelsenbeck and Ronquist 2001) using four analytical approaches: maximum parsimony (MP), maximum likelihood (ML), Bayesian inference of phylogeny (BA), and neighbor joining (NJ). MP trees were estimated using a branch-and-bound or a heuristic search algorithm with 100 replicates, with sequences added at random and tree bisection–reconnection branch swapping. ML analysis employed the best-fit model of nucleotide substitution estimated by MODELTEST (Posada and Crandall 1998), a heuristic search consisting of 10 replicates with taxa added randomly and tree bisection–reconnection branch swapping. The stability of phylogenetic hypotheses was assessed with bootstrap analyses (1000 replicates for MP and NJ and 100 replicates for ML). A Bayesian phylogenetic analysis (e.g., Huelsenbeck et al. 2001) was conducted using the model of nucleotide substitution estimated by MODELTEST. One out of every 100 trees was sampled for 500 000 generations and the strict consensus tree was computed with 1000 trees excluded as the burnin. We employed the incongruence length difference test (Farris et al. 1995) to examine the significance of conflict among data sets. The test was performed in PAUP* with the partition homogeneity test and with 1000 random bipartitions analyzed by tree bisection–reconnection branch swapping on 100 random sequence addition replicates. The homogeneity of base composition across taxa was assessed using the goodness-of-fit (χ^2) test implemented in PAUP*. The timing of invasions and radiations is based on COI clock calibration of 1.4%–2.2% sequence divergence per million years (Knowlton et al. 1993; Knowlton and Weigt 1998).

Results

Patterns of divergence

Pairwise sequence divergences were highly variable in both data sets and for all three genes. As expected, higher divergences were found for the fast-evolving COI gene than for the rRNA genes. For amphipods, Tamura–Nei nucleotide distances at COI ranged from 17% to 28% for comparisons between species, while divergences between "conspecific" populations from the Black and Caspian seas ranged from 2% to 7%. The mysids showed even higher divergences at COI with distances ranging from 19% to 49% (the lower values reflected intrageneric comparisons). Despite the very high nucleotide distances at COI in *Paramysis*, Poisson-corrected amino acid distances ranged from just 0% to 2%. Base frequencies were unequal, with the mitochondrial genes possessing a higher A–T content than the nuclear gene (Table 2). Base composition for the COI gene was homogenous across the amphipod taxa (p = 0.99) but was very heterogeneous among the mysids (p < 0.001) (Table 2). Among the three genes analyzed, the nuclear 28S gene had the highest transition to transversion ratio (1.6). The results of the partition homogeneity tests were not significant, as p values were greater than 0.05 in both groups (amphipods: p = 0.48; mysids: p = 0.45), suggesting congruence in phylogenetic signal among the genes. However, we analyzed the data sets both separately and in combination (Eernisse and Kluge 1993), enabling separate analysis for COI with a more extensive data set. The second round of analyses included a combination of COI and 16S for the mysids and a combination of COI and 28S for the amphipods. To test the monophyly of the Ponto–Caspian gammaroids, we introduced multiple outgroups in a third round of analyses.

Phylogenetic analyses

Mysids

The parsimony analyses of the COI data resulted in four equally parsimonious trees (tree length = 1066, consistency index = 0.55, homoplasy index = 0.45, retention index = 0.81). The topology of the strict consensus MP tree was similar to that of the NJ tree. The tree estimated in the Bayesian phylogenetic analyses differed from the MP and NJ phylo-

© 2005 NRC Canada

Fig. 2. (*a*) Strict consensus of 19 000 trees estimated in the Bayesian phylogenetic analysis (BA) for the cytochrome *c* oxidase subunit I (COI) gene for mysids. The numbers above the nodes indicate the Bayesian posterior probabilities. (*b*) Strict consensus of the four most parsimonious trees (tree length = 1066, consistency index = 0.55, homoplasy index = 0.45, retention index = 0.81) obtained using the maximum parsimony (MP) criterion for the COI gene. The numbers above the nodes indicate MP bootstrap support (1000 replicates), and the numbers below the nodes indicate neighbor-joining (NJ) bootstrap percentages (1000 replicates) for the nodes supported by both methods.

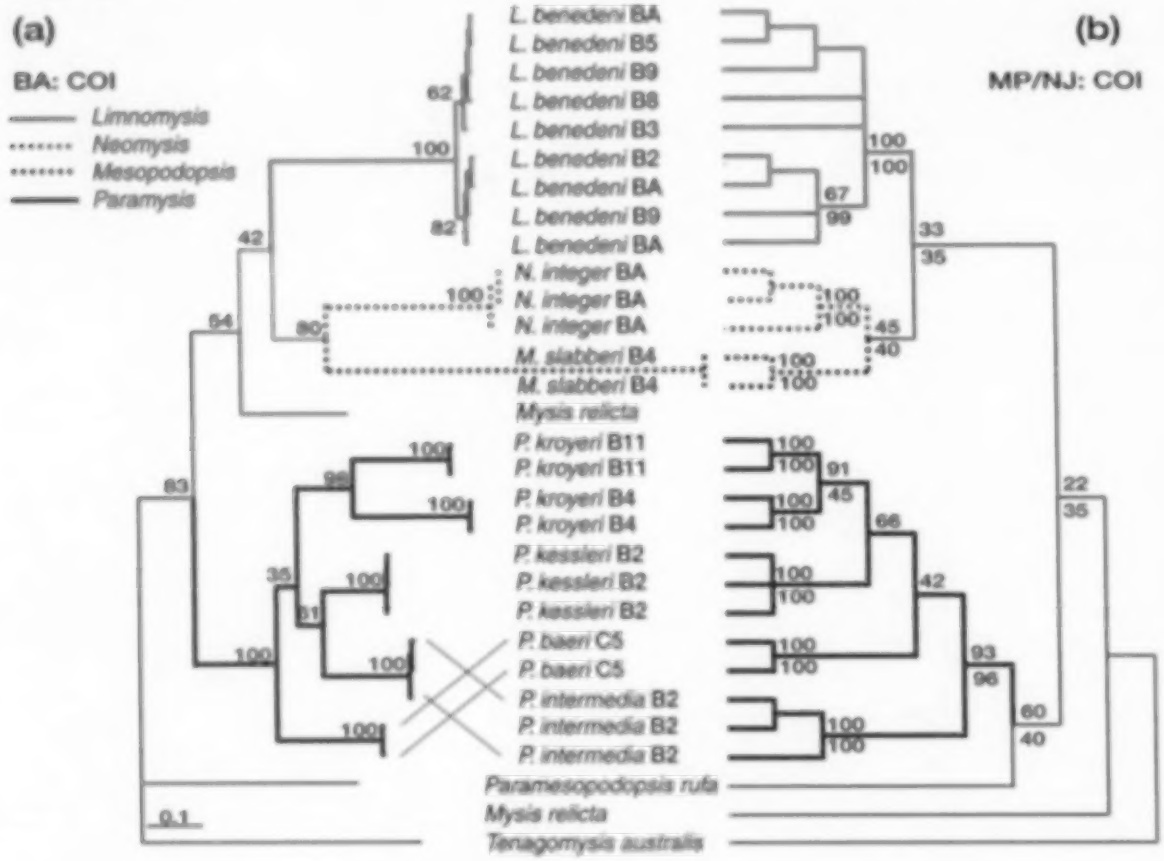

genies solely in the placement of *Mysis relicta*. By contrast, *Mysis relicta* was consistently placed as a sister group to *Paramysis* in all phylogenetic reconstructions based on only first and second codon positions (trees not shown). All analyses unambiguously supported the monophyly of the genus *Paramysis* and the affinity between *Mesopodopsis slabberi*, *Neomysis integer*, and *L. benedeni* (Fig. 2). Likewise, ML, BA, MP, and NJ analyses of the combined data set supported the monophyly of the five *Paramysis* species (Fig. 3). The rest of the genera clustered together with *L. benedeni* as sister taxon to the *Mesopodopsis slabberi* and *N. integer* group. Despite inconsistencies in the position of outgroup taxa, neither the data sets nor algorithms supported the monophyly of the Ponto-Caspian mysids with respect to the non-Ponto-Caspian taxa.

Amphipods

The strict consensus tree of the five most parsimonious trees (tree length = 900, consistency index = 0.51, homoplasy index = 0.49, retention index = 0.82) for the COI gene had a topology congruent with the trees estimated in both the Bayesian and NJ analyses (Figs. 4 and 5). All phylogenetic reconstructions supported the monophyly of the family Pontogammaridae as well as the monophyly of each of its genera (*Pontogammarus*, *Obesogammarus*, and *Dikerogammarus*). As predicted by morphologically based phylogenies, the genus *Echinogammarus* occupied a basal position. Within the family Pontogammaridae, *Dikerogammarus* was a sister taxon to the cluster formed by *Obesogammarus* and *Pontogammarus*. However, when the mitochondrial (COI) and nuclear (28S) genes were combined, the topology of the trees changed slightly with respect to the position of the genus *Dikerogammarus*, although statistical support for varying arrangements (bootstrap and Bayesian posterior probabilities) was weak. Additional phylogenetic analyses of the COI gene included multiple outgroups from four gammaroid families. The relationship between the ingroup taxa did not change in the BA and NJ analyses and there

© 2005 NRC Canada

Fig. 3. (*a*) Maximum likelihood (ML) phylogram (–ln likelihood = 6061.61) for the combined data sets (cytochrome *c* oxidase subunit I (COI) and 16S genes) for mysids. The numbers above the nodes indicate bootstrap support (100 replicates) followed by Bayesian posterior probabilities as percentages. (*b*) The most parsimonious tree (tree length = 1162, consistency index = 0.69, homoplasy index = 0.31, retention index = 0.48) obtained using the maximum parsimony (MP) criterion of the combined data sets (COI and 16S). The numbers above the nodes indicate MP bootstrap support followed by neighbor-joining (NJ) bootstrap percentages for the nodes supported by both methods (1000 replicates). BA, Bayesian phylogenetic analysis.

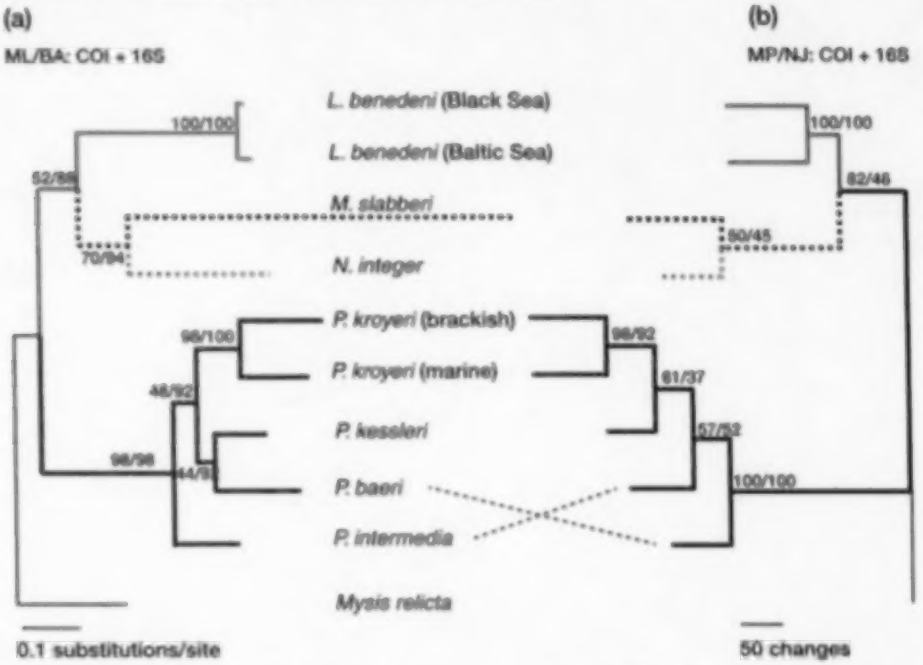

was increased statistical support for most of the clades with strong support for the monophyly of the Ponto–Caspian gammaroids, including the genus *Echinogammarus* (Fig. 6).

Discussion

Phylogenetic inferences

Ponto–Caspian mysids

All phylogenetic reconstructions in this study confirmed the monophyly of the genus *Paramysis*. However, these analyses did not fully resolve phylogenetic relationships among its component taxa (*Paramysis baeri*, *Paramysis kessleri*, *Paramysis kroyeri*, and *Paramysis intermedia*). Moreover, at a generic level, no single, completely resolved topology was favored by all analytical approaches. Certainly, MP and BA methods were not decisive owing to the low statistical support for deep nodes and the instability of the position of key taxa such as *Mysis relicta*. Although the relationship between the Ponto–Caspian genera *Limnomysis* and *Paramysis* and the related mysids (*Mysis relicta*, *N. integer*, and *Mesopodopsis slabberi*) was not resolved, the paraphyly of the Ponto–Caspian mysids (genera *Limnomysis* and *Paramysis*) was apparent, suggesting that there have been multiple invasions and radiations in the region.

The high COI divergences of 19%–27% within the *Paramysis* flock contrast with the very low allozyme distances (0.06) found by Väinölä (1995) for members of the Caspian *Mysis* species flock. In fact, a surprisingly high level of sequence divergence (24%) was found between two adjacent brackish (B11) – marine (B4) populations of *Paramysis kroyeri*. This value is higher than the mean COI divergence value of 11.3% among congeneric animal species (Hebert et al. 2003) and far higher than the mean intraspecific divergence of 1%–2% often recorded in the phylogeographic literature (Avise 2000).

Ponto–Caspian gammaroids

This study supports the monophyly of the Ponto–Caspian gammaroids (genera *Dikerogammarus*, *Echinogammarus*, *Obesogammarus*, and *Pontogammarus*) as well as the monophyly of each individual genus. In addition, this study confirms the monophyly of the family Pontogammaridae while refuting the monophyly of the family Gammaridae. Since all reconstruction methods and all data sets support a close phylogenetic relationship (sister groups) between members of the family Pontogammaridae and the two *Echinogammarus* species, the assignment of the Ponto–Caspian *Echinogammarus* to the family Pontogammaridae warrants consideration. Furthermore, the genus *Pontogammarus* is paraphyletic when *Pontogammarus* (*Euxinia*) *maeoticus* is treated as a member of the genus *Euxinia*, indicating that its assignment to a new genus is not supported by molecular data. Barnard and Barnard (1983) suggested that the Ponto–Caspian gammaroids originated from a fresh–brackish water *Gammarus*-type ancestor and that the evolutionary path fol-

© 2005 NRC Canada

Fig. 4. (*a*) Strict consensus of 9400 trees estimated in the Bayesian phylogenetic analysis (BA) for the cytochrome *c* oxidase subunit I (COI) gene for amphipods. The numbers above the nodes indicate the Bayesian posterior probabilities followed by the neighbor-joining (NJ) bootstrap percentages (1000 replicates) for the nodes supported by both methods. (*b*) Strict consensus of the five most parsimonious trees (tree length = 900, consistency index = 0.51, homoplasy index = 0.49, retention index = 0.82) obtained using the maximum parsimony (MP) criterion of the COI gene. The numbers above the nodes indicate bootstrap support greater than 50% (1000 replicates).

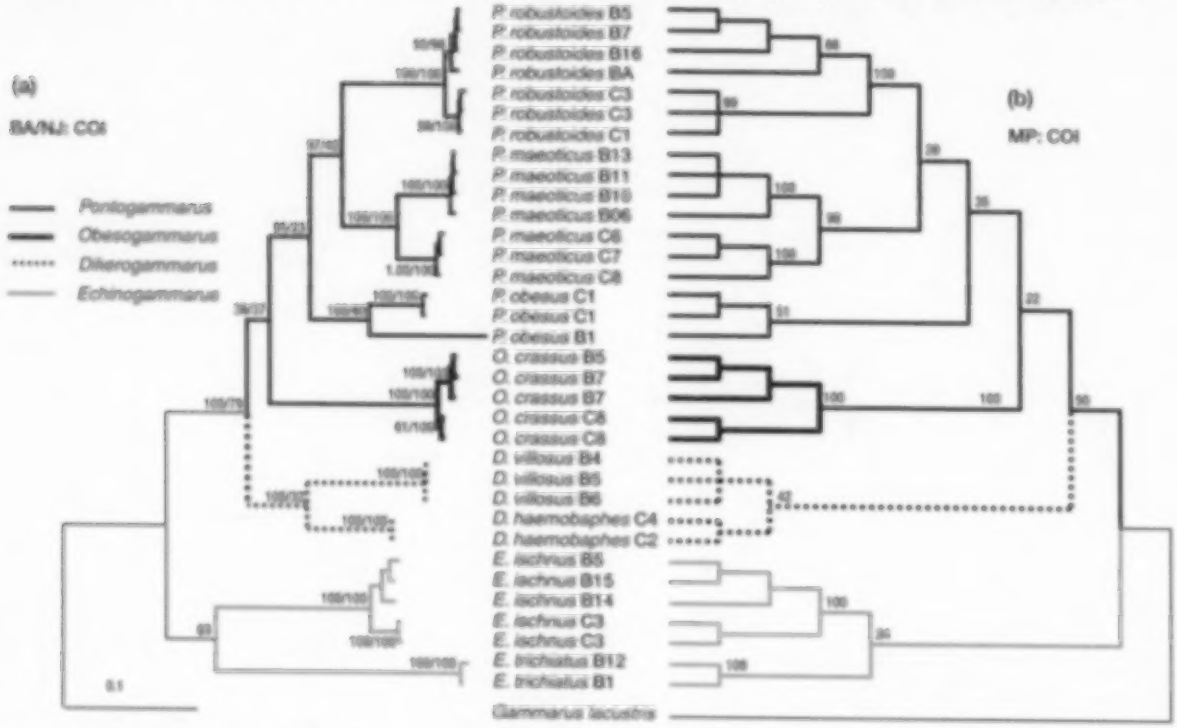

Fig. 5. (*a*) Maximum likelihood (ML) phylogram (–ln likelihood = 7616.56) for the total evidence (cytochrome *c* oxidase subunit I (COI) and 28S genes) for amphipods. The numbers above the nodes indicate bootstrap support (100 replicates) followed by the Bayesian posterior probabilities. (*b*) The most parsimonious tree (tree length = 1086, consistency index = 0.59, homoplasy index = 0.41, retention index = 0.51) obtained using the maximum parsimony (MP) criterion of the total evidence (COI and 28S). The numbers above the nodes indicate MP bootstrap support followed by neighbor-joining (NJ) bootstrap percentages for the nodes supported by both methods (1000 replicates). BA, Bayesian phylogenetic analysis.

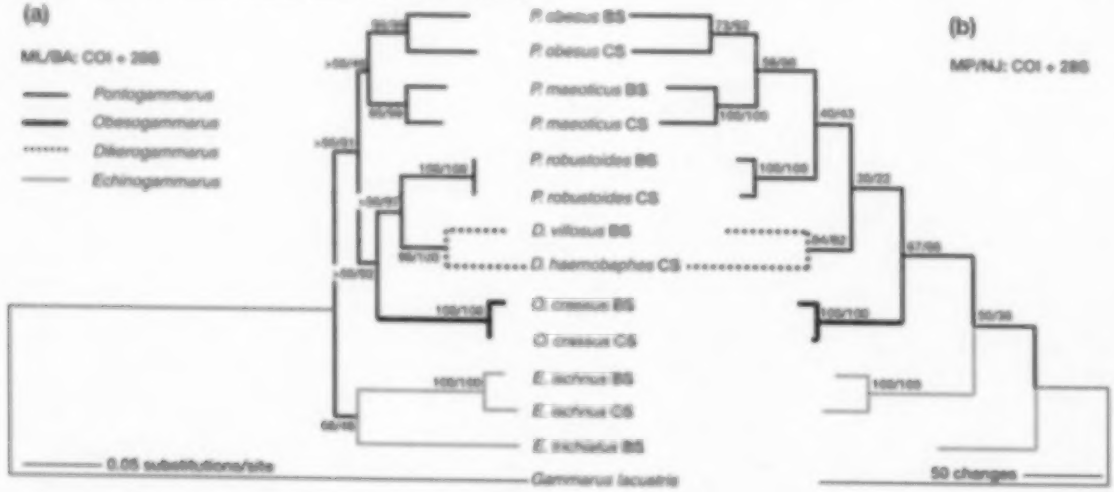

© 2005 NRC Canada

Fig. 6. Strict consensus tree estimated in the Bayesian phylogenetic analysis (BA) for the cytochrome *c* oxidase subunit I (COI) gene for amphipods. Numbers indicate the Bayesian posterior probabilities followed by the neighbor-joining (NJ) bootstrap percentages (1000 replicates) for the nodes supported by both methods.

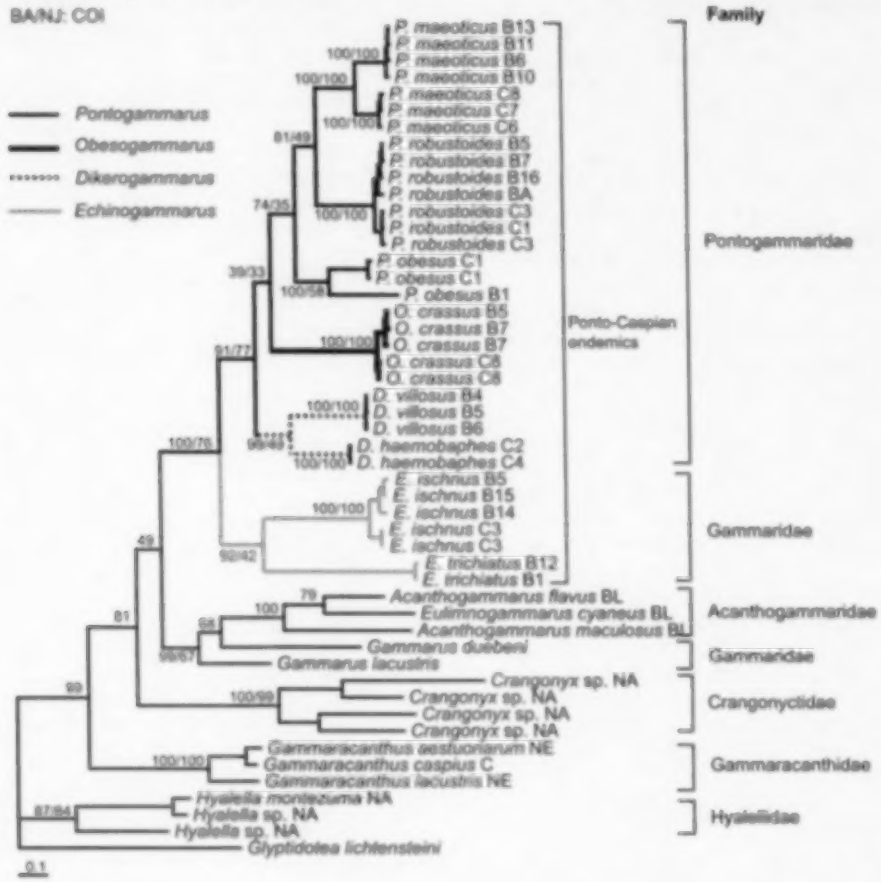

lowed either the *Echinogammarus–Dikerogammarus* line or the Baikalian lineages leading to *Eulimnogammarus* and *Gmelina*. While this study did not examine *Gmelina*, our data strongly suggest that the Ponto–Caspian gammarids derive from an *Echinogammarus*-type ancestor. Certainly, the Baikalian group represented in our phylogeny by the genera *Acanthogammarus* and *Eulimnogammarus* has no direct evolutionary link with the Ponto–Caspian gammarids. Recent studies of sequence diversity in the nuclear 18S gene in Baikalian amphipods have revealed the presence of two main clades (Sherbakov et al. 1998). One consists of benthic, mostly "unarmed" taxa, while the other includes predominantly taxa with more ornamental complexity (Sherbakov et al. 1998; Sherbakov 1999). More relevant to the present study is the old age of the Baikalian generic lineages, which based on the COI calibration for the Caribbean crabs (Schubart et al. 1998) appear to be as old as the lake itself (approximately 20–30 Mys; Sherbakov et al. 1998; Sherbakov 1999). Similarly, our estimates based on the snapping shrimp COI clock (Knowlton et al. 1993; Knowlton and Weigt 1998) suggest that the age of the Ponto–Caspian lineages is remarkably deep (approximately 8–16 Mys). It is likely that these lineages arose shortly after the origin of the basin (Paratethys and Sarmatian basins).

A consistent and marked genetic subdivision was detected at the "subspecific" level between populations of amphipods from the Black and Caspian seas reinforcing the role of geographic isolation and local refugia in lineage survival and evolution (Cristescu et al. 2003). For example, the level of COI divergence between populations of five amphipods (*Pontogammarus maeoticus*, *Pontogammarus robustoides*, *Pontogammarus obesus*, *Obesogammarus crassus*, and *Echinogammarus ischnus*) from the two basins varied from 2.3% to 11%, values that are significantly higher than those typical of intraspecific divergence (Avise 2000).

Geological and molecular reconciliation: age and sequence of invasions

When comparing the timing estimated by molecular results with geological evidence, we found that several cladogenesis events among amphipods and mysids appear concurrently and match various geological events. However,

© 2005 NRC Canada

these molecular clock estimates must be treated with the caution always accorded to these types of best estimates. Nevertheless, the COI divergences in this study support the conclusion that members of most peracarid species flocks diversified well in advance of the Pleistocene. While the close evolutionary relationship between members of the Caspian *Mysis* flock points to a recent (middle or late Pleistocene) intralacustrine origin (Väinölä 1995), and the extent of genetic divergence among the *Mysis relicta* species complex indicates a Pliocene radiation (Väinölä 1986; Väinölä et al. 1994; Dooh 2003), our COI data support a middle–late Miocene radiation for the *Paramysis* flock. Furthermore, it appears that the gammarid group radiated almost simultaneously. The timing provided by the COI clock corresponds to the extensive, brackish Paratethys and Sarmatian basins (16–10 and 10.5–8 Mys, respectively). These radiations have spanned a broad stretch of time, with estimates ranging from Miocene at the generic level to late Miocene throughout Pliocene at the congeneric level.

It appears that two major and contrasting evolutionary forces acted upon the gene pool of most Ponto–Caspian crustacean lineages. On one side, we observe an arresting morphological diversity between most members of species flocks (e.g., pontogammarids, paramysids, mysids, and onychopods), which is not necessarily associated with high genetic divergences, and on the other side, we detect sharp genetic subdivisions between morphologically uniform populations that inhabit ecologically distinctive habitats (Cristescu et al. 2003). A reassessment of the taxonomic status of the latter "species" is needed for a more inclusive view about the key evolutionary and ecological factors responsible for the plethora of endemics in the Ponto–Caspian region.

Acknowledgments

We thank Verginica Serban, Henk Ketelaars, and Igor Grigorovich for help with sample collection and taxon identification. We also thank Teresa Crease, Risto Väinölä, and Jonathan Witt for their thoughtful comments on the manuscript. This study was supported by grants from the Natural Sciences and Engineering Research Council of Canada and the Canada Research Chairs Program to P.D.N.H. and by an Ontario Graduate Scholarship to M.E.A.C.

References

Avise, J.C. 2000. Phylogeography. The history and formation of species. Harvard University Press, Cambridge, Mass.

Băcescu, M. 1940. Les Mysidacés des eaux roumaines: études taxonomique, morphologique, bio-géographique et biologique. Ann. Sci. Univ. Jassy, **26**: 453–804.

Băcescu, M. 1954. Crustacea: Mysidacea. Acad. Repub. Pop. Rom. Bucharest, **4**: 1–126.

Barnard, J.L., and Barnard, C.M. 1983. Freshwater Amphipoda of the world. I. Evolutionary patterns. Hayfield Associates, Mt. Vernon, Va.

Bousfield, E.L. 1977. A new look at the systematics of gammaroidean amphipods of the world. Crustaceana. Suppl. 4. *Edited by* E.J. Brill. Leiden, Netherlands. pp. 282–316.

Cărăuşu, S. 1943. Amphipodes de Roumanie — Gammarides de type Caspien. l'Institut de Recherches Piscicoles de Romanie. Imprimeria Nationala, Bucharest.

Cristescu, M.E.A., Hebert, P.D.N., and Oscin, T.M. 2003. Phylogeography of Ponto–Caspian crustaceans: a benthic–planktonic comparison. Mol. Ecol. **12**: 985–996.

Cristescu, M.E.A., Witt, J.D.S., Grigorovich, I.A., Hebert, P.D.N., and MacIsaac, H.J. 2004. Dispersal of the Ponto–Caspian amphipod *Echinogammarus ischnus*: invasion waves from the Pleistocene to the present. Heredity, **92**: 197–203.

Dooh, R.T. 2003. Patterns of genetic divergence in glacial relict crustaceans. M.Sc. thesis, University of Guelph, Ont.

Dumont, H.J. 1998. The Caspian Lake: history, biota, structure and function. Limnol. Oceanogr. **43**: 44–52.

Dumont, H.J. 2000. Endemism in the Ponto–Caspian fauna, with special emphasis on the Onychopoda (Crustacea). *In* Advances in ecological research. Ancient lakes: biodiversity, ecology and evolution. *Edited by* A. Rossiter and H. Kawanabe. Academic Press, London, UK. pp. 181–196.

Eernisse, D.J., and Kluge, A.G. 1993. Taxonomic congruence versus total evidence, and amniote phylogeny inferred from fossils, molecules, and morphology. Mol. Biol. Evol. **10**: 733–740.

Farris, J.S., Kallersjo, M., Kluge, A.G., and Bult, C. 1995. Testing significance of incongruence. Cladistics, **10**: 315–319.

Folmer, O., Black, M., Hoeh, W., Lutz, R., and Vrijenhoek, R. 1994. DNA primers for amplification of mitochondrial cytochrome *c* oxidase subunit I from diverse metazoan invertebrates. Mol. Mar. Biol. Biotechnol. **3**: 294–299.

Grigorovich, I.A., Therriault, T.W., and MacIsaac, H.J. 2003. History of aquatic invertebrate invasions in the Caspian Sea. Biol. Invasions, **5**: 103–115.

Gu, X., and Li, W.H. 1996. Bias-corrected paralinear and LogDet distances and tests of molecular clocks and phylogenies under nonstationary nucleotide frequencies. Mol. Biol. Evol. **13**: 1375–1383.

Hebert, P.D.N., Ratnasingham, S., and deWaard, J.R. 2003. Barcoding animal life: cytochrome *c* oxidase subunit 1 divergences among closely related species. Proc. R. Soc. Lond. B. Biol. Sci. **270**: 596–599.

Huelsenbeck, J.P., and Ronquist, F. 2001. MRBAYES: Bayesian inference of phylogenetic trees. Bioinformatics, **17**: 745–755.

Huelsenbeck, J.P., Ronquist, F., Nielsen, R., and Bollback, J.P. 2001. Bayesian inference of phylogeny and its impact on evolutionary biology. Science (Wash., D.C.), **294**: 2310–2314.

Karaman, G.S., and Barnard, J.L. 1997. Classificatory revisions in gammaridean Amphipoda (Crustacea). Part 1. Proc. Biol. Soc. Wash. **92**: 106–165.

Knowlton, N., and Weigt, L.A. 1998. New dates and new rates for divergence across the Isthmus of Panama. Proc. R. Soc. Lond. B Biol. Sci. **265**: 2257–2263.

Knowlton, N., Weigt, L.A., Solorzano, L.A., Mills, D.K., and Bermingham, E. 1993. Divergence in proteins, mitochondrial DNA, and reproductive compatibility across the Isthmus of Panama. Science (Wash., D.C.), **260**: 1629–1632.

Lake, J.A. 1994. Reconstructing evolutionary trees from DNA and protein sequences: paralinear distances. Proc. Natl. Acad. Sci. U.S.A. **91**: 1455–1459.

Martin, J.W., and Davis, G.E. 2001. An updated classification of the recent Crustacea. Natural History Museum, Los Angeles, Calif. Contrib. Sci. Ser. 39.

Mauchline, J. 1980. The biology of mysids. *In* Advances in marine biology. Vol. 18. *Edited by* J.H.S. Blaxter, F.S. Russell, and M. Yonge. Academic Press, London, UK. pp. 1–269.

© 2005 NRC Canada

Mordukhai-Boltovskoi, F.D. 1964. Caspian fauna beyond the Caspian Sea. Int. Rev. Gesamten Hydrobiol. **49**: 139–176.

Palumbi, S. 1996. Nucleic acids II: The polymerase chain reaction. *In* Molecular systematics. *Edited by* D. Hillis, B. Mable, and C. Moritz. Sinauer Associates, Inc., Sunderland, Mass. pp. 205–247.

Posada, D., and Crandall, K.A. 1998. Testing the model of DNA substitution. Bioinformatics, **14**: 817–818.

Schubart, C.D., Diesel, R., and Hedges, S.B. 1998. Rapid evolution to terrestrial life in Jamaican crabs. Nature (Lond.), **393**: 363–365.

Schwenk, K., Sand, A., Boersma, M., Brehm, M., Mader, E., Offerhaus, D., and Spaak, P. 1998. Genetic markers, genealogies and biogeographic patterns in the cladocera. Aquat. Ecol. **32**: 37–51.

Sherbakov, D.Yu. 1999. Molecular phylogenetic studies on the origin of biodiversity in Lake Baikal. Trends Ecol. Evol. **14**: 92–95.

Sherbakov, D.Yu., Kamaltynov, R.M., Ogarcov, O.B., and Verheyen, E. 1998. Patterns of evolutionary change in Baikalian gammarids inferred from DNA sequences (Crustacea, Amphipoda). Mol. Phylogenet. Evol. **10**: 160–167.

Swofford, D.L. 2001. PAUP* 4.0b10. Phylogenetic analysis using parsimony (*and other methods). Sinauer Associates, Inc., Sunderland, Mass.

Tamura, K., and Nei, M. 1993. Estimation of the number of nucleotide substitutions in the control region of mitochondial DNA in humans and chimpanzees. Mol. Biol. Evol. **10**: 512–526.

Taylor, D.J., Crease, T.J., and Brown, W.M. 1999. Phylogenetic evidence for a single long-lived clade of crustacean cyclic parthenogens and its implications for the evolution of sex. Proc. R. Soc. Lond. B Biol. Sci. **266**: 791–797.

Väinölä, R. 1986. Sibling species and phylogenetic relationships of *Mysis relicta* (Crustacea: Mysidacea). Ann. Zool. Fenn. **23**: 207–221.

Väinölä, R. 1995. Origin and recent endemic divergence of a Caspian *Mysis* species flock with affinities to the "glacial relict" crustaceans in boreal lakes. Evolution, **49**: 1215–1223.

Väinölä, R., Riddoch, B.J., Ward, R.D., and Jones R.I. 1994. Genetic zoogeography of the *Mysis relicta* species group (Crustacea: Mysidacea) in northwestern Europe and North America. Can. J. Fish. Aquat. Sci. **51**: 1490–1505.

Väinölä, R., Vainio, J.K., and Palo, J.U. 2001. Phylogeography of "glacial relict" *Gammaracanthus* (Crustacea, Amphipoda) from boreal lakes and the Caspian and White seas. Can. J. Fish. Aquat. Sci. **58**: 2247–2257.

Wetzer, R. 2001. Hierarchical analysis of mtDNA variation and the use of mtDNA for isopod systematics (Crustacea: Isopoda). Contrib. Zool. **70**: 23–39.

Witt, J.D.S., Blinn, D.W., and Hebert, P.D.N. 2003. The recent evolutionary origin of the phenotypically novel amphipod *Hyalella montezuma* offers an ecological explanation for morphological stasis in a closely allied species complex. Mol. Ecol. **12**: 405–413.

Zenkevitch, L. 1963. Biology of the seas of the USSR. George Allen & Unwin, London, UK.

© 2005 NRC Canada

Marine nitrogen in central Idaho riparian forests: evidence from stable isotopes

Akihiro Koyama, Kathleen Kavanagh, and Andrew Robinson

Abstract: Terrestrial and marine ecosystems are linked by the annual migration of salmonids. We examined the contribution of anadromous fish to foliar nitrogen (N) in central Idaho riparian forests where anadromous fish have been in sharp decline for approximately 30 years. To determine if the amount of N from anadromous fish carcasses can be assessed from conifer foliage, we fertilized seedlings with varying proportions of N from marine sources and analyzed their foliar $^{15}N/^{14}N$ ratio ($\delta^{15}N$). Also, to evaluate whether N obtained from marine sources was evident in riparian forests, we analyzed the $\delta^{15}N$ of conifer foliage, above and below waterfalls, along historically salmon-bearing and non-salmon-bearing streams and rivers in central Idaho. In the seedling study, the amount of marine N was positively correlated with foliar $\delta^{15}N$. Furthermore, we determined that foliar $\delta^{15}N$ values in riparian forests were explained by the historical occurrence of salmon. Foliar $\delta^{15}N$ declined significantly from bankside to upslope trees in transects along salmon-bearing streams and rivers, whereas there was no significant gradient along transects perpendicular to non-salmon-bearing reaches. We therefore conclude that marine nutrient sources have historically contributed to the N pool in riparian conifer forests and marine N persisted following 30 years of severe populations declines.

Résumé : La migration annuelle des salmonidés relie les écosystèmes marins et terrestres. Nous avons examiné la contribution des poissons anadromes à l'azote (N) des feuilles dans des forêts riveraines du centre de l'Idaho où les populations de poissons anadromes sont en fort déclin depuis une trentaine d'années. Afin de vérifier si la quantité de N provenant des carcasses de poissons anadromes peut être estimée à partir du feuillage des conifères, nous avons fertilisé des jeunes pousses avec diverses proportions de N d'origine marine et nous avons analysé le rapport $^{15}N/^{14}N$ ($\delta^{15}N$) de leurs feuilles. De plus, afin de vérifier si le N provenant de sources marines est décelable dans les forêts riveraines, nous avons analysé le $\delta^{15}N$ du feuillage de conifères, en amont et en aval de chutes, ainsi que le long de ruisseaux et de rivières qui, historiquement, ont eu ou non des populations de saumons. Dans l'étude des jeunes pousses, la quantité de N marin est en corrélation positive avec le $\delta^{15}N$ des feuilles. De plus, nous avons déterminé que le $\delta^{15}N$ des feuilles dans les forêts riveraines s'explique par la présence de saumons au cours des années. Le $\delta^{15}N$ des feuilles diminue significativement dans les transects s'étendant des arbres en bordure du cours d'eau vers les arbres en flanc de montagne dans les ruisseaux et rivières à saumons, alors qu'il n'y a pas de gradient significatif dans les transects perpendiculaires à la rive dans les sections qui ne contiennent pas de saumons. Nous concluons donc que les sources marines de nutriments ont contribué au cours des années au pool de N dans les forêts de conifères riveraines et que le N marin persiste malgré 30 années d'un important déclin des populations de saumons.

[Traduit par la Rédaction]

Introduction

Anadromous fish are an important component of the freshwater and terrestrial ecosystems where they migrate upstream to spawn. This annual migration of anadromous fish extends the interface between the ocean and terrestrial ecosystems up to 1000 km inland (Gross et al. 1998). One ecological function provided by this mass migration is the transport of marine-derived nutrients to freshwater and adjacent terrestrial ecosystems. Pacific salmon (*Oncorhynchus* spp.) and steelhead (*Oncorhynchus mykiss*) can be an important nutrient vector, since they gain the majority of their biomass in productive oceans and return to their oligotrophic natal streams to spawn and deposit their carcasses (Cederholm et al. 1999). Release of nutrients from decaying carcasses is likely for iteroparous steelhead because of their high mortality after spawning (Meehan and Bjornn 1991). It is important to consider the movement of materials from marine to terrestrial ecosystems because such spatial subsidies can influence community productivity through food web dynamics both directly and indirectly (Polis et al. 1997).

Quantifying the spatial subsidy by salmon at a specific point in the Columbia River basin is difficult, since accurate local spawning records are not always available. However, region-wide records can give us a clue of the overall magnitude of this nutrient subsidy. In the Columbia River basin, salmon have been spawning for at least 3000 years (Lichatowich 1999) in approximately 20 000 km of historically accessible stream and river habitat (Cederholm et al. 1999). Anadromous salmon and steelhead were estimated to

Received 12 January 2004. Accepted 7 September 2004. Published on the NRC Research Press Web site at http://cjfas.nrc.ca on 30 March 2005.
J17913

A. Koyama, K. Kavanagh,[1] and A. Robinson. Forest Resources Department, University of Idaho, Moscow ID 83844-1133, USA.

[1]Corresponding author (e-mail address: katyk@uidaho.edu).

 doi: 10.1139/F04-220 © 2005 NRC Canada

provide an annual gross input of organic material ranging from 77 to 103 million kilograms prior to the Euro-American settlement at the end of the nineteenth century (Gresh et al. 2000). Since each fresh carcass is approximately 3% nitrogen (N) (Larkin and Slaney 1997), it can be calculated that 2.3–3 million kilograms of N per annum was once deposited by decaying salmon carcasses throughout the entire Columbia River basin.

A proportion of the carcass material deposited into aquatic ecosystems is transferred to the adjacent riparian forests through several pathways. Transfer can occur either in the hyporheic zone (O'Keefe and Edwards 2003), through direct deposition of salmon carcasses and other aquatic components on the stream bank during a flood (Cederholm et al. 1989), through deposition of salmon carcasses carried by predators onto the riparian forest floor (Cederholm et al. 1989), or through the fecal matter of predators that have consumed spawning salmon, carcasses, or aquatic insects (Ben-David et al. 1998; Hilderbrand et al. 1999*a*). The historic amount of marine N delivered to the riparian terrestrial ecosystems at a given point is highly variable. However, assuming that approximately 2% (Ashkenas et al. 2004) of the N additions from carcass material is deposited within a 10-m strip along both banks of the rivers and streams, terrestrial N deposition rates would average 0.84–1.12 kg·ha^{-1}·year^{-1}. This estimate of terrestrial N deposition is not a definitive value but may useful for comparison with other levels of N inputs.

Several studies have explored the spatial subsidy of marine nutrients to terrestrial ecosystems. The contributions of marine carbon (C) and N were established using stable isotopes, since salmon are enriched in ^{13}C and ^{15}N relative to C and N from terrestrial sources. Nutrients from marine sources were found in fish (e.g., Kline et al. 1990), aquatic invertebrates (Bilby et al. 1996), terrestrial invertebrates (Hocking and Reimchen 2002), mammals (e.g., Ben-David et al. 1997*a*, 1997*b*; Hilderbrand et al. 1999*b*), lake sediments (Finney et al. 2000), and riparian vegetation (e.g., Bilby et al. 1996; Ben-David et al. 1998). All of these studies were located in regions with abundant salmon populations.

We know of no studies that experimentally test if the amount of N from anadromous fish carcasses can be assessed from the N isotopic composition of conifer foliage. This is an important initial step when using the N isotopic composition of conifer foliage to assess the proportion of the N pool from marine sources in riparian forests. The objectives of this study therefore were to characterize the relationship between foliar δ^{15}N and the proportion of marine N in a controlled environment, thus allowing the application of a mixing model, and to determine if the N deposited from salmon carcasses was detectable in the N isotopic composition of conifer foliage after 30 years of sharp decline or extirpation in wild salmon populations. The riparian forests in central Idaho present an opportunity to begin this exploration, since anadromous fish populations have precipitously declined or been extirpated for at least three decades (Hassemer et al. 1997) and N is often a limiting nutrient for terrestrial systems in this region (Moore et al. 1991). Also, conifer trees are long-lived and have low N turnover rates, so they can serve as a long-term depository of the isotopic composition of N inputs. We hypothesized that (1) the δ^{15}N value of conifer foliage of seedlings would increase as the proportion of N from marine sources increased, (2) the conifer foliage along historically salmon-bearing streams would have a higher δ^{15}N relative to non-salmon-bearing streams in the riparian forests of central Idaho, and (3) there would be a declining gradient in foliar δ^{15}N along transects from salmon-bearing riparian systems to upslope forests. We would not expect to observe such gradients in sites that have never been accessible to salmon.

Table 1. Description of the proportions of Alaska Fish Fertilizer (AFF) and Miracid applied to greenhouse-grown, 1-year-old *Pseudotsuga menziesii* seedlings prior to budbreak including the N isotope ratio (δ^{15}N) and percentage of N applied as organic N (%ON).

Fertilizer content	Total N applied to each seedling (mg)	δ^{15}N	%ON
100% AFF	18.9	10.23	96.2
30% AFF and 70% Miracid	18.9	2.96	29.1
10% AFF and 90% Miracid	18.9	0.88	9.6
100% Miracid	18.9	–0.15	0

Methods

Seedling experiment

To test hypothesis 1, we conducted a controlled fertilization study on eighty 1-year old Douglas-fir (*Pseudotsuga menziesii*) seedlings (0.43% N, 0.63‰ δ^{15}N) that were grown in 90-mL cavities of styroblock containers. The application of fertilizer to newly planted seedlings at our field sites was not possible because the sites were very remote and consistent seedling care throughout the growing season would not be possible. The conditions in the greenhouse were similar to field conditions in midspring when N uptake is high (mean temperature 17.25 °C, relative humidity 58%, moist soil). In mid-July 2002, at budbreak, each seedling was given 18.9 mg of N using combinations of two sources of N that reflected differing percentages of marine origin and different proportions of inorganic and organic N (Table 1). Fertilizer derived from ocean fish (Alaska Fish Fertilizer Co., Clackamas, Oregon) was used as a source of marine-derived organic N and Miracid (Scotts Miracle-Gro, Marysville, Ohio) was used as an inorganic N source. The amount of N was chosen to approximate a media C/N ratio of 35, which limits net N mineralization rates in media (Prescott et al. 2000), and thus limits N availability to seedlings. The low N level available to the seedling minimized N loss and fractionation upon uptake. Seedlings were randomly harvested in early October 2002 following a sufficient period for current-year needle elongation and budset. The current-year foliage, formed postfertilization, was dried in an oven at 70 °C for 24 h and finely ground for N isotope, C isotope, %N, and %C analysis at the Idaho Stable Isotope Laboratory, University of Idaho. We expressed foliar ^{15}N level as δ^{15}N values (Peterson and Fry 1987).

© 2005 NRC Canada

Fig. 1. Map showing sample sites along with the tributaries and mainstem dams of the Snake River in central Idaho. The transect along Elk Creek below (transect No. 3 in the figure) has not been accessible to salmon since 1971 because of Dworshak dam completion without fish passage.

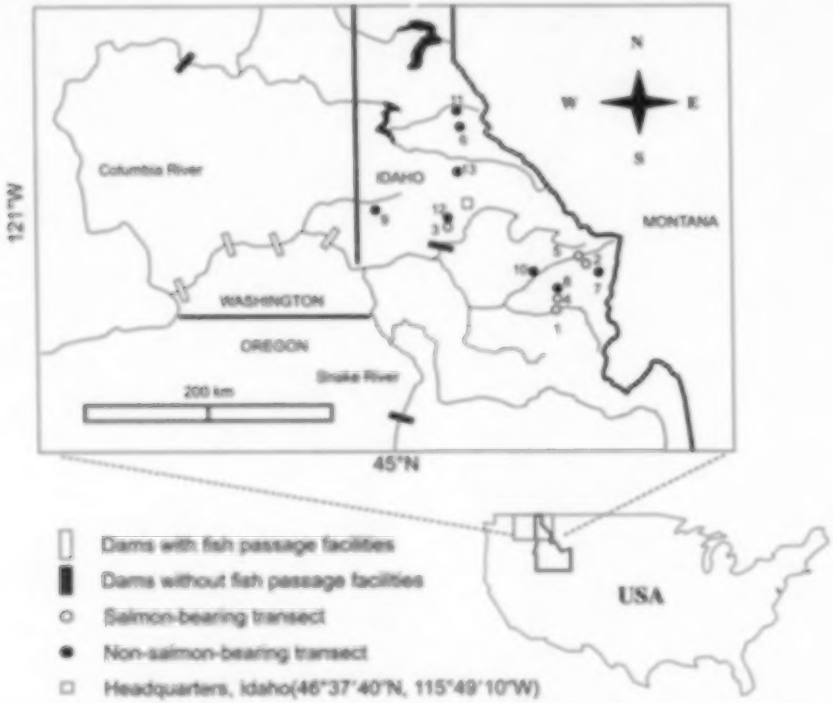

The application of known quantities of N to the soil as well as the initial soil $\delta^{15}N$ and N availability allowed comparison of actual foliar $\delta^{15}N$ with predicted values using a mixing model modified from Balesdent and Mariotti (1996):

$$(1) \qquad X = \frac{ab + cd}{100}$$

where X is predicted foliar $\delta^{15}N$, a is %N from Miracid, b is Miracid $\delta^{15}N$, c is %N from Alaska Fish Fertilizer, and d is Alaska Fish Fertilizer $\delta^{15}N$.

Field sample collection

To address hypotheses 2 and 3, we collected conifer foliage from three locations, bankside (adjacent to the stream), adjacent upslope (just above the floodplain, approximately 10–50 m), and upslope (an additional 100–150 m upslope), along transects perpendicular to streams and rivers in central Idaho (Fig. 1; Table 2). The actual distances between locations varied depending on the gradient of the transects and availability of sample trees. Sample trees were the dominant tree species on the site including Douglas fir, grand fir (*Abies grandis*), subalpine fir (*Abies lasiocarpa*), and ponderosa pine (*Pinus ponderosa*). Current-year foliage, which was growing in full sun, was obtained from the upper canopy and diameter at breast height (DBH; 1.37 m) was recorded for each sampled tree. Elevation and aspect were determined at each site. Foliar samples were collected in September 2000 and August and September 2001 and were transported to the laboratory on ice in a cooler and frozen until processed. The samples were processed for isotope analysis as above.

Five of the 13 transects were in riparian systems with historically salmon-bearing streams, and the other eight had significant waterfalls that are natural geologic barriers to salmon migration (T. Cochenhauer, Idaho Department of Fish and Game, 1540 Warner Avenue, Lewiston, ID 83501, USA, and the late Dr. T. Bjornn, University of Idaho, Moscow, ID 83843, USA, personal communications) (Table 2). All of the transects were located in forests at mid- to late-successional stages with less than 5% of the understory foliar biomass from N-fixing plants (based on ocular estimates) to avoid confounding the marine ^{15}N signal (Kohl and Searer 1980; Hobbie et al. 1999). Distance between transects above and below the waterfalls in streams varied from 2 to 4 km. This distance was necessary to eliminate marine N transport above waterfalls by vectors such as bears (Hilderbrand et al. 1999*a*) and to locate riparian and upslope forests with a similar steam morphology, tree species composition, and tree size as was sampled below the waterfall. In addition, we collected conifer foliage above and below a waterfall from a basin that was located above a primary waterfall that prevented marine N transport (i.e., Willow Creek above and below) to investigate a possible systematic error in foliar $\delta^{15}N$ ratios due to waterfall presence. Unfortunately, we were only able to locate one set of these unique conditions within central Idaho.

To assess the potential contribution of marine sources to foliar N (%MN) collected from salmon-bearing transects, we

© 2005 NRC Canada

Table 2. Characteristics and mean foliar $\delta^{15}N$ of transects located in central Idaho.

		Mean foliar $\delta^{15}N$ in location (‰)								
Transect[a]	Salmon[b]	B (SE)	AU (SE)	U (SE)	Coordinates	Elevation (m)	Aspect	Sampled coniferous species	Mean DBH (SE) (cm)	Transect No. in Fig. 1[c]
Selway River	Present	0.73 (1.22)	2.75 (0.27)	−1.83 (0.49)	46°03′ N, 115°18′ W	550	SW	PM, AG, PP	19.0 (2.6)	1
Warm Spring Creek below	Present	−1.01 (0.35)	−2.51 (0.36)	−5.50 (0.54)	46°26′ N, 114°52′ W	1090	E	AG	31.4 (3.6)	2
Elk Creek below	Present	−1.46 (0.11)	−3.58 (0.14)	−3.27 (0.29)	46°44′ N, 116°11′ W	700	W	PM, AG	12.9 (1.7)	3
Gedney Creek below	Present	−1.83 (0.52)	−2.66 (0.33)	−4.53 (0.14)	46°05′ N, 115°18′ W	670	E	PM, AG	14.7 (1.3)	4
Lochsa River	Present	−3.07 (0.21)	−4.06 (0.29)	−2.14 (0.31)	46°27′ N, 115°00′ W	951	NE	AG	32.3 (3.9)	5
Willow Creek above	Absent	−1.88 (0.30)	−2.09 (0.11)	−2.50 (0.28)	47°26′ N, 115°50′ W	1460	NE	PM, AL	32.9 (3.4)	6
Warm Spring Creek above	Absent	−1.89 (0.46)	−2.10 (0.23)	−2.33 (.0.33)	46°25′ N, 114°52′ W	1260	E	PM, AG	38.8 (3.1)	7
Gedney Creek above	Absent	−1.99 (0.25)	−0.92 (0.25)	−0.83 (0.46)	46°07′ N, 115°15′ W	1040	E	PM, AG, PP	12.2 (1.2)	8
Palouse River	Absent	−2.33	−3.69 (0.46)	−3.14 (0.18)	46°58′ N, 116°30′ W	990	SW	PM, AG	9.5 (1.1)	9
White Horse Creek above	Absent	−2.64 (0.44)	−3.83 (0.35)	−3.69 (0.28)	46°17′ N, 115°24′ W	910	NE	PM	31.3 (1.6)	10
Willow Creek below	Absent	−2.88 (0.20)	−3.06 (0.37)	−3.02 (0.34)	47°27′ N, 115°50′ W	1330	NE	PM, AG	29.5 (2.0)	11
Elk Creek above	Absent	−3.38 (0.22)	−3.23 (0.28)	−2.79 (0.36)	46°44′ N, 116°10′ W	830	W	PM, AG	9.5 (1.6)	12
Marble Creek	Absent	−3.48 (0.63)	−3.89 (0.21)	−3.02 (0.34)	47°10′ N, 116°06′ W	980	SW	PM, AG	10.6 (1.1)	13

Note: B, bankside; AU, adjacent upslope; U, upslope; SE, standard error; AL, *Abies lasiocarpa*; AG, *Abies grandis*; PM, *Pseudotsuga menziesii*; PP, *Pinus ponderosa*; DBH, diameter at breast height. $\delta^{15}N$ values have not been corrected for species and diameter.

[a]Above and below the waterfalls.

[b]Historical salmon presence or absence at the section of streams or rivers where transects were made.

[c]Numbers correspond to sample transect numbers in Fig. 1.

© 2005 NRC Canada

Fig. 2. Relationship between predicted and observed foliar $\delta^{15}N$ of *Pseudotsuga menziesii* seedlings fertilized with varying proportions of Alaska Fish Fertilizer and Miracid. Predictions of foliar $\delta^{15}N$ were calculated using a mixing model. The broken line is the 1:1 line and the solid line is the regression of predicted versus observed values ($y = 0.7282x + 0.0971$; $R^2 = 0.834$, $p < 0.0001$). Observed values of foliar $\delta^{15}N$ were measured on fully expanded foliage that emerged postfertilization. The sample size for each treatment is 5.

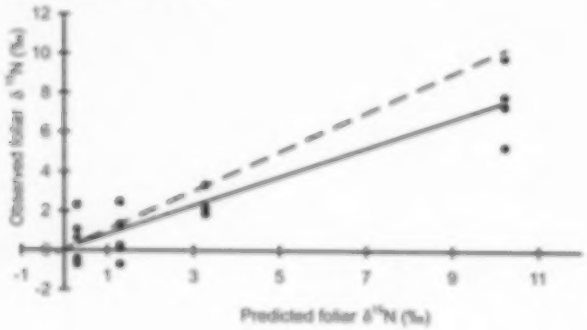

used a mixing model (Balesdent and Mariotti 1996) on select sites:

$$(2) \qquad \mathrm{MN}(\%) = \frac{b-u}{s-u} \times 100$$

where b is the mean $\delta^{15}N$ value for salmon-bearing bankside locations, u is the mean $\delta^{15}N$ value for upslope foliage, and s is the $\delta^{15}N$ value of N in a salmon carcass, 13.4‰ with standard deviation 0.9 and sample size 4 (Jacoby et al. 1999). At individual sites, values for b and u are derived from grand fir foliage from Elk Creek and Warm Spring Creek, since this species had enough samples (more than three) in both bankside and upslope to calculate error terms in the mixing model. In addition, to assess the uncertainty associated with the use of a mixing model, the 95% confidence intervals (CI) of the N proportions were calculated using IsoError (Phillips and Gregg 2001; Environmental Protection Agency 2003*a*).

Statistical analysis

The subsample size for our study is 209 individual foliage samples nested within 39 sampling locations (bankside, adjacent upslope, and upslope at each of 13 transects). A linear mixed-effects ANOVA, not to be confused with the mixing model in eqs. 1 and 2, was employed to construct models suitable for our statistical analysis. The independent variables in the model were species (fixed), salmon (fixed), DBH (fixed), location (as a fixed effect), interaction of salmon and location (fixed), interaction of DBH and location (fixed), interaction of DBH and conifer species (fixed), site (blocking, random), and location (blocking effect, nested within site, random). The foliar $\delta^{15}N$ values as the dependent variable in the model were transformed to provide homoscedasticity and normality of error effects. The root mean squared error, intralocation standard error (SE), and intrasite SE for the model were 0.259, 0.264, and 0.268, respectively. Estimated foliar $\delta^{15}N$ values were derived with the constructed model with coefficients for each independent variable. The estimated means reported are weighted to reflect the unbalanced sample design. We assessed the quality of these models with graphical diagnostics including normal quartile graphs of residuals and random effects and graphs of residuals against fitted values and compared them using the Akaike information criterion corrected for small sample sizes (Burnham and Anderson 1998). The statistical analyses were conducted using the S-PLUS® 6.1 software package (Insightful Corporation, Seattle, Washington).

Table 3. Foliar %N and C/N ratios of current-year foliage from *Pseudotsuga menziesii* seedlings receiving different proportions of Alaska Fish Fertilizer (AFF) and Miracid.

Fertilizer content	%N (SE)	C/N ratio (SE)
100% AFF	1.36 (0.12)	39.54 (3.12)
30% AFF and 70% Miracid	1.51 (0.19)	35.76 (3.57)
10% AFF and 90% Miracid	1.38 (0.19)	38.44 (5.04)
100% Miracid	1.49 (0.10)	35.03 (2.55)

Note: %N and C/N ratio are not statistically different among treatments ($p = 0.82$ and $p = 0.87$ in one-way ANOVA for %N and C/N ratio, respectively). SE, standard error.

Results

Seedling experiment

Increasing the percentage of N from fish carcasses resulted in an increase in foliar $\delta^{15}N$; however, this relationship was not 1:1 (Fig. 2). There was a significant difference in the slope ($p = 0.012$) but not in the intercept ($p = 0.89$) between the regression line and the 1:1 line (Fig. 2). When 100% marine N (Alaska Fish Fertilizer) was applied, the measured values were more depleted in ^{15}N relative to the predicted values (Fig. 2). There were no significant differences in %N or C/N ratios between treatments (Table 3).

Field experiment

The conifer foliage along historically salmon-bearing streams had a higher $\delta^{15}N$ relative to non-salmon-bearing streams ($p = 0.0071$) (Fig. 3). Furthermore, there was a declining gradient in foliar $\delta^{15}N$ along the transects from salmon-bearing bankside trees to adjacent upslope trees ($p < 0.0001$). No such gradient was found along non-salmon-bearing streams (Fig. 3).

Using the mean $\delta^{15}N$ values estimated from the model for salmon-bearing upslope locations as a baseline, mixing model (eq. 2) calculations indicate that 13% (±7.8% for 95% CI) of the total N is from marine sources across all of the salmon-bearing bankside locations. In addition, it was estimated that 11.7% (±4.7% for 95% CI) and 23.8% (±7.9% for 95% CI) of the N in conifer foliage was from marine sources at Elk Creek and Warm Spring Creek, respectively (Table 4). When foliar $\delta^{15}N$ values are compared between bankside and upslope on sites where the same conifer species were sampled, there were significant differences between bankside and upslope values on salmon-bearing streams (Elk Creek below and Warm Spring Creek below) (Table 5). However, there were no such significant differences in transects without salmon (Elk Creek above, Warm

© 2005 NRC Canada

Fig. 3. Foliar N isotope values estimated by a linear mixed-effects model for transects on salmon-bearing (open circles) and non-salmon-bearing stream reaches (solid circles) in central Idaho. The transects included three sampling locations: bankside (B), adjacent upslope (AU), and upslope (U). Bars represent standard error. The means are weighted to reflect the unbalanced sample design.

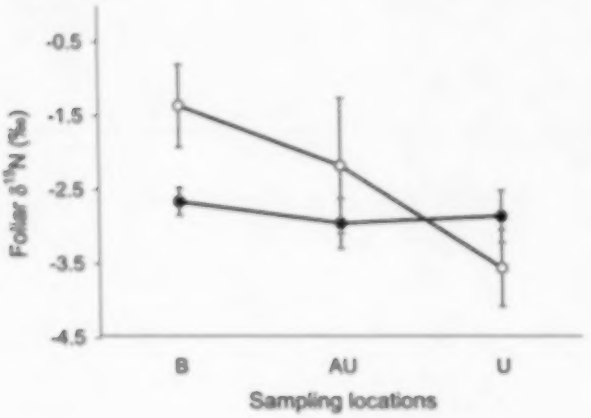

Spring Creek above, and Willow Creek above and below) (Table 5).

The intersite variability in baseline (i.e., upslope) foliar ^{15}N values was high, ranging from –5.50 (0.54) at Warm Spring Creek to –0.83 (0.54) at Gedney Creek (Table 2). The DBH of the sample trees is positively correlated with foliar ^{15}N level ($p < 0.0001$), but the effect is very small (the DBH coefficient is 0.0053). Species was also a statistically significant predictor ($p < 0.0001$), with *P. ponderosa* foliage having a higher $\delta^{15}N$ and grand fir foliage having the lowest $\delta^{15}N$ (Table 6). These effects were independent of the historic presence or absence of salmon carcasses and thus cannot explain the systematic relative differences in $\delta^{15}N$ values between salmon-bearing and non-salmon-bearing riparian foliage. Also, the location effects and the environmental and ecological effects were represented separately in the model. The distribution of the species was unbalanced with regard to location in some of the transects, but the model detected a location effect even after taking this into account. Our summary statistics are based on pooled data to simplify the comparison, but the hypothesis tests were based on unpooled data.

Discussion

Seedling foliar $\delta^{15}N$ reflected the percentage of N from marine sources, although there is a departure from the 1:1 line when 100% Alaska Fish Fertilizer was applied. This departure can be attributed to the preferential uptake of ^{14}N relative to ^{15}N when organic N in Alaska Fish Fertilizer was mineralized to inorganic N prior to seedling uptake or to retranslocation of N with a lower $\delta^{15}N$ value from older foliage, formed before the initialization of the fertilizer treatments, to the newly forming foliage. Current evidence suggests that retranslocation of N from older foliage to newer foliage is significant in seedlings (Proe et al. 2000)

Table 4. Estimated contribution of marine N to total N in *Abies grandis* foliage at two sites in central Idaho that historically had spawning salmon calculated from a mixing model.

	Foliar $\delta^{15}N$ (SD, *n*)		
Site	Bankside	Upslope	Mean marine N contribution (%) (±95% CI)
Elk Creek	–1.46 (0.24, 3)	–3.42 (0.68, 5)	11.7 (±4.7)
Warm Spring Creek	–1.01 (0.80, 4)	–5.50 (1.24, 4)	23.8 (±7.9)

Note: SD, standard deviation; *n*, number in sample; CI, confidence interval.

and thus a likely cause of a lower foliar $\delta^{15}N$ in the high marine N treatment than predicted from the mixing model. The $\delta^{15}N$ of the retranslocated N would be similar to the Miracid treatment (more negative), since the fertilizer applied before the treatment was Miracid.

The seedling trial results support our field observations of foliar $\delta^{15}N$. An increase in foliar $\delta^{15}N$ is evident on sites with a history of salmon carcass N inputs relative to sites without a contribution of marine N, and there is a declining trend in foliar $\delta^{15}N$ from bankside to upslope trees in salmon-bearing systems. These results are consistent with a significant contribution of marine N to the riparian forest ecosystems. Also, these results indicate that N retention rates are high enough to allow this signal to persist over 30 years of severely declining and extirpated salmon populations. However, in examining these results, it is important to consider other sources of variation in foliar ^{15}N that could also account for these patterns.

Species and DBH were significant sources of variation in foliar $\delta^{15}N$. Species differences in plant foliar $\delta^{15}N$ have been linked with differences in source N (Pate et al. 1993; Kielland et al. 1998), N availability (Michelsen et al. 1998), and the extent of mycorrhizal associations (Hobbie et al. 2000). Once we had controlled for variation due to site and location in the mixed-effects model, the differences detected in foliar $\delta^{15}N$ by species and DBH were consistent (i.e., species–location and DBH–location interactions were not statistically significant) across a wide range of upslope values. These results indicate that irrespective of cause, the relative difference in foliar $\delta^{15}N$ due to species and DBH is consistent between sites.

It is important to consider topographic variation when interpreting foliar $\delta^{15}N$ patterns, since several N processes can vary topographically. Variations in N processes in riparian areas can result in increasing foliar $\delta^{15}N$ patterns in riparian foliage relative to upslope foliage, thus making it difficult to distinguish salmon effects. These processes include (*i*) increasing presence of N-fixing species resulting in enrichment in riparian foliage (Helfield and Naiman 2002), (*ii*) high denitrification potential in riparian areas associated with favorable spawning habitat, which may result in enrichment in riparian foliage (Pinay et al. 2003), and (*iii*) high net nitrification potential in riparian areas, which can result in enrichment in riparian foliage (Garten 1993). We minimized the confounding effects of N fixation by sampling in areas

© 2005 NRC Canada

Table 5. Comparison in foliar $\delta^{15}N$ between bankside and upslope trees on sites with the same conifer species in bankside and upslope locations.

Site	Above or below waterfall	Salmon association	Species	Difference (bank mean – upslope mean)	Mean foliar $\delta^{15}N$ (SE, *n*)	
					Bankside	Upslope
Elk Creek	Below	Yes	AG	2.01	–1.46 (0.14, 3)	–3.47 (0.68, 5)*
	Above	No	AG	–0.73	–3.52 (0.39, 2)	–2.79 (0.4, 6)
Warm Spring Creek	Below	Yes	AG	4.49	–1.01 (0.4, 4)	–5.50 (0.62, 4)**
	Above	No	AG	0.57	–2.14 (0.33, 3)	–2.72 (0.60, 4)
Willow Creek	Above	No	PM	0.40	–1.82 (0.19, 3)	–2.22 (1.04, 5)
	Below	No	PM	–0.20	–2.58 (0.21, 6)	–2.39 (0.39, 4)

Note: AG, *Abies grandis*; PM, *Pseudotsuga menziesii*; SE, standard error; *, $p < 0.05$; **, $p < 0.01$.

Table 6. Estimated mean foliar N isotope values for current-year sun foliage by the linear mixed-effects model.

Species sampled	Sample size	Estimated foliage ^{15}N value	SE
Pinus ponderosa	6	–0.37	0.31
Pseudotsuga menziesii	94	–2.20	0.01
Abies lasiocarpa	16	–2.58	0.02
Abies grandis	93	–3.17	0.01

Note: All of the samples are pooled to obtain the values independent of presence–absence of salmon, sampling location (bankside, adjacent upslope, and upslope), diameter at breast height (DBH), and site. SE, standard error.

that had less than 5% of foliar biomass from N-fixing species.

Denitrification potential increases in poorly drained riparian soils. When denitrification occurs, the preferential loss of the more readily volatilized ^{14}N results in a higher percentage of ^{15}N remaining in the soil and thus a higher $\delta^{15}N$ value. This could be especially troublesome if the rate of denitrification varied in conjunction with the presence or absence of salmon. The spatial variation in soil denitrification potential in a western Alaska basin differed significantly between salmon spawning habitat and nonspawning habitat (Pinay et al. 2003). The lower gradient meandering spawning reaches were found to have finer textured soils with higher potential denitrification rates relative to the coarser soils along braided nonspawning reaches. In contrast, we sampled above and below waterfalls and we chose paired sites with similar geomorphic features; thus, we do not expect to see variations in denitrification patterns associated with spawning habitat. None of the streams that were sampled could be characterized as meandering or braided, and all were located in mountainous reaches with constrained channels. However, we cannot rule out denitrification, since we did not measure soil texture and moisture at any of our sites. However, one indication that denitrification was not a factor was that we did not see a change in foliar $\delta^{15}N$ in transects located above and below waterfalls where salmon were not present (Willow Creek) or at any other non-salmon-bearing sites.

Since high net nitrification potential in riparian areas can also result in enrichment in riparian foliage, we examined foliar $\delta^{15}N$ from salmon-bearing and non-salmon-bearing sites that had a sufficient sample of a single tree species throughout the transect for a direct comparison. The absolute differences in foliar $\delta^{15}N$ bankside to upslope were 2.01‰ (Elk Creek) and 4.49‰ (Warm Spring Creek) in our salmon-bearing streams relative to 0.73 (Elk Creek), 0.57‰ (Warm Spring Creek), 0.40‰ (Willow Creek above), and 0.20‰ (Willow Creek below) for the non-salmon-bearing sites. On the non-salmon-bearing sites, significant shifts in foliar $\delta^{15}N$ were not observed, thus indicating that there were no topographic shifts in net nitrification potential that could account for the difference in foliar $\delta^{15}N$ observed on salmon-bearing and non-salmon-bearing sites.

In summary, there were no major topographic differences between the salmon-bearing and non-salmon-bearing sites that were sampled, and there was an absence of increasing foliar $\delta^{15}N$ patterns in riparian foliage relative to upslope foliage in all of the non-salmon-bearing sites. The combination of these observations suggests that N processes did not vary significantly at our sampling sites and therefore would not be a likely cause of an increase in foliar $\delta^{15}N$ that we observed exclusively on salmon-bearing sites.

Once deposited, marine N cycles within riparian forest ecosystems, and our observations suggest high retention of this historical spatial nutrient subsidy. The retention of marine N on these sites is consistent with low N turnover rates characteristic of regions with xeric summers and cold winters (e.g., Fahey et al. 1985; Prescott 2002). However, to determine the rate of foliar isotope decline associated with the dramatic decline in marine N inputs, it is necessary to compare foliar isotopic composition of upslope and riparian forests on our sites with that on similar sites that still have abundant salmon. Unfortunately, since salmon have severely declined or been extirpated throughout Idaho for at least three decades (Hassemer et al. 1997; Isaak et al. 2003), we have no comparable riparian forests with relatively high salmon abundance. Therefore, we compared our absolute differences in foliar $\delta^{15}N$ levels from bankside to upslope with values published for riparian conifer forests outside the region where salmon are still abundant (i.e., coastal Alaska and Washington). Judged against upslope foliar $\delta^{15}N$ levels, bankside foliage with abundant salmon was enriched by 3.9‰ (Helfield and Naiman 2002), 4.0‰ (Helfield and Naiman 2001), and 4.5‰ (Hilderbrand et al. 1999*a*). Our absolute difference of 2.3‰ suggests that the signal may have diminished following decades of salmon decline, or perhaps the historic annual level of marine N inputs were lower. Another potential explanation could also be that

© 2005 NRC Canada

denitrification rates were higher on the more mesic coastal forests relative to more xeric sites in central Idaho, thus causing an additional enrichment in foliar $\delta^{15}N$ levels.

The level of N retention implies that N from salmon was an important input to riparian forest ecosystems; yet the degree of importance of marine N to net primary productivity is very difficult or impossible to measure directly. Problems assessing the importance of N inputs to forest productivity include controlling for spatial variation in environmental variables that limit tree growth and influence salmon abundance (Kirchoff 2003) as well as availability of long-term data on factors influencing tree density in riparian forests and thus individual tree size and productivity (Bilby et al. 2003). It has been theorized that foliar C/N ratios are a good indicator of the importance of marine N to subsidies to riparian forests, with low C/N ratios being indicative of significant marine derived inputs (Helfield and Naiman 2001). Helfield and Naiman (2001) reported that riparian trees in Alaska obtained N from spawning salmon, resulting in a decrease in C/N ratios compared with non-salmon-bearing sites (32.7 with SE = 1.46 versus 39.2 with SE = 2.01). Our C/N ratios of conifer foliage collected from bankside locations did not vary between salmon presence and absence (49.14 with SE = 2.57 versus 48.50 with SE = 0.91) and were much higher relative to those of Helfield and Naiman (2001). The lack of variation in C/N ratios on our site could be due to an increase in foliar biomass where historical N inputs were higher. This is consistent with a N-limited ecosystem and the findings of Balster and Marshall (2000) where 7 or 8 years after application of N fertilizer to interior *P. menziesii* forests, leaf area per unit ground area was 22%–25% higher on the fertilized plots compared with the unfertilized controls. The relatively high C/N ratio and increase in C/N ratio with salmon abundance in the Helfield and Naiman (2001) study are indicative of an ecosystem where N is no longer limiting, since you would expect the foliar N to be diluted by new growth if the N was limiting. It is evident that further long-term research under controlled conditions is needed to fully assess the primary productivity of salmon-bearing versus non-salmon-bearing riparian forests in N-limited interior riparian forests.

Our analysis of the input of N from salmon carcasses in central Idaho to riparian conifers represents a significant step forward in quantifying the spatial subsidy of terrestrial ecosystems from marine sources. This information will be essential in setting ecologically defensible salmon recovery goals (Peery et al. 2003) for sites that have had severe long-term declines in salmon populations. The analysis of $\delta^{15}N$ levels in terrestrial components, such as foliage from long-lived conifer species, allows for an integration of salmon inputs across several decades or centuries. Based on our results that conifer forests integrate long-term salmon nutrient inputs and that this signal persists for a long period of time, it may be possible to monitor cascading impacts of salmon extirpation by assessing $\delta^{15}N$ levels of riparian conifer foliage.

Acknowledgements

We thank Dr. P. Robinson, Dr. J. Marshall, Dr. D. Bennett, Dr. J. Lichatowich, Dr. B. Bond, Mr. D. Bradley, Dr. R. Waring, Dr. W. Minshall, and two unnamed referees for manuscript reviews; Dr. S. Perakis, Dr. K. Nadelhoffer, Peter Mika, Dr. Deborah Page-Dumroese, and Dr. Thomas DeLuca for discussion; R. Stickrod II of the Idaho Stable Isotope Laboratory for foliage sample analysis; T. Cochenhauer, R. Pangle, C. Chambers, M. Beasley, Dr. C. Moffitt, and the late Dr. T. Bjornn for field sampling and locating sites; and E. Strand for cartography.

References

Ashkenas, L.R., Johnson, S.L., Gregory, S.V., Tank, J.L., and Wolleim, W.M. 2004. A stable isotope tracer study of nitrogen uptake and transformation in an old-growth forest stream. Ecology, **85**: 1725–1739.

Balesdent, J., and Mariotti, A. 1996. Measurement of soil organic matter turnover using 13C natural abundance. *In* Mass spectrometry of soils. *Edited by* T.W. Boutton and S. Yamasaki. Marcel Dekker, New York. pp. 83–111.

Balster, N.J., and Marshall, J.D. 2000. Eight-year responses of light interception, effective leaf area index, and stemwood production in fertilized stands of interior Douglas-fir (*Pseudotsuga menziesii* var. *glauca*). Can. J. For. Res. **30**: 733–743.

Ben-David, M., Flynn, R.W., and Schel, D.M. 1997*a*. Annual and seasonal changes in diets of martens: evidence from stable isotope analysis. Oecologia, **111**: 280–291.

Ben-David, M., Hanley, T.A., Klein, D.R., and Schel, D.M. 1997*b*. Seasonal changes in diets of coastal and riverine mink: the role of spawning Pacific salmon. Can. J. Zool. **75**: 803–811.

Ben-David, M., Hanley, T.A., and Schell, D.M. 1998. Fertilization of terrestrial vegetation by spawning Pacific salmon: the role of flooding and predator activity. Oikos, **83**: 47–55.

Bilby, R.E., Fransen, B.R., and Bisson, P.A. 1996. Incorporation of nitrogen and carbon from spawning coho salmon into the trophic system of small streams: evidence from stable isotopes. Can. J. Fish. Aquat. Sci. **53**: 164–173.

Bilby, R.E., Beach, E.W., Fransen, B.R., and Walter, J.K. 2003. Transfer of nutrients from spawning salmon to riparian vegetation in western Washington. Trans. Am. Fish. Soc. **132**: 733–745.

Burnham, K.P., and Anderson, D.R. 1998. Model selection and inference. Springer-Verlag, New York.

Cederholm, C.J., Houston, D.B., Cole, D.L., and Scarlett, W.J. 1989. Fate of coho salmon (*Oncorhynchus kisutch*) carcasses in spawning streams. Can. J. Fish. Aquat. Sci. **46**: 1347–1355.

Cederholm, C.J., Kunze, M.D., Murota, T., and Sibatani, A. 1999. Pacific salmon carcasses: Essential contributions of nutrients and energy for aquatic and terrestrial ecosystems. Fisheries, **24**(10): 6–15.

Environmental Protection Agency. 2003. IsoError 1.04. Available from http://www.epa.gov/wed/pages/models/isotopes/isoerror1_04.htm [accessed 20 October 2003; updated 21 March 2005].

Fahey, T.J., Yavitt, J.B., Pearson, J.A., and Knight, D.H. 1985. The nitrogen cycle in lodgepole pine forests, southeastern Wyoming. Biogeochemistry, **1**: 257–275.

Finney, B.P., Gregory-Eaves, I., Sweetman, J., Douglas, M.S.V., and Smol, J.P. 2000. Impacts of climatic change and fishing on Pacific salmon abundance over the past 300 years. Science (Wash., D.C.), **290**: 795–799.

Garten, C.T. 1993. Variation in foliar ^{15}N abundance and the availability of soil nitrogen on Walker Branch Watershed. Ecology, **74**: 2098–2113.

© 2005 NRC Canada

Gresh, T., Lichatowich, J., and Schoonmaker, P. 2000. An estimation of historic and current levels of salmon production in the Northeast Pacific ecosystem: evidence of a nutrient deficit in the freshwater systems of the Pacific Northwest. Fisheries, **25**: 15–21.

Gross, H.P., Wurtsbaugh, W.A., and Luecke, C. 1998. The role of anadromous sockeye salon in the nutrient loading and productivity of Redfish Lake, Idaho. Trans. Am. Fish. Soc. **127**: 1–18.

Hassemer, P.F., Kiefer, S.W., and Petrosky, C.E. 1997. Idaho salmon: can we count every last one? *In* Pacific salmon and their ecosystems. *Edited by* D.J. Stouder, P.A. Bisson, and R.J. Naiman. Chapman and Hall, New York. pp. 113–126.

Helfield, J.M., and Naiman, R.J. 2001. Effects of salmon-derived nitrogen on riparian forest growth and implications for stream productivity. Ecology, **82**: 2403–2409.

Helfield, J.M., and Naiman, R.J. 2002. Salmon and alder as nitrogen sources to riparian forests in a boreal Alaskan watershed. Oecologia, **133**: 573–582.

Hilderbrand, G.V., Hanley, T.A., Robbins, C.T., and Schwartz, C.C. 1999a. Role of brown bears (*Ursus arctos*) in the flow of marine nitrogen into a terrestrial ecosystem. Oecologia, **121**: 546–550.

Hilderbrand, G.V., Schwartz, C.C., Robbins, C.T., Jacoby, M.E., Hanley, T.A., Arthur, S.M., and Servheen, C. 1999b. The importance of meat, particularly salmon, to body size, population productivity, and conservation of North American brown bears. Can. J. Zool. **77**: 132–138.

Hobbie, E.A., Macko, S.A., and Shugart, H.H. 1999. Interpretation of nitrogen isotope signatures using the NIFTE model. Oecologia, **129**: 405–415.

Hobbie, E.A., Macko, S.A., and Williams, M. 2000. Correlations between foliar $\delta^{15}N$ and nitrogen concentrations may indicate plant-mycorrhizal interactions. Oecologia, **122**: 273–283.

Hocking, M.D., and Reimchen, T.E. 2002. Salmon-derived nitrogen in terrestrial invertebrates from coniferous forests of the Pacific Northwest. BMC Ecology, **2**: 1–14.

Isaak, D.J., Thurow, R.F., Rieman, B.E., and Dunham, J.B. 2003. Temporal variation in synchrony among chinook salmon (*Oncorhynchus tshawytscha*) redd counts from a wilderness area in central Idaho. Can. J. Fish. Aquat. Sci. **60**: 840–848.

Jacoby, M.E., Hilderbrand, G.V., Servheen, C., Schwartz, C.C., Arthur, S.M., Hanley, T.A., Robins, C.T., and Michener, R. 1999. Trophic relations of brown and black bears in several North American ecosystems. J. Wildl. Manag. **63**: 921–929.

Kielland, K., Bunnett, B., and Schell, D. 1998. Intraseasonal variation in the $\delta^{15}N$ signature of taiga trees and shrubs. Can. J. For. Res. **28**: 485–488.

Kirchoff, M.D. 2003. Effects of salmon-derived nitrogen on riparian forest growth and implications for stream productivity: comment. Ecology, **84**: 3396–3399.

Kline, T.C., Jr., Goering, J.J., Mathisen, O.A., Poe, P.H., and Parker, P.L. 1990. Recycling of elements transported upstream by runs of Pacific salmon: I. $\delta^{15}N$ and $\delta^{13}C$ evidence in Sashin Creek, southeastern Alaska. Can. J. Fish. Aquat. Sci. **47**: 136–144.

Kohl, D.H., and Shearer, G. 1980. Isotopic fractionation associated with symbiotic N_2 fixation and uptake of NO_3^- by plants. Plant Physiol. **66**: 51–56.

Larkin, G.A., and Slaney, P.A. 1997. Implications of trends in marine-derived nutrient influx to south coastal British Columbia salmonid production. Fisheries, **22**: 16–24.

Lichatowich, J. 1999. Salmon without rivers. Island Press, Washington, D.C.

Meehan, W.R., and Bjornn, T.C. 1991. Salmonid distributions and life stories. Am. Fish. Soc. Spec. Publ. **19**: 47–82.

Michelsen, A., Quarmby, C., Sleep, D., and Jonasson, S. 1998. Vascular plant ^{15}N natural abundance in heath and forest tundra ecosystems is closely correlated with presence and type of mycorrhizal fungi in roots. Oecologia, **115**: 406–418.

Moore, J.M., Mika, P.G., and Vander Ploeg, J.L. 1991. Nitrogen fertilizer response of Rocky Mountain Douglas-fir by geographic area across the inland Northwest. West. J. Appl. For. **6**: 94–99.

O'Keefe, T.C., and Edwards, R.T. 2003. Evidence for hyporheic transfer and removal of marine-derived nutrients in a sockeye stream in southwest Alaska. Am. Fish. Soc. Symp. **34**: 99–107.

Pate, J.S., Stewart, G.R., and Unkovich, M. 1993. ^{15}N natural abundance of plant and soil components of a Banksia woodland ecosystem in relation to nitrate utilization, life form, mycorrhizal status and N_2-fixing abilities of component species. Plant Cell Environ. **16**: 365–373.

Peery, C., Kavanagh, K., and Scott, J.M. 2003. Pacific salmon in aquatic and terrestrial and aquatic ecosystems: setting biologically defensible recovery goals. BioScience, **53**: 622–623.

Peterson, B.J., and Fry, B. 1987. Stable isotopes in ecosystem studies. Annu. Rev. Ecol. Syst. **18**: 293–320.

Phillips, D.L., and Gregg, J.W. 2001. Uncertainty in source partitioning using stable isotopes. Oecologia, **127**: 171–179.

Pinay, G., O'Keefe, T.O., Edwards, R., and Naiman, R. J. 2003. Potential denitification activity in the landscape of a western Alaska drainage basin. Ecosystems, **6**: 336–343.

Polis, G.A., Anderson, W.B., and Holt, R.D. 1997. Toward and integration of landscape and food web ecology: the dynamics of spatially subsidized food webs. Annu. Rev. Ecol. Syst. **28**: 289–316.

Prescott, C.E. 2002. The influence of forest canopy on nutrient cycling. Tree Physiol. **22**: 1193–1200.

Prescott, C.E., Vesterdal, L., Pratt, J., Venner, K.H., de Montigny, L.M., and Trofymow, J.A. 2000. Nutrient concentrations and nitrogen mineralization in forest floors of single species conifer plantations in coastal British Columbia. Can. J. For. Res. **30**: 1341–1352.

Proe, M.F., Midwood, A.J., and Craig, J. 2000. Use of stable isotopes to quantify nitrogen, potassium and magnesium dynamics in young Scots pine (*Pinus sylvestris*). New Phytol. **146**: 461–469.

© 2005 NRC Canada

Summer and fall habitat of North Atlantic right whales (*Eubalaena glacialis*) inferred from satellite telemetry

Mark F. Baumgartner and Bruce R. Mate

Abstract: Satellite-monitored radio tags were attached to North Atlantic right whales (*Eubalaena glacialis*) in Grand Manan Basin of the lower Bay of Fundy during the summer and early fall seasons of 1989–1991 and 2000. Monte Carlo tests were used to examine the distribution of the tagged whales in space and time and with respect to a variety of environmental variables to characterize right whale habitat on their northern feeding grounds. These environmental variables included depth, depth gradient, climatological surface and bottom hydrographic properties, and remotely sensed surface temperature, chlorophyll concentration, and their respective horizontal gradients. Site fidelity in the Bay of Fundy was very low during 1989–1991 and high during 2000. When the tagged animals left the Bay, they did not frequently visit the deep basins of the Gulf of Maine and Scotian Shelf, where abundances of their primary copepod prey, *Calanus finmarchicus*, are thought to be high. Instead, right whales visited areas characterized by low bottom water temperatures, high surface salinity, and high surface stratification. No evidence was found that the tagged right whales associated with oceanic fronts or regions with high standing stocks of phytoplankton.

Résumé : Des baleines franches noires (*Eubalaena glacialis*) ont été munies d'étiquette radio et surveillées par satellite dans le bassin de Grand Manan dans la baie de Fundy inférieure durant l'été et le début de l'automne en 1989–1991 et en 2000. Des épreuves de Monte Carlo ont servi à étudier la répartition des baleines marquées dans l'espace et le temps et en fonction d'une gamme de variables environnementales afin de caractériser l'habitat des baleines franches noires sur leurs aires d'alimentation du nord. Les variables environnementales comprenaient la profondeur, le gradient de profondeur, les propriétés hydrographiques de la surface et climatologiques du fond, les températures de surface déterminées par senseur à distance et la chlorophylle, ainsi que leurs gradients horizontaux respectifs. La fidélité au site était très faible dans la baie de Fundy en 1989–1991, mais élevée en 2000. Quand les animaux marqués quittaient la baie, ils ne visitaient pas souvent le golfe du Maine et la plate-forme néoécossaise, où il existe, estime-t-on, de fortes abondances de *Calanus finmarchicus*, le copépode qui leur sert de proie principale. Au contraire, les baleines franches noires visitaient des régions caractérisées par une température froide des eaux du fond, une salinité élevée en surface et une forte stratification de surface. Il n'y a pas d'indications qui laissent croire que les baleines franches noires marquéeassocient à des fronts océaniques ou des régions contenanimportants stocks de phytoplancton.

[Traduit par la Rédaction]

Introduction

The North Atlantic right whale (*Eubalaena glacialis*) is one of the most highly endangered whales (Clapham et al. 1999) and recent population assessments indicate that about 300 individuals remain (International Whaling Commission (IWC) 2001). Recovery of this population after centuries of whaling and subsequent international protection in the 1930s has been slow or perhaps even nonexistent (IWC 2001). The hypothesized reasons for this lack of recovery have been numerous and include inbreeding, habitat degradation, competition for food, pollution, and human-caused mortality (IWC 2001). Knowlton and Kraus (2001) reported that 9 of the 19 known right whale mortalities during 1990–1999 were linked to ship strikes, and Kraus (1990) reported that 57% of photographed right whales bear scars from fishing-gear entanglement. At current mortality rates, population models suggest that the North Atlantic right whale will become extinct in the next two centuries (Caswell et al. 1999). To help mitigate human-caused mortality, information about the distribution and habitat of right whales is desperately needed.

Traditional, large-scale habitat studies have combined shipboard or aerial surveys with oceanographic observations to elucidate associations between cetaceans and the environment (e.g., Cetacean and Turtle Assessment Program (CETAP) 1982; Reilly 1990; Baumgartner et al. 2001). These studies are limited in spatial and temporal coverage by the expense of operating a research vessel for long peri-

Received 24 February 2004. Accepted 31 August 2004. Published on the NRC Research Press Web site at http://cjfas.nrc.ca on 12 April 2005.
J18002

M.F. Baumgartner.[1,2] 104 Ocean Administration Building, College of Oceanic and Atmospheric Sciences, Oregon State University, Corvallis, OR 97331, USA.
B.R. Mate. Coastal Oregon Marine Experiment Station, Hatfield Marine Science Center, Oregon State University, Newport, OR 97365, USA.

[1]Corresponding author (e-mail: mbaumgartner@whoi.edu).
[2]Present address: Biology Department, MS #33, Woods Hole Oceanographic Institution, Woods Hole, MA 02543, USA.

 doi: 10.1139/F04-238 © 2005 NRC Canada

ods of time. Radio tracking is a comparatively low-cost alternative that provides a unique, animal-based perspective that is only limited in spatial and temporal coverage by technological challenges such as attachment duration and battery life. To date, location data from satellite telemetry have been used largely in a descriptive fashion (e.g., where animals go, when they go there, and how long they stay) and have yet to be exploited profitably in a quantitative habitat study. These data, consisting only of dates and positions, seem simple, but statistical methods for exploring habitat associations with them are lacking. With the increasing availability of synoptic oceanographic information such as remotely sensed data, climatological data sets, and ocean model output, telemetry data can now be combined with a wealth of environmental data to investigate the habitat of marine animals.

We report here on a study of North Atlantic right whales equipped with satellite-monitored radio tags on their northern feeding grounds during the summer and early fall of 1989–1991 and 2000. We used Monte Carlo methods to examine the distribution of the tagged right whales in space and time and with respect to a variety of environmental variables. The environmental variables were chosen with specific hypotheses in mind. Right whales feed on older life stages of the copepod *Calanus finmarchicus* in every major high-use area of their feeding grounds in the northwestern Atlantic Ocean: Cape Cod Bay (Watkins and Shevill 1976; Mayo and Marx 1990), Great South Channel (Wishner et al. 1988, 1995; Beardsley et al. 1996), lower Bay of Fundy (Murison and Gaskin 1989; Woodley and Gaskin 1996; Baumgartner et al. 2003*a*), and Roseway Basin (Stone et al. 1988; Baumgartner et al. 2003*a*). Large concentrations of *C. finmarchicus* have been observed deep in the basins of the Scotian Shelf (Sameoto and Herman 1990), and modeling studies suggest that similarly large concentrations exist below 200 m in the deep Gulf of Maine basins (Lynch et al. 1998). We examined the hypothesis (denoted H1) that the tagged right whales use these basins to exploit the *C. finmarchicus* aggregations found there. Tidal mixing fronts are frequently observed in the study area (Ullman and Cornillon 1999) and we examined the hypothesis (H2) that the tagged right whales associate with these fronts because they provide improved feeding opportunities via the accumulation of biomass (Olson and Backus 1985; Epstein and Beardsley 2001). We also tested the hypothesis (H3) that the tagged right whales frequent areas with high surface chlorophyll concentrations because these conditions presumably provide feeding opportunities for their copepod prey.

Finally, we examined associations between the distribution of the tagged right whales and a variety of hydrographic properties. Baumgartner and Mate (2003) observed right whales foraging on discrete layers of *C. finmarchicus* stage-5 copepodites (C5) just above the bottom mixed layer in the lower Bay of Fundy and Roseway Basin, so we investigated associations between the tagged whales and bottom water properties. During studies in the Great South Channel (Wishner et al. 1988, 1995; Brown and Winn 1989; Beardsley et al. 1996) and the lower Bay of Fundy (Murison and Gaskin 1989; Woodley and Gaskin 1996), right whales have frequently been observed in stratified waters (but see Baumgartner et al. 2003*a*), so we also examined associations between the distribution of the tagged whales and surface stratification.

Materials and methods

Each right whale was tagged with a satellite-monitored radio transmitter and tracked via the Argos system carried aboard the US National Oceanic and Atmospheric Administration (NOAA) Polar Orbiting Environmental Satellites (POES). The tag consisted of a Telonics ST-3 (1989), ST-6 (1990–1991), or ST-15 (2000) UHF radio transmitter housed in a surface-mounted (1989–1991) or an implantable (2000) stainless-steel cylinder. A salt-water switch and microprocessor were used to conserve battery power by limiting transmissions to times when the tag was out of the water and when the NOAA POES were likely overhead. Further details about the tag design and deployment methods can be found in Mate et al. (1997, 1998, 1999). Right whales were also photographed and individually identified when possible (after Kraus et al. 1986).

The environmental data for this study came from either static or temporally varying gridded data sets. We constructed a digital bathymetry from a variety of sources, including NOAA National Ocean Service sounding data, $2'$ by $2'$ data from satellite altimetry (Smith and Sandwell 1997), and ETOPO 5 gridded bathymetry (National Geophysical Data Center 1988). Depth gradient was computed from the digital bathymetry to examine associations between right whales and sea-floor topography. Horizontal gradients for depth, sea surface temperature (SST), and surface chlorophyll concentration (see below) were computed as vector quantities by using a 3 by 3 pixel Sobel gradient operator (a weighted average of finite differences; Russ 1995), and for brevity, the scalar gradient magnitude will be referred to as the gradient.

Remotely sensed SSTs with a nominal resolution of 1.1 km were acquired from the University of Rhode Island's advanced very high resolution radiometer archive (Cornillon et al. 1987). Reliable automated cloud masking was performed by the University of Rhode Island on the 1989–1991 data only, so we masked SST values in the 2000 data set that were judged extreme within a fixed temporal (10 days) and spatial (36 km by 36 km) window about a pixel. Owing to the crudeness of this approach in 2000, only 1989–1991 SST data are presented; however, the results of our analyses using SST data from all years were similar. Raw ocean color radiance data for 2000 were acquired from the sea-viewing wide field-of-view sensor and processed into gridded estimates of surface chlorophyll concentration with a nominal resolution of 1.1 km using SeaDAS software (version 4.0) (Baith et al. 2001). Both SST and surface chlorophyll concentration were coregistered to a digital coastline by hand with an accuracy of approximately ±1 pixel. Oceanic fronts can often be observed from remotely sensed data as regions of coherent horizontal variability in either SST or surface chlorophyll concentration, so both SST and surface chlorophyll gradient were computed as proxies for the presence of oceanic fronts. To investigate whether right whales visit areas historically rich in oceanic fronts, we also examined a climatology of

© 2005 NRC Canada

monthly front-presence probabilities (Ullman and Cornillon 1999).

The hydrography of the Gulf of Maine and the Scotian Shelf is quite variable in space because of a variety of physical processes acting in a topographically complex region (Mountain and Jessen 1987). These processes include tidal mixing, slope water intrusions, wintertime convective and mechanical mixing, buoyancy forcing due to local and remote (e.g., St. Lawrence River) freshwater inputs, and stratification due to vernal warming. To examine associations between right whales and hydrographic features, a summertime climatology of surface temperature, salinity and stratification (density difference in the top 50 m of the water column), and bottom temperature and salinity was utilized (Loder et al. 1997).

Randomly generated simulated tracks were created from the observed Argos data for Monte Carlo tests (described below). For each tagged animal's track, 9999 corresponding simulated tracks were generated such that the initial location (tag-deployment site), the total distance traveled and the between-location distances and speeds for each simulated track were identical with those for the observed track, but the direction of travel between locations was randomly selected from a uniform distribution of angles between 0° and 360°. The simulated locations were not allowed to occur on land, but straight-line paths between locations were allowed to cross small islands. The static environmental data were spatially averaged within a radius of 7.5 km around each observed and simulated location. All remotely sensed data were first temporally averaged within ±1 day of a location-acquisition time and then spatially averaged within a radius of 7.5 km around an observed or simulated location. Spatially averaged front probabilities were computed from the monthly climatology that corresponded to the location-acquisition time. If the location was beyond the domain of the gridded environmental data set or, in the case of the remotely sensed variables, more than 50% of the data in the spatial average were missing because of cloud contamination, the environmental datum for that location was flagged as a missing value. The spatial averaging radius was chosen as 7.5 km based on accuracy tests reported in Mate et al. (1997). They found that 68% of the poorest quality Argos locations (class 0) were within 7.5 km of the true transmitter location. Even if the location error is negligible, a right whale could potentially move up to 6 km at a maximum swimming speed of 18 km·h^{-1} during a NOAA POES overpass that can take up to 20 min. Therefore, the 7.5-km radius also accounts for any location uncertainty due to movement of the tagged whale during a satellite overpass.

Right whales generally remained in the lower Bay of Fundy in 2000 (see Results) and so a second simulation data set was created to minimize confounding due to selection of this habitat. The lower Bay of Fundy is a well-known habitat for right whales, so movements occurring outside the Bay are of particular interest. For each tagged animal's track outside the Bay of Fundy, 9999 corresponding simulated tracks were generated. The first location in each simulated track was the last acquired location in the Bay of Fundy before the animal exited the Bay. As before, the total distance traveled outside the Bay and the between-location distances and speeds for the simulated tracks were identical with those for the observed track. Only the direction of travel between locations was randomly selected. The simulated track ended if and when the tagged animal returned to the Bay of Fundy. Separate simulated tracks were generated each time a tagged animal left the Bay.

We used Monte Carlo tests to determine if the tagged right whales' observed distribution in space and time and with respect to each of the environmental variables could have occurred by chance (i.e., by simply moving at random). The null hypothesis in all of these tests is that the tagged right whales' distribution is random. Rejection of the null hypothesis in a two-tailed test provides evidence for either resource selection (preference) or resource rejection (avoidance) and the p value from such a test is denoted p_2. The p value from a one-tailed test for resource selection is denoted p_U and the p value from a one-tailed tests for resource rejection is denoted p_L.

The first Monte Carlo test was conducted to determine if the tagged right whales preferred or avoided particular regions or topographic features in the study area. To accomplish this, the total number of locations occurring over a particular feature was tallied for all of the tagged right whales. For each of the 9999 simulated track sets (a set consisted of one simulated track for each of the tagged whales), the total number of locations over the topographic feature was similarly tallied. The total number of locations occurring over the feature is regarded as a statistic of interest and the 10 000 values for this statistic (9999 from the simulated track sets and 1 from the observed data) make up the sampling distribution of this statistic under the null hypothesis. Consider first a one-tailed test of resource selection. The null hypothesis is rejected if fewer than 5% of the 10 000 values in the sampling distribution are greater than or equal to the observed statistic. Rejection of the null hypothesis would suggest that the tagged right whales preferred the topographic feature in question, since more locations occurred there than expected. A one-tailed p value (p_U) can be assigned to the observed statistic as the fraction of values in the sampling distribution that are greater than or equal to the observed statistic. Similarly, the p value in a one-tailed test of resource rejection (p_L) can be assigned to the observed statistic as the fraction of values in the sampling distribution that are less than or equal to the observed statistic. A two-tailed p value for either resource selection or rejection (p_2) is constructed as the smaller of $2p_U$ and $2p_L$ (Manly 1997).

In addition to the number of locations occurring over a particular topographic feature, the number of individuals was also tested in the same manner as described above. Because the Bay of Fundy is a well-known high-use area, selection of this habitat was examined over time with one-tailed Monte Carlo tests of the numbers of locations and individuals occurring there in biweekly time intervals.

A two-dimensional frequency histogram was constructed to examine the null hypothesis of random spatial distribution. The study area was partitioned in 0.685° longitude by 0.5° latitude bins (nominally 56 km by 56 km) and separate one-tailed Monte Carlo tests were conducted on the numbers of locations and individuals in each bin. Bins containing significant results represent areas that the tagged right whales

© 2005 NRC Canada

Fig. 1. Map of the study area in eastern Canada and the USA, including location names. The 91-m (50 fathom) isobath is shown as a shaded line; basins are cross-hatched.

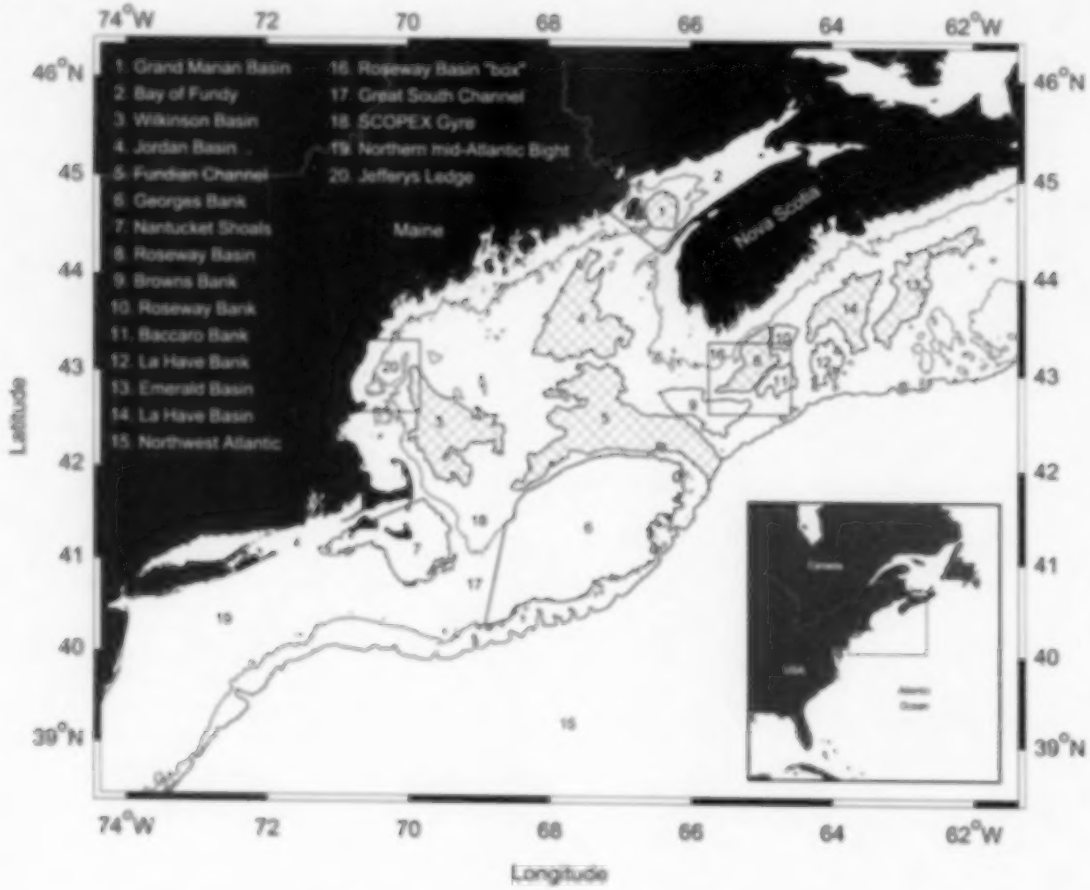

visited more than would be expected had they moved about at random.

Monte Carlo tests were also used to examine the null hypothesis that the tagged right whales were distributed randomly with respect to the environmental variables. Separate two-tailed Monte Carlo tests were conducted for the mean, standard deviation, skewness, and kurtosis of each environmental variable (Manly 1997). Significant results for any of these tests were interpreted as evidence that the tagged right whales' distribution was different from an expected distribution under the null hypothesis. To further examine the relationship between the tagged whales and the environmental variables, we constructed univariate frequency histograms for each variable and separate one-tailed Monte Carlo tests were conducted on the numbers of locations and individuals occurring in each histogram bin. Frequency histogram bin sizes were allowed to vary and were determined such that the average number of locations from the 10 000 values in the sampling distribution for each bin was the same. Plots of collocated temperature and salinity measurements are useful for investigating water masses, so we constructed a bivariate frequency histogram for bottom salinity and bottom temperature to investigate the tagged right whales' distribution with respect to bottom water masses. The two-dimensional bin sizes were fixed at 0.25 practical salinity units (psu) and 1 °C for bottom salinity and bottom temperature, respectively. Separate one-tailed Monte Carlo tests were conducted on the numbers of locations and individuals in each bin.

For the univariate and bivariate one-tailed tests of resource selection, all bins with observed counts greater than zero were considered as well as those in which two or more locations occurring in a bin could be found significant (i.e., where 5% or more of the values in the sampling distribution exceeded zero). Resource rejection in a one-tailed test could only be detected when fewer than 5% of the values in the sampling distribution (2.5% for a two-tailed test) were zero. To illustrate this constraint, consider the most extreme case of potential resource rejection when zero observed locations or individuals occur in an area. Then only 5% or fewer of the values in the sampling distribution can be zero if statistical significance of the observed result in a one-tailed test is to be achieved (i.e., $p_L < 0.05$). In other words, an area must be potentially visited often, but actually visited infrequently (or never at all) to successfully detect resource rejection.

In the analyses described above, many Monte Carlo tests are carried out to determine the significance of an area or a

© 2005 NRC Canada

Table 1. Summary data for each tag deployment, including the ID No. from the New England Aquarium (NEA) right whale catalog, tagging date, total number of locations, percentage of locations outside the Bay of Fundy (BOF), total (minimum) distance traveled (calculated as the sum of rhumb-line distances between Argos locations), and total duration of location acquisitions.

Tag ID No.	NEA ID No.	Tagging date	Total no. of locations	Locations outside BOF (%)	Total distance traveled (km)	Total duration (days)	Label (see Fig. 2)
1989							
843	1146	15 Oct. 1989	71	94.4	1511	21.2	A
1990							
840	1135	24 Aug. 1990	15	66.7	770	6.4	B
839	1140	24 Aug. 1990	108	88.0	3614	41.5	C
833	1981	25 Aug. 1990	25	0.0	367	10.6	D
825	1629	26 Aug. 1990	8	0.0	196	9.9	E
823	1421	12 Sept. 1990	137	97.8	3104	42.1	F
1991							
1 385	1243	27 Sept. 1991	6	83.3	218	7.9	G
1 386	1608	28 Sept. 1991	38	84.2	1787	23.7	H
1 387	1406	5 Oct. 1991	46	87.0	1321	21.4	I
2000							
848[a]		9 July 2000	5	60.0	504	23.1	J
4 174	2645	13 July 2000	63	3.2	1400	52.9	K
23 039[b]	2320	11 Aug. 2000	114	53.5	6006	125.8	L
10 829	2795	11 Aug. 2000	26	23.1	1547	66.0	M
1 387	2617	12 Aug. 2000	4	0.0	36	18.9	N
23 040	1114	12 Aug. 2000	14	35.7	708	18.9	O
824	1027	12 Aug. 2000	16	0.0	266	6.3	P
823	2310	12 Aug. 2000	24	4.2	513	23.2	Q
828	3030	12 Aug. 2000	39	61.5	2606	52.1	R

Note: Location data are shown in Fig. 2.

[a]Whale not yet identified; hence missing NEA ID No.

[b]Nonmigrating portion: the total number of locations was 101, 47.5% of locations were outside the BOF, the total distance traveled was 3718 km, and total duration was 94.8 days.

single environmental variable. This multiple testing increases the likelihood of obtaining a significant result when, in fact, the null hypothesis is true (i.e., increases the probability of identifying resource selection when there is none). Since our study is exploratory, with the goal of identifying potential habitat, this Type I error is more acceptable than a Type II error (i.e., failing to identify resource selection when, in fact, it exists). Therefore, we chose not to use a multiple-testing adjustment to the selected significance level of 0.05 (e.g., Bonferroni adjustment), relying instead on coherent patterns in the results to judge ecological significance.

Right whale habitat is characterized here as an area or oceanographic regime that is visited by individual whales many times or for extended periods (i.e., the analyses of locations), or as an area/regime that is visited by many whales (i.e., the analyses of individuals). The Argos position data do not contain any explicit information about behavior, so it is impossible to determine if tagged whales are foraging, resting, or just traveling slowly through an area identified as habitat. However, high metabolic rates and a large body mass suggest that right whales must feed often to satisfy their energetic requirements (CETAP 1982; Kenney and Winn 1986; Kenney et al. 1986). Therefore, we assume that the primary motivation for resource selection is the presence of exploitable concentrations of right whale prey. We acknowledge that other factors may play a role in governing movements (e.g., reproduction) and these will be considered here as appropriate, but the movements of the tagged whales will be interpreted largely in the context of feeding and the physical and biological oceanographic processes that make prey available to right whales.

Results

Thirty-five right whales were equipped with satellite-monitored radio tags in Grand Manan Basin of the lower Bay of Fundy during the summer or early fall seasons of 1989–1991 and 2000 (Fig. 1). Eighteen whales were tracked for 6 days or more (Table 1) and locations for these animals were acquired, on average, 2.1 times·day^{-1} for 20.5 days in 1989–1991 and 0.9 times·day^{-1} for 43.2 days in 2000. These location-acquisition rates varied because programmed transmission rates were reduced in 2000 to conserve battery power. Only the 18 whales shown in Table 1 were used in the analyses. This sample size precluded an investigation of habitat differences among sex, age, and reproductive classes. One of the whales (23 039 in 2000, New England Aquarium ID No. 2320) migrated from the northern feeding grounds in mid-November to the only known wintering area off the Florida–Georgia coast in the USA. The migration portion of this whale's track was omitted from the analysis, since we

© 2005 NRC Canada

Fig. 2. Argos-acquired locations for all tagged right whales (*Eubalaena glacialis*). Because of the large number of locations in the lower Bay of Fundy, locations there are indicated as solid circles. All locations for an individual animal outside the Bay of Fundy are denoted by the same letter. Summary data for each animal are included in Table 1. The 91-m (50 fathom) isobath and the features from Fig. 1 are shown.

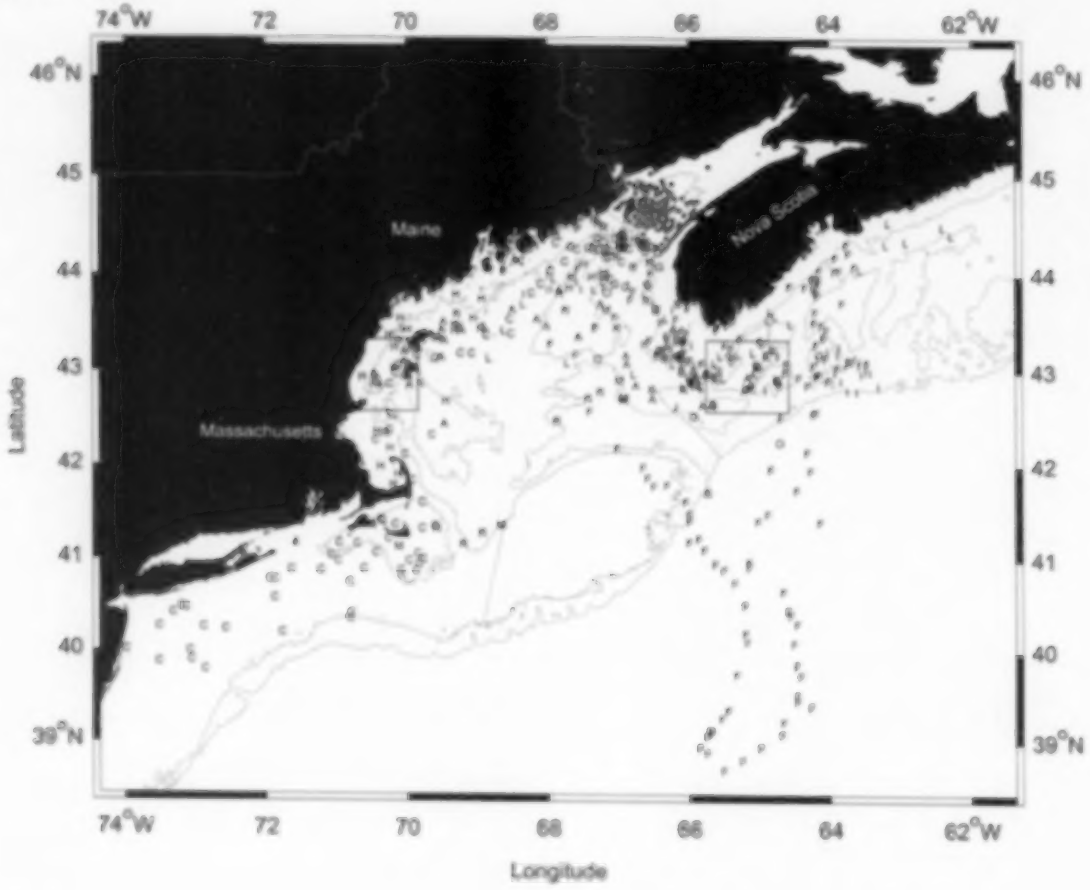

are concerned here only with habitat use on the northern feeding grounds. When the tagged right whales left the Bay of Fundy, they moved extensively throughout the Gulf of Maine, western Scotian Shelf, northern mid-Atlantic Bight, and on the continental slope at an average speed of 79 km·day^{-1} (Fig. 2).

During 1989–1991, only 16% of all acquired locations (71 of 454, $p_2 = 0.060$) occurred in the lower Bay of Fundy (Table 2). In contrast, 70% of all locations (203 of 292, $p_2 = 0.0008$) acquired in 2000 occurred in the lower Bay of Fundy (Table 2). To examine whether these differences were an artifact of the tag-deployment times (late August through mid-October in 1989–1991 and early July through early August in 2000), we conducted one-tailed Monte Carlo tests on the biweekly occurrence of locations and individuals in the Bay of Fundy (Table 3). These tests demonstrate that from late August to mid October, significantly more locations and individuals occurred in the Bay of Fundy during 2000 than expected. During the same period in 1989–1991, the observed number of locations in the Bay of Fundy was consistently less than the mean of the sampling distribution. Because right whales exhibited such strong selection for the lower Bay of Fundy in 2000, the simulation data set for track segments outside the Bay was used for all subsequent analyses.

The number of locations in the deep basins of the Gulf of Maine and Scotian Shelf for all years was quite low (37; Table 3) and there was some suggestive but inconclusive evidence that the tagged whales that moved out of the Bay of Fundy actually avoided these deep basins ($p_2 = 0.093$). The observed numbers of locations in the Fundian Channel (5) and Jordan Basin (19) were much lower than the mean of the sampling distribution (Table 4), though these results were not significant ($p_2 = 0.065$ and $p_2 = 0.21$, respectively). More of the tagged right whales (7 individuals) visited the banks of the southwestern Scotian Shelf than expected ($p_2 = 0.0012$), but only 4.5% of the locations outside the Bay of Fundy were found on these banks (22 of 491, $p_2 = 0.073$). Interpretation of the tagged right whales' use of Roseway Basin depended on the definition of where this basin is actu-

© 2005 NRC Canada

Table 2. Two-tailed Monte Carlo test results for the number (n) of locations or individuals that occurred in the Bay of Fundy.

	1989–1991				2000				All years			
	Locations (n_t = 454)		Individuals (n_t = 9)		Locations (n_t = 292)		Individuals (n_t = 9)		Locations (n_t = 746)		Individuals (n_t = 18)	
	n	μ	n	μ	n	μ	n	μ	n	μ	n	μ
Bay of Fundy	71	147.9	9	9.0	203***	71.0	9	9.0	274	218.9	18	18.0
Inside Grand Manan Basin	47	40.9	9	8.7	126***	24.4	9	9.0	173***	65.3	18	17.7
Outside Grand Manan Basin	24**	107.0	7	7.9	77	46.7	9	6.8	101	153.6	16	14.7

Note: μ is the mean number of locations or individuals in the Bay of Fundy from the sampling distribution, and n_t is the total number of locations or individuals. **, $0.01 > p \geq 0.001$; ***, $p < 0.001$.

Table 3. Results of one-tailed Monte Carlo tests of resource selection for the number (n) of locations or individuals that occurred in the Bay of Fundy during 2-week intervals.

	1989–1991				2000			
	Locations		Individuals		Locations		Individuals	
	n	μ	n	μ	n	μ	n	μ
1–15 July					6	5.3	2	2.0
15–29 July					2	0.5	1	0.2
29 July – 12 Aug.					11	3.1	3	2.2
12–26 Aug.	10	9.8	3	3.0	75*	40.4	7	6.3
26 Aug. – 9 Sept.	39	60.3	4	3.9	44**	15.7	6**	3.2
9–23 Sept.	3	25.1	1	1.7	33**	3.8	3**	0.8
23 Sept. – 7 Oct.	13	23.9	4	3.5	20**	1.5	2**	0.2
7–21 Oct.	6	19.6	2	1.9	12***	0.5	2***	0.1
21 Oct. – 4 Nov.	0	8.9	0	0.7	0	0.1	0	0.0
4–18 Nov.	0	0.2	0	0.1	0	0.0	0	0.0

Note: μ is the mean number of locations or individuals from the sampling distribution. *, $0.05 > p \geq 0.01$; **, $0.01 > p \geq 0.001$; ***, $p < 0.001$.

ally located. No more locations or individuals were found in the basin area bounded by the 130-m isobath than expected (region 8 in Fig. 1); however, significantly more locations (42, $p_2 = 0.041$) were found in the high-use area described by Mitchell et al. (1986) as Roseway Basin (region 16 in Fig. 1). More individuals (4) visited this area in 1989–1991 than expected ($p_2 = 0.040$) and more locations (12) occurred here in 2000 than expected ($p_2 = 0.035$). The locations acquired in 2000 were, however, from a single animal. The area around Jefferys Ledge, bounded to the south by 42°35′N, to the north by 43°20′N, to the east by 69°50′W, and to the west by the coast (after Weinrich et al. 2000), had more locations (32, $p_2 = 0.044$) and individuals (3, $p_2 = 0.024$) than expected in 1989–1991, but there was no evidence that this area was frequented or avoided in 2000. Nantucket Shoals was visited by three individuals ($p_2 = 0.023$) and more locations were acquired than expected (18, $p_2 = 0.025$); however, 16 of the 18 locations were from a single animal.

Significant concentrations of locations or individuals occurred in the western Gulf of Maine (north and west of Wilkinson Basin), on the southwestern Scotian Shelf, over Nantucket Shoals, in the northern mid-Atlantic Bight, and over the continental slope in the northwest Atlantic Ocean (Fig. 3). The latter three areas, however, were each predominantly occupied by only one animal (Fig. 2). The large number of locations between the mouth of the Bay of Fundy and Jordan Basin was not significantly higher than expected and appeared to be the result of the tagged animals using this region as a corridor when leaving from and returning to the Bay.

Monte Carlo tests of the mean, standard deviation, skewness, and kurtosis of the environmental variables suggest that the tagged right whales' distribution with respect to surface salinity, surface stratification, bottom temperature, bottom salinity, and SST gradient may differ from a random distribution (Table 5). The mean surface salinity ($p_2 = 0.0088$) and bottom temperature ($p_2 = 0.016$) were lower than expected, while the mean surface stratification ($p_2 = 0.023$) was higher than expected. The kurtosis of bottom salinity, surface stratification, and SST gradient was different than expected ($p_2 = 0.024$, $p_2 = 0.024$, and $p_2 = 0.032$, respectively). Although depth was not found to be significant for any of these statistics, the high mean depth (Table 5) suggests confounding by the few individuals that moved off the shelf into the very deep waters of the northwest Atlantic Ocean (Fig. 2; Table 4). When the 48 points occurring in this region were removed from the analysis, all of the observed statistics for depth became highly significant (mean: $\theta = 123.0$, $\mu = 312.7$, $p_2 = 0.0032$; standard deviation: $\theta = 53.5$, $\mu = 658.0$, $p_2 = 0.0002$; skewness: $\theta = -0.03$, $\mu = 5.49$, $p_2 = 0.0024$; kurtosis: $\theta = -0.58$, $\mu = 40.48$, $p_2 = 0.0068$).

The patterns of significant results for either locations or individuals in the univariate frequency histograms (shown as probability density functions in Fig. 4) suggest that the tagged whales' distributions with respect to surface salinity,

© 2005 NRC Canada

Table 4. Results of two-tailed Monte Carlo tests of the number (n) of locations or individuals that occurred in regions outside the Bay of Fundy.

	1989–1991				2000				All years			
	Locations (n_t = 391)		Individuals (n_t = 7)		Locations (n_t = 100)		Individuals (n_t = 7)		Locations (n_t = 491)		Individuals (n_t = 14)	
	n	μ	n	μ	n	μ	n	μ	n	μ	n	μ
Deep basins	26	56.1	5	5.4	11	15.6	3	3.7	37	71.6	8	9.1
Wilkinson Basin	9	5.3	3	1.0	0	1.7[a]	0	0.9[a]	9	7.0	3	1.9
Jordan Basin	13	30.3	4	4.7	6	7.4	2	2.8	19	37.8	6	7.5
Fundian Channel[b]	1	19.3	1	2.9	4	6.1	2	2.3	5	25.4	3	5.2
La Have Basin	3	0.8	1	0.2	0	0.2[a]	0	0.1[a]	3	1.0	1	0.3
Emerald Basin	0	0.4[a]	0	0.1[a]	1	0.1	1	0.1	1	0.5	1	0.2
Scotian Shelf Banks	18	5.3	4*	1.4	4	1.5	3*	0.8	22	6.8	7**	2.2
Browns Bank	4	3.8	2	1.1	2	1.1	2	0.6	6	4.9	4	1.8
Roseway Bank	0	0.3[a]	0	0.2[a]	1	0.1	1	0.1	1	0.4	1	0.2
Baccaro Bank	6	0.7	3**	0.3	0	0.2[a]	0	0.1[a]	6	0.9	3*	0.4
La Have Bank	8*	0.4	2*	0.2	1	0.1	1	0.1	9*	0.6	3**	0.3
Roseway Basin[c]	10	2.2	2	0.7	2	0.6	1	0.4	12	2.8	3	1.0
Roseway Basin[d]	30	7.9	4*	1.3	12*	2.0	1	0.9	42*	10.0	5	2.2
Jefferys Ledge	32*	3.5	3*	0.6	1	1.0	1	0.5	33*	4.4	4*	1.1
Georges Bank	4	13.1[a]	1	1.6[a]	0	4.7[a]	0	1.7[a]	4	17.9	1	3.3
Nantucket Shoals	16*	1.0	1	0.2	2	0.5	2	0.3	18*	1.5	3*	0.6
Northwest Atlantic Ocean	47	20.2	3	1.9	1	10.5[a]	1	1.9[a]	48	30.7	4	3.8

Note: Results were obtained using observed and simulated track segments outside of the Bay of Fundy. μ is the mean number of locations or individuals in these regions from the sampling distribution, and n_t is the total number of locations or individuals. *, $0.05 > p \geq 0.01$; **, $0.01 > p \geq 0.001$.

[a] p_U (see Materials and methods) could not be assessed because more than 2.5% of the values in the sampling distribution were zero.

[b] Includes Georges Basin and the Northeast Channel.

[c] Area enclosed by the 130-m isobath (region 8 of Fig. 1).

[d] High-use area observed in Blanford whaling records (Mitchell et al. 1986) (region 16 of Fig. 1).

surface stratification, bottom temperature, bottom salinity, and depth were indeed different than expected. The number of locations or individuals outside the Bay of Fundy was significantly greater than expected in waters of low surface salinity (Fig. 4*c*) and high surface stratification (Fig. 4*g*). The lowest two frequency histogram bins for surface salinity contained 29% of all locations (142 of 491), whereas the highest two bins for surface stratification contained 27% of all locations (134 of 491). Since surface salinity and surface stratification are correlated in the data, it is not surprising that the same subset of locations contributed to the significance of both of these variables. Significantly more locations or individuals were found in waters with low bottom temperatures (Fig. 4*f*) and the lowest two frequency histogram bins for this variable contained 25% of all locations (125 of 491). The pattern of significant results for bottom salinity is less coherent (Fig. 4*e*); however, it is worth noting that 37% of locations found inside the Bay of Fundy (102 of 274) fell within the range 33.21–33.39 psu (bins 2 and 3 in Fig. 4*e*). The number of locations or individuals in waters of 133–165 m depth (bins 2–4 in Fig. 4*a*) was also significantly greater than expected and 24% of locations inside the Bay of Fundy (66 of 274) were found in this depth range. Finally, there was no evidence to suggest that the tagged right whales occurred more frequently at higher climatological front probabilities (Fig. 4*j*), SST gradients (Fig. 4*k*), or surface chlorophyll gradients (Fig. 4*l*).

The results of the Monte Carlo tests for the bivariate frequency histogram of bottom temperature and bottom salinity (Fig. 5*a*) suggest that particular bottom water properties were selected by the tagged right whales. Significantly more locations were found in the warmest and freshest waters, but all of these locations were from the single animal that visited Nantucket Shoals. Several of the bins found in cool and moderately fresh bottom waters had more locations and individuals than expected. In total, 30% of all locations outside the Bay of Fundy were found in bottom waters of less than 6 °C and 33.75 psu (131, $p_U = 0.0005$) and more individuals were found in these bottom waters than expected (9, $p_U = 0.022$). This bottom water mass was also characterized by low surface salinities, high surface stratification, and depths between 75 and 175 m (Fig. 5*b*). In contrast, bottom waters above 6 °C and lower than 33.75 psu were characterized by high surface salinities, low surface stratification, and shallower depths (between 25 and 150 m). The deep basins had bottom waters above 6 °C and 33.75 psu and were characterized by greater depths and bimodal distributions of surface salinity and surface stratification. These bimodal distributions indicate the lower surface salinities and higher surface stratification over the deep basins of the Scotian Shelf (Emerald and La Have basins) and the high surface salinities and lower surface stratification over the deep basins of the Gulf of Maine (Wilkinson and Jordan basins and the Fundian Channel). Bottom waters below 6 °C and 33.75 psu occur in the western Gulf of Maine to the north and west of Wilkinson Basin, in the South Channel Ocean Productivity Experiment (SCOPEX) gyre, on the southwestern Scotian Shelf, and along the southern coast of Nova Scotia (Fig. 6).

© 2005 NRC Canada

Fig. 3. Distribution of Argos-acquired locations outside the Bay of Fundy (shaded circles) and the results of one-tailed Monte Carlo tests of resource selection for the corresponding spatial-frequency histogram. Boxes indicate two-dimensional bins in which Monte Carlo tests were conducted. A significant number of locations and (or) individuals ($p_U < 0.05$) were found in bins labeled with numbers. The label "1" indicates that only one individual occurred in the bin, but the number of locations was significantly higher than expected ($p_U < 0.05$). The observed number (n) of locations or individuals and the mean number (μ) of locations or individuals in the sampling distribution for all other labeled bins are shown in the inset table (*, $0.05 > p \geq 0.01$; **, $0.01 > p \geq 0.001$; ***, $p < 0.001$). The 91-m (50 fathom) and 200-m isobaths are shown.

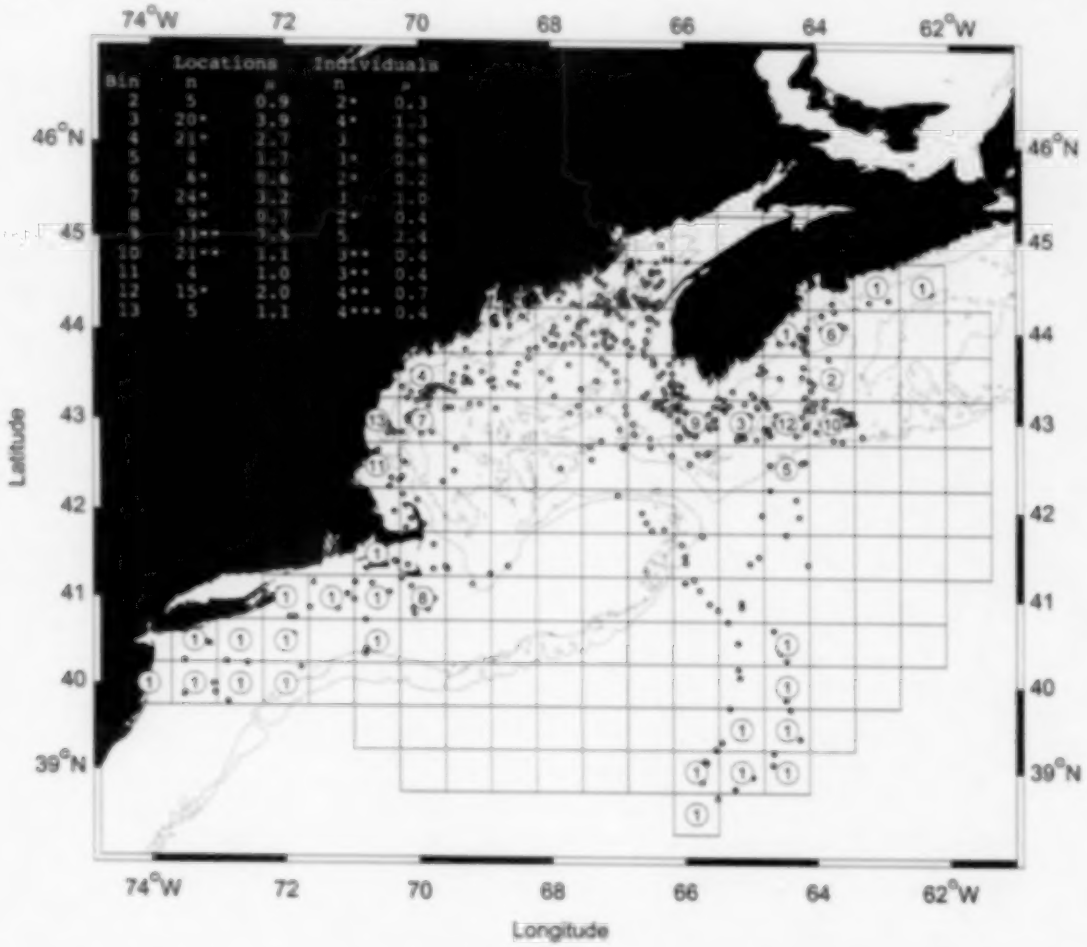

The areas that the tagged right whales visited more than expected (Fig. 3) correspond well to the spatial extent of these bottom waters.

Discussion

Upon exiting the lower Bay of Fundy, the tagged right whales moved extensively about the Gulf of Maine, Scotian Shelf, northern mid-Atlantic Bight, and the continental slope. Moving at an average speed of 79 km·day^{-1}, right whales could circumnavigate the entire Gulf of Maine (including a visit to Roseway Basin) and return to the Bay of Fundy in only 15 days. Individual movements were highly variable and no other area or oceanographic regime was used as much as the lower Bay of Fundy. Of the 14 tagged animals that left the Bay of Fundy, 50% returned to it before the tag stopped transmitting. Right whales have been observed during the summer and fall in some of the other areas frequently visited by the tagged animals, including the southwestern Scotian Shelf (Mitchell et al. 1986; Stone et al. 1988; CETAP 1982), the SCOPEX gyre (CETAP 1982), and the western Gulf of Maine (CETAP 1982; Payne et al. 1990; Weinrich et al. 2000).

The high site fidelity exhibited by tagged right whales in Grand Manan Basin in 2000 might suggest that food resources were abundant in that year compared with 1989–1991. In the summer and early fall of 1989, Woodley and Gaskin (1996) reported late-stage *C. finmarchicus* abundances of 1128 ± 637 copepods·m^{-3} (mean ± standard deviation) from 12 vertical tows near right whales in the basin. A single right whale was tagged in the same year and it left the Bay of Fundy soon after tagging and did not return during

© 2005 NRC Canada

Table 5. Results of two-tailed Monte Carlo tests of the observed mean, standard deviation, skewness, and kurtosis (θ) of each environmental variable.

	Mean		Standard deviation		Skewness		Kurtosis	
	θ	μ	θ	μ	θ	μ	θ	μ
Depth (m)	452.9	299.7	1099.1	632.6	3.27	5.73	9.32	44.14
Depth gradient ($m \cdot km^{-1}$)	8.18	7.37	13.94	9.72	8.86	6.55	108.23	64.14
Surface temperature (°C)	14.10	13.53	2.74	2.47	0.14	0.66	–0.57	0.36
Surface salinity (psu)	31.94**	32.18	0.54	0.41	0.29	0.41	1.20	6.54
Bottom temperature (°C)	6.93*	7.56	2.09	1.56	1.74	0.84	6.31	3.52
Bottom salinity (psu)	33.33	33.37	0.79	0.87	0.23	0.04	–0.29*	–0.87
Surface stratification ($kg \cdot m^{-3}$)	1.72*	1.36	0.92	0.78	–0.01	0.28	–1.29*	–0.78
Remotely sensed SST (°C)[a]	14.43	13.48	3.33	2.40	0.71	0.89	–0.10	1.51
Surface chlorophyll concn. ($mg \cdot m^{-3}$)[b]	2.60	2.67	2.16	2.55	3.28	2.80	14.22	10.29
Front probability	0.02	0.02	0.02	0.02	1.13	1.10	1.32	1.47
SST gradient ($°C \cdot km^{-1}$)[a]	0.14	0.14	0.06	0.06	1.10	1.68	0.51*	4.59
Chlorophyll gradient ($mg \cdot m^{-3} \cdot km^{-1}$)[b]	0.35	0.33	0.53	0.56	3.87	4.21	18.07	20.42

Note: Results were obtained using only observed and simulated track segments outside the Bay of Fundy for all years. μ is the mean statistic from the sampling distribution. SST, sea-surface temperature; psu, practical salinity units. *, $0.05 > p \geq 0.01$; **, $0.01 > p \geq 0.001$; ***, $p < 0.001$.

[a]1989–1991 data only.

[b]2000 data only.

the 21 days it was tracked. In 2000, Baumgartner et al. (2003*a*) observed late-stage *C. finmarchicus* abundances of only 457 ± 74 copepods·m^{-3} in Grand Manan Basin from three oblique bongo tows near right whales on long dives (a typical characteristic of feeding activity in this area). These low abundances were corroborated with numerous independent optical plankton counter (Herman 1988, 1992) measurements (Baumgartner et al. 2003*a*). The *C. finmarchicus* abundances in 2000 represented a minimum in 3 years of zooplankton monitoring near right whales in Grand Manan Basin from 1999 to 2001 (Baumgartner et al. 2003*a*). Although extreme caution is warranted when attempting to characterize zooplankton abundance for an entire season with only a few plankton samples, the available data tenuously suggest that right whales remain in Grand Manan Basin for reasons other than feeding. Social and sexual activity is common in the Bay (Kraus and Hatch 2001), therefore it is possible that right whales remain in the Bay for breeding opportunities even when food resources are low.

There was no evidence to support the hypothesis that right whales used the deep basins of the Gulf of Maine and the Scotian Shelf (H1). Moreover, there was suggestive but inconclusive evidence that they actually avoided these basins. Sameoto and Herman (1990) and Herman et al. (1991) reported very high abundances of late-stage *C. finmarchicus* below 200 m in the basins of the Scotian Shelf (up to 20 000 copepods·m^{-3}). Meise and O'Reilly (1996) demonstrated that the 10-year average total water column abundance of late-stage *C. finmarchicus* in the upper 200 m reaches a regional and annual maximum in the central Gulf of Maine in the summer and fall. Modeling results obtained by Lynch et al. (1998) suggest that high abundances of *C. finmarchicus* exist below 200 m in the Gulf of Maine basins. In light of these studies, it is somewhat surprising that right whales do not visit these basins more often. The basins have average depths of 210–250 m, which is 40%–67% greater than the average depth in the Bay of Fundy or in Roseway Basin (150 m). It is plausible that the deepest portions of the basins are inaccessible to right whales; however, we have observed right whales tagged with time–depth recorders diving to depths of 200 m in Grand Manan Basin (Baumgartner and Mate 2003). Furthermore, the satellite-monitored radio tag deployed in 1989 was equipped with a pressure sensor, and the maximum dive depth for the single whale on which it was used was between 272 and 306 m in Wilkinson Basin. Based on these observations, we think it is unlikely that right whales have diving limitations that would prevent them from exploiting *C. finmarchicus* concentrations below 200 m. Although right whales may be physiologically capable of reaching discrete layers of *C. finmarchicus* at these depths, they may still avoid foraging on these layers. Foraging at deeper depths affords less feeding time, and thus less energetic benefit per dive, than foraging at shallower depths (Baumgartner et al. 2003*a*).

Prey concentrations that are ecologically meaningful to right whales are difficult to measure at depth with plankton nets. The vertically integrated tows upon which the Meise and O'Reilly (1996) climatology is based can only provide an average water-column abundance of *C. finmarchicus*. This average abundance grossly underestimates the concentration of prey actually available to a right whale because the whales seek out and feed on prey that are distributed vertically in discrete layers (Baumgartner and Mate 2003). So despite the high total water-column abundances present in the Gulf of Maine basins, our results suggest that discrete, high concentrations of late-stage *C. finmarchicus* may not exist there. This is in contrast to the prediction of Lynch et al. (1998) that high concentrations of resting *C. finmarchicus* must exist below 200 m in these basins during the fall to explain the springtime distribution of younger stages of *C. finmarchicus*. We sampled Jordan and Wilkinson basins in the summer of 2001 with a vertically profiled optical plankton counter and did not observe any discrete, high concentration layers of *C. finmarchicus* below 200 m (M.F. Baumgartner, unpublished data). These layers were, however, readily observable at mid-depth near foraging right whales in Grand Manan Basin with the same instrument (Baumgartner and Mate 2003). The high concentrations ob-

© 2005 NRC Canada

Fig. 4. Results of one-tailed Monte Carlo tests of resource selection for univariate frequency histograms. The frequency histograms have been converted to probability density functions to facilitate visualization because the frequency-bin sizes vary. Hatching down to the left or down to the right indicates a significantly higher number of locations or individuals in the bin than expected ($p_U < 0.05$), respectively. The numerals denote the bins for which significant results were found. The observed number (n) of locations or individuals and the mean number (μ) of locations or individuals in the sampling distribution for all significant bins are shown in the inset table. Sea-surface temperatures (SST) and SST gradients are from 1989–1991 only and surface chlorophyll concentrations and chlorophyll gradients are from 2000 only.

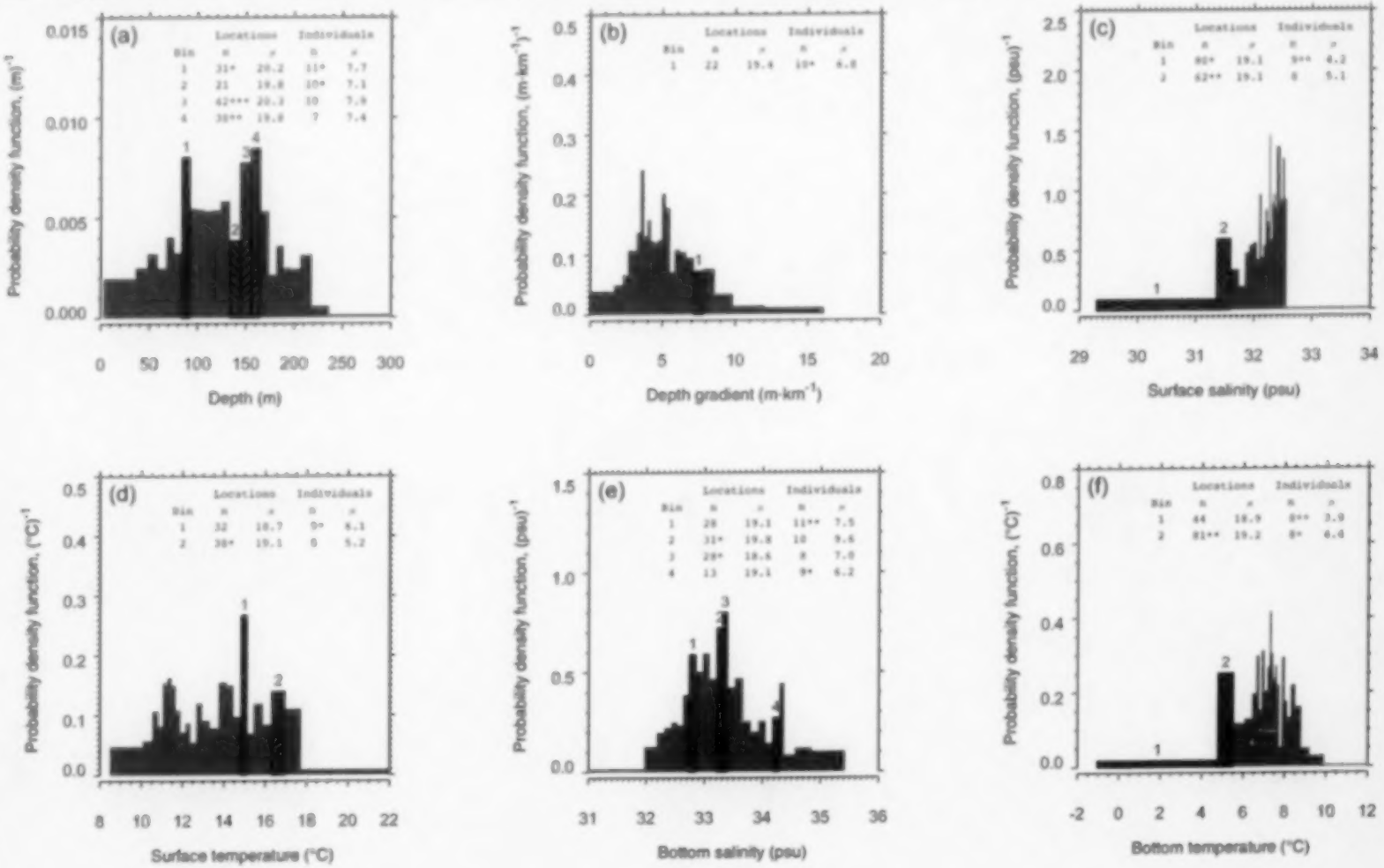

© 2005 NRC Canada

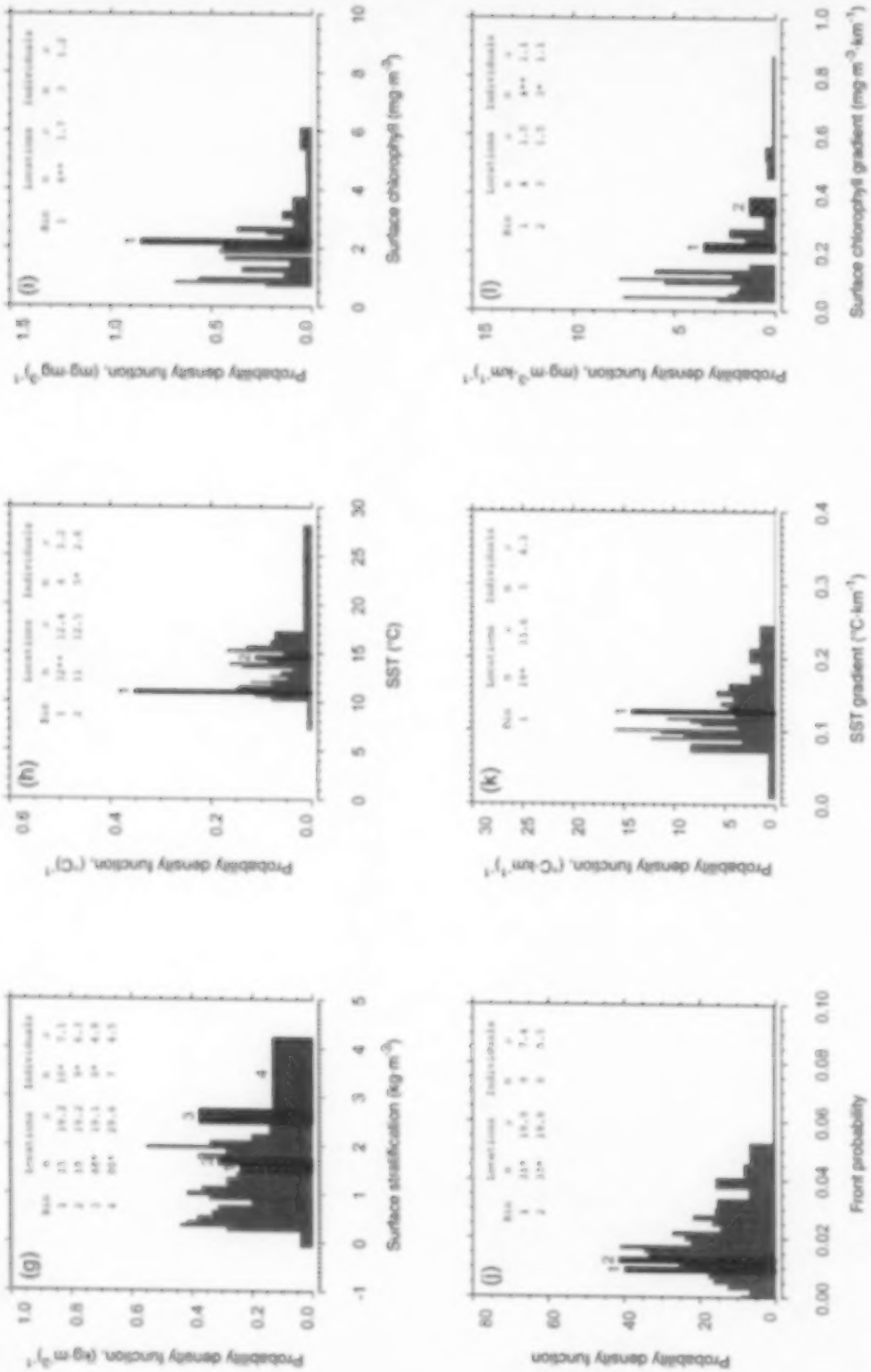

Fig. 4 (*Continued*).

© 2005 NRC Canada

Fig. 5. (*a*) Distribution of bottom salinity and temperature at Argos-acquired locations (shaded circles) and results of one-tailed Monte Carlo tests of resource selection for the corresponding bivariate frequency histogram. Boxes indicate two-dimensional bins in which Monte Carlo tests were conducted. Numerals denote bins in which a significant number of locations and (or) individuals ($p_U < 0.05$) were found. The label "1" indicates that only one individual occurred in the bin, but the number of locations was significantly higher than expected ($p_U < 0.05$). The observed number (n) of locations or individuals and the mean number (μ) of locations or individuals in the sampling distribution for all other labeled bins are shown in the inset table. (*b*) Distribution of bottom salinity and temperature at the same locations as in *a* with percent-frequency histograms of surface salinity (SSAL), surface stratification (STRAT), and depth (DEP) for locations in quadrants defined by bottom temperature (BT) < 6 °C and bottom salinity (BS) < 33.75 practical salinity units (psu) (lower left), BT ≥ 6 °C and BS < 33.75 psu (upper left), and BT ≥ 6 °C and BS ≥ 33.75 psu (upper right).

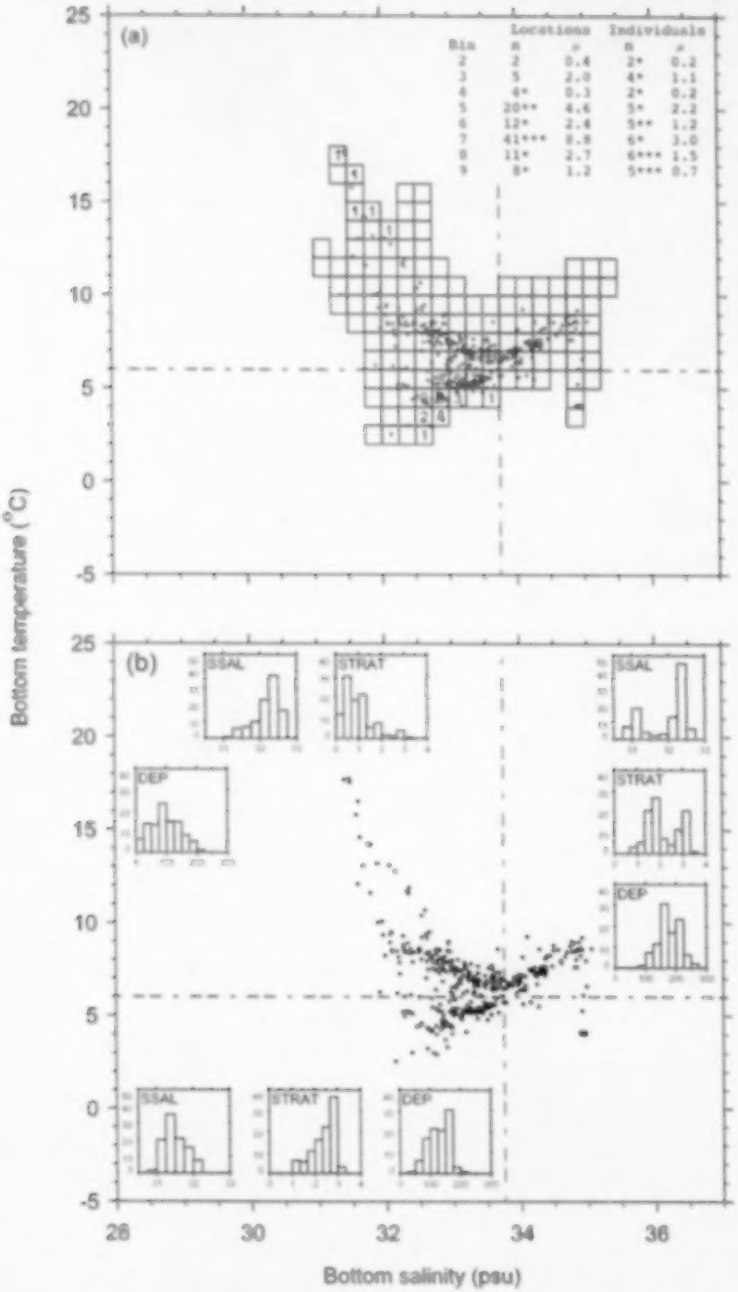

© 2005 NRC Canada

Fig. 6. Map of areas with bottom temperature less than 6 °C and bottom salinity less than 33.75 psu (cross-hatched). Shaded circles indicate Argos-acquired locations outside the Bay of Fundy. The 91-m (50 fathom) and 200-m isobaths are also shown.

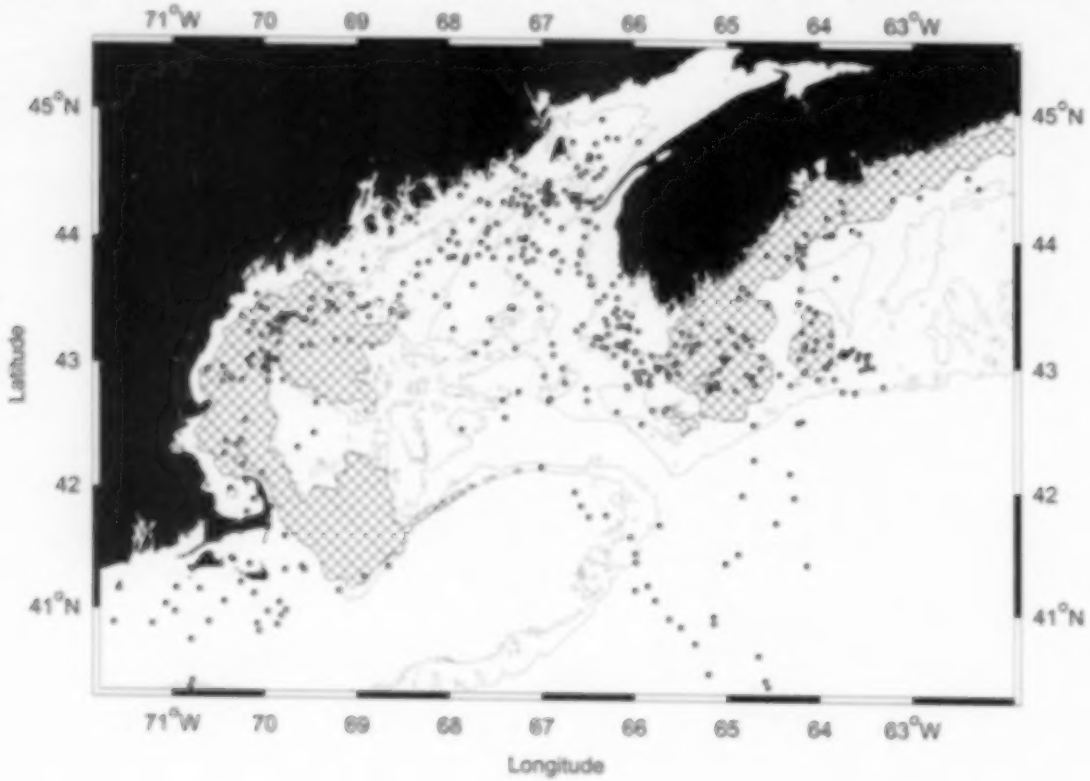

served by Sameoto and Herman (1990) and Herman et al. (1991) in the deep basins of the Scotian Shelf would certainly be attractive to right whales, but the paucity of Argos locations acquired there suggests that these concentrations may not be present every year.

There was no evidence to support the hypothesis that right whales associate with oceanic fronts or visit areas that are climatologically rich in fronts (H2). Despite the presence of a strong tidal mixing front along the western margin of Grand Manan Basin, Murison and Gaskin (1989) and Woodley and Gaskin (1996) found that right whales occupied the central basin, well away from this front. Brown and Winn (1989) observed that right whales were nearly always on the stratified side of a persistent tidal mixing front in the Great South Channel during the spring, but were a median 11.4 km away from it. Wishner et al. (1995) found dense concentrations of *C. finmarchicus* at the leading edge of a low-salinity plume during the 2 years of the SCOPEX study in the Great South Channel (Kenney and Wishner 1995), but Beardsley et al. (1996) found no evidence of a physical concentrating mechanism near a right whale feeding on very large aggregations of *C. finmarchicus* during that study. Baumgartner et al. (2003*a*) found no evidence of an association between right whale occurrence and oceanic fronts in the lower Bay of Fundy, but they did find evidence of such an association in Roseway Basin. While it is possible that fronts may aggregate prey in particular regions, our results suggest that oceanic fronts are not a common feature of right whale habitat.

There was no evidence to support the hypothesis that right whales frequent areas with high surface chlorophyll concentrations (H3). This is not particularly surprising when considered in the context of *C. finmarchicus* life history. When *C. finmarchicus* reach stage C5, they typically undertake an ontogenetic vertical migration to depth, where they enter a resting state (termed diapause) (Hirche 1996). *Calanus finmarchicus* C5 do not feed during diapause, relying on their considerable lipid reserves to support metabolism (although see Durbin et al. 1995). Female *C. finmarchicus* spawn the year's first generation (G1) of copepods in midwinter, which matures in early spring (Durbin et al. 1997, 2000). While some *C. finmarchicus* C5 enter diapause at this time, others remain at the surface to become the progenitors of the next generation of copepods (G2). The G2 generation reaches stage 4 or 5 by late spring or early summer. Some G2 animals may remain at the surface to spawn a third generation (G3), but the bulk of the *C. finmarchicus* population can be found at depth as C5 by summer. Baumgartner and Mate (2003) observed right whales foraging on deep layers of *C. finmarchicus* C5 in the lower Bay of Fundy and Roseway Basin during the summer. Moreover, diel vertical migration studies of *C. finmarchicus* in the lower Bay of Fundy carried out at that time indicate that the animals in

© 2005 NRC Canada

these layers have empty guts and do not migrate to the surface (Baumgartner et al. 2003*b*). Since phytoplankton abundance is irrelevant to nonfeeding *C. finmarchicus* C5 in diapause during the summer and early fall, right whale distribution is accordingly unrelated to surface chlorophyll concentration.

The tagged right whales' preference for waters with low bottom temperatures suggests that these conditions may improve feeding opportunities by promoting higher *C. finmarchicus* abundance or better quality food. Oceanic populations of *C. finmarchicus* typically migrate to several hundred metres depth (Miller et al. 1991), where the ambient temperature is typically only a few degrees Celsius. Continental-shelf populations, however, do not have access to such great depths and low temperatures. The lipid reserves upon which *C. finmarchicus* rely to survive starvation during diapause are depleted faster at higher temperatures because metabolic rates in resting stocks increase with temperature (Hirche 1983). The lower bottom temperatures found in the areas visited by the tagged right whales, therefore, may promote higher abundances by improving *C. finmarchicus* survivorship relative to the warmer bottom waters of the deep basins or the coastal environment. Meise and O'Reilly (1996) demonstrated that average water-column abundance of late-stage *C. finmarchicus* was negatively correlated with average water-column temperature in the summer and fall, suggesting that, indeed, lower temperatures improve survivorship of resting stocks. Sameoto and Herman (1990) reported a large decrease in Emerald Basin *Calanus* spp. over the winter and they raised the possibility (among others) that copepods could not survive diapause in the 8.5–10 °C waters at depth. For copepods that migrate to depth at the same time in the early summer, lipid reserves (and therefore energetic content) will be higher during the summer and fall in those animals that descend to colder waters. Therefore, right whales foraging in waters with lower bottom temperatures may also encounter higher quality food relative to what is available in waters with higher bottom temperatures.

The tagged whales visited areas with depths of roughly 150 m more frequently than expected. These areas can be characterized as shallow basins. The structure, hydrography, and physical processes of these basins may improve the availability, quality, and aggregation of *C. finmarchicus*, respectively, for foraging right whales. Shoal layers of prey allow longer feeding times for right whales relative to deeper layers and thus are more energetically favorable (Baumgartner et al. 2003*a*). In contrast to deeper basins, the shoal depths of shallow basins guarantee shoal layers of prey. While the bottom waters of deeper basins are warm because of slope water intrusions, lower temperatures prevail near the bottom of shallow basins. As discussed above, these conditions may improve survivorship and reduce oil depletion in resting *C. finmarchicus*, so prey abundance and quality may be enhanced in shallow basins. Strong tidal currents in the Gulf of Maine and Scotian Shelf act on the sea floor to generate turbulence and a well-mixed bottom layer. Baumgartner and Mate (2003) consistently found *C. finmarchicus* C5 in discrete layers just above this bottom mixed layer near feeding right whales in the lower Bay of Fundy and Roseway Basin. Unlike in very shallow regions, where the surface and bottom mixed layers interact and copepods may become uniformly distributed (e.g., Georges Bank, Nantucket Shoals), resting stocks of *C. finmarchicus* in shallow basins may be vertically aggregated between surface and bottom mixed layers. The tide also produces cyclonic circulation over shallow basins via tidal rectification, which, if sufficiently strong, may horizontally aggregate and retain *C. finmarchicus* as well. Tidal rectification generates a cyclonic gyre over Grand Manan Basin (Lynch et al. 1996) in which Woodley and Gaskin (1996) and Baumgartner et al. (2003*a*) suggest that late-stage *C. finmarchicus* are aggregated and made available to foraging right whales.

The spatial and temporal scales of the present study (hundreds of kilometres, tens of days) would be impossible to study using ship-based or aerial surveys. Even if these methods were viable, the rarity of right whale sightings over these spatial scales would make habitat analyses futile. Radio tracking provides direct observations of resource selection and is therefore a useful tool for studying right whale habitat at these larger spatial scales. Considering the large volume of tracking data for marine vertebrates collected to date, improving the statistical methods to analyze satellite-acquired locations and associated environmental data is a particularly fruitful avenue of research. With approaches such as those presented here, much can be learned about marine habitats with data already in hand.

Acknowledgments

We are grateful for assistance in the field by P. Duley, S. Kraus, B. Lagerquist, T. Martin, M.L. Mate, S. Nieukirk, J. Owen, D. Stahlke, F. Wenzel, and the New England Aquarium right whale group. We also received critical support from the chief scientists, Phil Clapham and Tim Cole, and the master, officers, and crew of the National Oceanic and Atmospheric Administration (NOAA) ship *Delaware II*. We thank R. Mesecar for tag design and development, T. Martin and T. Follett for technical support, and the New England Aquarium for identifying the tagged whales. P. Cornillon and R. Evans provided access to the University of Rhode Island's advanced very high resolution radiometer archive. We are particluarly grateful to J. Loder and D. Ullman for providing access to their respective hydrographic and front-probability climatologies. This study was supported by the Office of Naval Research, National Marine Fisheries Service, Oregon State University Marine Mammal Endowment, and the Space Grant and Earth System Science fellowship programs of the National Aeronautics and Space Administration.

References

Baith, K., Lindsay, R., Fu, G., and McClain, C.R. 2001. SeaDAS: data analysis system developed for ocean color satellite sensors. EOS Trans. Am. Geophys. Union, **82**: 202–205.

Baumgartner, M.F., and Mate, B.R. 2003. Summertime foraging ecology of North Atlantic right whales. Mar. Ecol. Prog. Ser. **264**: 123–135.

Baumgartner, M.F., Mullin, K.D., May, L.N., and Leming, T.D. 2001. Cetacean habitats in the northern Gulf of Mexico. Fish. Bull. **99**: 219–239.

© 2005 NRC Canada

Baumgartner, M.F., Cole, T.V.N., Clapham, P.J., and Mate, B.R. 2003*a*. North Atlantic right whale habitat in the lower Bay of Fundy and on the SW Scotian Shelf during 1999–2001. Mar. Ecol. Prog. Ser. **264**:137–154.

Baumgartner, M.F., Cole, T.V.N., Campbell, R.G., Teegarden, G.J., and Durbin, E.G. 2003*b*. Associations between North Atlantic right whales and their prey, *Calanus finmarchicus*, over diel and tidal time scales. Mar. Ecol. Prog. Ser. **264**:155–166.

Beardsley, R.C., Epstein, A.W., Chen, C., Wishner, K.F., Macaulay, M.C., and Kenney, R.D. 1996. Spatial variability in zooplankton abundance near feeding right whales in the Great South Channel. Deep-Sea Res. II, **43**: 1601–1625.

Brown, C.W., and Winn, H.E. 1989. Relationship between the distribution pattern of right whales, *Eubalaena glacialis*, and satellite-derived sea surface thermal structure in the Great South Channel. Cont. Shelf Res. **9**: 247–260.

Caswell, H., Fujiwara, M., and Brault, S. 1999. Declining survival probability threatens the North Atlantic right whale. Proc. Natl. Acad. Sci. U.S.A. **96**: 3308–3313.

Cetacean and Turtle Assessment Program. 1982. A characterization of marine mammals and turtles in the mid- and north Atlantic areas of the U.S. outer continental shelf. Final report, Bureau of Land Management, Washington, D.C., USA. (Rep. No. PB83215855, National Technical Information Service, Springfield, VA 22161, USA.)

Clapham, P.J., Young, S.B., and Brownell, R.L., Jr. 1999. Baleen whales: conservation issues and the status of the most endangered populations. Mamm. Rev. **29**: 35–60.

Cornillon P., Gilman, C., Stramma, L., Brown, O., Evans, R., and Brown, J. 1987. Processing and analysis of large volumes of satellite-derived thermal infrared data. J. Geophys. Res. **92**: 12 993 – 13 002.

Durbin, E.G., Campbell, R.G., Gilman, S.L., and Durbin, A.G. 1995. Diel feeding behavior and ingestion rate in the copepod *Calanus finmarchicus* in the southern Gulf of Maine during the late spring. Cont. Shelf Res. **15**: 539–570.

Durbin, E.G., Runge, J.A., Campbell, R.G., Garrahan, P.R., Casas, M.C., and Plourde, S. 1997. Late fall – early winter recruitment of *Calanus finmarchicus* on Georges Bank. Mar. Ecol. Prog. Ser. **151**: 103–114.

Durbin, E.G., Garrahan, P.R., and Casas, M.C. 2000. Abundance and distribution of *Calanus finmarchicus* on the Georges Bank during 1995 and 1996. ICES J. Mar. Sci. **57**: 1664–1685.

Epstein, A.W., and Beardsley, R.C. 2001. Flow-induced aggregation of plankton at a front: a 2-D Eulerian model study. Deep-Sea Res. II, **48**: 395–418.

Herman, A.W. 1988. Simultaneous measurement of zooplankton and light attenuance with a new optical plankton counter. Cont. Shelf Res. **8**: 205–221.

Herman, A.W. 1992. Design and calibration of a new optical plankton counter capable of sizing small zooplankton. Deep-Sea Res. **39**: 395–415.

Herman, A.W., Sameoto, D.D., Shunnian, C., Mitchell, M.R., Petrie, B., and Cochrane, N. 1991. Sources of zooplankton on the Nova Scotia Shelf and their aggregations within deep-shelf basins. Cont. Shelf Res. **11**: 211–238.

Hirche, H.-J. 1983. Overwintering *Calanus finmarchicus* and *Calanus helgolandicus*. Mar. Ecol. Prog. Ser. **11**: 281–290.

Hirche, H.-J. 1996. Diapause in the marine copepod, *Calanus finmarchicus* — a review. Ophelia, **44**: 129–143.

International Whaling Commission. 2001. Report of the workshop on status and trends of western North Atlantic right whales. J. Cetacean Res. Manag. Spec. Issue No. 2. pp. 61–87.

Kenney, R.D., and Winn, H.E. 1986. Cetacean high-use habitats of the northeast United States continental shelf. Fish. Bull. **84**: 345–357.

Kenney, R.D., and Wishner, K.F. 1995. The South Channel ocean productivity experiment. Cont. Shelf Res. **15**: 373–384.

Kenney, R.D., Hyman, M.A.M., Owen, R.E., Scott, G.P., and Winn, H.E. 1986. Estimation of prey densities required by western North Atlantic right whales. Mar. Mamm. Sci. **2**: 1–13.

Knowlton, A.R., and Kraus, S.D. 2001. Mortality and serious injury of northern right whales (*Eubalaena glacialis*) in the western North Atlantic Ocean. J. Cetacean Res. Manag. Spec. Issue No. 2. pp. 193–208.

Kraus, S.D. 1990. Rates and potential causes of mortality in North Atlantic right whales (*Eubalaena glacialis*). Mar. Mamm. Sci. **6**: 278–291.

Kraus, S.D., and Hatch, J.J. 2001. Mating strategies in the North Atlantic right whale (*Eubalaena glacialis*). J. Cetacean Res. Manag. Spec. Issue No. 2. pp. 237–244.

Kraus, S.D., Moore, K.E., Price, C.A., Crone, M.J., Watkins, W.A., Winn, H.E., and Prescott, J.H. 1986. The use of photographs to identify individual North Atlantic right whales (*Eubalaena glacialis*). Rep. Int. Whaling Comm. Spec. Issue No. 10. pp. 145–151.

Loder, J.W., Han, G., Hannah, C.G., Greenberg, D.A., and Smith, P.C. 1997. Hydrography and baroclinic circulation in the Scotian Shelf region: winter versus summer. Can. J. Fish. Aquat. Sci. **54**: 40–56.

Lynch, D.R., Ip, J.T.C., Naimie, C.E., and Werner, F.E. 1996. Comprehensive coastal circulation model with application to the Gulf of Maine. Cont. Shelf Res. **16**: 875–906.

Lynch, D.R., Gentleman, W.C., McGillicuddy, D.J., Jr., and Davis, C.S. 1998. Biological/physical simulations of *Calanus finmarchicus* population dynamics in the Gulf of Maine. Mar. Ecol. Prog. Ser. **169**: 189–210.

Manly, B.F.J. 1997. Randomization, bootstrap and Monte Carlo methods in biology. Chapman & Hall, London.

Mate, B.R., Nieukirk, S.L., and Kraus, S.D. 1997. Satellite-monitored movements of the northern right whale. J. Wildl. Manag. **61**: 1393–1405.

Mate, B.R., Gisiner, R., and Mobley, J. 1998. Local and migratory movements of Hawaiian humpback whales tracked by satellite telemetry. Can. J. Zool. **76**: 863–868.

Mate, B.R., Lagerquist, B.A., and Calambokidis, J. 1999. The movements of North Pacific blue whales off southern California and their southern fall migration. Mar. Mamm. Sci. **15**: 1246–1257.

Mayo, C.A., and Marx, M.K. 1990. Surface foraging behavior of the North Atlantic right whale, *Eubalaena glacialis*, and associated zooplankton characteristics. Can. J. Zool. **68**: 2214–2220.

Meise, C.J., and O'Reilly, J.E. 1996. Spatial and seasonal patterns in abundance and age-composition of *Calanus finmarchicus* in the Gulf of Maine and on Georges Bank: 1977–1987. Deep-Sea Res. II, **43**: 1473–1501

Miller, C.B., Cowles, T.J., Wiebe, P.H., Copley, N.C., and Grigg, H. 1991. Phenology in *Calanus finmarchicus*: hypotheses about control mechanisms. Mar. Ecol. Prog. Ser. **72**: 79–91.

Mitchell, E., Kozicki, V.M., and Reeves, R.R. 1986. Sightings of right whales, *Eubalaena glacialis*, on the Scotian Shelf, 1966–1972. Rep. Int. Whaling Comm. Spec. Issue No. 10. pp. 83–107.

Mountain, D.G., and Jessen, P.F. 1987. Bottom waters of the Gulf of Maine, 1978–1983. J. Mar. Res. **45**: 319–345.

Murison, L.D., and Gaskin, G.E. 1989. The distribution of right whales and zooplankton in the Bay of Fundy, Canada. Can. J. Zool. **67**: 1411–1420.

© 2005 NRC Canada

National Geophysical Data Center. 1988. Digital relief of the surface of the Earth. National Oceanic and Atmospheric Administration Data Announcement 88-MGG-02, Boulder, Color. Available from http://www.ngdc.noaa.gov/mgg/global/etopo5.html [accessed 3 April 2000; updated 27 December 2004].

Olson, D.B., and Backus, R.H. 1985. The concentrating of organisms at fronts: a cold-water fish and a warm-core Gulf Stream ring. J. Mar. Res. **43**: 113–137.

Payne, P.M., Wiley, D.N., Young, S.B., Pittman, S., Clapham, P.J., and Jossi, J.W. 1990. Recent fluctuations in the abundance of baleen whales in the southern Gulf of Maine in relation to changes in selected prey. Fish. Bull. **88**: 687–696.

Reilly, S.B. 1990. Seasonal changes in distribution and habitat differences among dolphins in the eastern tropical Pacific. Mar. Ecol. Prog. Ser. **66**: 1–11.

Russ, J.C. 1995. The image processing handbook. 2nd ed. CRC Press, Boca Raton, Fla.

Sameoto, D.D., and Herman, A.W. 1990. Life cycle and distribution of *Calanus finmarchicus* in deep basins on the Nova Scotia shelf and seasonal changes in *Calanus* spp. Mar. Ecol. Prog. Ser. **66**: 225–237.

Smith, W.H.F., and Sandwell, D.T. 1997. Global seafloor topography from satellite altimetry and ship depth soundings. Science (Wash., D.C.), **277**: 1957–1962.

Stone, G.S., Kraus, S.D., Prescott, J.H., and Hazard, K.W. 1988. Significant aggregations of the endangered right whale, *Eubalaena glacialis*, on the continental shelf of Nova Scotia. Can. Field-Nat. **102**: 471–474.

Ullman, D.S., and Cornillon, P.C. 1999. Satellite derived sea surface temperature fronts on the continental shelf off the northeast U.S. coast. J. Geophys. Res. **104**: 23 459 – 23 478.

Watkins, W.A., and Schevill, W.E. 1976. Right whale feeding and baleen rattle. J. Mammal. **57**: 58–66.

Weinrich, M.T., Kenney, R.D., and Hamilton, P.K. 2000. Right whales (*Eubalaena glacialis*) on Jeffreys Ledge: a habitat of unrecognized importance? Mar. Mamm. Sci. **16**: 326–337.

Wishner, K., Durbin, E., Durbin, A., Macaulay, M., Winn, H., and Kenney, R. 1988. Copepod patches and right whales in the Great South Channel off New England. Bull. Mar. Sci. **43**: 825–844.

Wishner, K.F., Schoenherr, J.R., Beardsley, R., and Chen, C. 1995. Abundance, distribution and population structure of the copepod *Calanus finmarchicus* in a springtime right whale feeding area in the southwestern Gulf of Maine. Cont. Shelf Res. **15**: 475–507.

Woodley, T.H., and Gaskin, D.E. 1996. Environmental characteristics of North Atlantic right and fin whale habitat in the lower Bay of Fundy, Canada. Can. J. Zool. **74**: 75–84.

© 2005 NRC Canada

Model averaging to estimate rebuilding targets for overfished stocks

Jon Brodziak and Christopher M. Legault

Abstract: Reducing overfishing and recovering overfished fish stocks is a challenging and important global problem. Rebuilding targets are essential ingredients for guiding overfished stocks to recovery. Having robust estimates of rebuilding targets is likely a necessary condition for effective long-term management of fishery resources. In this paper, we show how Bayesian model averaging can be applied to estimate rebuilding targets under alternative hypotheses about stock–recruitment dynamics. Using alternative hypotheses about stock–recruitment dynamics and environmental variation is important because using only a single hypothesis can lead to substantially different reference points and policy implications. The alternative hypotheses are augmented with prior information collected from meta-analyses of stock–recruitment data to construct a set of age-structured production models. We illustrate our approach using three overfished New England groundfish stocks. We fit alternative model likelihoods to observed data using Bayesian inference techniques. The Schwarz goodness-of-fit criterion was used to calculate model probabilities. Bayesian model averaging was used to estimate rebuilding targets that were robust to model selection uncertainty. Model-averaged estimates suggested that rebuilding targets for overfished stocks can be reasonably well determined if adequate prior information on stock productivity is available. Nonetheless, results had wide confidence intervals that reflected the underlying uncertainty in rebuilding targets.

Résumé : La réduction de la surpêche et la récupération des stocks de poissons surexploités sont des problèmes et des défis importants au niveau de la planète. Les objectifs de récupération sont essentiels pour guider le rétablissement des stocks surexploités. La détermination d'estimations robustes des objectifs de récupération est vraisemblablement une condition nécessaire pour une gestion efficace à long terme des ressources halieutiques. Nous démontrons, dans notre étude, que le calcul de moyennes de modèles bayésiens peut servir à estimer les objectifs de récupération sous diverses hypothèses de rechange au sujet de la dynamique du recrutement du stock. Il est important d'utiliser diverses hypothèses de rechange concernant la dynamique du recrutement du stock et la variation environnementale parce que l'utilisation d'une seule hypothèse peut mener à l'établissement de points de référence et de politiques de gestion très différents. Les diverses hypothèses de rechange sont modifiées sur la base d'informations a priori obtenues de méta-analyses des données de stock–recrutement pour obtenir une série de modèles de production structurés en fonction de l'âge. Nous illustrons notre méthodologie en l'appliquant à trois stock surexploités de poissons de fond de la Nouvelle-Angleterre. Nous ajustons les vraisemblances diverses des modèles au données observées à l'aide de techniques d'inférence bayésienne. Le critère d'ajustement de Schwarz sert à calculer les probabilités des modèles. La détermination des moyennes des modèles par techniques bayésiennes permet d'établir des objectifs de récupération qui sont robustes malgré l'incertitude associée à la sélection des modèles. Les estimations basées sur les moyennes des modèles laissent croire qu'il est possible d'établir assez bien des objectifs de récupération pour les stocks surexploités s'il existe une information préalable adéquate sur la productivité des stocks. Néanmoins, les résultats ont de grands intervalles de confiance, ce qui reflète l'incertitude sous-jacente aux objectifs de récupération.

[Traduit par la Rédaction]

Introduction

Worldwide, many fishery resources have been or are now being overfished (Garcia and Newton 1997; Pauly et al. 2002). Reducing overfishing and recovering overfished fish stocks is a challenging and important global problem (Hutchings et al. 1997; Rosenberg 2003). Biological rebuilding targets are an essential ingredient for guiding overfished stocks to recovery, since they provide the biological basis for managing fisheries to eliminate overfishing. Having robust estimates of rebuilding targets is likely a necessary condition for effective long-term management of fishery resources.

Estimating biological rebuilding targets can be a challenging task, however, because multiple factors can affect fish population dynamics. Why did a particular fish stock collapse? Was it due to recruitment overfishing or changing environmental conditions or some combination of both? These are fundamental questions that need to be addressed in any approach to estimate rebuilding targets. In the ideal scenario where the underlying population dynamics conform to a single known model, standard likelihood-based approaches can be used to draw inferences about rebuilding targets. More

Received 10 February 2004. Accepted 9 October 2004. Published on the NRC Research Press Web site at http://cjfas.nrc.ca on 13 April 2005.
J17968

J. Brodziak[1] and C.M. Legault. National Marine Fisheries Service, Northeast Fisheries Science Center, 166 Water Street, Woods Hole, MA 02543, USA.

[1]Corresponding author (e-mail: jon.brodziak@noaa.gov).

 doi: 10.1139/F04-199 © 2005 NRC Canada

often, however, uncertainty exists about the best approximating model. For example, the stock–recruitment relationship is highly variable for many stocks and uncertain given short time series of data. Similarly, changes in environmental conditions that coincide with decreases in recruitment may suggest serial correlation in stock–recruitment dynamics. Another uncertainty arises when time series of stock–recruitment observations are limited to a period when recruitment overfishing was occurring. As a result, the range of stock–recruitment data is truncated to reflect only low spawning stock sizes. This can lead to the perception that an overfished stock is less productive than it was in the past, the so-called shifting baseline syndrome (Pauly 1995). In this case, there may be insufficient contrast in spawning stock size to statistically estimate a stock–recruitment relationship without using auxiliary information to determine model parameters. One direct approach to addressing model uncertainty is to develop multiple working hypotheses (e.g., see Hilborn and Mangel 1997) and then apply model selection or model averaging for statistical inference (Hoeting et al. 1999; Burnham and Anderson 2002).

In this paper, we show how Bayesian model averaging can be applied to estimate rebuilding targets for overfished stocks under alternative hypotheses about stock–recruitment dynamics. Using alternative hypotheses about the stock–recruitment relationship and environmental variation is important because using a single hypothesis about stock–recruitment dynamics can lead to substantially different reference points and policy implications (see Myers et al. 1994). The alternative hypotheses are augmented with prior information collected from meta-analyses of stock–recruitment data to construct a set of age-structured production models (Shepherd 1982; Sissenwine and Shepherd 1987). We fit the alternative models to observed data using Bayesian inference techniques (e.g., see Ellison 2004). Markov Chain Monte Carlo (MCMC) simulation was used to calculate the posterior distribution of rebuilding targets. The Schwarz goodness-of-fit criterion was used to rank the alternative models and assign them probabilities for model averaging (Kass and Raftery 1995). When only one model is highly probable, model averaging will produce results that are similar to selecting a single model based on goodness-of-fit. In contrast, when several competing models have similar probabilities, selecting a single model may produce misleading inferences and underestimate uncertainty. To alleviate this possibility, Bayesian model averaging was applied (Hoeting et al. 1999) to estimate rebuilding targets that were robust to model selection uncertainty.

We illustrate our approach using three overfished groundfish stocks from Georges Bank: Atlantic cod (*Gadus morhua*), haddock (*Melanogrammus aeglefinus*), and yellowtail flounder (*Pleuronectes ferrugineus*). We begin by describing the construction of alternative age-structured production models to estimate rebuilding targets of S_{MSY} and F_{MSY}, the spawning biomass and fishing mortality rate associated with maximum sustainable yield (MSY), respectively. These rebuilding targets are a necessary component of harvest control rules for US marine fisheries. They also provide useful biological limits under a precautionary approach to fisheries management (Mace 2001). We then describe our statistical approach to estimate model parameters using Bayesian model averaging of objectively selected models. Model-averaged rebuilding target estimates are compared with existing values (Northeast Fisheries Science Center (NEFSC) 2002*a*). The model-averaged results suggest that rebuilding targets for these overfished stocks can be reasonably well determined despite model uncertainty if sufficient prior information on stock productivity is available. The sensitivity of estimated rebuilding targets to the selection of informative priors is also investigated and discussed.

Materials and methods

Stock–recruitment models

The stock–recruitment relationship is of fundamental importance for determining many biological rebuilding targets (Sissenwine and Shepherd 1987; Quinn and Deriso 1999; Williams and Shertzer 2003). In this study, Beverton–Holt (BH) and Ricker (RK) stock–recruitment models were chosen for constructing alternative MSY-based rebuilding target models. This choice provided two competing hypotheses about stock–recruitment dynamics: compensatory under the BH model and overcompensatory under the RK model. The flat-topped BH model is commonly used when fish survival at one or more early life history stages is density dependent. In contrast, the dome-shaped RK model is commonly used when spawner abundance has a negative impact on an early life history stage survival through cannibalism or other interactions. These models can produce substantially different biological reference points when applied to the same data set (Myers et al. 1994). We did not include depensatory stock–recruitment models because there was no clear evidence of depensation for the three overfished stocks under consideration. In recent years, spawning biomasses of both the Georges Bank haddock and yellowtail flounder stocks have increased at low fishing mortality rates, while cod biomass has remained stable owing to continued overfishing (NEFSC 2002*b*). As a result, both BH and RK models were used to describe expected equilibrium stock–recruitment conditions for the three Georges Bank stocks.

A modified BH curve was used for estimation:

$$(1)\qquad R = \frac{4z_{MAX}R_{MAX}S}{S_{MAX}(1 - z_{MAX}) + S(5z_{MAX} - 1)}$$

where S_{MAX} is the maximum observed spawning biomass or a proxy estimate, R_{MAX} is the recruitment expected at S_{MAX}, and z_{MAX} is the steepness of the modified BH curve computed as the ratio of R at 20% of S_{MAX} to R_{MAX}. In this context, S_{MAX} is simply a fixed spawning biomass at which to compute R_{MAX}. This reparameterization allowed us to choose a reasonable maximum observed spawning biomass for curve fitting in contrast with the asymptotic form of the BH curve $R = \alpha S/(\beta + S)$, where $R \to \alpha$ as $S \to \infty$. Parameters of the asymptotic curve are related to those of the modified curve by

$$(2)\qquad \alpha = \frac{4z_{MAX}R_{MAX}}{5z_{MAX} - 1} \quad \text{and} \quad \beta = \frac{S_{MAX}(1 - z_{MAX})}{5z_{MAX} - 1}$$

Given α and β, equilibrium spawning biomass as a function of fishing mortality (F) for the BH curve (S_{BH}) was

$$(3)\qquad S_{BH} = \alpha \mathrm{SPR}(F) - \beta$$

© 2005 NRC Canada

Values of S_{MAX}, the reference spawning biomass for the parameter R_{MAX}, were computed from available assessment data for each stock. Assessment estimates of spawning biomass and recruitment are available for Georges Bank cod since 1978 and for Georges Bank yellowtail flounder since 1973. Since both stocks were relatively abundant during the 1960s, as evidenced by time series of mean biomass per tow from the NEFSC spring and autumn surveys and fishery yields (NEFSC 2002*a*), we computed values of S_{MAX} using assessment estimates and earlier survey data. In particular, values of S_{MAX} were computed as the product of average spawning biomass from stock assessments times the ratio of average NEFSC autumn survey biomass indices during 1963–1970 to the same average during 1990–1999 (NEFSC 2002*a*). For Georges Bank cod, S_{MAX} = 104 200 mt, while for yellowtail flounder, S_{MAX} = 36 200 mt. Since Georges Bank haddock had a long time series of assessment estimates, we set S_{MAX} to be the maximum spawning biomass value in the stock–recruitment time series and S_{MAX} = 199 500 mt for haddock.

The form of the RK model used for parameter estimation was

$$R = aSe^{-bS} \tag{4}$$

where a is the slope at the origin and b is the strength of density dependence in the relationship. Given a and b, equilibrium spawning biomass as a function of F for the RK curve (S_{RK}) was

$$S_{RK} = \frac{1}{b}[\log(a\,\mathrm{SPR}(F))] \tag{5}$$

The rebuilding target for the three overfished stocks was defined to be the biomass that produces MSY (S_{MSY}), as mandated by the US Sustainable Fisheries Act of 1996. MSY is typically interpreted to be the long-term average yield that can be taken from a stock under existing environmental conditions. In this context, uncorrelated errors may be an appropriate for estimating rebuilding targets if environmental factors affect annual stock productivity in a random fashion. Alternatively, serially correlated errors may be appropriate if stock productivity is affected by low-frequency environmental forcing. We investigate both possible error structures below.

In this application, we chose to only model uncertainty in the stock–recruitment relationship. Other potential sources of uncertainty, such as variation in life history parameters, that might affect equilibrium spawning biomass per recruit or yield per recruit calculations (Appendix A) were not included, since recruitment largely determines the magnitude of S_{MSY} under the Sissenwine–Shepherd model (Sissenwine and Shepherd 1987). To see this, observe that S_{MSY} is the product of the spawning biomass per recruit at F_{MSY} ($\mathrm{SPR}(F_{MSY})$) and recruitment that produces MSY (R_{MSY}):

$$S_{MSY} = \mathrm{SPR}(F_{MSY})R_{MSY} \tag{6}$$

Next, observe that the variance of any equilibrium spawning biomass (S) can be approximated to first order (see Appendix A) as a function of spawning biomass per recruit (SPR) and recruitment (R) by

$$\mathrm{VAR}[S] \approx \left[\frac{\partial S}{\partial R}\right]^2 \sigma_R^2 + \left[\frac{\partial S}{\partial \mathrm{SPR}}\right]^2 \sigma_{\mathrm{SPR}}^2 = (\mathrm{CV}[R]^2 + \mathrm{CV}[\mathrm{SPR}]^2)(R \cdot \mathrm{SPR})^2 \tag{7}$$

where CV[R] and CV[SPR] are the coefficients of variation for recruitment and spawning biomass per recruit, respectively. If the coefficient of variation of the recruitment process is much larger than the coefficient of variation for spawning biomass per recruit, then the uncertainty due to recruitment dominates the variance in equilibrium spawning biomass and in particular S_{MSY}. This is a likely scenario for many marine fish stocks that have highly variable recruitment but relatively stable life history parameters and fishery selectivity parameters. Thus, modeling uncertainty in recruitment strength is a parsimonious choice for estimating rebuilding targets.

Error structures

Error structures are a fundamental component of our approach because they represent how one expects stock–recruitment data to vary about the expected relationship (see Likelihoods below). Observation errors for alternative stock–recruitment models were assumed to be multiplicative lognormal distributions. Multiplicative lognormal errors were used because this positively skewed distribution arises naturally when groundfish survival rates during early life history are affected by numerous independent random events represented as multiplicative log-scale effects. As the number of random events becomes large, the distribution of the mean of the log-scale multiplicative process approaches a normal random variable under the central limit theorem.

Observation errors for the stock–recruitment models were either a multiplicative lognormal or an autoregressive, multiplicative lognormal error structure with a lag of 1 year. The uncorrelated error term represented the common assumption that environmental forcing was independent through time. In contrast, the autoregressive error term represented serial correlation in random environmental forcing. The error terms were multiplied by the expected stock–recruitment curve, denoted as $f(S_i)$ for the ith data point, to obtain the observation error model

$$R_i = f(S_i)e^{\varepsilon_i} \tag{8}$$

For uncorrelated errors, the random shocks ε_i were independent and identically distributed Gaussian random variables with mean equal to $-\sigma^2/2$ and variance equal to σ^2. In this case, the mean was chosen to set the expected value of the multiplicative error term to unity and the error variance (σ^2) was a parameter to be estimated. For autoregressive lag 1 errors, the random shocks ε_i were distributed as

$$\varepsilon_i = \phi\varepsilon_{i-1} + w_i \tag{9}$$

where $|\phi| < 1$ and

$$w_i \sim N\left(-\frac{\sigma_w^2}{2}, \sigma_w^2\right)$$

© 2005 NRC Canada

In this case, the expected value of the multiplicative error term was unity and the autoregressive coefficient (ϕ) and error variance were additional parameters to be estimated.

Likelihoods

Likelihoods of the observed stock–recruitment data were constructed for the BH and RK models using the two competing hypotheses for error structures. The sample likelihood was conditioned on the assumed prior distributions (see Prior information below) and stock–recruitment model. Based on a total of n stock–recruitment data points (R_i, S_i), the log-likelihood ($\log L_{SR}$), using uncorrelated errors, was (Brodziak et al. 2001)

$$(10)\quad \log L(\underline{\theta}, \sigma^2) = -\frac{n}{2}\log(2\pi) - n\log\sigma - \sum_{i=1}^{n}\log R_i - \frac{1}{2\sigma^2}\sum_{i=1}^{n}\left(\log R_i - \log f(S_i) + \frac{\sigma^2}{2}\right)^2$$

Similarly, the log-likelihood for serially correlated errors (for a derivation, see Seber and Wild (1989) with $\sigma_w^2 = (1-\phi^2)\sigma^2$ was

$$(11)\quad \log L_{SR}(\underline{\theta}, \sigma^2, \phi) = -\frac{n}{2}\log(2\pi) - n\log\sigma_w - \sum_{i=1}^{n}\log R_i + \frac{1}{2}\log(1-\phi^2)$$
$$- \frac{1}{2\sigma_w^2}\sum_{i=2}^{n}\left(\log R_i - \phi\log R_{i-1} - \log f(S_i) + \phi\log f(S_{i-1}) + (1-\varphi)\frac{\sigma_w^2}{2}\right)^2 - \frac{(1-\phi^2)}{2\sigma_w^2}\left(\log R_1 - \log f(S_1) + \frac{\sigma_w^2}{2}\right)^2$$

Prior information

Using prior information is a key component of our approach to estimating rebuilding targets. In this context, prior information represents the accumulated scientific knowledge of the likely stock–recruitment dynamics of the three stocks. We chose to estimate rebuilding targets assuming either the absence or presence of such knowledge. To represent an absence of knowledge about the likely stock–recruitment dynamics, uninformative priors for stock–recruitment model parameters were chosen before inspecting the data. For each stock, we used very broad uniform prior distributions (π) for the square root of the error variance σ, autoregressive parameter ϕ, BH parameters $\log(R_0)$ and z (defined below), and RK parameters $\log(a)$ and b:

$$(12)\quad \pi_\sigma \sim U[0.0001, 4], \quad \pi_\phi \sim U[-1, 1]$$
$$\pi_{\log(R_0)} \sim U[-10, 100], \quad \pi_z \sim U[0.20001, 1]$$
$$\pi_{\log(a)} \sim U[-10, 10], \quad \pi_b \sim U[-1000000, 0]$$

Inferences about rebuilding targets using the uninformative priors were, in effect, based solely on the likelihood function.

In contrast, informative priors represented accumulated scientific knowledge of the likely stock–recruitment dynamics of the three stocks. Based on previous analyses (Brodziak et al. 2001; Brodziak 2002), it was recognized that there may be insufficient contrast in the stock–recruitment data to estimate either the steepness and unfished recruitment parameters of the BH curve or the slope at the origin of the RK curve. To resolve the issue of estimability, we borrowed from the strength of meta-analyses of numerous fish populations (Hilborn and Liermann 1998; Myers and Mertz 1998) to determine these parameters in an empirical Bayesian estimation framework (Gelman et al. 1995; Carlin and Louis 2000). In particular, we developed informative priors for steepness, slope at the origin, and unfished recruitment for each stock.

To include auxiliary information on the likely values of the steepness parameter for each of the three stocks, results from the Myers et al. (1999) meta-analysis of a large number of stock–recruitment data sets were used to determine appropriate prior distributions for the steepness parameter (z). These priors provided auxiliary information on the likely rate of increase in expected recruitment as spawning stock increases from low levels. Steepness was calculated relative to the unfished spawning stock size (S_0) and was related to unfished equilibrium recruitment (R_0) and the parameters of the asymptotic BH curve by

$$(13)\quad z = \frac{\frac{\alpha S_0 0.2}{(\beta + S_0 0.2)}}{R_0}$$

In general, values of S_0 and R_0 differed from S_{MAX} and R_{MAX}, since unfished stock size was not necessarily equal to the value of S_{MAX} as estimated from assessment data.

For each species, the prior on steepness for the BH curve was based on value of z reported for that species in Myers et al. (1999, table 1). The informative prior was assumed to be distributed as a Gaussian random variable with the constraint that $z \in [0.2,1]$ so that the logarithm of the prior on steepness (π_z) was

$$(14)\quad -\log\pi_z = 0.5\log(2\pi) + \log(\sigma_z) + \frac{(z-\mu_z)^2}{2\sigma_z^2}$$

The mean of the informative prior (μ_z) was taken to be the median point estimate for the species. The standard error of the informative prior (σ_z) was computed from the upper and lower values of the 60% confidence interval for steepness from Myers et al. (1999) and the assumption that the steepness was normally distributed. This produced informative priors for the steepness of Atlantic cod, haddock, and yellowtail flounder (Table 1; Fig. 1*a*).

We used the informative prior distributions for steepness to parameterize prior distributions for the mean slope at the origin parameter (a) of the RK model. This choice ensured that comparable assumptions were made for slope at the ori-

© 2005 NRC Canada

Table 1. Values of the mean and standard error of informative prior distributions for steepness, slope at the origin, and unfished recruitment.

	Steepness		Slope		Unfished recruitment (×1 000 000)		
Species	Mean	SE	Mean	SE	Mean	SE	Recruitment data
Atlantic cod	0.84	0.08	0.78	0.07	23.2	4.4	Top quartile of spawning biomass, 1978–2001
Haddock	0.74	0.11	1.25	0.19	75.2	5.6	1931–1960
Yellowtail flounder	0.75	0.07	4.39	0.41	101.2	3.4	Top quartile of spawning biomass, 1963–1998

Fig. 1. Uninformative (solid line) and informative priors for (*a*) stock–recruitment steepness and (*b*) the natural logarithm of unfished recruitment of Georges Bank Atlantic cod (dotted line), haddock (dashed line), and yellowtail flounder (dotted–dashed line).

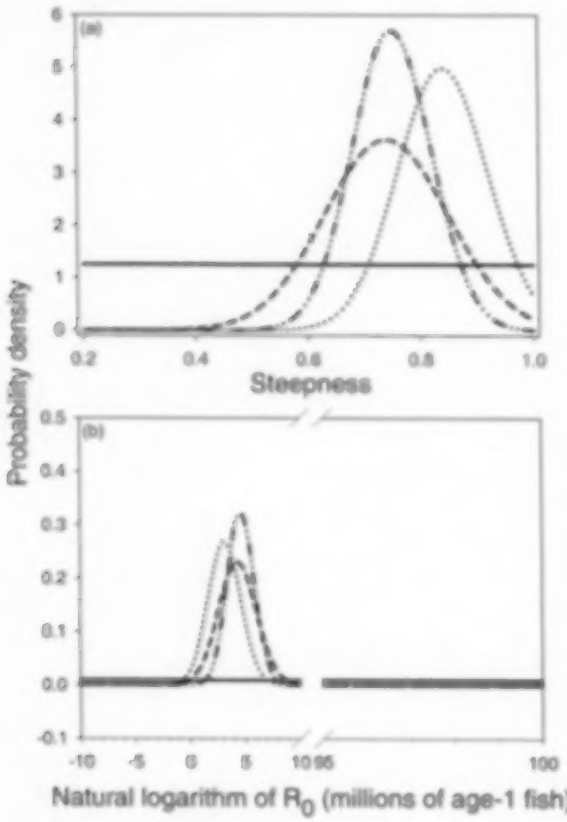

gin and steepness prior distributions under the alternative stock–recruitment hypotheses. The informative prior (π_z) for the slope at the origin parameter (a) of the RK curve was also assumed to be distributed as a normal random variable. For each stock, the mean of the informative prior on the slope at the origin was calculated from the mean of the informative prior for steepness. The relationship between steepness and slope was (see Myers et al. 1999)

$$(15) \quad a = \frac{4z}{(1-z)\,\mathrm{SPR}(0)}$$

The standard error of the informative prior (σ_a) was set by assuming that the informative priors for z and a had equal coefficients of variation. This determined the parameters of the informative priors for the slope at the origin of Atlantic cod, haddock, and yellowtail flounder (Table 1).

It was also recognized that there was limited information on unfished recruitment because the stock–recruitment time series were short in comparison with the historic periods of exploitation. For example, Georges Bank cod has been fished since the 1600s but the available stock–recruitment time series begins in 1978. Further, all three stocks were overfished throughout much of the stock–recruitment time series with many observations at relatively low spawning stock sizes. To alleviate potential bias due to the lack of observations at high spawning stock sizes, we used an empirical Bayesian approach (Carlin and Louis 2000) to set an informative prior based on the distribution of unfished recruitment. The informative prior for unfished recruitment (π_{R_0}) was also assumed to be normally distributed with the constraint that $R_0 > 0$. The mean (μ_R) and standard error (σ_R) of the informative prior for R_0 were determined using functional statistics of the empirical distribution of recruitment at high spawning stock size. In this case, we used what a panel of experts had previously judged to be an appropriate subset of observed stock–recruitment data (NEFSC 2002*a*). For Georges Bank haddock, recruitment values during 1931–1960 were used to determine the prior parameters (Table 1; Fig. 1*b*). This corresponded to the period of high fishery yields prior to the stock collapse in the early 1970s. For Georges Bank cod, recruitment data for spawning stock sizes in the top quartile of the spawning biomass distribution were used to determine the prior parameters. For Georges Bank yellowtail flounder, recruitment data for spawning biomass sizes in the top quartile of the hindcast spawning biomass distribution from Brodziak et al. (2001) were used to determine the prior parameters.

Informative priors were not developed for the density-dependence parameter b of the RK curve because there was no auxiliary information on the spawning stock size at which overcompensation would be expected to occur.

Alternative models

We constructed a set of 12 alternative probability models for estimating rebuilding targets using the stock–recruitment models, error structures, and assumptions about prior information. Each alternative represented a discrete hypothesis about stock dynamics and parameter estimability. The alternatives were formed as a Cartesian product of stock–recruitment curve, error structure, and assumptions about informative priors. For the BH curve, this led to eight alternative rebuilding target models (Table 2). For the RK curve, this led to four alternatives (Table 2). Under each of the alternative models, MSY-based rebuilding targets were calculated using the Sissenwine–Shepherd approach (Appendix A).

© 2005 NRC Canada

Table 2. Abbreviations of alternative rebuilding target models (model components indicated with a cross).

	Model abbreviation											
Model component	BH	ABH	RBH	RABH	ZBH	ZABH	RZBH	RZABH	RK	ARK	SRK	SARK
Stock–recruitment curve												
Beverton–Holt	×	×	×	×	×	×	×	×				
Ricker									×	×	×	×
Error structure												
Uncorrelated	×		×		×		×		×		×	
Correlated		×		×		×		×		×		×
Informative prior												
Unfished recruitment			×	×			×	×				
Steepness					×	×	×	×				
Slope at origin											×	×

Fig. 2. Schematic depiction of construction of (*a*) spawner per recuit, (*b*) recruit per spawner, (*c*) equilibrium spawning biomass, (*d*) yield per recruit, and (*e*) equilibrium yield curves using Georges Bank Atlantic cod as an example. Metric tons, t.

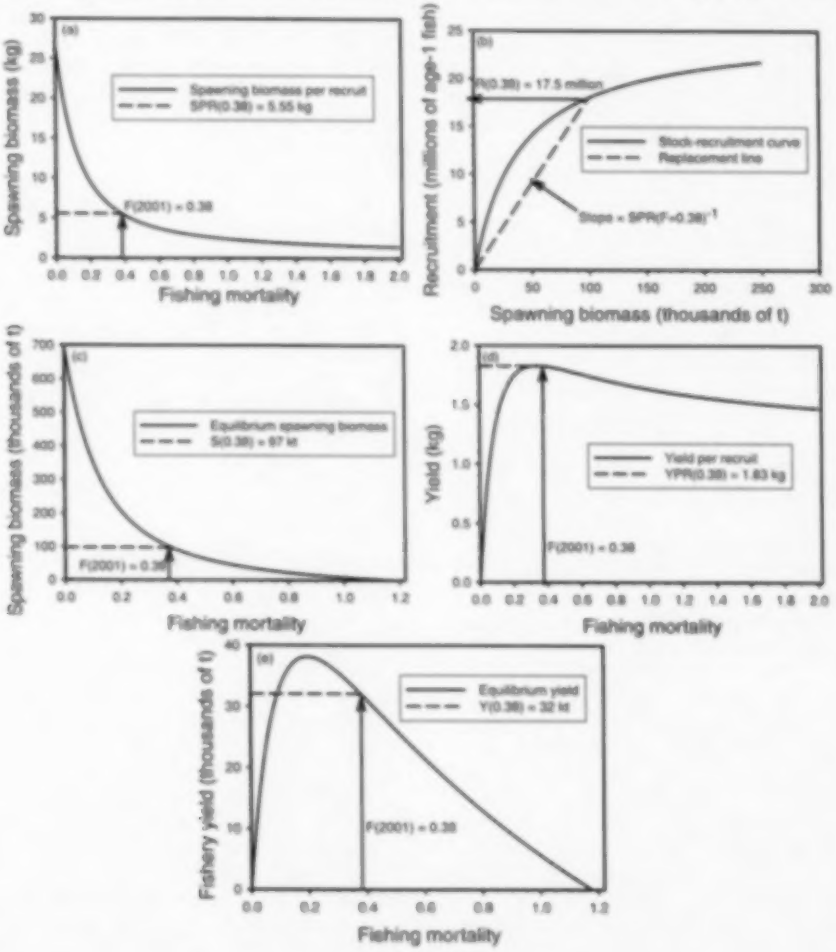

To illustrate the Sissenwine–Shepherd approach to computing rebuilding targets, consider the spawning biomass per recruit curve for Georges Bank cod (Fig. 2*a*) constructed using life history and fishery parameters in NEFSC (2002*b*). The point estimate of fishing mortality on this Atlantic cod stock in 2001 was $F_{2001} = 0.38$. At this value of F, the SPR(0.38) is about 5.55 kg·recruit^{-1}. The inverse of this SPR value is the slope of the stock replacement line at equilibrium (Fig. 2*b*). The intersection of the replacement line and the stock–recruitment curve is the equilibrium recruitment, $R(0.38)$,

© 2005 NRC Canada

which is roughly 17.5 million age-1 recruits at $F_{38\%}$. Equilibrium recruitment × spawning biomass per recruit equals equilibrium spawning biomass $S(0.38) = R(0.38)\mathrm{SPR}(0.38) =$ 17.5 million recruits × 5.55 kg·recruit^{-1} ≈ 97 000 metric tons (t) (Fig. 2*c*). Yield per recruit at an $F = 0.38$ is roughly 1.83 kg·recruit^{-1} (Fig. 2*d*). Multiplying equilibrium recruitment and yield per recruit (YPR) equals equilibrium yield, $Y(F)$. In this case, $Y(0.38) = R(0.38)\mathrm{YPR}(0.38) = 17.5$ million recruits × 1.83 kg·recruit^{-1} ≈ 32 000 t (Fig. 2*e*). Repeating this calculation over a range of feasible values, one can numerically determine the F that maximizes equilibrium yield; this is F_{MSY}.

Parameter estimation

Given the model likelihoods, priors, and observed stock–recruitment data, posterior distributions of rebuilding targets for statistical inference were calculated using standard numerical methods. We used a likelihood-based Bayesian simulation approach to compute model-averaged estimates of rebuilding targets. The AD Model Builder software package (Schnute et al. 1998; Otter Research Ltd. 2001) was used for maximizing the logarithm of the joint posterior distribution (L), where L_{SR} denotes the sample likelihood and Π denotes the joint prior distribution comprising uninformative or informative priors:

$$\log L = \log L_{\mathrm{SR}} + \log \Pi \tag{16}$$

Samples from the joint posterior distribution of rebuilding target estimates were generated in three steps. The first step was to compute most likely values (posterior modes) of model parameters for each of the 12 stock–recruitment models. The second step was to apply MCMC simulation to generate sequences of samples from the joint posterior distribution of parameters (Gilks et al. 1996). The AD Model Builder software performs MCMC sampling of model parameters using the Metropolis–Hastings algorithm (Gelman et al. 1995). In this implementation, the jumping kernel that determines the value of the next posterior sample has the same covariance matrix as the target (posterior) distribution. The covariance matrix is estimated from the observed information matrix evaluated at the posterior mode. For models that used uninformative prior distributions, the use of MCMC simulation was analogous to the use of a parametric boostrap to estimate the sampling distribution of the rebuilding targets. We ran two MCMC simulations (chains) of length 300 000 for each model using different random seeds. Two chains were needed to assess whether the simulated values converged to the posterior distribution. Each chain was thinned by selecting every 50th sample to eliminate the possibility of autocorrelation. Of the 6000 samples remaining after thinning, we excluded the first 1000 to burn-in the chain, which effectively eliminated any dependence on the initial condition (the most likely estimates of the rebuilding targets). This left 5000 simulated posterior samples for inference. Convergence of the MCMC chains was verified for each rebuilding target (S_{MSY}, F_{MSY}, and MSY) using a convergence diagnostic called the potential scale reduction factor (PSRF) (Gelman et al. 1995) and further verified using another diagnostic called the second-order central-moment reduction. The latter diagnostic does not require a normality assumption (Brooks and Gelman 1998). In practice, a PSRF value <1.2 provides confirmatory evidence that the chains have converged to the posterior distribution (Gelman et al. 1995).

The last step was to examine the results for credibility. In this case, three criteria were applied to determine whether the likelihood fits were consistent with auxiliary information and with respect to model goodness-of-fit measures. These criteria were used as a quality control check to ensure that the individual model outputs made sense (e.g., Schnute and Richards 2001). Although this required subjective judgment, it was necessary given the short time series of stock–recruitment data. A priori, we required that the estimated posterior mode from each model fit satisfy both the first- and second-order derivative conditions required for a strict maximum of L. Second, posterior samples with F_{MSY} values >2 (81% exploitation rate with natural mortality of $M = 0.2$) were not considered credible given the likely range of spawning biomass per recruit required for long-term sustainability (Mace and Sissenwine 1993). Last, we excluded models where the coefficient of variation of MSY, S_{MSY}, or F_{MSY} derived from posterior sampling exceeded 100%. In this case, an extremely high coefficient of variation indicated that one or more model parameters were not identifiable. The remaining models formed the set of credible models.

Goodness-of-fit criterion

We evaluated the relative likelihood of credible models using the Schwarz criterion (Schwarz 1978) (minus twice the Schwarz criterion is also called the Bayesian information criterion). This goodness-of-fit criterion allows one to compare the fits of alternative models to a data set. It is conceptually similar to the use of a multiple coefficient of determination to select a set of best predictor variables in multivariate regression. In our application, we used the Schwarz criterion to compare the fits of BH and RK models to stock–recruitment data. In general, if one wants to compare two alternative models M_j and M_k with parameter vectors $\boldsymbol{\theta}_j$ and $\boldsymbol{\theta}_k$ of dimension d_j and d_k using fixed data (D) with sample size n, the Schwarz criterion (SC_{jk}) is

$$\mathrm{SC}_{jk} = \log(L_{\mathrm{SR}}(D|\hat{\boldsymbol{\theta}}_j, M_j)) - \log(L_{\mathrm{SR}}(D|\hat{\boldsymbol{\theta}}_k, M_k)) - \frac{1}{2}(d_j - d_k)\log(n) \tag{17}$$

where $\hat{\boldsymbol{\theta}}_j$ and $\hat{\boldsymbol{\theta}}_k$ are the most likely values of the parameter vectors. The model with the greatest likelihood, as adjusted by a parameter penalty, provides the best fit to the data. For example, in eq. 17, a negative SC_{jk} value would indicate that model M_k provided a better fit because it had a larger log-likelihood adjusted by the parameter penalty than model M_j. Using the Schwarz criterion provided a single objective measure to judge each model's goodness-of-fit to the data.

The Schwarz criterion is related to Bayesian inference with several models. The Schwarz criterion is approximately equal to the natural logarithm of the Bayes factor (B_{jk}) (Kass and Raftery 1995). The Bayes factor provides a summary of the weight of evidence in favor of one scientific theory to another for a fixed data set. In particular, the Bayes factor is the ratio of the posterior odds of a hypothesis to its prior odds. When used for comparing competing models where each model has equal prior odds, the Bayes factor represents

© 2005 NRC Canada

the relative odds of one model versus another being true. One can approximate the Bayes factor for comparing alternative models M_j and M_k as

$$(18) \quad B_{jk} = \frac{\Pr(D|M_j)}{\Pr(D|M_k)} \approx \exp(SC_{jk})$$

where $\Pr(D|M_k)$ is the integrated likelihood of D under model M_k.

The Bayes factor measures the relative success of alternative models at predicting the observed data. The approximation in eq. 18 gives a reliable, if not exact (the value of $SC_{jk}/\log(B_{jk})$ approaches unity as n becomes arbitrarily large), measure of the weight of evidence in favor of one model versus another conditioned on the observed data (Kass and Raftery 1995). The strengths of the approximate Bayes factor are that it is easy to use and does not depend on the evaluation of prior distributions. In this context, minus twice the natural logarithm of the Bayes factor ($-2\log(B_{jk})$) measures the strength of evidence of model Mj versus model M_k on the same scale as a deviance or a likelihood ratio statistic. The quantity $-2\log(B_{jk})$ can be interpreted as the strength of evidence against model M_k (also known as the Bayesian information criterion; Kass and Raftery 1995): values of $-2\log(B_{jk})$ between 0 and 2 provide no evidence against M_k, values between 2 and 6 provide positive evidence against M_k, and values between 6 and 10 and >10 provide strong and very strong evidence against M_k, respectively. Given that it is the relative difference that determines the weight of evidence and not the actual value, we used the Schwarz criterion approximation to compute Bayes factors for all pairs of credible models.

Model probabilities

The Bayes factors of the credible models were used to rank the models and compute their relative probability conditioned on the available data. The Bayes factor and prior odds of model M_k were calculated relative to the best fitting credible model (M_0). In general, the prior odds (α_k) of M_k would be $\alpha_k = \Pr(M_k)/\Pr(M_0)$. In practice, we set the prior odds to be identically unity for all credible models, since there was a priori no reason to favor any one of the credible models. This choice implied that the relative model probabilities were determined by their approximate Bayes factors, which in turn depended on the likelihood functions. The posterior probability of each credible model was determined by its prior odds and Bayes factors via

$$(19) \quad \Pr(M_k|D) = \frac{\alpha_k B_{k0}}{\sum_j \alpha_j B_{j0}}$$

As a sensitivity analysis, the Akaike information criterion, was also used to compute model probabilities (see Brodziak et al. 2001; Burnham and Anderson 2002) and model-averaged rebuilding targets under the same numerical simulation approach.

Model averaging

The posterior distributions from the set of credible models were used to calculate robust rebuilding target estimates using Bayesian model averaging (Kass and Raftery 1995; Hoeting et al. 1999). Under this approach, averaging over all credible models can typically provide better predictive accuracy than using a single best-fitting model. The resulting model-averaged estimates explicitly accounted for model selection uncertainty among the credible models. To do this, we computed the model-averaged value of a rebuilding target, say S_{MSY}, from its conditional expectation under each model and the associated model probabilities:

$$(20) \quad E[S_{MSY}|D] = \sum_k E[S_{MSY}|D, M_k]\Pr(M_k|D)$$

The conditional expectation of S_{MSY} under model M_k was derived from its MCMC chain. Similarly, the posterior probability of model M_k was computed as the expected value of the MCMC sequences of Bayes factors $\{B_{jk}(1), B_{jk}(2),..., B_{jk}(5000)\}$ across models. In this case, the ordering of the samples of Schwarz criterion values $SC_{jk}(m)$ by model did not affect the calculated posterior probability, since the MCMC chains were independent samples from each individual model's posterior distribution.

Given the model-specific averages of S_{MSY}, we computed its model-averaged variance from its conditional variance and expectation under each model along with the associated model probability by

$$(21) \quad \mathrm{VAR}[S_{MSY}|D] = \sum_k (\mathrm{VAR}[S_{MSY}|D, M_k] + E[S_{MSY}|D, M_k]^2)\Pr(M_k|D) - E[S_{MSY}|D]^2$$

In eq. 21, the conditional variance of S_{MSY} under model M_k was computed from its MCMC chain and the other terms were taken from eq. 20.

Sensitivity analyses

We conducted sensitivity analyses to assess the relative importance of the choice of mean values for the informative priors under each alternative model. These analyses were expected to show which stock–recruitment parameters had the largest effect on rebuilding target estimates. Four separate analyses of sensitivity to informative priors were conducted: mean value of steepness prior, mean value of unfished recruitment prior, mean value of slope at the origin prior, and combination of mean values of steepness and unfished recruitment priors. In each sensitivity analysis, we recomputed the posterior modes of MSY, F_{MSY}, and S_{MSY} using an alternative set of values for the prior mean for each of the three stocks. This was done for both uncorrelated and serially correlated errors. For each analysis, the variance of the prior was set so that the coefficient of variation was constant and equal to the value in the original analysis of each stock. For the sensitivity analysis of the steepness prior, the set of values of μ_h was $Z = \{0.25, 0.35, 0.45, 0.55, 0.65, 0.75, 0.85, 0.95\}$. A corresponding set of values for the prior mean of the slope at the origin prior μ_α was determined using eq. 15 along with the expected value of unfished spawning biomass per recruit ($SPR(F = 0)$) for each stock. For the sensitivity analysis of the unfished recruitment prior, we used a set of multipliers M ranging from –50% to +50% of the original mean μ_R; the set of multipliers was $M = \{0.5, 0.6, 0.7, 0.8, 0.9, 1, 1.1, 1.2, 1.3, 1.4, 1.5\}$. In the combined sensitivity analysis of the steepness and unfished recruitment priors, we

© 2005 NRC Canada

Table 3. Coefficients of variation (%) of maximum sustainable yield (MSY), spawning stock to produces MSY (S_{MSY}), and fishing mortality to produce MSY (F_{MSY}) from posterior sampling for Georges Bank Atlantic cod, haddock, and yellowtail flounder under each alternative rebuilding target model (credible models indicated in bold).

	BH	ABH	**RBH**	**RABH**	ZBH	ZABH	**RZBH**	**RZABH**	RK	ARK	**SRK**	SARK
Georges Bank cod												
MSY	795	644	15	19	428	1447	15	18	100	322	65	393
S_{MSY}	839	509	19	22	445	1463	18	20	101	314	66	393
F_{MSY}	9	19	13	21	13	17	11	14	8	29	1	1
Georges Bank haddock												
MSY	2470	803	10	15	649	886	10	13	235	312	250	296
S_{MSY}	2437	835	14	22	706	965	12	16	239	318	253	289
F_{MSY}	25	64	33	59	20	41	24	44	23	29	15	14
Georges Bank yellowtail flounder												
MSY	856	194	5	9	554	301	5	6	210	381	613	409
S_{MSY}	960	248	6	13	617	307	5	7	253	544	643	428
F_{MSY}	15	27	9	27	11	15	8	13	23	45	8	8

Table 4. Model-averaging results for MSY (thousands of metric tons), S_{MSY} (thousands of metric tons), and F_{MSY} (per year) based on Markov Chain Monte Carlo sampling for Georges Bank Atlantic cod.

Model	Posterior model probability $[-2\log(B_{A})]$[a]	MSY	S_{MSY}	F_{MSY}	Evidence against model
RBH	0.34 [1.4]	37.4 (5.6)	193.7 (36.2)	0.21 (0.03)	None
RABH	0.15 [3.5]	35.4 (6.8)	176.1 (39.3)	0.23 (0.05)	Positive
RZBH	0.33 [1.4]	37.4 (5.6)	188.7 (33.6)	0.22 (0.02)	None
RZABH	0.16 [3.4]	35.8 (6.4)	172.7 (34.6)	0.23 (0.03)	Positive
SRK	0.01 [8.9]	46.2 (30.3)	87.5 (57.4)	0.69 (0.01)	Strong
Model average		36.9 (6.8)	184.7 (38.2)	0.23 (0.06)	
80% credibility interval		(28.2, 45.6)	(135.8, 233.6)	(0.15, 0.31)	

Note: Conditional expectations by model and model-averaged values of MSY, S_{MSY}, and F_{MSY} appear with the associated standard error in parentheses along with 80% credibility intervals for model-averaged results. The average value of twice the natural logarithm of the approximate Bayes factor appears in square brackets after each posterior model probability. Models: RBH, informative recruitment prior with uncorrelated Beverton–Holt; RABH, informative recruitment prior with autocorrelated Beverton–Holt; RZBH, informative recruitment and steepness priors with uncorrelated Beverton–Holt; RZABH, informative recruitment and steepness priors with autocorrelated Beverton–Holt; SRK, informative slope at origin prior with uncorrelated Ricker.

[a]Values may not sum to unity due to rounding.

used the set of all possible combinations of Z and M; this was the set $Z \otimes M$ with a total of 88 elements.

Results

Convergence diagnostics indicated that the individual MCMC simulations converged for all of the alternative models. As a result, posterior modes were judged to be estimable for each alternative model and stock. The calculated PSRF values for the estimands MSY, S_{MSY}, and F_{MSY} were approximately 1.00 in all cases except for the F_{MSY} values of Georges Bank cod using the BH (PSRF = 1.59) and ABH (PSRF = 1.18) models. In these two cases, the models were not identifiable (see below) and were not used for model averaging. Overall, the convergence diagnostics indicated that the MCMC samples converged in probability to the joint posterior distribution of the rebuilding targets. Identical results were obtained using the alternative convergence diagnostic based on the second-order central-moment reduction factor.

Many of the alternative models did not have identifiable parameters based on the coefficients of variation of MSY, S_{MSY}, and F_{MSY} (Tables 2 and 3). For Georges Bank cod, the set of credible models was {RBH, RABH, RZBH, RZABH, SRK}. For Georges Bank haddock and yellowtail flounder, the set of credible models was {RBH, RABH, RZBH, RZABH}. Thus, virtually all of the identifiable models were BH. In contrast, virtually all of the RK models were found to be noncredible based on the coefficient of variation criterion.

Model-averaged estimates of MSY, S_{MSY}, and F_{MSY} were tabulated from the posterior means and model probabilities of credible models for each stock. For Georges Bank cod, most of the credible models were BH models with an informative prior on unfished recruitment (Table 3; Fig. 3a). None of the posterior samples had values of $F_{MSY} > 2$. Of the four credible models, the RBH and RZBH models were most probable (Table 4). These two uncorrelated models used uninformative and informative priors on steepness but produced very similar rebuilding targets. The corresponding RABH and RZABH models with serially correlated errors were approximately half as likely as the uncorrelated ones. The least probable model was the RK with an informative prior on slope at the origin. There was strong evidence

© 2005 NRC Canada

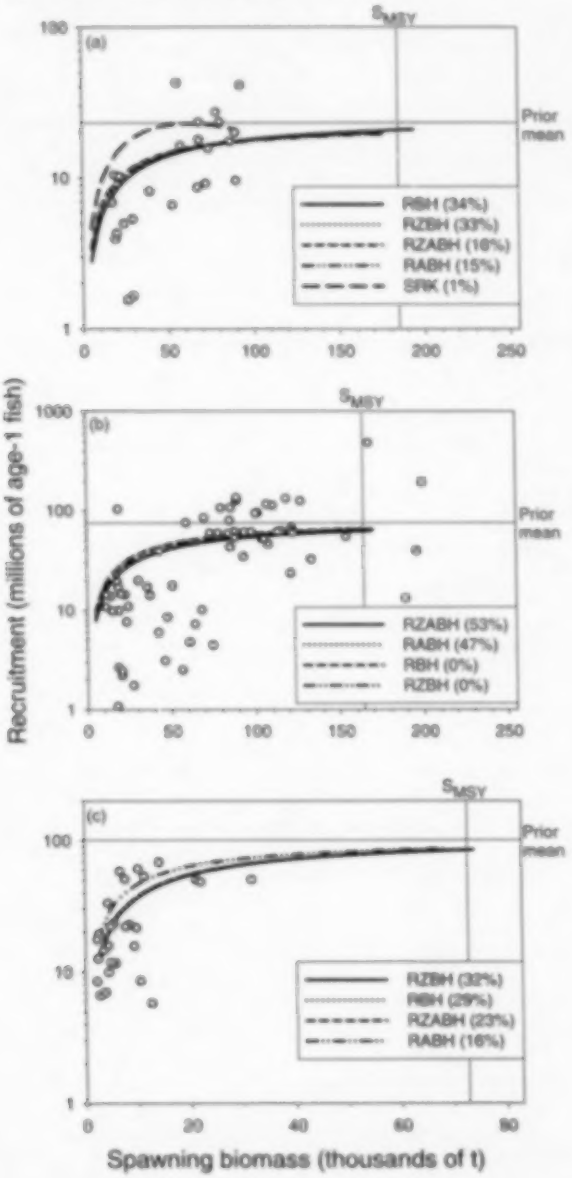

Fig. 3. Observed stock–recruitment data (circles), credible models and their approximate probabilities (%), model-averaged estimates of the spawning biomass to produce MSY (S_{MSY}, vertical line), and prior mean of unfished recruitment (horizontal line) for (*a*) Georges Bank Atlantic cod, (*b*) haddock, and (*c*) yellowtail flounder. Metric tons, t.

against this model, as it had roughly a 1% chance of being correct conditioned on the available data. Model-averaged values and standard errors of S_{MSY}, F_{MSY}, and MSY were computed over the set of credible models (Table 4). For comparison, the calculated 80% credibility intervals of the model-averaged rebuilding targets overlapped the current rebuilding targets for Georges Bank cod (NEFSC 2002*a*) of S_{MSY} (216.8 kt), F_{MSY} (0.18), and MSY (35.2 kt).

Georges Bank haddock model-averaging results differed from those of cod. For this stock, the most probable models were serially correlated with informative priors on unfished recruitment (RZABH and RABH) (Table 3; Fig. 3*b*). A few of the posterior samples were excluded from model averaging because they had values of $F_{MSY} > 2$. The percentages of samples excluded were 0.14% for RBH, 2.42% for RABH, 0.04% for RZBH, and 0.38% for RZABH. These four BH models were almost equally likely, although the one with an informative prior on steepness was slightly more probable (Table 5). There was strong evidence against the corresponding uncorrelated models (RZBH and RBH), which had a very low probabilities of being true conditioned on the available data. For haddock, the model-averaged values and associated standard errors of S_{MSY}, F_{MSY}, and MSY were computed and compared with current rebuilding targets. For Georges Bank haddock, the 80% credibility intervals overlapped the current rebuilding targets (NEFSC 2002*a*) of F_{MSY} (0.26) and MSY (52.9 kt) but did not overlap that for S_{MSY} (250.3 kt).

Model-averaging results for Georges Bank yellowtail flounder results were similar to those for cod since the credible models were the same for both stocks, except for the RK model deemed credible for cod but not for yellowtail flounder. For yellowtail flounder, none of the posterior samples had values of $F_{MSY} > 2$. Of the four credible models, the uncorrelated BH models with informative priors on unfished recruitment (RZBH and RBH) were most probable, as was the case for cod (Table 3; Fig. 3*c*). However, the difference between the model probabilities of the corresponding serially correlated models (RZABH and RABH) was smaller for yellowtail flounder than for cod (Table 6). There was some positive evidence against the autocorrelated models, which had similar odds of being true. In contrast with cod and haddock, the available yellowtail flounder data were relatively uninformative to discern among the credible models. The model-averaged values of S_{MSY}, F_{MSY}, and MSY were similar to the individual model results, since there was little difference among the individual model predictions (Table 6). In comparison with existing rebuilding targets for Georges Bank yellowtail flounder (NEFSC 2002*a*), the 80% credibility intervals of the model-averaged rebuilding targets did not overlap current rebuilding targets of S_{MSY} (58.8 kt), F_{MSY} (0.25), and MSY (12.9 kt).

Sensitivity analyses showed that the rebuilding targets were substantially affected by the steepness prior (Fig. 4). Sensitivity analyses on the effect of the mean of the steepness prior for BH models showed different patterns across stocks as well. The posterior mode of MSY showed a nonlinear decrease as steepness increased. In magnitude, estimates of MSY were over 100-fold greater than existing MSY estimates at low steepnesses below 0.5 for each stock. These estimates became more consistent with observed annual yields (30 000, 9000, and 4000 t during 1980–1999 for cod, haddock, and yellowtail flounder, respectively) and MSY estimates (35 000, 53 000, and 13 000 t for cod, haddock, and yellowtail flounder, respectively) as the mean steepness increased (Fig. 4). However, the steepness at which this occurred differed among stocks. Estimates of MSY for uncorrelated and autocorrelated errors were similar at high steepnesses, although uncorrelated estimates tended

© 2005 NRC Canada

Table 5. Model-averaging results for MSY (thousands of metric tons), S_{MSY} (thousands of metric tons), and F_{MSY} (per year) based on Markov Chain Monte Carlo sampling for Georges Bank haddock.

Model	Posterior model probability [$-2\log(B_{\Delta})$][a]	MSY	S_{MSY}	F_{MSY}	Evidence against model
RBH	0.00 [19.6]	55.7 (5.6)	164.0 (23.3)	0.54 (0.17)	Very strong
RABH	0.47 [1.3]	53.8 (7.9)	158.5 (33.6)	0.59 (0.31)	None
RZBH	0.00 [19.3]	54.4 (5.2)	170.8 (20.4)	0.48 (0.11)	Very strong
RZABH	0.53 [0.9]	51.8 (6.5)	169.1 (26.2)	0.48 (0.19)	None
Model average		52.7 (7.3)	164.3 (30.2)	0.53 (0.26)	
80% credibility interval		(43.4, 62.0)	(125.6, 203.0)	(0.20, 0.86)	

Note: Conditional expectations by model and model-averaged values of MSY, S_{MSY}, and F_{MSY} appear with the associated standard error in parentheses along with 80% credibility intervals for model-averaged results. The average value of twice the natural logarithm of the approximate Bayes factor appears in square brackets after each posterior model probability. Models: RBH, informative recruitment prior with uncorrelated Beverton–Holt; RABH, informative recruitment prior with autocorrelated Beverton–Holt; RZBH, informative recruitment and steepness priors with uncorrelated Beverton–Holt; RZABH, informative recruitment and steepness priors with autocorrelated Beverton–Holt.

[a]Values may not sum to unity due to rounding.

Table 6. Model-averaging results for MSY (thousands of metric tons), S_{MSY} (thousands of metric tons), and F_{MSY} (per year) based on Markov Chain Monte Carlo sampling for Georges Bank yellowtail flounder.

Model	Posterior model probability [$-2\log(B_{\Delta})$][a]	MSY	S_{MSY}	F_{MSY}	Evidence against model
RBH	0.29 [1.4]	22.5 (1.1)	73.0 (4.1)	0.36 (0.03)	None
RABH	0.16 [3.2]	23.5 (2.1)	68.5 (8.9)	0.42 (0.12)	Positive
RZBH	0.32 [1.1]	22.3 (1.0)	73.9 (3.8)	0.35 (0.03)	None
RZABH	0.23 [2.2]	22.4 (1.4)	73.4 (5.2)	0.36 (0.05)	Positive
Model average		22.6 (1.4)	72.7 (5.7)	0.37 (0.06)	
80% credibility interval		(20.8, 24.4)	(65.4, 80.0)	(0.29, 0.45)	

Note: Conditional expectations by model and model-averaged values of MSY, S_{MSY}, and F_{MSY} appear with the associated standard error in parentheses along with 80% credibility intervals for model-averaged results. The average value of twice the natural logarithm of the approximate Bayes factor appears in square brackets after each posterior model probability. Models: RBH, informative recruitment prior with uncorrelated Beverton–Holt; RABH, informative recruitment prior with autocorrelated Beverton–Holt; RZBH, informative recruitment and steepness priors with uncorrelated Beverton–Holt; RZABH, informative recruitment and steepness priors with autocorrelated Beverton–Holt.

[a]Values may not sum to unity due to rounding.

to be at or above autocorrelated ones. The sensitivity results for S_{MSY} were very similar to those for MSY. The S_{MSY} decreased as steepness increased and uncorrelated estimates tended to be at or above autocorrelated ones. In contrast, there was a more linear increase in the posterior mode estimate of F_{MSY} with mean steepness across stocks (Fig. 4). Further, the autocorrelated estimates of F_{MSY} showed a more pronounced response to changes in steepness than the uncorrelated estimates. Overall, MSY and S_{MSY} estimates were more sensitive to the steepness parameter.

Were rebuilding targets sensitive to the informative prior values for unfished recruitment under a BH model? Yes, the effect of the prior mean for unfished recruitment had an important effect on the rebuilding target estimates that varied among stocks (Fig. 5). The estimates of MSY and S_{MSY} generally increased with increasing unfished recruitment but the rate of increase differed among stocks. Uncorrelated estimates of both MSY and S_{MSY} were similar to autocorrelated estimates (Fig. 5). In contrast, estimates of F_{MSY} decreased with increasing unfished recruitment. Uncorrelated and autocorrelated estimates of F_{MSY} were similar for cod and yellowtail flounder but differed for haddock. Further, as unfished recruitment increased, MSY and S_{MSY} increased, while F_{MSY} decreased. Overall, the unfished recruitment parameter had a smaller effect on rebuilding target estimates than the steepness parameter.

Analyses also showed that estimated rebuilding targets were sensitive to the informative prior values for slope at the origin under an RK model. Sensitivity analyses of the effect of slope at the origin on rebuilding targets showed different patterns across stocks (Fig. 6), except for yellowtail flounder at low slope values. The estimates of MSY and S_{MSY} increased steadily with increasing slope, although the estimate of S_{MSY} for yellowtail flounder peaked at an intermediate slope value with autocorrelated errors. Uncorrelated and autocorrelated estimates of MSY and S_{MSY} were also similar, except for yellowtail flounder at low slope values (Fig. 6). The estimates of F_{MSY} tended to increase to the maximum allowable F ($F = 2$) as slope increased for all stocks. Uncorrelated posterior modes of F_{MSY} were noncredible for mean slope priors of 10 or greater for both haddock and yellowtail flounder. There was very little difference between uncorrelated and autocorrelated estimates of F_{MSY} for cod and haddock. Overall, rebuilding target estimates were more sensitive to the slope at the origin priors than the unfished recruitment priors.

Were estimated rebuilding targets sensitive to the informative prior values for steepness and unfished recruitment priors under a BH model with uncorrelated errors? Yes, the rebuilding targets were sensitive to the joint effects of both priors. Sensitivity analyses of the joint effects of steepness and unfished recruitment priors using uncorrelated errors

© 2005 NRC Canada

Fig. 4. Sensitivity analyses of posterior modes of maximum sustainable yield (MSY, thousands of metric tons), spawning biomass to produce MSY (S_{MSY}, thousands of metric tons), and fishing mortality to produce MSY (F_{MSY}) to choice of mean steepness for a Beverton–Holt stock–recruitment curve using uncorrelated (solid line) and autocorrelated (broken line) errors.

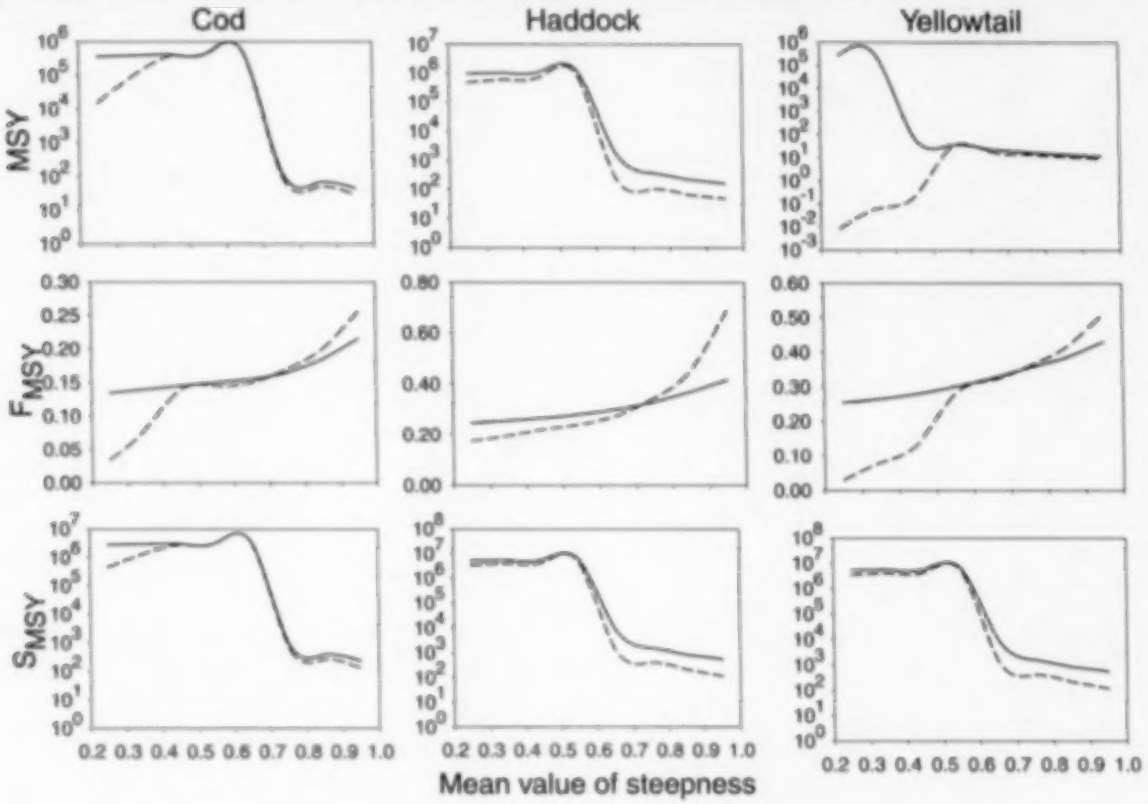

(Fig. 7) showed that the range of effects differed among stocks. Estimates of MSY and S_{MSY} were strongly affected by the unfished recruitment prior but were less sensitive to the choice of steepness prior. For fixed steepness, the estimated values of MSY and S_{MSY} were largely determined by unfished recruitment. MSY estimates had a slight negative correlation between steepness and unfished recruitment, while S_{MSY} estimates had a slight positive correlation (Fig. 7). In contrast, F_{MSY} estimates were strongly affected by the steepness prior. The F_{MSY} estimates appeared to have a moderate positive correlation between steepness and unfished recruitment. For a fixed value of unfished recruitment, steepness largely determined the estimated value of F_{MSY}. Thus, for uncorrelated errors, both MSY and S_{MSY} were determined by unfished recruitment, while F_{MSY} estimates were determined by steepness.

Estimated rebuilding targets were also sensitive to the informative prior values for steepness and unfished recruitment using correlated errors. Sensitivity analyses of the joint impacts of steepness and unfished recruitment using autocorrelated errors showed some similarities across stocks (Fig. 8). The estimated posterior modes of MSY were affected by both steepness and unfished recruitment. There was a negative correlation between steepness and unfished recruitment effects on MSY and this relationship was nonlinear for cod and yellowtail flounder (Fig. 8). The effects of steepness and unfished recruitment on F_{MSY} estimates were similar across stocks. In this case, the steepness prior was much more important than the unfished recruitment prior. There was a slight positive correlation between steepness and unfished recruitment effects at high steepness and low unfished recruitment values. Estimates of S_{MSY} for all three stocks were strongly affected by unfished recruitment (Fig. 8) and there was a moderate positive correlation between steepness and unfished recruitment effects on S_{MSY}.

Comparison of the results of sensitivity analyses using uncorrelated and autocorrelated error structures showed that the choice of error structure was important for these stocks. MSY estimates using uncorrelated errors were dependent on the unfished recruitment prior and were generally larger than estimates using autocorrelated errors. Estimates of MSY using autocorrelated errors were dependent on both steepness and unfished recruitment (Fig. 8). They also exhibited a stronger negative correlation between steepness and unfished recruitment effects and had a nonlinear response surface for cod and yellowtail flounder. Estimates of F_{MSY} using uncorrelated and autocorrelated were both strongly affected by the steepness prior (Figs. 7 and 8). Estimates of F_{MSY} were also higher using uncorrelated errors than estimates using autocorrelated errors. There was a stronger positive cor-

© 2005 NRC Canada

Fig. 8. Sensitivity analyses of posterior modes of maximum sustainable yield (MSY, thousands of metric tons), spawning biomass to produce MSY (S_{MSY}, thousands of metric tons), and fishing mortality to produce MSY (F_{MSY}) to choice of prior mean multiplier of unfished recruitment for a Beverton–Holt stock–recruitment curve using uncorrelated (solid line) and autocorrelated (broken line) errors.

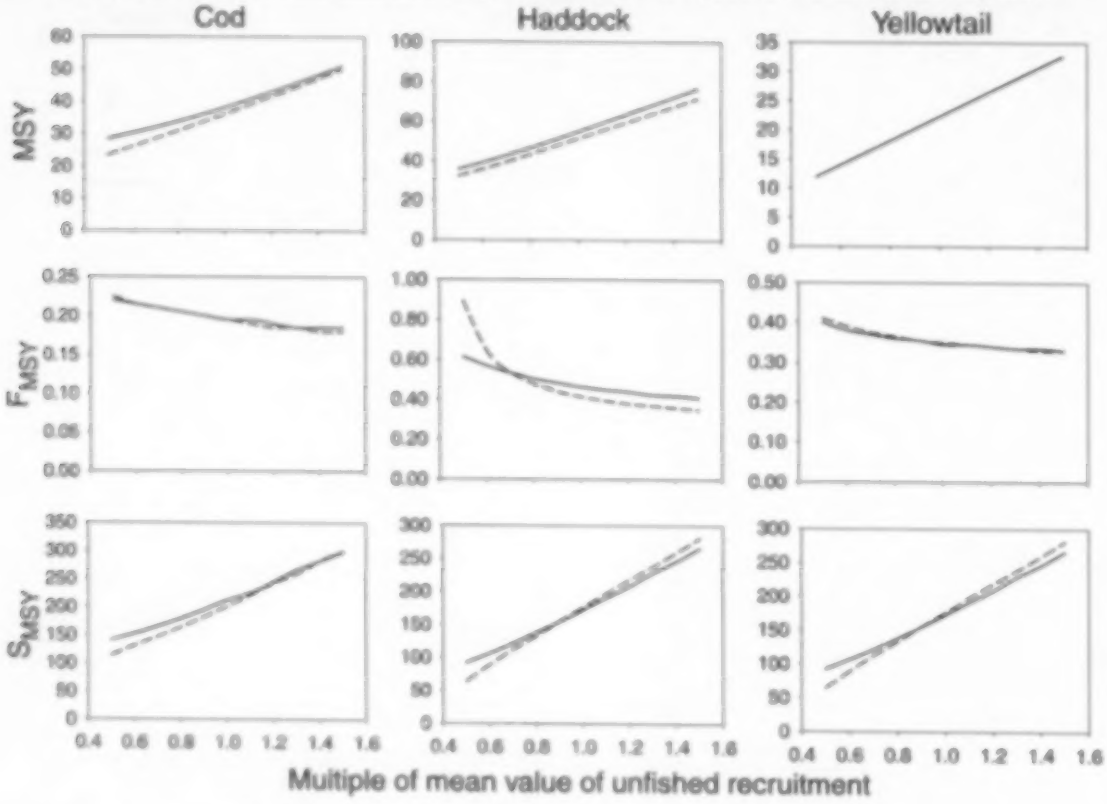

relation between steepness and unfished recruitment effects using uncorrelated errors. Estimates of S_{MSY} using uncorrelated and autocorrelated errors were strongly dependent on the unfished recruitment prior (Figs. 7 and 8). Steepness and unfished recruitment effects were more positively correlated and showed some nonlinearity at high unfished recruitment using autocorrelated errors. The S_{MSY} estimates using uncorrelated errors also tended to be lower than estimates using autocorrelated errors. Overall, rebuilding target estimates were more sensitive to priors with correlated versus uncorrelated errors.

Discussion

Model-averaging results placed almost all of the probability mass on the BH model for the three Georges Bank stocks. This suggested that the BH relationship was an adequate compensatory hypothesis given sufficient prior information on unfished recruitment. This relationship has a sound theoretical basis as a model of stock–recruitment dynamics and arises naturally when density-dependent effects are critical at some early life history stage (e.g., see Quinn and Deriso 1999). This model can also arise as a result of stock adaptation to balance predation and foraging risk in a variable environment (Walters and Korman 1999). Without sufficient prior information, however, none of the BH models were identifiable for any of the stocks. This emphasizes the importance of including as much relevant information as possible when evaluating rebuilding targets for overfished stocks.

In contrast, model-averaging results showed limited support for the overcompensatory stock–recruitment hypothesis for all three stocks. This finding is consistent with observed food habits information for these three stocks, which show very little incidence of cannibalism (one possible mechanism to generate overcompensation) for haddock and none for yellowtail flounder (NEFSC 2002*a*). Interestingly, Georges Bank cod, which exhibits an increasing incidence of cannibalism with ontogeny (Link and Garrison 2002), was the only stock that had positive probability for an RK model. However, that model was also the least probable (1%) model for cod.

Our illustration of model averaging to compute rebuilding targets was limited to contrasting a pair of two-parameter stock–recruitment models that can produce vastly different rebuilding target values with similar values of the goodness-of-fit criterion (Myers et al. 1994). When using model averaging in practice, it will be necessary to modify the hypotheses to match the specific situation. Investigating different stock–recruitment models, such as the hockey stick (Barrowman and Myers 2000) or curves that exhibit depensation, and using error structures that reflect expected dynamics un-

© 2005 NRC Canada

Fig. 6. Sensitivity analyses of posterior modes of maximum sustainable yield (MSY, thousands of metric tons), spawning biomass to produce MSY (S_{MSY}, thousands of metric tons), and fishing mortality to produce MSY (F_{MSY}) to choice of mean slope at the origin for a Ricker stock–recruitment curve using uncorrelated (solid line) and autocorrelated (broken line) errors.

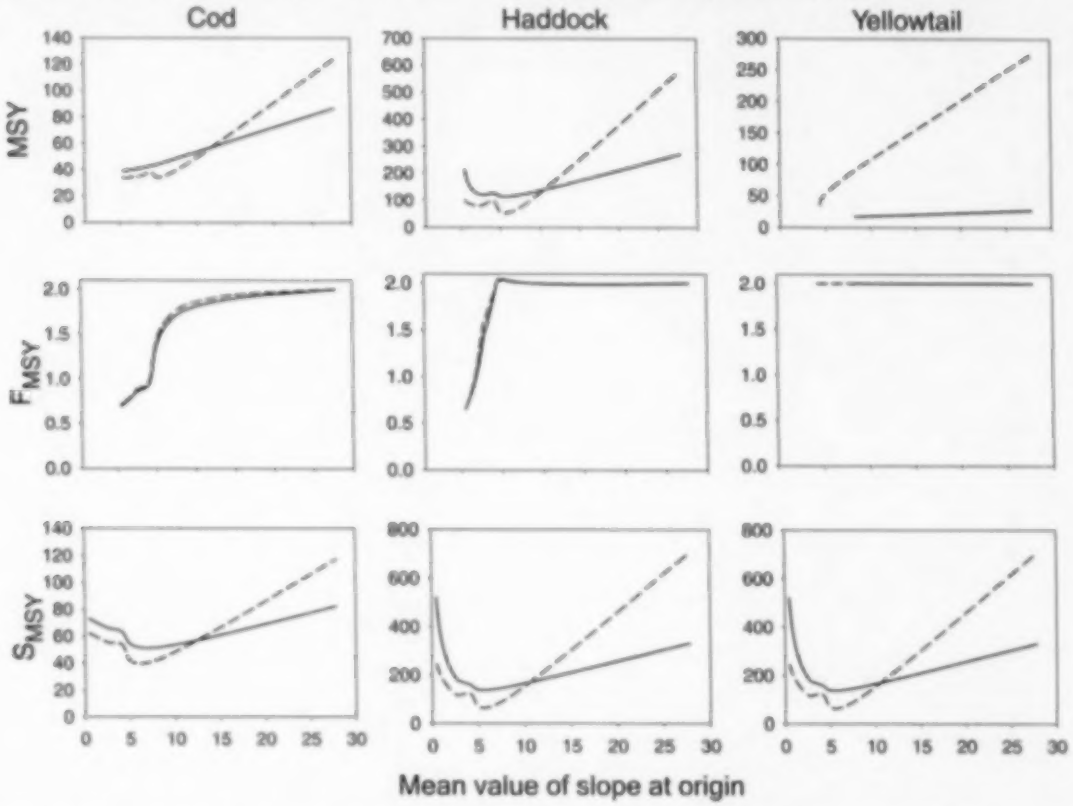

der alternative hypotheses may be necessary. In this context, it is the shape of the curves, their biological plausibility, and the estimability of model parameters that are of paramount importance. It may be difficult to identify stock–recruitment models that have similar shapes using short time series. This emphasizes the importance of choosing an appropriate set of models to average over when applying model-averaging techniques (Hoeting et al. 1999).

While we used a Bayesian approach for model averaging, a frequentist approach based on multiple-model inference and model averaging using bootstrapped Akaike weights could also have been applied (Anderson et al. 2001; Burnham and Anderson 2002). In this context, our use of informative priors is conceptually equivalent to applying a penalty function to a likelihood to constrain parameter estimates (e.g., Edwards 1992). For comparison, a sensitivity analysis using the Akaike criterion instead of the Schwarz criterion produced virtually identical model-averaged rebuilding targets for all three stocks. This was not surprising, since both criteria are based on the sample likelihood adjusted with a parameter penalty. Although our choice of a cutoff coefficient of variation of 100% on key model parameters to eliminate nonidentifiable models was subjective, sensitivity analyses using a higher cutoff of 200% produced identical rebuilding targets for haddock and yellowtail flounder. For cod, the uncorrelated RK model became credible using a 200% cutoff. However, the model-averaged rebuilding target estimates changed by less than 0.5%. Overall, this suggested that the model-averaging approach was robust to the choice of goodness-of-fit and model identifiability criteria.

Although the concept of MSY has its limitations (Larkin 1977), the expected fishing mortality that produces MSY has proven to be a useful limit rebuilding target for precautionary single-species management (Mace 2001). Similarly, the expected spawning biomass that produces MSY provides a useful goal for implementing an ecosystem approach to fisheries management with multiple performance measures (Brodziak and Link 2002). We also note that the model-averaging approach can be applied with other reference points that depend on stock–recruitment models, such as biomass limits for recruitment overfishing (Myers et al. 1994) and fishing limits defined by the slope of the stock–recruitment relationship at the origin (ICES 1997). While it has been argued that it may be useful to eventually move away from model-based estimates of reference points (e.g., Hilborn 2002), we believe that rebuilding targets can provide satisfactory management advice provided that uncertainties about the stock–recruitment relationship are explicitly addressed. Furthermore, we recommend using multiple working hypotheses to address fundamental uncertainties. In this context, model averaging offers a structured alternative to estimating rebuilding targets when there are several compet-

© 2005 NRC Canada

Fig. 7. Sensitivity analyses of posterior modes of maximum sustainable yield (MSY, thousands of metric tons), spawning biomass to produce MSY (S_{MSY}, thousands of metric tons), and fishing mortality to produce MSY (F_{MSY}) to choice of mean steepness and multiplier of mean unfished recruitment for a Beverton–Holt stock–recruitment curve using uncorrelated errors.

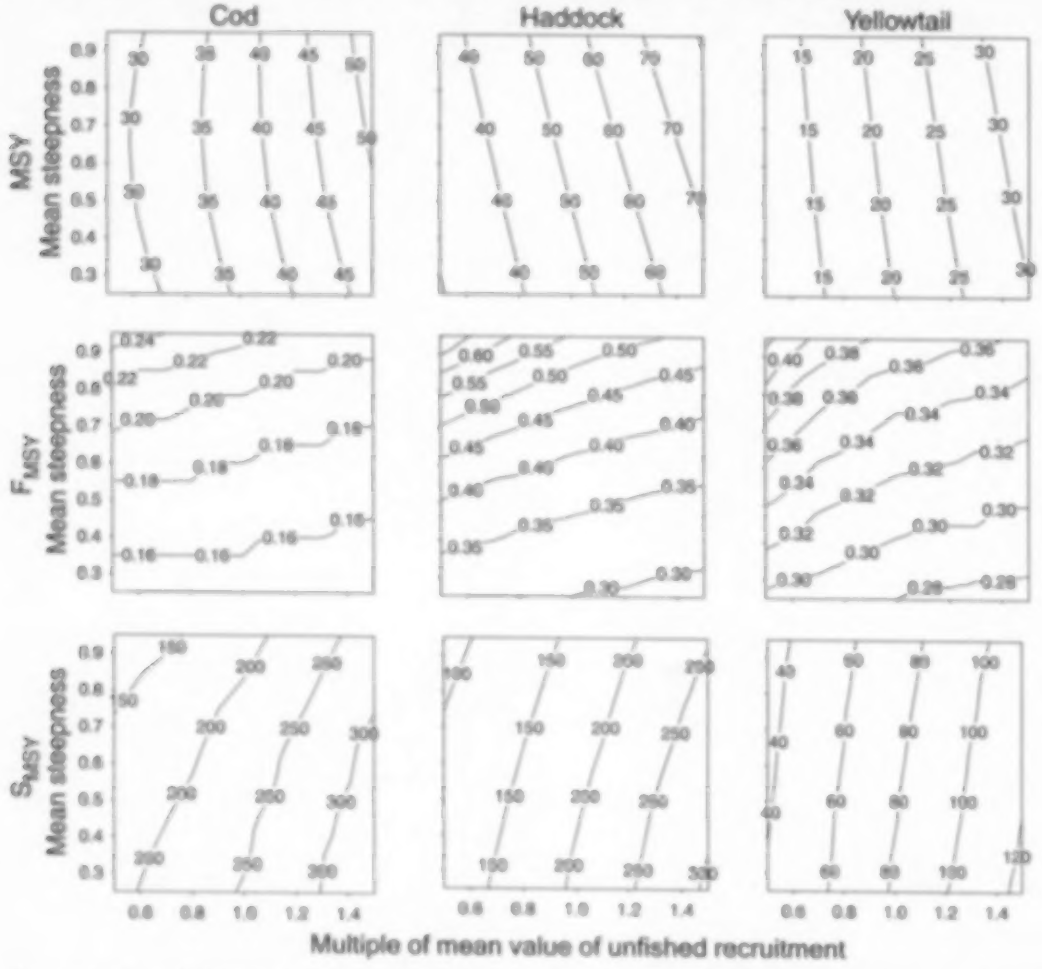

ing hypotheses about stock dynamics in an objective manner.

Model averaging results for the three groundfish stocks had wide confidence intervals that reflected the underlying uncertainty in rebuilding targets. Although some differences existed between the results of this study and existing biological rebuilding targets (e.g., haddock F_{MSY} and S_{MSY} and yellowtail flounder MSY, F_{MSY}, and S_{MSY}), it is important to recognize that our results are only an illustration of the technical approach. In particular, our results could not logically supplant the existing biological rebuilding targets, which have undergone extensive peer review and stakeholder scrutiny and, as a result, have been judged to constitute the best available science for the current fishery management plan to manage New England groundfish. Nonetheless, it is clear that management advice for these three stocks would be robust to apparent differences. Fishing mortality on the Georges Bank cod stock needs to be reduced and the stock needs to be rebuilt to a larger spawning biomass (NEFSC 2002*b*). In contrast, the Georges Bank haddock and yellowtail flounder stocks were rebuilding in recent years at historically low fishing mortality rates (NEFSC 2002*b*). Furthermore, although the model-averaged estimate F_{MSY} for Georges Bank haddock in this study is roughly twice the current rebuilding target, it is imprecisely determined with a coefficient of variation of roughly 50%. It is interesting that this stock produced an average annual yield of 50 kt when fished at an average F of roughly 0.5 over three decades even though smaller mesh was utilized (Sissenwine and Shepherd 1987). At least historically, the haddock stock was resilient and productive at relatively high fishing mortalities. Nonetheless, the fundamental uncertainty in the rebuilding target estimates emphasizes the need to manage adaptively by monitoring progress towards stock recovery and reevaluating rebuilding targets as appropriate. This uncertainty would be reduced by observations of recruitment at high stock sizes if stock recovery plans are successful.

Our model-averaging results could also be applied to estimate rebuilding trajectories for these overfished stocks using a standard projection framework (e.g., Brodziak et al. 1998)

© 2005 NRC Canada

Fig. 8. Sensitivity analyses of posterior modes of maximum sustainable yield (MSY, thousands of metric tons), spawning biomass to produce MSY (S_{MSY}, thousands of metric tons), and fishing mortality to produce MSY (F_{MSY}) to choice of mean steepness and multiplier of mean unfished recruitment for a Beverton–Holt stock–recruitment curve using autocorrelated errors.

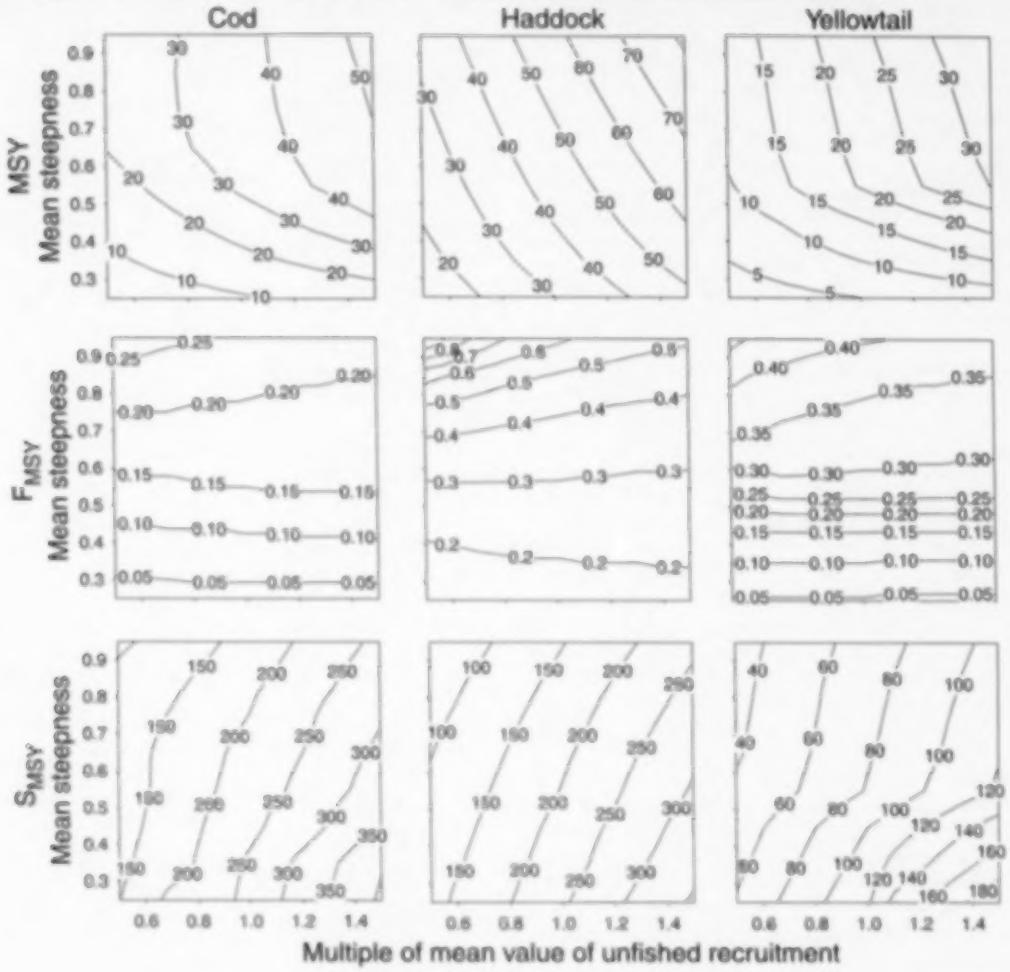

in a straightforward manner. In particular, one can randomly select a credible stock–recruitment model in proportion to its model probability and then draw a set of model parameters from the joint posterior distribution of the selected model. If low-frequency environmental forcing is important, it will be incorporated into the projections through one or more autocorrelated models. In this way, the simulation directly reflects the model-averaging estimates — a useful simplification when addressing the large number of uncertainties that may be important for forecasting (e.g., Patterson et al. 2001). On the other hand, it is important to not overinterpret the reliability of recruitment predictions, especially if nonstationarity in stock–recruitment dynamics due to either environmental forcing or depensatory effects appears evident. In practice, it is advisable to assess whether there are trends in observed production of recruits per spawner in recent years. If strong time trends are apparent, a single stock–recruitment model fit with autocorrelated errors may not provide a satisfactory short-term approximation and other structural approaches, such as randomly resampling recent recruitment observations, may have better predictive accuracy.

The results of the sensitivity analyses provide some guidance on the potential effects of choices for informative priors on steepness, slope at the origin, or unfished recruitment. In general, we found that steepness priors with mean values below 0.5 (well outside the probable range of the informative prior) led to noncredible results for MSY and S_{MSY}, regardless of the whether an uncorrelated or autocorrelated error structure was used. In contrast, changes in unfished recruitment priors produced a more linear response in rebuilding target estimates. Slope at origin priors also produced noncredible results (e.g., $F_{MSY} > 2$) at higher mean slopes. This is likely due to an intrinsic lack of model identifiability when an overcompensatory stock–recruitment curve is combined with a high slope at the origin. In particular, RK and similarly shaped curves can produce deterministic chaos. Combining this deterministic feature with short time series

© 2005 NRC Canada

of highly variable stock–recruitment data may make parameter identification difficult. Our results also showed that MSY and S_{MSY} were strongly dependent on unfished recruitment, while F_{MSY} was strongly dependent on steepness. Thus, the overall magnitude of recruitment had a more pronounced effect on the magnitude of yield and stock biomass, while the rate of increase of the stock–recruitment curve near the origin had a greater effect on the fishing mortality rate. In comparison, the choice of error structure had a less pronounced effect in most cases, although autocorrelation introduced more nonlinearity in the response to steepness and unfished recruitment. Last, it was evident that the sensitivity of rebuilding targets differed among stocks, which emphasizes the importance of measuring differences in life history parameters and the time series of available stock and recruitment observations.

Model averaging is a general technique for ecological investigations that can be used to produce robust parameter estimates when model uncertainty is important (Johnson and Omland 2004). This approach could be applied to rebuilding target estimation for many commercially exploited stocks that have age-structured assessment data. One common problem of rebuilding target estimation is lack of knowledge about the steepness parameter of the stock–recruitment relationship (Williams and Shertzer 2003). We believe that the use of meta-analyses such as Myers et al. (1999) provides the best alternative when time series of stock–recruitment data are short and have high intrinsic variance, a common situation in assessment data worldwide. Another common problem with rebuilding target estimation is the lack of stock–recruitment data at high spawning stock sizes. Our use of informative priors for unfished recruitment based on observed recruitment distributions directly addresses this problem. In fact, our results show that it may not be possible to reliably estimate rebuilding targets for stocks with a long history of overfishing unless prior information on steepness or unfished recruitment is available. Overall, this underscores the importance of being explicit about the treatment of model and parameter uncertainty, especially when conflicts arise over appropriate rebuilding targets for overfished stocks (e.g., see Greene 2002).

Acknowledgments

We thank Jim Bence, Fred Serchuk, and two anonymous referees for their helpful comments on the draft manuscript.

References

Anderson, D.R., Burnham, K.P., and White, G.C. 2001. Kullback–Leibler information in resolving natural resource conflicts when definitive data exist. Wildl. Soc. Bull. **29**: 1260–1270.

Barrowman, N.J., and Myers, R.A. 2000. Still more spawner–recruitment curves: the hockey stick and its generalizations. Can. J. Fish. Aquat. Sci. **57**: 665–676.

Brodziak, J. 2002. In search of optimal harvest rates for west coast groundfish. N. Am. J. Fish. Manag. **22**: 258–271.

Brodziak, J., and Link, J. 2002. Ecosystem-based fishery management: what is it and how can we do it? Bull. Mar. Sci. **70**: 589–611.

Brodziak, J., Rago, P., and Conser, R. 1998. A general approach for making short-term stochastic projections from an age-structured fisheries assessment model. *In* Proceedings of the International Symposium on Fishery Stock Assessment Models for the 21st Century. *Edited by* F. Funk, T. Quinn II, J. Heifetz, J. Ianelli, J. Powers, J. Schweigert, P. Sullivan, and C.-I. Zhang. Alaska Sea Grant College Program, University of Alaska, Fairbanks, Alaska.

Brodziak, J.K.T., Overholtz, W.J., and Rago, P.J. 2001. Does spawning stock affect recruitment of New England groundfish? Can. J. Fish. Aquat. Sci. **58**: 306–318.

Brooks, S.P., and Gelman, A. 1998. General methods for monitoring convergence of iterative simulations. J. Comput. Graph. Stat. **7**: 434–455.

Burnham, K.P., and Anderson, D. 2002. Model selection and multimodel inference. Springer-Verlag, New York.

Carlin, B.P., and Louis, T.A. 2000. Bayes and empirical Bayes methods for data analysis. Chapman and Hall, New York.

Edwards, A.W.F. 1992. Likelihood. Johns Hopkins University Press, Baltimore, Md.

Ellison, A.M. 2004. Bayesian inference in ecology. Ecol. Lett. **7**: 509–520.

Garcia, S.M., and Newton, C. 1997. Current situations, trends and prospects in world capture fisheries. *In* Global trends: fisheries management. *Edited by* E.K. Pikitch, D.D. Huppert, and M.P. Sissenwine. Am. Fish. Soc. Symp. **20**: 3–27.

Gelman, A., Carlin, J.B., Stern, H.S., and Rubin, D.B. 1995. Bayesian data analysis. Chapman and Hall, New York.

Gilks, W.R., Richardson, S., and Spiegelhalter, D.J. 1996. Markov Chain Monte Carlo in practice. Chapman and Hall, New York.

Greene, K. 2002. Bigger populations needed for sustainable harvests. Science (Wash., D.C.), **296**: 1229–1230.

Hilborn, R. 2002. The dark side of reference points. Bull. Mar. Sci. **70**: 403–408.

Hilborn, R., and Liermann, M. 1998. Standing on the shoulders of giants: learning from experience in fisheries. Rev. Fish Biol. Fish. **8**: 273–283.

Hilborn, R., and Mangel, M. 1997. The ecological detective. Princeton University Press, Princeton, N.J.

Hoeting, J.A., Madigan, D., Raftery, A.E., and Volinsky, C.T. 1999. Bayesian model averaging: a tutorial. Stat. Sci. **14**: 382–401.

Hutchings, J.A., Walters, C., and Haedrich, R.L. 1997. Is scientific inquiry incompatible with government information control? Can. J. Fish. Aquat. Sci. **54**: 1198–1210.

ICES. 1997. Report of the study group on the precautionary approach to fisheries management. ICES CM 1997/Assess 7.

Johnson, J.B., and Omland, K.S. 2004. Model selection in ecology and evolution. Trends Ecol. Evol. **19**: 101–108.

Kass, R.E., and Raftery, A.E. 1995. Bayes factors. J. Am. Stat. Assoc. **90**: 773–795.

Larkin, P. 1977. An epitaph for the concept of maximum sustained yield. Trans. Am. Fish. Soc. **106**: 1–11.

Link, J.S., and Garrison, L.P. 2002. Trophic ecology of Atlantic cod *Gadus morhua* on the northeast US continental shelf. Mar. Ecol. Prog. Ser. **227**: 109–123.

Mace, P.M. 2001. A new role for MSY in single-species and ecosystem approaches to fisheries stock assessment and management. Fish Fish. **2**: 2–32.

Mace, P.M., and Sissenwine, M.P. 1993. How much spawning per recruit is enough? *In* Risk evaluation and biological reference points for fisheries management. *Edited by* S.J. Smith, J.J. Hunt, and D. Rivard. Can. Spec. Publ. Fish. Aquat. Sci. No. 120. pp. 101–118.

Myers, R.A., and Mertz, G. 1998. Reducing uncertainty in the biological basis of fisheries management by meta-analysis of data from many populations: a synthesis. Fish. Res. **37**: 51–60.

© 2005 NRC Canada

Myers, R.A., Rosenberg, A.A., Mace, P.M., Barrowman, N.J., and Restrepo, V.R. 1994. In search of thresholds for recruitment overfishing. ICES J. Mar. Sci. **51**: 191–205.

Myers, R., Bowen, K.G., and Barrowman, N. 1999. Maximum reproductive rate of fish at low population sizes. Can. J. Fish. Aquat. Sci. **56**: 2404–2419.

NEFSC. 2002*a*. Working Group Report, re-evaluation of biological reference points for New England groundfish. Ref. Doc. 02-04. National Marine Fisheries Service, Northeast Fisheries Science Center, Woods Hole, Mass. Available at http://www.nefsc.nmfs.gov/nefsc/publications/crd/crd0204/.

NEFSC. 2002*b*. Assessment of 20 northeast groundfish stocks through 2001. A report of the Groundfish Assessment Review Meeting (GARM), Woods Hole, Massachusetts, 8–11 October 2002. Ref. Doc. 02-16. National Marine Fisheries Service, Northeast Fisheries Science Center, Woods Hole, Mass. Available at http://www.nefsc.nmfs.gov/nefsc/publications/crd/crd0216/.

Otter Research Ltd. 2001. An introduction to AD Model Builder 6.0.2 for use in nonlinear modeling and statistics. Otter Research Ltd., Box 2040, Sidney, BC V8L 3S3, Canada.

Patterson, K.P., Cook, R., Darby, C., Gavaris, S., Kell, L., Lewy, P., Mesnil, B., Punt, A., Restrepo, V., Skagen, D.W., and Stefansson, G. 2001. Estimating uncertainty in fish stock assessment and forecasting. Fish Fish. **2**: 125–157.

Pauly, D. 1995. Anecdotes and the shifting baseline syndrome of fisheries. Trends Ecol. Evol. **10**: 430.

Pauly, D., Christensen, V., Guénette, S., Pitcher, T.J., Sumaila, U.R., Walters, C.J., Watson, R., and Zeller, D. 2002. Towards sustainability in world fisheries. Nature (Lond.), **418**: 689–695.

Quinn, T.J., II, and Deriso, R.B. 1999. Quantitative fish dynamics. Oxford University Press, New York.

Rosenberg, A.A. 2003. Managing to the margins: the overexploitation of fisheries. Front. Ecol. Environ. **1**: 102–106.

Schnute, J.T., and Richards, L.J. 2001. Use and abuse of fishery models. Can. J. Fish. Aquat. Sci. **58**: 10–17.

Schnute, J.T., Richards, L.J., and Olsen, N. 1998. Statistics, software, and fish stock assessment. *In* Proceedings of the International Symposium on Fishery Stock Assessment Models for the 21st Century. *Edited by* F. Funk, T. Quinn II, J. Heifetz, J. Ianelli, J. Powers, J. Schweigert, P. Sullivan, and C.-I. Zhang. Alaska Sea Grant College Program, University of Alaska, Fairbanks, Alaska.

Schwarz, G. 1978. Estimating the dimension of a model. Ann. Stat. **6**: 461–464.

Seber, G.A., and Wild, C.J. 1989. Nonlinear regression. Wiley, New York.

Shepherd, J.G. 1982. A versatile new stock–recruitment relationship for fisheries, and the construction of sustainable yield curves. J. Cons. Int. Explor. Mer, **40**: 67–75.

Sissenwine, M.P., and Shepherd, J.G. 1987. An alternative perspective on recruitment overfishing and biological reference points. Can. J. Fish. Aquat. Sci. **44**: 913–918.

Walters, C.J., and Korman, J. 1999. Linking recruitment to trophic factors: revising the Beverton–Holt model from a life history and multispecies perspective. Rev. Fish Biol. Fish. **9**: 187–202.

Williams, E.H., and Shertzer, K.W. 2003. Implications of life-history invariants for biological reference points used in fishery management. Can. J. Fish. Aquat. Sci. **60**: 710–720.

Appendix A

Spawning biomass per recruit and yield per recruit

Spawning biomass and yield per recruit calculations are two basic components of the rebuilding target models. We used a standard approach for computing spawning biomass and yield per recruit curves (Gabriel et al. 1989). Life history and fishery data for the spawning biomass and yield per recruit calculations were collected from NEFSC (2002*b*) for all three stocks.

Spawning biomass per recruit (SPR) is the sum of expected spawning biomass at age per recruit as a function of survival at age over a cohort's life span. Given a fish stock with $A - 1$ true ages and a plus-group consisting of fish age A and older, SPR depends on spawning weight at age ($W_{S,a}$), fraction mature at age (D_a), natural mortality (M), fishery selectivity at age (P_a), fishing mortality (F), and total mortality at age (Z_a). Note that Z_a is related to M, P_a, and F by $Z_a = M + FP_a$. The probability of a fish surviving to spawn at age a, where a fraction of natural mortality (C_M) and fishing mortality (C_F) occurs before spawning, is the probability of surviving to age a times the probability of surviving to the beginning of the spawning season. Summing the product of the survival to spawn probabilities and the average spawning weights over all age-classes gives an expression for SPR:

$$\text{(A1)}\quad \mathrm{SPR} = \sum_{a=1}^{A-1} D_a W_{S,a} \exp\left(-C_M M - (a-1)M - C_F P_a F - F\sum_{k=1}^{a-1} P_k\right) + D_A W_{S,A} \frac{\exp\left(-C_M M - (A-1)M - C_F P_A F - F\sum_{k=1}^{A-1} P_k\right)}{1 - \exp(-Z_A)}$$

Similarly, yield per recruit (YPR) is the sum of expected yields at age per recruit as a function of survival at age over a cohort's life span. YPR is calculated in an analogous manner as the sum of the product of the probability of survival to age a, the probability that a fish is captured at age a, and the average landed weight at age (W_a):

$$\text{(A2)}\quad \mathrm{YPR} = \sum_{a=1}^{A-1} \frac{W_a P_a F}{Z_a}(1 - \exp(-Z_a)) \exp\left(-(a-1)M - F\sum_{k=1}^{a-1} P_k\right) + \frac{W_A P_A F}{Z_A} \exp\left(-(A-1)M - F\sum_{k=1}^{A-1} P_k\right)$$

Rebuilding target model

We used the Sissenwine–Shepherd age-structured production model to estimate rebuilding targets (Shepherd 1982; Sissenwine and Shepherd 1987). This deterministic equilibrium model requires estimates of spawning biomass per recruit, yield per recruit, and stock–recruitment curves to construct estimates of S_{MSY}. To apply this model to a given fish stock, output recruitment (R) and input spawning stock (S) under a stock–recruitment curve (f) are assumed to be in equilibrium with

© 2005 NRC Canada

respect to a constant fishing mortality rate F. In particular, R is a function of spawning stock, $R = f(S, \theta)$, where θ is the parameter vector of the stock–recruitment curve. At equilibrium, the product of spawning biomass per recruit at F, denoted by $SPR(F)$, and R equals S, i.e., $S(F) = SPR(F)f(S, \theta)$. Solving this equation for S in terms of F and θ implicitly determines equilibrium recruitment as $R(F) = f[S(F), \theta]$. Thus, equilibrium yield (Y) at fishing mortality F is the product of yield per recruit at F ($YPR(F)$) and R, i.e., $Y(F) = YPR(F)R(F)$. The maximum value of $Y(F)$ can be numerically determined by searching over a grid of F values. This determines MSY, S_{MSY}, and F_{MSY}.

Approximate variance of equilibrium spawning biomass

In this section, an expression for the approximate variance of equilibrium spawning biomass is derived. Equilibrium spawning biomass (S^*) is the product of equilibrium recruitment (R^*) and spawning biomass per recruit (SPR^*) at the equilibrium fishing mortality:

$$S^* = R^* SPR^* \quad \text{(A3)}$$

A first-order Taylor series expansion of S^* as a function of R^* and SPR^* approximates the variance of equilibrium spawning biomass ($VAR[S^*]$) in terms of the variances of equilibrium recruitment ($VAR[R^*]$) and spawning biomass per recruit at the equilibrium fishing mortality ($VAR[SPR^*]$) as

$$VAR[S^*] \approx \left(\frac{\partial S^*}{\partial R^*}\right)^2 VAR[R^*] + \left(\frac{\partial S^*}{\partial SPR^*}\right)^2 VAR[SPR^*] \quad \text{(A4)}$$

From eq. A3, the partial derivatives of equilibrium spawning biomass with respect to equilibrium recruitment and spawning biomass per recruit are

$$\frac{\partial S^*}{\partial R^*} = SPR^* \quad \text{and} \quad \frac{\partial S^*}{\partial SPR^*} = R^* \quad \text{(A5)}$$

At equilibrium, the expected values of recruitment and spawning biomass per recruit are constant and equal to R^* and SPR^*. As a result, the coefficients of variation of equilibrium recruitment ($CV[R^*]$) and spawning biomass per recruit at equilibrium fishing mortality ($CV[SPR^*]$) are

$$CV[R^*] = \frac{\sqrt{VAR[R^*]}}{R^*} \quad \text{(A6)}$$

and

$$CV[SPR^*] = \frac{\sqrt{VAR[SPR^*]}}{SPR^*}$$

Solving for R^* and SPR^* in eq. A6 and substituting this result along with eq. A5 into eq. A4 gives the approximate variance of equilibrium spawning biomass in terms of the coefficients of variation of R^* and SPR^* in eq. 7.

Appendix references

Gabriel, W., Sissenwine, M., and Overholtz, W. 1989. Analysis of spawning stock biomass per recruit: an example for Georges Bank haddock. N. Am. J. Fish. Manag. **9**: 383–391.

NEFSC. 2002b. Assessment of 20 northeast groundfish stocks through 2001. A report of the Groundfish Assessment Review Meeting (GARM), Woods Hole, Massachusetts, 8–11 October 2002. Ref. Doc. 02-16. National Marine Fisheries Service, Northeast Fisheries Science Center, Woods Hole, Mass. Available at http://www.nefsc.nmfs.gov/nefsc/publications/crd/crd0216/.

Shepherd, J.G. 1982. A versatile new stock–recruitment relationship for fisheries, and the construction of sustainable yield curves. J. Cons. Int. Explor. Mer, **40**: 67–75.

Sissenwine, M.P., and Shepherd, J.G. 1987. An alternative perspective on recruitment overfishing and biological reference points. Can. J. Fish. Aquat. Sci. **44**: 913–918.

© 2005 NRC Canada

Metal bioaccumulation and oxidative stress in yellow perch (*Perca flavescens*) collected from eight lakes along a metal contamination gradient (Cd, Cu, Zn, Ni)[1]

Anik Giguère, Peter G.C. Campbell, Landis Hare, and Carole Cossu-Leguille

Abstract: Links among metal exposure, metal accumulation, and metal-induced effects were explored in indigenous yellow perch (*Perca flavescens*) collected from eight lakes located along a metal concentration gradient in two mining regions. Fish exposure to Cd, Cu, Ni, and Zn was estimated on the basis of calculated free metal ion concentrations in lake waters. Hepatic metal concentrations were determined and various markers of oxidative stress were measured to assess metal effects in liver cells. Accumulated metals were not consistently related to ambient free metal ion concentrations, possibly because of unaccounted for fluctuations in lake water metal concentrations. Accumulated metals were associated with limited oxidative stress in perch livers, as evidenced by reductions in glutathione concentrations and glutathione reductase activities. However, this stress appeared to be minor, since increasing hepatic Cu concentrations were associated with reduced lipid peroxidation, a response opposite to that predicted from basic principles. Our results suggest that oxidative stress will not have direct repercussions on the health of the perch at the individual level. We speculate that the observed increase in metallothionein concentrations with increasing accumulated metals might afford protection against reactive oxygen species.

Résumé : Des spécimens de perchaude jaune (*Perca flavescens*), récoltés dans huit lacs localisés le long d'un gradient de contamination métallique dans deux régions minières, ont permis d'explorer les liens entre l'exposition aux métaux, leur bioaccumulation et la manifestation de stress oxydatif. L'exposition à quatre métaux (Cd, Cu, Ni et Zn) a été évaluée en dosant les métaux dissous dans chaque lac et en calculant les concentrations d'ions métalliques libres. Les concentrations de métaux et de divers indicateurs de stress oxydatif ont été mesurées dans le foie des poissons, pour y évaluer la bioaccumulation et les effets induits par les métaux accumulés. Les métaux accumulés dans le foie étaient associés à une baisse de la concentration de glutathion et de l'activité de l'enzyme glutathion réductase, suggérant un certain stress oxydatif. Ce stress semble cependant limité, la peroxydation lipidique ayant diminué en fonction de la concentration hépatique en Cu, une réponse contraire aux prédictions. D'après nos résultats, le stress oxydatif ne devrait pas avoir de répercussions directes sur les perchaudes au niveau des individus. Il est possible que l'augmentation des concentrations en métallothionéine, qui se produit le long du gradient de contamination, confère une certaine protection contre les espèces réactives responsables du stress oxydatif.

Introduction

Effects of chemical contaminants can be viewed as occurring at various levels of biological organization, extending from the biochemical level to the physiology of individual organisms and ultimately to the levels of populations, communities, and the ecosystem. Alteration of biochemical systems should underlie and precede effects at higher levels of organization, rendering them potentially useful for monitoring the effects of environmental contamination (Stegeman et al. 1989). Recent reviews (Eason and O'Halloran 2002; Handy et al. 2003) have highlighted the importance of using a weight of evidence approach to assess deterioration of ecosystem health using suites of measurements at the molecular, cellular, physiological, population, and ecosystem levels.

We have been using this approach to evaluate the effects of metals on the health of indigenous yellow perch (*Perca flavescens*) collected in various lakes along a Cd, Cu, Ni, and Zn exposure gradient (reviewed by Campbell et al. 2003). Recently, we demonstrated that some hepatic metals

Received 3 February 2004. Accepted 12 November 2004. Published on the NRC Research Press Web site at http://cjfas.nrc.ca on 12 April 2005.
J17950

A. Giguère, P.G.C. Campbell,[2] and L. Hare. Institut national de la recherche scientifique – Eau, Terre et Environnement (INRS–ETE), Université du Québec, 490 de la Couronne, Québec, QC G1K 9A9, Canada.
C. Cossu-Leguille. Laboratoire EBSE, Faculté des Sciences, Université de Metz, rue du Général Delestraint, F 57070 Metz, France.

[1]Contribution No. 41 from the Metals in the Environment Research Network (www.mite-rn.org).
[2]Corresponding author (e-mail: peter_campbell@inrs-ete.uquebec.ca).

 doi: 10.1139/F04-224 © 2005 NRC Canada

were only partially detoxified by binding to metallothionein (MT) or sequestration in granules and that metal accumulation could be detected in metal-sensitive cytosolic proteins and organelles (A. Giguère, L. Hare, and P.G.C. Campbell, unpublished data). Likely as a consequence of this partial detoxification, metal-induced toxic effects on the fish were observed at the organ, individual, population, and community levels. The present project was designed to complete this picture by determining if there are metal-induced effects in the same indigenous yellow perch at the cellular level through measurements of various markers of oxidative stress and to verify if the eventual responses are proportional to metal exposure.

Biochemical endpoints associated with oxidative stress have long been considered as markers for environmental impact assessment and are recognized as useful in the identification of subtle and early effects of contaminants (Di Guilio et al. 1989; Stegeman et al. 1989; Vasseur and Cossu-Leguille 2003). However, the vast majority of experiments designed to study the mechanisms by which environmental contaminants induce oxidant-mediated responses have been carried out in the laboratory; studies of such responses in free-living organisms are rare, and the existing studies have tended to focus on organic xenobiotics. Few researchers have used measurements of markers of oxidative stress to monitor the effects of exposure of indigenous fish to metals (Rodríguez-Ariza et al. 1993; Lopes et al. 2001; Farag et al. 2003).

To quantify metal exposure and accumulation in indigenous yellow perch, we measured metal concentrations in lake water and metals and other variables in the livers of fish collected from eight lakes located along a Cd, Cu, Ni, and Zn gradient in mining regions in Quebec (Rouyn-Noranda) and Ontario (Sudbury), Canada. Biochemical measurements in perch livers included an indicator of lipid peroxidation (malondialdehyde), the activities of two enzymatic antioxidants (glutathione reductase and glutathione peroxidase), along with the concentration of a nonprotein antioxidant, glutathione. To relate these responses to metal exposure and (or) accumulation, we used regression analyses.

Materials and methods

Study area

Water samples and fish were collected from a total of eight lakes varying in their metal concentrations (especially Cd, Cu, Ni, and Zn). Four lakes in the vicinity of Rouyn-Noranda and four lakes located near Sudbury were sampled in June 2001 (Table 1). These two regions have been subjected to inputs of acidic and metal-rich materials from nearby mining and smelting operations (Sudbury: Ni and Cu; Rouyn-Noranda: Cu, Pb, and Zn).

Metal exposure quantification

Water samples were collected in the epilimnion of each of the eight studied lakes using duplicate in situ diffusion samplers (consisting of eight contiguous cells of 4 mL each) separated from lake water by a 0.2-µm nominal pore size polysulfone membrane (Pall Gelman Sciences HT-200, Pall Corporation, East Hills, New York). The two samplers were suspended 1 m above the lake bottom and at least 1.5 m under the surface in the epilimnion of each lake. They were re-

Table 1. Total dissolved metal concentrations, [M], and free metal ion concentrations, $[M^{2+}]$, dissolved organic C, [DOC], and pH in the epilimnetic water of the studied lakes.

Lake	[Cd] (nmol·L^{-1})	[Cu] (nmol·L^{-1})	[Ni] (nmol·L^{-1})	[Zn] (nmol·L^{-1})	$[Cd^{2+}]$ (nmol·L^{-1})	$[Cu^{2+}]$ (nmol·L^{-1})	$[Ni^{2+}]$ (nmol·L^{-1})	$[Zn^{2+}]$ (nmol·L^{-1})	[DOC] (mg·L^{-1})	[Ca] (µmol·L^{-1})	pH
Default	6.7	180	10	1100	2.3	0.025	4.9	379	5.3	420	7.46
Wavy	1.5	110	900	120	1.2	11	752	100	2.8	40	5.01
Hannah	2.4	370	2500	50	1	0.44	1603	24	3.7	270	7.02
Raft	1.7	130	1820	160	0.88	0.094	1284	80	2.6	90	6.68
Laurentian	0.6	140	840	30	0.26	0.075	518	12	4.6	110	6.37
Osisko	1.6	140	20	110	0.25	<0.001	2.9	3.4	3.1	640	9.54
Vaudray	0.5	42	10	60	0.03	0.001	2.1	5.9	8.8	80	7.20
Opasalica	0.3	33	10	20	0.02	<0.001	3.1	1.7	7.7	220	7.75
Ratio max./min.	22	11	250	55	115	>1×10^5	763	223	3	16	3.4×10^4

Note: The free Cd^{2+}, Cu^{2+}, Zn^{2+}, and Ni^{2+} concentrations were estimated with the Windermere Humic Aqueous Model (WHAM 6.0.1) from total dissolved metal concentrations (including Al and Fe), concentrations of inorganic ligands and organic C, and pH of the water.

© 2005 NRC Canada

trieved after an equilibration period of 3 days and sampled immediately; earlier work had shown that a 3-day period was sufficient to achieve equilibrium between the diffusion samplers and ambient lake water (A. Tessier and R. De Vitre, INRS – Eau, Terre et Environnement, Université du Québec, 490 de la Couronne, Québec, QC G1K 9A9, Canada, unpublished data). Subsamples for analysis of trace metals (Cd, Cu, Zn, Ni, Al, and Fe), major cations (Ca^{2+}, Mg^{2+}, Na^+, and K^+), major anions (SO_4^{2-}, NO_3^-, and Cl^-), and organic and inorganic C were removed from each sampler. Temperature and pH were also measured in water collected 0.5 m under the surface, above the samplers, at the time of retrieval. Analyses of Al, Ca, Fe, and Zn were performed by inductively coupled plasma – atomic emission spectrometry (Varian Vista AX, Varian Inc., Mulgrave, Victoria, Australia). Cadmium, Cu, and Ni were measured using a graphite furnace atomic absorption spectrophotometer equipped with a graphite tube atomizer (PerkinElmer Simaa 6000, PerkinElmer, Uberlingen, Germany) and an autosampler (PerkinElmer model AS-72). Certified reference water samples (riverine water reference material NIST 1643d, National Institute of Standards and Technology, Gaithersburg, Maryland) were also analysed for metals during each analytical run; measured trace metal concentrations were consistently within the certified range for each element. Average concentrations were calculated for each sampler (three cells in each diffusion sampler) resulting in two average concentrations for each lake. Metal speciation at equilibrium was calculated with the Windermere Humic Aqueous Model (WHAM version 6.0.1) (Centre for Hydrology and Ecology 2001; Tipping 1998). This model calculates the equilibrium distribution of a metal among various dissolved inorganic and organic forms (free metal ion, hydroxo-complexes, sulphato-complexes, carbonato-complexes, chloro-complexes, and metals bound to natural dissolved organic matter). Required input data include the total dissolved metal concentrations (including Fe and Al), the total concentrations of inorganic ligands, and the ambient pH. The WHAM model uses semiempirical complexation constants determined from metal titration data obtained under given chemical conditions (ionic strength, metal to ligand ratios, etc.) that can differ from those observed in natural systems. Concentrations of fulvic and humic acids, also required as input data to the model, were estimated from our measurements of dissolved organic C, assuming that humic substances contain 50% C (Tipping et al. 1988) and that the ratio of humic to fulvic acids is 1:9 (Oliver et al. 1983). The original database of inorganic complexation constants provided with WHAM 6.0.1 was compared with recommended values in the US National Institute of Standards and Technology database (Martell and Smith 2001) and modified as necessary.

Fish collection and tissue metal analysis

Yellow perch were collected in June 2001 from the eight studied lakes using a seine net and were kept alive in aerated coolers at a density of ~6 fish·L^{-1} for a period of <3 h, after which they were killed with a blow to the head and immediately dissected. Livers were kept in acid-washed plastic containers and held in liquid nitrogen until analysis. We collected juvenile fish of similar size (7–10 g) to minimize variability related to fish age (Giguère et al. 2004). Two observers evaluated the age of a subsample of 10–18 fish from each lake from a section of the longest ray of the dorsal fin. This procedure yields ages similar to those determined from otoliths (otoliths and the ray of the dorsal fin were compared in yellow perch of all sizes collected in a single lake and in juvenile fish collected in eight lakes: both structures yielded similar results in fish of <3 years old (A. Giguère, L. Hare, and P.G.C. Campbell, unpublished data)).

Liver metal analysis

Livers from 16 perch were combined for each replicate sample (N = 3 replicates per lake) and were homogenized in 0.9% NaCl (purity 99.999%, Alfa Aesar No. 10862, Alfa Aesar, Ward Hill, Massachusetts) using a Potter-Elvehjem homogenizer equipped with a glass pestle (Cole-Parmer U-04368, Labcor, Anjou, Quebec). An aliquot was then taken from the whole homogenate. This aliquot was digested in nitric acid (Fisher Scientific Ltd., Nepean, Ontario, trace metal grade) (~3 mL acid·g tissue^{-1}) in an autoclave at 120–125 °C (1.1–1.3 kg·cm^{-2}) for 3 h. Cooled digestates were then diluted 10-fold with ultrapure water. Certified reference material (lobster hepatopancreas; NRCC TORT-1, Ottawa, Ontario) was submitted to the same procedure. Concentrations of Cd, Cu, and Zn were measured by inductively coupled plasma – atomic emission spectrometry (Varian Vista AX). Blanks indicated negligible contamination (N = 15): Cd < 0.33 µg·L^{-1}, Cu < 0.61 µg·L^{-1}, and Zn = 0.3 µg·L^{-1}. The recovery of TORT-1 reference samples (N = 12) was within the certified range for Cd (100.5 ± 3.8% (SD)) and within 15% of the certified values for Cu (88.6 ± 3.6%) and Zn (89.1 ± 4.3%). Concentrations of Ni were measured with a graphite furnace atomic absorption spectrophotometer (PerkinElmer Simaa 6000, with Zeeman background correction). Digestion blanks indicated negligible Ni contamination (Ni < 0.11 µg·L^{-1}, N = 5). Measurements of Ni in TORT-1 reference samples (N = 2) were within the certified range (95.1%).

Biochemical assays

After thawing on ice, tissues for all biochemical assays were mechanically homogenized. To limit enzymatic protein degradation, we performed all homogenate manipulations at ~4 °C in an ice-cold buffer. All reagents used for buffer preparation were of ACS grade or the equivalent, unless specified otherwise.

Lipid peroxidation was quantified by measuring malondialdehyde concentrations according to the colorimetric method of Sunderman et al. (1985) using tetraethoxypropane (97%) (Sigma T8282, Sigma Chemical Co., St. Louis, Missouri) as an internal standard. This method is based on the reaction of thiobarbituric acid with malondialdehyde and related chromogens. Three livers per replicate (five replicates) were homogenized in KCl (154 mmol·L^{-1}, 3 mL·g tissue wet weight^{-1}) for malondialdehyde analyses.

Glutathione-dependent oxidoreductase enzymes were analysed on the basis of kinetic enzymatic reactions as monitored by spectrophotometric methods. The activity of selenium-independent glutathione peroxidase was measured according to the method of Lawrence and Burk (1976). Reactant concentrations were optimized for perch liver tissues by using 0.2 mmol reduced NADPH·L^{-1}, 1 mmol EDTA·L^{-1}, 1.6 U

© 2005 NRC Canada

glutathione reductase·mL^{-1}, 1 mmol NaN_3·L^{-1}, 5.5 mmol glutathione (GSH, γ-L-glutamyl-L-cysteinyl-glycine)·L^{-1}, and 8 mmol cumene hydroperoxide ($C_6H_5C(CH_3)_2OOH$)·L^{-1}. For the measurement of glutathione peroxidase, five livers per replicate (four replicates) were pooled and homogenized in phosphate buffer (50 mmol·L^{-1}, pH 7, 9 mL·g tissue wet weight^{-1}) containing 1 mmol EDTA·L^{-1}. The activity of glutathione reductase was determined according to the method described by Carlberg and Mannervik (1985), optimized for perch liver by using 30 mmol reduced glutathione (GSH)·L^{-1}. For the measurement of glutathione reductase, five livers per replicate (four replicates per lake) were pooled and homogenized in phosphate buffer (0.2 mol·L^{-1}, pH 7, 9 mL·g tissue wet weight^{-1}) containing 2 mmol EDTA·L^{-1}.

For the measurement of reduced and oxidized glutathione, six livers per replicate (five replicates) were pooled and homogenized in a solution of $HClO_4$ (10%) and EDTA (2 mmol·L^{-1}), with a ratio of 2 mL·g tissue wet weight^{-1}; this solution prevents the oxidation of the glutathione sulphydryl group. The homogenates were then centrifuged at 10 000*g* for 5 min. Reduced and oxidized glutathione were measured in the supernatant using reversed phase liquid chromatography followed by a postcolumn derivatization with *o*-phthalaldehyde according to a method adapted from Leroy et al. (1993) by Cossu et al. (2000). The reduced form (GSH) was evaluated directly after injection of the deproteinized sample; to evaluate total glutathione content (GSH plus GSSG), the biological samples were first reduced using 3.3 mmol dithiothreitol·L^{-1} for 1 h in the dark before injection. Oxidized glutathione (GSSG) levels were determined specifically by forming an adduct between the reduced glutathione contained in the biological sample and *N*-ethylmaleimide: deproteinized samples were incubated with 1.6 mmol *N*-ethylmaleimide·L^{-1} for 5 min at 0 °C and then reduced by dithiothreitol, as described earlier, before the injection. The direct GSSG concentration measure corresponded well to the difference between total (GSH plus GSSG) and reduced (GSH) glutathione concentrations (on average 99.9 ± 0.4% (SD) similarity).

Proteins were measured according to the method of Bradford (1976) using bovine albumin (fraction V, Sigma No. A-4503) as the standard. For this analysis, five livers per replicate (four replicates) were pooled and homogenized in phosphate buffer (0.1 mol·L^{-1}, pH 7.0, 7–16 mL·g tissue wet weight^{-1}).

We also indirectly estimated the concentration of MT-like proteins in the cytosol of the perch livers. Sixteen livers were combined for each replicate sample (N = 3 replicates per lake) and were homogenized in 0.9% NaCl (purity 99.999%, Alfa Aesar No. 10862) at a dilution of 1:2 (*w*/*w*) using a 2-mL Potter-Elvehjem homogenizer equipped with a glass pestle (Cole Parmer U-04368). This homogenate was centrifuged at 100 000*g* for 60 min at 4 °C to yield supernatant S1, which corresponded to the cytosol. The separation of the MT-like proteins from other cytosolic proteins was performed according to Wallace et al. (2003) by (*i*) heating supernatant S1 at 80 °C for 10 min, (*ii*) cooling it on ice for an hour, and (*iii*) centrifuging it at 50 000*g* for 10 min at 4 °C. The heat-stable MT-like proteins remain in the final supernatant (S2). MT concentrations were back-calculated from the concentrations of Cd, Cu, and Zn in the final supernatant S2 using an MT binding capacity of seven atoms of Cd and Zn and 12 atoms of Cu per MT molecule (hepatic [MT] = [Zn in S2]/7 + [Cd in S2]/7 + [Cu in S2]/12). If some of the MT were free in the cytosol, i.e., unbound to metals or undersaturated, this indirect method would underestimate total MT concentrations. However, in practice, hepatic metal concentrations are in excess relative to the concentration of MT binding sites. Given the very high in vitro affinity of MT for metals (stability constants for Cd–MT complexes of ~10^{22} and for Zn–MT of ~10^{18}), appreciable concentrations of unsaturated MT are highly unlikely.

Calculations and statistics

Condition factors were calculated as (WL^{-3}) × 100, where W is fish body weight (grams) and L is fish fork length (centimetres). The exact value of the exponent was calculated to be 2.96 ± 0.07 (SE) ($P < 0.001$) from the nonlinear regression $W = aL^b$ fitted to the data obtained from a previous study on perch of various sizes collected from Lake Osisko (Giguère et al. 2004). Condition factors were calculated from 120 to 300 fish from each lake (Dufault, 298; Hannah, 122; Opasatica, 198; Osisko, 198; Vaudray, 125; Laurentian, 125; Raft, 125; Wavy, 125). Liver somatic indices were calculated as the ratio of liver wet weight (grams) to total body wet weight (grams) for five replicates of three pooled samples from each lake (i.e., one replicate is the weight of three pooled wet livers divided by the weight of the corresponding three pooled whole fish).

Relationships between variables were initially examined in bivariate scatterplots. When bivariate plots indicated a possible linear relationship, a simple regression model was tested using the Statistica computer program (StatSoft Inc. 1999). When bivariate plots appeared to be nonlinear, nonlinear regression models with least-squares fitting were tested using the Sigmaplot computer program (SPSS Inc. 2000); the explained variances were compared with those obtained from a simple regression model. For each of the significant relationships presented (a P level of 0.05 as the threshold for statistical significance), we verified if the residuals were normally distributed and if some outlier values biased the regression coefficients. The proportionality between hepatic Zn and Cd concentrations was tested using simple linear correlation (Pearson's r) and no outliers were identified when the scatterplot of the correlation was examined.

Results

Metal exposure and bioaccumulation

Important gradients in ambient free metal ion (M^{2+}) concentrations between the least and most contaminated lakes were found for the four studied metals (Table 1). Measurements of dissolved Ni concentrations confirmed that this metal only exceeded background levels in the lakes located in the Sudbury area (Hannah, Laurentian, Raft, and Wavy).

Hepatic Ni concentrations were significantly related (r^2 = 0.53, P = 0.04) to free Ni^{2+} concentrations (Fig. 1*d*). In contrast, total Cd, Cu, and Zn accumulations in the liver were not significantly related ($P > 0.05$) to the corresponding ambient free metal ion concentrations (Figs. 1*a*–1*c*) or to total dissolved metal concentrations (data not shown). We tested

© 2005 NRC Canada

Fig. 1. Relationships between metal concentrations in the livers of yellow perch (*Perca flavescens*) and free metal ion concentrations in lakes from the Rouyn-Noranda area (●) and in lakes from the Sudbury area (○). The broken line in Fig. 1*a* represents the former relationship obtained with fish collected in 2000 in Rouyn-Noranda. Each point represents data for fish collected from a single lake in 2001 (mean ± SD, $N = 3$ composite samples of 16 individuals). Lakes: DU, Dufault; LA, Laurentian; HA, Hannah; OP, Opasatica; OS, Osisko; RA, Raft; VA, Vaudray; WA, Wavy.

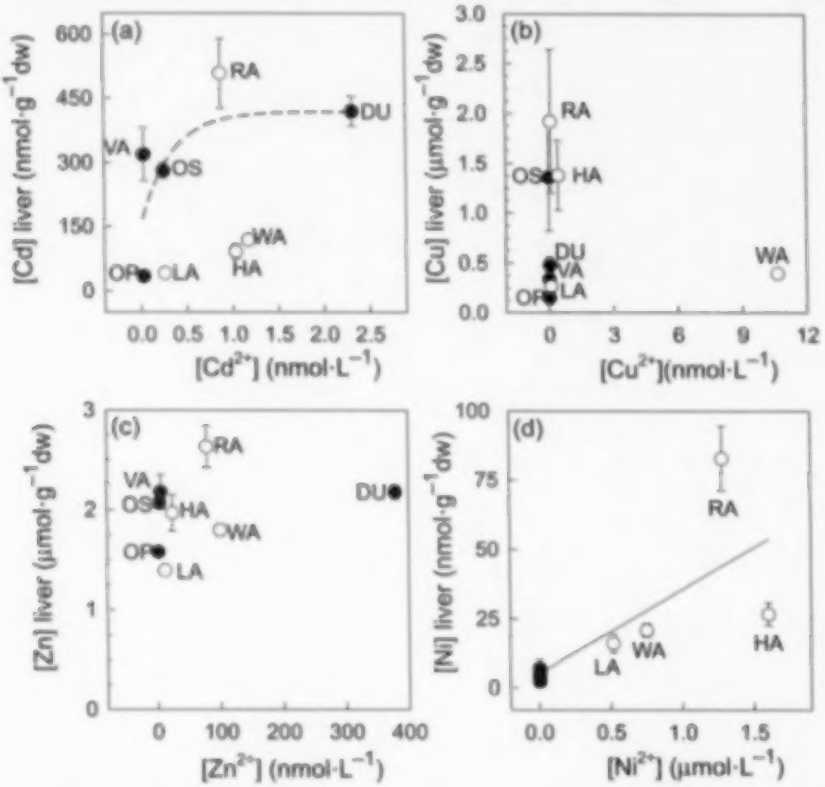

possible competition between M^{2+} concentrations and Ca^{2+}, H^+, or other metals at biological uptake sites to explain the lack of significant relationships between aqueous Cd, Cu, and Zn and the concentrations of these metals in perch (as explained in Giguère et al. 2004). Taking into account such potential ionic competition did not yield significant relationships between hepatic and aqueous metal concentrations. For Cd bioaccumulation (Fig. 1*a*), the exposure–accumulation relationships appear to differ between the two sampling regions. The concentrations of Cd in perch livers from the Rouyn-Noranda area reached a maximum of ~400 nmol·g dry weight^{-1} (Fig. 1*a*), which is similar to that observed for fish sampled from eight lakes the previous year (Giguère et al. 2004; the four Rouyn-Noranda lakes in the present study are a subset of the original group of eight lakes). For fish sampled in Sudbury, such a trend is not apparent, likely because hepatic metal concentrations in fish collected in Wavy and Hannah (Fig. 1*a*, open circles) are low in comparison with those from the other lakes.

Fish age

Average age (± SD) of the fish collected from each lake was 1 year old for Dufault (1.2 ± 0.4, $N = 15$), Hannah (1.0 ± 0.0, $N = 15$), Laurentian (1.3 ± 0.6, $N = 14$), and Osisko (1.1 ± 0.3, $N = 10$) and 2 years old for Opasatica (2.2 ± 0.4, $N = 14$), Raft (2.3 ± 0.9, $N = 14$), Wavy (1.5 ± 0.7, $N = 15$), and Vaudray (1.5 ± 0.5, $N = 18$).

Lipid peroxidation and antioxidant defences

Lipid peroxidation results in the production of a complex mixture of lipid degradation by-products (malondialdehyde and other aldehydes) (Roméo et al. 2000). We evaluated lipid peroxidation in liver cells using the concentrations of one of these lipid peroxidation by-products, malondialdehyde (also referred to as TBARS in some studies because of the assay method, which involves the use of thiobarbituric acid). Although malondialdehyde concentrations tended to decrease as all hepatic metal concentrations increased, the only significant relationship was between malondialdehyde and hepatic Cu concentrations ($P < 0.05$) (Fig. 2*b*). The two sampling regions contributed equally to this relationship.

Overall, for the two sampling regions, we observed significant negative relationships between total glutathione concentrations (GSH plus GSSG) and hepatic Cd (Fig. 3*a*) or Zn concentrations (Fig. 3*c*); comparable relationships were not significant for Cu and Ni concentrations. Furthermore, GSH concentrations in the liver decreased as hepatic Cd or Zn concentrations increased (Figs. 4*a* and 4*c*) but they were not related to hepatic Cu or Ni concentrations (Figs. 4*b* and 4*d*). Note that hepatic Cd and Zn concentrations showed a

© 2005 NRC Canada

Fig. 2. Relationships between the concentrations of malondialdehyde (MDA) and metals in the livers of yellow perch (*Perca flavescens*) collected in lakes near Rouyn-Noranda (●) and Sudbury (○). Each point represents data for fish collected in a single lake (mean ± SD, $N = 5$ composite subsamples of three individuals). Lakes: DU, Dufault; LA, Laurentian; HA, Hannah; OP, Opasatica; OS, Osisko; RA, Raft; VA, Vaudray; WA, Wavy. Regression in Fig. 2*b*: $y = 139x^{0.3}$ ($r^2 = 0.61$, $P = 0.02$).

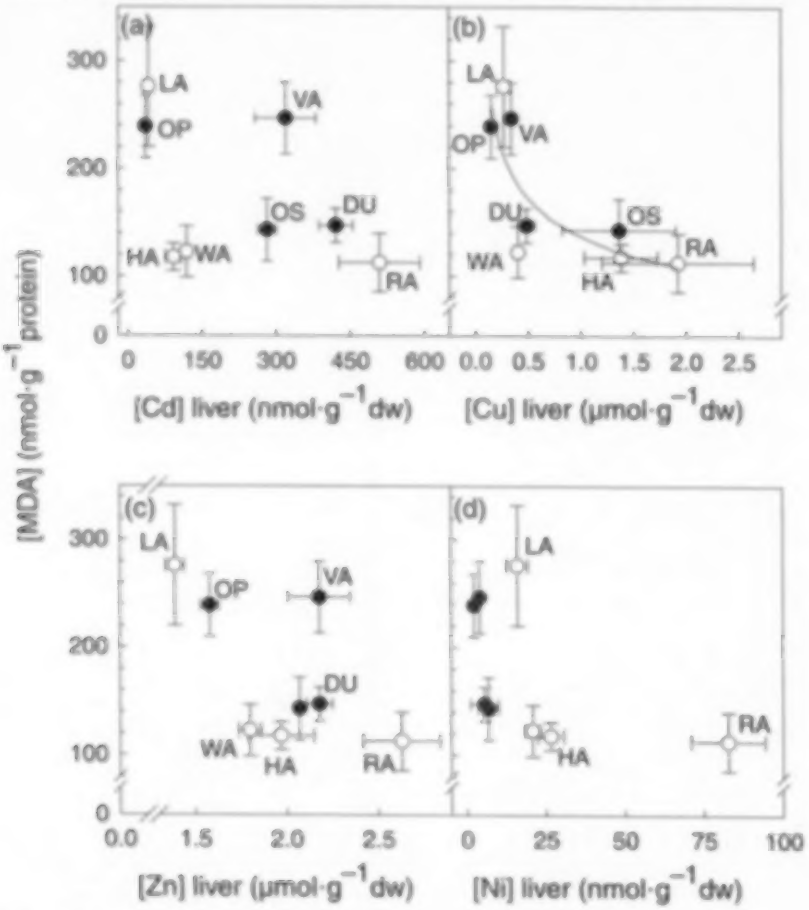

strong positive correlation (Pearson's correlation coefficient of 0.92, $P < 0.005$), a result that precludes the unambiguous identification of one or the other metal as the causative factor. On further examination of the data, it is clear that the negative relationship between GSH concentrations and hepatic Cd or Zn concentrations can be ascribed solely to the lakes from the Sudbury area (Fig. 4). Indeed, hepatic GSH in the fish collected from the Sudbury lakes was linked to the concentrations of each of the four metals, including Cu and Ni. In contrast, metal exposure did not appear to affect hepatic glutathione concentrations in perch from the Rouyn-Noranda lakes.

Concentrations of GSSG were not related to any of the measured hepatic metal concentrations in the pooled regions (results not shown). However, whereas hepatic GSSG was unrelated to metal concentrations in the fish collected in Sudbury, it tended to decrease with increases in hepatic Cd or Zn concentrations in the fish collected from the Rouyn-Noranda lakes. To integrate these two responses, we calculated the ratio of GSH to GSSG concentrations; the ratio varied between 0.9 (Opasatica) and 4.6 (Vaudray and Laurentian). A general decreasing trend in the value of this ratio with increasing metal concentrations was observed in the livers of fish collected in the Sudbury lakes, whereas it tended to increase with increasing hepatic metal levels in perch collected in the Rouyn-Noranda lakes (results not shown).

In the livers of fish from the combined sampling regions, glutathione reductase activity decreased as liver Cu concentrations increased (Fig. 5*b*), whereas it was not linked to concentrations of liver Cd, Zn, or Ni (Figs. 5*a*, 5*c*, and 5*d*). In fish collected in the Sudbury region, this decrease in glutathione reductase activity was observed for all four metals. However, none of the measured hepatic metal concentrations helped explain the variability of glutathione peroxidase activity in the liver (results not shown), which varied between 2.6 ± 0.2 (SD) and 3.5 ± 0.9 U·g protein^{-1}. An increase in MT concentrations with the sum of the concentrations of Cd, Cu, and Zn in the whole liver was also observed (Fig. 6).

For the two sampling regions, fish condition factor decreased with an increase in the natural logarithm of hepatic

© 2005 NRC Canada

Fig. 3. Relationships between the sum of the concentrations of reduced and oxidized glutathione (GSH + GSSG) and metals in the livers of yellow perch (*Perca flavescens*) collected in lakes near Rouyn-Noranda (●) and Sudbury (○). Each point represents data for fish from a single lake (mean ± SD, $N = 5$ composite subsamples of six individuals). Lakes: DU, Dufault; LA, Laurentian; HA, Hannah; OP, Opasatica; OS, Osisko; RA, Raft; VA, Vaudray; WA, Wavy. Regression in Fig. 3a: $r^2 = 0.81$, $P = 0.002$; regression in Fig. 3c: $r^2 = 0.73$, $P = 0.007$.

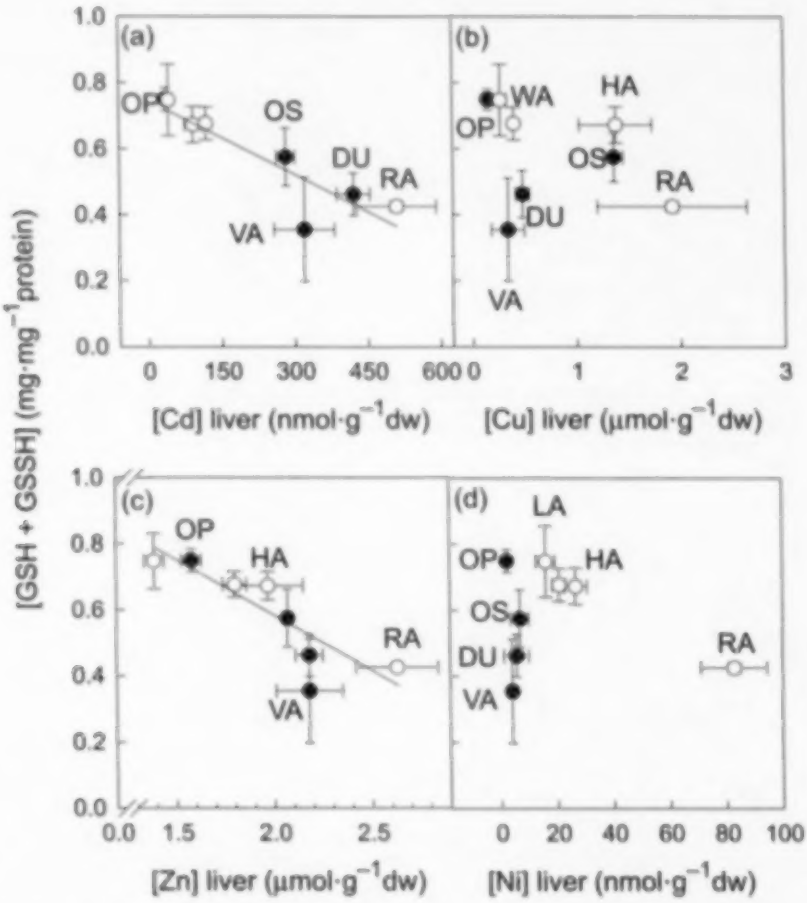

Ni concentrations ($r^2 = 0.58$, $P = 0.03$) (Fig. 7*a*); fish condition was not related to the concentration of any other hepatic metal. The liver somatic index did not vary greatly and was unrelated to any of the hepatic metal concentrations (Fig. 7*b*).

Discussion

Metal exposure and bioaccumulation

In an initial study of yellow perch from eight lakes in the Rouyn-Noranda area, we were able to explain most of the interlake variability in metal bioaccumulation (Cd, Cu, and Zn) in terms of changes in the concentrations of the ambient free metal ion and Ca (Giguère et al. 2004). However, using these same variables, we could not explain the trends in metal bioaccumulation in the present study, which included four new lakes from the Sudbury area. The influence of metal bioavailability on the exposure–bioaccumulation relationships was minimized by measuring concentrations of dissolved organic C and inorganic ligands, together with pH, to calculate the ambient free metal ion concentrations. Similarly, given that hardness cations (Ca^{2+} and Mg^{2+}) and the proton (H^+) are known to inhibit trace metal uptake by a variety of aquatic organisms, we took into account possible competition from these cationic species for binding to metal uptake sites (Croteau et al. 1998; Di Toro et al. 2001). The influence of the metabolic status of the studied species (age, water temperature, and reproductive cycles) was also minimized by collecting fish of the same age-class (1–2 years old) at the same time of the year (June). Lastly, the variation that could be due to metals in various food types was minimized by collecting an age-class of yellow perch that is recognized as uniformly planktivorous in Rouyn-Noranda lakes (Sherwood et al. 2002). However, despite all of these considerations, aqueous metal exposure could not explain hepatic metal bioaccumulation in perch collected across the two sampling areas.

If dietary exposure to metals were important for wild fish (Giguère et al. 2004), then relationships between aqueous exposure and bioaccumulation might well be masked by the influence of the food vector. In such cases, exposure–

© 2005 NRC Canada

Fig. 4. Relationships between the concentrations of glutathione (GSH) and metals in the livers of yellow perch (*Perca flavescens*) collected in lakes near Rouyn-Noranda (●) and Sudbury (○). Each point represents data for fish collected in a single lake (mean ± SD, $N = 5$ composite subsamples of six individuals). Lakes: DU, Dufault; LA, Laurentian; HA, Hannah; OP, Opasatica; OS, Osisko; RA, Raft; VA, Vaudray; WA, Wavy. Regression in Fig. 4a: $r^2 = 0.52$, $P = 0.04$; regression in Fig. 4c: $r^2 = 0.53$, $P = 0.04$.

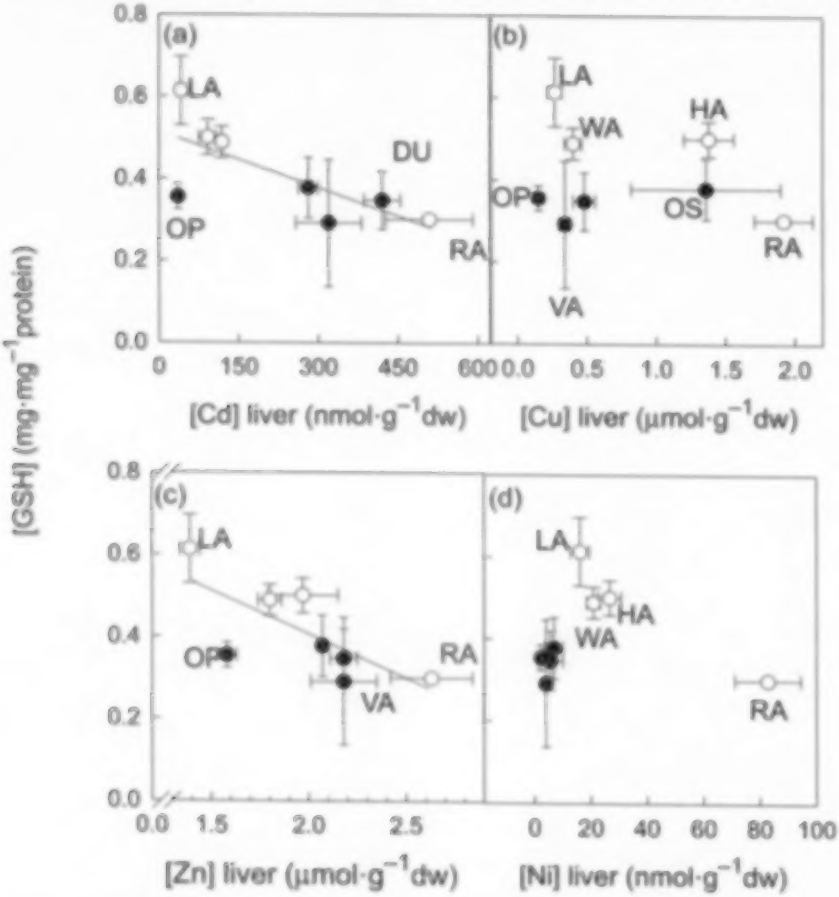

bioaccumulation relationships might be improved by taking into account differences in prey type and prey metal concentrations among lakes (Croteau et al. 2003). Also, we cannot exclude possible genetic differences among fish populations in the various lakes. Note, too, that different metal mixtures are present in the lakes of the two sampling regions: the Rouyn-Noranda lakes are contaminated mostly by Cd and Zn, whereas the Sudbury lakes are contaminated mostly by Cd, Cu, and Ni. These different exposure regimes could lead to physiological differences in the handling of metals by perch, but this research area has been little investigated.

Another complication inherent in the study of field-exposed organisms is that metal concentrations in lake water vary over time. Metal concentrations in fish organs will not fluctuate as rapidly as those in lake water. This lag between exposure and accumulation is more important in the liver, which integrates exposure over a long period of time, than in the organs responsible for uptake such as the gills and gastrointestinal tract. For example, when juvenile yellow perch were transplanted from an uncontaminated reference lake to a metal-contaminated lake, hepatic Cd concentrations in the transplanted fish still had not reached the levels measured in the indigenous fish after 30 days of exposure (L. Kraemer, INRS – Eau, Terre et Environnement, 490 de la Couronne, Québec, QC G1K 9A9, Canada, personal communication). Consequently, a 3-day mean measure of ambient Cd^{2+} concentrations, as determined in the present study, would not necessarily represent the true seasonal exposure regime. Lastly, attempting to predict trace element concentrations in animal organs based on those in water may be too simplistic; this approach is insensitive to changes in the pathway of metal accumulation and ignores the internal redistribution of metals as well as the physiological condition of the animal and changes in mechanisms of metal excretion as bioaccumulated metal concentrations increase.

Lipid peroxidation

Lipid peroxides are formed from the oxidative deterioration of polyunsaturated lipids in the membranes of cells and organelles. Lipid peroxidation by-products, such as malondialdehyde, are used as indicators of increases in the concentrations of cellular reactive oxygen species and as

© 2005 NRC Canada

Fig. 5. Relationships between the activity of glutathione reductase and metals in the livers of yellow perch (*Perca flavescens*) collected in lakes near Rouyn-Noranda (●) and Sudbury (○). Each point represents data for fish collected in a single lake (mean ± SD, $N = 4$ composite subsamples of five individuals). Lakes: DU, Dufault; LA, Laurentian; HA, Hannah; OP, Opasatica; OS, Osisko; RA, Raft; VA, Vaudray; WA, Wavy. Regression in Fig. 5*b*: $r^2 = 0.52$, $P = 0.04$.

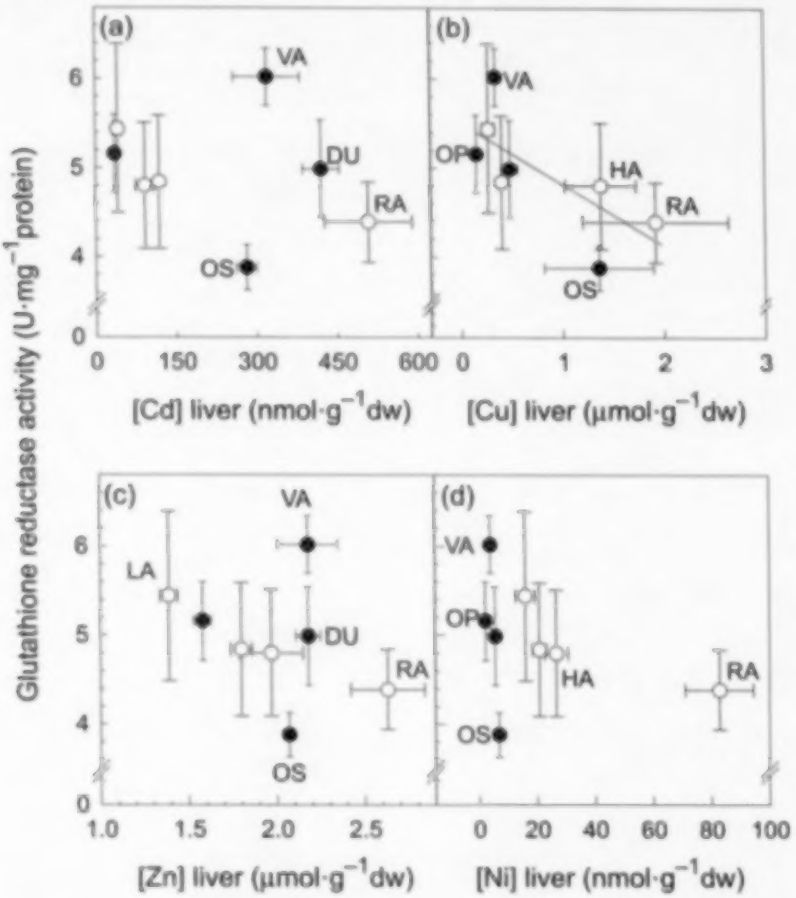

signs of cellular injuries in general (Christie and Costa 1984). Diverse contaminants can initiate lipid peroxidation, including metals and some organic contaminants. One might predict that among Cd, Cu, and Zn, Cu would be the most likely to enhance lipid peroxidation (Di Guilio et al. 1989). Indeed, in biological systems, Cu will readily cycle between the cupric (Cu^{2+}) and the cuprous (Cu^{+}) oxidation states, an activity that has been associated with the generation of hydroxyl radicals ($^{\bullet}OH$) (Halliwell and Gutteridge 1984). In principle, Ni^{2+} and Ni^{3+} may also undergo redox cycling, especially when bound to peptides, and thus catalyze the reduction of hydrogen peroxide leading to hydroxyl radical generation (Torreilles and Guerin 1990). Metals such as Cd or Zn can also indirectly affect the intracellular redox balance and enhance lipid peroxidation of cells, since they can inhibit antioxidant enzymes (Pruell and Engelhardt 1980; Reddy et al. 1981) and inactivate glutathione (Christie and Costa 1984).

In the present study, however, increasing hepatic Cu concentrations were associated with reduced lipid peroxidation, as estimated from malondialdehyde concentrations, a response opposite to the one predicted from basic principles. Most studies to date on the effects of metals on lipid peroxidation in fish have been performed in the laboratory. Some have reported increases in lipid peroxidation with increasing metal exposure (in the liver following a chronic waterborne Cd exposure of Atlantic croaker (*Micropogonias undulatus*): Wofford and Thomas 1988; in the liver following a chronic waterborne Pb exposure of Indian catfish (*Heteropneustes fossilis*): Chaurasia and Kar 1999; in the kidney following a Cu intraperitoneal injection of sea bass (*Dicentrarchus labrax*): Roméo et al. 2000; in the plasma following a diet-borne Ni exposure of lake trout (*Salvelinus namaycush*): Ptashynski et al. 2001). Other workers have reported no significant response in the liver following either a waterborne or diet-borne exposure (to Cd, Cu, Pb, and Zn in rainbow trout (*Oncorhyncus mykiss*): Farag et al. 1994; to Cd in Atlantic croaker: Thomas and Wofford 1993) or after intraperitoneal administration of the metals (rainbow trout: Tort et al. 1996; sea bass: Roméo et al. 2000).

There have been few studies in which the oxidative stress generated by exposure to metals was measured in indigenous

© 2005 NRC Canada

Fig. 6. Estimated metallothionein (MT) concentrations in the liver cytosol of juvenile yellow perch (*Perca flavescens*) collected in four lakes located in the Sudbury area and in four lakes in the Rouyn-Noranda area in relation to the total concentration of Cd, Cu, and Zn in the whole liver. Lakes: DU, Dufault; LA, Laurentian; HA, Hannah; OP, Opasatica; OS, Osisko; RA, Raft; VA, Vaudray; WA, Wavy. MT concentrations were estimated from Cd, Cu, and Zn concentrations measured in the metallothionein-like subcellular fraction separated using differential centrifugation. An MT-binding capacity of seven atoms of Cd and Zn and 12 atoms of Cu per MT molecule was used to perform the calculation.

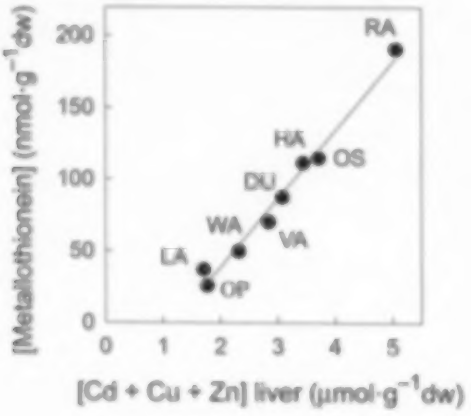

fish. Farag et al. (1995) reported an increase in hepatic lipid peroxidation in brown trout (*Salmo trutta*) exposed in nature to Cd, Cu, and As, even though they measured hepatic Cd concentrations 20-fold lower and Cu concentrations fivefold lower than those measured in yellow perch in the present study. However, in a second study, Farag et al. (2003) reported a similar increase in lipid peroxidation in rainbow trout having hepatic Cd, Cu, and Zn concentrations similar to those that we measured in perch. In contrast, Rodríguez-Ariza et al. (1993) measured a reduction in the concentration of malondialdehyde in indigenous mullet (*Mugil* sp.) exposed to a combination of Cu (hepatic concentrations slightly higher than those measured in the present study), Fe, and organic contaminants, i.e., the same response that we observed for perch. This hormesis-like response could reflect a stimulation of antioxidant mechanisms to a level exceeding the strict needs of the cells to counter the increase in reactive oxygen species resulting from exposure to Cu. In agreement with this model, Rodríguez-Ariza et al. (1993) measured increases in antioxidant enzyme activities (including glutathione reductase and glutathione peroxidase) that could explain the corresponding decrease in malondialdehyde concentrations measured in exposed fish. We also measured several antioxidants to test this possibility, and these results are discussed below.

Antioxidant defences

Various endogenous antioxidants protect against the propagation of oxyradical reactions in organisms: enzymatic antioxidants, including glutathione reductase and glutathione peroxidase, and nonenzymatic antioxidants such as ascorbic acid, glutathione, and tocopherols.

Enzymatic antioxidants

Glutathione reductase supplies reducing equivalents in the form of reduced glutathione and thus is responsible for maintaining an optimum GSH to GSSG ratio (or redox status), the value of which could serve as a biomarker (Bus and Gibson 1979; Stegeman et al. 1989) (Fig. 8). The normal value of this ratio varies among taxa, i.e., it is ~10 in rat liver cells (Kosower and Kosower 1978), 3–5 in the digestive gland of a freshwater bivalve (Cossu et al. 2000), and ~30 in the liver of rainbow trout (Lange et al. 2002). We measured ratios of 1–5 in yellow perch. Because ours is the first report of measurements for this species, we cannot determine if the ratios that we observed indicate a perturbation of the liver cells' glutathione status or if they are within the acceptable range for this species.

To our knowledge, the only study in which glutathione reductase activity was measured in fish exposed to metals is that of Rodríguez-Ariza et al. (1993), who reported enhanced activities of this enzyme following exposure to multiple xenobiotics. In the present study, however, the measured glutathione reductase activities did not help to explain the hormesis-like response in malondialdehyde concentrations, since they did not increase with increasing metal concentrations but rather decreased with increasing hepatic Cu concentrations. This decrease in glutathione reductase activity might reflect metal binding to the enzyme functional group. For example, Christie and Costa (1984) demonstrated that Cu^{2+} could inhibit glutathione reductase activity in vitro. Reductase activity could also be affected by a decrease in the concentration of its second substrate, NADPH; Brigelius (1985) reported that oxidative stress could lower NADPH concentrations. Furthermore, the activity of the enzyme glucose-6-phosphate dehydrogenase, which catalyzes the reduction of $NADP^+$ to NADPH (Fig. 8), remained low in summer in yellow perch livers collected from contaminated lakes, whereas higher levels were measured in perch from the reference lakes (Levesque et al. 2002).

Glutathione peroxidase can limit the propagation of reduced reactive oxygen species by reducing lipid hydroperoxides to stable alcohols and by removing hydrogen peroxide formed in the cytosol (Bus and Gibson 1979). Generally, the activity of antioxidant enzymes such as glutathione peroxidase is induced in the liver following the exposure of fish to metals (waterborne exposure to Cu or Zn in carp (*Cyprinus carpio morpha*): Radi and Matkovics 1988; waterborne and diet-borne exposure to Cu, Fe, and organic contaminants in indigenous grey mullet: Rodríguez-Ariza et al. 1993; waterborne exposure to Cd in Nile tilapia (*Oreochromis niloticus*): Almeida et al. 2002). This induction can serve as an important acclimation mechanism under these conditions (Di Guilio et al. 1989). However, several authors also reported a status quo in glutathione peroxidase activity in the liver of fish following metal exposure (three fish species following a whole-lake Cd addition experiment: Palace and Klaverkamp 1993; chronic waterborne Cd exposure of rainbow trout: Palace et al. 1993). In the present study, exposure to metals did not appear to affect the activity of gluta-

© 2005 NRC Canada

Fig. 7. Relationships between (*a*) the condition factor of indigenous yellow perch (*Perca flavescens*) and the natural logarithm of total hepatic Ni concentrations and (*b*) the hepatosomatic index and total hepatic Ni concentrations in yellow perch sampled in lakes near Rouyn-Noranda (●) and Sudbury (○).

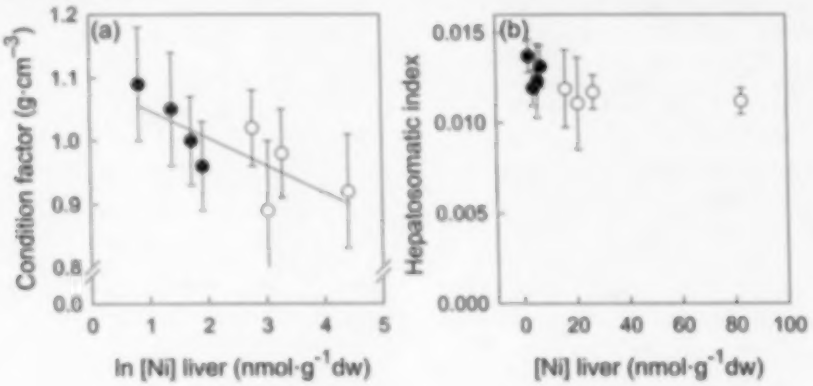

thione peroxidase, and thus, the response of this antioxidant cannot help to explain the decreasing concentrations of malondialdehyde with increasing hepatic Cu concentrations.

Glutathione

Glutathione is a sulphydryl-rich tripeptide that serves several vital functions, including scavenging reactive oxygen species, serving as a substrate for glutathione peroxidase, and maintaining the intracellular redox balance and essential thiol status of proteins (Stegeman et al. 1989) (Fig. 8). Given its known affinity for "soft" metal ions, it can also act as an intracellular metal chelator, thereby preventing the electrophilic interaction of metals with essential cellular structures (Maracine and Segner 1998).

We could find no reports in which GSH concentrations had been measured in indigenous fish that were chronically exposed to metals in their natural habitat, but there have been a number of laboratory investigations of metal–GSH relationships. Most such studies report an increase in hepatic GSH concentrations following exposure to Cd, whether exposure was performed in vitro (Schlenk and Rice 1998), in vivo through intraperitoneal administration (rainbow trout: Tort et al. 1996), or following chronic waterborne exposure (mullet: Thomas et al. 1982; Thomas and Wofford 1984; blue tilapia (*Oreochromis aureus*): Allen 1995). A few investigators have reported no variation in hepatic GSH concentrations following either in vitro exposure (to Zn: Schlenk and Rice 1998) or waterborne exposure (to Cd in Atlantic croaker: Thomas and Wofford 1993; to Cd or Zn in rainbow trout: Lange et al. 2002).

In the present study, GSH concentrations and total glutathione (GSH plus GSSG) concentrations tended to decrease in response to increasing metal concentrations (Cd and Zn) in the perch liver, and thus, variations in GSH do not help explain the hormesis-like decrease in malondialdehyde concentrations with increasing hepatic Cu concentrations. We note, however, that there are differences between our study regions. In Sudbury, the decrease in total glutathione (GSH plus GSSG) concentrations with increasing hepatic Cd and Zn was due to a reduction in GSH concentrations, whereas in Rouyn-Noranda, it was due to a reduction in GSSG concentrations. Glutathione concentrations were uniformly low in fish from lakes having high aqueous metal concentrations, which suggests that GSH is kept at low levels in the presence of excess metals. In contrast, GSH concentrations in fish from reference lakes varied widely, suggesting that other factors (such as variable nutrition) may have influenced GSH concentrations in these uncontaminated lakes. Luoma (1996) reported a similar type of trend in a marine system, i.e., the scope for growth of bivalves varied greatly at low metal concentrations but was uniformly low at high metal concentrations.

We consider three mechanisms that might explain the observed decrease in GSH concentrations with increasing hepatic metal concentrations (Cd, Cu, Zn, and (or) Ni) in Sudbury lakes. First, whereas GSH concentrations tended to decrease with increasing hepatic metal concentrations in Sudbury fish, there was also a concomitant trend towards a decrease in glutathione reductase activity with increasing metal concentrations (Cu and (or) Ni). Furthermore, glutathione concentrations tended to increase with the activity of glutathione reductase in fish from Sudbury lakes. These observations support a model of cytotoxicity in which exposure to metals inhibits the activity of the enzyme glutathione reductase, leading to a reduction in the concentrations of GSH. It should, however, be pointed out that this model is undermined by the observation that fish collected in the Rouyn-Noranda lakes did not experience an equivalent decrease in GSH concentrations with increasing Cu, whereas they did exhibit decreasing glutathione reductase activity with increasing Cu concentrations. Second, the redox cycling of Cu^{+} and Cu^{2+} or of Ni^{2+} and Ni^{3+} (or peptide-bound Ni) could directly catalyze the reduction of hydrogen peroxide, leading to free oxygen radical generation in the livers of fish sampled from the Sudbury lakes. The increase in reactive oxygen species following Cu and (or) Ni exposure would result in an oxidation of glutathione. Aside from well-documented lipid peroxidation in animals exposed to Cu (discussed above), there are several reports of GSH concentrations and glutathione reductase activity in the liver and kidney of rats following intraperitoneal administration of Ni (reviewed in Chakrabarti and Bai 1999). Lastly, the forma-

© 2005 NRC Canada

Fig. 8. Some antioxidant defence mechanisms against reactive oxygen species in animal cells. Lipid peroxidation chain reactions are illustrated at the bottom: the lipid radical $^{\bullet}L$ reacts readily with oxygen to produce the peroxy radical L-OO$^{\bullet}$. This radical can remove a hydrogen from another polyunsaturated lipid, LH, yielding a lipid hydroperoxide, lipid-OOH, and a new $^{\bullet}L$, which can then continue the chain reaction, propagating additional L-OOH and $^{\bullet}L$. Figure modified from Bus and Gibson (1979) and Stegeman et al. (1989).

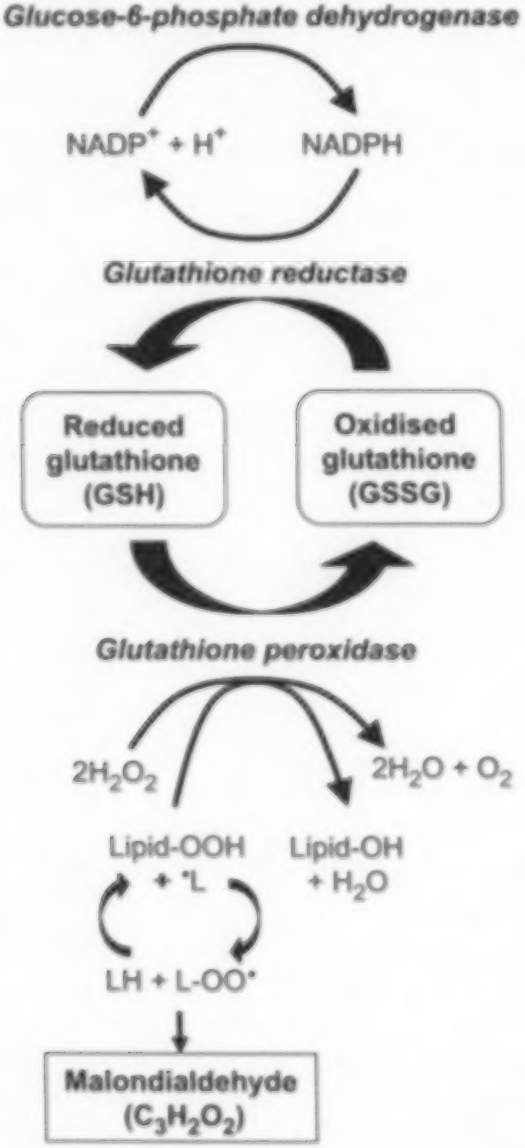

tion of glutathione conjugates with soft metals such as Hg, Cd, and Cu could be responsible for a reduction in the efficacy of glutathione as an antioxidant, since it has a high affinity for these metals (Maracine and Segner 1998; Lange et al. 2002). However, such binding cannot explain the observed decrease in GSH concentrations along the metal gradient; the GSH assay involves a preliminary acidification step, and thus, both free GSH and metal-bound GSH are measured.

MTs

The concentrations of MT-like proteins in perch increased with increasing hepatic metal concentrations (cf. Laflamme et al. 2000). Elevated MT levels could explain in part the apparent hormetic response whereby malondialdehyde concentrations decrease as hepatic Cu concentrations increase. Indeed, MTs are characterized by an important proportion of cysteinyl residues (~30%), which serve as ligands for metal chelation but also trap reactive oxygen species (particularly $^{\bullet}OH$) efficiently (Sato and Bremner 1993). MTs may be induced in response to oxidative stress (reviewed in Sato and Bremner 1993) or protect against oxidative stress once induced by metal exposure, as has been demonstrated by in vitro studies on various fish cell lines (Kling et al. 1996; Schlenk and Rice 1998; Wright et al. 2000). In their review of the antioxidant role of MTs, Viarengo et al. (2000) suggested that MT can act not only by inactivating reactive oxygen species but also by reducing cytosolic levels of prooxidant metals such as Cu and Fe and by releasing Zn, which is known to play a role in stabilizing cell membranes. Thomas et al. (1986), using human erythrocytes, demonstrated that as the thiolate bonds in MT are oxidized, metals that were initially bound to them are released. If MTs were truly responsible for the observed reduction in oxidative stress, they would therefore have a second beneficial effect in metal-exposed perch besides their well-documented role of metal sequestration.

Condition factor and hepatosomatic index

The observed reduction of the condition factor of yellow perch with increasing liver Ni concentrations signals deterioration in the health of the fish exposed to Ni relative to fish from reference lakes. This result coincides with an increase in the concentrations of Ni bound to metal-sensitive subcellular fractions, namely the enzymes fraction, observed in perch from contaminated lakes (A. Giguère, L. Hare, and P.G.C. Campbell, unpublished data). A metal exposure related decrease in condition factor was also observed in other studies on perch collected in metal-contaminated lakes (Rouyn-Noranda: Laflamme et al. 2000; Levesque et al. 2002; Giguère et al. 2004; Sudbury: Eastwood and Couture 2002; Rajotte and Couture 2002; Audet and Couture 2003). Whereas Giguère et al. (2004) related decreasing condition factors to Cd only (among three metals), the other studies did not relate this trend to the concentration of any particular metal. The condition factor of native fish reflects their energy reserves such as stored liver glycogen and body fat (Goede and Barton 1990). Sherwood et al. (2000) indeed measured a lower specific growth rate in yellow perch from contaminated lakes in Rouyn-Noranda relative to those from reference lakes, suggesting that these fish experienced greater energetic costs. In addition, Levesque et al. (2002) observed altered glycogen reserve cycling and an inability to increase the lipid levels in yellow perch from our most contaminated lakes, which may have contributed to the observed decrease in condition factor.

© 2005 NRC Canada

Results from the present study provide further support for the use of condition factors as an indicator of effects in metal-contaminated yellow perch but do not support the use of the hepatosomatic index as a means to this end (Couture and Rajotte 2003).

In summary, yellow perch are a promising sentinel organism for metal contamination in Canadian lakes, since they are distributed across the country and they are relatively tolerant to metals and low pH. However, the lack of a relationship between free metal ion concentrations in the lake water and metal concentrations in the livers of the yellow perch calls for further research to establish the limits of this species as a sentinel organism. Along with measurements of accumulated metals, a characterization of the metal exposure regime for at least a complete summer, together with an evaluation of metal concentrations in organisms constituting food for juvenile perch, appear to be the key steps towards a better understanding of metal accumulation in indigenous perch.

Oxidative stress seems to be well controlled in indigenous yellow perch exposed to metals. Indeed, levels of a lipid peroxidation by-product, malondialdehyde, revealed a hormesis-like response in these fish, even though the levels of two antioxidants, glutathione reductase and glutathione, were depressed. Other indicators of lipid peroxidation, such as lysosomal membrane stability, could be monitored to confirm this unexpected response.

MT-like proteins appear to have contributed significantly towards reducing the concentrations of a lipid peroxidation by-product, malondialdehyde, in metal-exposed fish. These proteins have been extensively studied for their detoxification properties, but based on our observations, future studies interested in oxidative stress generated by metals should also consider measuring concentrations of MT for its antioxidant qualities.

The potential of malondialdehyde and glutathione concentrations or of the activities of glutathione reductase and glutathione peroxidase as biomarkers of metal-induced effects is not evident from our results. We measured contradictory responses for these various endpoints in metal-exposed yellow perch. Some of these biomarkers seem to be sensitive to metal exposure (glutathione and glutathione reductase), whereas one did not respond to exposure (glutathione peroxidase) and the other responded in the opposite direction from what was expected (malondialdehyde). It thus appears from our results that accumulated metals may have caused oxidative stress in the livers of indigenous yellow perch, but the decrease in malondialdehyde concentrations along the metal gradient suggests that this stress was controlled by various antioxidants at the cellular level and that thus it was probably not directly responsible for major deleterious effects at the whole-fish level. The added metabolic cost for controlling oxidative stress levels could, however, be indirectly responsible for deleterious effects in the exposed fish.

Acknowledgements

A grant from the Metals in the Environment Research Network supported this project. The Société de la Faune et des Parcs de l'Abitibi-Témiscamingue (Government of Quebec) provided invaluable logistical support. The technical assistance of Sophie Cooper and Amélie Cliche in the field is gratefully acknowledged. Michelle Geoffroy-Bordeleau helped with metal analyses. P.G.C. Campbell is supported by the Canada Research Chair program.

References

Allen, P. 1995. Changes in tissue glutathione levels in the cichlid *Oreochromis aurrus* (Steindachner) following long term exposure to mercury, cadmium and lead. *In* Toxicological and environmental chemistry. *Edited by* O. Hutzinger. Gordon and Breach Science Publishers, Kuala Lumpur, Malaysia. pp. 1–12.

Almeida, J.A., Diniz, Y.S., Marques, S.F.G., Faine, L.A., Ribas, B.O., Burneiko, R.C., and Novelli, E.L.B. 2002. The use of the oxidative stress responses as biomarkers in Nile tilapia (*Oreochromis niloticus*) exposed to in vivo cadmium contamination. Environ. Int. **27**: 673–679.

Audet, D., and Couture, P. 2003. Seasonal variations in tissue metabolic capacities of yellow perch (*Perca flavescens*) from clean and metal-contaminated environments. Can. J. Fish. Aquat. Sci. **60**: 269–278.

Bradford, M.M. 1976. A rapid method for the quantification of microgram quantities of proteins utilizing the principle of protein–dye binding. Anal. Biochem. **72**: 248–254.

Brigelius, R. 1985. Mixed disulfides: biological functions and increase in oxidative stress. *In* Oxidative stress. *Edited by* H. Sies. Academic Press, London, UK. pp. 243–272.

Bus, J.S., and Gibson, J.E. 1979. Lipid peroxidation and its role in toxicology. Rev. Biochem. Toxicol. **1**: 125–149.

Campbell, P.G.C., Hontela, A., Rasmussen, J.B., Giguère, A., Gravel, A., Kraemer, L., Kovesces, J., Lacroix, A., Levesque, H., and Sherwood, G. 2003. Differentiating between direct (physiological) and food-chain mediated (bioenergetic) effects on fish in metal-impacted lakes. Hum. Ecol. Risk Assess. **9**: 847–866.

Carlberg, I., and Mannervik, B. 1985. Glutathione reductase. Methods Enzymol. **113**: 484–490.

Centre for Hydrology and Ecology. 2001. Windermere Humic Aqueous Model (WHAM). Natural Environment Research Council, Windermere, UK.

Chakrabarti, S.K., and Bai, C. 1999. Role of oxidative stress in nickel chloride-induced cell injury in rat renal cortical cells. Biochem. Pharmacol. **58**: 1501–1510.

Chaurasia, S.S., and Kar, A. 1999. An oxidative mechanism for the inhibition of iodothyronine 5′-monodeiodinase activity by lead nitrate in the fish, *Heteropneustes fossilis*. Water Air Soil Pollut. **111**: 417–423.

Christie, N.T., and Costa, M. 1984. In vitro assessment of the toxicity of metal compounds. IV. Disposition of metals in cells: interactions with membranes, glutathione, metallothionein, and DNA. Biol. Trace Elem. Res. **6**: 139–158.

Cossu, C., Doyotte, A., Babut, M., Exinger, A., and Vasseur, P. 2000. Antioxidant biomarkers in freshwater bivalves, *Unio tumidus*, in response to different contamination profiles of aquatic sediments. Ecotoxicol. Environ. Saf. **45**: 106–121.

Couture, P., and Rajotte, J.W. 2003. Morphometric and metabolic indicators of metal stress in wild yellow perch (*Perca flavescens*) from Sudbury, Ontario: a review. J. Environ. Monit. **5**: 216–221.

Croteau, M.-N., Hare, L., and Tessier, A. 1998. Refining and testing a trace metal biomonitor (*Chaoborus*) in highly acidic lake. Environ. Sci. Technol. **32**: 1348–1353.

© 2005 NRC Canada

Croteau, M.-N., Hare, L., and Tessier, A. 2003. Difficulties in relating Cd concentrations in the predatory insect *Chaoborus* to those of its prey in nature. Can. J. Fish. Aquat. Sci. **60**: 800–808.

Di Giulio, R.T., Washburn, P.C., Wenning, R.J., Winston, G.W., and Jewell, C.S. 1989. Biochemical responses in aquatic animals: a review of determinants of oxidative stress. Environ. Toxicol. Chem. **8**: 1103–1123.

DiToro, D.M., Allen, H.E., Bergman, H.L., Meyer, J.S., Paquin, P.R., and Santore, R.C. 2001. Biotic ligand model of the acute toxicity of metals. 1. Technical basis. Environ. Toxicol. Chem. **20**: 2383–2396.

Eason, C., and O'Halloran, K. 2002. Biomarkers in toxicology versus ecological risk assessment. Toxicology, **181–182**: 517–521.

Eastwood, S., and Couture, P. 2002. Seasonal variations in condition and liver metal concentrations of yellow perch (*Perca flavescens*) from a metal contaminated environment. Aquat. Toxicol. **58**: 43–56.

Farag, A.M., Boese, C.J., Woodward, D.F., and Bergman, H.L. 1994. Physiological changes and tissue metal accumulation in rainbow trout exposed to foodborne and waterborne metals. Environ. Toxicol. Chem. **13**: 2021–2029.

Farag, A.M., Stansbury, M.A., Hogstrand, C., MacConnell, E., and Bergman, H.L. 1995. The physiological impairment of free-ranging brown trout exposed to metals in the Clark Fork River, Montana. Can. J. Fish. Aquat. Sci. **52**: 2038–2050.

Farag, A.M., Skaar, D., Nimick, D.A., MacConnell, E., and Hogstrand, C. 2003. Characterizing aquatic health using salmonid mortality, physiology, and biomass estimates in streams with elevated concentrations of arsenic, cadmium, copper, lead, and zinc in the Boulder River watershed, Montana. Trans. Am. Fish. Soc. **132**: 450–467.

Giguère, A., Campbell, P.G.C., Hare, L., McDonald, D.G., and Rasmussen, J.B. 2004. Influence of lake chemistry and fish age on cadmium, copper, and zinc concentrations in various organs of indigenous yellow perch (*Perca flavescens*). Can. J. Fish. Aquat. Sci. **61**: 1702–1716.

Goede, R.W., and Barton, B.A. 1990. Organismic indices and an autopsy-based assessment as indicators of health and condition of fish. Am. Fish. Soc. Symp. **8**: 93–108.

Halliwell, B., and Gutteridge, M.C. 1984. Oxygen toxicity, oxygen radicals, transition metals and disease. Biochem. J. **219**: 1–14.

Handy, R.D., Galloway, T.S., and Depledge, M.H. 2003. A proposal for the use of biomarkers for the assessment of chronic pollution and in regulatory toxicology. Ecotoxicology, **12**: 331–343.

Kling, P., Erkell, L.J., Kille, P., and Olsson, P.-E. 1996. Metallothionein induction in rainbow trout gonadal (RTG-2) cells during free radical exposure. Mar. Environ. Res. **42**: 33–36.

Kosower, N.S., and Kosower, E.M. 1978. The glutathione status of cells. Int. Rev. Cytol. **54**: 109–160.

Laflamme, J.-S., Couillard, Y., Campbell, P.G.C., and Hontela, A. 2000. Interrenal metallothionein and cortisol secretion in relation to Cd, Cu, and Zn exposure in yellow perch, *Perca flavescens*, from Abitibi lakes. Can. J. Fish. Aquat. Sci. **57**: 1692–1700.

Lange, A., Ausseil, O., and Segner, H. 2002. Alterations of tissue glutathione levels and metallothionein mRNA in rainbow trout during single and combined exposure to cadmium and zinc. Comp. Biochem. Physiol. C Comp. Pharmacol. Toxicol. **131**: 231–243.

Lawrence, R.A., and Burk, R.F. 1976. Glutathione peroxidase activity in selenium-deficient rat liver. Biochem. Biophys. Res. Commun. **71**: 952–958.

Leroy, P., Nicolas, A., Wellman, M., Michelet, F., Oster, T., and Siest, G. 1993. Evaluation of *o*-phthalaldehyde as bifunctional fluorogenic post-column reagent for glutathione in LC. Chromatographia, **36**: 130–134.

Levesque, H.M., Moon, T.W., Campbell, P.G.C., and Hontela, A. 2002. Seasonal variation in carbohydrate and lipid metabolism of yellow perch (*Perca flavescens*) chronically exposed to metals in the field. Aquat. Toxicol. **60**: 257–267.

Lopes, P.A., Pinheiro, T., Santos, M.C., Mathias, M.D., Collares Pereira, M.J., and Viegas Crespo, A.M. 2001. Response of antioxidant enzymes in freshwater fish populations (*Leuciscus alburnoides* complex) to inorganic pollutants exposure. Sci. Total Environ. **280**: 153–163.

Luoma, S.N. 1996. The developing framework of marine ecotoxicology: pollutants as a variable in marine ecosystems? J. Exp. Mar. Biol. Ecol. **200**: 29–55.

Maracine, M., and Segner, H. 1998. Cytotoxicity of metals in isolated fish cells: importance of the cellular glutathione status. Comp. Biochem. Physiol. A Comp. Physiol. **120**: 83–88.

Martell, A.E., and Smith, R.M. 2001. NIST Critically selected stability constants of metal complexes v. 6.0. National Institute of Standards and Technology, Gaithersburg, Md.

Oliver, B.G., Thurman, E.M., and Malcolm, R.L. 1983. The contribution of humic substances to the acidity of colored natural waters. Geochim. Cosmochim. Acta, **47**: 2031–2035.

Palace, V.P., and Klaverkamp, J.F. 1993. Variation of hepatic enzymes in three species of freshwater fish from Precambrian Shield lakes and the effect of cadmium exposure. Comp. Biochem. Physiol. C Comp. Pharmacol. Toxicol. **104**: 147–154.

Palace, V.P., Majewski, H.S., and Klaverkamp, J.F. 1993. Interactions among antioxidant defences in liver of rainbow trout (*Oncorhynchus mykiss*) exposed to cadmium. Can. J. Fish. Aquat. Sci. **50**: 156–162.

Pruell, R.J., and Engelhardt, F.R. 1980. Liver cadmium uptake, catalase inhibition and cadmium-thionein production in the killifish (*Fundulus heteroclitus*) induced by the experimental cadmium exposure. Mar. Environ. Res. **3**: 101–111.

Ptashynski, M.D., Pedlar, R.M., Evans, R.E., Wautier, K.G., Baron, C.L., and Klaverkamp, J.F. 2001. Accumulation, distribution and toxicology of dietary nickel in lake white fish (*Coregonus clupeaformis*) and lake trout (*Salvelinus namaycush*). Comp. Biochem. Physiol. C Comp. Pharmacol. Toxicol. **130**: 145–162.

Radi, A.A.R., and Matkovics, B. 1988. Effects of metal ions on the antioxidant enzyme activities, protein contents and lipid peroxidation of carp tissue. Comp. Biochem. Physiol. C Comp. Pharmacol. Toxicol. **90**: 69–72.

Rajotte, J.W., and Couture, P. 2002. Effects of environmental metal contamination on the condition, swimming performance, and tissue metabolic capacities of wild yellow perch (*Perca flavescens*). Can. J. Fish. Aquat. Sci. **59**: 1296–1304.

Reddy, C.C., Scholz, R.W., and Massaro, E.J. 1981. Cadmium, methylmercury, mercury, and lead inhibition of calf liver glutathione *S*-transferase exhibiting selenium-independent glutathione peroxidase activity. Toxicol. Appl. Pharmacol. **61**: 460–468.

Rodríguez-Ariza, A., Peinado, J., Pueyo, C., and Lòpez-Barea, J. 1993. Biochemical indicators of oxidative stress in fish from polluted littoral areas. Can. J. Fish. Aquat. Sci. **50**: 2568–2573.

Roméo, M., Bennani, N., Gnassia-Barelli, M., Lafaurie, M., and Girard, J.P. 2000. Cadmium and copper display different responses towards oxidative stress in the kidney of the sea bass *Dicentrarchus labrax*. Aquat. Toxicol. **48**: 185–194.

Sato, M., and Bremner, I. 1993. Oxygen free radicals and metallothionein. Free Radical Biol. Med. **14**: 325–337.

© 2005 NRC Canada

Schlenk, D., and Rice, C.D. 1998. Effect of zinc and cadmium treatment on hydrogen peroxide-induced mortality and expression of glutathione and metallothionein in a teleost hepatoma cell line. Aquat. Toxicol. **43**: 121–129.

Sherwood, G.D., Rasmussen, J.B., Rowan, D.J., Brodeur, J., and Hontela, A. 2000. Bioenergetic costs of heavy metal exposure in yellow perch (*Perca flavescens*): in situ estimates with a radiotracer (^{137}Cs) technique. Can. J. Fish. Aquat. Sci. **57**: 441–450.

Sherwood, G.D., Kovecses, J., Hontela, A., and Rasmussen, J.B. 2002. Simplified food webs lead to energetic bottlenecks in polluted lakes. Can. J. Fish. Aquat. Sci. **59**: 1–5.

SPSS, Inc. 2000. Sigmaplot 2000 for Windows. SPSS, Inc., Chicago, Ill.

StatSoft, Inc. 1999. Statistica for Windows. StatSoft, Inc., Tulsa, Okla.

Stegeman, J.J., Brouwer, M., Di Giulio, R.T., Förlin, L., Fowler, B.A., Sanders, B.M., and Van Veld, P.A. 1989. Molecular responses to environmental contamination: enzyme and protein synthesis as indicators of chemical exposure and effect. *In* Biomarkers. *Edited by* R.J. Hugget, R.A. Kimerle, P.M.J. Mehrle, and H.L. Bergman. Lewis Publishers, Boca Raton, Fla. pp. 235–333.

Sunderman, F.W., Marzouk, A., Hopfer, S.M., Zaharia, O., and Reid, M.C. 1985. Increased lipid peroxidation in tissues of nickel chloride-treated rats. Ann. Clin. Lab. Sci. **15**: 229–236.

Thomas, J.P., Bachowski, G.J., and Girotti, A.W. 1986. Inhibition of cell membrane lipid peroxidation by cadmium- and zinc-metallothioneins. Biochim. Biophys. Acta, **884**: 448–461.

Thomas, P., and Wofford, H.W. 1984. Effects of metals and organic compounds on hepatic glutathione, cysteine, and acid soluble thiol levels in mullet (*Mugil cephalus* L.). Toxicol. Appl. Pharmacol. **76**: 172–182.

Thomas, P., and Wofford, H.W. 1993. Effects of cadmium and Arochlor 1254 on lipid peroxidation, glutathione peroxidase activity, and selected antioxidants in Atlantic croaker tissues. Aquat. Toxicol. **27**: 159–178.

Thomas, P.T., Wofford, H.W., and Neff, J.M. 1982. Effect of cadmium on glutathione content of mullet (*Mugil cephalus*) tissues. *In* Physiological mechanisms of marine pollutant toxicity. *Edited by* W.B. Vernberg, A. Calabrese, F.P. Thurberg, and F.J. Vernberg. Academic Press, New York. pp. 109–125.

Tipping, E. 1998. Humic ion-binding model VI: an improved description of the interactions of protons and metal ions with humic substances. Aquat. Geochem. **4**: 3–48.

Tipping, E., Backes, C.A., and Hurley, M.A. 1988. The complexation of protons, aluminium and calcium by aquatic humic substances: a model incorporating binding-site heterogeneity and macroionic effects. Water Res. **22**: 597–611.

Torreilles, J., and Guerin, M.-C. 1990. Nickel(II) as a temporary catalyst for hydroxyl radical generation. FEBS Lett. **272**: 58–60.

Tort, L., Kargacin, B., Torres, P., Giralt, M., and Hidalgo, J. 1996. The effect of cadmium exposure and stress on plasma cortisol, metallothionein levels and oxidative status in rainbow trout (*Oncorhynchus mykiss*) liver. Comp. Biochem. Physiol. C Comp. Pharmacol. Toxicol. **114**: 29–34.

Vasseur, P., and Cossu-Leguille, C. 2003. Biomarkers and community indices as complementary tools for environmental safety. Environ. Int. **28**: 711–717.

Viarengo, A., Burlando, B., Ceratto, N., and Panfoli, I. 2000. Antioxidant role of metallothioneins: a comparative overview. Cell. Mol. Biol. **46**: 407–417.

Wallace, W.G., Lee, B.-G., and Luoma, S.N. 2003. Subcellular compartmentalization of Cd and Zn in two bivalves. I. Significance of metal-sensitive fractions (MSF) and biologically detoxified metal (BDM). Mar. Ecol. Prog. Ser. **249**: 183–197.

Wofford, H.W., and Thomas, P. 1988. Effects of xenobiotics on peroxidation of hepatic microsomal lipids from striped mullet (*Mugil cephalus*) and Atlantic croaker (*Micropogonias undulatus*). Mar. Environ. Res. **24**: 285–289.

Wright, J., George, S., Martinez Lara, E., Carpene, E., and Kindt, M. 2000. Levels of cellular glutathione and metallothionein affect the toxicity of oxidative stressors in an established carp cell line. Mar. Environ. Res. **50**: 503–508.

© 2005 NRC Canada

Invasion of an estuarine transition zone by *Dreissena polymorpha* veligers had no detectable effect on zooplankton community structure

Gesche Winkler, Pascal Sirois, Ladd E. Johnson, and Julian J. Dodson

Abstract: Large numbers of the filter-feeding larval stage of zebra mussels (*Dreissena polymorpha*) (veligers) have been advected into the estuarine transition zone (ETZ) of the St. Lawrence River. In 1994, they became the dominant member of the tidal freshwater zooplankton assemblage of the ETZ (and subsequently the true estuarine assemblage) during summer months. These changes in community structure have not, however, been reflected in changes in the abundance of preinvasion taxa. Abundance of potential planktonic competitors such as rotifers and the cladoceran *Bosmina longirostris* fluctuated between years but did not decline following the invasion. Only densities of the copepod *Eurytemora affinis* declined in 2000 and 2001, but this could not be definitively associated with the invasion. Synchronous variation among different zooplankton groups suggests that environmental forcing related to or correlated with temperature anomalies is the major cause of interannual variation in the abundance of zooplankton taxa. The negative correlation between veliger abundance and salinity indicates that the ETZ acts as a sink for the larval stages of the zebra mussel. Their precise fate remains uncertain, but our study suggests that this invasion has had little or no impact on this pelagic community in spite of the numerical dominance of veligers.

Résumé : Un grand nombre de larves véligères à alimentation par filtration de la moule zébrée (*Dreissena polymorpha*) ont été entraînées par advection dans la zone de transition estuarienne (ZTE) du fleuve Saint-Laurent. En 1994, elles sont devenues l'élément dominant des peuplements intertidaux de zooplancton de la ZTE (pour former ensuite le véritable peuplement estuarien) durant les mois d'été. Cependant, ces changements de structure de communauté n'entraînent pas de changements d'abondance des taxons présents avant l'invasion. L'abondance des compétiteurs planctoniques potentiels, tels que les rotifères et le cladocère *Bosmina longirostris*, fluctue d'une année à l'autre, mais il n'y a pas eu de déclin après l'invasion. Seules les densités du copépode *Eurytemora affinis* ont diminué en 2000 et 2001, mais le déclin ne peut être clairement associé à l'invasion. L'existence de variations synchrones parmi les différents groupes du zooplancton laisse croire que le forçage environnemental associé aux anomalies de température, ou en corrélation avec elles, est la cause principale de la variation d'abondance des taxons du zooplancton. La corrélation négative entre l'abondance des véligères et la salinité indique que la ZTE agit comme un puits pour les stades larvaires de la moule zébrée. Leur sort exact reste incertain, mais notre étude laisse croire que cette invasion a eu peu ou pas d'impact sur la communauté pélagique, malgré la dominance numérique des véligères.

[Traduit par la Rédaction]

Introduction

By far the most influential invader of the Laurentian lake and river complex in recent times has been the zebra mussel (*Dreissena polymorpha*) (Griffiths et al. 1991). Since first observed in North America in the late 1980s, this invasive bivalve has successfully colonized many freshwater ecosystems (Johnson and Carlton 1996) including the entire length of the St. Lawrence River (Mellina and Rasmussen 1994*a*, 1994*b*). While human activities are responsible for much of this secondary spread (Johnson and Carlton 1996), the rapidity of the downstream spread was largely due to the planktotrophic life cycle of this species, which includes a feeding larval stage (the veliger) that spends weeks in the water column (Martel et al. 1995). Owing to the high fecundity of this species, veligers can reach high densities (Ram and McMahon 1996) and then be transported hundreds of kilometres downstream during the planktonic period.

In contrast with the extensive research effort on the ecological impact of benthic populations of this invasive bivalve on native planktonic and benthic communities (e.g., Great Lakes (Vanderploeg et al. 2002) and the Hudson, Mississippi, and St. Lawrence rivers (Ricciardi et al. 1997; Pace et al. 1998; James et al. 2000)), little is known about the ecological impact of the planktonic phase of the life cycle. Veligers are known to filter-feed nanoplankton in a size range of 2–10 µm (Bernier 2003), and high densities of veligers could thus compete with other filter-feeders exploiting similar particle size ranges, such as rotifers (4–17 µm), cladocerans (4–28 µm), and copepods (2 to >150 µm) (Arndt 1993; Cyr and Curtis 1999; Zimmermann-Timm 2002).

Received 23 January 2004. Accepted 12 November 2004. Published on the NRC Research Press Web site at http://cjfas.nrc.ca on 9 April 2005.
J17930

G. Winkler,[1] L.E. Johnson, and J.J. Dodson. Département de biologie et Québec – Océan, Université Laval, Québec, QC G1K 7P4, Canada.
P. Sirois. Département des sciences fondamentales, Université du Québec à Chicoutimi, Chicoutimi, QC G7H 2B1, Canada.

[1]Corresponding author (e-mail: gesche.winkler@giroq.ulaval.ca).

 doi: 10.1139/F04-230 © 2005 NRC Canada

Whereas the effect of filter-feeding by veligers can be far less than that of dense populations of adult mussels in areas of shallow, rocky bottoms (e.g., western Lake Erie (MacIsaac et al. 1992)), their effects elsewhere may be substantially greater depending on levels of productivity and the abundance of competing organisms, both benthic and planktonic.

The St. Lawrence Middle Estuary includes the estuarine transition zone (ETZ) where distinct physical properties such as estuarine recirculation, semidiurnal stratification and mixing, sediment entrapment, and high turbidity act as major factors organizing the aquatic biota. Estuarine circulation and entrapment result in elevated primary production at the head of the ETZ (Vincent et al. 1994, 1996; Frenette et al. 1995), while heterotrophic processes dominate farther downstream. Both processes show strong spatial and trophic coupling (Winkler et al. 2003). The plankton community of the ETZ, including primary producers, herbivores, and planktivores, is longitudinally organized across the frontal gradient of the transition zone.

The ETZ is a key element of the estuarine ecosystem because of its unique combination of upstream and downstream properties (Vincent and Dodson 1999). For the St. Lawrence River, it is still unknown to what extent this sensitive interface between the freshwater and marine areas of this large river–estuarine ecosystem is vulnerable to environmental perturbation. Estuaries are the receiving end of lentic systems, and thus, environmental stressors can be the result of the integration and accumulation of upstream processes including chemical pollution, sediment loading, and discharge modification. Whereas some stressors might be mitigated en route (e.g., sedimentation of suspended solids), others become progressively compounded as one moves downstream. This problem is often the case for the biological pollution that results from the introduction of nonnative species, which are inevitably spread downstream.

The potential impact of veligers on the planktonic communities of the ETZ is thus difficult to predict but may depend on both the precise biological and physical conditions of the zooplankton assemblage. In the 1970s (Bousfield et al. 1973), 1980s (Laprise and Dodson 1994), and again in the 1990s (Winkler et al. 2003), three distinct assemblages of zooplankton were recognized in the ETZ that are mainly controlled by average salinity and the degree of water column stratification: (*i*) a freshwater assemblage characterized by the cladoceran *Bosmina longirostris* and the amphipod *Gammarus tigrinus* found around and upstream of Île d'Orléans in warmer, well-mixed waters of salinities <1.6 psu (practical salinity units), (*ii*) a true estuarine assemblage dominated by the copepod *Eurytemora affinis* and the mysid *Neomysis americana* that occurs downstream of Île d'Orléans in weakly stratified waters of salinities between 0.5 and 6 psu, and (*iii*) a euryhaline–marine assemblage characterized by copepods (*Calanus* spp.), the mysid *Mysis littorales*, and euphausids (*Thysanoessa* spp. and *Meganyctiphanes norvegica*), which is found farther downstream in colder and more stratified waters with salinities >6 psu. Zooplankton biomass peaks in the true estuarine assemblage (Bousfield et al. 1973; Laprise and Dodson 1994) and provides a rich food resource for larval and juvenile fish, including rainbow smelt (*Osmerus mordax*) and Atlantic tomcod (*Microgadus tomcod*) (Dauvin and Dodson 1990; Laprise and Dodson 1990; Sirois and Dodson 2000).

Normally, the higher salinities of estuarine conditions would protect this ecosystem from upstream freshwater invaders, but the combination of high discharge (sixth highest in the world), geomorphology, and extreme tides produces an estuary that extends for 540 km and thus lacks abrupt salinity changes. Moreover, the exact salinity tolerance of zebra mussels is not yet well established, but it is clear that both benthic and planktonic stages are capable of surviving in low-salinity waters (adults up to 8 psu (Mackie and Kilgour 1992; Walton 1996) and veligers up to 4 psu (Wright et al. 1996)). This concern is particularly pertinent to the ETZ where retention processes could lead to elevated densities of veligers and nanoplankton dynamics play an important role (Frenette et al. 1995; Barnard et al. 2003).

In this study, we examined the impact of the zebra mussel invasion on zooplankton in the ETZ of the St. Lawrence River. We proposed that the potential for competition between veligers and other filter-feeders exploiting similar particle size ranges may have caused changes in the abundance of some zooplankton species and hence altered zooplankton community structure. The objective of this study was thus to document changes in the abundance of zebra mussel veligers and other zooplankton species at the head of the ETZ of the St. Lawrence Middle Estuary during the invasion. The distribution and abundance of *D. polymorpha* veligers and certain preinvasion species of the zooplankton community were assessed along the salinity gradient to detect changes in the three distinct zooplankton assemblages of the ETZ. Sampling cruises conducted in 1993 (preinvasion) and 1994 and 1995 (invasion) enabled us to detect the time of the massive arrival of veligers in the estuary, and further sampling was conducted in 2000 and 2001 (postinvasion) to assess if any changes have occurred since then that could be attributed to the presence of veligers in the transition zone.

Material and methods

Study site

The St. Lawrence Middle Estuary is located from 50 to 230 km downstream of the city of Québec and encompasses a salinity range of 0–25 psu (Fig. 1). Three channels (northern, middle, and southern) run through this part of the estuary. A combination of semidiurnal, lunar tides ranging from 3 to 5 m in amplitude, and freshwater discharge varying between 18 164 and 8863 $m^3 \cdot s^{-1}$ from May to August (Ministère de l'environnement Canada, Service météorologique) creates strong estuarine circulation. Because of the lateral variation in bathymetry (a deep northern channel and shallower middle and southern channels are separated by islands, sand banks, and shallow shoals), salt water intrudes farther upstream in the northern channel of the estuary, creating both along- and cross-estuary salinity gradients (Simons 2004). The water column is generally well mixed and partially stratified with stratification that varies on tidal and subtidal scales (Simons 2004). Mean current velocities exceed 0.6–3 $m \cdot s^{-1}$, and hydrodynamic trapping of inorganic and organic particles owing to estuarine circulation is responsible for high turbidity in this area (D'Anglejan 1981).

© 2005 NRC Canada

Fig. 1. Average position of isoclines (psu) and location of stations sampled in the northern and southern channels of the St. Lawrence Middle Estuary in 1993, 1994, 1995, 2000, and 2001. Symbols represent only average positions among field surveys, as the exact location of stations was determined on each occasion according to surface salinity. Indeed, certain stations could be representative of more than one assemblage depending on the tidal conditions.

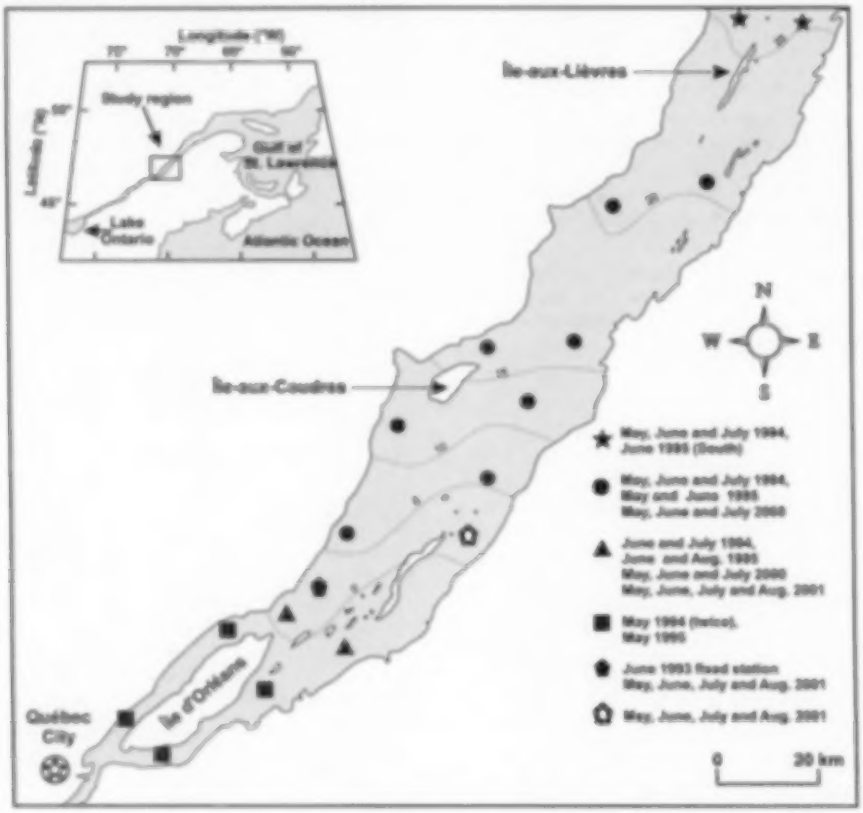

Data

The data used in this study were obtained from several studies that differed in their major objectives, and thus, sampling protocols varied between years. To render the data comparable, we imposed the well-documented preinvasion structure of zooplankton assemblages (Bousfield et al. 1973; Laprise and Dodson 1994; Winkler et al. 2003) on the data sets to form three putative zooplankton assemblages: tidal fresh water, true estuarine, and euryhaline–marine. We assessed the inter- and intra-group structure of these three assemblages with a nonmetric multidimensional scaling (MDS) analysis. Intergroup structure was analysed to test if the putative assemblages were distinct whereas intragroup structure was analysed to assess the contribution of each taxon in explaining within-assemblage similarity. To reveal the impact of veligers on the transition zone zooplankton community, we compared preinvasion (1993), invasion (1994 and 1995), and postinvasion (2000 and 2001) periods.

Preinvasion zooplankton community

To describe the preinvasion state of the zooplankton community, we used data obtained over a 76.5-h period from 22 to 26 June 1993 at a fixed sampling station located in the north channel of the St. Lawrence estuary 10 km downstream of Île d'Orléans (Winkler et al. 2003). Sampling was conducted every 1.5-h period covering a salinity range from 0 to 6 psu. Zooplankton samples were collected using a 0.5-m standard net (63-μm mesh size). For a detailed description of sampling and laboratory procedures, see Winkler et al. (2003). For the purposes of this paper, we only used data from surface samples taken by 5-m vertical tows in the surface layer.

Invasion (1994 and 1995) and postinvasion (2000 and 2001) periods

Field surveys were conducted in 1994 (24–26 May, 20–22 June, and 15 and 16 July), in 1995 (25–27 May, 27 and 28 June, and 14 August), and in 2000 (30 May – 4 June, 23–25 June, 11 and 12 July, and 24–26 July). A grid of 10–16 stations along the salinity gradient was sampled for each survey (Fig. 1). Stations were determined by real-time measures of surface salinity (i.e., a Lagrangian sampling design). In 2001, we sampled two stations at the head of the transition zone (freshwater <0.6 psu) and two stations in the transition zone (0.6–6 psu) each week from 22 May to 31 July. For all sampling, salinity and temperature profiles were measured using a SeaBird Seacat profiler (Sea-logger SBE-19, SeaBird Electronics, Inc., Bellevue, Washington). Zooplankton

© 2005 NRC Canada

were collected by 5-m vertical tows in the surface layer with a 0.5-m standard net (63-µm mesh size). In 1994 and 1995, samples were preserved in 4% buffered formaldehyde. In 2000 and 2001, 95% ethanol was used and changed once in the first week after the first preservation to prevent the solution from becoming too acidic (Butler 1992). The following species and taxa were identified: veligers of *D. polymorpha*, rotifers, *B. longirostris*, calanoid copepods *E. affinis* and *Acartia* sp. (other, rarely occurring calanoid copepods were pooled and identified as "other calanoids"), cyclopoid copepods (mainly *Cyclops* sp.), harpacticoid copepods (mainly *Ectinosoma curticorne*), and nauplii (includes all copepod species). To distinguish *D. polymorpha* veligers, we used cross-polarized light (Johnson 1995). Abundances were evaluated from subsamples, counting a minimum of 10% of the total sample volume with densities expressed per litre of filtered water.

Statistical analysis

Prior to statistical analysis, we grouped our zooplankton samples into three distinct zooplankton assemblages (see above) according to salinity: (*i*) tidal freshwater from 0 to 0.5 psu, (*ii*) true estuarine from 0.6 to 6 psu, and (*iii*) euryhaline–marine waters >6 psu. We combined June and July data to represent the summer zooplankton community during the period of the highest abundance of *D. polymorpha* veligers. To visualize the distribution and variability of these three putative zooplankton communities over the sampling sites, we used MDS (Legendre and Legendre 1998; Clarke and Warwick 2001) on transformed data ($\log(x + 1)$). Data were transformed to reduce bias resulting from highly abundant species. Bray–Curtis similarities were calculated to create an MDS representation of the yearly zooplankton assemblages as a function of the three predetermined salinity categories. This technique reduces a multidimensional scatter plot into a lower number of dimensions while preserving the maximum amount of variation in the data, thus allowing relationships between individual points to be more easily visualized. Each data point represents the abundance of all taxa in the zooplankton community at one sampling site at a specific time. To test differences between zooplankton assemblages, we used analysis of similarities (ANOSIM). This analysis operates on a similarity matrix. Zooplankton assemblages are considered very different in their species composition when similarities within an assemblage are greater than those between the assemblages. The ANOSIM statistic R is based on the difference of mean ranks between assemblages and within assemblages. The ANOSIM R value shows the degree of distinctness as follows: well separated ($R > 0.75$), overlapping but clearly different ($R > 0.5$), and barely separable at all ($R < 0.25$) and value 0 indicating completely random grouping. The statistical significance of the observed R is assessed by permutation of the grouping vector to obtain the empirical distribution of R under a null model (Clarke 1993; Clarke and Warwick 2001). A similarity of percentages routine (SIMPER) was used to assess the contributions of different taxa to observed within-assemblage similarity. Nonmetric MDS, ANOSIM, and SIMPER were performed using the PRIMER v5 program (PRIMER-E Ltd., Plymouth, UK).

Even though our sampling grids are spatially structured, spatial autocorrelation was negligible. The sampling stations for each cruise were chosen according to salinity and not to geographic position (e.g., a Langrangian sampling design). Strong tidal currents mixed the water mass from one station to another and from one day to the next. The large distances between stations further assured the sampling of different water masses. Nevertheless, to avoid any bias associated with spatial autocorrelation, we visually verified if adjacent points in the MDS plots were sampled on the same day. In such cases, data from these stations were averaged (3% of all data points).

Kendall's rank correlation coefficient τ was used to measure the best match of biotic and environmental similarity matrices for the years 1993, 1994, 1995, 2000, and 2001. Differences in the estimates of abundance of each taxon between years for the three zooplankton assemblages were tested using a Kruskal–Wallis ANOVA and Tukey's test for multiple comparisons of unequal sample sizes (Zar 1996). As abiotic factors can govern the distribution and abundance of zooplankton (Viitasalo 1992; Dippner et al. 2000), we used air temperature and discharge (Ministère de l'environnement Canada, Service météorologique) measured and estimated at Québec (located approximately 40 km from the ETZ) as indicators of weather conditions in the years of the study. We calculated the mean monthly temperature and mean monthly discharge of 1993–2001 to define the monthly temperature anomalies for each year that we sampled zooplankton, i.e., 1993–1995, 2000, and 2001. We did the same calculation for mean monthly zooplankton abundance of the tidal freshwater and true estuarine assemblages.

Results

Occurrence of *D. polymorpha* veligers in zooplankton assemblages

Sampling in the mid-1990s detected for the first time *D. polymorpha* veligers in the ETZ. Whereas no veligers were found in 1993, large numbers (up to 138 veligers·L^{-1}) were found starting in 1994 when the relative abundance of veligers at the head of the transition zone (i.e., in the tidal freshwater assemblage) increased from 20% to 80% of the zooplankton between May and July (Figs. 2*a*–2*c*). Similar patterns were seen over the next 7 years with the proportion of veligers reaching 75% by June in 1995 and similarly high proportions of veligers in June (80%–90%) and July (70%–90%) of 2000 and 2001 (Figs. 2*a*–2*c*). Peak abundances always occurred in June: 293 veligers·L^{-1} in 1995, 127 veligers·L^{-1} in 2000, and 353 veligers·L^{-1} in 2001. In August, the proportion of veligers diminished whereas rotifers and nauplii dominated (Fig. 2*d*). Absolute densities of veligers (30–70 veligers·L^{-1}) in the tidal freshwater zone in August were much lower than in June and July (70–235 veligers·L^{-1}). The composition of the true estuarine zooplankton assemblage was also affected by the invasion. Beginning in 1994, veligers were present in May, but only in 2001 were they the dominant component of this assemblage (Fig. 2*e*). The dominant taxa in the true estuarine zooplankton assemblage in June and July from 1993 to 1995 were copopods (especially *E. affinis* and nauplier stages). However, this pattern changed in 2000 and 2001 when veligers were numerically dominant (Figs. 2*f* and 2*g*).

© 2005 NRC Canada

Fig. 2. Seasonal and annual differences in zooplankton community structure for each assemblage. Zooplankton composition in the tidal freshwater assemblage in (*a*) May, (*b*) June, (*c*) July, and (*d*) August, in the true estuarine assemblage in (*e*) May, (*f*) June, (*g*) July, and (*h*) August, and in the euryhaline–marine assemblage in (*i*) May, (*j*) June, (*k*) July, and (*l*) August during preinvasion (1993), invasion (1994 and 1995), and postinvasion (2000 and 2001). No column indicates that data for that date were not available.

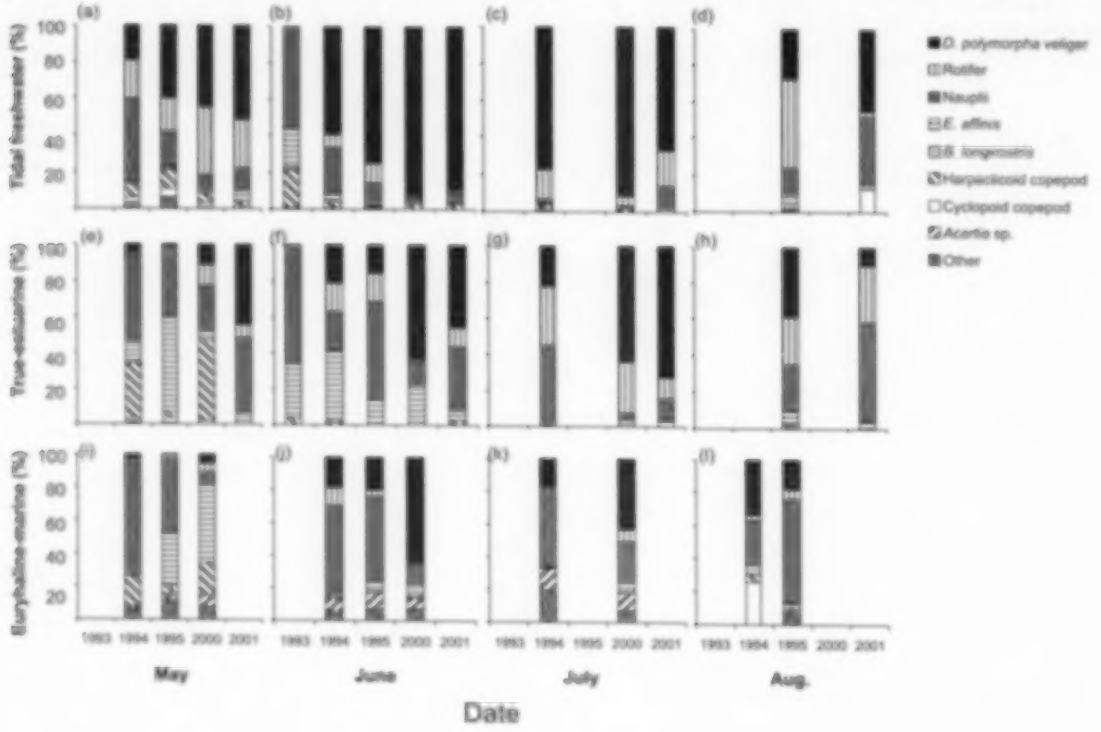

In the euryhaline–marine zooplankton assemblage, veligers contributed <20% and copepod species dominated, except in June and July 2000, when the veliger contribution was 60% and 40%, respectively. No data for 1993 and 2001 were available for this zooplankton assemblage. The rest of the assemblage consisted primarily of copepod species, especially nauplier stages. *Eurytemora affinis* was particularly abundant in May of two years (1995 and 2000) whereas *Acartia* was more common in June and July (Figs. 2*i*–2*l*), especially in 2000.

Comparison of putative zooplankton assemblages

Species contribution to similarity (SIMPER), MDS, and ANOSIM assessed both within-assemblage and between-assemblage similarity for all sampling stations in 1993, 1994, 1995, 2000, and 2001 for the three zooplankton assemblages. In 1993, before the invasion, most of the within-assemblage similarity was due to nauplii and *E. affinis* for both tidal freshwater and true estuarine assemblages (Table 1). During the invasion period, most of the within-assemblage similarity in the tidal freshwater assemblage was due to *D. polymorpha* veligers (51% and 38% in 1994 and 1995, respectively) (Table 1) whereas in the true estuarine assemblage, nauplii still accounted for much of the within-assemblage similarity (32% and 34%, respectively) (Table 1). In contrast, during the postinvasion period (2000 and 2001), both the tidal freshwater and true estuarine assemblages were dominated by *D. polymorpha* veligers, which were largely responsible for the within-assemblage similarity in both assemblages (Table 1).

General patterns in the MDS plots were similar for all years. The freshwater assemblage was adjacent to the true estuarine assemblage, which in turn was next to the euryhaline–marine assemblage (Fig. 3). However, the detailed structure of the assemblages was different between years and between analyses with and without *D. polymorpha* veligers. Overall global *R* increased when veligers were excluded from the analysis except in 2000. During the preinvasion period (1993), the tidal freshwater and true estuarine assemblages were significantly different (Table 2; Fig. 3*a*) with an average dissimilarity of 40%, mostly because of differences in mean abundance of nauplii and *E. affinis* between the two assemblages. In 1994 at the start of the invasion phase, the calculated ANOSIM *R* between the tidal freshwater and estuarine assemblages did not differ (ANOSIM *R* inferior to 0.25) in cases both with and without veligers. In contrast, ANOSIM *R* in 1995 was high (but not significant) when veligers were included in the analysis, indicating a strong difference between the assemblages. However, when veligers were excluded, the difference between these two assemblages mostly disappeared. Furthermore, none of the ANOSIM *R* for these two years were significant

© 2005 NRC Canada

Table 1. Average within-assemblage similarities (%) of the three putative zooplankton assemblages and the contribution of most important taxa (%) for all years.

Year	Tidal fresh water	%	True estuarine	%	Euryhaline–marine	%
1993	Average similarity	67	Average similarity	84		
	Nauplii	47	Nauplii	53		
	Eurytemora affinis	25	*Eurytemora affinis*	40		
	Harpacticoid copepods	21				
	Bosmina longirostris	5				
1994	Average similarity	57	Average similarity	67	Average similarity	52
	Dreissena veligers	51	Nauplii	32	Nauplii	56
	Rotifers	19	Rotifers	28	*Dreissena* veligers	15
	Harpacticoid copepods	11	*Dreissena* veligers	23	Other	14
					Acartia sp.	12
1995	Average similarity	83	Average similarity	75	Average similarity	49
	Dreissena veligers	38	Nauplii	34	Nauplii	57
	Nauplii	23	*Eurytemora affinis*	29	Other	17
	Rotifers	16	*Dreissena* veligers	23	*Dreissena* veligers	13
	Eurytemora affinis	14	Rotifers	11	*Acartia* sp.	6
2000	Average similarity	72	Average similarity	70	Average similarity	46
	Dreissena veligers	78	*Dreissena* veligers	64	*Dreissena* veligers	55
	Harpacticoid copepods	8	Nauplii	12	Nauplii	19
	Rotifers	7	*Eurytemora affinis*	10	Others	10
	Eurytemora affinis	3	Rotifers	10	*Eurytemora affinis*	10
2001	Average similarity	64	Average similarity	69		
	Dreissena veligers	40	*Dreissena* veligers	40		
	Nauplii	18	Nauplii	31		
	Rotifers	18	*Eurytemora affinis*	14		
	Hapacticoid copepods	8	Rotifers	11		

owing to small sample sizes ($n = 4$ in 1994 and $n = 2$ in 1995). During the postinvasion phase, we found the tidal freshwater and true estuarine assemblages to be different in 2000 but not in 2001 because of high variability within both assemblages in 2001 (Figs. 3*c* and 3*d*; Table 2) (ANOSIM $R < 0.25$). When veligers were excluded, ANOSIM R decreased and there were no differences between the two assemblages in 2000 whereas ANOSIM R slightly increased. in 2001. The euryhaline–marine assemblage always showed significant differences from the two upstream assemblages whether veligers were included or not in the calculations (Figs. 3*b*–3*d*; Table 2).

Kendall's rank correlations between the similarity matrices for biotic and environmental patterns revealed that salinity seemed to be far more important in determining zooplankton distribution than temperature (Table 3). These correlations appear to be due to patterns of abundance of *D. polymorpha* veligers, rotifers, *B. longirostris*, and cyclopoid copepods, which reached the highest levels in the freshwater assemblage and were negatively correlated with salinity and positively correlated with temperature (Table 4). The abundance of *E. affinis*, the characteristic species of the true estuarine assemblage, was positively correlated with temperature but not with salinity, as it reached maximum abundance at midrange salinities. Nauplii were weakly correlated with temperature (positive) and salinity (negative) because of the fact that this group included several copepod species distributed throughout the estuary. *Acartia* sp. was strongly positively correlated with salinity and negatively correlated with temperature, reflecting its strong affinity to the euryhaline–marine assemblage (Table 4).

Interannual variation in the abundance of individual groups of zooplankton

Mean abundances of the invader (*D. polymorpha* veligers) and most of the preinvasion taxa (rotifers, nauplii, *E. affinis*, and cyclopoid copepods) varied significantly between years mostly in the tidal freshwater and true estuarine assemblages. In contrast, mean abundances of harpacticoid copepods did not differ between years in either zooplankton assemblage (Table 5). For *D. polymorpha* veligers, there was no increasing trend with time after the initial invasion (Fig. 4*a*), and in fact, a significantly lower mean abundance was found in the tidal freshwater group in 2000. In the true estuarine group, mean abundance of veligers was always lower but generally showed a trend in interannual variation similar to that observed in the tidal freshwater group (Fig. 4*b*). No interannual variation in mean abundance of veligers occurred in the euryhaline–marine assemblage (Table 5).

No rotifers were found in 1993 whereas they were abundant in all subsequent years. Their mean abundance varied significantly between years and paralleled the pattern of veliger abundance in the tidal freshwater and true estuarine assemblages, with their abundance in 2000 being the lowest of the postinvasion years (Figs. 4*c* and 4*d*; Table 5).

Mean abundance of nauplii varied significantly between years and zooplankton assemblages (Table 5). Mean abundance of nauplii was highest in 1995 and lowest in 2000 as was the case for other taxa of the tidal freshwater and true estuarine assemblages (Figs. 4*e* and 4*f*; Table 5). The abun-

© 2005 NRC Canada

Fig. 3. Nonmetric multidimensional scaling (MDS) plots for three zooplankton assemblages (tidal fresh water (▲), true estuarine (▼), and euryhaline–marine (■) in the St. Lawrence Middle Estuary (June and July data pooled) during (*a*) preinvasion in 1993, invasion from (*b*) 1994 to (*c*) 1995, and postinvasion from (*d*) 2000 to (*e*) 2001. The stress of the MDS plots varied between years: 0.04 (1995), 0.08 (1993, 1994, and 2000), and 0.16 (2001).

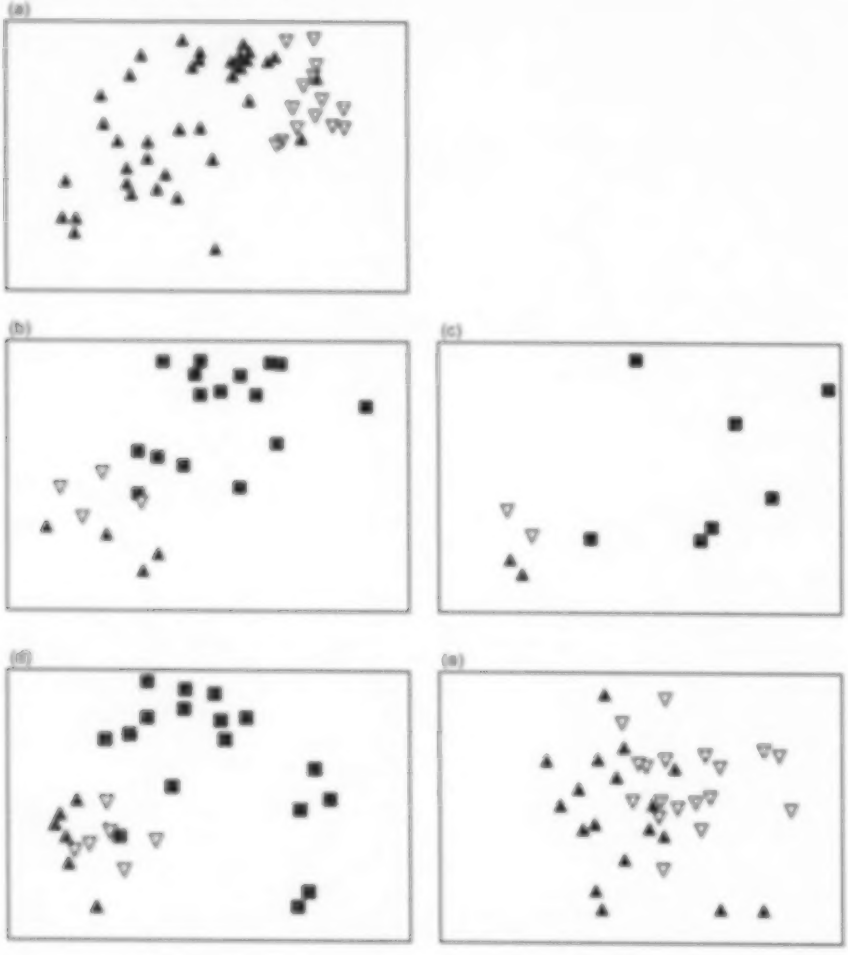

dance of *E. affinis* declined progressively after the invasion of *D. polymorpha* in the tidal freshwater and true estuarine assemblages, with the lowest abundance in the true estuarine assemblage occurring in 2000 (Figs. 4*g* and 4*h*; Table 5). Mean abundance of *B. longirostris* in the tidal freshwater assemblage did not differ significantly between years (Table 5) owing largely to high variability between replicates in each year. In the true estuarine group, mean abundance was significantly higher in 1994 than in all other years. Harpacticoid copepods did not show any significant difference in mean abundance between years in any assemblage (Table 5). Abundance of cyclopoid copepods was highly variable between years, and maximum abundance occurred in the tidal freshwater group in 2001 (Table 5). *Acartia* sp. occurred only in the euryhaline–marine group and its mean abundance was significantly lowest in 2000 (Table 5). In general, the abundance patterns observed over time all showed broadly similar trends, although they differed in amplitude: elevated from 1993 to 1995, down in 2000, and then up again in 2001 (Fig. 4). This alone suggests that there was no major impact of the veliger invasion on interannual variation.

Interannual variability: air temperature and discharge

In all years of the study, mean air temperature varied between months and years (Fig. 5*a*). Relatively warm temperatures in June 1994 and 1995 coincided with relatively high zooplankton abundances in this month whereas relatively low temperatures in June 1993 and 2000 and July 2000 coincided with relatively low abundances (Figs. 5*c*–5*j*). In the other months and years, this pattern was not so evident, suggesting that temperature is not the only factor in explaining interannual variability in abundance. Variability in mean discharge between years and months was also high, characterizing 1993 and 1994 as high-flow years and 1995 and 2001 as low-flow years (Fig. 5*b*). In high-flow year 1994, veliger abundance was below the overall mean, and in low-flow year

© 2005 NRC Canada

Table 2. Results of ANOSIM including and excluding veligers from the analysis.

	ANOSIM global R (p level)			ANOSIM R (p level)	
Year	Veligers included in the analysis	Veligers excluded from the analysis	Pairwise test assemblages	Veligers included in the analysis	Veligers excluded from the analysis
1993		**0.319 (0.001)**	Fresh water – estuarine		**0.319 (0.001)**
1994	**0.512 (0.001)**	**0.525 (0.001)**	Fresh water – estuarine	0.188 (0.171)	0.094 (0.23)
			Fresh water – marine	**0.691 (0.002)**	**0.654 (0.001)**
			Estuarine–marine	**0.504 (0.001)**	**0.548 (0.003)**
1995	**0.443 (0.013)**	**0.522 (0.013)**	Fresh water – estuarine	0.75 (0.33)	0.25 (0.667)
			Fresh water – marine	**0.656 (0.028)**	**0.727 (0.028)**
			Estuarine–marine	**0.532 (0.023)**	**0.643 (0.028)**
2000	**0.346 (0.001)**	**0.285 (0.001)**	Fresh water – estuarine	**0.413 (0.002)**	0.091 (0.21)
			Fresh water – marine	**0.521 (0.002)**	**0.377 (0.001)**
			Estuarine–marine	**0.337 (0.009)**	**0.288 (0.009)**
2001	**0.208 (0.001)**	**0.249 (0.001)**	Fresh water – estuarine	**0.208 (0.001)**	**0.249 (0.001)**

Note: ANOSIM R varies from –1 to +1, with a value of 0 indicating completely random grouping. Statistical significance of the observed R is assessed by permutation and shown in parentheses. Significant R values are shown in boldface.

Table 3. Environmental variables yielding the best match of biotic and abiotic similarity matrices as measured by Kendall's rank correlation coefficient τ for the years 1993, 1994, 1995, 2000, and 2001.

	τ	
Year	Salinity	Temperature
1993	0.453	0.144
1994	0.538	0.364
1995	0.517	0.546
2000	0.584	0.381
2001	0.146	0.233

Table 4. Kendall's correlation coefficients τ between zooplankton abundance and physical variables of all 165 samples collected in the estuarine transition zone (ETZ) in 1993, 1994, 1995, 2000, and 2001.

	τ	
	Water temperature	Salinity
Dreissena polymorpha veligers	**0.6**	**–0.52**
Rotifers	**0.25**	**–0.18**
Nauplii	**0.16**	**–0.17**
Eurytemora affinis	**0.17**	–0.15
Bosmina longirostris	**0.29**	**–0.24**
Harpacticoid copepods	0.03	**–0.20**
Cyclopoid copepods	**0.17**	**–0.22**
Acartia sp.	**–0.32**	**0.44**

Note: All values greater than 0.15 or less than –0.15 (boldface) represent significant correlations at the $p < 0.05$ level.

2001, veliger abundance in both the tidal freshwater and true estuarine groups was higher than average in all three months. However, in the other taxa, no consistent pattern between abundance and discharge occurred (Figs. 5*e*–5*j*).

Discussion

Data limitation

The mining of data sets collected over many years that were initially collected to meet objectives at times quite different from those of this study inevitably involves a disparate collection of sampling strategies and techniques. Thus, not all previous data sets were appropriate for the present analysis and the interpretation of those that were appropriate was complicated by the limitations of specific data sets. Data from the preinvasion phase are limited to sampling at a fixed station in June 1993. Nevertheless, sampling at a fixed station in this highly dynamic estuary permitted the intensive sampling of water masses varying between 0 and 6 psu, which is equivalent to the spatial sampling of stations deployed over approximately 15 km of the middle estuary. Earlier work in the middle estuary is not quantitatively comparable with the data that we present here. In 1971, Bousfield et al. (1973) sampled the ETZ, but with a bigger mesh size (158 µm instead of 63 µm), thus missing potential nauplii and rotifers. The study by Laprise and Dodson (1994) from the late 1980s only examined *E. affinis* and *B. longirostris* and abundances were estimated semiquantitatively; smaller zooplankton were not counted. These data sets were thus unsuitable for integration into our analysis.

Veliger invasion

Although the distribution of adult zebra mussels had reached at least into the intertidal zone of the St. Lawrence Estuary at Levis as early as 1992 (Mellina and Rasmussen 1994*a*), veligers were not detected in our sampling of the ETZ of the St. Lawrence River in 1993 and were only first observed there in 1994, at which time and thereafter they occurred in great numbers. Despite the spatial limitation of the 1993 sampling, we are confident in our observation of the absence of veligers in 1993. Although adult zebra mussels had already been documented along the St. Lawrence River down to the western tip of the Île d'Orléans in 1992, their abundance was very low (a maximum of 1631 individuals·m^{-2} at Port de Bécancour and 287 individuals·m^{-2} at Île d'Orléans (Costan and de Lafontaine 2000). The combination of low adult densities throughout the St. Lawrence River with the dilution of larvae by high river outflow proba-

© 2005 NRC Canada

Table 5. Kruskal–Wallis ANOVA calculated for the abundance of each taxon for factor "years" and post hoc multiples comparisons (Tukey's test after Dunn for unequal sample size) for each taxon in each salinity group.

Taxon	Salinity group	*df*	*N*	*H*	*p*	Multiple comparisons test (years)				
Dreissena polymorpha veliger	Tidal fresh water	4	61	56.9	<0.001	1995	2001	1994	2000	1993
	True estuarine	4	40	29.2	<0.001	2001	1995	2000	1994	1993
	Euryhaline–marine	2	40	1.3	0.513					
Rotifer	Tidal fresh water	4	61	54.8	0.000	1995	1994	2001	2000	1993
	True estuarine	4	40	29.7	<0.001	1995	1994	2001	2000	1993
	Euryhaline–marine	2	40	4.2	0.118					
Naupfii	Tidal fresh water	4	61	16.8	0.002	1995	2001	1993	1994	2000
	True estuarine	4	40	20.7	<0.001	1995	1993	1994	2001	2000
	Euryhaline–marine	2	40	19.3	<0.001			1995	1994	2000
Eurytemora affinis	Tidal fresh water	4	61	16.6	0.002	1995	1993	2001	1994	2000
	True estuarine	4	40	21.4	<0.001	1995	1993	1994	2001	2000
	Euryhaline–marine	2	40	14.3	0.002			2000	1995	1994
Bosmina longirostris	Tidal fresh water	4	61	8.1	0.085					
	True estuarine	4	40	14.6	0.005	1994	2000	1993	2001	1995
	Euryhaline–marine	2	40	1.0	0.600					
Harpacticoid copepods	Tidal fresh water	4	61	4.1	0.389					
	True estuarine	4	40	7.2	0.126					
	Euryhaline–marine	2	40	0.1	0.955					
Cyclopoid copepods	Tidal fresh water	4	61	34.0	<0.001	2001	1994	1993	1995	2000
	True estuarine	4	40	6.5	0.165					
	Euryhaline–marine	2	40	12.7	0.002			1994	1995	2000
Acartia sp.	Tidal fresh water	4	61	0.0	1.000					
	True estuarine	4	40	0.0	1.000					
	Euryhaline–marine	2	40	7.0	0.029			1994	1995	2000

Note: Post hoc multiples comparisons were not conducted in the case of nonsignificance (multiple comparisons test column left blank). The degrees of freedom (df), number of samples (*N*), *H* statistic, and significance levels (*p*) are shown. In multiple comparisons tests, years are ordered by decreasing ranks from left to right and nonsignificant differences among years are underlined.

bly left veliger densities below our ability to detect them until 1994. The data for all years after 1993 always indicated that maximum abundances of veligers occurred in June and July in the tidal freshwater region of the middle estuary. Thus, even if present in 1993, the abundance of veligers must have been very low. Otherwise, veligers would have been easily detectable in the June 1993 samples.

Densities of veligers were much higher than at upstream sites in the fluvial part of the river where the peak abundance in early July was 40 veligers·L^{-1} (de Lafontaine et al. 1995). Veligers are estimated to drift at a rate of 250–500 km·week^{-1} in the fluvial part of the St. Lawrence River (Costan and de Lafontaine 2000), suggesting a high advective loss from these fluvial habitats. In contrast, tidal influence farther downstream could prolong residence time, and net drift distance could be shortened (i.e., the concept of persistence (Speirs and Gurney 2001)). This combination of advection and retention may explain the high observed veliger abundance at the head of the transition zone and may thus reflect the reproduction from the ensemble of established upstream populations. In contrast, local production in the ETZ is likely to be relatively small because of limited

© 2005 NRC Canada

Fig. 4. Interannual variation in mean summer abundance (June and July pooled) in the tidal freshwater group of (*a*) *Dreissena polymorpha*, (*c*) rotifers, (*e*) nauplii, and (*g*) *Eurytemora affinis* and the true estuarine group of (*b*) *D. polymorpha*, (*d*) rotifers, (*f*) nauplii, and (*h*) *E. affinis* during preinvasion (1993), invasion (1994 and 1995), and postinvasion (2000 and 2001). Bars represent standard errors, and letters above the bars indicate significant differences from multiple comparisons.

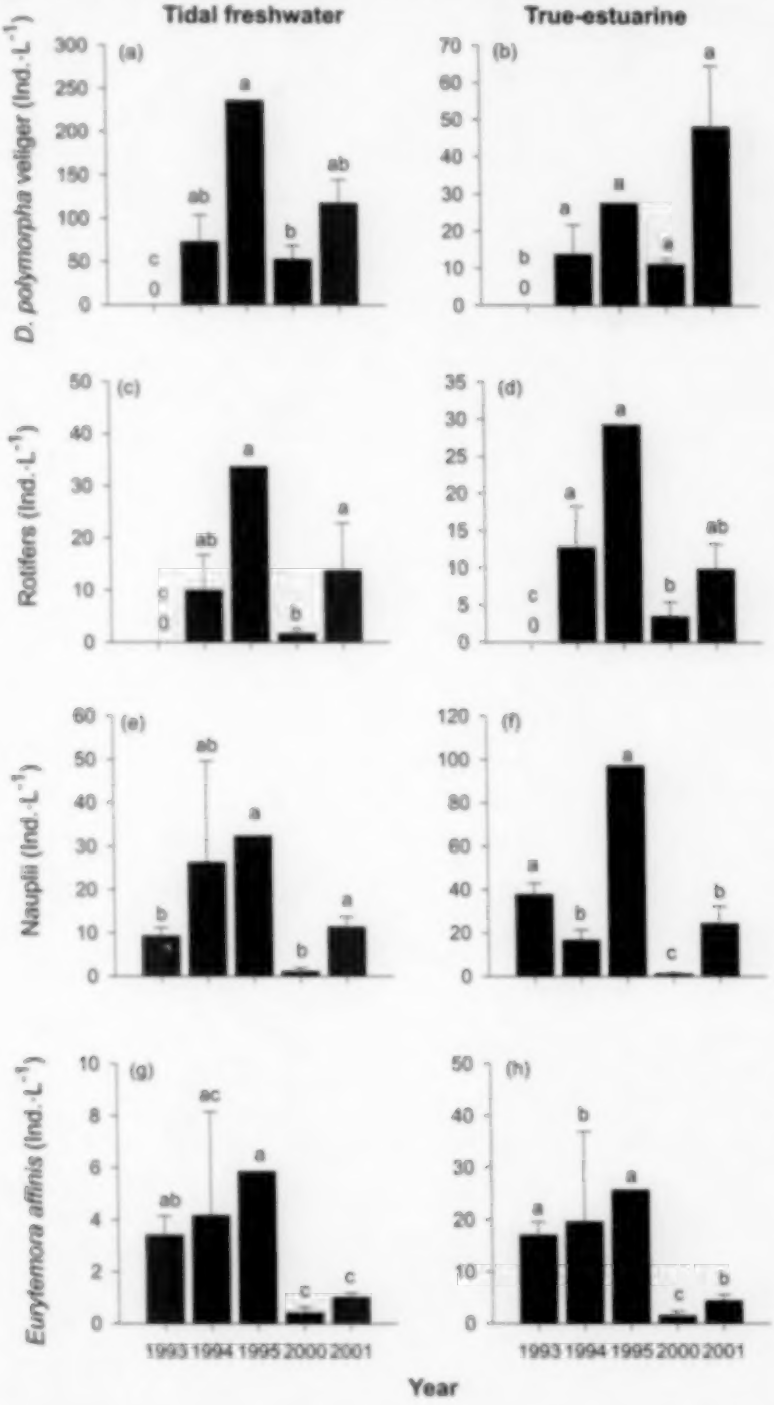

© 2005 NRC Canada

Fig. 5. Monthly air temperature, discharge anomalies at Québec, and monthly zooplankton abundance anomalies in the tidal freshwater and true estuarine groups for the years 1993–1995, 2000, and 2001. An asterisk indicates that data for that month were not available.

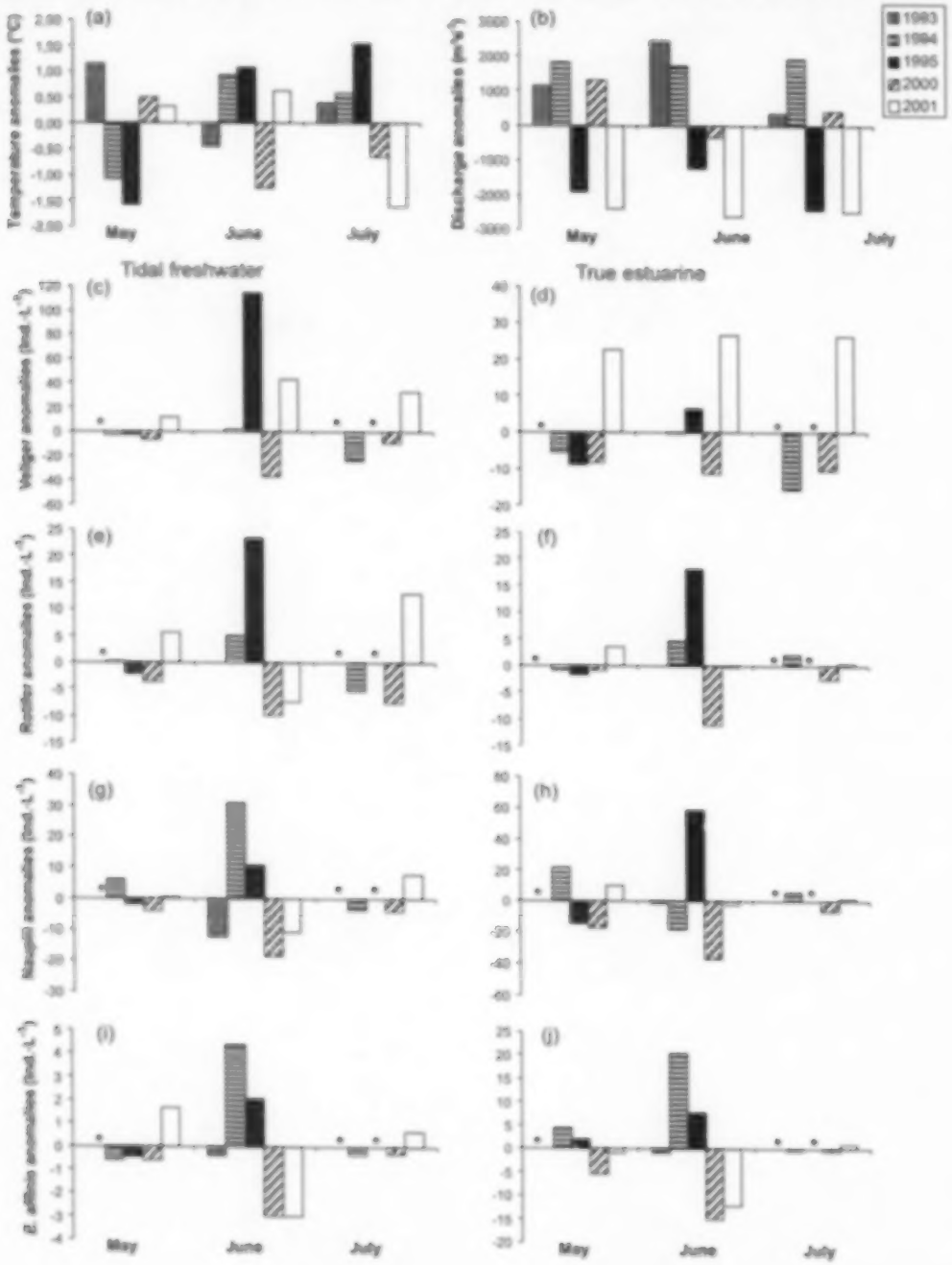

distribution and low population densities at the head of the ETZ (Costan and de Lafontaine 2000; A. Casper, Québec–Océan, Pavillon Vachon, Université Laval, Québec, QC G1K 7P4, Canada, unpublished data). Mean veliger abundance in 1994, 1995, 2000, and 2001 did not show any consistent trend with time of invasion, and the high interannual

© 2005 NRC Canada

variability in veliger abundance may be simply due to changes in reproduction of upstream populations as well as in the river discharge controlling advection of veligers (see below).

Effect of the invasion on individual zooplankton species

Interannual variation in the abundance of the preinvasion zooplankton in the tidal freshwater and true estuarine assemblages did not appear to be related to the invasion of veligers in the ETZ. Abundance patterns of preinvasion taxa were more or less rising and falling in synchrony, with changes in relative amplitude that suggested that other factors are responsible for the interannual variation (see below). An exception might be the copepod *E. affinis* where abundance in the postinvasion phase (2000 and 2001) was lower than in the preinvasion and invasion periods, but it is unclear if this decline in abundance was directly or indirectly caused by the invasion. Density variation found in this study corresponded to the densitiy range (0.01–3 *E. affinis*·L^{-1}) found in the early 1970s (Bousfield et al. 1973) and 1980s (Laprise and Dodson 1994). Although both species are filter-feeders, exploitative competition for food between *E. affinis* and *D. polymorpha* veligers is highly unlikely, as their ability to ingest particles differs. Veligers appear to be limited to particles sizes ≤10 µm (Bernier 2003) whereas *Eurytemora* spp. ingest particles ranging from 1 to 200 µm, including free-living and attached bacteria (Boak and Goulder 1983), phytoplankton (Uitto 1996), seston (Poulet 1978), and micro- and macro-aggregates (Zimmermann-Timm 2002). In the middle estuary, a high percentage of free-living autotrophs form aggregates with increases in salinity >2 psu, suggesting that food availability is reduced for veligers (Barnard et al. 2003). In contrast, food resources for *E. affinis* are probably unlimited because of their omnivorous behaviour and ability to exploit a vast size range of prey.

In contrast, the abundance of rotifers (e.g., *Keratella* sp.) closely paralleled that of the veligers, including their absence in samples from 1993. Rotifers, feeding most efficiently on protists in the 4- to 17-µm size range (Arndt 1993), seem to have very similar food requirements to *D. polymorpha* veligers (Bernier 2003), and isotopic ($\delta^{15}N$) studies indicate that both taxa occupy the same trophic level (Martineau et al. 2004). The invasion by the veligers did not, however, appear to have any negative effect on rotifers, as there was no obvious decline in their abundance. Competition for food resources may not exist in the ETZ because of its high primary production (Frenette et al. 1995; Vincent et al. 1996) and the relatively low abundance of rotifers (260 rotifers·L^{-1} compared with 900–1000 rotifers·L^{-1} reported from upstream sites (Thorp and Casper 2002, 2003)). Furthermore, veliger abundance in the ETZ was positively correlated with Chl *a* and protist abundance, suggesting that food limitation is unlikely (Barnard et al. 2003).

The total absence of rotifers in the 1993 samples should be interpreted with caution. Winkler et al. (2003) could not find rotifers in these samples in spite of the fact that they occurred in the digestive tracts of mysids collected at the same time. Thus, we are certain that rotifers were present in the ETZ in 1993 but suspect that they were not detectable owing to very low densities. In addition, sampling efforts in 1993 were focussed on a 3-day period in June and thus are not representative of the entire summer.

Bosmina longirostris also showed no decline with the invasion of *D. polymorpha* veligers in the system. Abundance ranged between 0.1 and 3.6 individuals·L^{-1} depending on sampling site, month, and year. In earlier sampling campaigns in the 1970s, 2 individuals·L^{-1} were found in the tidal freshwater region but declined with increasing salinity in the true estuarine zone (0.2 individual·L^{-1}) (Bousfield et al. 1973), and in the 1980s, Laprise and Dodson (1994) found 0.1–1 individual·L^{-1} in the tidal freshwater assemblage. In terms of possible trophic interactions with veligers and rotifers, *B. longirostris* is potentially a superior competitor for protists. Their feeding size spectrum (4–45 µm) is broader and completely encompassed the feeding range of the latter taxa (Bogdan and Gilbert 1982; Cyr and Curtis 1999). Moreover, stable isotope analysis indicates that *B. longirostris* is situated on a higher trophic level than either rotifers or veligers (Martineau et al. 2004), suggesting that there is little overlap in food resources between them.

Overall, then, there is little evidence for competitive interactions between zooplankton species, and we suggest that the ETZ is still able to support a high level of zooplankton standing stock despite the invasion of *D. polymorpha* veligers in this ecosystem. There was nevertheless substantial interannual variation in the abundance of preinvasion taxa, but we assert that this variation is more likely due to forcing by the physical environment (e.g., discharge and weather) and biological properties of the zooplankton taxa (food conditions, reproduction, predation, and mortality) than to the massive occurrence of *D. polymorpha* veligers in the system. For example, all taxa, including *D. polymorpha* veligers, showed the highest abundance in 1995 and the lowest abundance in 2000 compared with all other years. These extremes coincided with negative temperature anomalies in 2000 and positive ones in 1995 measured at Québec. Furthermore, cumulative degree-days in the tidal freshwater section in May, June, and July reflected the same patterns (data not shown). Without a longer time series of data from the ETZ, it is not possible to more rigorously evaluate changes in the preinvasion and invasion communities. However, in the Baltic Sea, interannual variability during spring and summer of small copepods (*Acartia* spp. and *E. affinis*) was controlled by climate variability (Viitasalo 1992; Dippner et al. 2000).

Weak relationships between monthly discharge and abundance of preinvasion species suggest that discharge is a minor factor driving interannual variation. In contrast, the negative correlations between the abundance of veligers and discharge support the idea that discharge may affect veligers directly by controlling advective losses (and thus the persistence of veliger populations), the position of the saltwater–freshwater front, the extent of estuarine recirculation, and the hydraulic and particle residence times (Pace et al. 1992; Jassby et al. 1995; Speirs and Gurney 2001). Thus, the higher discharge may lead to a lower residence time of veligers owing to high net advective outflow.

Biotic factors are also likely to influence zooplankton dynamics and may be partly responsible for interannual variation in abundance. Population growth and egg production in copepods are dependent on food resources, and population size may be impaired by mortality (i.e., predation) (Heinle et

© 2005 NRC Canada

al. 1977; Plourde and Runge 1993; Peitsch et al. 2000).

Effect of the veliger invasion on zooplankton assemblages

Relative dominance of *D. polymorpha* veligers showed a tendency to increase in all zooplankton assemblages from the initial to the postinvasion phase. Whereas there was no evidence that the arrival of veligers in the ETZ has affected the abundance of zooplankton species living there, they have changed the statistical characteristics and distinctiveness of the three zooplankton assemblages (tidal fresh water, true estuarine, and euryhaline–marine) distributed longitudinally along the ETZ of the St. Lawrence Middle Estuary. During the initial stages of the invasion (1994 and 1995), the tidal freshwater assemblage was dominated by *D. polymorpha* veligers whereas copepods were mostly responsible for the within-assemblage structure of the true estuarine and euryhaline–marine assemblages. Statistically, these two assemblages could not be discriminated, but this is most likely due to the low numbers of sampling sites in both assemblages. During the postinvasion phase, veligers made the greatest contribution to the within-group similarity in all assemblages, and by 2001, the tidal freshwater assemblage could not be discriminated from the true estuarine assemblage. Furthermore, the exclusion of veligers from the analysis revealed a random distribution between the tidal freshwater and true estuarine assemblages in all years, except 2001 in which a slight difference between the two assemblages occurred. Our results suggest that the distinction between the tidal freshwater and true estuarine assemblages is highly dependent on sample size, abundance of contributing taxa, and within-assemblage variability. In consequence, to reveal finer differences between zooplankton assemblages, it is necessary to increase the resolution of community structure by documenting the abundance of separate species instead of multispecies groups such as nauplii and rotifers, cyclopoid copepods, and harpacticoid copepods. Different species integrated in these taxa may have obscured differences in community structure.

The strong correlations between biotic and abiotic patterns suggest that the physical environment controls the longitudinal distribution and composition of the zooplankton assemblages in the middle estuary. Both temperature and salinity play a role, but the high correlations between zooplankton abundance and salinity suggest that it is the primary factor explaining the distribution of zooplankton, supporting the conclusions of previous studies of the ETZ of this estuary (Laprise and Dodson 1994; Barnard et al. 2003; Winkler et al. 2003).

The ETZ as a sink for *D. polymorpha* veligers

Veliger densities decreased significantly from the tidal freshwater to the euryhaline–marine assemblage, illustrating that the ETZ acts as a sink for the larval stage. As adult densities are quite low (maximum of 670 mussels·m^{-2}, occurring in patches on hard substrate) in the ETZ (A. Casper, Québec–Océan, Pavillon Vachon, Université Laval, Québec, QC G1K 7P4, Canada, unpublished data), this pattern is undoubtedly the result of high rates of mortality rather than high settlement. The strong negative correlation with salinity suggests that osmotic stress is an important mortality factor, and this conclusion is consistent with other laboratory and field studies. A parallel field survey in the ETZ found that the greatest decrease in veliger density in the ETZ occurred at around 2 psu (Barnard et al. 2003). Feeding rates in the laboratory declined linearly between 0 and 5 psu (Bernier 2003), and lethal salinity levels have been estimated at 4–4.5 psu (Kilgour et al. 1994; Wright et al. 1996). Alternatively, the high discharge and tides of the ETZ produce strong currents (up to 3 m·s^{-1}) and high turbulent mixing (1 m^2·s^{-1}) (Laprise and Dodson 1989), resulting in shear forces and turbulence that can increase mortality of veligers (Horvath and Lamberti 1999). The strong estuarine circulation also creates high turbidity (up to 400 nephelometric turbidity units), but veliger feeding activity is much less affected by turbidity relative to salinity in laboratory studies (Bernier 2003). Finally, there is also the possibility that predation rates might be high. Larval fish, however, do not appear to feed on veligers (H. Yoneksma, Québec–Océan, Pavillon Vachon, Université Laval, Québec, QC G1K 7P4, Canada, unpublished data). Predation by the dominant mysid *N. americana* has been observed on veligers in the ETZ (G. Winkler, unpublished data), but it remains unknown if this predation is sufficient to limit veliger abundance.

In summary, the veligers of the zebra mussel have seasonally dominated the zooplankton communities of the ETZ of the St. Lawrence Estuary, especially in the tidal freshwater portion, since 1994. This invasion appears, however, to have had little impact on individual zooplankton species. Comparisons of the interannual variation in abundance of potential competitors such as rotifers, *E. affinis*, and *B. longirostris* showed little indirect evidence of any competitive effect, (e.g., declines in abundance over time or a negative relationship with the abundance of veligers). Much interannual variation was observed in the abundance of individual species but appears to reflect variation in the abiotic environment such as temperature rather than the *D. polymorpha* invasion. The addition of this invader has, however, changed the statistical characterization of zooplankton community structure in the tidal freshwater and true estuarine assemblages because of its numerical dominance. Although the functioning of this ecosystem seems not to have been impaired by this invasion and it is still able to support the zooplankton community, the veligers have changed its nature by playing a numerically dominant but noninteractive role. In effect, their presence is transitory, as the abundance of veligers is both temporally limited by the reproduction of upstream populations and spatially limited by the strong salinity gradient that appears to be largely responsible for the decline downstream of veliger abundance in the ETZ. Thus, the ETZ of the St. Lawrence Estuary acts as a veliger sink.

Acknowledgements

The authors are deeply indebted to the many people who contributed to the sampling program and data analysis. We thank the crew members of the *Mondax* and *Willie DeRaspe* for their help in the field. Special thanks are extended to B. Laberge, F. Benichou, S. Roy, C. Fasulo, A. van den Eede, M. Davy, and K. Philippot for their assistance in the laboratory and field. We also thank A. Casper and C. Barnard for helpful discussions. This research was supported by grants

© 2005 NRC Canada

from the Natural Sciences and Engineering Research Council of Canada to J.J.D. and L.E.J. This is a contribution to the program of Québec–Océan (Groupe interinstitutionnel de recherches océanographiques du Québec), formerly GIROQ.

References

Arndt, H. 1993. Rotifers as predators on components of the microbial web (bacteria, heterotrophic flagellates, ciliates) — a review. Hydrobiologia, **255**: 231–246.

Barnard, C., Frenette, J.J., and Vincent, W.F. 2003. Planktonic invaders of the St. Lawrence estuarine transition zone: environmental factors controlling the distribution of zebra mussel veligers. Can. J. Fish. Aquat. Sci. **60**: 1245–1257.

Bernier, S. 2003. Efficacité et sélectivité alimentaire des larves de la Moule zébrée: effets potentiels sur le réseau alimentaire de la zone de transition estuarienne du St-Laurent. M.S. thesis, Université Laval, Québec, Que.

Bonk, A.C., and Goulder, R. 1983. Bacterioplankton in the diet of the calanoid copepod *Eurytemora* sp. in the Humber Estuary. Mar. Biol. **73**: 139–149.

Bogdan, K.G., and Gilbert, J.J. 1982. Seasonal patterns of feeding by natural populations of *Keratella*, *Polyarthra*, and *Bosmina*: clearance rates, selectivities and contributions to community grazing. Limnol. Oceanogr. **27**: 918–934.

Bousfield, E.L., Filteau, G., O'Neill, M., and Gentes, P. 1973. Population dynamics of zooplankton in the middle St. Lawrence Estuary. *In* Estuarine research. Vol. 1. Chemistry, biology, and the estuarine system. *Edited by* L.E. Cronin. Academic Press, Inc., New York.

Butler, J.L. 1992. Collection and preservation of material for otolith analysis. *In* Otolith microstructure examination and analysis. *Edited by* D.K. Stevenson and S.E. Campana. Can. Spec. Publ. Fish. Aquat. Sci. No. 117. pp. 13–17.

Clarke, K.R. 1993. Non-parametric multivariate analysis of changes in community structure. Aust. J. Ecol. **18**: 117–143.

Clarke, K.R., and Warwick, R.M. 2001. Change in marine communities: an approach to statistical analysis and interpretation. 2nd ed. Plymouth Marine Laboratory, Plymouth, UK.

Costan, G., and de Lafontaine, Y. 2000. Présence de la moule zébrée dans le Saint-Laurent: à suivre. Environnement Canada, Centre Saint-Laurent, Montréal, Que.

Cyr, H., and Curtis, J.M. 1999. Zooplankton community size structure and taxonomic composition affects size-selective grazing in natural communities. Oecologia, **118**: 306–315.

D'Anglejan, B. 1981. On the advection of turbidity in the St. Lawrence middle estuary. Estuaries, **4**: 2–15.

Dauvin, J.-C., and Dodson, J.J. 1990. Relationship between feeding incidence and vertical and longitudinal distribution of rainbow smelt larvae (*Osmerus mordax*) in a turbid well-mixed estuary. Mar. Ecol. Prog. Ser. **60**: 1–12.

de Lafontaine, Y., Lapierre, L., Henry, M., and Grégoire, Y. 1995. Abondances des larves de moule zébrée (*Dreissena polymorpha*) et de quagga (*Dreissena bugensis*) aux abords des centrales hydroélectriques de Beauharnois, les Cèdres et Rivière des Prairies. Rapport scientifique et technique St-14. Environment Canada, Région du Québec, Conservation de l'environnement, Centre Saint-Laurent, Montréal, Que.

Dippner, J.W., Kornilovs, G., and Sidrevics, L. 2000. Long-term variability of mesozooplankton in the Central Baltic Sea. J. Mar. Syst. **25**: 23–31.

Frenette, J.J., Vincent, W.F., Dodson, J.J., and Lovejoy, C. 1995. Size-dependent variations in phytoplankton and protozoan community structure across the St. Lawrence River transition region. Mar. Ecol. Prog. Ser. **120**: 1–3.

Griffiths, R.W., Schloesser, D.W., Leach, J.H., and Kovalak, W.P. 1991. Distribution and dispersal of the zebra mussel (*Dreissena polymorpha*) in the Great Lakes region. Can. J. Fish. Aquat. Sci. **48**: 1381–1388.

Heinle, D.R., Harris, R.P., Ustach, J.F., and Flemer, D.A. 1977. Detritus as food for estuarine copepods. Mar. Biol. **40**: 341–353.

Horvath, T.G., and Lamberti, G.A. 1999. Mortality of zebra mussel, *Dreissena polymorpha*, veligers during downstream transport. Freshw. Biol. **42**: 69–76.

James, W.F., Barko, J.W., Davis, M., Eakin, H.L., Rogala, J.T., and Miller, A.C. 2000. Filtration and excretion by zebra mussels: implications for water quality impacts in Lake Pepin, upper Mississippi River. J. Freshw. Ecol. **15**: 429–437.

Jassby, A., Kimmerer, W., Monismith, S., Armor, C., Cloern, J., Powell, T., Schubel, J., and Vendlinski, T. 1995. Isohaline position as a habitat indicator for estuarine populations. Ecol. Appl. **5**: 272–289.

Johnson, L.E. 1995. Enhanced early detection and enumeration of zebra mussel (*Dreissena* spp.) veligers using cross-polarised light microscopy. Hydrobiologia, **312**: 139–146.

Johnson, L.E., and Carlton, J.T. 1996. Post-establishment spread in large-scale invasions: dispersal mechanisms of the zebra mussel *Dreissena polymorpha*. Ecology, **77**: 1686–1690.

Kilgour, B., Mackie, G.L., Baker, M.A., and Keppel, R. 1994. Effects of salinity on the condition and survival of zebra mussels (*Dreissena polymorpha*). Estuaries, **17**: 385–393.

Laprise, R., and Dodson, J.J. 1989. Ontogeny and importance of tidal vertical migration in the retention of larval smelt *Osmerus mordax* in a well-mixed estuary. Mar. Ecol. Prog. Ser. **55**: 101–111.

Laprise, R., and Dodson, J.J. 1990. The mechanism of retention of pelagic tomcod, *Microgadus tomcod*, larvae and juveniles in the well-mixed part of the St. Lawrence Estuary. Environ. Biol. Fishes, **29**: 293–302.

Laprise, R., and Dodson, J.J. 1994. Environmental variability as a factor controlling spatial patterns in distribution and species diversity of zooplankton in the St. Lawrence estuary. Mar. Ecol. Prog. Ser. **107**: 67–81.

Legendre, P., and Legendre, L. 1998. Numerical ecology. Elsevier Science Publishers BV, Amsterdam, Netherlands.

MacIsaac, H.J., Sprules, W.G., Johannsson, O.E., and Leach, J.H. 1992. Filtering impacts of larval and sessile zebra mussels (*Dreissena polymorpha*) in western Lake Erie. Oecologia, **92**: 30–39.

Mackie, G.L., and Kilgour, B.W. 1992. Effects of salinity on growth and survival of zebra mussels (*Dreissena polymorpha*). J. Shellfish Res. **11**: 230.

Martel, A., Hynes Teresa, M., and Buckland-Nicks, J. 1995. Prodissoconch morphology, planktonic shell growth, and size at metamorphosis in *Dreissena polymorpha*. Can. J. Zool. **73**: 1835–1844.

Martineau, C., Vincent, W., and Frenette, J.J. 2004. Primary consumers and particulate organic matter: isotopic evidence of strong selectivity in the estuarine transition zone. Limnol. Oceanogr. **49**: 1679–1686.

Mellina, E., and Rasmussen, J.B. 1994*a*. Occurrence of zebra mussel (*Dreissena polymorpha*) in the intertidal region of the St. Lawrence estuary. J. Freshw. Ecol. **9**: 81–84.

Mellina, E., and Rasmussen, J.B. 1994*b*. Patterns in the distribution and abundance of zebra mussel (*Dreissena polymorpha*) in rivers and lakes in relation to substrate and other physicochemical factors. Can. J. Fish. Aquat. Sci. **51**: 1024–1036.

Pace, M.L., Findlay, S.E.G., and Lints, D. 1992. Zooplankton in

© 2005 NRC Canada

advective environments: the Hudson River community and a comparative analysis. Can. J. Fish. Aquat. Sci. **49**: 1060–1069.

Pace, M.L., Findlay, S.E.G., and Fischer, D. 1998. Effects of an invasive bivalve on the zooplankton community of the Hudson River. Freshw. Biol. **39**: 103–116.

Peitsch, A., Knepcke, B., and Bernat, N. 2000. Long-term investigation of the distribution of *Eurytemora affinis* (Calanoida; Copepoda) in the Elbe Estuary. Limnologica, **30**: 175–182.

Plourde, S., and Runge, J.A. 1993. Reproduction of the planktonic copepod *Calanus finmarchicus* in the Lower St. Lawrence Estuary — relation to the cycle of phytoplankton production and evidence for a *Calanus* pump. Mar. Ecol. Prog. Ser. **102**: 217–227.

Poulet, S.A. 1978. Comparison between five coexisting species of marine copepods feeding on naturally occurring particulate matter. Limnol. Oceanogr. **23**: 1126–1143.

Ram, J.L., and McMahon, R.F. 1996. Introduction: the biology, ecology, and physiology of zebra mussels. Am. Zool. **36**: 239–243.

Ricciardi, A., Whoriskey, F.G., and Rasmussen, J.B. 1997. The role of the zebra mussel (*Dreissena polymorpha*) in structuring macroinvertebrate communities on hard substrata. Can. J. Fish. Aquat. Sci. **54**: 2596–2608.

Simons, R. 2004. Circulation and zooplankton retention in the estuarine transition zone of the St. Lawrence Estuary. Ph.D. thesis, Stanford University, Stanford, Calif.

Sirois, P., and Dodson, J. 2000. Influence of turbidity, food density and parasites on the ingestion and growth of larval rainbow smelt *Osmerus mordax* in an estuarine turbidity maximum. Mar. Ecol. Prog. Ser. **193**: 167–179.

Speirs, D.C., and Gurney, W.S.C. 2001. Population persistence in rivers and estuaries. Ecology, **82**: 1219–1237.

Thorp, J.H., and Casper, A.F. 2002. Potential effects on zooplankton from species shifts in planktivorous mussels: a field experiment in the St. Lawrence River. Freshw. Biol. **47**: 107–119.

Thorp, J.H., and Casper, A.F. 2003. Importance of biotic interactions in large rivers: an experiment with planktivorous fish, dreissenid mussels and zooplankton in the St. Lawrence River. River Res. Appl. **19**: 265–279.

Uitto, A. 1996. Summertime herbivory of coastal mesozooplankton and metazoan microplankton in the northern Baltic. Mar. Ecol. Prog. Ser. **132**: 47–56.

Vanderploeg, H.A., Nalepa, T.F., Jude, D.J., Mills, E.L., Holeck, K.T., Liebig, J.R., Grigorovich, I.A., and Ojaveer, H. 2002. Dispersal and emerging ecological impacts of Ponto-Caspian species in the Laurentian Great lakes. Can. J. Fish. Aquat. Sci. **59**: 1209–1228.

Viitasalo, M. 1992. Mesozooplankton of the Gulf of Finland and northern Baltic Proper — a review of monitoring data. Ophelia, **35**: 147–168.

Vincent, W.F., and Dodson, J.J. 1999. The St. Lawrence River, Canada–USA: the need for an ecosystem-level understanding of large rivers. Jpn. J. Limnol. **60**:29–50.

Vincent, W., Bertrand, N., and Frenette, J.J. 1994. Photoadaptation to intermittent light across the St. Lawrence Estuary freshwater–saltwater transition zone. Mar. Ecol. Prog. Ser. **110**: 2–3.

Vincent, W.F., Dodson, J.J., Bertrand, N., and Frenette, J.J. 1996. Photosynthetic and bacterial production gradients in a larval fish nursery: the St. Lawrence River transition zone. Mar. Ecol. Prog. Ser. **139**: 227–238.

Walton, W.C. 1996. Occurrence of zebra mussel (*Dreissena polymorpha*) in the oligohaline Hudson River, New York. Estuaries, **19**: 612–618.

Winkler, G., Dodson, J.J., Bertrand, N., Thivierge, D., and Vincent, W.F. 2003. Trophic coupling across the St. Lawrence River estuarine transition zone. Mar. Ecol. Prog. Ser. **251**: 59–73.

Wright, D.A., Setzler Hamilton, E.M., Magee, J.A., and Harvey, H.R. 1996. Laboratory culture of zebra (*Dreissena polymorpha*) and quagga (*D. bugensis*) mussel larvae using estuarine algae. J. Gt. Lakes Res. **22**: 46–54.

Zar, J.H. 1996. Biostatistical analysis. Prentice Hall, Upper Saddle River, N.J.

Zimmermann-Timm, H. 2002. Characteristics, dynamics and importance of aggregates in rivers — an invited review. Int. Rev. Gesamten Hydrobiol. **87**: 197–240.

© 2005 NRC Canada

Physical fluxes, pelagic ecosystem structure, and larval fish survival in Hauraki Gulf, New Zealand

John R. Zeldis, John Oldman, Sira L. Ballara, and Laura A. Richards

Abstract: The ecosystem supporting snapper (*Pagrus auratus*) larvae was studied during three spring–summer (November–January 1985–1988) spawning seasons in Hauraki Gulf, New Zealand. Upwelling-favourable winds caused more incursion of shelf water into the Gulf in 1985–1986 and 1986–1987 than in 1987–1988, but in the first two seasons, the winds were relatively weak. Stronger winds in 1987–1988 drove greater vertical diffusivity and correlated with greater mixed-layer primary biomass and productivity. Effects of vertical mixing appeared to dominate horizontal incursion of upwelled shelf water in supporting upper water column productivity. The more productive 1987–1988 season had greater abundances of nauplii, copepodites, adult copepods, cladocerans, chaetognaths, hydromedusae, decapod larvae, and numerous larval fish taxa (including snapper). There was much higher survival of snapper between the late-stage egg and post-first-feeding larval stages in 1987–1988, which correlated spatially and temporally with high larval prey densities. Neither higher egg production, fewer predators, nor less horizontal advection accounted for these strong larval snapper cohorts. We hypothesize that larval competence improved within the superior larval feeding environment, reducing predatory losses. The ecosystem response to wind mixing may partially explain the correlation of sea temperatures with recruitment, previously observed for the Hauraki Gulf snapper stock.

Résumé : Nous avons étudié l'écosystème qui alimente les larves de pagres (*Pagrus auratus*) durant trois périodes de fraye au printemps et à l'été (novembre à janvier, 1985–1988) dans le golfe d'Hauraki, Nouvelle-Zélande. Des vents favorisant les affleurements ont provoqué plus d'incursions dans le golfe d'eau provenant de la plate-forme continentale en 1985–1986, et en 1986–1987 qu'en 1987–1988, bien que les vents aient été relativement faibles durant les deux premières saisons. Des vents plus forts en 1987–1988 ont causé une diffusivité verticale plus importante et sont reliés à une biomasse et une productivité primaires plus élevées dans la couche de mélange. Les effets du brassage vertical semblent surpasser l'incursion horizontale d'eau d'affleurement en provenance de la plate-forme continentale comme soutien de la productivité dans la partie supérieure de la colonne d'eau. La saison plus productive de 1987–1988 a vu de plus grandes abondances de nauplies, de copépodites, de copépodes adultes, de cladocères, de chétognathes, d'hydroméduses, de larves de décapodes et de larves de plusieurs taxons de poissons, dont les pagres. La survie des pagres depuis la fin du stade oeuf jusqu'aux stades larvaires qui suivent la première alimentation a été plus importante en 1987–1988, ce qui est relié dans le temps et dans l'espace à de fortes densités de proies pour les larves. La présence de ces fortes cohortes de larves de pagres ne s'explique ni par une production accrue d'oeufs, ni par une réduction des prédateurs, ni par une diminution de l'advection horizontale. Nous posons l'hypothèse selon laquelle la compétence des larves s'est améliorée dans un milieu alimentaire enrichi, ce qui a réduit les pertes par prédation. La réaction de l'écosystème au brassage par le vent peut peut-être expliquer en partie la corrélation entre la température de la mer et le recrutement, observée antérieurement chez le stock de bagres du golfe d'Hauraki.

[Traduit par la Rédaction]

Introduction

The Hauraki Gulf in northeastern New Zealand (Fig. 1) supports the country's largest and most valuable stock of snapper (*Pagrus auratus*) (Sparidae) (Annala et al. 2002). Annual recruitment of 1-year-old (1+) snapper to this fishery has varied eightfold over a 12-year time series of trawl surveys (Annala et al. 2002) and is correlated (r = 0.89) with surface sea temperature in the Gulf during the late larval and early juvenile period. Snapper are serial spawners, with females releasing batches of eggs daily into the coastal plankton (<35 m depth) from early October (spring) to February (summer), with the most intense spawning in November and December (Scott et al. 1993; Zeldis and Francis 1998). This extended period of egg production could allow interannual variation in intensity of larval settlement if poor or favour-

Received 24 March 2004. Accepted 22 November 2004. Published on the NRC Research Press Web site at http://cjfas.nrc.ca on 13 April 2005.
J18046

J.R. Zeldis.[1] National Institute of Water and Atmospheric Research, P.O. Box 8602, Riccarton, Christchurch, New Zealand.
J. Oldman. National Institute of Water and Atmospheric Research, Gate 10 Silverdale Road, Hamilton, New Zealand.
S.L. Ballara. National Institute of Water and Atmospheric Research, P.O. Box 14-901, Kilbirnie, Wellington, New Zealand.
L.A. Richards. P.O. Box 958, Nelson, New Zealand.

[1]Corresponding author (e-mail: j.zeldis@niwa.co.nz).

 doi: 10.1139/F04-209 © 2005 NRC Canada

Fig. 1. Location and bathymetry of (*a*) northeast North Island shelf and Hauraki Gulf within New Zealand and (*b*) detail of Hauraki Gulf with grid sampling locations (circles). Larger circles are stations illustrated in Figs. 5*a*–*c* and 6*a*–*c*. The broken lines are the northern (NB) and eastern (EB) boundaries used for the flux calculations in the circulation model.

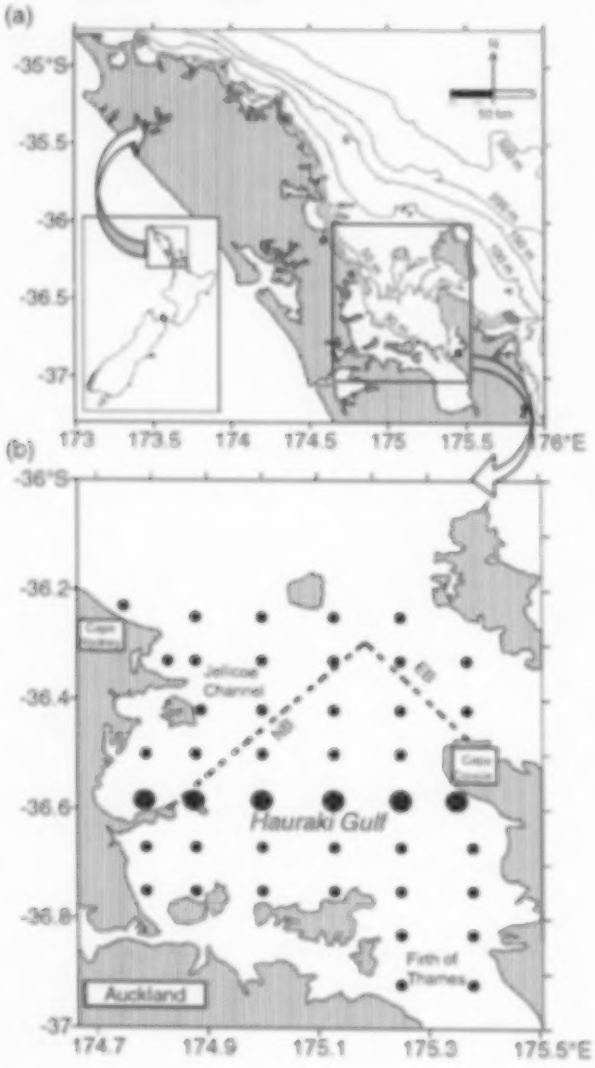

able conditions for egg and larval survival persist for lengthy periods through the spawning season. There is evidence that this occurs in the Gulf snapper stock: using back-calculated settlement dates from otolith check rings, Francis (1994) showed that periods of successful settlement have in some years been brief and in other years extended over much of the spawning season. Similar results have been obtained for *P. auratus* in Spencer Gulf, Australia (Fowler and Jennings 2003). This suggests that a component of snapper recruitment variability may originate within the presettlement phase.

Given the correlation of recruitment with a physical ecosystem variable (temperature) and the possible importance of the presettlement phase in recruitment, the object of our study was to evaluate whether snapper presettlement dynamics were linked to interannual variation in the "ecosystem state" of the Hauraki Gulf and whether physical conditions and prey and predator fields favourable for larval cohort development varied between these states. There is evidence that the ecosystem state of the Hauraki Gulf does vary interannually in response to physical forcing. Upwelling and downwelling over the adjacent continental shelf are favoured by northwesterly and southeasterly along-shelf winds, respectively (Sharples and Greig 1998; Zeldis et al. 2004), and cause variation in nutrient supply and phytoplankton assemblages (Chang et al. 2003; Zeldis 2004). The strength of the mean wind also varies (Gordon 1985), potentially causing variation in vertical mixing regimes with consequent effects on productivity. Both wind direction and wind strength have an interannual signal related to El Niño – Southern Oscillation, with weaker, predominately westerly winds during summer in El Niño periods (Gordon 1985).

We surveyed three consecutive November–January snapper spawning seasons in 1985–1986, 1986–1987, and 1987–1988. Here, we first assess the wind climate and hydrographic structure of the region over this time frame and model the coincident wind-forced horizontal exchange fluxes between the shelf and Gulf and vertical fluxes through the water column. We then assess the coincident structures, abundances, and productivities of Gulf phytoplankton and zooplankton assemblages and consider whether they were driven by the variations in physical fluxes. Finally, we examine variation in fish larval abundance, particularly of snapper, as a function of advection, fish egg abundance, and predators and prey of the larvae and conclude by considering the results in the context of the snapper temperature–recruitment relationship.

Methods

Meteorology and hydrography

Wind speed and direction data were acquired from Auckland Airport, a near sea level, fully exposed meteorological station southwest of the inner Hauraki Gulf (Fig. 1). Along-shelf wind stresses were calculated by adding 30° to the raw bearings, to align the along-shelf component parallel to the coast, and calculating the stress component as described in Sharples and Greig (1998). Vertical profiles of temperature, salinity, and density were made on station grids across the Gulf (Fig. 1) during November–January 1985–1986, 1986–1987, and 1987–1988 using a Guildline conductivity–temperature–depth (CTD) pump-hose assembly (these three survey periods are hereafter referred to as "seasons" in reference to the three snapper spawning seasons surveyed). In 1985–1986, the grids did not include the inner Firth of Thames and were occupied once per month. In 1986–1987 and 1987–1988, the grids were occupied twice per month and extended farther south into the Firth of Thames. All sampling was done in daylight between 06:00 and 20:00.

To determine tidal- and wind-forced water fluxes into and out of the Gulf during the three seasons, a calibrated hydrodynamic model (3DD) of the Gulf was used (Black et al.

© 2005 NRC Canada

2000). The hydrodynamic model was set up with the eastern water level clamped to mean sea level and a geostrophic boundary condition for the northern boundary. This boundary condition assumes that across-shelf water levels are in geostrophic balance with the along-shelf low-frequency currents. Wind records from Auckland Airport for each of the three seasonal simulation periods were used to apply an additional slope on the northern boundary associated with the across-shelf wind stress. For each period, the water flux normal to northern and eastern Gulf boundaries (Fig. 1) was derived. To determine dispersal rates of larval fish during each month of each of the three seasons, the transport/dispersion model P3DD was used. P3DD uses the output from 3DD to advect particles within the model domain. The model was calibrated against field measurements (current meter, dye tests, and CTD) of horizontal and vertical diffusivity of conservative plumes (outfalls) in the Hauraki Gulf. The model was able to accurately simulate plume movement under a range of wind conditions for periods of up to 1 month (Beca-Steven Ltd. 1992; Bell et al. 1999). Five tracer release sites were chosen within the snapper spawning area (using Zeldis and Francis 1998), and for each site, a simulation was carried out whereby larval particles were released continuously at surface (0–5 m), mid- (15–20 m), and bottom (25–30 m) depths and allowed to advect and disperse for 8 days. Trajectories were very similar for the different release depths, so only middepth results (the depth of maximum larval snapper density (Kingsford and Atkinson 1994)) are shown here.

To examine the effects of winds on water column mixing, a measure of mixing energy added to the column by the wind stress was made using E_m (watts per square metre = joules per second per square metre) = $0.0015\rho_a C_{10} U_{10}^3$, where ρ_a is the air density (taken as 1.2 kg·m^{-3}), U_{10} is the wind speed 10 m above the sea surface, and C_{10} is the surface drag coefficient for such winds (Mann and Lazier 1991). The daily mixing energy was estimated for the period from the start of surveys (taken as 10 November) to their end in January (taken as 20 January). We also estimated E_m for the period 1 September – 20 January in each season to include the spring growth period (Chang et al. 2003). Prediction of the amount of deepening of the mixed layer by the wind energy was made using the mean rate of potential energy added per hour to the water column (Mann and Lazier 1991). Finally, the coefficient of vertical eddy diffusivity, K_z (per metre) was calculated from wind and CTD data using $K_z = 0.25\varepsilon N^{-2}$ (Denman and Gargett 1983) where ε is the rate of dissipation of turbulent kinetic energy (proportional to the cube of wind speed calculated using mean wind speed on the day of each CTD cast) and N is the buoyancy frequency.

Phytoplankton, zooplankton, and larval fish sampling and analyses

Water samples were taken at grid stations using the CTD–hose assembly at standard depths (1, 10, 25, 40, and 60 m below the surface in 1985–1986 and 1, 10, 15, 20, 25, 35, 45, and 55 m in 1986–1987 and 1987–1988). Fluorescence, chlorophyll *a* (Chl *a*), and Lugol iodine-preserved phytoplankton compositions were determined as described in Zeldis et al. (1995). Lugol samples were acquired only in December 1985 and in November and December of 1986–1987 and 1987–1988 from inner Gulf stations. Zooplankton >100 µm were collected using the CTD–hose assembly at all grid stations in 1985–1986 and at alternate grid stations in 1986–1987 and 1987–1988 by directing the pump flow through a 100-µm-mesh net on deck. The zooplankton samples were combined over all depths on each pump profile and preserved in 4% formaldehyde. In the laboratory, subsamples were taken with a large-bore pipette, taxa were enumerated until at least 100 individuals of the most common organism were counted, and numbers per cubic metre were calculated by scaling for subsampling the pump flow rate and the pumping time. Fish eggs, fish larvae, and other zooplankton (>365 µm) were collected at each grid station using double-oblique, water column integrated hauls of a plankton net (mouth diameter 80 cm, 365-µm mesh) fitted with a flowmeter and preserved in 4% formaldehyde. In the laboratory, all snapper larvae were removed and measured (standard length) using electronic measuring devices on dissecting microscopes. The samples were then split to one eighth of their original size and all subsampled fish larvae and five common fish egg species (including snapper eggs) were counted. From this subsample, other zooplankton taxa were enumerated until at least 100 individuals of the most common organism were counted. Numbers per cubic metre were calculated by scaling for subsampling and the volume filtered. Snapper eggs were grouped into six morphological stages illustrated in Crossland (1980). Preserved snapper larvae were assigned approximate ages using age-at-length data for cultured snapper (Pankhurst et al. 1991). The larval lengths were corrected for shrinkage by comparing the lengths of preserved larvae at particular morphological stages with published lengths of live snapper larvae at those stages (Pankhurst et al. 1991; Kingsford and Atkinson 1994).

To enable a comparison of phytoplankton photosynthesis between the seasons, we used the Chl *a* values on each profile to estimate the light attenuation for each standard depth interval by employing the empirical relationship of Riley (1956) of average Chl *a* concentration (milligrams per cubic metre) to light attenuation: $k' = 0.04 + 0.0088\text{Chl} + 0.054\text{Chl}^{2/3}$. Gross carbon uptake ($P_g$) was estimated for each depth interval using the parameterization P_g (milligrams carbon per hour) = $P_{max} I/(I_k + I)$Chl, where P_{max} is the maximum photosynthesis, I is the light intensity in the depth interval, and I_k is the light intensity at the junction of the initial slope of P versus I and P_{max} (Parsons et al. 1984). The P_{max} was obtained from P versus I experiments made in the Hauraki Gulf in 1998–2000 (P_{max} = 3.0; M. Gall, NIWA, Christchurch, New Zealand, personal communication). I_k was set at 40% of surface irradiance, and surface irradiance was set as a constant using representative photosynthetically active radiation profile data collected in the surveys of Chang et al. (2003) in the inner Hauraki Gulf in January 1997 using CTD. The irradiance characteristics of the three seasons were assessed and compared using daily mean pyrometer data from the meteorological station at Cape Rodney (Fig. 1*b*).

Abundance differences among taxa of mesozooplankton, fish larvae, and fish eggs between the three seasons were analysed with ANOVA. For the zooplankton, the taxon counts used were those from the net mesh (100 or 365 µm)

© 2005 NRC Canada

that caught the greater numbers per cubic metre on average, across the grids. The data from both grids occupied in each month in 1986–1987 and 1987–1988 were combined. The counts at each station were $\ln(x + 1)$ transformed prior to analysis and were adherent to normal and satisfied Cochran's C test for homogeneity of variance. The relationships of the nine month-by-season groups of stations in multivariate space were analysed using canonical discriminate function (CDF) analyses for the 100- and 365-μm zooplankton, fish larvae, and fish eggs. The object was to determine if some month-by-season groups clustered more closely together than others, given measurements of the abundances of the species at each station and their a priori assignment to their monthly and seasonal groupings (Manly 1986). Standardised canonical coefficients were examined to ensure that the CDFs had zero mean and within-class pooled variances were equal to 1. The station scores for each group on the first two CDF axes were plotted against each other and the centroids of the resulting scatter calculated to visualise the relationships of the groups.

To test for differences in survival of snapper from the egg to the larval stage across the three spawning seasons, we estimated the survey means of ratios of larval to egg abundances at each station. This analysis was made using abundances of late-stage eggs (stages 5 and 6 summed), which were within about 10 h of hatching (Crossland 1980). Estimates of abundances of late-stage eggs at the time of larval hatching were calculated using egg abundance curves, fitted by distance-weighted, least-squares regression to mean late-stage abundances from each grid survey. The median age of larvae in each grid survey was used to back-calculate the egg abundance on the date the larvae were hatched. The ratios were $\ln(x + 1)$ transformed prior to analysis, after multiplying the larval abundances by 100 to minimize the effect of adding 1, were adherent to normal, and satisfied Cochran's C test for homogeneity of variance. The means of larval to egg ratios for each survey were compared within months across seasons using ANOVA.

Results

Meteorology, hydrography, and horizontal and vertical fluxes

Along-shelf wind stress over the region was predominately from the northwest in 1985–1986 and 1986–1987 (Fig. 2), whereas in 1987–1988, stresses were more evenly balanced between episodes of northwest and southeast, with greater incidence of southeast stress than previous seasons. The predominance of northwest winds in 1985–1986 and 1986–1987 was favourable for upwelling on the shelf, such that more incursion of shelf bottom water would be expected through Jellicoe Channel and into the Gulf than in 1987–1988 (Zeldis et al. 2004). The incursions were evident as higher salinity water in Jellicoe Channel (ref. Fig. 1*b*) near the seabed in all months of the first two seasons than in 1987–1988. In November, the central Gulf and Jellicoe Channel were occupied by water with salinity >35.2 ppt in the first two seasons, whereas in 1987–1988, this area had salinity predominately <35.2 ppt. Salinities increased in summer (December–January) in all years but were higher in the first two seasons (>35.3 ppt) than in 1987–1988 (>35.2 ppt). The circulation modelling showed the time sequence of incursions (Fig. 3) that formed the higher salinity Gulf water masses in the first two seasons and the lower salinity water mass of the third. In 1985, deep layer fluxes through the northern model boundary (Fig. 1*b*) into the Gulf were strongly positive in October, became neutral during November, but then were followed in December by a strong positive flux through to the end of the simulation in January. During 1986–1987, the northern boundary deep layer flux was steadily positive up to early December followed by neutral fluxes for the rest of the simulation. In 1987–1988, the northern boundary had an initial period of weak positive and then negative deep layer flux followed by a brief positive flux and then a flat or negative trend through to the end of the simulation.

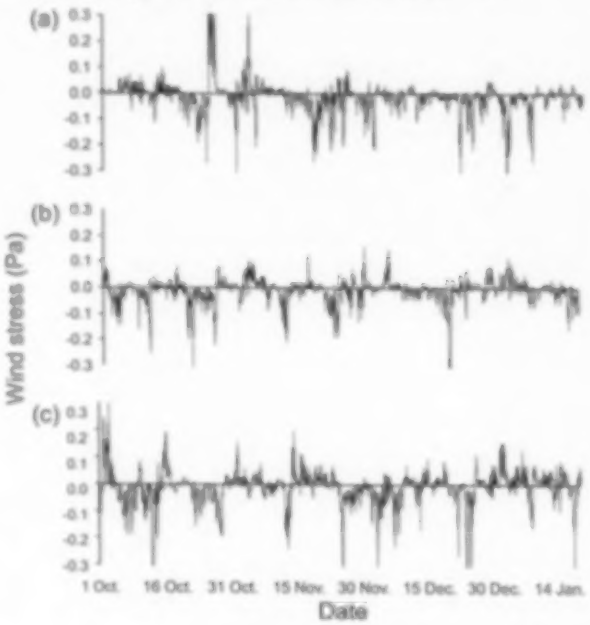

Fig. 2. Hourly mean along-shelf wind stress from Auckland Airport for 1 October – 20 January for (*a*) 1985–1986, (*b*) 1986–1987, and (*c*) 1987–1988. Negative wind stress is from the northwest and positive stress is from the southeast.

In addition to the differing wind stress directions, there were differences in wind speeds among the three seasons (Table 1). Between October and the end of the survey period (20 January), there were fewer low-wind days and more frequent high-wind days in 1987–1988 than in the previous two seasons, with days of high winds (>7 $m \cdot s^{-1}$) about 40% more frequent in 1987–1988 than in the other seasons. This was reflected in Fig. 2: in 1987–1988, in addition to strong wind events with westerly components, there were frequent events with strong easterly components, unlike the previous two seasons. This resulted in more wind mixing energy added to the water column (Fig. 4). From mid-September to mid-October, energy addition in 1987 exceeded that in the previous two seasons considerably. Thereafter, until mid-November, energy addition was about equal among the seasons but then in the third season again became more energetic until the end of surveying in late January. For 1 September – 20 January (i.e.,

© 2005 NRC Canada

Fig. 3. Cumulative sum plots of flux through the northern boundary of the circulation model (Fig. 1*b*) in the near-surface (0–2 m), subsurface (5–15 m), and deep (15–50 m) layers during the (*a*) 1985–1986, (*b*) 1986–1987, and (*c*) 1987–1988 simulations. An increasing cumulative sum indicates that the net flux is to the south, a decreasing cumulative sum indicates that the net flux is to the north, and a flat plot shows that the net flux is zero.

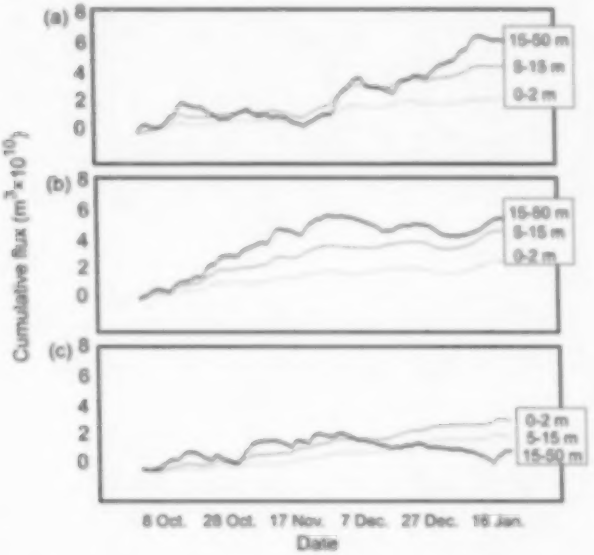

Table 1. Daily wind speed frequencies from 1 October to 20 January 1985–1986, 1986–1987, and 1987–1988.

Wind speed ($m \cdot s^{-1}$)	1985–1986	1986–1987	1987–1988
>1–2	2	6	1
>2–3	12	7	7
>3–4	28	22	12
>4–5	18	19	12
>5–6	19	20	19
>6–7	6	14	20
>7–8	8	10	14
>8–9	8	4	5
>9–10	6	6	11
>10–11	1	3	9
>11–12	3	1	1
>12–13	1	0	0
>13–14	0	0	0
>14–15	0	0	1
<4 (%)	38	31	18
>7 (%)	29	34	54

Note: The last two rows are the percentage of days within each season with speeds <4 $m \cdot s^{-1}$ (i.e., Beaufort 3: gentle breeze or less) and >7 $m \cdot s^{-1}$ (Beaufort 5: fresh breeze or greater).

from the start of the spring growth period until the end of surveys) in the three respective seasons, energy deviated by –0.12, –0.54, and +0.66 $J \cdot m^{-2} \cdot h^{-1}$ from the wind energy averaged across all three periods. For the actual survey period (10 November – 20 January) in each season, average energy deviated by –0.31, –0.39, and +0.70, respectively,

Fig. 4. Cumulative mean daily wind mixing power added to the water column by wind stress for 1 September – 20 January in 1985–1986 (circles), 1986–1987 (diamonds), and 1987–1988 (squares). The days of the three grid surveys in 1985–1986 and the six grid surveys in 1986–1987 and 1987–1988 are shown as solid symbols.

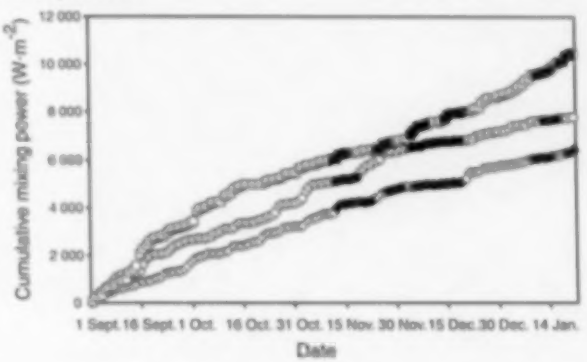

from the average wind energy across all three survey periods. The absolute differences among these deviations indicated that the energy added the Gulf water column by wind was higher in 1987–1988, by approximately 1 $J \cdot m^{-2} \cdot h^{-1}$, than in the previous two seasons.

The additional wind mixing energy of 1987–1988 generated somewhat deeper mixed-layer depths that season and less middle to upper water column stratification (Table 2; Fig. 5), although the differences from the previous seasons were generally not large. The moderate mixed-layer deepening was consistent with that expected from the addition of potential energy of 1 $J \cdot m^{-2} \cdot h^{-1}$ to the column (Mann and Lazier 1991). However, the higher wind energy in 1987–1988 caused considerably greater vertical diffusivity (K_z) in the water columns in that season than in 1985–1986 and 1986–1987 (Fig. 5; Table 2), both in the mixed layer and in the pycnocline. These K_z values lead to the prediction that, because of wind mixing energy, the mixed layer would have turned over through a 10-m eddy length scale in about 10 h in 1987–1988, while the same turnover would have required about 20 h in 1985–1986 and 24 h in 1986–1987 (Mann and Lazier 1991). For the stratified pycnocline below the mixed layer, the same turnover would have taken about 4 days in 1987–1988 but 10 and 13 days in 1985–1986 and 1986–1987, respectively.

Variation in phytoplankton, zooplankton, and ichthyoplankton

Similar to the physical fluxes, phytoplankton varied strongly between the three seasons. In 1985–1986 and 1986–1987, Chl *a* concentration was low in the mixed layer and higher below it, while in 1987–1988, the inverse occurred (Fig. 6; Table 2). These reciprocal distributions meant that it was not uncommon for column-integrated Chl *a* in the first two seasons to rival that of 1987–1988 (Table 2) owing to high concentrations deep in the column (e.g., December 1986 in Fig. 6*b*). However, estimated photosynthesis (Table 2) was much higher in 1987–1988, both integrated to the depth of 1% surface irradiance and, especially, integrated to the bottom of the mixed layer. This was caused by the high

© 2005 NRC Canada

Table 2. Means (1 SE) for each month in 1985–1986, 1986–1987, and 1987–1988 of the mixed layer depth (MLD), coefficient of vertical diffusivity (K_z) shallower than the MLD and deeper than the MLD to the bottom, mean Chl *a* concentration shallower than the MLD and deeper than the MLD to the bottom, Chl *a* integrated to the bottom, estimated gross phytoplankton photosynthesis (P_g) integrated to the depth of 1% of surface irradiance (Z_{eu}) and to the MLD, mean daily solar radiation, and mean water temperature. Averages for each season are also shown.

Month and year	MLD (m)	$K_z \leq$ MLD ($\times 10^{-3}$ m^2·s^{-1})	$K_z >$ MLD ($\times 10^{-4}$ m^2·s^{-1})	Chl *a* ≤ MLD (μg·L^{-1})	Chl *a* > MLD (μg·L^{-1})	Integrated Chl *a* (mg·m^{-2})	P_g integrated to Z_{eu} (mg C·m^{-2}·h^{-1})	P_g integrated to MLD (mg C·m^{-2}·h^{-1})	Solar radiation (MJ·m^{-2}·day^{-1})	Temperature (°C)
November 1985	14.0 (1.4)	1.2 (0.11)	1.5 (0.13)	0.36 (0.04)	0.68 (0.06)	17.5 (2.3)	17.8 (1.4)	9.1 (1.2)	22.6 (1.1)	16.64 (0.02)
December 1985	13.5 (1.3)	1.3 (0.13)	1.4 (0.12)	0.59 (0.08)	1.69 (0.19)	36.5 (5.5)	23.7 (1.6)	15.0 (2.1)	24.9 (1.5)	17.47 (0.03)
January 1986	5.7 (0.4)	0.3 (0.05)	0.4 (0.02)	0.27 (0.03)	1.10 (0.10)	26.2 (2.8)	19.5 (1.5)	4.3 (0.4)	21.8 (1.5)	19.20 (0.06)
Average	11.0 (0.8)	1.1 (0.07)	1.0 (0.05)	0.42 (0.04)	1.16 (0.08)	26.6 (2.3)	20.3 (0.9)	10.8 (1.1)	23.1 (0.8)	17.82 (0.03)
November 1986	15.1 (0.7)	1.3 (0.08)	1.3 (0.06)	0.81 (0.06)	1.73 (0.10)	35.2 (3.1)	28.7 (1.5)	19.6 (1.6)	21.9 (1.0)	16.61 (0.02)
December 1986	11.6 (0.6)	0.4 (0.03)	0.4 (0.03)	1.28 (0.13)	2.87 (0.15)	57.6 (4.7)	34.0 (2.2)	23.9 (2.5)	21.8 (1.5)	17.60 (0.02)
January 1987	10.6 (0.9)	1.8 (0.17)	1.2 (0.09)	0.65 (0.05)	0.94 (0.05)	20.1 (1.6)	21.4 (1.5)	13.5 (1.4)	21.2 (1.3)	20.12 (0.03)
Average	12.8 (0.5)	1.1 (0.07)	0.9 (0.06)	0.93 (0.05)	1.98 (0.08)	39.8 (2.3)	28.9 (1.1)	19.8 (1.2)	21.6 (0.7)	17.71 (0.02)
November 1987	15.0 (0.9)	2.2 (0.15)	2.7 (0.16)	2.19 (0.05)	2.04 (0.06)	62.5 (2.3)	50.4 (1.0)	42.6 (1.3)	20.5 (1.4)	16.62 (0.02)
December 1987	14.9 (0.9)	3.4 (0.22)	3.2 (0.25)	2.24 (0.06)	1.51 (0.07)	52.4 (2.2)	48.9 (1.2)	43.1 (1.7)	22.0 (1.3)	17.29 (0.03)
January 1988	14.9 (0.9)	2.7 (0.18)	2.7 (0.21)	0.93 (0.04)	0.90 (0.04)	25.8 (1.5)	27.1 (1.6)	20.6 (1.7)	25.7 (1.0)	18.64 (0.02)
Average	14.9 (0.5)	2.7 (0.10)	2.8 (0.12)	1.77 (0.04)	1.49 (0.04)	46.6 (1.6)	41.9 (1.0)	35.1 (1.1)	22.7 (0.7)	17.50 (0.02)

© 2005 NRC Canada

Fig. 5. (*a–c*) Vertical diffusivity (K_z) interpolated on a vertical section across the Hauraki Gulf (large circles in Fig. 1*b*) for each month and (*d–f*) scatterplots of K_z values over all water column profiles for each month in (*a* and *d*) 1985–1986, (*b* and *e*) 1986–1987, and (*c* and *f*) 1987–1988. In Figs. 5*a–5c*, the shading shows K_z, the heavy line shows the average depth (m) of the bottom of the mixed layer across the section, and the contour lines show density (kg·m^{-3}).

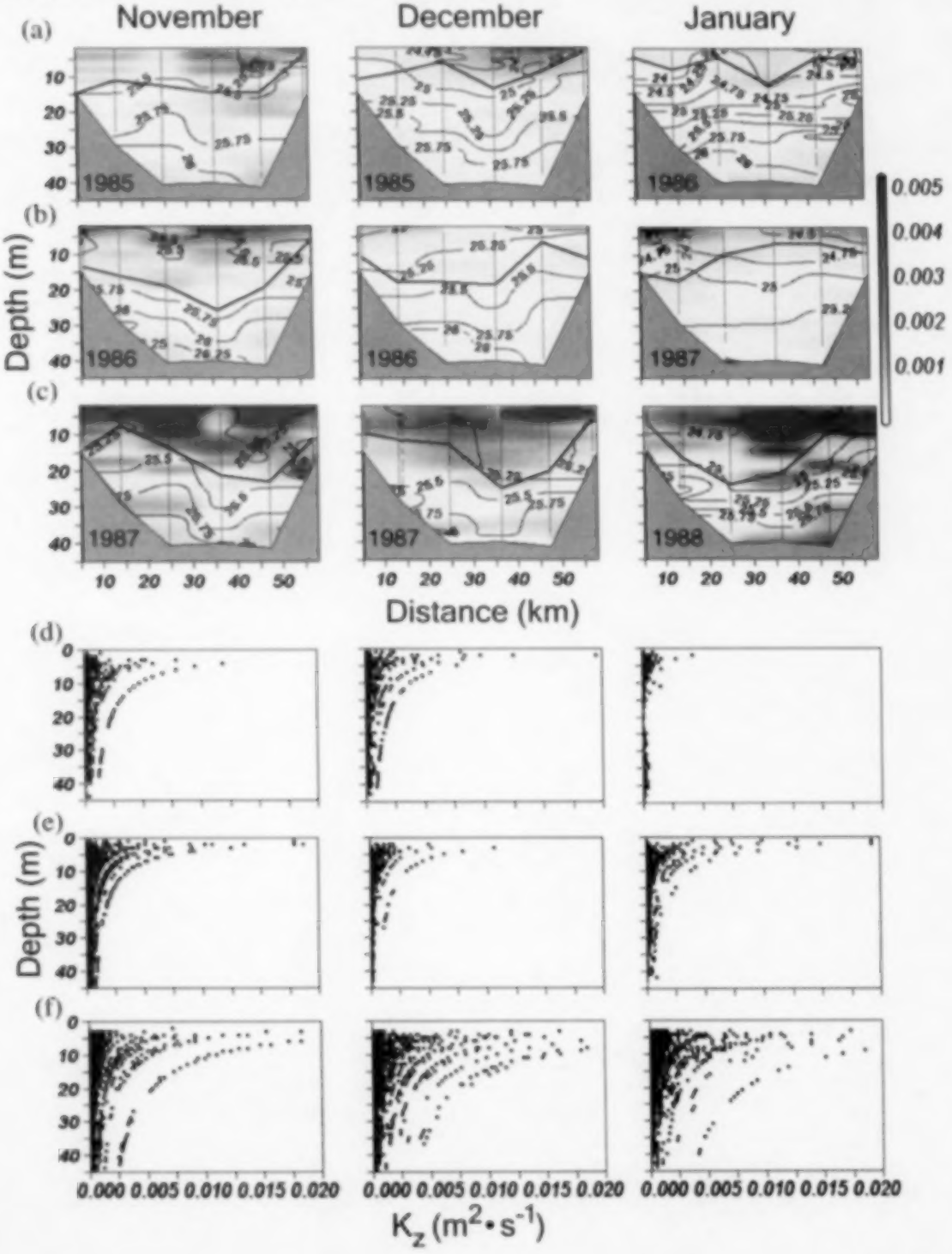

© 2005 NRC Canada

Fig. 6. Chl *a* concentration interpolated on a vertical section across the Hauraki Gulf (large circles in Fig. 1*b*) for each month, and plots of all Chl *a* water column profiles during each month in (*a* and *d*) 1985–1986, (*b* and *e*) 1986–1987, and (*c* and *f*) 1987–1988. In Figs. 6*a*–6*c*, the shading shows Chl *a* and the line shows the average depth (m) of the bottom of the mixed layer across the section.

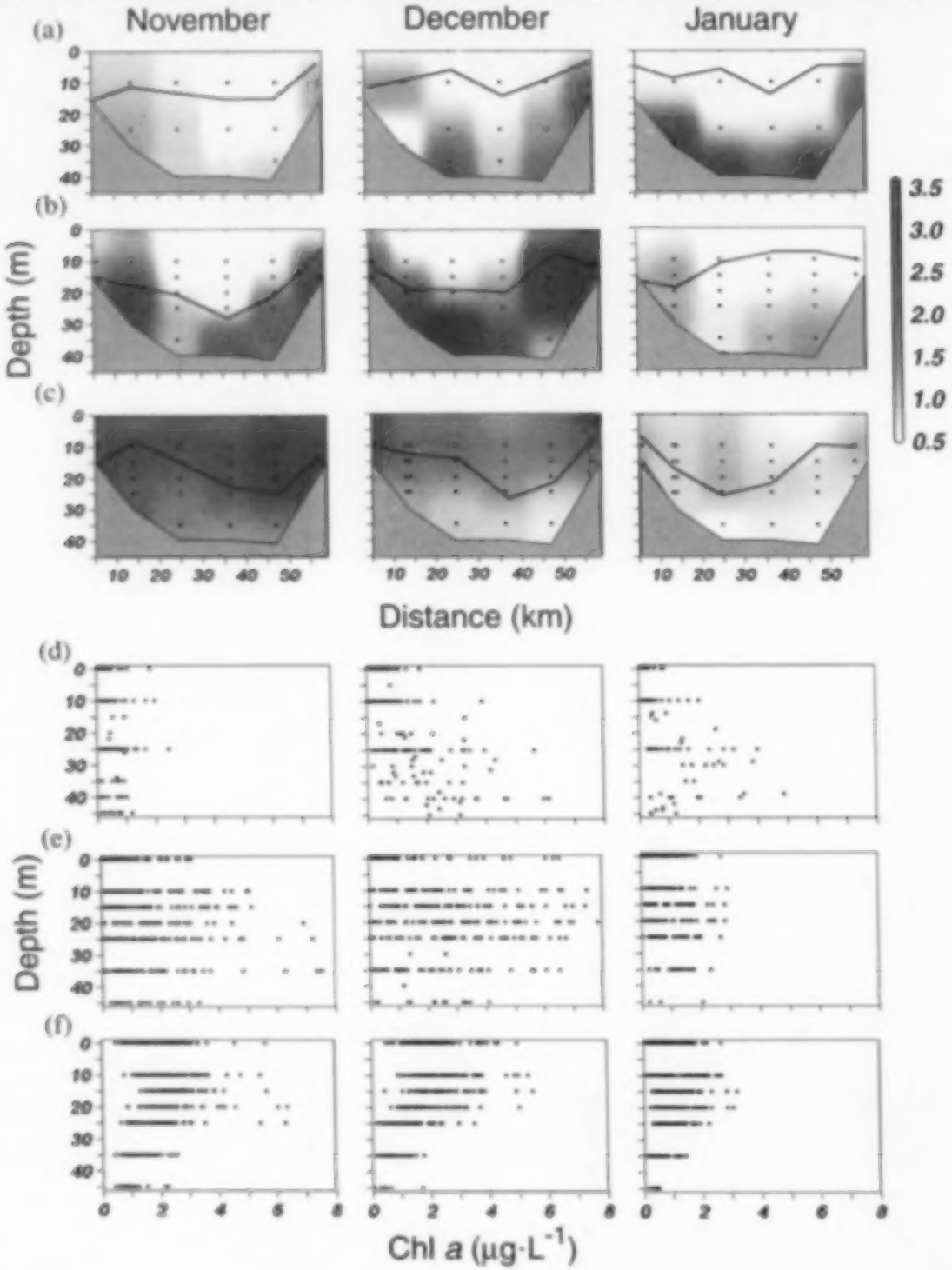

© 2005 NRC Canada

Table 3. Arithmetic mean proportions of diatom, dinoflagellate, and nanoflagellate carbon in samples of phytoplankton in December 1985, November–December 1986, and November–December 1987.

Year	Diatoms	Dinoflagellates	Nanoflagellates	Dinoflagellates + nanoflagellates	*n*
1985	0.65	0.27	0.08	0.35	14
1986	0.67	0.17	0.16	0.33	31
1987	0.41	0.38	0.21	0.59	43
p	<0.0001	<0.0001	0.018	<0.0001	

Note: *p* is the probability that proportions in each taxonomic group were equal between years tested by ANOVA, dinoflagellates + nanoflagellates is the mean proportions of dinoflagellates and nanoflagellates summed within samples, and *n* is sample number in each season. Proportions were arcsine square root transformed prior to analysis.

Table 4. Arithmetic mean concentrations (individuals·m^{-3}) of mesozooplankton for November, December, and January month groups across the three seasons captured in 100- and 365-µm-mesh nets.

	November			December			January		
Net mesh and taxon	1985	1986	1987	1985	1986	1987	1986	1987	1988
100 µm									
Nauplii	1091b	1911b	5918a	1966b	2057b	9646a	1886b	2015b	7607a
Copepodites	1330b	2119b	2670a	2156b	3416b	7962a	2915b	2722b	11328a
Euterpina	112c	264b	1363a	245a	208ab	181b	279a	710a	209ab
Corycaeus	123b	248b	940a	196b	297a	236b	269a	327a	456a
Oithona	220a	454a	510a	1663a	290b	783ab	1621b	3174ab	2616a
Temora	172a	66a	142a	189a	317a	375a	449b	353c	3889a
Clausocalanus	250a	62b	21c	152a	186a	55b	181a	277a	121b
Paracalanus	85a	203a	472a	808a	373a	481b	1165a	554a	606a
Oncaea	4a	6a	2b	16b	15b	25a	23b	2b	61a
Bivalve larvae	178b	762b	3397a	981b	1216b	2848a	293b	3490a	3391a
Gastropod larvae	21b	143a	178a	47a	91a	246a	87a	143a	180a
Penilia	10a	114a	168a	86a	605a	37b	5698b	1961b	17326a
Oikopleura	40c	188b	1526a	392b	392a	530ab	1217a	331b	915b
365 µm									
Salps	21b	1433a	1c	806a	793a	0b	80a	2b	0b
Sagitta	36b	4c	42a	2b	5b	99a	2c	7b	117a
Medusae	<1c	<1b	4a	<1b	<1b	2a	<1c	1b	17a
Nyctiphanes	7b	20a	12a	41ab	20b	38a	59a	22b	21c
Reptant larvae	9c	13b	51a	39b	10b	82a	12a	3b	12a
Natant larvae	2c	4b	12a	4b	4b	43a	8c	10b	57a

Note: Means within each species and month group with different letters are significantly different (Student–Neuman–Keuls post hoc tests, $\alpha \leq 0.05$), with concentrations decreasing from a to c.

concentrations of Chl *a* in the mixed layer of the third season, where higher light levels were received (after accounting for attenuation). There was no consistent pattern in variation in solar radiation in the Gulf region (Table 2) among the three seasons, showing that the variation in photosynthesis was not a function of varying incident radiation. Finally, there were significant differences in the taxonomic compositions of the phytoplankton assemblages among the three seasons. In November–December of the first two years, 65–67% of phytoplankton carbon was diatoms compared with 41% in November–December 1987 (Table 3). There was nearly twice the percentage of flagellated cells (dinoflagellates plus nanoflagellates) in 1987 than in 1985 and 1986. The ratio of diatom to total phytoplankton carbon was positively correlated with depth ($r^2 = 31\%$, $p < 0.001$) in November–December of the second season, with the predicted proportion of carbon in diatoms equal to 0.46 at the surface and 0.86 at 30 m. This relationship was non-significant ($p = 0.54$) in 1987. Too few samples were available at shallow depths to perform this analysis in 1985.

Among the zooplankton, naupliar and copepodite copepods were three to six times more abundant in 1987–1988 than in the previous two seasons (Table 4). This occurred throughout the Gulf sampling area (Fig. 7*a*). Among other 100-µm-net zooplankton, the copepod *Temora turbinata* and especially the cladoceran *Penilia avirostris* increased each year in January (summer) but did so much more in 1988 (Table 4) in the inner Gulf. The copepods *Euterpina acutifrons* and *Corycaeus aucklandicus* and the appendicularian *Oikopleura* spp. were most abundant in November 1987 as were bivalve larvae in November and December 1987. In contrast, the copepod *Clausocalanus* was more common in the first two seasons than in 1987–1988. Results were more variable for less abundant taxa (e.g., the copepod *Paracalanus* and gastropod larvae). The CDF analysis for 100-µm-net zooplankton detected a strong spring to

© 2005 NRC Canada

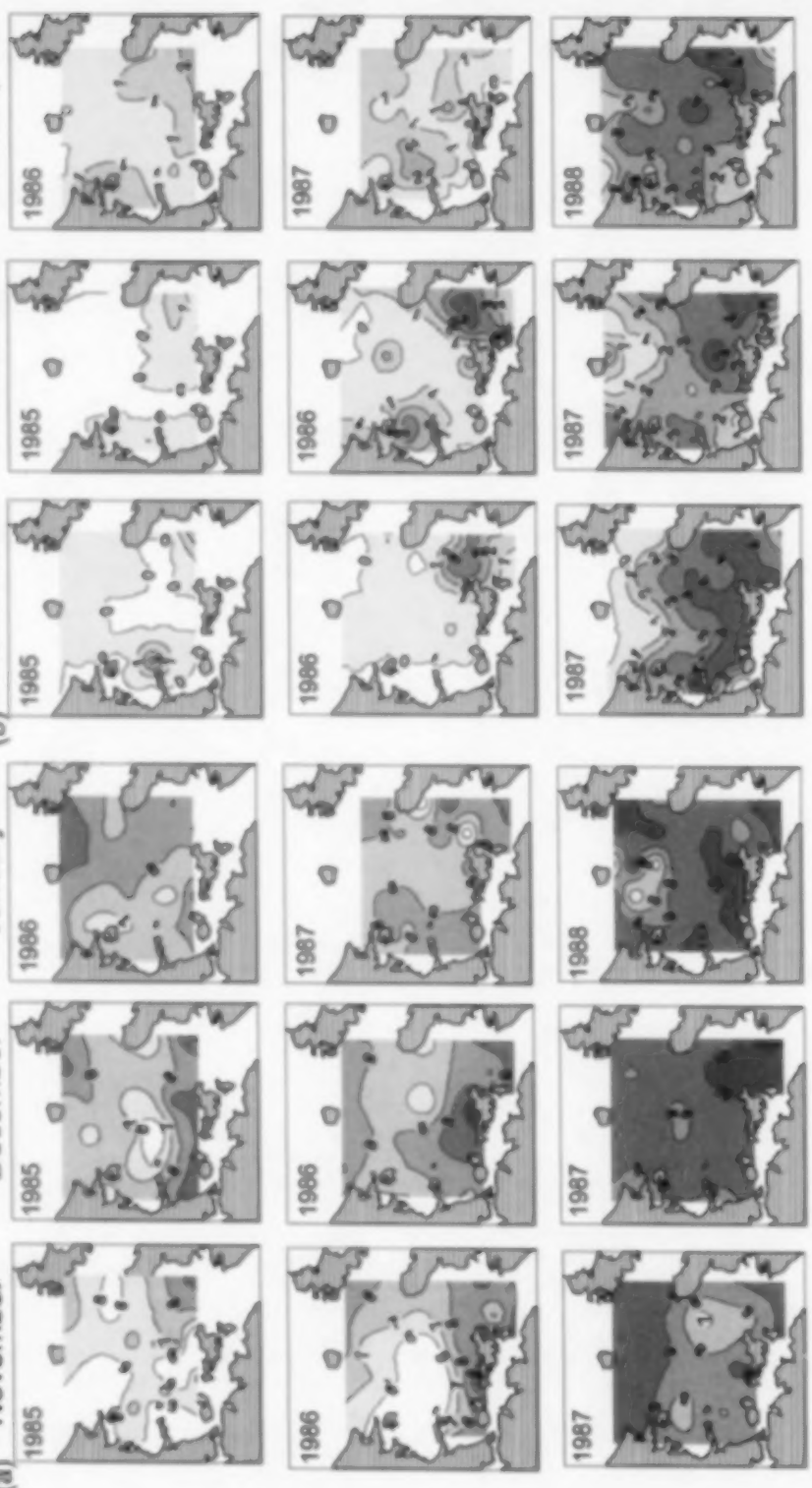

Fig. 7. Abundances of (*a*) summed copepod nauplii and copepodites (m^{-3}) and (*b*) snapper (*Pagrus auratus*) larvae ($100\ m^{-3}$) for each month and season. Contours are natural logarithms. For reference, ln(1) through ln(11) correspond to the arithmetic values 3, 7, 20, 55, 148, 403, 1097, 2981, 8103, 22 026, and 59 874, respectively.

© 2005 NRC Canada

summer trend through the abundance data, separating the three months in a consistent fashion on CDF1 (Fig. 8*a*). CDF2 captured interannual variation, with all months in 1987–1988 separated from all months in 1985–1986 and 1986–1987 (which clustered more closely together). The larger 365-μm-net zooplankton also showed differences among the three seasons (Table 4). Salps (*Thalia democratica*) were abundant in December 1985 and in November and December 1986 but were virtually absent in all of 1987–1988. The holoplanktonic predators *Sagitta* spp. (Chaetognatha) and hydromedusae were always more abundant in 1987–1988, as were reptant and natant decapod (crab and shrimp) larvae, in almost all months. The CDF analysis for 365-μm-net zooplankton (Fig. 8*b*) showed no strong monthly separation but did show consistent separation of 1987–1988 months from those of the previous two seasons on CDF1.

The larvae of numerous fish species were also most abundant in 1987–1988 (Table 5). Snapper larvae, in particular, were 4–30 times more abundant than in the previous two seasons and were distributed widely across the inner Gulf in 1987–1988 (Fig. 7*b*), similar to nauplii and copepodites (Fig. 7*a*). In the first two seasons, snapper larvae were caught only in low numbers, mainly in the outer Firth of Thames (Fig. 1*b*) or the western Gulf. Six other larval fish taxa had significantly greater abundances in 1987–1988 for at least two of the three months sampled in each season (Table 5). This included the three most abundant taxa: jack mackerel (*Trachurus novaezelandiae*), blue mackerel (*Scomber australasicus*), and anchovy (*Engraulis australis*). The CDF analysis for fish larvae (Fig. 8*c*) showed that the predominate pattern of abundance variation was between seasons, as shown by the separation of 1987–1988 from the previous two seasons, irrespective of month, on CDF1. In contrast with the larval fish, there was no consistent temporal pattern in fish egg abundance for the five dominant taxa that were identified and counted (Table 5). Only anchovy showed consistent between-season differences, with low egg numbers in the first season. The CDF analysis for fish eggs (Fig. 8*d*) showed that differences in abundance were relatively small and less consistently ordered by month or season, with the centroids of station scores tightly clustered and intermingled. For snapper, the large between-season differences in larval abundances, compared with the relatively small differences in their late-stage egg abundances, resulted in mean larval to egg ratios that were always much greater in 1987–1988 than in 1985–1986 and 1986–1987 (Table 6).

Undersampling of the youngest snapper larvae by the plankton net occurred (Fig. 9), owing no doubt to extrusion of the weakly ossified yolk sac and early first feeding stages (Atkinson 1987) through the 365-μm-mesh nets. Because of extrusion, the abundances of larvae younger than 6–8 days of age were extremely inaccurately sampled (by many-fold). However, by about 8 days of age, the larvae appeared to be more fully recruited to the net, for this was when abundance-at-age curves peaked and started to decline (Fig. 9). By this age (approximately 3–4 days after the start of larval feeding, see Discussion), large differences in cohort strength between 1987–1988 and the previous two seasons had been established.

Most snapper larval development took place in the inner Hauraki Gulf (Fig. 7*b*), which is where the spawning of this

Fig. 8. Centroids of station scores of the first two CDFs of the analyses for (*a*) 100-μm net zooplankton, (*b*) 365-μm net zooplankton, (*c*) fish larvae, and (*d*) fish eggs. The rings encircle the 3 months of each season, with squares indicating 1985–1986, triangles indicating 1986–1987, and circles indicating 1987–1988. The percentages of total variance explained by the functions are shown in parentheses on the axes.

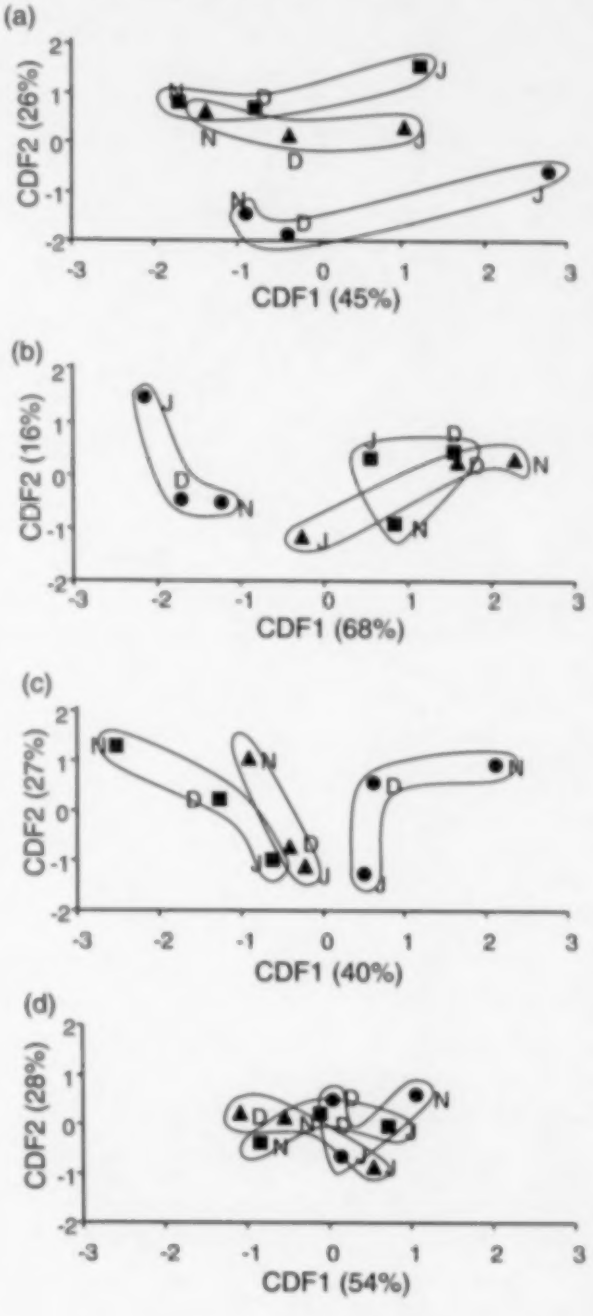

© 2005 NRC Canada

Table 5. Arithmetic mean concentrations (individuals·100 m^{-3}) of fish larvae and eggs for November, December, and January month groups across the three seasons.

	November			December			January		
	1985	1986	1987	1985	1986	1987	1986	1987	1988
Fish larvae									
Snapper	2b	3b	32a	<1c	8b	30a	3b	4b	33a
Blue mackerel	2b	2b	34a	13b	16b	51a	17a	7b	55a
Jack mackerel	17c	29b	170a	23b	72b	249a	86a	32b	125a
Crested flounder	2b	3b	12a	1c	5b	14a	4a	5a	11a
Speckled sole	<1c	3b	10a	0b	0b	2a	0b	2a	4a
Flounder	<1b	<1b	3a	0a	0a	1a	0a	0a	0a
Spotted stargazer	<1b	1b	3a	0b	1a	2a	1b	1a	2a
Triplefin	1c	9b	25a	2b	1b	28a	1a	1ab	2a
Opalfish	<1a	<1a	<1a	<1b	<1b	1a	<1a	<1a	<1a
Ahuru	<1a	<1a	2a	<1b	<1b	1a	<1b	<1b	2a
Anchovy	10c	12b	30a	3b	46a	37a	22b	37b	63a
Pilchard	110a	40b	30b	9b	2b	54a	3a	1b	8a
Fish eggs									
Snapper	190b	268a	437a	147b	466b	282a	56a	29a	49a
Blue mackerel	20b	178ab	356a	182a	27b	248a	41a	4b	10a
Jack mackerel	215c	970b	1757a	1184a	771a	784b	441a	193ab	84a
Flatfish	50b	103b	353a	57b	76b	113a	116a	111b	98c
Anchovy	28b	194a	178a	29b	191a	166a	64b	211a	193a

Note: Means within each species and month group with different letters are significantly different (Student–Neuman–Keuls post-hoc tests, $\alpha \leq 0.05$), with concentrations decreasing from *a* to *c*.

Table 6. Mean ratios of snapper (*Pagrus auratus*) larvae (×100) to late-stage snapper eggs, and mean late-stage egg concentrations (95% confidence intervals) for the grid surveys made in each month and season.

	Larvae to late-stage eggs ratio	Late-stage eggs (100 m^{-3})
Mid-November 1985	1.2b	91 (84)
Mid-November 1986	3.1b	94 (67)
Late November 1986	5.4b	173 (124)
Mid-November 1987	100.2a	130 (66)
Late November 1987	64.2a	214 (72)
Mid-December 1985	0.2c	59 (35)
Early December 1986	3.7bc	151 (167)
Mid-December 1986	13.0b	15 (11)
Early December 1987	34.2a	109 (53)
Mid-December 1987	40.3a	62 (24)
Mid-January 1986	9.8b	30 (15)
Mid-January 1987	26.5b	13 (7)
Late January 1987	17.9b	11 (6)
Mid-January 1988	114.3a	35 (17)
Late January 1988	155.4a	11 (9)

Note: Ratios within each month group with different letters are significantly different (Student–Neuman–Keuls post hoc tests, $\alpha \leq 0.05$), with ratios decreasing from *a* to *c*.

stock is centred (Zeldis and Francis 1998). This indicated that larvae were not drifting in residual currents far from spawning areas during development. Larval drift simulations verified this: residual drift of larval tracers from the five representative larval release sites over 8 days postspawning (by which time the larval cohorts had greatly diverged in strength; Fig. 9) was small with respect to the size of the whole ichthyoplankton sampling grid (Fig. 10, cf. Fig. 1*b*). Only 5% of larvae drifted farther than 20 km from any of the five release sites, irrespective of season. This was well within the survey sampling area, which had an approximately 80-km-long north–south axis (Fig. 1*a*).

Discussion

Hauraki Gulf hydrography and phytoplankton

The shelf circulation in the northern approaches to the Hauraki Gulf is highly responsive to winds, with upwelling and downwelling responses to along-shelf winds from the northwest and southeast, respectively (Sharples and Greig 1998; Black et al. 2000; Zeldis et al. 2004). During upwelling, these flows have a cross-shelf, onshore component near the seabed, transporting shelf water with relatively high salinity and nitrate concentration into the Hauraki Gulf through Jellicoe Channel (Zeldis 2004). In contrast, southeast wind stress causes offshore near-bed flows and outflow of Gulf waters at Jellicoe Channel. In our study, northwest along-shelf wind stress prevailed for much of the November–January periods of 1985–1986 and 1986–1987. Consistent with the above studies, this corresponded to higher salinity, shelf-affiliated water near the seabed in the Hauraki Gulf and its approaches and greater modelled shelf water flux into the Gulf than in 1987–1988, when northwest stress was more balanced by southeast stress.

The incursions of 1985–1986 and 1986–1987 correlated with Chl *a* maxima deep in the water column, composed primarily of diatoms. In 1987–1988, when there was less shelf–Gulf exchange, there were greater proportions of dinoflagellates and nanoflagellates. Similarly, Chang et al. (2003)

© 2005 NRC Canada

Fig. 9. Snapper (*Pagrus auratus*) larval abundance-at-age frequencies for each month and season for (*a*) November, (*b*) December, and (*c*) January 1985–1986 (diamonds), 1986–1987 (squares), and 1987–1988 (triangles).

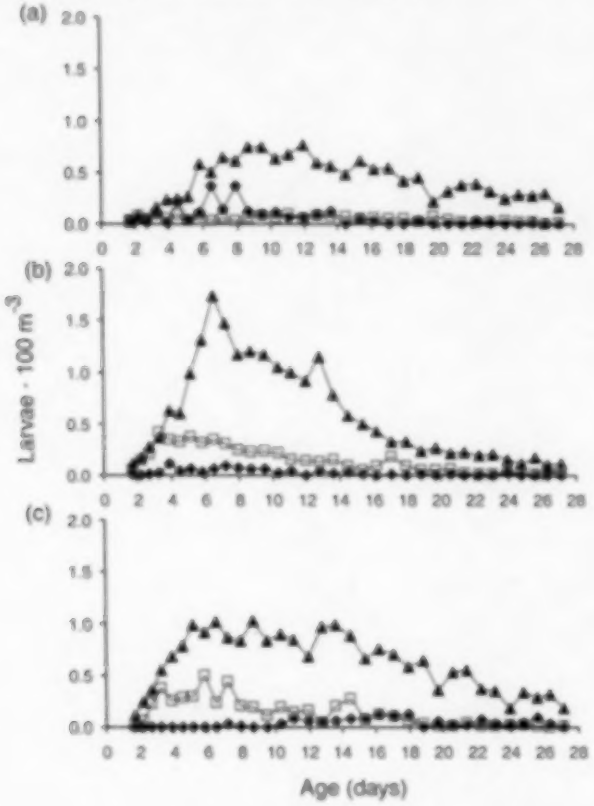

observed that when incursions of near-bed shelf water moved into the Hauraki Gulf, a layer of large cells (>20 μm) was found in the Gulf pycnocline, with a high proportion of diatoms. They concluded that diatom growth within the layer was fostered in situ by the elevated nitrate concentration associated with the incursion and the capacity for diatoms to grow at low light levels (Chan 1980). When the Gulf was not strongly influenced by shelf water incursions, Chang et al. (2003) found primarily dinoflagellates and nanoflagellates growing in the assemblage. Maddock and Taylor (1984) also identified a characteristic diatom assemblage in Jellicoe Channel, which periodically appeared in a subsurface layer and was associated with advected shelf water and westerly winds.

The phytoplankton of 1987–1988 also differed strongly from that of the previous two seasons in vertical distribution and productivity, which we believe reflected the action of higher wind mixing power and vertical diffusivity. It is possible that a component of this involved cell accumulation in low-turbulence, deep layers in the first two seasons, where low production and decay rates may have sustained deep Chl *a* maxima (reviewed in Mann and Lazier 1991). However, the much greater upper water column productivity rates estimated for 1987–1988 indicate that it was high growth rates that maintained high mixed-layer Chl *a* concentrations that season. In addition to maintaining cells in suspension, we surmise that this was sustained by mixing of nutrients from the pycnocline into the more euphotic mixed layer, consistent with experiments comparing biologically and physically based vertical flux estimates (e.g., Epply et al. 1979) in stratified coastal waters. These have shown that "vertical eddy diffusion is the responsible agent in the transport of nitrate to the mixed layer, and is a controlling factor in primary production" (Mann and Lazier 1991).

Zeldis (2004) showed that along-shelf wind stress from the northwest increased shelf water incursion into the Gulf and near-bed nitrate concentration, so it was likely that near-bed nitrate concentration would often have been greater in the first two seasons than in 1987–1988. However, effects of vertical mixing appeared to have dominated this horizontal advective effect for mixed-layer primary biomass and production. There were extremely low Chl *a* levels in November 1985, when both horizontal advection and vertical diffusivity were low, followed by a substantial increase in deep-layer Chl *a* concentration in December 1985, after the onset of incursion. However, vertical mixing was still low, and there was only minor elevation of mixed-layer Chl *a* concentration and productivity. In November and early December 1986, during persistent incursion, deep-layer Chl *a* concentrations were higher than in 1985, as was productivity. However, relative to 1987, mixing was still weak, and upper column Chl *a* concentration and productivity were much lower. The results suggest that nutrient levels in the Gulf during nonupwelling conditions (e.g., 1987–1988) are sufficient to sustain substantial upper column production, if there is sufficient supply to the mixed layer.

Zooplankton abundance and the lower food web

The 1987–1988 season sustained greater abundance of most zooplankton taxa than 1985–1986 or 1986–1987. The exceptions were shelf-affiliated taxa that were more common in the first two seasons and reflected the entrainment of shelf-affiliated zooplankton into the Gulf, when westerly winds predominated (Jillett 1971). The salp *T. democratica* was abundant in December 1985 and November and December 1986 in the western Gulf, and while it is normally a shelf-affiliated species (Jillett 1971), it probably arose when overwintering individuals were advected into Gulf waters. Although capable of exerting high population grazing rates (Zeldis et al. 1995), it is unlikely that salps were the main factor in creating low mixed-layer Chl *a* in the first two seasons: low Chl *a* concentrations were already present in November 1985, before the proliferation of salps, and salps were never abundant in the southeastern Gulf, Firth of Thames, or the outer Gulf, where low mixed-layer Chl *a* concentrations were regularly observed in the first two seasons. Also, relatively low mixed-layer Chl *a* concentrations and productivity occurred in January 1986 and 1987, when salps were rare or absent. Another shelf-affiliated taxon, the copepod *Clausocalanus* spp., was more abundant in the first two seasons, again reflecting the shelf water entrainment.

Apart from these taxa, Gulf zooplankton assemblages were not greatly different in species composition between years, suggesting that altered in situ production of the Gulf assemblage, rather than advection of a wholly distinct shelf

© 2005 NRC Canada

Fig. 10. Contours of relative snapper (*Pagrus auratus*) larval concentrations during drift from five representative Hauraki Gulf snapper spawning sites in the middle water column for the first 8 days posthatch. The shades on the greyscale indicate proportions of larvae originally released remaining within that contour after 8 days of drift.

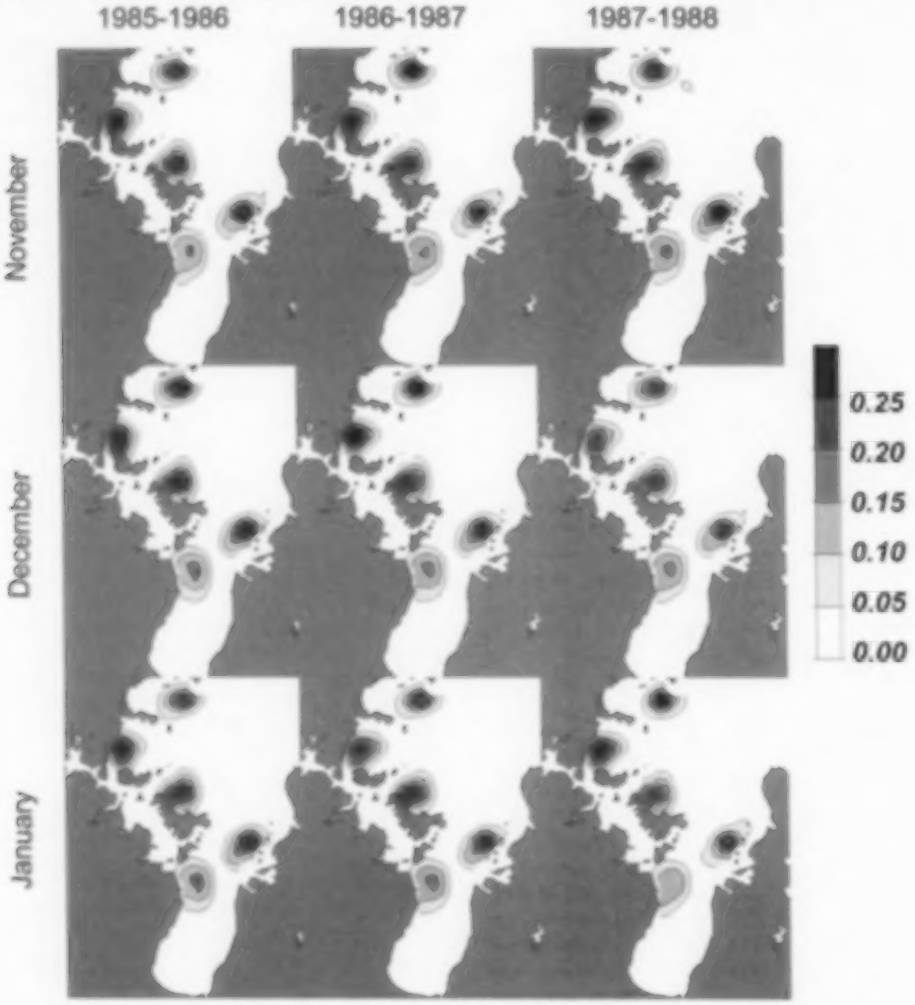

assemblage, had the greatest effects on abundance. This was supported by the slow turnover of the Gulf water volume, even in higher flux years. Integrating the modelled 1985–1986 and 1986–1987 northern boundary fluxes yielded a turnover time of the Gulf volume (9.4×10^{10} m^3) of about 81 days, not inconsistent with 69 days estimated using a water and salt mass-balance budget (data collected in 1996–1997 and recalculated from Zeldis and Smith 1999). Gulf copepods at these temperatures (approximately 17 °C) would have had approximately 2- to 3-week generation times (Huntley and Lopez 1992), much less than these turnover times, suggesting that in situ effects on zooplankton abundance dominated advective effects. Food limitation of zooplankton productivity may explain their abundance variation between the seasons. Hansen et al. (1997), in a meta-analysis of feeding and growth of copepods, found that the half-saturation food concentration of ingestion rate was approximately 240 μg C·L^{-1}. Assuming a C:Chl *a* ratio of 50, this implies a half-saturation Chl *a* concentration for copepod feeding of approximately 5 μg Chl *a*·L^{-1}, well above averages in the Gulf during this study and indicating that ingestion rates of Gulf copepods were not saturated. Although column-integrated Chl *a* stocks in the first two seasons were in some months similar to those of 1987–1988, mixed-layer stocks and euphotic zone and mixed-layer productivities were always considerably greater in 1987–1988. Given that it is not uncommon for mesozooplankton to feed predominately on the productivity maximum in the mixed layer (Longhurst and Herman 1981; Mann and Lazier 1991), this suggests that 1987–1988 presented better conditions for sustaining mesozooplankton production.

Diet may also have played a part. In laboratory and mesocosm studies, diatom diets have been shown to be deleterious to copepod oogenesis, hatching, and naupliar produc-

© 2005 NRC Canada

tion (reviewed in Miralto et al. 1999; Nejstgaard et al. 2001), although this is contentious and has yet to be demonstrated in the field (see Irigoien et al. 2002 and references therein). From a nutritional standpoint, however, dinoflagellates and nanoflagellates have been shown to be considerably more nutritious than diatoms (in terms of carbon and nitrogen constituents) on a Chl *a* or volume-specific basis (Chan 1980; Hitchcock 1982; Rey et al. 2001), suggesting that the productive and dense assemblages rich in these flagellates observed in 1987–1988 would have been favourable for secondary production.

Ichthyoplankton abundance and sources of early life mortality

For many fish species, 1987–1988 produced the most larvae. This included snapper larvae, which were far more abundant that season. Greater advection of snapper larvae out of the survey area was not the reason for their lower abundance in 1985–1986 and 1986–1987, as shown by the larval drift modelling. Drift and mixing of snapper larvae in the Gulf were slow relative to the times required for cohort strengths to diverge between seasons (approximately 8 days posthatch), consistent with the long turnover times estimated for the Gulf water mass (discussed above). Early life mortality for the larval fish was, however, very high in all years, judging by the great differences in mean abundances of eggs and larvae and considering the differing longevities of these two groups. Predation is known to be an important part of this, at least for snapper. In a Hauraki Gulf snapper egg production survey (see table 2 in Zeldis and Francis 1998), mortality of snapper eggs between spawning and hatching averaged about 83%, and calculations from our data using egg and 8-day-old larval abundances show that approximately 98% of larvae were eliminated between hatching and 8 days old in the season when larval survival was highest (1987–1988). It is likely that predation caused much of this mortality because much of this interval is prior to, and coincident with, first feeding.

However, there is evidence to suggest that mortality was not related solely to predation. First, invertebrate predators of ichthyoplankton were not more abundant in the years of low larval fish abundance. Chaetognaths, hydromedusae, and crustaceans (including copepods and decapod larvae) have been found to predate larval fish (Turner et al. 1985; Paradis et al. 1996; Sulkin et al. 1998), and they were always significantly, and usually much more, abundant in 1987–1988, the year of highest larval fish abundance. Although Paradis and Pepin (2001) concluded that invertebrates were insignificant predators of larval fish (based on low modelled encounter rates), Brewer et al. (1984) and Rilling and Houde (1999) found negative correlations of fish larval abundance and invertebrate predator densities. Among planktivorous fish, adult jack mackerel occurred in 85% of the trawls in Hauraki Gulf trawl surveys made in November 1986 and 1987 (Kendrick and Francis 2002) and accounted for large numbers of planktonic eggs in our study. However, adult jack mackerel abundances measured in these trawl surveys did not correlate with variation in zooplankton and larval fish densities between spawning seasons (292 $kg \cdot km^{-2}$ trawled in 1986 versus 423 $kg \cdot km^{-2}$ in 1987, non-significantly different at $p = 0.60$). It was notable also that the egg abundances for planktivorous blue mackerel, jack mackerel, and anchovy had no systematic patterns of increased abundance in the first two seasons relative to 1987–1988, suggesting no increase in spawner biomasses in those seasons, nor were their eggs distributed differently across the Gulf between these seasons (J.R. Zeldis, unpublished data).

Second, the snapper larva to egg ratios compared between seasons showed that abundance of late-stage eggs did not explain the much greater larval snapper numbers in 1987–1988. Mean abundances of late-stage eggs were not greatly different between seasons, but those of 8-day-old larvae were. This suggests that if predation mortality caused the interannual variation in larval snapper abundance, it would have had to have operated at a greater rate on larvae, but not on eggs, in the first two seasons than in 1987–1988. This could have happened if susceptibility of larvae to predation increased with poorer nutrition at the start of feeding at 3–4 days posthatch (Pankhurst et al. 1991). Such covariation of predation and nutrition is potentially a strong determinant for larval survival (Bailey and Houde 1989), wherein the proximate cause of mortality is predation but the ultimate cause is food limitation (Taggart and Leggett 1987).

The nutritional environment for snapper larvae did appear to be better in 1987–1988 because it sustained a much more abundant community of prey, particularly naupliar and copepodite copepods, cladocerans, and bivalve larvae. Significantly, the spatial distributions of these taxa overlapped extensively with larval snapper nursery areas, and larval drift patterns during the first 8 days posthatch showed that these relationships between prey and larvae were temporally stable over the first-feeding period. First-feeding snapper larvae take prey up to 450 µm long and older larvae take prey up to 1100 µm long including the above prey types (Atkinson 1987, J.R. Zeldis, personal observation). Gaining food at first feeding is particularly important for snapper larvae because they are at the small end of the spectrum of size-at-hatch among teleosts (Miller et al. 1988). In culture, when starved from the age of first feeding (3–4 days posthatch), they stop swimming and lose condition rapidly, starving to death in 3–4 days (Pankhurst et al. 1991). They feed visually but have only weakly developed optical acuity and a short reactive distance to prey (Pankhurst 1994), such that successful capture requires that prey be relatively dense or encountered frequently (Pankhurst et al. 1991). This suggests a potential role for the greater wind energy of 1987–1988 in enhancing encounter rates between larval fish and their prey (Rothschild and Osborn 1988; Sundby and Fossum 1990). Average wind speeds in the three seasons were 5.1, 4.9, and 6.5 $m \cdot s^{-1}$, respectively, and naupliar densities were approximately four times greater in the third season. As an exercise to compare contact rates between the seasons, we can assume parameter values for naupliar and larval swimming speeds and distance of separation equal to those used by Sundby and Fossum (1990): 0.02 $cm \cdot s^{-1}$, 0.2 $cm \cdot s^{-1}$, and 5 cm, respectively. Our values of root mean square turbulent velocities (Rothschild and Osborn 1988) derived from the above wind speeds suggest a modest increase in physically forced larval contact rate with prey (about 21%) in the

© 2005 NRC Canada

1987–1988 season. However, this increases to 500% when linearly scaled by the approximately fourfold greater naupliar prey density (Davis et al. 1991).

The abundant conditions of the third season occurred across the dominant components of Hauraki Gulf mesozooplankton (including its holo- and meroplanktonic, herbivorous, omnivorous, and predatory components) as well as across most of its guild of larval fish, as detected by repeated sampling over a very extensive survey area (4500 km^2) for a protracted period (3 months) in each season. We saw responses of the phytoplankton to physical processes in the water column that were consistent with mechanisms of mixing and nutrient and light supply and large changes in secondary communities consistent with the variations in primary biomass and production. The scale of these effects and their correlation with physical processes would suggest that the most parsimonious explanation for the variation in mesozooplankton assemblage abundance among the three seasons were "bottom-up" effects. Primary among these were the positive effects of wind-driven mixing energy, which promoted greater primary production and mixed-layer primary biomass.

It is not possible to ascertain from this study whether or not amelioration of predation was the sole reason for strong fish larval survival in the third season. It is very difficult to separate the effects of food limitation and fish predation on larval fish survival (Pepin et al. 2003). Many factors come into play, not least the requirement to balance sampling effort at small scales, to reveal growth and mortality dynamics, with wide-scale sampling, to reveal the generality of processes and to account for processes with temporal lags (Taggart and Leggett 1987; Baumann et al. 2003). Baumann et al. (2003) demonstrated that past history (in terms of larval drift) must be accounted for in explaining a larval cohort's survivorship. They showed using particle tracking that in their case, larval growth rates and survivorship did not correlate with prey abundance, while larval survival was negatively related to predatory fish abundance. In contrast, we have shown that increased success of larval snapper was correlated with high prey abundance, after accounting for drift, up to the age by which larval cohort strength was determined. We hypothesise that within the richer community of the third season, first-feeding snapper larvae (which suffer rapid loss of competency upon starvation) were exposed to better prey fields and had improved competency and therefore fewer predation losses. Although we cannot test this hypothesis with our present results, it is consistent with Rilling and Houde (1999) who showed that larval growth was correlated with prey density and that mortality rate declined with increasing growth rate (however, see Pepin et al. 2003). Our results indicate that further research on the effects of vertical mixing and horizontal advection on the physical microstructure, nutrient, and production fluxes in the Hauraki Gulf would be beneficial. Research should also assess the growth and mortality reactions of larval fish assemblages, coincident with predator behaviour and abundance.

Snapper larval abundance, juvenile recruitment, and temperature

Our results support Francis' (1994) suggestion that part of interannual variation in snapper recruitment could be driven by variable production of late-stage larvae. Francis (1994) showed strong negative correlations between larval period duration (and hence exposure to larval mortality) and sea temperature, which he suggested could lower cumulative mortality at higher temperatures. This could be a component of the temperature–recruitment relationship for this snapper stock (see Introduction), wherein cool spawning season temperatures correlate with weaker recruitment. However, this does not explain our observations, which were obtained during three spawning seasons with very similar mean sea temperatures.

We observed that when there was increased wind-driven vertical mixing in the Hauraki Gulf, late-stage snapper larval production increased greatly. This also could be a component of the temperature–recruitment relationship. El Niño conditions in summer in northern New Zealand usually bring cool sea temperatures (Greig et al. 1988), westerly wind conditions, and weaker overall wind strengths (Gordon 1985). Although the second season of our study was during a moderate El Niño, it did not have significantly cooler sea temperatures than the other seasons. However, along with the first season, it was characteristic of typical El Niño summer conditions with respect to its weak, predominately westerly winds and a lack of easterlies. The larval dynamics that we demonstrate under these conditions may indicate effects to be expected during a negative El Niño – Southern Oscillation and a role for late larval production in guiding 0+ snapper recruit strength.

Acknowledgements

We thank Gary Voss, Jon Ingerson, Joy Jay, Dean Christophers, Mike Stevenson, and the officers and crews of the RVs *James Cook* and *Kaharoa* for technical assistance and Dr. Janet Grieve for reviews (all of the National Institute of Water and Atmospheric Research). The work was completed under contract CO1X0027 from the New Zealand Foundation for Research, Science, and Technology.

References

Annala, J.H., Sullivan, K.J., O'Brien, C.J., Smith, N.W.McL., and Varian, S.J.A. (Comps.) 2002. Report from the Fishery Assessment Plenary, May 2002: stock assessments and yield estimates. National Institute of Water and Atmospheric Research Library, Wellington, New Zealand.

Atkinson, M.H. 1987. Ontogenetic patterns in presettlement *Chrysophyrs auratus* (Sparidae). M.Sc. thesis, University of Auckland. National Institute of Water and Atmospheric Research Library, Wellington, New Zealand.

Bailey, K.M., and Houde, E.D. 1989. Predation on early developmental stages of marine fishes and the recruitment problem. Adv. Mar. Biol. **25**: 1–83.

Baumann, H., Pepin, P., Davidson, F.J.M., Mowbray, F., Schnack, D., and Dower, J.F. 2003. Reconstruction of environmental histories to investigate patterns of larval radiated shanny (*Ulvaria subbifurcata*) growth and selective survival in a large bay of Newfoundland. ICES J. Mar. Sci. **60**: 243–258.

Beca-Steven Ltd. 1992. North Shore sewerage facilities treatment and disposal: Hauraki Gulf oceanographic study. Report prepared for the North Shore City Council by Beca-Steven Ltd. National Institute of Water and Atmospheric Research Library, Hamilton, New Zealand.

© 2005 NRC Canada

Bell, R.G., Oldman, J.W., Turner, S.J., Gibbs, M.M., MacDonald, I., and Mills, G. 1999. Oceanographic and water quality investigations for the North Shore City outfall: assessment of environmental effects. National Institute of Water and Atmospheric Research client report NSC90201/3. National Institute of Water and Atmospheric Research Library, Hamilton, New Zealand.

Black, K.P., Bell, R.G., Oldman, J.O., Carter, G.S., and Hume, T.M. 2000. Features of 3-dimensional barotropic and baroclinic circulation in the Hauraki Gulf, New Zealand. N.Z. J. Mar. Freshw. Res. **34**: 1–28.

Brewer, G.D., Kleppel, G.S., and Dempsey, M. 1984. Apparent predation on ichthyoplankton by zooplankton and fishes in nearshore waters of southern California. Mar. Biol. **80**: 17–28.

Chan, A.T. 1980. Comparative physiological study of marine diatoms and dinoflagellates in relation to irradiance and cell size. II. Relationship between photosynthesis, growth and carbon/chlorophyll *a* ratio. J. Phycol. **16**: 428–432.

Chang, F.H., Zeldis, J., Gall, M., and Hall, J. 2003. Seasonal and spatial variation of phytoplankton assemblages, biomass and cell size from spring to summer across the New Zealand northeastern continental shelf. J. Plankton Res. **25**: 737–758.

Crossland, J. 1980. The number of snapper, *Chrysophrys auratus* (Forster), in the Hauraki Gulf, based on egg surveys in 1974–75 and 1975–76. Fish. Res. Bull. 22. National Institute of Water and Atmospheric Research Library, Wellington, New Zealand.

Davis, C.S., Flierl, G.R., Wiebe, P.H., and Franks, P.J.S. 1991. Micropatchiness, turbulence and recruitment in plankton. J. Mar. Res. **49**: 109–151.

Denman, K.L., and Gargett, A.E. 1983. Time and space scales of vertical mixing and advection of phytoplankton in the upper ocean. Limnol. Oceanogr. **28**: 801–815.

Eppley, R.W., Renger, E.H., and Harrison, W.G. 1979. Nitrate and phytoplankton production in southern California coastal waters. Limnol. Oceanogr. **24**: 483–494.

Fowler, A.J., and Jennings, P.R. 2003. Dynamics in 0+ recruitment and early life history for snapper (*Pagrus auratus*, Sparidae) in South Australia. Mar. Freshw. Res. **54**: 941–956.

Francis, M.P. 1994. Duration of larval and spawning periods in *Pagrus auratus* (Sparidae) determined from otolith daily increments. Environ. Biol. Fishes, **39**: 137–152.

Gordon, N.D. 1985. The southern oscillation: a New Zealand perspective. J. R. Soc. N.Z. **15**: 137–155.

Greig, M.J., Ridgeway, N.M., and Shakespeare, B.S. 1988. Sea surface temperature variations at coastal sites around New Zealand. N.Z. J. Mar. Freshw. Res. **22**: 391–400.

Hansen, P.J., Bjornsen, P.K., and Hansen, B.W. 1997. Zooplankton grazing and growth: scaling within the 2–2000 µm body size range. Limnol. Oceanogr. **42**: 687–704.

Hitchcock, G.L. 1982. A comparative study of the size-dependent organic composition of marine diatoms and dinoflagellates. J. Plankton Res. **4**: 363–377.

Huntley, M.E., and Lopez, M.D.G. 1992. Temperature-dependent production of marine copepods: a global synthesis. Am. Nat. **140**: 210–242.

Irigoien, X., et al. 2002. Copepod hatching success in marine ecosystems with high diatom concentrations. Nature (Lond.), **419**: 387–389.

Jillett, J.B. 1971. Zooplankton and hydrology of Hauraki Gulf New Zealand. N.Z. Dep. Sci. Ind. Res. Bull. **204**.

Kendrick, T.H., and Francis, M.P. 2002. Fish assemblages in the Hauraki Gulf, New Zealand. N.Z. J. Mar. Freshw. Res. **36**: 699–717.

Kingsford, M.J., and Atkinson, M.H. 1994. Increments in otoliths and scales: how they relate to the age and early development of reared and wild larval and juvenile *Pagrus auratus* (Sparidae). Aust. J. Mar. Freshw. Res. **45**: 1007–21.

Longhurst, A.R., and Herman, A.W. 1981. Do oceanic zooplankton aggregate at, or near, the deep chlorophyll maximum? J. Mar. Res. **39**: 353–356.

Maddock, L., and Taylor, F.J. 1984. The application of multivariate statistical methods to phytoplankton counts from the Hauraki Gulf, New Zealand. N.Z. J. Mar. Freshw. Res. **18**: 309–322.

Manly, B.F.J. 1986. Multivariate statistical methods: a primer. Chapman and Hall, London, UK.

Mann, K.H., and Lazier, J.R.N. 1991. Dynamics of marine ecosystems. Biological–physical interactions in the oceans. Blackwell Scientific Publications, Cambridge, Mass.

Miller, T.J., Crowder, L.B., Rice, J.A., and Marchall, E.A. 1988. Larval size and recruitment mechanisms in fishes: toward a conceptual framework. Can. J. Fish. Aquat. Sci. **45**: 1657–1670.

Miralto, A., Barone, G., Romano, G., Poulet, S.A., Ianora, A., Russo, G.L., Buttino, I., Mazzarella, G., Laabir, M., Cabrini, M., and Giacobbe, M.G. 1999. The insidious effect of diatoms on copepod reproduction. Nature (Lond.), **402**: 173–176.

Nejstgaard, J.C., Hygum, B.H., Naustvoll, L.-J., and Bamstedt, U. 2001. Zooplankton growth, diet and reproductive success compared in simultaneous diatom- and flagellate–microzooplankton-dominated blooms. Mar. Ecol. Prog. Ser. **221**: 77–91.

Pankhurst, P.M. 1994. Age-related changes in the visual acuity of larvae of New Zealand snapper, *Pagrus auratus*. J. Mar. Biol. Assoc. U.K. **74**: 337–349.

Pankhurst, P.M., Montgomery, J.C., and Pankhurst, N.W. 1991. Growth, development and behaviour of artificially reared larval *Pagrus auratus* (Bloch & Schneider, 1801) (Sparidae). Aust. J. Mar. Freshw. Res. **42**: 391–398.

Paradis, A.R., and Pepin, P. 2001. Modeling changes in the length frequency distributions of fish larvae using field estimates of predator abundance and size distributions. Fish. Oceanogr. **10**: 217–234.

Paradis, A.R., Pepin, P., and Brown, J.A. 1996. Vulnerability of fish eggs and larvae to predation: review of the influence of the relative size of prey and predator. Can. J. Fish. Aquat. Sci. **53**: 1226–1235.

Parsons, T.R.,Takahashi, Masayuki, T., and Hargrave, B. 1984. Biological oceanographic processes. Pergamon Press, Oxford, U.K.

Pepin, P., Dower, J.F., and Davidson, F.J.M. 2003. A spatially explicit study of prey–predator interactions in larval fish: assessing the influence of food and predator abundance on larval growth and survival. Fish. Oceanogr. **12**: 19–33.

Rey, C., Harris, R., Irigoien, X., Head, R., and Carlotti, F. 2001. Influence of algal diet on growth and ingestion of *Calanus helgolandicus* nauplii. Mar. Ecol. Prog. Ser. **216**: 151–165.

Riley, G.A. 1956. Oceanography of Long Island Sound 1952–54. IX. Physical oceanography. Bull. Bingham Oceanogr. Collect. Yale Univ. **15**: 15–46.

Rilling, G.C., and Houde, E.D. 1999. Regional and temporal variability in growth and mortality of bay anchovy, *Anchoa mitchilli*, larvae in Chesapeake Bay. Fish. Bull. **97**: 555–569.

Rothschild, B.J., and Osborn, T.R. 1988. Small scale turbulence and plankton contact rates. J. Plankton Res. **10**: 465–474.

Scott, S.G., Zeldis, J.R., and Pankhurst, N.W. 1993. Evidence of daily spawning in natural populations of the New Zealand snapper *Pagrus auratus* (Sparidae). Environ. Biol. Fishes, **36**: 149–156.

Sharples, J., and Greig, M. 1998. Tidal currents, mean flows, and upwelling on the northeast shelf of New Zealand. N.Z. J. Mar. Freshw. Res. **32**: 215–231.

Sulkin, S., Lehto, J., Strom, S., and Hutchinson, D. 1998. Nutri-

© 2005 NRC Canada

tional role of protists in the diet of the first stage larvae of the Dungeness crab *Cancer magister*. Mar. Ecol. Prog. Ser. **169**: 237–242.

Sundby, S., and Fossum, P. 1990. Feeding conditions of Arcto-Norwegian cod larvae compared with the Rothschild–Osborn theory on small-scale turbulence and plankton contact rates. J. Plankton Res. **12**: 1153–1162.

Taggart, C.T., and Leggett, W.C. 1987. Short-term mortality in post-emergent larval capelin *Mallotus villosus*. II Importance of food and predatory density, and density dependence. Mar. Ecol. Prog. Ser. **41**: 219–229.

Turner, J.T., Tester, P.A., and Hettler, W.F. 1985. Zooplankton feeding ecology. Mar. Biol. **90**: 1–8.

Zeldis, J.R. 2004. New and remineralised nutrient supply and ecosystem metabolism on the northeastern New Zealand continental shelf. Continental Shelf Res. **24**: 563–581.

Zeldis, J., and Francis, R.I.C.C. 1998. A daily egg production method estimate of snapper biomass in Hauraki Gulf, New Zealand. ICES J. Mar. Sci. **55**: 522–534.

Zeldis, J.R., and Smith, S.V. 1999. Water, salt and nutrient budgets for Hauraki Gulf, New Zealand. *In* Australasian estuarine systems: carbon, nitrogen and phosphorus fluxes. *Edited by* S.V. Smith. LOICZ Rep. Stud. **12**.

Zeldis, J.R., Davis, C.S., James, M., Booth,W., Ballara, S., and Chang, H. 1995. Salp grazing: effects on phytoplankton abundance, vertical distribution and species composition in a coastal habitat. Mar. Ecol. Prog. Ser. **126**: 267–283.

Zeldis, J.R., Walters, R.A., Greig, M.J.N., and Image, K. 2004. Circulation over the northeastern New Zealand continental slope, shelf and adjacent Hauraki Gulf, from spring to summer. Continental Shelf Res. **24**: 543–561.

© 2005 NRC Canada

Can vessel monitoring system data also be used to study trawling intensity and population depletion? The example of Australia's northern prawn fishery

Roy Deng, Cathy Dichmont, David Milton, Mick Haywood, David Vance, Natasha Hall, and David Die

Abstract: We explore the potential of using data from Australia's northern prawn fishery (NPF) vessel monitoring system(s) (VMS) to examine trawl track, trawling intensity, and stock depletion due to trawling. We simulate VMS data by subsampling global positioning system (GPS) fixes from the NPF fishing vessels at different polling intervals to examine their accuracy in describing trawl tracks. The results of the simulations suggest that VMS data with polling intervals longer than 30 min cannot accurately estimate trawl tracks. The analysis of high-polling-frequency VMS data collected in four (later reduced to three) 6 nautical mile × 6 nautical mile grids that historically received high levels of fishing effort showed that trawling was not random and some areas were trawled up to 28 times in the tiger prawn fishing season and the impact varied among years. The results of a catch-depletion analysis suggest that fishery catch-per-unit-effort and cumulative catch may not be proportional to overall target-species biomass in areas with highly aggregated trawl effort. The VMS data also showed a large number of trawls can occur in productive areas and that trawling impacts on benthos may be quite marked.

Résumé : Nous examinons la possibilité d'utiliser les données de du système de surveillance des navires (VMS) de la pêche crevettière du nord de l'Australie (NPF) pour étudier les pistes de chalutage, l'intensité du chalutage et l'épuisement des stocks dû au chalutage. Nous simulons les données VMS en sous-échantillonnant les coordonnées des navires de pêche NPF obtenues par le système de positionnement global (GPS) à différents intervalles d'échantillonnage afin de déterminer leur précision pour décrire les pistes de chalutage. Les résultats de nos simulations indiquent que des données VMS basées sur des intervalles d'échantillonnage supérieurs à 30 min ne permettent pas d'estimer correctement les pistes de chalutage. L'analyse de données VMS échantillonnées à fréquence plus élevée (HPF) obtenues sur quatre grilles (réduites subséquemment à trois) de 6 × 6 milles marins, qui ont, dans le passé, traditionnellement été soumises à des pressions de pêche élevées, montre que le chalutage ne se fait pas au hasard et que certaines régions sont soumises à jusqu'à 28 fois au chalutage durant la saison de pêche de la crevette tigrée et que l'impact varie d'une année à l'autre. Les résultats d'une analyse d'épuisement des captures indiquent que les captures par unité d'effort de cette pêche et les captures cumulées peuvent ne pas être proportionnelles à la biomasse globale de l'espèce visée dans les régions où l'importance du chalutage est fortement concentrée. Les données VMS montrent aussi qu'il peut se produire un important chalutage dans les zones productives et que les impacts du chalutage sur le benthos peuvent être très considérables.

[Traduit par la Rédaction]

Introduction

Current prawn (shrimp) stock assessment models do not explicitly take into account small-scale spatial variation in prawn distribution (Fu and Quinn 2000; Dichmont et al. 2003). Most stock assessments assume that fishing effort is randomly distributed within the known fishing grounds (Hilborn and Walters 1992). However, with the advent and wide use of vessel monitoring system(s) (VMS) in many fisheries, there is great potential to utilize the VMS data to improve spatially explicit fishery models (Die and Ellis 1999). If prawn trawling is nonrandom and aggregated in areas of high abundance of the target species, it is possible that catch-per-unit-effort (CPUE) is not proportional to over-

Received 26 September 2003. Accepted 1 September 2004. Published on the NRC Research Press Web site at http://cjfas.nrc.ca on 13 April 2005.
J17765

R. Deng,[1] **C. Dichmont, D. Milton, M. Haywood, D. Vance, and N. Hall.** Marine Research, Commonwealth Scientific and Industrial Research Organisation, P.O. Box 120, Cleveland, QLD 4163, Australia.
D. Die. Cooperative Institute for Marine and Atmospheric Studies, Rosenstiel School of Marine and Atmospheric Science, University of Miami, 4600 Rickenbacker Causeway, Miami, FL 33149, USA.

[1]Corresponding author (e-mail: roy.deng@csiro.au).

 doi: 10.1139/F04-219 © 2005 NRC Canada

all biomass. This may affect the management advice that is given on the basis of the target-species assessments. As well, studies through the world are showing that the seabed can be repeatedly trawled each year (Rijnsdorp et al. 1998; Schratzberger and Jennings 2002). The impacts of repeated trawling are cumulative and vary among taxa (Poiner et al. 1998; Tanner 2003). Some benthic fauna, such as sponges, might be severely impacted by a single trawl, whilst others (algae, bryozoans, Pennatulacea) might be able to withstand several repeated trawls, but their vulnerability increases with successive trawls (Poiner et al. 1998).

VMS data may also be useful in assessing the effects of trawling on the benthic communities throughout a fishery. To date, these effects have been examined mainly at a small scale with experimental manipulations. This is due to the fact that most experiments are only cost effective at a scale of a few square kilometres. For example, Poiner et al. (1998) repeatedly trawled six 2.7 km long and 30 m wide tracks in the Great Barrier Reef region to simulate commercial fishing of the same ground. In this case we may be able to use VMS data to link these small-scale experiments at a single time with fishery-wide trawl effects over several years.

The northern prawn fishery (NPF) is the most valuable nationally managed trawl fishery in Australia and covers about 800 000 km^2 of northern Australian waters. At the end of 2002, about 100 trawlers were operating in the NPF and caught about 4600 t of banana prawns (*Penaeus merguiensis* and *Penaeus indicus*) and 2000 t of tiger prawns (*Penaeus esculentus* and *Penaeus semisulcatus*). Trawl fisheries such as the NPF are coming under increasing pressure to demonstrate that their impacts on target and bycatch species and on the benthic communities are sustainable. This requires an understanding of the distribution and scale of trawl effort (Poiner et al. 1998; Tuck et al. 1998).

The fishing methods used to capture banana and tiger prawns are quite different. In the NPF, banana prawns form dense aggregations visible as muddy stains from the air where their position is recorded by fishing company spotter planes or on the fishing vessel's echo sounders. These aggregations are fished intensively during daylight for the first couple of weeks of the fishing season each year (April). When catch rates decline to a level where it is no longer economically viable to continue fishing for banana prawns, the fishers switch to targeting tiger prawns. Tiger prawns do not aggregate to the same degree as banana prawns and are generally only catchable by demersal trawl gear at night, when they are active. During daylight, tiger prawns tend to bury themselves in the substrate.

Although tiger prawns do not form dense schools like banana prawns, their distribution across the seabed is not uniform and the fishers employ a searching strategy to enable them to identify and target areas of high tiger prawn abundance. NPF fishing vessels are equipped with twin otter trawls and when fishing for tiger prawns, a single trawling operation lasts between 3 and 4 h. A small (4 m head rope length) beam or otter trawl known as try gear is generally operated between the two main fishing nets. The try gear is retrieved every 30–40 min, allowing the fishers to monitor their catch rates without retrieving the main gear. When they are satisfied with the catch rate from the try gear they will turn the vessel around and retrace the vessel's track, hoping to reproduce or better the catch rate. This practice is facilitated by the use of a global positioning system (GPS) and plotters that record the vessel's position every minute and allow the fishers to annotate their electronic charts, recording prawn catches, areas of untrawlable ground, or places that have produced high catches. The GPS and plotter technology, which was introduced into this fishery in 1998, has increased fishing power in this fishery significantly (Robins et al. 1998).

Satellite-based VMS technology has been operating in fisheries around the world for several years (Drouin 2001). It was mainly introduced as a surveillance system to ensure that fishers comply with seasonal and spatial closures (Australian Fisheries Management Authorities (AFMA) website: http://www.afma.gov.au/). However, it has potential uses in assessing stock and evaluating the ecosystem impacts of trawling. The approach developed for the NPF would be applicable to most trawl fisheries in other countries. VMS provides trawl location data at greater spatial resolution than those that could normally be collected from logbooks. Potentially, these data could be applied to problems at both fine and coarse scales, thus bridging the gap between small-scale environmental-impact studies and fishery-wide stock assessment. Similarly, GPS is now widely used throughout many fisheries. Robins et al. (1998) found that the use of GPS and plotter systems has increased the catch of prawn trawl fisheries by enabling the fishers to target schools more accurately. Because coarser VMS data can be treated as a subset of the finer GPS data set, GPS data are a critical data source for examining the accuracy of trawl tracks through simulation of VMS data.

VMS data can be used to assess a potential environmental or fishery impact and determine its spatial extent. One of our objectives is to evaluate the capacity of VMS data to be incorporated into spatial aspects of applied fisheries research in the NPF tiger prawn fishery. As VMS data are mainly designed for surveillance purposes, the polling frequency varies widely among fisheries. We need to examine VMS to find the lowest polling frequency that can be used to describe the trawl track without significant bias. Another objective is to apply VMS data to stock assessment and evaluation of trawling impacts. A potential use of VMS data is in population-depletion analysis to estimate population size or better define fishery assessment model parameters by linking trawl position with logbook catch data. Many current stock-assessment models assume that target-species CPUE is linearly proportional to biomass (Hilborn and Walters 1992). This may not be the case in these highly aggregated and intensively fished areas. The catch or CPUE of trawl fisheries can be affected by gear saturation, where fishers negatively impact each other's CPUE by fishing intensively in a small area. On the other hand, in highly aggregatory species this linearity between CPUE and biomass can also be affected because fishers can maintain a high CPUE by continuing to move and to target aggregations, although the overall abundance of the stock may be decreasing. Therefore, we wanted to test the hypothesis that the decline rate of the depletion curve in highly aggregated fishing areas is artificially higher or lower than that in randomly fished areas (Fig. 1).

© 2005 NRC Canada

Fig. 1. Expected types of fishing patterns in trawl fisheries. (*a*) Random: this plot shows all the vessel monitoring system(s) (VMS) records for one 6 nmi × 6 nmi grid for August–September 1998. (*b*) Aggregated: this plot shows all the VMS records for another 6 nmi × 6 nmi grid for August–September 1998. (*c* and *d*) The corresponding hypothesized rates of depletion of random and aggregated patterns, respectively, when it is assumed that catch-per-unit-effort (CPUE) is linearly related to biomass.

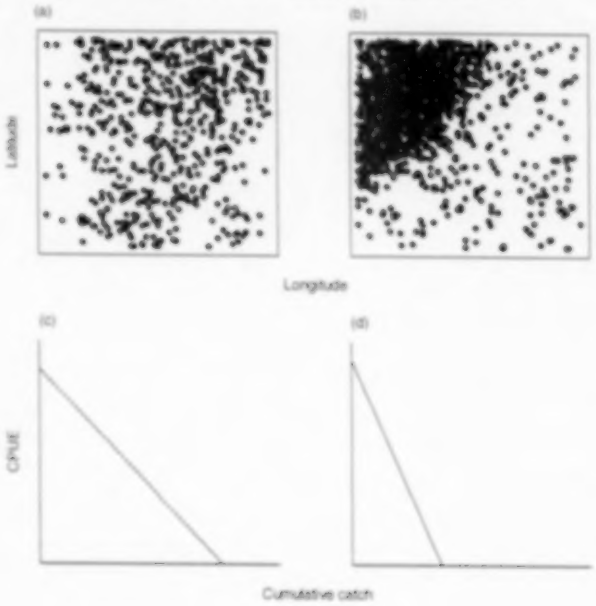

Materials and methods

To assess the feasibility of undertaking studies of trawling intensity with VMS data, there are several steps in the analysis. The different data sets and their resolution/coverage are described in Table 1. Initially, an acceptable approximation of each trawl track has to be identified by comparing tracks obtained from GPS data with simulated VMS fixes taken at a range of polling frequencies. Then high-polling-frequency VMS (HPFVMS) data were collected and used to calculate trawling intensity. Once this has been calculated, the vessel logbook catch records have to be matched with the trawl tracks in order to undertake a population-depletion analysis. In this case, the coverage of the HPFVMS data was too small, so the standard-frequency VMS data needed to be joined to the data set.

We define one trawl track as one vessel trawling during a single night, as the NPF in the relevant period is a nighttime trawl fishery. An onboard GPS can provide positional data at high frequency (e.g., 1–5 s) and a set of fine-scale GPS records from a trawler can be treated as a continuous trawl track. Since GPS data from past trawls are a valuable record, they are usually retained by the skipper and are not freely available. A few skippers have made their GPS data available to us. These positional data are recorded at intervals of approximately 100 m (equivalent to approximately 1 min at a trawling speed of 3 kn (1 kn = 1.85 km/h)) and the track calculated from this can be treated as "true" vessel track.

A VMS consists of three main components: the tracking unit on board the vessel, the transmission medium, and the base station. The tracking unit has its own integrated GPS and is programmed to send positional data to the base station via the transmission medium (communication satellites) at regular intervals. Reports from the boat can also be automatically collected at a predetermined location or time (AFMA website: http://www.afma.gov.au/). In the Australian NPF, VMS is a requirement for all catcher, carrier, and processor vessels (AFMA website: http://www.afma.gov.au/). It would be ideal to acquire the VMS data at the same fine scale as GPS data for research purposes. However, transmission of these data from the vessel to the base station via satellite is quite expensive, consequently VMS data are generally transmitted much less frequently. This allows government agencies to collect information on trawl location at a reasonable cost. Therefore, the routine VMS data in the NPF vary widely in resolution and in most cases are quite coarse. Under the auspices of this research, we collected HPFVMS data from the deliberately selected areas, each a 6 nautical mile (nmi) × 6 nmi grid square, at a polling frequency of 20 min for 2 years (1998 and 1999). Four areas were originally selected but one area was subsequently closed to fishing. These areas were chosen from the AFMA daily logbook records because historically they were all subject to a high level of effort. We also used the same years' routine VMS data as the auxiliary data set for this research.

Logbooks in the NPF are filled in daily and the fishers are obliged to give the position where their largest catch was made each night. The data are reported at a coarse scale of a single catch and location value per 24 h of fishing. However, fishers usually trawl 3–4 shots per night when targeting tiger prawns. Each logbook record contains the vessel's name, the vessel identity number, the date, the catch of each target species group, and the location at which the largest catch in the night was obtained. Logbook data from two fishing seasons from August to October in 1998 and 1999 were used.

As VMS data are much more detailed than we need, some data preprocessing had to be conducted to eliminate nonfishing records. From fishers' GPS records we also determined that one of the three areas (grid A) contained significant amounts of untrawlable ground, whereas the other two were relatively free of untrawlable ground.

Accuracy of trawl tracks at various polling frequencies

To compare characteristics of tracks recorded at a variety of different polling intervals, we characterized each track in terms of (*i*) track area (TA): the area that would be covered if trawling occurred in a straight line between successive points (no overlap); (*ii*) area passed once (AP1): the area of track referenced once only; (*iii*) percent area passed once (PAP1): the ratio of the area passed once to the corresponding track area. As well, we assume that the vessel maintains approximately the same speed when fishing. The relationships among these characteristics are as follows:

$$(1) \qquad PAP1 = AP1 \times 100/TA$$

© 2005 NRC Canada

Table 1. Summary of data sets used in this study.

Data set	Abbreviation	Spatial resolution	Temporal resolution	Spatial coverage	Temporal coverage	Objective(s)
Satellite-based vessel monitoring system data	VMS	Depends on temporal resolution	From minutes to hours	Northern prawn fishery (NPF)	1998 and 1999	Population-depletion analysis
High-polling-frequency vessel monitoring system data	HPFVMS	2000 m	≤20 min	Three 6 nmi × 6 nmi grids	August–October of 1998 and 1999	Trawling-intensity calculation; population-depletion analysis
Global positioning system data	GPS	100 m	1 min	100 night tracks from 4 skippers	1998	Input for simulation VMS data at various polling frequencies
Vessel daily catch record data	Logbook	Various	1 day	NPF	1998 and 1999	Population-depletion analysis

We defined a trawl track as the path of a vessel recorded by a GPS over a single night's fishing (approximately 14 h) and this will approximate the true track. One hundred GPS-recorded trawl tracks from four vessels at polling intervals of 1 min (about 100 m apart) were analysed. We assumed that the vessels travelled in a straight line between adjacent points. This assumption is reasonable when one considers the size of the vessels, the length of trawl wire between the nets and the vessel, and typical turning radii of vessels engaged in trawling. A typical NPF trawler is between 20 and 25 m long, the ratios of trawl wire length to water depth used in this fishery are approximately 5:1, which corresponds to between 75 and 200 m of trawl wire, and the turning radius of a vessel whilst trawling is typically between 100 and 200 m. To produce a trawl track between point locations, it was assumed that trawl width was 30 m (based on standard trawl gear used in the fleet) and that the vessels trawled in a straight line between adjacent (1 min interval) points. We interpolated longitudinal and latitudinal coordinates for the outer extents of a 30 m wide rectangle (15 m each side of the vessel) between the VMS points.

Each of the longitudinal and latitudinal coordinates was assigned to a corresponding central cell reference with dimensions of 0.001 decimal degrees (approximately 11.7 m by 11.7 m). A file containing these cell references was written with the condition that the cell reference has not previously been recorded for neighbouring interpolated points. By doing this check, it could be assumed that each cell was only recorded once per pass. We summed the passes in each cell and used the frequency of passes in subsequent spatial analyses. Each track could then be described by its characteristics.

Trawling intensity

We calculated the trawling intensity in the selected grids with real HPFVMS data collected by AFMA. Based on the results of the GPS data simulations that the shorter polling interval had less chance of underestimating track area, three 6 nmi × 6 nmi grids (A, B, and C) were selected for polling at intervals of less than 20 min. These grids in the southern Gulf of Carpentaria represented the most intensively fished areas in the NPF at that time. The plots of polls from these areas represent two types of fishing patterns: random and aggregated. For this analysis, three data sets were combined: HPFVMS data, daily logbook catch data, and routine VMS data. The HPFVMS data were used to estimate trawling intensity, which is the number of times a particular piece of seabed is passed over by a trawl.

Owing to the costs, the VMS data do not record whether the vessel is fishing or in transit. This information can only be inferred from the vessel speed, calculated from the distance travelled between adjacent polling points and the time taken. Unless the vessel is travelling in a straight line between adjacent polling points, velocity calculated in this manner will always be underestimated. The following decision rules were used to exclude the records where fishing was not taking place: (*i*) vessel in a nonfishing location (port, seasonal- or permanent-closure areas); (*ii*) vessel whose speed was >4 kn (considered to be in transit), as trawling speed is usually about 3.2–3.5 kn and transit speed over large distances is usually >7 kn; (*iii*) vessel at anchor, as the location does not change for several hours; and (*iv*) daytime

© 2005 NRC Canada

records (0800–1800), as daytime fishing is banned in the NPF during the period tested. Given that vessels transit at higher speeds than those used for trawling and that anchoring or transiting is most likely to happen during the daytime, when fishing is banned, there is only a small chance that nontrawl data were retained after these restrictions were applied.

The following assumptions were also made: (*i*) the vessels travel in a straight line between polls; (*ii*) trawling width is 15 m on both sides of the vessel; (*iii*) one trawl track (30 m wide) is the trace of one vessel for one fishing night.

This third assumption allows VMS data and logbook data to be linked through a unique combination of vessel name and date identifier common to the logbook and VMS data. In this way, the catches in logbooks can be attached to a track and thus enable us to undertake depletion analyses.

The simulations of trawl tracks with HPFVMS data were undertaken in a geographical information systems (GIS) package (ArcInfo®; Environmental Systems Research Institute, Inc. 1982–2002). The VMS information was in the form of a series of positional fixes (points). These points were loaded into the GIS and converted into separate lines, each representing a vessel's track for a night of fishing. To characterize the area of the seabed trawled, the lines were buffered 15 m either side to model the width of a typical pair of NPF trawl nets. In this manner, the area trawled each night by a vessel was represented by a 30 m wide "strip". These strips were overlaid in the GIS and the trawling intensity at each point of the seabed was estimated by counting the strips overlying it.

Population-depletion analysis

The depletion analysis required routine VMS data, HPFVMS data, and logbook data. To undertake depletion analyses, we needed to link the logbook catches with the tracks calculated from HPFVMS. Logbooks give the single position where the vessel's largest catch was made each night. However, a night's fishing often extends beyond a single grid and therefore the routine VMS data for adjacent grids were also used to link the VMS and logbook data beyond the HPFVMS grids. The challenge was to combine all these data sets, which are recorded at different spatial and temporal scales. The result is that there is not enough information to determine which part of the catch was obtained within the trawl track.

The different spatial and temporal scales of the VMS and logbook data meant that the catch could not be accurately linked to the specific fishing grids chosen, but could only be associated with a larger, relatively loosely defined area that the vessel covered each night (based on its VMS plots). Furthermore, when plotting the position from HPFVMS data within the 6 nmi × 6 nmi grids that have catch allocated from the logbook data, the logbook position for the highest catch of the day did not always correspond to the vessel's position obtained from the VMS. Knowledge of the catch made within a specific area is required for biomass-depletion analyses.

These mismatches of VMS and logbook positions meant that the fishing areas to which the effort refers had to be carefully identified. As we described above, HPFVMS data were confined strictly to the three research grids. Often only one record of a track fell inside the grid. To define the full area trawled by all fishers that entered the research grids in that day, we needed to define a new, bigger area. We used a convex-hull method to define the fished area using the HPFVMS with the linked VMS and logbook position data for the relevant tracks. The convex hull is the smallest convex polygon containing all the points (both VMS and logbook positions of vessels that entered the grid and its 3 nmi vicinity). This can most easily be visualized by imagining pins being inserted at all observed points and a tightly fitting rubber band placed to enclose all the points. However, single outlying points can easily double the size of the fishing area and often these points were the less reliable logbook positions. For this reason we finally defined the area more conservatively by using a one-peel convex hull. This means removing the points that defined the outer extent of the convex hull and using the convex hull of the next outer set of fixes instead. We selected logbook records (the number of vessels varied from 12 to 46 depending on area and year) from the database that fell into the convex hulls, allocated the catches along with the efforts estimated by HPFVMS, and calculated the target prawn CPUE to plot the graph of CPUE against cumulative catch to assess whether or not there was a depletion of the biomass with increasing cumulative catch.

Table 2. Summary of track parameter estimates for the trawl tracks generated from GPS data.

	Track area (km^2)	Total area trawled once (km^2)	Percent area passed once
Mean	3.92	2.84	73.00
SD	0.4	0.63	16.17
Maximum	4.71	4.07	99.94
Minimum	2.05	1.09	26.58

Results

The grids chosen showed fishing that was either more randomly distributed (Fig. 1*a*) or heavily aggregated (Fig. 1*b*).

Accuracy of trawl tracks at various polling frequencies

The GPS data showed that the trawl tracks varied in shape, length, and degree of overlap (Table 2). These results can be explained by looking at examples of the trawl patterns. The "area trawled once" is only a small percentage of the convex-hull area. In general, a smaller area would be expected if tracks overlap (Fig. 2). In contrast, the track on the left-hand side of Fig. 2 is more open and extends across the diagonal and consequently has a much lower degree of overlap.

We calculated track areas and areas passed once. The mean values for track area and area passed once for all the tracks were plotted for each of the simulated polling intervals. Assuming that the values for 1-min-interval data are as accurate as possible, we have plotted the values for the other time intervals as proportions of the values for the 1-min-interval data. The results show that all simulated polling intervals underestimate the track area and area passed once,

© 2005 NRC Canada

Fig. 2. Two examples of fishing tracks from a single night of fishing obtained from vessel global positioning system (GPS) data. The track on the right has a high degree of overlap and the track on the left has a low degree of overlap.

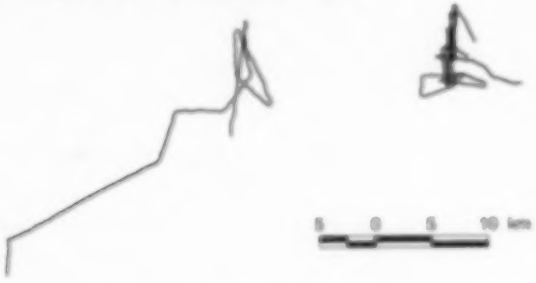

Fig. 3. Comparison of track area (solid line) and area passed once (broken line) calculated from simulated VMS data polled at a range of frequencies up to 120 min.

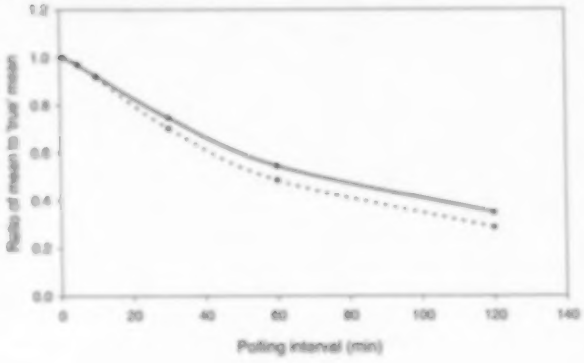

and the error increases with time interval (Fig. 3). At a 30-min polling interval, the estimates are around 70% of the true (1-min-interval data) track. Moreover, when the polling interval was set at 20 min, both estimates are above 80% of the true track. However, at 2-h intervals, the estimates are as low as 30%–40% of the true track (Fig. 3) and the loss of precision is quite marked (Fig. 4). An example of the loss of information is shown in Fig. 4, where the points from one night's fishing, recorded by GPS plotter, were subsampled ("polled") at 30- and 120-min intervals. At the 120-min level of subsampling, all sign of the intensely aggregated part of the night's fishing effort has been lost.

The distributions of "percent area trawled" against "number of passes" covered by a realistic number of trawl passes (100, 200, or 400) were calculated. The distributions for the "true" (1 min interval) estimate fitted the distribution most closely at the highest level of fishing effort (Fig. 5*a*). For the fishing effort at 100 trawls, the distribution of trawling intensities calculated from 120 min interval simulation underestimated the percent area trawled once, was close at 200 trawls, and overestimated with 400 trawls. The greatest proportion of the grid had not been passed even once (Fig. 5). As the effort in the grids increased, a greater proportion of the area had been trawled multiple times (Fig. 5*d*).

The results presented in this paper assume that the width of the trawl track corresponds to that of the trawl gear that follows a straight line between sequential polling points. The issue is that the assumption of a straight line between two closely polled points 2 h apart is less accurate than the same assumption made for points 2 min apart. Another method was attempted that calculated the swept area that would be covered in the polling interval and then adjusted the width accordingly (*i.e.*, points that were closer together may have had a wider area of influence, as the vessel did not trawl in a straight line, whereas points that were farther apart in a short time would cover an area similar in width to the gear. These results are not presented, as the new method is computationally complex and did not change the results.

Trawling-intensity analysis

The spatial distribution of trawling intensity in the chosen areas highlights the changes in fishing patterns in the different years for the same grid. The spatial distributions of trawling intensity in grid A over the 2 consecutive years were similar, but the number of fishing tracks differed (134 in 1998, 82 in 1999). This suggests that prawn abundance remained above an economic threshold during the 2 years, although the fishing patterns in the first year were less aggregated than in the second year. In the other two areas, grid B and grid C, the spatial distribution of trawling intensities changed dramatically, as did the numbers of fishing tracks in the grids. The number of fishing tracks in grid B decreased from 239 to 4 and in grid C from 96 to 16 between 1998 and 1999. This suggests that biomass in these areas had declined significantly (Fig. 6).

Population-depletion analysis

Defining the "areas fished" when the VMS data and logbook data are spatially and temporally consistent is a critical factor for depletion experiments. In our study, we found that fishing patterns in grid A (Fig. 6) were aggregated during both 1998 and 1999, with relatively high levels of fishing effort. The depletion curve declined more slowly in 1998 than in 1999 and the total catch from this grid in 1999 was less than half of that in 1998. In 1998, the fishing pattern in grid B appeared aggregated and the level of effort was relatively high. The depletion trend shows the steepest decline among all of the curves. In 1999, grid B showed a dramatic decline in both fishing effort and CPUE, which might imply a heavy depletion of biomass in either 1998 or 1999. In grid C, the fishing pattern appeared to be less aggregated in 1998 and the depletion curves declined at a rate intermediate between those of grid A and grid B. In 1999, grid C exhibited the same problem of a large decline in fishing effort and CPUE (Fig. 7) and this result is not well summarized by a straight-line model.

Discussion

Accuracy of trawl tracks at various polling frequencies

HPFVMS can be used to accurately represent the trawl tracks of fishing vessels in the NPF, where fishing effort is often highly aggregated. However, the accuracy of the approach is limited by the polling frequency. This is because, at low polling frequencies, trawlers are unlikely to be travelling in straight lines between polling sites and so a straight-line linear interpolation may give incorrect estimates of the

© 2005 NRC Canada

Fig. 4. Original GPS track data recorded at a polling interval of 1 min (*a*) compared with simulated VMS tracks generated by subsampling the GPS track at polling intervals of 30 min (*b*) and 120 min (*c*).

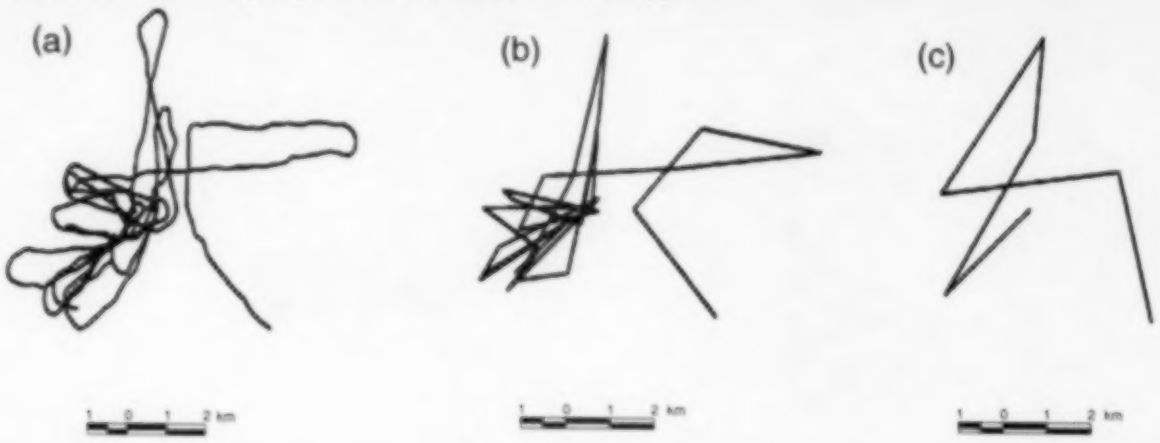

Fig. 5. Percent area trawled versus the number of times each 11.7 m × 11.7 m cell was trawled over a range of levels of effort and polling intervals. (*a*) Different track densities per grid. (*b*) 100 tracks per grid. (*c*) 200 tracks per grid. (*d*) 400 tracks per grid. In *b*, *c*, and *d*, the solid line represents the "true", 1-min interval and the broken line represents the 120-min interval.

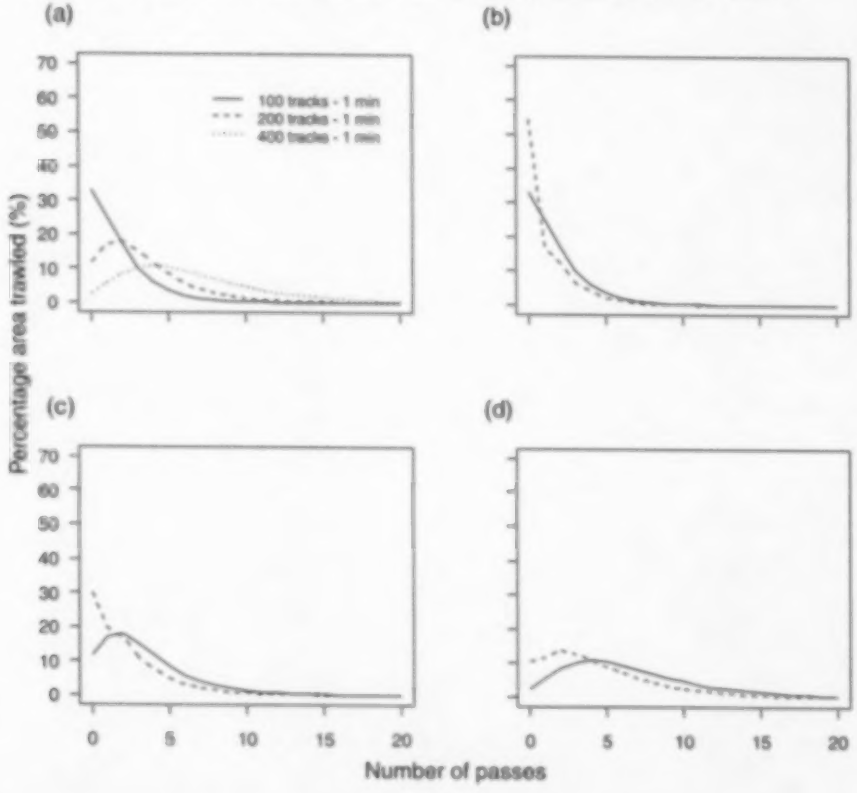

distribution of the effort. Even at relatively short polling frequencies (e.g., 30 min), biases occur and these biases increase as the polling frequency decreases. Calculations of the actual area trawled and the area trawled once or multiple times become progressively smaller than the most accurate estimates as polling frequency decreases. If analyses are concerned with effects at small spatial scales, such as studies of the impacts of trawling on the benthos, VMS polling intervals >30 min will result in serious bias of the estimated track areas. The linear interpolation also results in some error in the calculation of track parameters, especially when there is a significant change in direction. When vessels turn

© 2005 NRC Canada

Fig. 6. Distribution of trawling intensities in grids A–C from high-polling-frequency VMS (HPFVMS) data in 2 consecutive years.

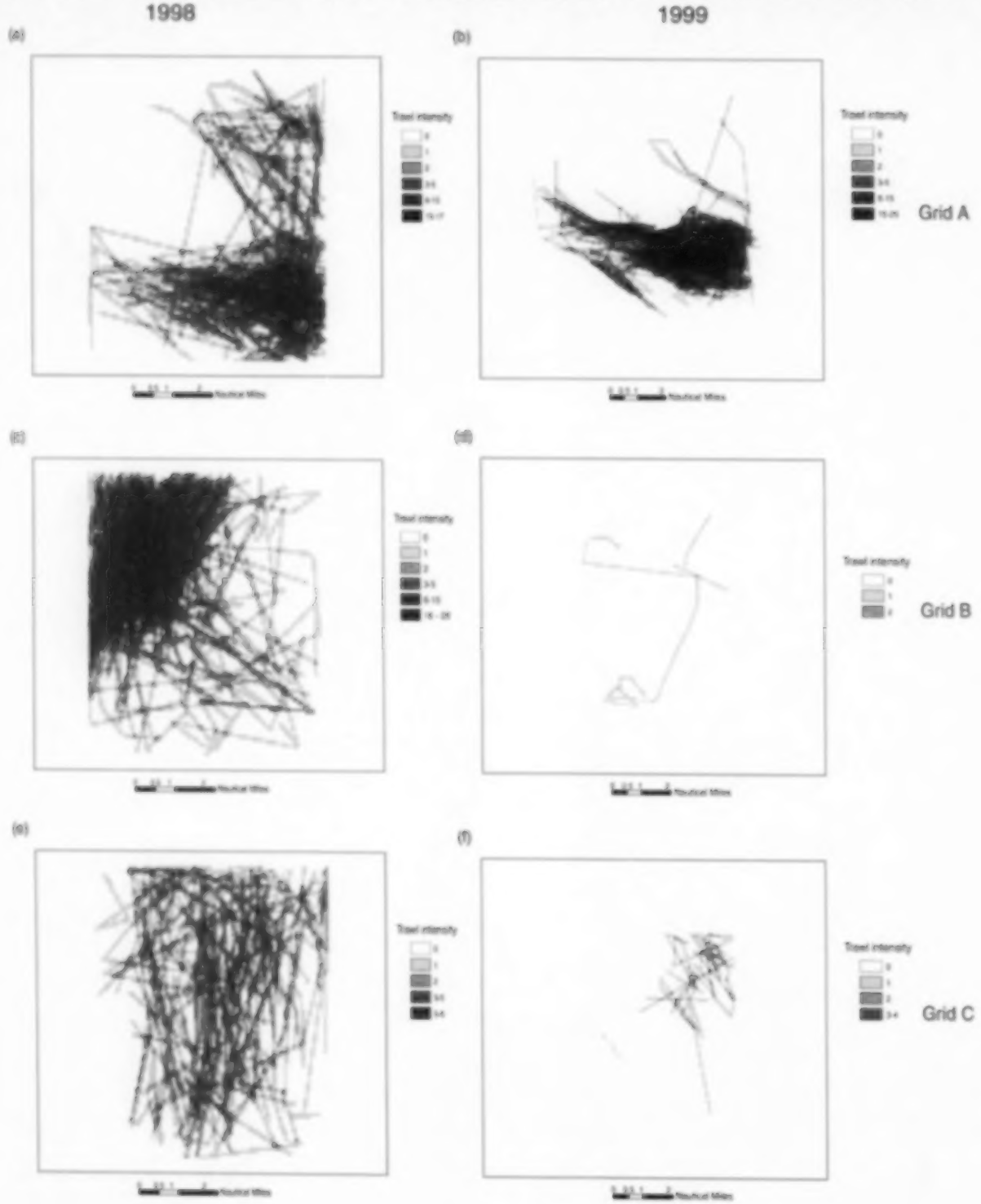

© 2005 NRC Canada

Fig. 7. Comparison of depletion curves in three grids during the 1998 and 1999 fishing seasons. Each point on the graphs represents daily CPUE for each grid.

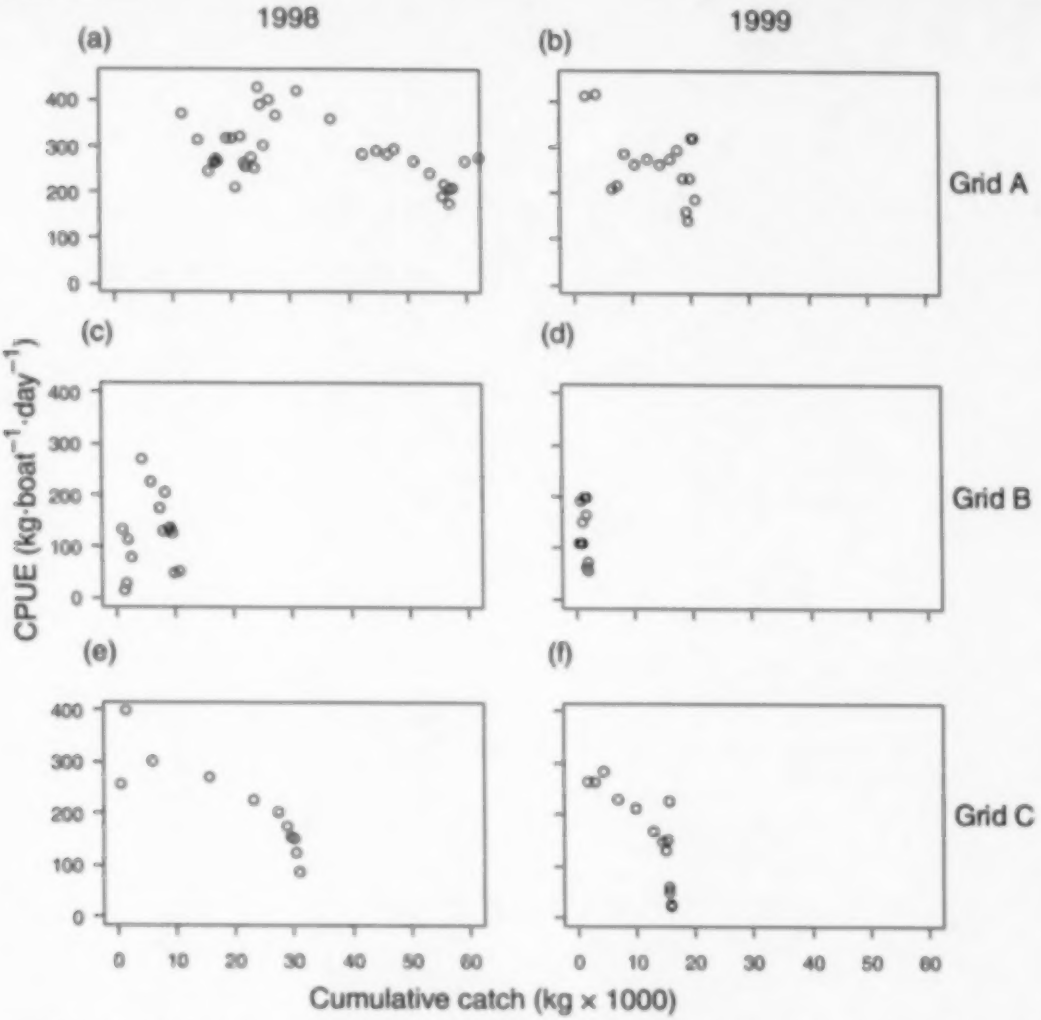

sharply, points are not allocated to the outside of the turn and although effort was made to exclude double counting of cells along the inside of the track, not all cases were eliminated. By assigning points to cells, we also limited the resolution of the estimation to around 12 m.

In most instances, fishers in the NPF vary their trawling patterns daily, depending on the degree of aggregation of the prawns and the success of the skipper in finding the aggregations. The relationship between the real trawl track and that estimated from low-frequency VMS polling depends largely upon the trawl pattern, so the track area and other parameters cannot be predicted from an estimate of the initial position and low-frequency VMS fixes (>30 min). In cases when the polling interval exceeded 30 min, enough information is lost for the characteristics of the trawl track to be significantly distorted. This suggests that the current VMS data collected routinely in the NPF cannot be used directly to estimate trawling-behaviour parameters.

It is difficult to advise as to one polling interval at which the results become significantly biased in all situations. If a polling interval was to be recommended, other factors including cost, physical polling limitations, form of data storage, and purpose of data collection must also be considered. Also, the scale at which the polled data were to be used would be an important determinant. However, we have shown that combining high- and low-polling-frequency data can enhance the accuracy of the analyses and increase the number of applications for which these data could be useful.

Comparing distributions of trawling intensities made from HPFVMS data (Fig. 8) and GPS data, the patterns of HPFVMS data were similar to the patterns from the analysis of the 1-min-interval method. This implies that the HPFVMS data themselves and the method used to analyse them were close to the true situation. For the grids sampled, the more aggregated the sample, the greater the proportion of highly trawled areas (Fig. 8). This suggests that specific areas within

© 2005 NRC Canada

Fig. 8. Distribution of trawling intensities based on HPFVMS data for 1998 (*a*) and 1999 (*b*). The solid line represents grid A, the broken line represents grid B, and the dotted line represents grid C.

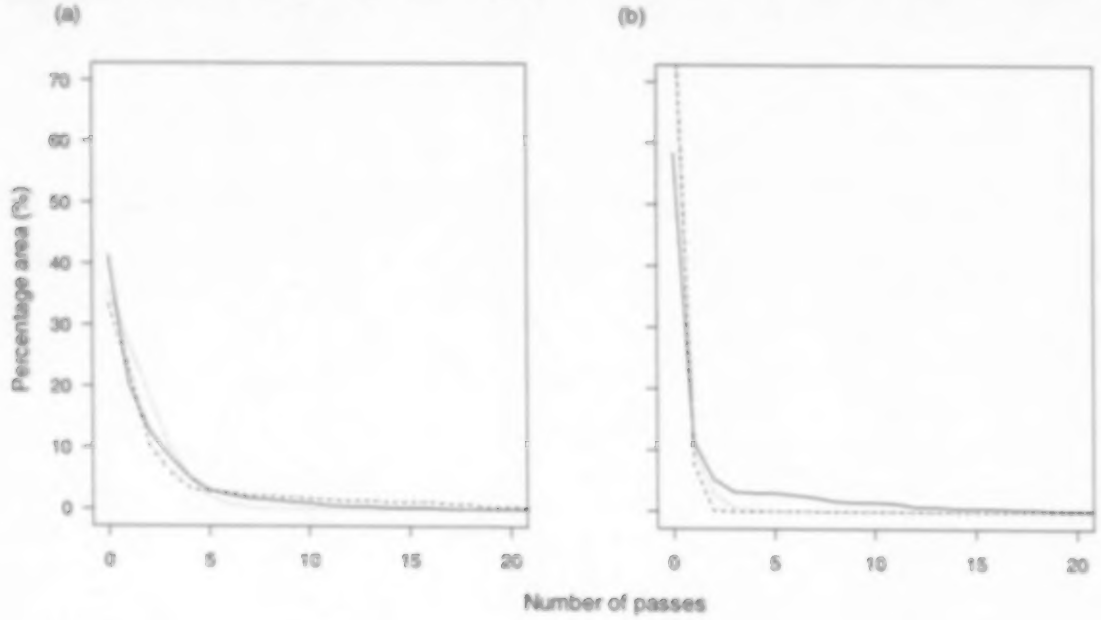

each grid are being targeted. Also, greater fishing effort coverage causes the distribution to flatten out.

Trawling intensity and population-depletion analysis

We found that we could realistically calculate trawling intensity only when the polling frequency was less than 20 min. However, the cost of obtaining and processing such large volumes of data for a large number of vessels is prohibitive. This makes it extremely difficult to undertake large-scale trawling-intensity studies with this approach. Rather, a more realistic approach to assessing trawl impacts on seabed biota would be to combine HPFVMS of areas of affordable size with repeat trawl experiments in the same area.

Three grids (6 nmi × 6 nmi) of HPFVMS data were collected during this study. Establishing reliable links between the VMS and logbook data was a complex operation because the two data sets have different spatial and temporal scales. Daily positions recorded in logbooks represent the locations of the highest catch on a specific fishing day, whereas the VMS records vessel locations (but no catch) at preset polling times. Generally, we found that there were four potential types of relationship between logbook data and HPFVMS records for one vessel on one day. These varied from complete compatibility to the case where the logbook placed the vessel in the nominated grid but the VMS showed that the vessel was elsewhere. We analysed 1999 logbook records falling inside the three 6 nmi × 6 nmi grids. In grid A, 64 of 70 logbook records matched HPFVMS records and 6 records not at all. In grid B, 4 of 5 matched and 1 not at all, and in grid C, 21 of 32 matched and 11 not at all. There are cases where the vessel's logbook location is too far away from the HPFVMS grid for a single night's trawling.

In cases where there were minor disagreements between VMS and logbook locations, this imprecision might not affect the accuracy of the analysis because the logbook records were very close to the "grid" and might represent partial input from the area fished. For cases where there is no agreement, the logbook position is either a mistake or a deliberate misrepresentation by the skipper. However, it is not possible to use only the HPFVMS data from specific grids because a night's fishing usually extends beyond a 6-min-interval grid.

To better define the spatial coverage of a night's fishing by vessels that entered the grid, we added the routine VMS records of relevant vessels. Furthermore, we added untrawlable fishing ground information to the GIS in order to better understand the fishers' behaviour in the grid. The combination of routine VMS, logbook, and HPFVMS data was used to define the area fished. Since this area need not be square, we used a convex-hull method to define the outer boundary of trawled areas. A one-peel convex hull was applied to remove the effect of outliers, such as logbook records that placed the vessel very far from the assumed correct VMS records of that vessel. We found that only by combining the logbook, routine VMS, and HPFVMS data could we adequately solve this problem. These difficulties in defining the depletion area would be common to many fisheries in Australia and the world.

The results of our depletion analysis did not always conform to the commonly held assumption of a linear relationship between CPUE and available biomass (Hilborn and Walters 1992). This relationship is widely assumed in many fishery-stock assessments. We have also shown a difference in depletion rate between highly aggregated and non-aggregated fishing patterns. This could be due to differences in biomass or habitats in each area, or to migration, but also may be related to trawling intensity. Although there are several scale issues in applying the depletion analysis, the point

© 2005 NRC Canada

is that these data are useful. Clearly there are difficulties with using a single data source, especially logbook data. We show that VMS data would therefore greatly enhance any depletion analyses.

The rates of depletion of two neighbouring fishing grids were often very dissimilar. However, the amount of effort in a grid is a major factor in the success of these analyses, as there needs to be enough effort to cause a population decline. In these two grids, fishing effort in 1998 was sufficient for an effective depletion experiment to be undertaken. The absolute CPUE is generally lower in grid B and its CPUE is also low early in the season. The decline rate of depletion was much higher in grid B than in grid C. One reason for this higher decline rate could be the highly aggregated fishing as per our hypothesis. The effort levels in these two grids in 1999 were not sufficient to yield useful results in a depletion analysis.

The fishing pattern in grid A in 1998 and 1999 indicates that trawling was aggregated. The decline rates of depletion in this grid during both years have similar trends but different extents. The decline rate of depletion was steeper in 1999 than in 1998. There are two possible reasons: either the fishing pattern was more highly aggregated in 1999 than in 1998 or the tiger prawn biomass was reduced between 1998 and 1999. Considering that effort dropped significantly between years (from 134 to 82 days), the decrease in the decline rate of depletion is most likely attributable to a reduction in prawn biomass.

Our estimate of the number of repeat trawls allows us to quantify the effects of repeat trawling on benthos. This is an important issue in any trawl fishery (Jennings et al. 2001). Our data show that trawlers target some areas heavily, so there is the potential for impacts on both the target species and sessile benthos to occur. Many fishing activities involving bottom trawling can cause chronic and widespread disturbance to the seabed in shelf seas (Schratzberger and Jennings 2002). Trawling and dredging can alter, remove, or destroy the complex, three-dimensional physical structure of benthic habitats by the direct removal of biological (e.g., sponges, hydroids, bryozoans, amphipod tubes, shell aggregates, and sea grass) and topographic (e.g., sand depressions and boulders) features (Turner et al. 1999; Jennings et al. 2001). According to Poiner et al. (1998), the average depletion rate of one trawl was 7% for all sessile benthos classes, 9% for mobile benthos, and 10% for fish. It is noticeable that in some grids we found that fishing was extremely intensive in some areas (up to 28 trawls over the same ground). This suggests that most benthos has probably been removed from some areas, based on the level of impact found by Poiner et al. (1998) (Table 3). However, Poiner et al.'s (1998) study was based on the Great Barrier Reef, in areas with a lot of sessile epibenthos, and much of the NPF has soft, unstructured sediments with different benthic assemblages. Thus, the effects of trawling on these assemblages may be quite different. The less stable the substrate, the less likely it is that the impacts of trawling would be severe, because the species assemblages there are more likely to be opportunistic species that colonize quickly following natural disturbances.

In summary, we found that VMS polling at an interval of less than 20 min represents an acceptable estimate of the real track of a trawl without substantial bias. HPFVMS data have greatly increased our ability to monitor fishing activity and are particularly valuable when calculating trawl intensities for fine-scale analysis of fishing impacts. We have also shown that by combining fishery logbook catch records, HPFVMS data, and routine VMS data, a localized population-depletion analysis can be undertaken. Our depletion analyses hint towards supporting the hypothesis that the rate of depletion will be more rapid in highly aggregated fishing areas than in randomly fished areas. It is difficult, though, to scale this result to the whole fishery, but it does suggest that trawl-fishery CPUE and available biomass may not be directly proportional when fishing effort is highly aggregated. Even so, VMS data are essential to the success of this analysis. Finally, the VMS data have demonstrated that a large number of repeated trawls can occur in productive areas and that the effect of this trawling may be quite marked and should be investigated.

Table 3. Estimated rate of removal of nontarget organisms in each of three NPF fishing grids (A, B, and C) based on the results of repeated trawl experiments in similar habitats (Poiner et al. 1998).

Year and grid	Trawling intensity (*N*)	Percent area trawled	Total removal rate (%)		
			Sessile benthos	Mobile benthos	Fish
1999					
A	1	27.1	7	9	10
	2	12.9	14	17	19
	3–5	22.0	20–30	25–38	27–41
	6–15	32.6	35–66	43–76	47–79
	16–25	5.5	69–84	78–91	81–93
B	1	99.0	7	9	10
	2	1.0	14	17	19
C	1	74.7	7	9	10
	2	21.1	14	17	19
	3–4	4.2	20–25	25–31	27–34
1998					
A	1	34.8	7	9	10
	2	21.7	14	17	19
	3–5	28.4	20–30	25–38	27–41
	6–15	14.9	35–66	43–76	47–79
	16–17	0.2	69–71	78–80	81–83
B	1	34.2	7	9	10
	2	15.9	14	17	19
	3–5	18.7	20–30	25–38	27–41
	6–15	38.8	35–66	43–76	47–79
	16–28	5.7	69–87	78–93	81–95
C	1	42.2	7	9	10
	2	29.5	14	17	19
	3–5	26.8	20–30	25–38	27–41
	6–8	1.6	35–44	43–53	47–57

Acknowledgments

We thank the AFMA for providing the VMS data and the NPF skippers for making their GPS data available to us. Thanks also go to Fiona Manson and Janet Bishop for processing the NPF logbook data, Nick Ellis for his simulation

© 2005 NRC Canada

guidance, Bill Venables for his advice on data analyses, and Yimin Ye, Nick Ellis, Neil Loneragan, and an anonymous reviewer for their suggestions for improving the paper.

References

Dichmont, C.M., Punt, A.E., Deng, A., Dell, Q., and Venables, W. 2003. Application of a weekly delay-difference model to commercial catch and effort data for tiger prawns in Australia's Northern Prawn Fishery. Fish. Res. **65**: 335–350.

Die, D., and Ellis, N. 1999. Aggregation dynamics in penaeid fisheries: banana prawns (*Penaeus merguiensis*) in the Australian Northern Prawn Fishery. Mar. Freshw. Res. **50**: 667–675.

Drouin, M. 2001. Vessel Monitoring Systems gain ground. Pac. Fish. **22**: 31

Environmental Systems Research Institute, Inc. 1982–2002. ArcInfo®. Version 8.2. Help manual of ARC [computer program]. Environmental Systems Research Institute, Inc., Redlands, Calif.

Fu, C., and Quinn, T.J., II. 2000. Estimability of natural mortality and other population parameters in a length-based model: *Pandalus borealis* in Kachemak Bay, Alaska. Can. J. Fish. Aquat. Sci. **57**: 2420–2432.

Hilborn, R., and Walters, C.J. (*Editors*). 1992. Quantitative fisheries stock assessment: choice, dynamics and uncertainty. Chapman and Hall, London.

Jennings, S., Kaiser, M.J., and Reynolds, J.D. 2001. Marine fisheries ecology. Blackwell Science, Oxford.

Poiner, I.R., Glaister, J., Pitcher, C.R., Burridge, C.Y., Wassenberg, T.J., Gribble, N., et al. 1998. Final report on effects of trawling in the far northern section of the Great Barrier Reef: 1991–1996. Division of Marine Research, Commonwealth Scientific and Industrial Research Organisation, Cleveland, Qld.

Rijnsdorp, A.D., Buys, A.M., Storbeck, F., and Visser, E.G. 1998. Micro-scale distribution of beam trawl effort in the southern North Sea between 1993 and 1996 in relation to the trawling frequency on the sea bed and the impact on benthic organisms. ICES J. Mar. Sci. **55**: 403–419.

Robins, C.M., Wang, Y.-G., and Die, D. 1998. The impact of global positioning systems and plotters on fishing power in the northern prawn fishery, Australia. Can. J. Fish. Aquat. Sci. **55**: 1645–1651.

Schratzberger, M., and Jennings, S. 2002. Impacts of chronic trawling disturbance on megafaunal communities. Mar. Biol. (Berl.), **141**: 991–1000.

Tanner, J.E. 2003. The influence of prawn trawling on sessile benthic assemblages in Gulf St. Vincent, South Australia. Can. J. Fish. Aquat. Sci. **60**: 517–526

Tuck, I.D., Hall, S.J., Robertson, M.R., Armstrong, E., and Basford, D.J. 1998. Effects of physical trawling disturbance on a previously unfished sheltered Scottish sea loch. Mar. Ecol. Prog. Ser. **162**: 227–242.

Turner, S.J., Thrush, S.F., Hewitt, J.E., Cummings, V.J., and Funnell, G. 1999. Fishing impacts and the degradation or loss of habitat structure. Fish. Manag. Ecol. **6**: 401–420.

© 2005 NRC Canada

Chemical tags in otoliths indicate the importance of local and distant settlement areas to populations of a temperate sparid, *Pagrus auratus*

Paul A. Hamer, Gregory P. Jenkins, and Bronwyn M. Gillanders

Abstract: Understanding geographic origins of fish is essential to the management of fisheries and protection of critical juvenile habitats. We used natural chemical tags (Mn, Sr, and Ba), characterized from otoliths of 0+ snapper (*Pagrus auratus*) (approximately 1–3 months postsettlement), to determine the origins of 1- and 2-year-old (subadult) fish about to recruit to the Victorian fishery. We sampled subadults from eight areas across 700 km of coastline and within the major Victorian fishery, Port Phillip Bay. Maximum likelihood analyses indicated for both cohorts that most subadults in Port Phillip Bay and a significant proportion from west Victorian coastal waters had settled within Port Phillip Bay. The contribution of the Port Phillip Bay settlement area to coastal populations, however, decreased with distance to the west, varied between cohorts, and was negligible at locations over 200 km to the east of the bay. Comparison of elemental tags between 0+ fish of known settlement origin and the subadults indicated that unknown settlement areas may have contributed recruitment to one of the cohorts. These results have highlighted the importance of local settlement areas to sustaining the major Victorian fishery, but small juveniles can migrate large distances from this settlement area and contribute to coastal populations.

Résumé : Il est nécessaire de bien connaître l'origine géographique des poissons afin d'aménager la pêche et de protéger les habitats essentiels pour les jeunes. Nous avons utilisé des étiquettes chimiques naturelles (Mn, Sr, Ba) déterminées dans les otolithes de pagres (Pagrus auratus) d'âge 0+ (environ 1–3 mois après leur établissement territorial) afin de déterminer l'origine des poissons âgés de 1–2 ans (subadultes) au moment où ils contribuent au recrutement de la pêche commerciale de l'état de Victoria. Nous avons échantillonné les subadultes dans huit régions le long de 700 km de côtes et dans la baie de Port Phillip, le site principal de pêche commerciale de l'état. Des analyses de vraisemblance maximale indiquent que, dans les deux cohortes, la majorité des subadultes de la baie de Port Phillip et un pourcentage significatif des subadultes des eaux côtières de l'ouest de l'état de Victoria s'étaient établis dans la baie de Port Phillip. Néanmoins, la contribution de la zone d'établissement de la baie de Port Phillip diminue en fonction de la distance vers l'ouest, elle varie d'une cohorte à l'autre et elle devient négligeable dans les régions situées à plus de 200 km à l'est de la baie. La comparaison des étiquettes chimiques des poissons d'âge 0+ dont le lieu d'établissement est connu et de celles des subadultes indique que plusieurs régions d'établissement territorial inconnues peuvent avoir contribué au recrutement d'une des cohortes. Nos résultats mettent en lumière l'importance des régions locales d'établissement territorial pour le maintien de la pêche commerciale principale de l'état de Victoria, mais les jeunes de petite taille peuvent migrer sur de grandes distances depuis cette région d'établissement territorial pour contribuer au recrutement des populations côtières.

[Traduit par la Rédaction]

Introduction

The adult stages of many fish species show broad and continuous distributions, whereas young juveniles are confined to discrete geographic areas such as estuaries and sheltered bays (Beck et al. 2001). For exploited species, determining which juvenile areas are the major sources of older individuals is critical for understanding population dynamics and for ensuring protection of critical juvenile habitats (Beck et al. 2001; Gillanders et al. 2003). To make these assessments, methods

Received 19 December 2003. Accepted 16 November 2004. Published on the NRC Research Press Web site at http://cjfas.nrc.ca on 13 April 2005.
J17886

P.A. Hamer[1,2] **and G.P. Jenkins.** Department of Primary Industries Research Victoria, Marine and Freshwater Systems, P.O. Box 114, Queenscliff, VIC 3225, Australia, and Department of Zoology, University of Melbourne, Parkville, VIC 3052, Australia.
B.M. Gillanders. Southern Seas Ecology Laboratories, Darling Building DP418, School of Earth and Environmental Sciences, University of Adelaide, Adelaide, SA 5005, Australia.

[1]Corresponding author (e-mail: Paul.Hamer@dpi.vic.gov.au).
[2]Mailing address: Department of Primary Industries Research Victoria, Marine and Freshwater Systems, P.O. Box 114, Queenscliff, VIC 3225, Australia.

 doi: 10.1139/F04-221 © 2005 NRC Canada

Fig. 1. Map of Australia (inset *a*) and the Victorian coast showing locations where subadult snapper (*Pagrus auratus*) were collected. Sites where samples were collected within Port Phillip Bay are indicated by the circles in inset *b*. Numbers associated with the site labels indicate which cohort/age was sampled at the particular site; 2 indicates the 2000 cohort and 1 indicates the 2001 cohort.

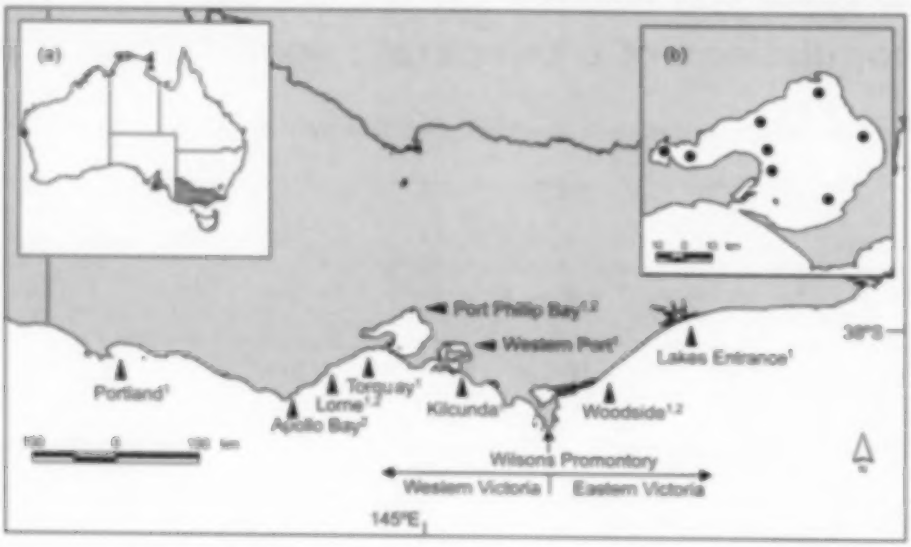

of tracking the movement of individual fish between the juvenile and adult life stages are necessary. Traditional methods, such as manual tagging and recapture (Sanders 1974; Kleider et al. 1987; Walker et al. 2000), are unlikely to be suitable for quantifying connectivity between the juvenile and adult stages. This is because of the difficulty in tagging large numbers of very small juveniles, high juvenile mortality rates, and spatial biases in tagging and recapture effort (Kearney 1989).

Research on otolith chemistry has demonstrated that the chemical composition of these calcified structures, situated in the inner ear of teleost fish, may provide a natural tag (Gillanders and Kingsford 1996; Campana 1999; Campana and Thorrold 2001). A number of studies have shown that juvenile fish collected from different geographic areas can be distinguished based on the chemistry of their otoliths (Thorrold et al. 1998; Gillanders and Kingsford 2000; Rooker et al. 2001). Furthermore, development of fine-scale sampling techniques, such as laser ablation (Fowler et al. 1995; Russo et al. 2002), has enabled chemical tags characterized from small juveniles to be identified within the otoliths of older migratory fish, thus indicating their geographic origin. This methodology has now been used to determine natal homing rates of marine fish and the contributions of different juvenile sources to mixed populations of adults (Gillanders and Kingsford 1996; Thorrold et al. 2001; Gillanders 2002).

Understanding the sources of recruitment to localized fisheries is particularly critical. If recruitment is dependent on one or a few sources, as opposed to many sources, increased protection of the few source habitats, and the juveniles originating from them, will be essential to the sustainable management of the local fishery. Snapper (*Pagrus auratus* (Sparidae)) support important commercial and recreational fisheries throughout southern Australia, New Zealand, and Japan (Kailola et al. 1993; Francis 1995; Fujita et al. 1996). Regional variation in the life history characteristics of snapper can be an important influence on the geographic nature of fisheries for this species. In some regions, the juvenile stages occur within estuaries and the adults occur in ocean waters (Ferrell and Sumpton 1996; Gillanders 2002). In this situation, the fishery is largely based on oceanic adults that are derived from a variety of different source estuaries (Gillanders 2002), and changes in the contributions of one or a few source estuaries may have limited impact on the adult fishery. However, some of the most important snapper fisheries are localized within large bays and gulfs where all life stages can be found together, and the fishery may be highly dependent on local sources (Kailola et al. 1993; Francis 1995; Fowler and Jennings 2003).

Port Phillip Bay, Victoria (Fig. 1), provides an example of a highly localized snapper fishery, where all life stages are found together (Coutin et al. 2003; Hamer and Jenkins 2004). Although there is a small coastal fishery, and snapper do migrate between Port Phillip Bay and coastal waters, greater than 80% of the Victorian catch comes from Port Phillip Bay (Coutin et al. 2003). Our previous work has identified a number of larval settlement areas along the Victorian coast (Hamer et al. 2003; Hamer and Jenkins 2004). Although most of these areas are situated in eastern Victoria, Port Phillip Bay in western Victoria is by far the largest known settlement area (Fig. 1). It is currently not known whether larval settlement in Port Phillip Bay is the primary source of older snapper within this bay or whether migration of small juveniles out of this bay is important for sustaining populations in coastal waters. Over the past 15 years, the deeper habitats where snapper larvae settle within Port Phillip Bay have changed significantly owing to the impacts of introduced pest species, while pollution from industries and the large population base around the bay provides further threats to habitat quality. These factors, coupled with high exploitation of juveniles and strong annual variation of larval settlement within the bay (Hamer and Jenkins 2004), demonstrate the importance of understanding how the Victorian

© 2005 NRC Canada

snapper fishery depends on the settlement areas within Port Phillip Bay.

The current study is therefore aimed at assessing the contribution of the Port Phillip Bay settlement area to snapper populations in Victorian waters, with particular emphasis on the population within Port Phillip Bay. Previously, we identified chemical tags in the otoliths of recently settled snapper (approximately 1–3 months postsettlement, hereafter termed 0+) of two cohorts (years) that distinguished between individuals from Port Phillip Bay and those from all other known settlement areas (Hamer et al. 2003). The tag for Port Phillip Bay was largely based on the higher levels of Ba found in the otoliths of 0+ snapper from Port Phillip Bay (Hamer et al. 2003). The chemical tag for this bay was not consistent among cohorts over long time scales. This implied that we could only use elemental tags from 0+ fish to determine the settlement origins of older fish from the same cohorts (Hamer et al. 2003). In this study, we utilize the previously characterised 0+ elemental tags to determine the settlement origins of age-1+ and age-2+ fish (hereafter termed subadults) from the 2000 and 2001 cohorts. By sampling subadults in Port Phillip Bay and at various locations along a broad stretch of the Victorian coastline (approximately 700 km), we quantify the importance of the Port Phillip Bay settlement area to recruitment of subadult snapper both within Port Phillip Bay and along the Victorian coast. Further, by comparing the results for two cohorts, we investigate whether the importance of this source is consistent among year and age classes.

Methods

Tags of settlement origin

The multi-elemental tags used to indicate the settlement origins of subadults were characterized previously by sampling otoliths of 0+ fish collected from bays and inlets along the Victorian coast where settlement of snapper larvae was known to occur (Hamer et al. 2003). Our earlier work indicated that the major differences in otolith chemistry of 0+ snapper were between fish that settled within Port Phillip Bay and those from the other known settlement areas, which were poorly discriminated from each other (Hamer et al. 2003). In the current study, we have used two sets of baseline otolith chemistry data to determine the settlement origins of subadults. One data set represented elemental compositions of 0+ snapper that had settled within Port Phillip Bay, the other represented fish that had settled in areas outside the bay. Strong discrimination (100% and 85% for the 2000 and 2001 cohorts, respectively) between these two baseline groups has previously been shown and is not a consideration of the current study (Hamer et al. 2003).

Sampling of subadult snapper

We collected age-2+ and age-1+ snapper from the 2000 and 2001 cohorts based on their size, which is a good estimator of age for young snapper in Victorian waters (i.e., 1+ fish = 13–19 cm total length, 2+ fish = 19–25 cm total length; Coutin et al. 2003). The ages were confirmed by counting annual increments after the otoliths were sectioned (Francis et al. 1992). These fish would recruit to the fishery over the coming 2 years upon reaching 27 cm total length. Samples were collected on an opportunistic basis from March through to May 2002. We employed several collection methods, including line fishing, fish traps, and trawling. For Port Phillip Bay, to ensure that our sample was representative of the entire bay, we collected similar numbers of subadults from eight areas (Fig. 1). For the 2000 cohort (age 2+), coastal samples were obtained from two locations in western Victoria (hereafter, western Victoria refers to west of Wilsons Promontory) (Fig. 1) and one location in eastern Victoria (hereafter, eastern Victoria refers to east of Wilsons Promontory) (Fig. 1). For the more abundant 2001 cohort (age 1+), samples were obtained from four coastal locations in western Victoria, two in eastern Victoria, and also from within Western Port Bay, situated about 60 km east of Port Phillip Bay (Fig. 1). To prevent any school-related biases, samples were composed of fish from at least two sampling events in each area.

Otolith preparation

We took particular care to ensure that all otoliths from the subadult fish were stored, prepared, and analysed using the same methods that were applied to analyses of 0+ fish during characterization of baseline elemental tags (see Hamer et al. 2003). Briefly, the sagittal otoliths were cleaned of adhering tissues, rinsed with Milli-Q water, air dried, and then mounted in epoxy resin (Struers epofix). Transverse sections of 350 µm were taken through the primordial region with a diamond saw lubricated with Milli-Q water. The otoliths were polished with lapping film and then mounted on acid-cleaned microscope slides with epoxy resin doped with In as a resin indicator. Once cured, the otolith slides were sonicated for 3 min in Milli-Q water, further rinsed with copious amounts of Milli-Q water, and then dried in a laminar flow cabinet before storage in sealed containers.

Otolith analyses

Otoliths were analysed with a Merchantek LUV 266™ Nd:YAG ultraviolet laser microprobe operated in Q switched mode in conjunction with a Finnigan MAT ELEMENT™ high-resolution inductively coupled plasma mass spectrometer. We conducted our analyses at the Earth Sciences Department of Monash University, Melbourne, Australia, with the same instrument used to characterize the 0+ elemental tags (Hamer et al. 2003). The analytical methodology and instrument operating parameters were identical to those described in Hamer et al. (2003). For both studies, calibration was achieved using the National Institute of Standards 612 standard. The isotopes ^{55}Mn, ^{88}Sr, and ^{138}Ba were collected along with ^{44}Ca, which was used as the internal standard (Hamer et al. 2003). Otoliths were prepared in haphazard order and analysed in a randomized blocks fashion with respect to capture location to further eliminate any bias resulting from instrument drift (Hamer et al. 2003). Detection limits were similar between studies and all samples were above detection for each isotope. To check precision between the earlier identification of elemental tags in 0+ fish (Hamer et al. 2003) and the current study, we reanalysed a pressed pellet of crushed snapper otoliths. Similar results were obtained for both analysis periods (mean, standard error for earlier study/current study, n = 45, data are micrograms per gram: Mn:

© 2005 NRC Canada

2.21, 0.06/2.13, 0.05; Sr: 1950, 182/1808, 152; Ba: 5.50, 0.05/5.33, 0.07).

To identify the settlement area tags in sectioned otoliths of subadult fish, as for the 0+ fish (Hamer et al. 2003), we averaged the elemental concentrations across three ablations of approximately 100 µm diameter on each otolith. The positions of the three ablations were standardized so as to approximate the same area (time) of otolith deposition that was analysed for tag characterization in 0+ otoliths (Hamer et al. 2003). To estimate these areas, we measured the distances from the cores to the ablation craters of 100 randomly selected 0+ otoliths that were analysed during the tag characterization phase (Hamer et al. 2003). These measurements provided minimum and maximum distances along the three standardized growth axes, within which the region of otolith relevant to the 0+ tags would be located. While temporal matching between sampling of the subadult and 0+ otoliths may not be exact, our previous work suggests that small-scale temporal variation had little effect on tag composition (Hamer et al. 2003).

Statistical analyses

Settlement origins of subadults

We used a maximum likelihood estimation approach (MLA) (Millar 1987, 1990*a*, 1990*b*) to determine the contributions of the different settlement areas to the mixed samples of subadults. Analyses were performed using the HISEA program (Millar 1990*b*; http://www.stat.auckland.ac.nz/~millar/). The baseline groups for these analyses were the multi-elemental tags (Mn, Sr, and Ba) determined from otoliths of 0+ fish from each cohort by Hamer et al. (2003). Data for all elements were transformed to $\log_{10}(x + 1)$ to meet univariate normality and to reduce the weight of the Sr data (Millar 1990*a*). Bootstrapping, with 100 resamplings of the baseline and mixed sample data, was used to estimate the average and standard deviation of the proportions of the mixed samples belonging to each of the baseline groups (Millar 1987).

Comparisons of subadult and 0+ baseline tags

Confidence in the accuracy of estimations of mixed-stock origins requires the assumption that all possible sources that could contribute to the mixed stock have been included in the baseline data (Wood et al. 1987; Campana 1999). While all currently known settlement areas were included in our 0+ baseline data, it is possible that unknown settlement areas may have been missed during our previous work and therefore not included in our baseline data. If unknown settlement areas contributed to recruitment of subadults, this may show up as elemental tags in subadults that do not match any of the 0+ baseline groups (i.e., Milton et al. 1997). To investigate this possibility, we used canonical variate plots to compare the multi-elemental tag compositions among otoliths of subadults and the 0+ fish of known settlement origins.

Results

Settlement origins of subadults

2000 cohort at age 2+

The MLA for the 2000 cohort estimated that 96% of the fish sampled within Port Phillip Bay had settled within this bay (Fig. 2*a*). Similarly, it was estimated that between 95% and 100% of fish sampled in west Victorian coastal waters had actually settled in Port Phillip Bay (Fig. 2*a*). For the location in eastern Victoria, however, it was estimated that only 15% of the fish sampled could have settled in Port Phillip Bay (Fig. 2*a*). At this location, most individuals were derived from the other settlement areas, which were predominantly east Victorian estuaries (see Hamer et al. 2003). Standard deviations for the mean estimations of mixed-stock origin from MLA ranged from 0% to only 9%. This indicated that the estimations of mean contributions of the different settlement sources were a good measure of their true contributions (Fig. 2*a*).

2001 cohort at age 1+

The MLA for the 2001 cohort estimated that around 80% of the fish sampled within Port Phillip Bay were fish that had settled within this bay (Fig. 2*b*). For the areas sampled in west Victorian coastal waters and Western Port, the estimated proportion of subadults that settled in Port Phillip Bay ranged from 15% in Western Port to 62% at the coastal site of Lorne (Fig. 2*b*). Subadults that settled in Port Phillip Bay made no contribution to the 2001 cohort at the eastern Victorian sites (Fig. 2*b*). The contribution that subadults from settlement areas in Port Phillip Bay made to coastal populations declined with distance to the west of the bay, from an estimated 60% at the nearest coastal sites, Torquay and Lorne, to 30% at the farthest, Portland (Figs. 1 and 2*b*). Compared with the 2000 cohort, in the 2001 cohort, there was considerable variability around the estimate of the proportion of subadults derived from the Port Phillip Bay settlement area (Fig. 2*b*). The standard deviation around the mean of the MLA estimates ranged from 12% to 20% for western Victorian coastal areas and Western Port and was 10% for Port Phillip Bay (Fig. 2*b*). In contrast, the standard deviation of the mean MLA estimates for the two east Victorian sites remained low at 4% (Fig. 2*b*).

Comparisons of subadult and 0+ baseline tags

2000 cohort at age 2+

The element tags identified in subadults of the 2000 cohort sampled from Port Phillip Bay and the coastal waters off western Victoria were mostly distributed within the 95% confidence ellipse around the data for 0+ fish known to have settled in Port Phillip Bay (Figs. 3*a* and 3*b*). Similarly, the elemental tags identified in subadults from eastern Victorian coastal waters were mostly within the 95% confidence ellipse around the data for 0+ fish known to have originated from settlement areas outside Port Phillip Bay (Fig. 3*c*). These comparisons support high confidence in the MLA estimations of the contribution that the Port Phillip Bay settlement area made to the 2000 cohort (Fig. 2*a*).

2001 cohort at age 1+

Elemental tags identified in otoliths of subadults of the 2001 cohort in Port Phillip Bay were distributed within or just outside the 95% confidence ellipse for data from 0+ fish known to have settled in Port Phillip Bay (Fig. 4*a*). A similar result was also obtained for a large proportion of subadults from western Victorian coastal waters (Fig. 4*b*). However, unlike the 2000 cohort, a significant number of

© 2005 NRC Canada

Fig. 2. Results of maximum likelihood analyses indicating the percentage of subadult snapper (*Pagrus auratus*) from different Victorian locations that originated from settlement areas in Port Phillip Bay. (*a*) 2000 cohort/age 2+; (*b*) 2001 cohort/age 1+. The bars are the average percentages estimated from 100 resamplings of the baseline and mixed-sample data and the error bars represent 1 SD of these estimates. The numbers above each bar indicate the sample size with the standard deviation in parentheses.

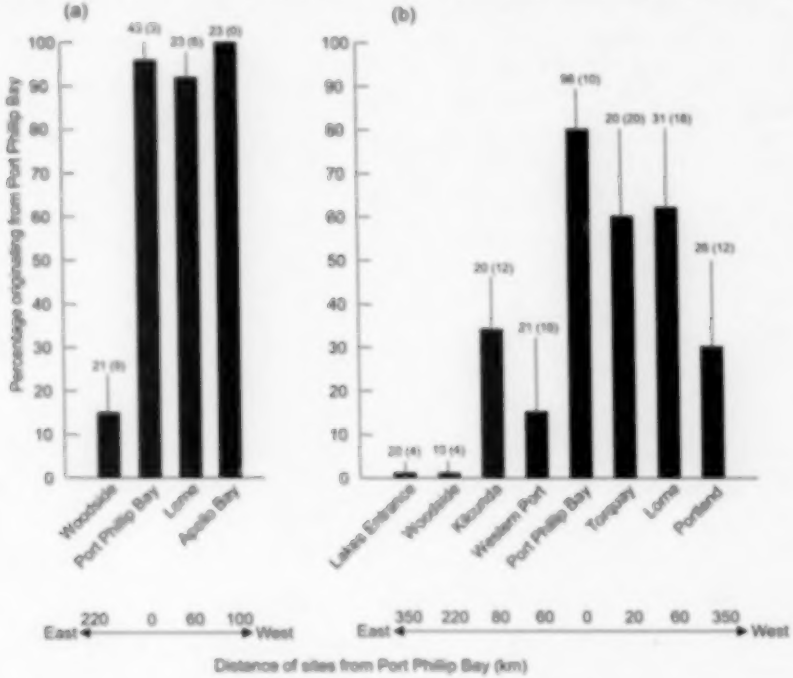

subadults from west Victorian coastal waters and Western Port displayed elemental tags that were not within the ellipses for either 0+ baseline group or were intermediate between the two baseline groups (Figs. 4*b* and 4*c*). The elemental tags identified in subadults from eastern Victoria were, however, mostly distributed within the confidence ellipse around the data for 0+ fish from settlement areas outside Port Phillip Bay (Fig. 4*d*). Subadults from western Victoria and Western Port with elemental tags outside the baseline groups would partly explain the lower confidence (higher standard deviations, Fig. 2*b*) in the MLA estimates of Port Phillip Bay's contribution to these areas. These outlying elemental tags may be indicative of another settlement area that was not included in our 0+ baseline data.

Discussion

The discovery of natural chemical tags in otoliths has provided a new method for investigating connectivity among juvenile source areas and adult populations (Gillanders and Kingsford 1996; Campana 1999; Thorrold et al. 2001). While a number of studies have reported natural chemical tags in otoliths of juvenile fish, there are currently few studies that have applied these natural tags to determining the origins of older fish (Milton et al. 1997; Thorrold et al. 2001; Gillanders 2002).

We determined the settlement origins of two cohorts of subadult snapper by identifying natural chemical tags that were incorporated into their otoliths shortly (within a few months) after larval settlement. For both cohorts, the majority of snapper about to recruit into the major Victorian fishery, Port Phillip Bay, had settled within this bay. Furthermore, for both cohorts, a significant proportion of subadults from western Victorian coastal waters displayed otolith tags that indicated that they had migrated from settlement areas within Port Phillip Bay. While there was evidence that some subadults had migrated large distances west (approximately 350 km) from their original settlement area of Port Phillip Bay, there was little evidence for similar long-distance migrations in an easterly direction. The subadults sampled in eastern Victorian coastal waters were dominated by individuals with elemental tags indicating that they had migrated out of eastern Victorian estuaries. These results are consistent with previous tag and recapture studies that have suggested very low mixing of adult snapper between Port Phillip Bay and eastern Victorian waters but significant mixing of adult snapper between Port Phillip Bay and western Victorian coastal waters (Coutin et al. 2003). Our results increase the knowledge of snapper movement behaviour by demonstrating a previously unknown high level of juvenile (at least 1 year of age) migration from Port Phillip Bay to western Victorian coastal waters.

Although the major sources of subadults for the populations in Port Phillip Bay and eastern Victoria were similar between cohorts, the contribution of the Port Phillip Bay settlement area to populations in western Victorian waters varied between the cohorts. We found that while migrants from the Port Phillip Bay settlement area dominated the 2000 cohort at 2 years of age, in western Victorian waters, their contribution to the 2001 cohort at 1 year of age was about 50% lower. Movement of snapper out of Port Phillip Bay is sug-

© 2005 NRC Canada

Fig. 3. The 2000 cohort: canonical variate plots comparing multi-elemental tags (Mn, Sr, and Ba) identified within the otoliths of subadult snapper (*Pagrus auratus*) with those of the 0+ baseline groups of known settlement origin. Ellipses are 95% confidence ellipses around the data for the two baseline groups. Open circles, 0+ from settlement areas outside Port Phillip Bay; crosses, 0+ from settlement areas within Port Phillip Bay; solid circles, subadults of unknown origin. (*a*) Subadults sampled from Port Phillip Bay; (*b*) subadults from locations in west Victorian coastal waters; (*c*) subadults sampled from east Victorian coastal waters. Elements that contributed the most variation to the data (canonical loadings) are indicated adjacent to each axis.

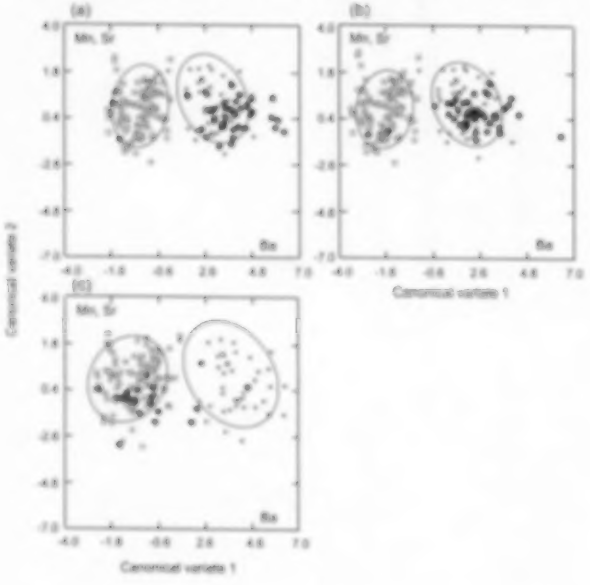

Fig. 4. The 2001 cohort: canonical variate plots comparing multi-elemental tags (Mn, Sr, and Ba) identified within the otoliths of subadult snapper (*Pagrus auratus*) with those of the 0+ baseline groups of known settlement origin. Ellipses are 95% confidence ellipses around the data for the two baseline groups. Open circles, 0+ from settlement areas outside Port Phillip Bay; crosses, 0+ from settlement areas in Port Phillip Bay; solid circles, subadults of unknown origin. (*a*) Subadults sampled from Port Phillip Bay; (*b*) subadults sampled from all locations in west Victorian coastal waters; (*c*) subadults sampled in Western Port; (*d*) subadults sampled from all locations in east Victorian coastal waters. Elements that contributed the most variation to the data (canonical loadings) are indicated adjacent to each axis.

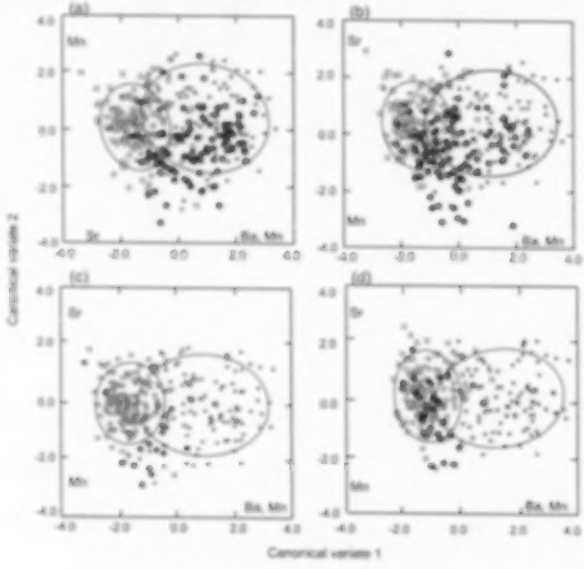

gested to increase with age (Coutin et al. 2003); therefore, higher rates of migration out of Port Phillip Bay with increasing age could partly explain the observed differences between the cohorts. Although age-related variation in migration rates may have been important, the high proportion of the 2001 cohort in western Victoria and Western Port that did not possess the Port Phillip Bay elemental tag does indicate that other settlement area(s) contributed to recruitment in these areas.

The locations of alternative settlement areas that contributed to populations in western Victoria remain unclear. We believe, however, that it is unlikely that the known settlement areas outside Port Phillip Bay, which include a number of estuaries and inlets in eastern Victoria and Western Port Bay in western Victoria (see Hamer et al. 2003), are contributing significantly to populations in western Victoria. This is because recruitment of 0+ snapper in Western Port is very low, and although some subadults sampled in Western Port may have originated there, this source is unlikely to have contributed significantly to coastal populations (Hamer and Jenkins 2004). Furthermore, the MLA results demonstrated that the contribution of settlement areas, other than Port Phillip Bay, to populations in western Victoria actually increased in a westerly direction, away from the known settlement areas in eastern Victoria and Western Port. Portland, the location most distant to the west, had the highest proportion of subadults derived from settlement areas other than Port Phillip Bay. These observations would contradict any suggestion that the alternative settlement area or areas contributing recruitment to western Victorian populations were in fact the known settlement areas in eastern Victoria.

The canonical variate plots that compared the elemental tags identified in subadult otoliths with those from the 0+ baseline fish supported the existence of an alternative settlement source that was not sampled by Hamer et al. (2003). Numerous subadults from the 2001 cohort in western Victoria displayed elemental tags either not closely matched to the baseline groups or intermediate between the two baseline groups. Closer inspection of the data for the 0+ fish of known settlement origins also suggested that most subadults with outlying tag compositions were not closely matched to any individual component (i.e., bay or inlet) of our composite baseline groups. We ensured that sampling conditions and preparation methods were consistent between analyses of subadult and 0+ otoliths, and we are therefore confident that these differences in tag compositions were not related to variations in analytical procedures. Rather, we suggest that these differences may be indicative of an alternative settlement area(s) that was not sampled during earlier development of the baseline settlement area tags.

© 2005 NRC Canada

Snapper are thought to spawn in coastal waters and Port Phillip Bay (Niera et al. 2000; Coutin et al. 2003). We hypothesize that the alternative settlement area may be the coastal habitats along the west Victorian coast. Although our previous attempts to sample 0+ snapper from western Victorian coastal waters failed, this may have been due to low sampling effort and their naturally low density (Hamer et al. 2003). While oceanic nursery areas for 0+ snapper are unknown in Australian waters, they do occur in New Zealand (Francis 1995). It was interesting that recruitment of 0+ snapper in western Victoria was 10 times stronger for the 2001 than for the 2000 cohort (Hamer and Jenkins 2004). This suggests that conditions were highly favourable for recruitment of 0+ snapper in the summer–autumn of 2001 (Hamer and Jenkins 2004). It is possible that during the strong recruitment year of 2001, there was significant recruitment of 0+ snapper to marginal coastal habitats but that this did not occur in the poor recruitment year of 2000.

We are confident that if snapper larvae were settling into oceanic habitats along the western Victorian coast, they would not have incorporated elemental tags similar to those of Port Phillip Bay settlers, therefore possibly biasing MLA estimates of the contributions of the Port Phillip Bay settlement area. This is because analyses of water samples taken during the period of tag incorporation showed that water chemistry varied strongly between Port Phillip Bay and Victorian coastal waters. In particular, levels of Ba (the most important element for discrimination of Port Phillip Bay settlers) in coastal waters were half those determined for Port Phillip Bay (i.e., 5 $\mu g \cdot L^{-1}$ in coastal waters and 12 $\mu g \cdot L^{-1}$ in Port Phillip Bay) (P.A. Hamer, unpublished data), and incorporation of Ba into otoliths is positively correlated with ambient levels for 0+ snapper (P.A. Hamer, unpublished data) and a range of other species (Bath et al. 2000; Milton and Chenery 2001; Elsdon and Gillanders 2003).

Our results build on a previous study of snapper in another region of Australia that also used natural otolith tags (Gillanders 2002). This previous study showed that recruitment of 2-year-old snapper to one particular coastal region was derived predominantly from the nearest estuarine settlement areas (Gillanders 2002). However, unlike the current study, the narrow geographic range over which the older migratory fish were sampled prevented detailed investigation of the contributions that individual settlement areas made to populations at distant coastal locations. Our results supported the idea that local settlement areas were the most important, but they also demonstrated that long-distance and directional migration of young snapper occurred. For example, migrants from settlement areas in Port Phillip Bay contributed about 60% of the 2001 cohort at Lorne, 60 km to the west of the bay, whereas at Western Port Bay and Kilcunda, roughly the same distance to the east, they only contributed 20–30%. Differences between cohorts in the contribution of the Port Phillip Bay settlement area to coastal populations also implied that sampling of multiple cohorts might be required to comprehensively understand the importance of particular settlement areas. Our comparison between chemical tags identified in subadults and the 0+ baseline fish was also important in indicating the possible existence of a previously unknown settlement area(s) in ocean waters that now requires further investigation. Future sampling of older fish will be required to determine whether this alternative source eventually contributes to the snapper population within Port Phillip Bay.

In summary, the demonstration that subadult snapper in Port Phillip Bay are largely sourced from larval settlement within the bay, and that this source is also important for populations in western Victorian coastal waters, has important implications for ongoing management of this fishery. The long-term future of this fishery will depend on maintaining the habitats required for larval settlement and survival of small juveniles and careful management of the exploitation of juvenile and subadult fish within Port Phillip Bay. This information could not have been obtained with any other currently available mass-marking techniques.

Acknowledgments

Many thanks go to the anglers who helped with collection of subadult snapper and to J. Tsiros for assistance with laser ablation inductively coupled plasma mass spectrometry. We thank S. Campana for assistance with maximum likelihood analyses and C. Del Solar for assistance with sample preparation. This study was funded by a grant awarded to G.P.J. from the Fisheries Research and Development Corporation, Canberra, Australia (1999/34), and Fisheries Victoria.

References

Bath, G.E., Thorrold, S.R., Jones, C.M., Campana, S.E., McLaren, J.W., and Lam, J.W.H. 2000. Strontium and barium uptake in aragonitic otoliths of marine fish. Geochim. Cosmochim. Acta, **64**: 1705–1714.

Beck, M.W., Heck, K.L., Able, K.W., Childers, D.L., Eggleston, D.B., Gillanders, B.M., Halpern, B., Hays, C.G., Hoshino, K., Minello, T.J., Orth, R.J., Sheridan, P.F., and Weinstein, M.P. 2001. Conservation, and management of estuarine and marine nurseries for fish and invertebrates. BioScience, **51**: 633–664.

Campana, S.E. 1999. Chemistry and composition of fish otoliths: pathways, mechanisms and applications [review]. Mar. Ecol. Prog. Ser. **188**: 263–297.

Campana, S.E., and Thorrold, S.R. 2001. Otoliths, increments, and elements: keys to a comprehensive understanding of fish populations? Can. J. Fish. Aquat. Sci. **58**: 30–38.

Coutin, P.C., Cashmore, S., and Sivakumuran, K.P. 2003. Assessment of the snapper fishery in Victoria. Final report No. 97/127 to Fisheries Research and Development Corporation, Canberra, Australia. Marine and Freshwater Resources Institute, Queenscliff, Victoria.

Elsdon, T.S., and Gillanders, B.M. 2003. Relationships between water and otolith elemental concentrations in juvenile black bream, *Acanthopagrus butcheri*. Mar. Ecol. Prog. Ser. **260**: 263–272.

Ferrell, D., and Sumpton, W. 1996. Assessment of the fishery for snapper (*Pagrus auratus*) in Queensland and New South Wales. Final report No. 93/074 to Fisheries Research and Development Corporation, Canberra, Australia. Queensland Department of Primary Industries, Deception Bay, Queensland.

Fowler, A.J., and Jennings, P.R. 2003. Dynamics in 0-age recruitment and early life-history for snapper (*Pagrus auratus*, Sparidae) in South Australia. Mar. Freshw. Res. **54**: 941–956.

Fowler, A.J., Campana, S.E., Jones, C.M., and Thorrold, S.R. 1995. Experimental assessment of the effect of temperature and

© 2005 NRC Canada

salinity on elemental composition of otoliths using laser ablation ICPMS. Can. J. Fish. Aquat. Sci. **52**: 1431–1441.

Francis, M.P. 1995. Spatial and seasonal variation in the abundance of juvenile snapper, *Pagrus auratus*, in the northwestern Hauraki Gulf. N.Z. J. Mar. Freshw. Res. **29**: 201–218.

Francis, R.I.C.C., Paul, L.J., and Mulligan, K.P. 1992. Ageing of adult snapper (*Pagrus auratus*) from otolith annual ring counts: validation by tagging and oxytetracycline injection. Aust. J. Mar. Freshw. Res. **43**: 1069–1089.

Fujita, S., Tojima, T., Yamasaki, A., Uchino, K., and Kuwahara, A. 1996. Management of the red sea bream, *Pagrus major*, resource in the western Japan Sea. No. 45. Japan Fisheries Resources Conservation Association, Tokyo, Japan.

Gillanders, B.M. 2002. Connectivity between juvenile and adult fish populations: do adults remain near their recruitment estuaries? Mar. Ecol. Prog. Ser. **240**: 215–223.

Gillanders, B.M., and Kingsford, M.J. 1996. Elements in otoliths may elucidate the contribution of estuarine recruitment to sustaining coastal reef populations of a temperate reef fish. Mar. Ecol. Prog. Ser. **141**: 13–20.

Gillanders, B.M., and Kingsford, M.J. 2000. Elemental fingerprints of otoliths of fish may distinguish estuarine 'nursery' habitats. Mar. Ecol. Prog. Ser. **201**: 273–286.

Gillanders, B.M., Able, K.W., Brown, J.A., Eggleston, D.B., and Sheridan, P.F. 2003. Evidence of connectivity between juvenile and adult habitats for mobile marine fauna: an important component of nurseries. Mar. Ecol. Prog. Ser. **247**: 281–295.

Hamer, P.A., and Jenkins, G.P. 2004. High levels of recruitment variability in time and space of a temperate sparid, *Pagrus auratus*. Mar. Freshw. Res. **55**: 1–11.

Hamer, P.A., Jenkins, G.P., and Gillanders, B.M. 2003. Otolith chemistry of juvenile snapper, *Pagrus auratus*, in Victorian waters: natural chemical tags and their temporal variation. Mar. Ecol. Prog. Ser. **263**: 261–273.

Kailola, P.J., Williams, M.J., Stewart, P.C., Reichelt, R.E., McNee, A., and Grieve, C. 1993. Australian Fisheries Resources. Bureau of Resource Sciences and the Fisheries Research and Development Corporation, Canberra, Australia.

Kearney, R.E. 1989. Keynote address: tagging — solution or problem? *In* Tagging — solution or problem? Proceedings No. 5. Australian Society for Fish Biology Tagging Workshop, 21–22 July 1988, Sydney, Australia. *Edited by* D.A. Hancock. Australian Society for Fish Biology, Sydney, New South Wales.

Kleiber, P., Argue, A.W., and Kearney, R.E. 1987. Assessment of Pacific skipjack tuna (*Katsuwonus pelamis*) resources by estimating standing stock and components of population turnover from tagging data. Can. J. Fish. Aquat. Sci. **44**: 1122–1134.

Millar, R.B. 1987. Maximum likelihood estimation of mixed fishery composition. Can. J. Fish. Aquat. Sci. **44**: 583–590.

Millar, R.B. 1990a. Comparison of methods for estimating mixed stock fishery composition. Can. J. Fish. Aquat. Sci. **47**: 2235–2241.

Millar, R.B. 1990b. A versatile computer program for mixed stock fishery composition. Can. Tech. Rep. Fish. Aquat. Sci. No. 1753.

Milton, D.A., and Chenery, S.R. 2001. Sources of uptake of trace metals in otoliths of juvenile barramundi (*Lates calcarifer*). J. Exp. Mar. Biol. Ecol. **264**: 47–65.

Milton, D.A., Chenery, S.R., Farmer, M.J., and Blaber, S.J.M. 1997. Identifying the spawning estuaries of the tropical shad, *Terubok tenualosa toli*, using otolith microchemistry. Mar. Ecol. Prog. Ser. **153**: 283–291.

Niera, F.J., Jenkins, G.P., Longmore, A., and Black, K.P. 2000. Spawning and larval recruitment processes of commercially important species in coastal waters off Victoria 1997–1998. Final report No. 96/116 to Fisheries Research Development Corporation, Canberra, Australia. Marine and Freshwater Resources Institute, Queenscliff, Victoria.

Rooker, J.R., Secor, D.H., Zdanowicz, V.S., and Tomoyuki, I. 2001. Discrimination of northern bluefin tuna from nursery areas in the Pacific ocean using otolith chemistry. Mar. Ecol. Prog. Ser. **218**: 275–282.

Russo, R.E., Mao, X., Liu, H., Gonzalez, J., and Mao, S. 2002. Laser ablation in analytical chemistry — a review. Talanta, **57**: 425–451.

Sanders, M.J. 1974. Tagging indicates at least two stocks of snapper *Chrysophrys auratus* in south-east Australian waters. N.Z. J. Mar. Freshw. Res. **8**: 371–374.

Thorrold, S.R., Jones, C.M., Campana, S.R., McLaren, J.W., and Lam, J.W.H. 1998. Trace element signatures in otoliths record natal river of juvenile American shad (*Alosa sapidissima*). Limnol. Oceanogr. **43**: 1826–1835.

Thorrold, S.R., Latkoczy, C., Swart, P.K., and Jones, C.M. 2001. Natal homing in a marine fish metapopulation. Science (Wash., D.C.), **291**: 297–299.

Walker, T.I., Taylor, B.L., and Brown, L.P. 2000. Southern shark tag database project. Final report No. 96/162 to Fisheries Research and Development Corporation, Canberra, Australia. Marine and Freshwater Resources Institute, Queenscliff, Victoria.

Wood, C.C., McKinnell, S., Mulligan, T.J., and Fournier, D.A. 1987. Stock identification with maximum-likelihood mixture model: sensitivity analysis and application to complex problems. Can. J. Fish. Aquat. Sci. **44**: 866–881.

© 2005 NRC Canada

Escaping the tyranny of the grid: a more realistic way of defining fishing opportunities

Trevor A. Branch, Ray Hilborn, and Eugenia Bogazzi

Abstract: A large part of fishing behavior is choosing where to fish. Trawl skippers usually choose between known fishing opportunities, which are observed as groups of trawls that are conducted in the same portion of a fishing ground, or go exploratory fishing. We outline a simple clustering method based on Euclidean distances between trawls that offers a more realistic way of defining fishing opportunities than grid cells or statistical areas. The resulting cluster tree of trawls is divided into individual groups of trawls (fishing opportunities) using a recommended cut point. Our method correctly classified simulated trawls into fishing opportunities. Fishing opportunities were obtained for vessels in the British Columbia groundfish trawl fishery; each vessel usually fished at a wide variety (mean 26, standard deviation 16, range 2–69) of fishing opportunities. Within each fishing opportunity, trawls generally caught similar species. In the Argentina scallop fishery, our method was able to divide exploratory from regular fishing trawls, with obvious applications for catch-per-unit-effort calculations. Our method could also be used to detect positional errors in data from these fisheries. Fishing opportunities could provide indications of how fishermen might react to marine protected areas and to the imposition of quotas on multispecies fisheries.

Résumé : Une part importante du comportement de pêche consiste à décider où pêcher. Les capitaines de chalutiers choisissent ordinairement entre des occasions de pêche connues, ce qui s'observe quand des groupes de chalutiers sont actifs dans un même secteur d'un territoire de pêche ou quand ils font de la pêche exploratoire. Nous présentons une méthode simple de groupement basée sur les distances euclidiennes entre les chalutiers qui fournit une méthode plus réaliste de définir les occasions de pêche que les cellules d'une grille ou les zones statistiques. L'arbre des groupements produit est divisé en groupes individuels de chalutiers (occasions de pêche) à l'aide d'un point de coupure suggéré. Notre méthode classifie correctement des chalutiers simulés en occasions de pêche. Les occasions de pêche ont été obtenues pour les navires de la flotte de chalutage des poissons de fond de la Colombie-Britannique; chaque navire pêche généralement à une variété d'occasions de pêche (moyenne 26, écart type 16, étendue 2–69). Lors d'une même occasion de pêche, les chalutiers capturent généralement des espèces semblables. Dans la pêche commerciale de pétoncles de l'Argentine, notre méthode nous a permis de distinguer les chalutages exploratoires des chalutages ordinaires, ce qui a des conséquences sur les calculs des captures par unité d'effort. Notre méthode pourrait aussi servir à détecter les erreurs de position dans les données de ces pêches. Les occasions de pêche peuvent aussi fournir des renseignements sur la réaction possible des pêcheurs aux zones marines protégées et à l'imposition de quotas dans les pêches plurispécifiques.

[Traduit par la Rédaction]

Introduction

Understanding the behavior of fishermen is essential if we wish to examine the impact of management regimes like individual transferable quotas (ITQs) and marine protected areas (MPAs) on fisheries. One of the most basic elements of fishing behavior is the choice of when and where to deploy fishing gear: a skipper chooses between conducting exploratory fishing and fishing at competing fishing opportunities. We define fishing opportunities to be small areas over which the skipper of a vessel frequently trawls, i.e., groups of trawls that are consistently placed over the same geographic area (Fig. 1). These trawls should have a tight cluster of start positions and a tight cluster of end positions. Trawls that are in opposite directions can still belong to the same fishing opportunity if they cover the same ground (i.e., the start and end positions are switched). However, trawls starting in the same position, but conducted in opposite di-

Received 31 March 2004. Accepted 13 September 2004. Published on the NRC Research Press Web site at http://cjfas.nrc.ca on 13 April 2005.
J18056

T.A. Branch[1,2] **and R. Hilborn.** Box 355020, School of Aquatic and Fishery Sciences, University of Washington, Seattle, WA 98195-5020, USA.
E. Bogazzi. Instituto Nacional de Investigación y Desarrollo Pesquero, P.O. Box 175, Mar del Plata B7602HSA, Argentina, and Consejo Nacional de Investigaciones Científicas y Técnicas (CONICET), Mar del Plata, Argentina.

[1]Present address: Department of Mathematics and Applied Mathematics, University of Cape Town, Rondebosch, 7701, Western Cape, South Africa.
[2]Corresponding author (e-mail: tbranch@maths.uct.ac.za).

 doi: 10.1139/F04-232 © 2005 NRC Canada

Fig. 1. Trawls comprising types of fishing opportunities (*a*–*g*) overlaid by a regular grid: *a*, fishing opportunity with a tight cluster of start positions and end positions but with start positions in grid cells A1 and A2; *b* and *c*, two fishing opportunities with similar start positions but conducted in opposite directions; *d*, fishing opportunity comprising trawls covering the same ground but conducted in opposite directions; *e* and *f*, two fishing opportunities with the same start positions but different trawl lengths; *g*, fishing opportunity comprising circular trawls.

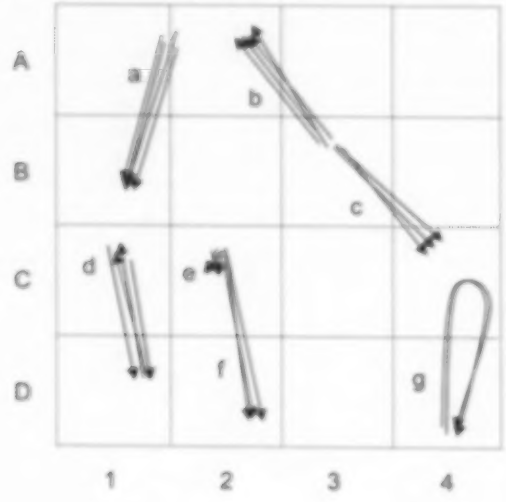

rections, would belong to different fishing opportunities. Some fishing opportunities could therefore be long and thin (for long trawls), and others could be small and round (e.g., short trawls or "circular" trawls that involve a midway 180° turn). For ease of presentation, we describe our method of defining fishing opportunities as if it only applied to trawlers. However, with minor modifications, our method could be applied to vessels using longlines, pots, gill nets, and other types of fishing gear.

As defined above, fishing opportunities are similar to what might be called fishing grounds. However, we consider fishing grounds to be larger regions that are fished by many vessels, whereas fishing opportunities represent vessel-specific methods of catching fish within these fishing grounds. Thus, for each fishing opportunity, a skipper will have previous knowledge gained through fishing (or from other skippers) about likely catch rates, species mix, optimal fishing months, appropriate gear, and the probable costs of fishing. Based on their knowledge, one skipper might only conduct short trawls in summer in the northern part of a fishing ground to target a skate species, while another vessel fishing in the same fishing ground may always conduct long winter trawls that traverse most of fishing ground and catch a wide mix of species. In this paper, we therefore define fishing opportunities to be vessel specific so that they can be related directly to fishermen behavior. In reality, fishing grounds often include areas that are untrawlable (i.e., too steep or rough), limiting the number of available fishing opportunities. We therefore consider it likely that some fishing opportunities will be frequented by multiple vessels.

We are unaware of papers that have examined fishermen behavior at the level of fishing opportunities; most published studies just divide the available space into statistical areas (e.g., Gillis et al. 1993; Mistiaen and Strand 2000; Cabrera and Defeo 2001) or into grid cells based on lines of latitude or longitude (e.g., Campbell and Hand 1999; Dorn 2001; Hannah 2003). Grid cells may be a reasonable approximation in a randomly spread out fishery that uses traps or pots to catch a sedentary resource (e.g., Swain and Wade 2003) but work poorly for trawlers. Simply put, long trawls do not fit conveniently into rectangular cells. True fishing opportunities may be split over several grid cells because the cells are defined independently of geographical features. Grid cells are either too big and include multiple fishing opportunities (e.g., the 5° × 5° cells used by Campbell and Hand (1999)) or too small, resulting in trawls that extend across many grid cells (e.g., 0.5 km × 0.5 km cells in Zimmerman (2003)). Cells that are too small require an algorithm to assign effort and catches from each trawl across several grid cells. Statistical areas can be improvement over grid cells, since they are often based on fishing effort but are usually too vast to be anything but broad indicators of fishermen behavior: some statistical areas encompass 25 000 km^2 (Holland and Sutinen 2000).

There are two published papers that offer reasonable approaches to defining fishing opportunities. Walters and Bonfil (1999) analyzed catch data from the British Columbia groundfish trawl fishery (B.C. fishery), first assigning trawls to 1 nautical mile square grid cells (using start positions), then smoothing catches over adjacent cells, and finally grouping grid cells with similar multispecies catches into 19 irregularly shaped fishing grounds. However, their grouping procedure was subjective and presumably time consuming and produced fishing grounds that were much larger than typical trawl lengths in the fishery. The resultant fishing grounds probably included multiple fishing opportunities, each fished by different skippers and containing different mixtures of species. An alternative approach was taken by Pelletier and Ferraris (2000) in their study of a small-scale marine fishery off Senegal. They censused canoe owners and produced a map of 28 known fishing locations, named by local fishermen according to either geography or fishing direction. They therefore provided the most realistic definition of fishing opportunities by reflecting local knowledge and fishing patterns, but their approach would be time consuming to apply to most fisheries.

In this paper, we present an objective and straightforward clustering method for allocating trawls to different fishing opportunities. We show how easily this approach scales to trawl length by analyzing data from a groundfish trawl fishery with long trawls and from a scallop fishery with short trawls. We provide recommendations on the appropriate spatial scale of fishing opportunities based on the characteristics of the fishery. We apply our method to the B.C. fishery to show how the species composition differs among fishing opportunities in a fishery where it is important to match multispecies catches to individual species quotas and to the Patagonian scallop fishery to discriminate between exploratory trawls and regular fishing trawls. We also note that this

© 2005 NRC Canada

method allows for the easy identification of positional errors in fisheries databases.

Methods

Clustering individual trawls

Both start and end positions of trawls are important when defining fishing opportunities. We used Euclidean distance to measure the geographically closeness of individual trawls. The Euclidean distance for a given pair of trawls was defined as a combination of the distance between the two start positions and the distance between the two end positions, thus using as inputs the start latitudes, start longitudes, end latitudes, and end longitudes (all in decimal degrees) of each trawl. Before calculating Euclidean distance, two adjustments were made to the input data. First, longitudes were multiplied by the cosine of the latitude to ensure that latitudes and longitudes were both in the same distance units. This is because lines of longitude are closer together than lines of latitude, except at the equator:

$$(1)\qquad \mathrm{lon}^{\mathrm{start}} = \mathrm{lon}^{\mathrm{start}} \cos\left(\frac{\mathrm{lat}^{\mathrm{start}}}{360} 2\pi\right), \quad \mathrm{lon}^{\mathrm{end}} = \mathrm{lon}^{\mathrm{end}} \cos\left(\frac{\mathrm{lat}^{\mathrm{end}}}{360} 2\pi\right)$$

Second, all trawls were reoriented by swapping the start and end positions of trawls that pointed southwards to ensure that trawls that were conducted in opposite directions over the same ground would be clustered together. We note that trawls in the eastward and westward directions may occasionally be incorrectly reoriented using this method. However, we consider this to be a relatively minor issue, since this problem would only arise if there were a group of eastward-facing (or westward-facing) trawls, some of which pointed slightly northward and some slightly southward. Of course, if most trawls in a fishery were in the eastward (or westward) direction, it would be sensible to reorient trawls by swapping the start and end positions of trawls that point eastwards.

The Euclidean distance ($D_{i,j}$) between the ith trawl and the jth trawl is therefore given by

$$(2)\qquad D_{ij} = \sqrt{(\mathrm{lon}_i^{\mathrm{start}} - \mathrm{lon}_j^{\mathrm{start}})^2 + (\mathrm{lon}_i^{\mathrm{end}} - \mathrm{lon}_j^{\mathrm{end}})^2 + (\mathrm{lat}_i^{\mathrm{start}} - \mathrm{lat}_j^{\mathrm{start}})^2 + (\mathrm{lat}_i^{\mathrm{end}} - \mathrm{last}_j^{\mathrm{end}})^2}$$

We clustered trawls using hierarchical agglomerative clustering based on the Euclidean distances between each pair of trawls (see Appendix A). In this method, all trawls are initially assigned to single-trawl clusters, and then clusters are progressively joined by minimizing the average dissimilarity between members of clusters (Venables and Ripley 1999, pp. 336–338) until all clusters have been combined into a cluster tree (Fig. 2).

Obtaining fishing opportunities using a cut point

Once the cluster tree was obtained, we chose a particular Euclidean distance cut point to divide the cluster tree into individual clusters of trawls (Fig. 2). Each cluster of trawls has similar start positions and similar end positions, thus matching our definition of a fishing opportunity. Not all resulting clusters will contain multiple trawls. A trawl that was conducted far from other trawls will be classified into a cluster by itself, i.e., it is a solitary trawl. Solitary trawls are the result of either exploratory fishing or database error.

The choice of cut point determines the balance between fishing opportunities and solitary trawls. A cut point that is too small will produce many apparent fishing opportunities and many solitary trawls but will subdivide the real fishing opportunities; conversely, a cut point that is too large will group even distant trawls into a few fishing opportunities. We developed a rule-of-thumb cut point leading to the clustering of groups of trawls that are closer together than the median trawl length in the fishery. First, the median trawl length in the fishery ($\bar{d}$) (kilometres) was converted to latitudinal degrees (d) using the constants 360 (degrees around the earth) and 40 075 (circumference of the earth in kilometres). Then, we note that if two trawls have start points that are d distance apart and end points that are d distance apart, eq. 1 implies that the Euclidean distance between the two trawls will be $\sqrt{2}d$, giving finally

$$(3)\qquad d = \frac{360}{40\,075}\bar{d}, \quad \mathrm{cutpoint} = \sqrt{2}d$$

For fisheries with very short trawl lengths, the mean distance between successive starting positions may be a better estimate of $\bar{d}$ than trawl length itself. In other fisheries, the spatial autocorrelation in the resource may provide a good estimate for $\bar{d}$; methods to estimate this distance are provided in Vignaux (1996) and Dorn (1997). One final method would be to estimate the fraction of trawls that were exploratory and then find the cut point that produces that fraction of solitary trawls.

Effect of different cut point values on simulated trawl data

To illustrate the effect of different cut point values, we simulated trawls and applied our clustering method to assign trawls to fishing opportunities. The simulated trawls were generated using the following method. (*i*) For each fishing opportunity, generate the mean start position ($\mathrm{lat}^{\mathrm{start}}$, $\mathrm{lon}^{\mathrm{start}}$) within the bounds of the fishing area, mean trawl direction (θ), and mean trawl distance (r) (kilometres). (*ii*) Calculate the mean end position ($\mathrm{lat}^{\mathrm{end}}$, $\mathrm{lon}^{\mathrm{end}}$) of that fishing opportunity:

$$(4)\qquad \begin{aligned} \mathrm{lat}^{\mathrm{end}} &= \frac{360}{40\,075} r \sin\theta + \mathrm{lat}^{\mathrm{start}} \\ \mathrm{lon}^{\mathrm{end}} &= \frac{360}{40\,075} r \cos\theta \cos\left(\frac{\mathrm{lat}^{\mathrm{start}} + \mathrm{lat}^{\mathrm{end}}}{2}\right) + \mathrm{lon}^{\mathrm{start}} \end{aligned}$$

© 2005 NRC Canada

Fig. 2. Example cluster tree obtained from 30 simulated trawls illustrating the fishing opportunities obtained with a cut point of 0.25. The numbers underneath each individual trawl indicate the fishing opportunity to which the trawl was assigned. For example, those labelled "8", "5", and "7" are solitary trawls, whereas the 10 trawls labelled "1" all belong to the same fishing opportunity.

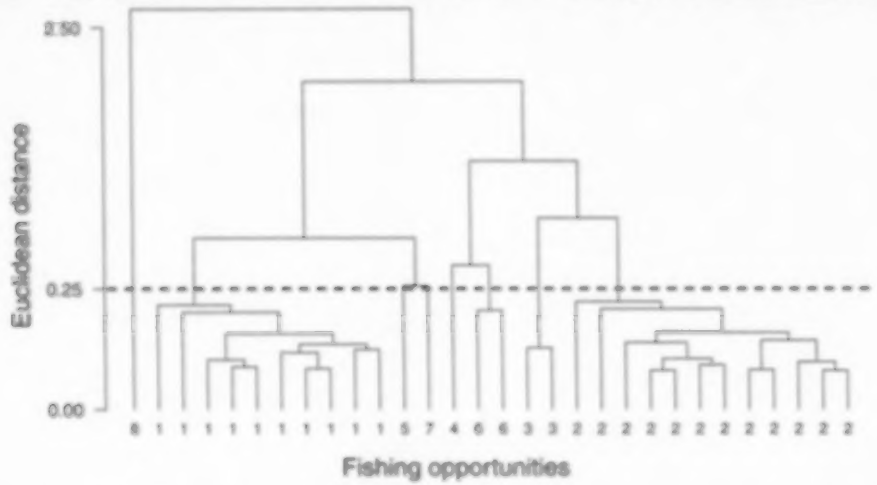

(*iii*) For each trawl within a fishing opportunity, generate a start position from a bivariate normal distribution (with variance–covariance matrix $\boldsymbol{\Sigma}$) around the mean start position. (*iv*) Generate an end position for each trawl around the mean end position. This procedure ignores the curvature of the earth, but the bias is slight.

The parameter values used for the simulated trawls were drawn from the following distributions:

$$
\begin{aligned}
&\text{lat}^{\text{start}} \sim U(41°, 43°)\\
&\text{lat}^{\text{start}} \sim U(124°, 124.3°)\\
&\theta \sim U(60°, 120°)\\
&r \sim \text{randomly drawn from actual trawl distances in B.C. groundfish fishery}\\
&\boldsymbol{\Sigma} = \begin{bmatrix} 0.002 & 0 \\ 0 & 0.0004 \end{bmatrix}
\end{aligned}
\tag{5}
$$

The implication of these parameters was that the simulated fishery was off the coast of Oregon and conducted within a narrow longitudinal band typical of a fishery confined to a particular depth range. We simulated 40 solitary trawls and four fishing opportunities containing 30, 40, 50, and 60 trawls, respectively. The simulated trawls were assigned to fishing opportunities using cut points of 0.01, 0.15, 0.2, 0.5, and 2.

Multispecies catches in fishing opportunities in the B.C. groundfish fishery

We applied our clustering method to observer data from the B.C. fishery to illustrate the species composition and number of fishing opportunities for a multispecies fishery. This fishery comprises 50–70 active vessels fishing for over 40 commercially valuable species governed by ITQs (Turris 2000).

We extracted trawl start and end positions and species catches from the observer database PacHarv for the 1996–2001 fishing years. Pacific hake (*Merluccius productus*) fishing trips (>50% Pacific hake caught during the trip) were eliminated because Pacific hake schools are not consistently found in the same location, although nonhake midwater trawls were retained. Trawls that lacked start or end positions were also deleted. The resulting database included 105 375 trawls, although no vessel conducted more than 3500 trawls. We obtained vessel-specific fishing opportunities for the 70 vessels that conducted the greatest number of trawls during 1996–2001. Based on speed and trawl duration, the median trawl distance in the fishery was 10.8 km, suggesting a cut point of 0.14 from eq. 2. We rounded this value upward to 0.15 for the analyses. Five of the resulting fishing opportunities were randomly selected for graphical display. From each of these fishing opportunities, we randomly selected 15 trawls and plotted catch proportions in each trawl for those species that cumulatively represented >95% of the catch.

Classifying trawls as exploratory or regular fishing in the Patagonian scallop fishery

The Patagonian scallop (*Zygochlamys patagonica*) commercial fishery started in 1996 and has grown to one of the most important scallop fisheries in the world, with annual landings of 6000 metric tons of muscle meat. The fleet is small: four vessels operated by two companies. The main fishing area is on the Argentine continental shelf (39°S–45°S) at depths of 80–195 m. Each trip lasts 20–40 days, and vessels can complete 40–60 trawls per day using two otter trawl nets. Nearly all trawls were 6–14 min long in the data that we analyzed.

We used observer data from a single trip (737 trawls) in 1995 during an experimental fishing program instigated by one of the vessels in the fishery. Observers onboard recorded trawl positions, speed, and duration of trawls in addition to recorded catches. Trawls with missing start or end positions were eliminated, leaving 614 trawls. Catch data at the indi-

© 2005 NRC Canada

vidual trawl level were not available for 357 trawls, leaving 257 trawls from which catch-per-unit-effort (CPUE) could be calculated. Trawls in this fishery are typically very short compared with the time taken for the gear to be deployed and hauled, and so the median distance between start positions of successive trawls (1.2 km) was used to suggest a cut point of 0.014. We used a higher cut point of 0.02 in the analyses because some trawls had been excluded and because skippers space out their trawls on the scallop grounds to avoid trawling over the same area twice. Solitary trawls were assumed to be exploratory; fishing opportunities with two to four trawls were "likely exploratory", and opportunities with five or more trawls were classified as "regular fishing". Relatively few trawls were classified as likely exploratory, so these trawls were grouped with the exploratory trawls. For the trawls with catch data, the average CPUE (metric tons per square kilometre) was calculated for exploratory and regular fishing trawls. To test whether the mean CPUE in regular fishing trawls was higher than in exploratory trawls, we used a randomization test. Assuming x exploratory trawls and y regular fishing trawls, we repeated the following procedure 1 million times: (*i*) randomly select with replacement one set of x and one set of y CPUE values from the 257 trawls, (*ii*) calculate the mean CPUE for these two sets, and (*iii*) test whether the difference in mean CPUE is greater than the observed difference in CPUE.

Finding positional errors

The clustering method outlined above is intended to find groups of trawls that have start and end positions that are geographically close together. For a given trawl, if there is an error in either the start or the end position, that trawl is likely not to be clustered together with any other trawls. The larger the error, the greater will be the Euclidean distance (eq. 1) between that trawl and all other trawls. Therefore, once a cluster tree based on Euclidean distance has been obtained, solitary trawls are likely to be those with positional errors, especially if a high cut point (relative to the recommended cut point) is used to divide the cluster tree into fishing opportunities. To test whether using a high cut point would uncover positional errors, we carefully examined the solitary trawls resulting from cut points of 1.0 in the B.C. fishery and 0.5 in the Patagonian scallop fishery, i.e., cut points around an order of magnitude greater than recommended.

Results

Applying different cut point values to simulated trawl data

Recommended cut points calculated from the sets of simulated trawls ranged from 0.10 to 0.17. We present the cluster tree (Fig. 3) and fishing opportunities obtained for different cut point values (Fig. 4) for a single set of simulated trawls. When the cut point was too small (0.01), almost all of the trawls were classified as solitary; for a slightly higher cut point (0.05), the four simulated fishing opportunities were subdivided into multiple small fishing opportunities. Values near the recommended cut point (0.15 and 0.20) best recreated the simulated fishing opportunities, although some of the simulated solitary trawls were grouped together into fishing opportunities. When the cut point was larger (0.5), the four simulated fishing opportunities were joined into two groups, and at a cut point of 2, all simulated trawls were considered to belong to a single fishing opportunity.

Consistent multispecies catches from fishing opportunities in the British Columbia groundfish fishery

A representative cluster tree from a single vessel in the B.C. fishery shows the typically large number of fishing opportunities (32 for this vessel) with ≥15 trawls at a cut point of 0.15 (Fig. 5). The number of fishing opportunities per vessel (for the top 70 vessels) ranged from 2 to 69 (mean 26, SD 16). In total, 1804 fishing opportunities were identified. Species composition differed greatly among the randomly selected fishing opportunities. In some, one or two species dominated the catches, with longspine thornyhead (*Sebastolobus altivelis*) and shortspine thornyhead (*Sebastolobus alascanus*) always caught in one opportunity (Fig. 6, opportunity A), rock sole (*Pleuronectes bilineatus*) in another (Fig. 6, opportunity C), and arrowtooth flounder (*Atheresthes stomias*) and yellowtail rockfish (*Sebastes flavidus*) in a third (Fig. 6, opportunity E). In contrast, ≥10 species were caught in each of the other two opportunities, where only abundant species like spiny dogfish (*Squalus acanthias*) and arrowtooth flounder were caught often (Fig. 6, opportunities B and D).

These five fishing opportunities typified the 1804 fishing opportunities obtained from all vessels. It should be noted that we included both bottom and midwater trawls in our analysis, so that it is not surprising that the occasional trawl caught midwater species like yellowtail rockfish (e.g., Fig. 6, opportunity E) in amongst trawls catching mainly demersal species. Some fishing opportunities (not represented in Fig. 6) also included occasional trawls from closely adjacent shallower (or deeper) waters. In addition, the tonnage caught in each trawl also varied considerably, although this is masked somewhat by plotting proportions in Fig. 6.

Classifying trawls as exploratory or regular fishing in the Patagonian scallop fishery

In the Patagonian scallop fishery, there was an obvious distinction between exploratory (one to four trawls per fishing opportunity) and regular fishing (five or more trawls per opportunity) trawls. Regular fishing trawls clustered together at small cut point values, whereas exploratory trawls were quite dissimilar from other trawls (Fig. 7). At a cut point of 0.02, 13 fishing opportunities (with five or more trawls each) were identified, but 12 of these were grouped into a southern fishing ground containing 75% of the total trawls (Fig. 8). The 13th fishing opportunity contained only five trawls and may have been an area that initially seemed promising but proved not to be commercially viable. Overall, 24% of the trawls were classified as exploratory (19% were solitary trawls) and 76% were classified as regular fishing trawls. For the trawls with CPUE information, 30% (77 trawls) were classified as exploratory and 70% (180 trawls) as regular fishing. The mean trawl duration was similar between exploratory (9.7 min, SD 2.6 min) and regular fishing trawls (9.8 min, SD 2.4 min), but CPUE was almost four times

© 2005 NRC Canada

Fig. 3. Cluster tree obtained from start and end positions of simulated trawls. Trawls that are contained in fishing opportunities (containing 10 trawls at a cut point of 0.15) are identified by a bar just below the *x* axis. The *y* axis is plotted on a square root scale to better show the detail of relationships between clusters at small Euclidean distances (in degrees).

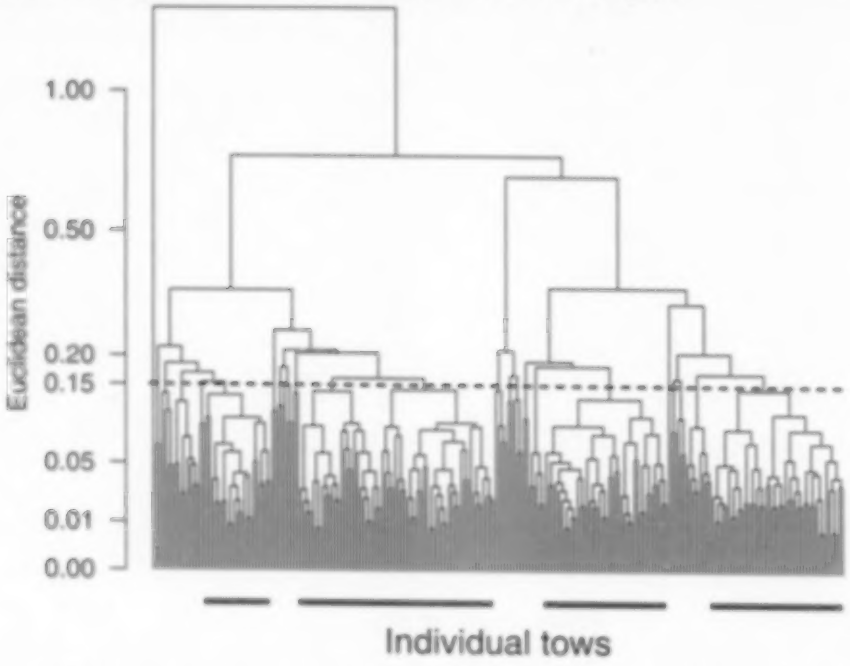

Fig. 4. Fishing opportunities obtained using different cut point values from the cluster tree in Fig. 3. The simulated trawl data are shown in the leftmost panel. Light gray trawls represent randomly distributed solitary trawls; trawls in simulated fishing opportunities are displayed in different shades, with a distinctive shade for each opportunity. The other six panels represent fishing opportunities obtained from the simulated data for different cut points (0.01°–2°). Again, gray trawls are solitary trawls, and each fishing opportunity is represented by a different, randomly allocated, shade.

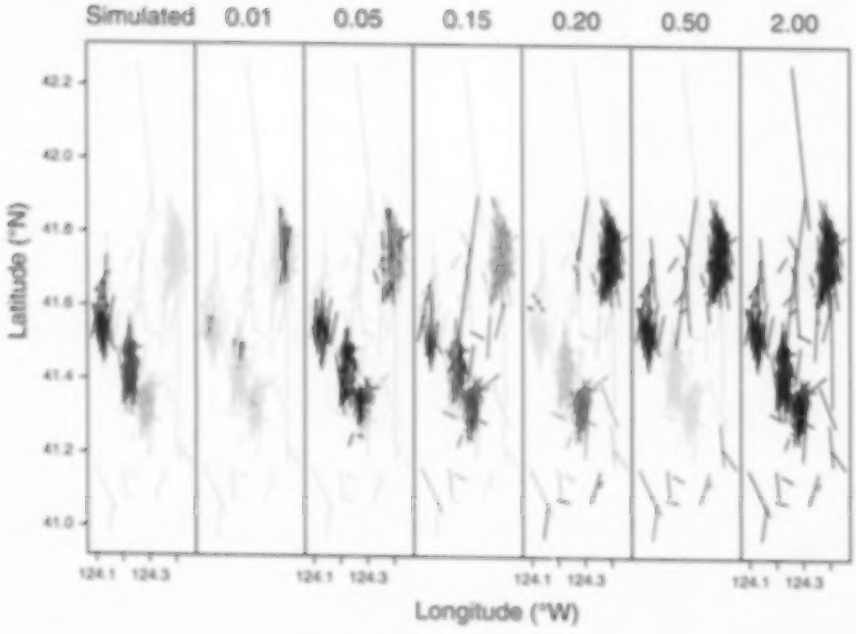

© 2005 NRC Canada

Fig. 5. Cluster tree obtained from start and end positions of a single vessel (not the entire fleet) in the British Columbia groundfish trawl fishery based on trawls from 1996 to 2001. Fishing opportunities with ≥15 trawls at a cut point of 0.15 are identified by a bar just below the *x* axis. The *y* axis is plotted on a square root scale.

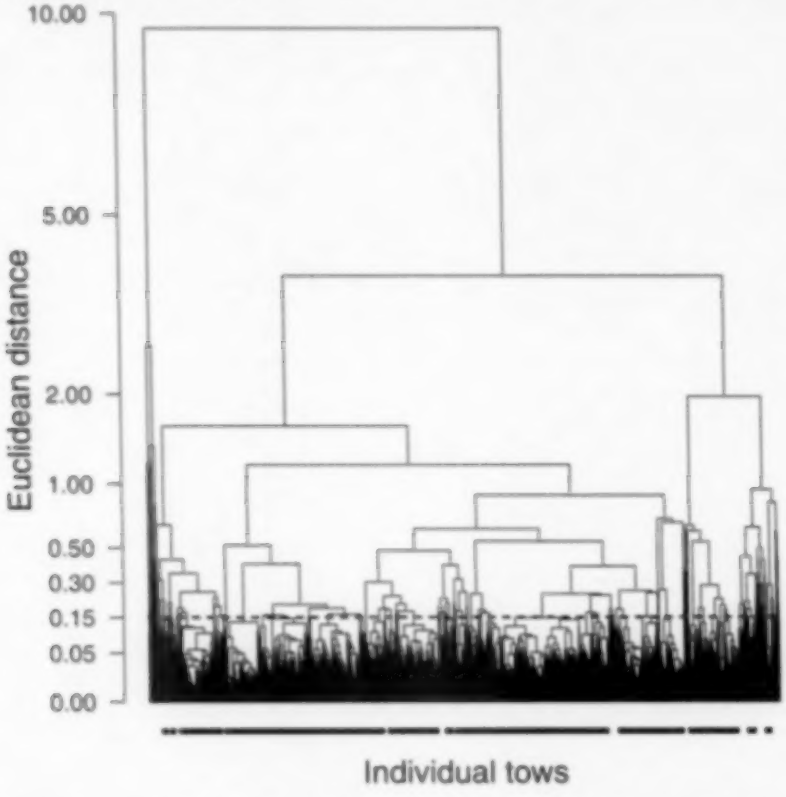

higher for the regular fishing trawls: 39.1 t·km^{-2} (SD 23.4) versus 10.6 t·km^{-2} (SD 13.8). This difference in CPUE was highly significant ($p < 10^{-6}$, randomization test).

Finding positional errors

In both fisheries, positional errors were identified. In the B.C. fishery, trawls had already been carefully screened for implausible distances between the start and end position, and so only 30 possible errors were flagged (0.03% of the total). Of these, five were definite errors, being located on land ($n = 4$) or traversing multiple depth contours ($n = 1$). 17 were possible errors, being found in very shallow waters close to land ($n = 13$) or far offshore ($n = 4$), and the remaining eight trawls may have been exploratory trawls. In the Patagonian scallop fishery, four trawls were classified as possible errors (0.6% of the total); in each case, the errors were obvious, with distances of around 0.5° (two trawls), 1°, and 2° between the start and end latitudes, much further than the vessels would have steamed during a single trawl.

Discussion

How do skippers choose where to fish? The answer depends on the scale of the fishing areas that are considered and how they are defined. In most fisheries, skippers can tell you the names of their favorite fishing locations, places where they return to year after year because they know catch rates of their target species will be high there. We call these locations fishing opportunities. At each fishing opportunity, the mix of species caught depends on the bottom topography (steep or flat) and the substrate type (e.g., rocky or muddy) of that location. Skippers learn which gear to use and what time of the year to fish at each fishing opportunity; therefore, fishing opportunities are best defined as vessel specific. Furthermore, since learning is a function of historical search patterns and exploratory behavior, each skipper will have information about a specific set of fishing opportunities, although information sharing among skippers may broaden the range of available fishing opportunities.

We define fishing opportunities using a clustering algorithm that groups trawls that all start in a similar position and end in a similar position. According to this operational definition, fishing opportunities may also be termed fishing grounds (if defined with a large cut point), hot spots, or track lines, except that these terms imply that the time of the year and choice of gear type are irrelevant. Our use of "opportunities" carries the connotation that fishing opportunities play an integral role in location choice, although we recognize that location choice also depends on a wide range of other factors. The clustering method that we use is simple enough to implement using three commands in R (itself a freely available software package). We show that fishing op-

© 2005 NRC Canada

Fig. 6. Species compositions recorded in individual trawls in five randomly selected fishing opportunities in the British Columbia groundfish trawl fishery. For each opportunity, 15 trawls were selected at random, and the most important species (summing to >95% of the total catch) in those trawls were plotted.

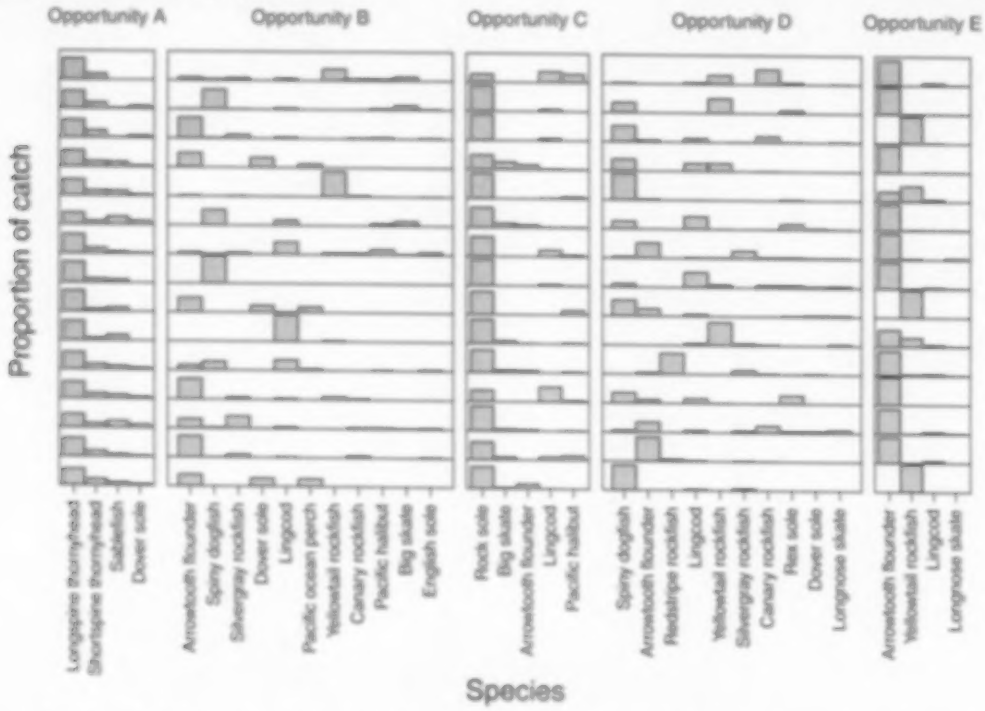

portunities can be identified from simulated data, the B.C. fishery (which has relatively long trawls), and the Patagonian scallop fishery (characterized by very short trawls).

Fishing opportunities are a finer scale grouping than "métiers" or "fishing tactics", which are groupings of vessels or trips (not trawls) defined using fishing location, gear, time of the year, and target species (Biseau and Gondeaux 1988; Biseau 1998; Pelletier and Ferraris 2000). These methods rely on multivariate statistics, which can be complicated and produce impractical results (Biseau 1998). Métiers correspond to much larger regions than true fishing opportunities, although the fishing locations for the Senegalese fishery in Pelletier and Ferraris (2000) are quite realistic. Métiers may be useful for the classification of vessels or trips, especially when detailed trawl-by-trawl data are unavailable, but are less useful when trying to analyze why a skipper chose to fish at a particular location.

An alternative to grouping trawls into fishing opportunities is to extract and use individual trawls directly. For example, Vignaux et al. (1998) outlined how to produce fine-scale (i.e., at a resolution finer than individual trawls) mapping of fish biomass using a Bayesian maximum entropy method, and Rijnsdorp et al. (1998) used automatic position recorders (data recorded every 6 min) to estimate the proportion of fishing grounds that have been disturbed multiple times by trawls. These methods could be usefully linked with fishing opportunities: once groups of trawls within each fishing opportunity have been identified, these trawls could be analyzed to produce maps of species distribution and habitat disturbance within the most heavily fished areas.

A key feature of our definition of fishing opportunities is the cut point. A small cut point will produce many fishing opportunities each containing few trawls; a large cut point will group many trawls into just a few fishing opportunities. Recommended cut points can be obtained from the mean trawl length, intertrawl distance, or the level of autocorrelation in the underlying fish populations or habitat types. Although recommended cut points provided reasonable characterizations of fishing opportunities for the examples in this paper, these values should only be seen as recommendations and may not be appropriate for all fisheries. In our experience, cut points at or slightly above the recommended value provide reasonable characterizations of fishing opportunities, while cut points below the recommended value tend to induce splitting.

Our method of determining fishing opportunities has straightforward data requirements: the start and end position of individual trawls. Many fisheries record these data in the form of logbooks or observer data. However, some fisheries record only the start position of each trawl. Fishing opportunities could be defined using just the start position using our method, but a number of additional issues arise when interpreting the results: (*i*) trawls that start in the same position but travel in opposite directions would be grouped together, (*ii*) trawls that cover the same ground but are conducted in opposite directions (start and end positions swapped) would be separated into two opportunities, (*iii*) circular trawls that end near their starting positions (Vignaux 1996; Gillis 1999) would be classified together with linear trawls, and (*iv*) an algorithm would be needed to map fishing effort from the

© 2005 NRC Canada

Fig. 7. Cluster tree obtained from a single trip by one vessel in the Patagonian scallop (*Zygochlamys patagonica*) fishery. Regular fishing trawls, those in opportunities with five or more trawls at a cut point of 0.02, are identified by a bar just below the *x* axis. The *y* axis is plotted on a square root scale.

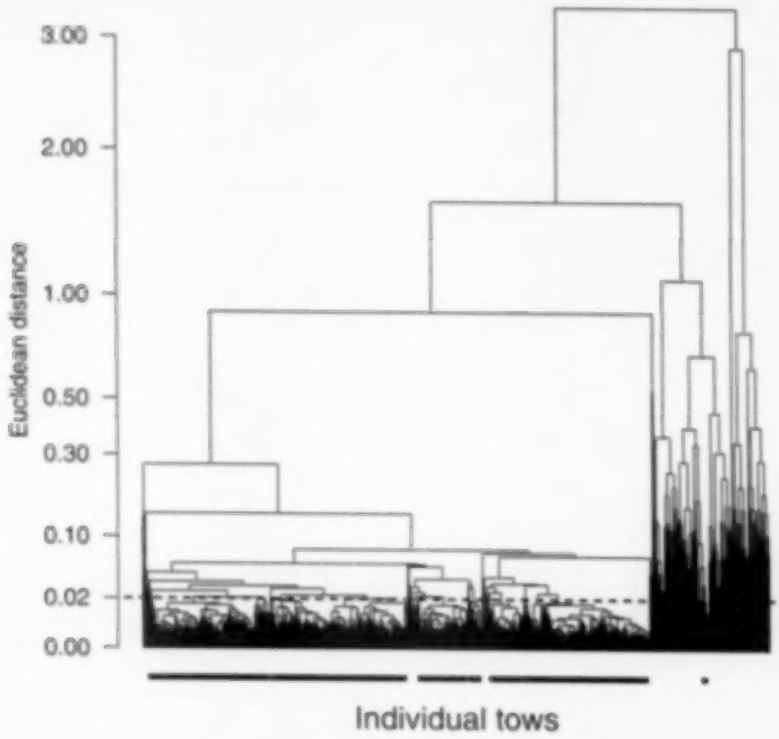

starting position to adjacent areas — many grid-based studies have distributed effort in circles around the starting points (e.g., Walters and Bonfil 1999; Hannah 2003), even though the actual effort is typically linearly distributed because of bottom topography. These problems plague grid-based analyses of fishing data, and we much prefer analyzing data that include both start and end positions, when they are available.

In the B.C. fishery, total catches are limited by quotas under the ITQ program. Vessel owners should therefore seek to maximize their profits by exactly catching their quota holdings, reducing costs, and landing species when market prices peak. Knowledge about species distribution and abundance in different fishing opportunities accordingly gains great value. Our analysis of the B.C. fishery shows that the average skipper trawled in 26 different fishing opportunities (≥15 trawls in each), although this varied greatly (2–69) among the top 70 vessels. Skippers in this fishery visit substantially more locations than were reported for Icelandic skippers fishing cod, who generally visited only a few locations and were considered to be not very innovative (Durrenberger and Pálsson 1986). Their study focused on locations that were 225 km^2 but noted that each location might contain a number of small "fishing spots", which would more likely correspond to our fishing opportunities. The great number of target species in the B.C. fishery probably also motivates skippers to fish in a wide variety of fishing opportunities. Although 1804 fishing opportunities were identified in total in this paper, many were likely duplicated among the vessels, so that the effective total was probably substantially lower.

Trawls within each fishing opportunity in the B.C. fishery caught fairly predictable mixes of species. However, huge quantities of one species were occasionally landed, demonstrating the highly variable returns even within a fishing opportunity. We were able to identify fishing opportunities dominated by (for example) thornyheads, rock sole, and arrowtooth flounder, while in other fishing opportunities, a wide range of species are caught. Sometimes midwater and bottom trawls were included in the same fishing opportunity if they were colocated; these two types of trawls could instead be analyzed separately if trawl gear data are available or separated a posteriori based on catch composition. More problematic was the occasional inclusion of shallow-water and deepwater trawls in the same fishing opportunity, especially where the topography was steep and these habitats were close together. We tried including depth as an additional clustering variable; however, despite careful scaling, distant trawls at the same depth sometimes clustered together, and the addition of depth as a factor made the method unnecessarily complicated. The majority of trawls in a fishing opportunity were at similar depths even when only latitude and longitude were used in the clustering process.

Like most sedentary species, Patagonian scallop is a spatially structured resource because of larval drift and settlement. At the outset of this fishery, trawling was characterized by random search (exploratory fishing) alternated with systematic trawling (regular fishing, like a sewing pattern) once high-

© 2005 NRC Canada

Fig. 8. Distribution of start locations of trawls from a single trip in the Patagonian scallop (*Zygochlamys patagonica*) fishery. Distinctions are made between trawls that are classified as exploratory (one trawl per fishing opportunity) (plus signs), probable exploratory (two to four trawls per opportunity) (triangles), and regular fishing (five or more trawls per opportunity) (circles). Latitude and longitude have been omitted for confidentiality reasons, but the tick mark labels are placed 0.5° apart.

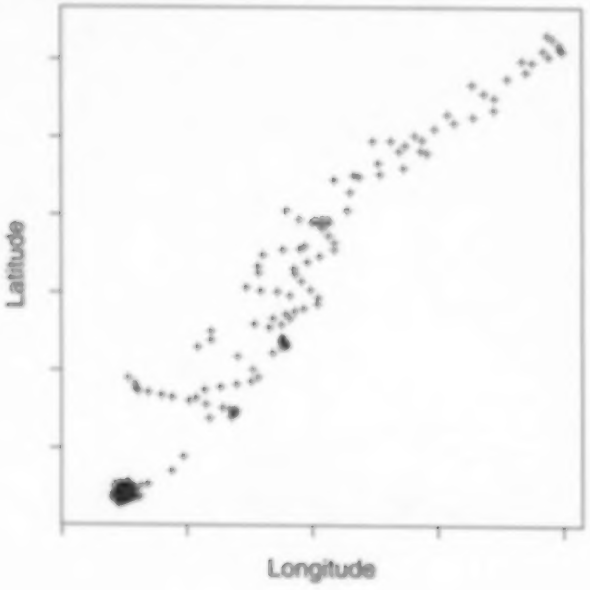

density areas were encountered. This pattern of exploitation on sedentary resources can lead to serial depletion, with the densest patches being exploited first, resulting in hyperstability in CPUE indices (Hilborn and Walters 1992, pp. 187–191). When calculating CPUE and modelling local profitability and depletion in this fishery, it is therefore important to distinguish between exploratory trawls and regular fishing trawls. Using the method outlined in this paper, it was easy to separate out exploratory and regular fishing trawls in the Patagonian scallop fishery. As expected, regular fishing trawls were characterized by far greater catch rates, four times higher, than exploratory trawls. Any measure of overall CPUE in the fishery would therefore be skewed if the proportion of trawls that are exploratory changed over time (as might be expected in a maturing fishery). Furthermore, sequential depletion of the resource could be masked unless CPUE from each fishing opportunity was calculated separately.

An unexpected benefit of our method of determining fishing opportunities was that positional errors in the database were easy to detect. The trawls that were flagged usually included obvious positional errors, like being on land or having an estimated speed beyond the capabilities of the vessels. Since this was not the central focus of our study, we did not investigate this method further, but it would be instructive to measure the usefulness of this method by comparing the error rate in a randomly selected set of trawls (acting as a control) with those in a set of trawls that have been flagged by this method.

Although we have applied our method for defining fishing opportunities to bottom trawlers that catch fish reliably found at given locations, our method would also be useful for other types of fisheries. For example, fishing opportunities might also be useful in mobile pelagic fisheries, where our method could separate exploratory trawls from regular fishing trawls, provided data from different time periods are analyzed separately. The number of trawls within each fishing opportunity would then be an indicator of the overall size of the fish aggregation that was targeted. When calculating CPUE for pelagic species, the total time spent searching for aggregations could be inferred from the total time and the time devoted to trawls on aggregations.

We see many uses of fishing opportunities in addition to those that have been outlined in this paper. For example, models of MPAs currently make very general assumptions about displaced fishing effort, which could be avoided by basing MPA models on fishing opportunities as follows. Assume that a skipper fishes in n fishing opportunities,with n_i trawls in each fishing opportunity i. A proposed MPA would close some of these fishing opportunities to fishing. Then, it would be relatively simple to redistribute the trawls formerly conducted inside the MPAs to those remaining outside the MPAs, with some adjustment for increased costs. When applied to all vessels, the resulting redistribution of effort could be used as a starting point for future predictions of the effects of MPAs. Of course, actual changes are likely to be much more complicated than this simple starting point might suggest.

An additional use of fishing opportunities is an application to multispecies fisheries that are constrained by small allowable catches on some species. This kind of situation is currently responsible for the closure of large swathes of the US West Coast groundfish fishery owing to overfishing of a few species. Classical models predict that when sustained catches are taken from a multistock (or multispecies) fishery, those species with low growth rates will diminish towards commercial extinction (Ricker 1958; Paulik et al. 1967). However, these models assume spatial homogeneity in abundance and hence equal catchability among stocks (or species). In reality, each fishing opportunity has a particular mix of species, and placing catch limits on one species will merely shift fishing effort from fishing opportunities where that species is likely to be caught to fishing opportunities where it is less abundant. There is evidence for these shifts in the B.C. fishery, where total allowable catches were reduced for a few species (generally those with low productivity) when ITQs were introduced. Catches of those species declined to match total allowable catches, but catches of other species in the fishery remained constant, suggesting that skippers were able to shift their fishing effort to alternative fishing opportunities where other species dominated.

In conclusion, fishing opportunities are a natural way of defining where fishermen choose to fish and can be easily determined from positional data. Many useful patterns of behavior can be inferred from fishing opportunities, but we have limited ourselves to examples from two fisheries. The analysis of the B.C. fishery demonstrates how catch information from a multispecies fishery can be partitioned to pro-

© 2005 NRC Canada

vide a useful basis to predict changes in fishing effort resulting from reductions in total allowable catches for some species. Data from the Patagonian scallop fishery indicate that exploratory and regular fishing can be separated and that such separation is necessary to avoid biases in CPUE trends and estimates. We also show that database errors in positions can be isolated using fishing opportunities.

Fishing opportunities will be most useful where predictive models need to include fishermen behavior to be realistic. MPAs and other types of management will induce changes in fishing behavior as skippers reallocate their fishing effort from areas rendered less profitable by the regulations to previously less desirable places. We hope that a focus on fishermen behavior will address the comments made by (Hilborn 1985) about fisheries management: "This sad litany of fisheries disasters can be ascribed to poor understanding of the dynamics of fishermen, how they fish, and how they invest". Fisheries scientists still largely concentrate on fish and less on fishermen. Fishing opportunities provide a way of redressing this imbalance, thus hopefully ensuring that the right numbers of fishermen are allowed to chase after the right number of fish in the right places.

Acknowledgements

T.A.B. was funded by National Marine Fisheries Service (NMFS) grant NA07FE0473 and by the South African National Research Foundation. We owe a debt of gratitude to Rick Stanley, Norm Olsen, and Kate Rutherford for preparing and providing the British Columbia groundfish observer database (PacHarv). Rick Stanley also assisted with useful insights about the operation of the B.C. fishery. Arni Magnusson, Carolina Minte-Vera, and Jason Cope gave advice on clustering methods, R programming, and Microsoft Access. We thank Jody Brauner, Carolina Minte-Vera, André Punt, Ian Stewart, and Teresa Turk for helpful comments on earlier versions of this manuscript.

References

Biseau, A. 1998. Definition of a directed fishing effort in a mixed-species trawl fishery, and its impact on stock assessments. Aquat. Living Resour. **11**: 119–136.

Biseau, A., and Gondeaux, E. 1988. Apport des méthodes d'ordination en typologie des flottilles. J. Cons. Int. Explor. Mer, **44**: 286–296.

Cabrera, J.L., and Defeo, O. 2001. Daily bioeconomic analysis in a multispecific artisanal fishery in Yucatan, Mexico. Aquat. Living Resour. **14**: 19–28.

Campbell, H.F., and Hand, A.J. 1999. Modeling the spatial dynamics of the U.S. purse-seine fleet operating in the western Pacific tuna fishery. Can. J. Fish. Aquat. Sci. **56**: 1266–1277.

Dorn, M.W. 1997. Mesoscale fishing patterns of factory trawlers in the Pacific hake (*Merluccius productus*) fishery. Calif. Coop. Oceanic Fish. Invest. Rep. **38**: 77–89.

Dorn, M.W. 2001. Fishing behavior of factory trawlers: a hierarchical model of information processing and decision-making. ICES J. Mar. Sci. **58**: 238–252.

Durrenberger, P., and Pálsson, G. 1986. Finding fish: the tactics of Icelandic skippers. Am. Ethnol. **13**: 213–229.

Gillis, D.M. 1999. Behavioral inferences from regulatory observer data: catch rate variation in the Scotian Shelf silver hake (*Merluccius bilinearis*) fishery. Can. J. Fish. Aquat. Sci. **56**: 288–296.

Gillis, D.M., Peterman, R.M., and Tyler, A.V. 1993. Movement dynamics in a fishery: application of the ideal free distribution to spatial allocation of effort. Can. J. Fish. Aquat. Sci. **50**: 323–333.

Hannah, R.W. 2003. Spatial changes in trawl fishing effort in response to footrope diameter restrictions in the U.S. West Coast groundfish trawl fishery. N. Am. J. Fish. Manag. **23**: 693–702.

Hilborn, R. 1985. Fleet dynamics and individual variation: why some people catch more fish than others. Can. J. Fish. Aquat. Sci. **42**: 2–13.

Hilborn, R., and Walters, C.J. 1992. Quantitative fisheries stock assessment: choice, dynamics and uncertainty. Chapman and Hall, New York.

Holland, D.S., and Sutinen, J.G. 2000. Location choice in New England trawl fisheries: old habits die hard. Land Econ. **76**: 133–150.

Mistiaen, J.A., and Strand, I.E. 2000. Location choice of commercial fishermen with heterogeneous risk preferences. Am. J. Agric. Econ. **82**: 1184–1190.

Paulik, G.J., Hourston, A.S., and Larkin, P.A. 1967. Exploitation of multiple stocks by a common fishery. J. Fish. Res. Board Can. **24**: 2527–2537.

Pelletier, D., and Ferraris, J. 2000. A multivariate approach for defining fishing tactics from commercial catch and effort data. Can. J. Fish. Aquat. Sci. **57**: 51–65.

Ricker, W.E. 1958. Maximum sustained yields from fluctuating environments and mixed stocks. J. Fish. Res. Board Can. **15**: 991–1006.

Rijnsdorp, A.D., Buys, A.M., Storbeck, F., and Visser, E.G. 1998. Micro-scale distribution of beam trawl effort in the southern North Sea between 1993 and 1996 in relation to the trawling frequency of the sea bed and the impact on benthic organisms. ICES J. Mar. Sci. **55**: 403–419.

Swain, D.P., and Wade, E.J. 2003. Spatial distribution of catch and effort in a fishery for snow crab (*Chionoecetes opilio*): tests of predictions of the ideal free distribution. Can. J. Fish. Aquat. Sci. **60**: 897–909.

Turris, B.R. 2000. A comparison of British Columbia's ITQ fisheries for groundfish trawl and sablefish: similar results from programmes with differing objectives, designs and processes. *In* Use of property rights in fisheries management. FAO Fish. Tech. Pap. 404/1. FishRights 99 Conference. *Edited by* R. Shotton. FAO, Fremantle, Western Australia. pp. 254–261.

Venables, W.N., and Ripley, B.D. 1999. Modern applied statistics with S-PLUS. 3rd ed. Springer, New York.

Vignaux, M. 1996. Analysis of spatial structure in fish distribution using commercial catch and effort data from the New Zealand hoki fishery. Can. J. Fish. Aquat. Sci. **53**: 963–973.

Vignaux, M., Vignaux, G.A., Lizamore, S., and Gresham, D. 1998. Fine-scale mapping of fish distribution from commercial catch and effort data using maximum entropy tomography. Can. J. Fish. Aquat. Sci. **55**: 1220–1227.

Walters, C.J., and Bonfil, R. 1999. Multispecies spatial assessment models for the British Columbia groundfish trawl fishery. Can. J. Fish. Aquat. Sci. **56**: 601–628.

Zimmerman, M. 2003. Calculation of untrawlable areas within the boundaries of a bottom trawl survey. Can. J. Fish. Aquat. Sci. **60**: 657–669.

Appendix A. Computational aspects.

To emphasize the simplicity of this analysis, the public software program R can be used with just three lines of code

© 2005 NRC Canada

(R Development Core Team 2003; available free from www.r-project.org) to assign trawls to fishing opportunities. We assume that an array X has been produced that has rows representing individual trawls and columns containing the start and end latitudes and longitudes in decimal degrees. We assume that longitudes have already been multiplied by cos(latitude) and the trawls reoriented to point northwards (these two steps can be trivially conducted in Microsoft® Excel). Given X, the following R code will produce a vector Y, which contains the number of the fishing opportunity that each trawl belongs to, at a cut point of 0.15.

```
distance <- dist(X, method="euclidean")
cluster.tree <- hclust(distance,
                       method="average")
Y <- cutree(cluster.tree, h=0.15)
```

In R, there is a limitation on the maximum number of trawls, n, that can be clustered (n = 5000 for computers with 512 megabytes of RAM). This limitation arises because the Euclidean distances must be calculated between each pair of trawls, thus requiring an intermediate triangular matrix of about $n^2/2$ elements to be kept in memory, i.e., in computer science terminology, the algorithm has $O(n^2)$ memory requirements. In most fisheries, this factor will not limit analyses for single vessels but can be a problem if the method is applied to the entire fleet. We suggest partitioning the trawls into groups before clustering. Partitioning algorithms exist that have $O(n)$ storage requirements, such as the K-means method (Hartigan and Wong 1979). This method was used by (He et al. 1997) to partition 46 961 longline sets into groups, before conducting a hierarchical cluster analysis on each of the groups. In R, it took less than 20 s to partition the British Columbia groundfish trawl fishery data (115 060 trawls) into 200 clusters, each containing <2500 trawls. The centroids of these partitions can be specified beforehand to divide the fishery into geographic regions.

References

Hartigan, J.A., and Wong, M.A. 1979. A K-means clustering algorithm. Appl. Stat. **28**: 100–108.

He, X., Bigelow, K.A., and Boggs, C.H. 1997. Cluster analysis of longline sets and fishing strategies within the Hawaii-based fishery. Fish. Res. **31**: 147–158.

R Development Core Team. 2003. R: a language and environment for statistical computing. R Foundation for Statistical Computing, Vienna, Austria.

© 2005 NRC Canada

Is metabolic rate a reliable predictor of growth and survival of brown trout (*Salmo trutta*) in the wild?

D. Álvarez and A.G. Nicieza

Abstract: In salmonids, there seems to be a positive correlation between standard metabolic rate and growth rate under artificial rearing conditions. Several recent studies have suggested that phenotypic correlations between physiological or behavioural traits and developmental or life history responses might be common when assayed in low-complexity habitats but rare in those with a high degree of spatiotemporal complexity. This study provides the first test of the connection between metabolic and growth rates of juvenile brown trout (*Salmo trutta*) in natural streams. In two out of four streams, there was no relationship between metabolic rates and subsequent growth, whereas in the two others, growth and metabolic rates were negatively correlated. Furthermore, survival rates were either unaffected or negatively correlated with metabolic rates. These results reveal complex relationships between metabolic rate, growth, and environmental variability and suggest that (*i*) in the wild, negative selection on high metabolic rates may result from both juvenile mortality and reduced growth rates, (*ii*) the conclusions derived from laboratory experiments are not directly applicable to natural populations, and (*iii*) the correlations between metabolic rate and growth can prove useful after selection of the appropriate spatial and temporal scales.

Résumé : Il semble exister chez les salmonidés une corrélation positive entre le taux de métabolisme standard et le taux de croissance dans les conditions artificielles d'élevage. Plusieurs études récentes laissent croire que les corrélations phénotypiques entre les caractéristiques physiologiques ou comportementales, d'une part, et les réactions du développement ou du cycle biologique, d'autre part, peuvent être communes dans les habitats à complexité réduite, mais rares dans ceux qui possèdent une complexité spatio-temporelle élevée. Notre étude fournit une première évaluation du lien entre les taux de métabolisme et de croissance chez de jeunes truites brunes (*Salmo trutta*) dans des cours d'eau naturels. Dans deux des quatre cours d'eau, il n'y a pas de relation entre les taux de métabolisme et la croissance subséquente, alors que dans les deux autres, il y a une corrélation négative entre les taux de croissance et de métabolisme. De plus, les taux de survie ne sont pas affectés par les taux de métabolisme ou alors ils sont liés par une corrélation négative. Ces résultats révèlent l'existence de relations complexes entre le taux de métabolisme, la croissance et la variabilité de l'environnement; ils indiquent que (*i*) en nature, la sélection négative des taux de métabolisme élevés peut être due tant à la mortalité juvénile qu'à la réduction des taux de croissance, (*ii*) les conclusions obtenues dans les expériences de laboratoire ne sont pas directement applicables aux populations naturelles et (*iii*) les corrélations entre le taux de métabolisme et la croissance peuvent s'avérer utiles une fois qu'on a choisi les échelles spatiales et temporelles appropriées.

[Traduit par la Rédaction]

Introduction

Rapid growth during larval and juvenile stages has multiple positive effects on fitness components (Roff 1992; Godin 1997; Sogard 1997). In fishes, higher growth rates are often associated with a larger body size, which in turn implies higher social status and competitive advantages (Harwood et al. 2002). One of the physiological traits most closely correlated with growth is the standard metabolic rate (SMR) (Priede 1985). There is evidence that intrapopulation variation in the onset of exogenous feeding can be associated with individual differences in metabolic rate (Metcalfe et al. 1995), and further, this could determine relationships between SMR and growth.

An exhaustive understanding of the link between metabolic and growth rates is important because a tight relationship between them would have applications in artificial selection for fast-growing genotypes or to characterize population life history. On the other hand, the causal paths between metabolism, social status, and growth remain obscure. The timing of the start of exogenous feeding seems to be correlated with fish dominance, and usually the fish that begin feeding earlier have greater competitive abilities than those initiating exoge-

Received 13 July 2004. Accepted 18 November 2004. Published on the NRC Research Press Web site at http://cjfas.nrc.ca on 14 April 2005.
J18220

D. Álvarez[1,2] and A.G. Nicieza. Unidad de Ecología, Departamento de Biología de Organismos y Sistemas, Universidad de Oviedo, E-33071 Oviedo, Spain.

[1]Corresponding author (e-mail: d.alvarez@bio.gla.ac.uk).
[2]Present address: Fish Biology Group, Division of Environmental and Evolutionary Biology, Graham Kerr Building, Institute of Biomedical and Life Sciences, University of Glasgow, Glasgow G12 8QQ, UK.

 doi: 10.1139/F04-223 © 2005 NRC Canada

Fig. 1. Schematic representation of the relationship between standard metabolic rate (SMR) and growth rate. Hypothetically, SMR might exert a direct effect on growth rate or an indirect effect through its influence on dominance and competitive ability (represented by the central chain). The net direct effect is the result of potential negative effects (costs of maintenance and collateral activity associated with high SMR) and positive effects (positive correlation between SMR and metabolic scope). Alternatively, a significant correlation between SMR and growth rate can arise if both of these are correlated with a third variable, even if there is no causal path between SMR and growth rate.

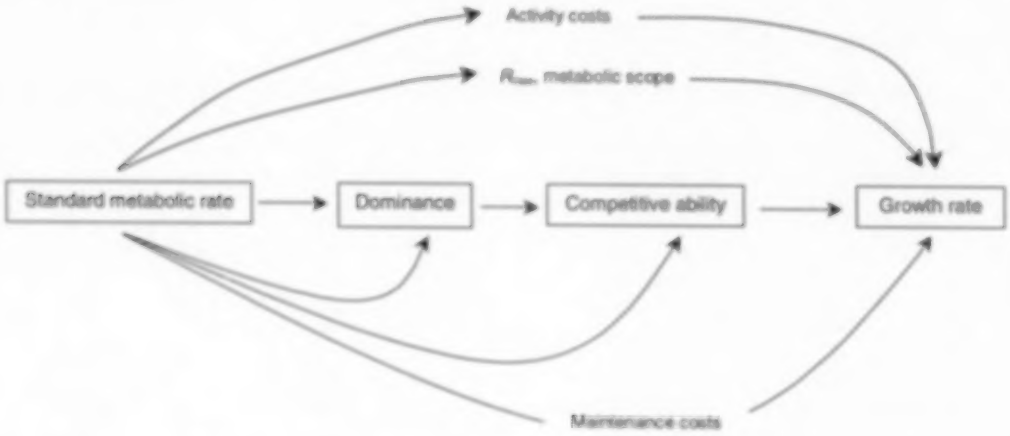

nous feeding later (Metcalfe and Thorpe 1992; Cutts et al. 2001). In addition, dominance could be mediated by priority effects, since those individuals who start feeding first also are the first ones to settle on the feeding grounds (O'Connor et al. 2000; Harwood et al. 2003*b*). These intermediate links make it difficult to know whether SMR has a direct influence on growth or, by contrast, the observed correlation is the product of a chain of effects (Fig. 1).

The potential influences of SMR on survival are less predictable. Assuming a positive effect of SMR on dominance and growth (Nakano 1995; Alanära et al. 2001), individuals with higher metabolic rates would have a greater chance of survival where competition for resources is intense. However, lower SMRs can be advantageous during periods of imposed inactivity and confer resistance to starvation and stressful conditions (Peters 1983; Harshman et al. 1999; Muller and Diamond 2001). Therefore, we could expect the effect that SMR can have on survival to be intrinsically context dependent.

The vast majority of studies examining the consequences of metabolic rates for fish growth were based on laboratory experiments where animals are maintained under a restricted set of environmental conditions and fed ad libitum (e.g., Metcalfe et al. 1995; Metcalfe 1998; Yamamoto et al. 1998). In most cases, these studies have evidenced significant positive correlations among dominance, metabolic rate, and growth (Metcalfe et al. 1995; Yamamoto et al. 1998). There is no doubt that artificial and natural environments differ in a series of important characteristics (Price 1999) that could determine how metabolic rates affect growth and survival (e.g., spatial structure, fish density, spatial and temporal distribution of food, or predation pressure). However, only a few studies have examined the relationship between dominance and growth in the wild and none between SMR and growth in the wild. The results advanced by field studies suggest very different outcomes from that observed in captivity. For example, activity and sex of juvenile Atlantic salmon (*Salmo salar*) explained a substantial part of the variance in growth rates, but there was not a significant correlation between dominance and growth (Martin-Smith and Armstrong 2002). Moreover, the links between size and social status and growth, well established in laboratory conditions, did not persist when the fish were released into their natural stream (Harwood et al. 2003*a*). This lack of a positive correlation between social status and growth in the wild may be explained by the spatiotemporal variability in resources, interspecific interactions, or the presence of predators (Harwood et al. 2003*a*). The aim of this paper was to investigate to what extent metabolic rate (SMR) can predict growth rate and survival of juvenile brown trout (*Salmo trutta*) in the wild.

Materials and methods

Juvenile trout (age 0+) were collected by electrofishing from Rivers Comeya, Orbiandi, Santianes, and Huerna. These rivers are located in the Cantabrian range, northern Spain (Table 1), and were sampled between 22 September and 10 November 1999 (Comeya, Orbiandi, and Santianes) and 18 December 2000 (Huerna). Fish were transferred to the laboratory and held under a natural photoperiod in 80-L tanks with dechlorinated tap water at 14.9 ± 0.1 °C. We selected this temperature because it is within the range of optimum temperatures for growth reported for this species in the study area (Ojanguren et al. 2001). All the tanks were provided with airstones to ensure oxygen saturation. Animals were allowed to acclimatize to laboratory conditions for 8 days prior to measuring metabolic rates. During that time, they were fed ad libitum with frozen chironomid larvae (MBF Bvba, Essen, Belgium). All of the fish fed actively within 24 h from arrival to the laboratory and no fish showed evident signs of stress (dark coloration, quietness, hyperventilation, lack of feeding motivation). The number of fish sampled from

© 2005 NRC Canada

Table 1. Location and physical characteristics of the study sections.

River	Location	Altitude (m above sea level)	Channel width (m)	Bedrock	Cover (%)	Summer discharge ($L \cdot s^{-1}$)
Orbiandi	43°16′N, 5°03′W	790	0.3–1.3	Calcareous	0–5	6.2
Comeya	43°17′N, 4°59′W	845	0.5–2.8	Calcareous	0	58.0
Santianes	43°25′N, 5°02′W	140	1.0–2.0	Siliceous	90–100	26.0
Huerna	43°01′N, 5°51′W	600	4.0–7.0	Calcareous	90–100	267.7

Table 2. Sample sizes and means ± 1 SD for size of the fish sampled for SMR and experimental conditions (flow through the chambers and temperature) during the respirometry trials.

Population	n	Fork length (mm)	Mass (mg)	Flow ($L \cdot h^{-1}$)	Temperature (°C)
Comeya	113	64.19±8.16	2519±957	0.39±0.09	14.8±0.3
Orbiandi	24	69.52±6.44	3263±1031	0.41±0.04	14.6±0.8
Santianes	50	63.59±6.63	2456±848	0.29±0.06	14.8±0.1
Huerna	160	66.32±9.32	2730±1160	0.35±0.05	14.8±0.1

each population varied between 24 and 173. Fish body size was similar in the four studied streams (Table 2).

Oxygen consumption rates

Measurement of oxygen consumption was conducted by flow-through respirometry. The system consisted of 20 replicate flow-through cylindrical chambers (15 mm × 100 mm) immersed in a water bath maintained at constant temperature (14.9 ± 0.1 °C) and supplied with oxygen-saturated water at the same temperature from a header tank. To measure metabolic rates, we placed single fish inside each of the 20 chambers. For each group, the flow rate of the water was adjusted to the average size of the fish (Table 2) to obtain at most a 20% reduction in the oxygen content of the water running through the chamber while maintaining a minimum flow to ensure a correct measurement of oxygen consumption (Steffensen 1989). The flow through each chamber was measured by weighing the amount of water (±0.001 g) dripping from the outflow during 120 s. After initial adjustment, the flow remained constant throughout each test. Water entering the chambers passed through an ultraviolet sterilizer, which prevented the oxygen levels from being reduced by bacterial respiration. In addition, we used a blank tube containing water but not fish. The difference in oxygen concentration between inflow and outflow water in this tube was negligible in all cases. To ensure complete gastric evacuation, we deprived all of the fish of food for 48 h prior to entering the chambers. Then, they were held for an additional 15-h acclimation period inside the chambers before measuring oxygen consumption. This ensured that the fish stabilized at a steady rate of oxygen consumption (Drud Jordan et al. 2001). The fish were kept in darkness and remained quiescent throughout the trials. The oxygen consumption of fish under these strict conditions is termed standard metabolic rate.

Oxygen saturation was measured using a microcathode oxygen electrode (model 1302) (Strathkelvin Instruments Ltd., Glasgow, Scotland) connected to an oxygen meter (model 781) (Strathkelvin Instruments Ltd.). Water samples (5 mL) were slowly drawn into a hypodermic syringe and injected into a thermostatted cell (MC 100) (Strathkelvin Instruments Ltd.) containing the oxygen electrode. The electrode was calibrated against air-saturated water (obtained from the header tank) and against a solution having zero oxygen saturation (sodium sulphite in 0.01 mol sodium tetraborate·L^{-1}). This protocol is widely used in studies on aquatic ectotherms (Metcalfe et al. 1995; McCarthy 2001; Butterworth et al. 2004). A respirometry run involved the sequential measurement of water samples from 20 individual fish, and trials involved three runs per group. This resulted in three measurements of SMR per individual fish. We conducted a fourth reading when any of the first three measures was abnormally high (e.g., as a consequence of fish moving during the measurement). In all cases, the coefficient of variation of the three measures used was less than 15%. The time between two consecutive tests for a single fish varied between 60 and 90 min, thus allowing for total renewal of the water in the chamber. All of the tests were conducted between 09:00 and 14:00 to control for potential influences of circadian variation. SMRs were calculated as

$$Vo_2 = V_w \Delta C_w$$

where Vo_2 (micrograms per hour) is the rate of oxygen consumption, V_w is the flow rate (litres per hour) of water through the chamber, and ΔC_w is the difference in oxygen concentration between the inflow and outflow water.

Growth rates and survival in the wild

The fish were measured for fork length (±0.01 mm) and mass (±0.1 g) and marked individually with biocompatible fluorescent elastomer (Visible Implant Elastomer, Northwest Marine Technology, Inc., Shaw Island, WA 98286) prior to releasing them into their natal streams. The trout from Rivers Comeya, Orbiandi, and Santianes were released within 10 days from the end of the respirometry trials. Huerna fish (n = 131) were released into a small tributary of River Huerna (Arroyo de la Foz, 42°59′N, 5°51′W, 1430 m above sea level). Because of ice cover and adverse meteorological conditions in the area, these fish were held in laboratory tanks until 19 April 2001. During the extended period of captivity, they were fed ad libitum with frozen chironomid larvae and salmonid fish food (Trouvit, TROUW ESPAÑA SA, energy content 17.66 kJ·g^{-1}) and used to provide an estimation of growth in an artificial environment. Growth rates in captivity were estimated for a single period of 90 days at a temperature

© 2005 NRC Canada

of 14.99 ± 0.1 °C. River Comeya was electrofished on two occasions: December 1999 (51 days from the time of release) and June 2000 (after 247 days). The experimental sections in Rivers Santianes and Orbiandi were sampled in March 2000 (148 days) and June 2000 (222 days), respectively. The Arroyo de la Foz was electrofished on 20 June 2001 (62 days). All the recaptured fish were measured, weighed, and then released at the capture sites. Comeya and Orbiandi are small source–sink rivers (i.e., these run underground upstream the "source" and downstream the "sink" points) containing closed populations. Downstream dispersal is physically possible in Arroyo de la Foz and River Santianes, but the experimental sections were located above large waterfalls that likely prevent high migration rates.

Data analysis

The relationship between SMR and growth rate was evaluated by regression analysis. The variable used to describe growth was the increase in body mass over a given period. Since the period over which growth was measured is the same for the fish captured at a given time in a particular river, the analyses based on total mass increments and those based on average daily increments provide the same results. Mass increments (ΔW) were calculated as the difference between final and initial wet mass ($W_f - W_i$). Both growth rates and metabolic rates can change with body mass. Therefore, mass increments were regressed on initial masses (W_i). SMRs were regressed on the body mass at the time of the respirometry trials, and the ensuing residuals of SMR (rSMR) and ΔW (rΔW) were used for the regression analyses. The relationships between survival rate and rSMR were examined by using χ^2 tests (Yates' correction for continuity applied) to compare the numbers of recaptured fish having positive and negative residuals. All analyses were done with the SPSS v.11.0.1 statistical package (SPSS Inc., Chicago, Illinois).

Results

River Comeya was sampled on December 1999 and June 2000. In December, a total of 21 fish (18.5%) were recaptured. There was a significant negative relationship between rSMR and growth (rΔW) over a 51-day period ($R^2 = 0.28$, $P = 0.015$, $n = 21$) (Fig. 2*a*). In June, the sample consisted of 26 fish, of which only five had been captured in December. In this case, there was no relationship between rSMR and rΔW ($R^2 = 0.006$, $P = 0.71$, $n = 26$) (Fig. 2*b*). Initial body mass did not explain a significant portion of the variance in mass increase either in December ($R^2 = 0.013$, $P = 0.39$, $n = 21$) or in June ($R^2 = 0.024$, $P = 0.21$, $n = 26$). At least, 42 fish could be categorized as alive after 51 days in the stream (21 of these were captured in June 2000 but not in December 1999). Seemingly, survival was related to size-corrected metabolic rate: 29 out of 42 fish had negative residuals, whereas only 13 with positive rSMR were recaptured ($\chi^2 = 5.35$, df = 1, $P = 0.02$). This bias increased when considering only the fish recaptured after 247 days (20 negative, six positive; $\chi^2 = 6.50$, d.f = 1, $P = 0.01$). There was no difference in initial size (mass at release) between recaptured and nonrecaptured trout (Mann–Whitney *U* test, $P = 0.96$, $n = 113$).

The rate of recapture in River Santianes was 24% ($n = 11$). The regression analysis indicated a negative significant relationship between rSMR and rΔW over a 148-day period ($R^2 = 0.37$, $P = 0.04$, $n = 11$) (Fig. 2*c*). In addition, mass gain was positively correlated with initial mass ($R^2 = 0.69$, $P = 0.0004$, $n = 11$). The ratio of negative to positive rSMR did not deviate significantly from the unity (seven negative versus four positive; $\chi^2 = 0.36$, df = 1, $P = 0.55$), and there was no difference in initial size between recaptured and nonrecaptured trout (Mann–Whitney *U* test, $P = 0.72$, $n = 50$).

In River Orbiandi, 9 out of 24 fish released were recaptured after 222 days. There was no significant relationship between rSMR and growth ($R^2 = 0.021$, $P = 0.70$, $n = 9$) (Fig. 2*d*), nor was survival rate dependent on rSMR ($\chi^2 = 1.78$, df = 1, $P = 0.18$). Again, there was no difference in initial size between recaptured and nonrecaptured trout (Mann–Whitney *U* test, $P = 0.49$, $n = 24$).

Fish from River Huerna showed different growth patterns in captivity and in the wild (Fig. 3). For the captivity period, the relationship between growth and SMR was positive and significant ($R^2 = 0.05$, $P = 0.010$, $n = 119$). However, there was no relationship between residual metabolic rate and growth over a 62-day period when returned to the stream ($R^2 < 0.001$, $P = 0.97$, $n = 37$). A total of 37 fish were recaptured (28%), and the number of individuals with negative residuals for SMR exceeded that with positive residuals (23 versus 14), but this ratio did not indicate that survival in the wild could be associated with metabolic rate ($\chi^2 = 1.73$, df = 1, $P = 0.19$). Growth in the stream was positively correlated with size at release ($R^2 = 0.35$, $P < 0.0005$, $n = 37$), and recaptured fish were larger than the rest of the group (Mann–Whitney *U* test, $P < 0.0005$, $n = 131$).

Fig. 2. Relationship between residuals of standard metabolic rate and residuals of mass increase in three wild populations of brown trout (*Salmo trutta*): (*a*) River Comeya (winter); (*b*) River Comeya (spring); (*c*) Rriver Santianes; (*d*) River Orbiandi.

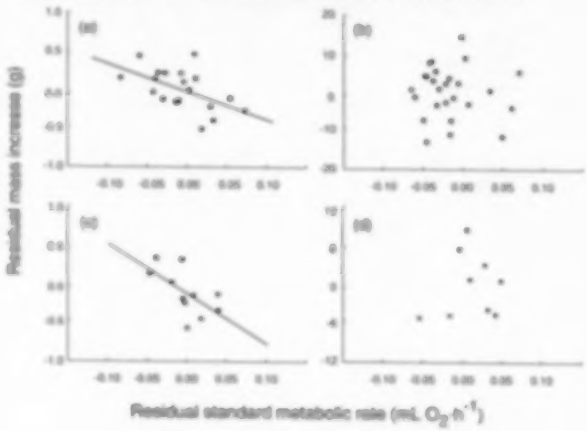

Discussion

This study provides the first analysis of the relationships between growth and SMR of brown trout in natural streams. The results presented here do not agree with previous laboratory studies that demonstrated a positive correlation between SMR and growth (e.g., Cutts et al. 1998; Huuskonen and Karjalainen 1998; Yamamoto et al. 1998). In two rivers, there was no correlation between growth and metabolic

© 2005 NRC Canada

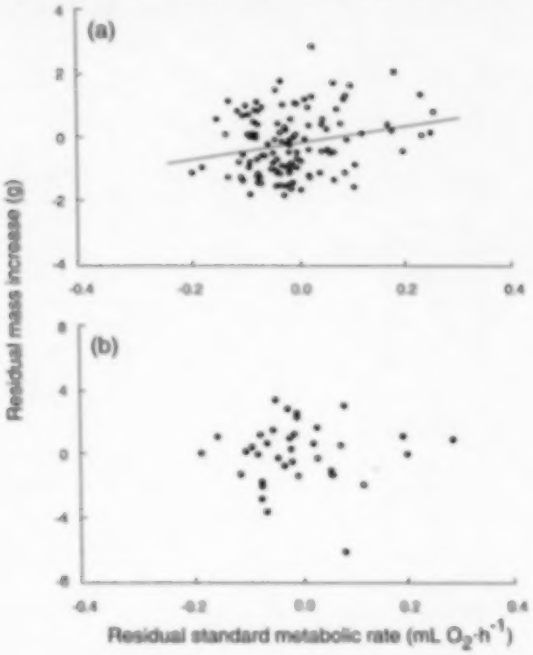

Fig. 3. Relationship between residuals of standard metabolic rate and residual mass increase of juvenile brown trout (*Salmo trutta*) from River Huerna (*a*) in captivity and (*b*) in the wild.

rates, whereas in two others, there was a negative correlation, suggesting that fish with relatively low metabolic rates could grow faster than fish with higher rates in a variety of situations. Similarly, survival rates were either unaffected or negatively affected by increasing metabolic rates.

In general, it is assumed that there is a positive correlation between basal or maintenance metabolic rates and dominance or social status (Röskaft et al. 1986; Metcalfe et al. 1995; McCarthy 2001). In addition, there is evidence that dominant individuals grow faster than subordinates under laboratory conditions (Li and Brocksen 1977; Metcalfe et al. 1989) and in the wild (Nakano 1995; Höjesjö et al. 2002). Nevertheless, these results contrast with a number of studies conducted in natural or near-natural streams that report a lack of correlation between growth and dominance (Cutts et al. 2001; Martin-Smith and Armstrong 2002; Harwood et al. 2003*a*), and this may be due to an energetic cost of dominance (Röskaft et al. 1986; Bryant and Newton 1994). In fact, the costs associated with high aggression rates could offset the increased food intake associated with a higher competitive ability (Cutts et al. 2001) and nonaggressive fish can grow as fast as dominants (Höjesjö et al. 2002; also see Vøllestad and Quinn 2003). Also, the relationship between dominance and growth rate can be weak or reverse under conditions of high spatiotemporal variability in resources and high habitat complexity (Martin-Smith and Armstrong 2002; Harwood et al. 2003*a*).

Seemingly, trout with higher SMRs did not have higher survival. Rather, it seems that under some circumstances, fish with relatively low SMR can have a greater life expectancy. The relationship between recapture rate and SMR in River Comeya may reveal selective mortality of the fish with higher metabolic rates over the winter season. It should be pointed out that here, we used a correspondence between recapture rate and survival rate and this ignores potential emigration from the study sections. However, there is no reason to expect a serious bias, since this stream contains a closed population due to the existence of a sink from which the river flows underground and because most juvenile fish remain within the same area for the first two years of life (D. Álvarez and A.G. Nicieza, unpublished data). There are several possible scenarios under which natural selection might hamper fish with high SMRs. First, selection for reduced metabolic rates may be strong where resources are limiting or the environmental conditions are stressful (Harshman et al. 1999; Mueller and Diamond 2001). During periods of potential nutritional stress (such as winter or drought episodes), fish with higher SMRs will face a higher risk of exhausting energy reserves than individuals with lower energetic requirements for subsistence. Similarly, an eventual fall in oxygen levels will kill those individuals with the highest SMRs first. Second, high-SMR individuals are often high-status or highly aggressive fish (Metcalfe et al. 1995; Cutts et al. 2001; D. Álvarez, A.G. Nicieza, and J. Östergren, unpublished data). Both defense of the top hierarchy and intrinsic aggressiveness seem to be concomitant with the risk of injury and significant costs in terms of either energy expended during agonistic contests or loss of feeding opportunities (Turnbull et al. 1998; Nicieza and Metcalfe 1999; Harwood et al. 2002). Therefore, the costs of being aggressive can indirectly generate negative relationships between metabolic rate and growth or survival rate. Third, predation risk can reduce the level of agonistic interactions and thereby the strength of social hierarchies, thus allowing subordinate individuals to gain access to more profitable feeding sites (Reinhardt 1999), and environmental perturbations such as spates and droughts could play a similar role in destabilizing social hierarchies (Sloman et al. 2001). Thus, the positive relationship between growth and metabolic rates under conditions of high environmental stability may not translate to small rivers where severe changes in water levels are frequent and predation pressure can be intense.

All of the experimental sections used in this study were located in very small brooks that are seemingly exposed to great levels of temporal variation in environmental conditions. For instance, because of their small water bodies and absence of cover, in Orbiandi and Arroyo de la Foz, temperature can change up to 10 °C within 6 h during summer. Comeya lacks cover, but its larger size and underground sources prevent such large fluctuations. Drought effects can be severe in Santianes and, especially, Orbiandi because of either direct mortality associated with drying of the lower sections or reduced food availability. Predation on fry and young-of-the-year fish may be eventually important in Comeya and Orbiandi owing to the existence of large cannibalistic trout in these streams but not in Santianes and Arroyo de la Foz. It seems clear that these conditions can exert a strong influence on survival, which could explain the higher survival expectations of individuals with relatively low metabolic rates in Comeya. Such a tendency was not seen in Orbiandi, but this could be due to a reduced sample size.

In two rivers (Comeya and Santianes), we found a negative correlation between rSMR and growth. A possible inter-

© 2005 NRC Canada

pretation of this result is that the spatiotemporal variation in resources and environmental conditions characteristic of small rivers could be responsible for a breakdown of the chain of links (e.g., dominance, competitive ability) connecting SMR and growth rate. Even so, if metabolic scopes were positively correlated with SMRs (e.g., Priede 1985), one should expect a positive effect on growth. Therefore, the data presented here suggest that, in natural conditions, the energetic costs of maintenance and collateral activities (e.g., fighting, exploratory behaviour, territoriality) may offset or reverse the potential benefits of a high rSMR. Furthermore, the fact that the significant correlation observed in Comeya disappeared during the second growing season and the fact that the other significant negative correlation (Santianes) was evidenced before the onset of the most favourable period for growth reveal that there is not a predictable trend or that the influence of metabolic rate on growth can be predictable but seasonally variable.

The dichotomy between natural and low-complexity human-made environments was patent when comparing the growth of the same fish in hatchery tanks (positive correlation between SMR and growth) and after release in Arroyo de la Foz (SMR and growth uncorrelated). The positive correlation between growth and metabolic rate of the fish from River Huerna during the captivity period supports the results obtained in previous studies (Cutts et al. 1998; Huuskonen and Karjalainen 1998; Yamamoto et al. 1998). Strikingly, this relationship vanished when the same fish were released in the wild. The unpredictability of resources is one of the factors that may disrupt the relationship between growth and dominance in Atlantic salmon (Harwood et al. 2003*a*). In artificial environments, unlimited and spatially predictable resources may confer a clear competitive advantage for fish with the higher metabolic rates because energy is available in excess to maintain their high energetic requirements. In artificial environments, the relationship between dominance and growth depends on the availability and predictability of the food sources (Metcalfe and Thorpe 1992; Huntingford and García de Leániz 1997).

Our results suggest, therefore, that the relationship between SMR and growth is mainly determined by the variability of the environment. If the spatial distribution of resources is predictable, individuals with a high basal metabolism will benefit from resource monopolization, regardless of whether resources are abundant or reduced, and will grow faster than low-SMR fish (Metcalfe and Thorpe 1992; Huuskonen and Karjalainen 1998; Yamamoto et al. 1998). If resources are predictable, but either too scant (i.e., even dominant individuals have a negative energetic balance) or abundant and homogeneously distributed (i.e., absence of competition), dominance costs are expected to overcome benefits, and subordinate, low-SMR individuals will grow faster. Finally, if the spatial and temporal distribution of resources is unpredictable, the superior competitive availability of high-SMR individuals, if any, does not translate into a greater energy intake compared with low-SMR individuals, whereas the higher costs that they incur will redound in slower growth rates (Martin-Smith and Armstrong 2002; Harwood et al. 2003*a*). The main conclusion emerging from this study is that SMR cannot be used as a general predictor of growth or survival in the wild. However, the results suggest that SMR could be a reliable predictor of growth rate on a local scale or when growth is measured over short (i.e., within-season) time intervals. Additional research will be required to confirm this possibility.

Acknowledgements

We thank the staff of Picos de Europa National Park and Dirección General de Recursos Naturales y Protección Ambiental (Principau d'Asturies) for providing authorization to work in the study rivers and especially Mario Quevedo, Felipe Reyes-Gavilán, Ataulfo Martínez, and Antón Fernández for their assistance in field work. Two anonymous reviewers provided useful comments on an earlier version of the manuscript. This study was funded by contracts FAIR-CT95-0009 and FAIR-CT97-3498 and grant MCYT-AGL2000-3181-CE.

References

Alanärа, A., Burns, M.D., and Metcalfe, N.B. 2001. Intraspecific resource partitioning in brown trout: the temporal distribution of foraging is determined by social rank. J. Anim. Ecol. **70**: 980–986.

Bryant, D.M., and Newton, A.V. 1994. Metabolic costs of dominance in dippers, *Cinclus cinclus*. Anim. Behav. **48**: 447–455.

Butterworth, K.G., Grieshaber, M.K., and Taylor, A.C. 2004. Behavioural and physiological responses of the Norway lobster, *Nephrops norvegicus* (Crustacea: Decapoda), to sulphide exposure. Mar. Biol. **144**: 1087–1095.

Cutts, C.J., Metcalfe, N.B., and Taylor, A.C. 1998. Aggression and growth depression in juvenile Atlantic salmon: the consequences of individual variation in standard metabolic rate. J. Fish Biol. **52**: 1026–1037.

Cutts, C.J., Adams, C.E., and Campbell, A. 2001. Stability of physiological and behavioural determinants of performance in Artic char (*Salvelinus alpinus*). Can. J. Fish. Aquat. Sci. **58**: 961–968.

Drud Jordan, A., Jungersen, M., and Steffensen, J.M. 2001. Oxygen consumption of East Siberian cod: no support for the metabolic cold adaptation theory. J. Fish Biol. **59**: 818–823.

Godin, J-G.J. 1997. Behavioural ecology of teleost fishes. Oxford University Press, Oxford, UK.

Harshman, L.G., Hoffmann, A.A., and Clark, A.G. 1999. Selection for starvation resistance in *Drosophila melanogaster*: physiological correlates, enzyme activities and multiple stress responses. J. Evol. Biol. **12**: 370–379.

Harwood, A.J., Armstrong, J.D., Griffiths, S.W., and Metcalfe, N.B. 2002. Sympatric association influences within-species dominance relations among juvenile Atlantic salmon and brown trout. Anim. Behav. **64**: 85–95.

Harwood, A.J., Armstrong, J.D., Metcalfe, N.B., and Griffiths, S.W. 2003*a*. Does dominance status correlate with growth in wild stream-dwelling Atlantic salmon (*Salmo salar*)? Behav. Ecol. **14**: 903–908.

Harwood, A.J., Griffiths, S.W., Metcalfe, N.B., and Armstrong, J.D. 2003*b*. The relative influence of prior residence and dominance on the early feeding behaviour of juvenile Atlantic salmon. Anim. Behav. **65**: 1141–1149.

Höjesjö, J., Jonhsson, J.I., and Bohlin, T. 2002. Can laboratory studies on dominance predict fitness of young brown trout in the wild? Behav. Ecol. Sociobiol. **52**: 102–108.

© 2005 NRC Canada

Huntingford, F.A., and García de Leániz, C. 1997. Social dominance, prior residence and the acquisition of profitable feeding sites in juvenile Atlantic salmon. J. Fish Biol. **51**: 1009–1014.

Huuskonen, H., and Karjalainen, J. 1998. A preliminary study on the relationships between otolith increment width, metabolic rate and growth in juvenile whitefish (*Coregonus lavaretus* L.). Arch. Hydrobiol. **142**: 371–383.

Li, H.W., and Brocksen, R.W. 1977. Approaches to the analysis of energetic cost of intraspecific competition for space use by rainbow trout (*Salmo gairdneri*). J. Fish Biol. **11**: 329–341.

Martin-Smith, K.M., and Armstrong, J.D. 2002.Growth rates of wild stream-dwelling Atlantic salmon correlate with activity and sex but not dominance. J. Anim. Ecol. **71**: 413–423.

McCarthy, I.D. 2001. Dominance and competitive ability are related to metabolic asymmetry in juvenile rainbow trout. J. Fish Biol. **59**: 1002–1014.

Metcalfe, N.B. 1998. The interaction between behaviour and physiology in determining life history patterns in Atlantic salmon. Can. J. Fish. Aquat. Sci. **55**(Suppl. 1): 93–103.

Metcalfe, N.B., and Thorpe, J.E. 1992. Anorexia and defended energy levels in over-wintering juvenile salmon. J. Anim. Ecol. **61**: 175–181.

Metcalfe, N.B., Huntingford, F.A., Graham, W.D., and Thorpe, J.E. 1989. Early social staus and the development of life-history strategies in Atlantic salmon. Proc. R. Soc. Lond. B Biol. Sci. **236**: 7–19.

Metcalfe, N.B., Taylor, A., and Thorpe, J.E. 1995. Metabolic rate, social status and life-history strategies in Atlantic salmon. Anim. Behav. **49**: 431–436.

Mueller, P., and Diamond, J. 2001. Metabolic rate and environmental productivity: Well-provisioned animals evolved to run and idle fast. Proc. Natl. Acad. Sci. U.S.A. **98**: 12 550 – 12 554.

Nakano, S. 1995. Individual differences in resource use, growth and emigration under the influence of a dominance hierarchy in fluvial red-spotted masu salmon in a natural habitat. J. Anim. Ecol. **64**: 75–84.

Nicieza, A.G., and Metcalfe, N.B. 1999. Cost of rapid growth: risk of aggression is high for fast-growing salmon. Funct. Ecol. **13**: 793–800.

O'Connor, K.I., Metcalfe, N.B., and Taylor, A.C. 2000. The effects of prior residence on behaviour and growth rates in juvenile Atlantic salmon (*Salmo salar*). Behav. Ecol. **11**: 13–18.

Ojanguren, A.F., Reyes-Gavilán, F.G., and Braña, F. 2001. Thermal sensitivity of growth, food intake and activity of juvenile trout. J. Therm. Biol. **26**: 165–170.

Peters, R.H. 1983. The ecological implications of body size. Cambridge University Press, Cambridge, UK.

Price, E.O. 1999. Behavioral development in animals undergoing domestication. Appl. Anim. Behav. Sci. **65**: 245–271.

Priede, I.G. 1985. Metabolic scope in fishes. *In* Fish energetics: new perspectives. *Edited by* P. Tytler and P. Calow. Croom Helm, London, UK. pp. 33–64.

Reinhardt, U.G. 1999. Predation risk breaks size-dependent dominance in juvenile coho salmon (*Oncorhynchus kisutch*) and provides growth opportunities for risk-prone individuals. Can. J. Fish. Aquat. Sci. **56**: 1206–1212.

Roff, D.A. 1992. The evolution of life histories — theory and analysis. Chapman and Hall, London, UK.

Röskaft, E., Järvi, T., Bakken, M., Bech, C., and Reinertsen, R.E. 1986. The relationship between social status and resting metabolic rate in great tits (*Parus major*) and pied flycatchers (*Ficedula hypoleuca*). Anim. Behav. **34**: 838–842.

Sloman, K.A., Taylor, A.C., Metcalfe, N.B., and Gilmour, K.M. 2001. Effects of an environmental perturbation on the social behaviour and physiological function of brown trout. Anim. Behav. **61**: 325–333.

Sogard, S.M. 1997. Size-selective mortality in the juvenile stage of teleost fishes: a review. Bull. Mar. Sci. **60**: 1129–1157.

Steffensen, J.F. 1989. Some errors in respirometry of aquatic breathers: how to avoid and correct for them. Fish Physiol. Biochem. **6**: 49–59.

Turnbull, J.F., Adams, C.E., Richards, R.H., and Robertson, D.A. 1998. Attack site and resultant damage during aggressive encounters in Atlantic salmon (*Salmo salar*) parr. Aquaculture, **159**: 345–353.

Vøllestad, L.A., and Quinn, T.P. 2003. Trade-off between growth rate and aggression in juvenile coho salmon, *Oncorhynchus kisutch*. Anim. Behav. **66**: 561–568.

Yamamoto, T., Ueda, H., and Higashi, S. 1998. Correlation among dominance status, metabolic rate and otolith size in masu salmon. J. Fish Biol. **52**: 281–290.

© 2005 NRC Canada

Habitat-specific biomass, survival, and growth of rainbow trout (*Oncorhynchus mykiss*) during summer in a small coastal stream

Bret C. Harvey, Jason L. White, and Rodney J. Nakamoto

Abstract: We observed significant habitat-scale variation in the density, survival, and growth of 811 passive integrated transponder tagged rainbow trout (*Oncorhynchus mykiss*) enclosed for 63–68 days at natural density in 59 individual habitats (pools and riffles) in a small coastal California stream in summer 2001. The initial habitat-scale densities of trout were positively related to both depth and cover, although by the end of the experiment, the influence of cover on density was less apparent. Survival varied substantially, but with no clear relationship to any of the physical factors that we measured. Mean growth was density dependent, positively influenced by habitat depth, and also increased downstream within the 2-km study reach. The overall change in trout biomass over the experiment was also negatively related to fish density and positively influenced by habitat depth. Individual growth within habitats appeared to be unrelated to body size. The positive influences of water depth and distance downstream on trout growth in this experiment suggest that management actions that increase dry season discharge and limit aggradation will benefit salmonids in small streams.

Résumé : Il existe à l'échelle de l'habitat une variation significative de la densité, de la survie et de la croissance chez 811 truites arc-en-ciel (*Oncorhynchus mykiss*) munies d'étiquettes PIT (transpondeurs intégrés passifs) placées pour 63–68 jours à des densités naturelles dans 59 habitats individuels (profonds et rapides) dans un petit cours d'eau de la côte californienne durant l'été 2001. À l'échelle de l'habitat, la densité initiale des truites est en corrélation positive à la fois avec la profondeur et les abris, bien que vers la fin de l'expérience l'influence des abris sur la densité ait été moins apparente. La survie varie considérablement, sans qu'il n'y ait de relation claire avec aucun des facteurs physiques que nous avons mesurés. La croissance moyenne est reliée à la densité, elle est influencée positivement par la profondeur de l'habitat et elle augmente vers l'aval dans la zone d'étude de 2 km. Le changement global de biomasse des truites durant l'expérience est en relation négative avec la densité et en relation positive avec la profondeur de l'habitat. La croissance individuelle dans chacun des habitats ne semble pas reliée à la taille. Les effets positifs de la profondeur de l'eau et de la distance vers l'aval sur la croissance des truites dans notre expérience laissent croire que, dans la gestion des petits cours d'eau, les actions qui favorisent l'augmentation du débit pendant la saison sèche et limitent l'alluvionnement sont bénéfiques aux saumons.

[Traduit par la Rédaction]

Introduction

Both resource managers and fish ecologists seek greater ability to predict the effects of changes in habitat on the population dynamics of stream fishes. Although knowledge of the distribution of fish among habitat types is useful in addressing this issue, the effort to predict the population-level consequences of habitat changes will benefit from a clearer understanding of the habitat-specific rates of key processes that affect population dynamics, such as survival and growth rates. These rates are likely to be site and taxon specific. While valuable data on the habitat-specific survival and growth of stream salmonids have been collected (e.g., Lonzarich and Quinn 1995; Kruzic et al. 2001; Rosenfeld and Boss 2001), further efforts to quantify habitat-specific vital rates should be very useful in building and evaluating predictive models linking habitat availability and population dynamics.

One complicating consideration in measuring habitat-specific survival and growth is their likely density dependence. Although habitat selection typically results in unequal densities of fish among habitat types, to date, most relevant studies have contrasted survival and growth among habitat types using constant fish densities (e.g., Lonzarich and Quinn 1995; Kruzic et al. 2001; Rosenfeld and Boss 2001). Measuring the survival and growth of fish at natural habitat-specific densities should provide useful complementary information, particularly for spatially explicit models that in-

Received 10 April 2004. Accepted 19 November 2004. Published on the NRC Research Press Web site at http://cjfas.nrc.ca on 14 April 2005.
J18067

B.C. Harvey,[1] J.L. White, and R.J. Nakamoto. USDA Forest Service, Pacific Southwest Research Station, 1700 Bayview Drive, Arcata, CA 95521, USA.

[1]Corresponding author (email: bch3@humboldt.edu).

 doi: 10.1139/F04-225 © 2005 NRC Canada

clude habitat selection by individual fish (e.g., Railsback and Harvey 2002). Such models appear particularly well suited to predicting the consequences of habitat changes for fish population dynamics. Documenting patterns in the distribution, survival, and growth of fish at a relatively fine spatial scale should be useful in evaluating these models by examining their ability to reproduce the patterns.

In this study, we quantified the habitat-specific natural distribution, survival, and growth of rainbow trout (*Oncorhynchus mykiss*) in a small coastal stream, with the objective of relating these variables to the physical characteristics of individual habitats. In selecting models to fit the data for survival and growth, we focused on the significance of water depth and cover (reviewed by Allouche 2002) and initial biomass (Keeley 2001). Finally, our experimental approach allowed examination of the relationship between body size and individual growth within habitat units, which has varied in previous studies of stream salmonids (Nakano et al. 1991; Martin-Smith and Armstrong 2002; Harwood et al. 2003). Greater understanding of this variation should also inform current efforts to link habitat characteristics and fish population dynamics using individual-based models.

Materials and methods

Study site

Jacoby Creek drains into Humboldt Bay in northwestern California. The 2-km study reach for this research lies within the Arcata City Forest in the upper drainage (watershed area 10 km^2 at the top of the reach and 15 km^2 at the bottom) at an elevation of ~250 m. The active stream channel in the reach averages about 4 m wide and alternates between shallow riffles and moderately deep pools (maximum depth ~1.5 m) over gravel and cobble substrate. Except for one bedrock-confined section, the gradient in the reach rarely exceeds 2%.

The climate of the region produces wet winters (mean annual rainfall >120 cm) and dry summers. US Geological Survey gage data over about 9 years (1955–1964) yielded average discharge at the bottom of the study reach of 0.90 $m^3 \cdot s^{-1}$ in winter and <0.05 $m^3 \cdot s^{-1}$ in summer. Annual maximum discharge averaged about 10 $m^3 \cdot s^{-1}$ for the same period. Turbidity can exceed 1000 nephelometric turbidity units (NTU) during storms and averages 35 NTU in winter and <5 NTU in summer. Water temperature ranges 7–12 °C in winter and 9–14 °C in summer. During this experiment (mid-July to late September), water temperature averaged 12.2 °C at the upper end of the study reach and 11.9 °C at the bottom.

Coast redwood (*Sequoia sempervirens*) and Douglas-fir (*Pseudotsuga menziesii*) constitute the majority of the forest cover in the watershed, although red alder (*Alnus rubra*) and bigleaf maple (*Acer macrophyllum*) dominate much of the riparian zone. Stink currant (*Ribes bracteosum*), western elderberry (*Sambucus cerulea*), and thimbleberry (*Rubus parviflorus*) preponderate in the riparian understory.

The study reach lies upstream of several natural barriers to upstream passage of fish. The reach contains an unexploited, naturally reproducing population of rainbow trout, the only fish species present. Coastal giant salamanders (*Dicamptodon tenebrosus*), tailed frog tadpoles (*Ascaphus truei*), and red-legged frog tadpoles (*Rana aurora*) complete the aquatic vertebrate assemblage.

Experiment setup and analysis

In mid-July 2001, we selected 59 experimental units to cover the range of available habitats in the study reach. The experiment included 29 complex pools (pools with moderate to extensive cover, including two pools dominated by logjams), 17 simple pools (pools with little or no cover), and 13 riffles (including one unique 48-m-long, high-gradient section) — about half the habitats in the reach. We enclosed each unit by blocking the upstream and downstream boundaries with plastic fencing (6-mm mesh) buried at least 10 cm in the substrate and supported by metal stakes. For pools, we included approximately 1.5 m of the upstream riffle in the fenced area to provide fish full access to the inflow. Overall, units averaged 18 m in length (range 7–48 m) and 66 m^2 in area (range 21–215 m^2).

After completing the fencing, we captured fish naturally occurring in each unit using multiple-pass electrofishing. We recorded wet mass to the nearest 0.01 g and fork length (FL) to the nearest millimetre and inserted a passive integrated transponder (PIT) tag in each fish >75 mm FL. We chose the 75-mm threshold for tagging to minimize tag-related mortality and because fish ≤ 75 mm were rare. Following measurement and tagging, fish were released back into the unit. Aside from crews visiting the units once or twice each week to clean debris from the fences, fish remained undisturbed for the next 63–68 days. To complete the experiment in late September 2001, we again employed multiple-pass electrofishing in the experimental units to recapture surviving fish. To evaluate electrofishing efficiency at the end of the experiment, we captured fish in 23 of the units and held them in net boxes overnight and then resampled the units the following day.

Response variables analyzed included experimental-unit-specific measures of initial and final biomass, survival, mean growth, maximum growth, and change in biomass. Maximum growth refers to the highest growth rate by an individual within an experimental unit. These estimates excluded age-0 fish because they were sampled inefficiently at the start of the experiment and some were small enough to pass through enclosure fences. We also analyzed biomass, survival, and growth variables for the subset of fish that we estimated had a high probability of being mature (individuals ≥130 mm FL). We quantified fish biomass as grams per metre of stream length to focus on the amount of stream network occupied. Also, because post-age-0 salmonids in streams rarely occupy shallow habitat with low water velocity, we anticipated that depth and flow characteristics in wide units would not lead to significant increases in useable habitat at the relatively low discharges during the experiment. Survival was estimated as the proportion of tagged fish remaining at the end of the experiment. Mass data from recaptured tagged fish allowed calculation of mean specific growth rate ($SGR = [(\ln M_t - \ln M_0)/t] \times 100$, where M_t is the final mass (grams), M_0 is the initial mass, and t is the growth period (days)).

To calculate initial and final biomass, we needed to incorporate estimates for fish that we did not capture during electrofishing; this required several steps. To estimate the

© 2005 NRC Canada

number of fish in a unit at the start of the experiment, we divided the total catch at the start by the proportion of tagged fish in the catch at the end of the experiment (a measure of our efficiency at the start). Initial biomass was estimated by multiplying the estimated number of uncaught fish at the start by the mean mass for a given unit and adding that value to the biomass of captured fish. To estimate the number of fish in a unit at the end of the experiment, we used the information from the 23 units that we electrofished on consecutive days to calculate a mean bias for the single-day, multiple-pass depletion estimates for each of three habitat types (complex pool, simple pool, and riffle). We assumed that total catch after 2 days of sampling in the 23 units reflected the actual number of fish in those units. We then adjusted the depletion estimates from the units sampled on only one day by the appropriate habitat-type specific bias estimate calculated from collections over 2 days, multiplied the estimated number of uncaught fish by the mean mass for a given unit, and added that value to the measured mass to produce an estimate of the total biomass at the end of the experiment.

To describe physical conditions in each unit, we measured cover and depth at a minimum of 50 points located every 0.5 m along 5–10 equally spaced transects. We measured cover using methods similar to those described in Kinsolving and Bain (1990): We counted the number of submerged object surfaces in a 0.5-m-wide cross-sectional cell centered on each sampling point. Solid objects ≥10 cm in any cross-sectional dimension and >3 cm from the stream substrate (woody debris and unembedded boulders and cobbles) were considered three surfaces. Objects ≥10 cm that did not provide overhead cover for fish (e.g., embedded boulders) and objects <10 cm in any cross-sectional dimension but >3 cm from the substrate were considered single surfaces. A cell with fine substrate and no larger objects was considered to have zero surfaces. From these data, we computed the proportion of 0.5-m-wide cells with ≥1 surface (cover density) and the mean of the nonzero values (cover complexity) for each unit. We used the product of cover density and cover complexity to quantify an index of cover availability. Because of its particular significance as a component of fish habitat in many forested watersheds, we also measured the area of each unit containing large woody debris (>10 cm in diameter) and expressed this area as a percentage of the total area of the unit for the analyses. To summarize the depth data, we computed the proportion of the points in each unit where depth exceeded 20 cm (depth > 20). We used this measure because previous studies indicate that 20 cm is a meaningful threshold for predation risk for stream fish from wading and diving predators (e.g., Power 1984).

We analyzed the data by constructing linear regression models with initial biomass, survival, mean growth, maximum growth, biomass accrual, and ending biomass as separate dependent variables. Depth > 20, the cover index, and the longitudinal position of the experimental units in the study reach were included as independent variables in all analyses. The longitudinal position of the experimental units was included because of previous observations that stream position can affect the distribution and growth of salmonids (e.g., Harvey 1998). The initial log-transformed fish biomass in the experimental units was included in the analyses of survival, growth, and biomass accrual because the density dependence of survival and growth in stream salmonids has been observed previously (Keeley 2001). The set of candidate models for each response variable included all combinations of the three or four independent variables outlined above. Thus, each independent variable was included in the same number of candidate models in the analysis of a given response variable. We also conducted exploratory analyses that included the area of large woody debris as an independent variable, with an emphasis on contrasting results from models with the amount of large woody debris versus the cover index as independent variables.

We evaluated the sets of candidate models developed for each response variable using Akaike's information criterion adjusted for small sample sizes (AIC_c), as suggested by Burnham and Anderson (2002). Models within two AIC units of the best approximating model were considered worthy of consideration. We assessed the importance of individual independent variables by summing the Akaike weights (w_i) of all candidate models that included a given variable (Burnham and Anderson 2002). Akaike weights quantify the evidence that a given model is the best approximating model, assuming that the best approximating model is among the candidate models. We assumed equal prior probabilities for all candidate models in calculating Akaike weights.

The experiment also provided data that allowed us to quantify relationships between body size and growth rate. Both specific growth rate and absolute growth rate (grams per day) were used as measures of growth. We included the second measure to provide comparability with several previous measurements of growth variation among individual stream salmonids (Nakano et al. 1991; Nakano 1995; Armstrong et al. 1999). Also to provide comparability with previous studies, we limited the analysis to experimental units where we recaptured 4–12 individuals. We modeled individual growth as a function of the experimental unit occupied and the log(rank) of individuals within the units, with fish rank assigned in descending order of initial mass. Previous observations have often revealed strong correspondence between body size and dominance status in salmonids (e.g., Nakano 1995).

Results

At the start of the experiment, we captured and tagged a total of 811 fish from 56 of the 59 experimental units and none from the other three. We estimated that 82% of the fish in the experimental units were captured at the start of the experiment and 99% at the end. Taking initial capture efficiencies into account, the unit-specific initial density estimates averaged three fish greater than the total catch for the 56 units where we captured fish. At the end of the experiment, the final density estimate equaled the final catch for all but nine units. Excluding age-0 fish from the analyses probably did not strongly influence results, as age-0 fish constituted only 4% of total fish biomass at the end of the experiment. Final biomass ranged 0–61 $g \cdot m^{-1}$ or 0–17 $g \cdot m^{-2}$. The upper end of this range corresponded to 0.9 $fish \cdot m^{-2}$ and a percent habitat saturation (Grant et al. 1998) of 90%. The three independent physical variables that we focused on for the analyses were not highly correlated (depth > 20 and cover index, $r = 0.23$,

© 2005 NRC Canada

Fig. 1. Best-approximating model of mid-July rainbow trout (*Oncorhynchus mykiss*) biomass in habitats of Jacoby Creek in summer 2001 from a set of candidate models that included all combinations of water depth, cover availability, and the position of the units in the 2-km study reach.

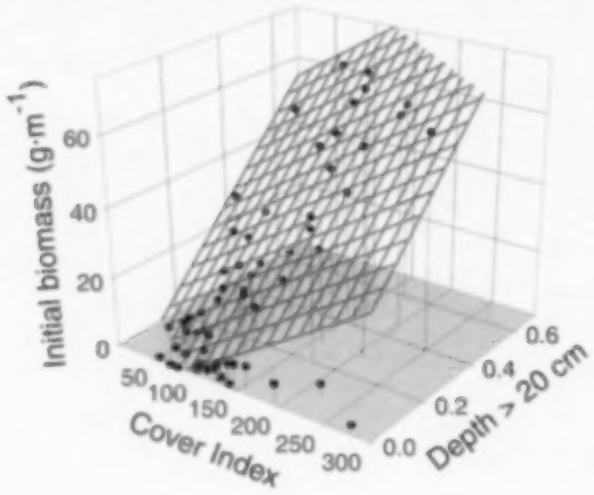

Fig. 2. Best-approximating model of final (late September) rainbow trout (*Oncorhynchus mykiss*) biomass in habitats of Jacoby Creek enclosed for 63–68 days. While the best-approximating model contains only a positive relationship with habitat depth, the relationship is graphed in three dimensions to facilitate comparison with Fig. 1.

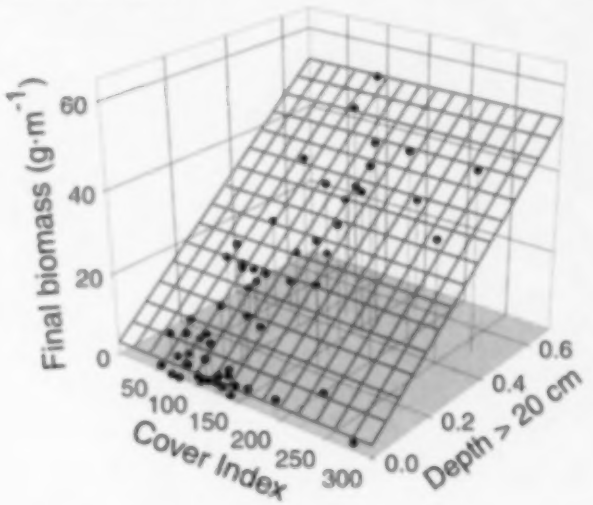

$p = 0.09$; depth > 20 and position in the reach, $r = -0.04$, $p = 0.75$; cover index and position in the reach, $r = -0.21$, $p = 0.12$). As expected, the cover index and the area of large woody debris (as a percentage of total area) were relatively strongly correlated ($r = 0.59$). The area of large woody debris was also correlated with depth ($r = 0.51$) but unrelated to position in the reach ($r = 0.05$).

Depth > 20 and cover index both positively influenced the initial biomass of trout in the experimental units, and both factors contributed to the best-approximating model ($r^2 = 0.73$) (Fig. 1) among the seven possible combinations of the independent variables: depth > 20, cover index, and position in the study reach. Summation of Akaike weights for all models including specific independent variables revealed strong support for both depth > 20 ($\Sigma w_i > 0.99$) and the cover index ($\Sigma w_i = 0.95$) being included in the best-approximating model. Analysis of the initial distribution of mature fish yielded a similar result: one model worthy of consideration that included positive relationships with both depth > 20 and cover availability ($r^2 = 0.68$). In this analysis, depth > 20 again had the strongest possible support for inclusion in the best-approximating model ($\Sigma w_i > 0.99$), while the cover index also had substantial support ($\Sigma w_i = 0.81$).

For final trout biomass, a positive relationship with depth > 20 provided the best-approximating model ($r^2 = 0.68$) (Fig. 2), when we again considered models including all combinations of depth, cover, and position in the reach. Unlike the results for starting biomass, the cover index had minimal support for inclusion in the best-approximating model ($\Sigma w_i = 0.03$). Depth > 20 alone also provided the best-approximating model ($r^2 = 0.66$) of the final biomass of mature fish, and cover index again had almost no support for inclusion in the best-approximating model ($\Sigma w_i < 0.01$).

In contrast with the analyses of trout biomass, none of the models that we constructed well represented survival within

Fig. 3. Survival of rainbow trout (*Oncorhynchus mykiss*) in habitats of Jacoby Creek versus cover availability.

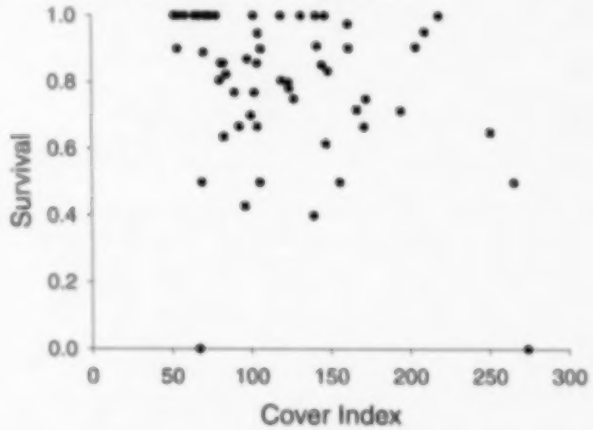

experimental units. In the best-approximating model ($r^2 = 0.09$), survival of all tagged fish declined with increasing cover (Fig. 3), while in a second model worthy of consideration ($\Delta AIC_c = 0.32$, $r^2 = 0.14$), survival was negatively related to cover and positively related to depth > 20. Analysis of the survival of mature fish yielded similar results in that none of the models performed well but a negative relationship with cover provided the best fit ($r^2 = 0.08$). Otters (*Lutra canadensis*) preyed on at least 11 fish in eight experimental units, as indicated by PIT tags found in otter scat. The amount of cover did not appear to influence predation by otters, in that the mean cover index for units where otters preyed on fish matched the mean cover index for the 59 experimental units in the experiment. The mean depth of the

© 2005 NRC Canada

Fig. 4. Mean growth of rainbow trout (*Oncorhynchus mykiss*) in habitats of Jacoby Creek versus initial biomass. The best-approximating model of mean growth included this negative relationship with initial density along with the positive influence of habitat depth and increasing growth downstream.

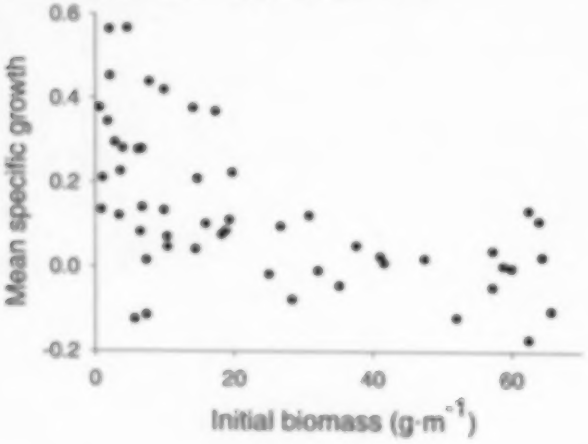

eight units where otters preyed on PIT-tagged fish slightly exceeded the mean depth of all 59 units in the experiment. Body size did not detectably influence survival: in habitats with <100% survival, the average sizes of fish recaptured and not recaptured did not differ (paired t test, $p = 0.20$, $n = 44$). Overall, surviving fish averaged 117 mm FL at the start of the experiment, while fish that we did not recover averaged 115 mm FL. Support for the accuracy of the survival estimates comes from (*i*) relatively strong estimates of initial and final capture efficiencies and (*ii*) the absence of any problems with the integrity of the enclosures over the course of the experiment (e.g., increases in stream stage or disruption of the fences).

Mean growth of trout was best described by a relatively complicated model that included negative relationships with initial biomass and the distance of the units from the bottom of the study reach and a positive relationship with depth > 20 ($r^2 = 0.57$). Although initial biomass by far provided the best single-factor model of mean growth ($r^2 = 0.41$) (Fig. 4) and had the strongest possible support for inclusion in the best-approximating model ($\Sigma w_i > 0.99$), both position in the reach ($\Sigma w_i = 0.92$) and depth > 20 ($\Sigma w_i = 0.72$) also had considerable support. In contrast, maximum growth of trout was best described by a model that included a negative relationship with distance upstream and a negative relationship with cover availability ($r^2 = 0.35$) (Fig. 5). Support for the importance of position of the units in the reach to maximum growth exceeded 0.99, while support for cover availability was substantially less ($\Sigma w_i = 0.65$). Initial biomass alone was unrelated to the maximum growth of trout ($r^2 = 0.05$), and this variable had relatively weak support for inclusion in the best-approximating model ($\Sigma w_i = 0.24$).

For mature fish, a single-factor model with a negative relationship between mean growth and the initial biomass of fish provided the best fit to the data ($r^2 = 0.30$). The data set did not provide any strong models of maximum growth by mature fish. The best-approximating model included a negative influence of initial biomass and a positive effect of depth > 20 ($r^2 = 0.16$), but several other models including initial biomass achieved similar AIC_c values.

Fig. 5. Best-approximating model of maximum growth of individual rainbow trout (*Oncorhynchus mykiss*) in habitats of Jacoby Creek.

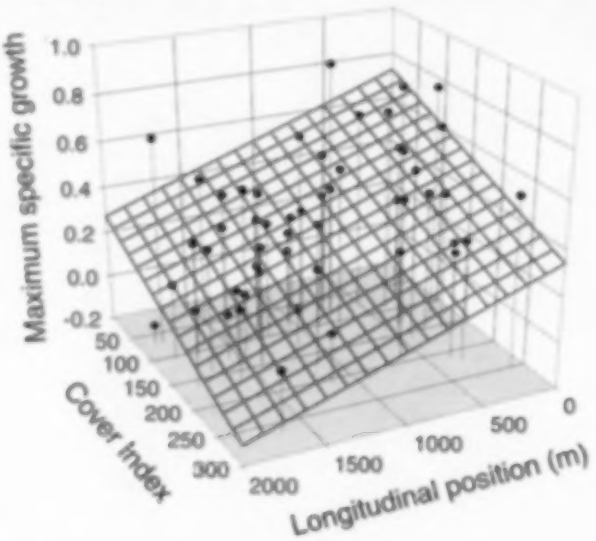

Fig. 6. Best-approximating model of the change in mass within habitats of Jacoby Creek over 63–68 days in summer 2001 from a set of candidate models that included all combinations of initial biomass, habitat depth, cover availability, and the position of the units in the 2-km study reach.

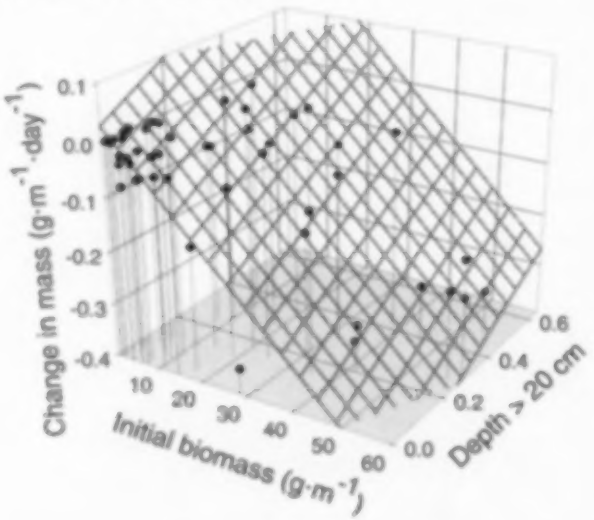

The change in trout biomass within habitats during the experiment was best approximated by a model that included both a negative effect of initial biomass and a positive effect of depth > 20 ($r^2 = 0.79$) (Fig. 6). The same two variables represented the change in biomass of mature fish even more strongly ($r^2 = 0.85$). For both all tagged fish and mature fish,

© 2005 NRC Canada

Table 1. Best-approximating models representing relationships between rainbow trout (*Oncorhynchus mykiss*) parameters and physical characteristics of habitats in Jacoby Creek as measured by AIC_c.

Response variable	Independent variable(s)	Δ_i	r^2
All post-age-0 fish			
Initial biomass	Depth > 20 (+), LWD (+)	0.0	0.79
	Depth > 20 (+), cover index (+)	15.9	0.73
Final biomass	Depth > 20 (+)	0	0.68
Mean specific growth	Depth > 20 (+), initial biomass (–), distance upstream (–)	0.0	0.57
Maximum specific growth	Distance upstream (–), cover index (–)	0.0	0.35
Change in total biomass	Initial biomass (–), depth > 20 (+)	0.0	0.79
Mature fish			
Initial biomass	Depth > 20 (+), LWD (+)	0.0	0.74
	Depth > 20 (+), cover index (+)	14.1	0.68
Final biomass	Depth > 20 (+)	0.0	0.66
Mean specific growth	Initial biomass (–)	0.0	0.30
Change in total biomass	Initial biomass (–), depth > 20 (+)	0.0	0.85

Note: Models of survival and the maximum specific growth of mature fish are not presented because none explained a substantial portion of the variation. LWD, proportion by area covered by large woody debris. For comparison, models that separately included LWD and the cover index are both listed for initial biomass. Otherwise, for all response variables listed, no other models were within two AIC_c units of the best-approximating model. Δ_i indicates the difference in AIC_c between models.

AIC_c results did not yield any other models worthy of consideration among the total of 15, which included all possible combinations of initial biomass, longitudinal position, depth, and cover as independent variables. The negative relationship between biomass accrual and initial biomass is not surprising given the relatively low survival observed: loss of biomass via mortality overwhelmed any changes in the total biomass in the units due to changes in individual mass.

Exploration of the data a posteriori suggested that the relationships described above were, in general, not highly dependent on the particular parameters selected to represent variables of interest. For example, mean depth within the experimental units and depth > 20 were strongly correlated ($r = 0.96$), and models using the former measure of depth had similar explanatory power to those using depth > 20 (r^2 values within 0.05–0.10, although consistently lower for mean depth). Similarly, expression of density on an areal basis (grams per square metre) produced results parallel to those with density as grams per metre. For example, the best model of initial density as grams per square metre included the same independent variables as the model described above for density as grams per metre, although with $r^2 = 0.67$ rather than 0.73.

Models with the area of large woody debris as an independent variable in place of the cover index yielded slightly different results in several cases. The models of the initial distribution of fish that included the area of large woody debris in place of the cover index provided better fits to the data for both all post-age-0 fish and adult fish (Table 1). Unlike the cover index, the area of large woody debris was completely unrelated to our estimates of survival ($r^2 < 0.01$) and did not contribute to the best approximating models of maximum growth ($\Sigma w_i = 0.14$). However, like the cover index, the area of large woody debris did not contribute to the best-approximating models of final biomass, mean growth, or the change in biomass over the experiment.

Fig. 7. Patterns in absolute growth by individuals versus their rank by body mass within individual experimental units. For clarity, the graph includes only those nine pools where the number of recaptured fish ranged from four to seven. Symbols distinguish groups of fish by experimental unit. Three sets of points are offset slightly for clarity.

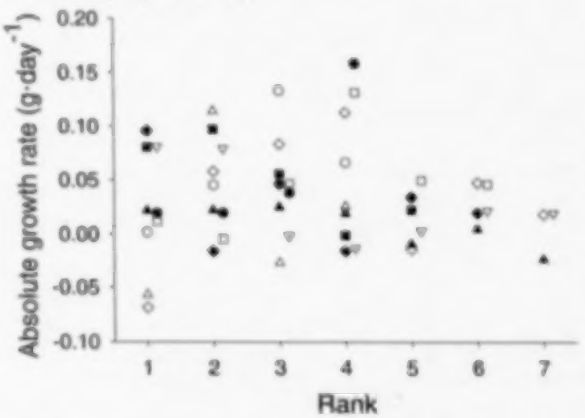

The growth rate of individual fish was not strongly related to their relative size within pools (Fig. 7). As expected from the unit-scale analysis of growth, variation among units accounted for substantial variation in specific growth rate of individuals ($r^2 = 0.37$). However, a model with log(rank) as an additional independent variable yielded a similar r^2 (0.41), and the modest influence of log(rank) on specific growth rate was positive. The analysis of individual absolute growth also revealed significant variation among units but no meaningful relationship with log(rank). Inspection of data for individual habitats did not reveal any examples of markedly higher growth by the largest tagged fish.

© 2005 NRC Canada

Discussion

The best-approximating model of the initial distribution of rainbow trout among units in this study corresponded to a variety of habitat-scale observations of positive relationships between salmonid density and both water depth and physical cover in pool–riffle stream channels (e.g., Heggenes et al. 1991; Inoue et al. 1997; Inoue and Nakano 1998). However, with fish movement prevented, the final distribution of trout biomass in the experiment appeared to be less related to cover availability. This change appeared to be driven primarily by a weak negative relationship between cover and fish survival.

Lack of support for the hypothesis that cover availability enhances survival of stream fish does not conflict with several previous studies. For example, Spalding et al. (1995) found that the survival of coho salmon (*Oncorhynchus kisutch*) in seminatural channels was unrelated to the amount of woody debris in the form of brush. Lonzarich and Quinn (1995) found that while survival of juvenile salmonids tended to be higher in seminatural channels with woody debris added compared with those without debris, the effect was not detectable statistically (in contrast with the beneficial effect of deeper water on survival). Boss and Richardson (2002) observed that the addition of cover enhanced survival of cutthroat trout (*Oncorhynchus clarki*) by >50% in one stream but found uniformly high survival across cover treatments in a smaller stream during the same experiment. Harvey and Stewart (1991) observed a strong effect of cover in the form of masonry blocks on the survival of minnows in shallow stream pools in an 11-day experiment, but such an effect might not persist over longer time periods, when the need to feed would more strongly influence habitat selection by fish. The need for fish to both avoid predators and acquire food probably contributes to repeated observations that water depth enhances survival (Harvey and Stewart 1991; Lonzarich and Quinn 1995; weak support from this study) and less consistent observations that cover enhances survival. Relatively deep habitats may enhance both predator avoidance and food acquisition, while some forms of cover can reduce feeding efficiency (Wilzbach et al. 1986).

This experiment's results for fish survival cannot be considered conclusive; several issues raise challenges to reliable estimation of the influence of habitat features on the survival of stream fish. Predation pressure exhibits significant spatiotemporal variation, as evidenced by Boss and Richardson's (2002) different findings in two vicinal streams during one experiment. While otters affected fish survival in Jacoby Creek in 2001, they did not appear to influence another summer experiment at the same study site in 2003, where survival in similar experimental units approached 100% over about the same part of the year (B.C. Harvey, J.L. White, and R.J. Nakamoto, unpublished data). Given the potential rates of piscivory by otters (Dolloff 1993), the presence–absence of this predator could profoundly influence experimental results. Assuming that the effects of different habitat features (e.g., water depth and amount and kinds of cover) on predation risk are dependent on both the identity and the density of predators, consistency among studies of survival's habitat dependence would not be expected. Another issue complicating estimation of habitat-specific survival is the potential influence of prey density on predation risk. Researchers have usually contrasted survival among experimental units in streams by using equal initial densities of fish (e.g., Harvey and Stewart 1991; Spalding et al. 1995; Boss and Richardson 2002). This approach may not accurately reflect predation risk at natural densities, if, for example, an artificially high density of prey attracts predators to patches, and this effect is not offset by reduced per capita risk for prey due to the elevated density. Our finding of weak relationships between habitat features and survival for fish at natural densities may be due in part to selection of habitats by fish that incorporates the risk of predation. A final caveat regarding efforts to estimate the influence of habitat features on survival is that habitat-scale estimates may not well represent survival probabilities for individuals: risk may vary on a finer spatial scale and (or) among individuals depending on their body size, social status, or innate ability to avoid predators.

This experiment extends observations of density-dependent growth in stream salmonids among whole streams (e.g., Vøllestad et al. 2002) and stream reaches (e.g., Jenkins et al. 1999; Bohlin et al. 2002) down to the scale of individual habitats. Our finding of density-dependent growth among habitats differs from observations by Jenkins et al. (1999) at a similar spatial scale over a similar range in density, but probably for reasons anticipated by those authors: (*i*) perhaps in contrast with the experimental units in Jenkins et al. (1999), conditions in Jacoby Creek during this study generated significant habitat-scale variation in food availability and (*ii*) unlike Jenkins et al. (1999), we prevented movement among habitats such that fish experienced consistent relative densities on that scale. Similar to previous research (Jenkins et al. 1999), neither survival nor maximum growth of individuals exhibited significant relationships with density.

In contrast with fish density, both water depth and distance downstream positively influenced the mean growth of fish. As noted above, the positive influence of greater water depth on growth may be enhanced by relatively low predation risk and its potential effects on food acquisition. To some extent, the gradient in water depth in this data set reflects a riffle to pool transition; Rosenfeld and Boss (2001) recently documented that pools can provide more energetically favorable habitats than riffles for post-age-0 salmonids in small streams. The influence of reach position on growth may reflect the value of higher discharge, even though discharge at the downstream end of the study reach did not exceed 0.05 $m^3 \cdot s^{-1}$ during the experiment. Small differences in discharge in headwater streams may lead to significant differences in food availability for trout by promoting more extensive invertebrate drift through increased production and higher water velocities at riffle–pool transitions.

The lack of a relationship between relative body size and growth rate within individual habitats in this experiment contrasts sharply with observations of masu salmon (*Oncorhynchus masou*) in a Japanese stream (Nakano et al. 1991; Nakano 1995) but coincides with recent studies revealing no relationship between dominance status and individual growth in juvenile Atlantic salmon (*Salmo salar*) (Martin-Smith and Armstrong 2002; Harwood et al. 2003). Differences among physical settings in the degree to which fish can affect food acquisition by other individuals may partly explain the varia-

© 2005 NRC Canada

tion in these results. During our experiment, the upstream ends of most pools in Jacoby Creek probably did not offer microhabitats with adequate depths and velocities to allow large fish to consume disproportionate amounts of drifting food. In habitats where the spatial distribution of food is unpredictable and (or) relatively homogenous, a positive relationship between growth and body size may not be expected (Armstrong et al. 1999). Indeed, Armstrong et al. (1999) found a negative relationship between growth and fish length for juvenile Atlantic salmon in an artificial riffle. Armstrong et al. (1999) suggested that the cost of dominance for fish near carrying capacity may have contributed to the negative relationship that they observed. Relatively high predation risk for fish in our experiment also may have influenced patterns in individual growth. The addition of a predator eliminated the growth advantage for larger masu salmon fry within instream enclosures (Reinhardt et al. 2001), which corresponds to observations that wariness of salmonids increases with body size (Grant and Noakes 1987), suggesting that predation risk can enhance feeding opportunities for subdominant fish.

This experiment has several implications for fish habitat management and efforts to model relationships between habitat and population dynamics. The positive influences of water depth and distance downstream on trout growth in this experiment suggest the value of higher discharge and the harm of extreme aggradation in stream channels during periods of seasonally low discharge. Large woody debris must be considered a key feature in many salmonid-bearing streams, given its influence on water depth by forming pools (e.g., Fausch and Northcote 1992) and documented value to stream salmonids during the wet season (e.g., Quinn and Peterson 1996). However, this experiment did not reveal strong dry season benefits of wood per se. That our measurements of fish survival probably depended on a predator that may be only an occasional visitor to the study site and that individual growth appeared to be unrelated to body size in contrast with previous observations in headwater stream pools both suggest significant challenges in modeling relationships between stream habitat and fish population dynamics.

Acknowledgements

Donald Ratcliff, Don Ashton, and Ryan Fogerty provided field assistance. Tom Lisle, Frank McCormick, and Peggy Wilzbach reviewed the manuscript. Mark Andre provided access to the City of Arcata's Jacoby Creek Forest.

References

Allouche, S. 2002. Nature and functions of cover for riverine fish. Bull. Fr. Pêche Piscic. **365/366**: 297–324.

Armstrong, J.D., Huntingford, F.A., and Herbert, N.A. 1999. Individual space use strategies of wild juvenile Atlantic salmon. J. Fish Biol. **55**: 1201–1212.

Bohlin, T., Sundström, L.F., Johnsson, J.I., Höjesjö, J., and Pettersson, J. 2002. Density-dependent growth in brown trout: effects of introducing wild and hatchery fish. J. Anim. Ecol. **71**: 683–692.

Boss, S.M., and Richardson, J.S. 2002. Effects of food and cover on the growth, survival, and movement of cutthroat trout (*Oncorhynchus clarki*) in coastal streams. Can. J. Fish. Aquat. Sci. **59**: 1044–1053.

Burnham, K.P., and Anderson, D.R. 2002. Model selection and multimodel inference: a practical information-theoretic approach. Springer-Verlag New York, Inc., New York.

Dolloff, C.A. 1993. Predation by river otters (*Lutra canadensis*) on juvenile coho salmon (*Oncorhynchus kisutch*) and Dolly Varden (*Salvelinus malma*) in southeast Alaska. Can. J. Fish. Aquat. Sci. **50**: 312–315.

Fausch, K.D., and Northcote, T.G. 1992. Large woody debris and salmonid habitat in a small coastal British Columbia stream. Can. J. Fish. Aquat. Sci. **49**: 682–693.

Grant, J.W.A., and Noakes, D.L.G. 1987. Escape behaviour and use of cover by young-of-the-year brook trout, *Salvelinus fontinalis*. Can. J. Fish. Aquat. Sci. **44**: 1390–1396.

Grant, J.W.A., Steingrímsson, S.O., Keeley, E.R., and Cunjak, R.A. 1998. Implications of territory size for the measurement and prediction of salmonid abundance in streams. Can. J. Fish. Aquat. Sci. **55**(Suppl. 1): 181–190.

Harvey, B.C. 1998. Influence of large woody debris on retention, immigration, and growth of coastal cutthroat trout (*Oncorhynchus clarki clarki*) in stream pools. Can. J. Fish. Aquat. Sci. **55**: 1902–1908.

Harvey, B.C., and Stewart, A.J. 1991. Fish size and habitat depth relationships in headwater streams. Oecologia, **87**: 336–342.

Harwood, A.J., Armstrong, J.D., Metcalfe, N.B., and Griffiths, S.W. 2003. Does dominance status correlate with growth in wild stream-dwelling Atlantic salmon (*Salmo salar*)? Behav. Ecol. **14**: 902–908.

Heggenes, J., Northcote, T.G., and Peter, A. 1991. Seasonal habitat selection and preferences by cutthroat trout (*Oncorhynchus clarki*) in a small, coastal stream. Can. J. Fish. Aquat. Sci. **48**: 1364–1370.

Inoue, M., and Nakano, S. 1998. Effects of woody debris on the habitat of juvenile masu salmon (*Oncorhynchus masou*) in northern Japanese streams. Freshw. Biol. **40**: 1–16.

Inoue, M., Nakano, S., and Nakamura, F. 1997. Juvenile masu salmon (*Oncorhynchus masou*) abundance and stream habitat relationships in northern Japan. Can. J. Fish. Aquat. Sci. **54**: 1331–1341.

Jenkins, T.M., Jr., Diehl, S., Kratz, K.W., and Cooper, S.D. 1999. Effects of population density on individual growth of brown trout in streams. Ecology, **80**: 941–956.

Keeley, E.R. 2001. Demographic responses to food and space competition by juvenile steelhead trout. Ecology, **82**: 1247–1259.

Kinsolving, A.D., and Bain, M.B. 1990. A new approach for measuring cover in fish habitat studies. J. Freshw. Ecol. **5**: 373–378.

Kruzic, L.M., Scarnecchia, D.L., and Roper, B.B. 2001. Comparison of midsummer survival and growth of age-0 hatchery coho salmon held in pools and riffles. Trans. Am. Fish. Soc. **130**: 147–154.

Lonzarich, D.G., and Quinn, T.P. 1995. Experimental evidence for the effect of depth and substrate on the distribution, growth, and survival of stream fishes. Can. J. Zool. **73**: 2223–2230.

Martin-Smith, K.M., and Armstrong, J.D. 2002. Growth rates of wild stream-dwelling Atlantic salmon correlate with activity and sex but not dominance. J. Anim. Ecol. **71**: 413–423.

Nakano, S. 1995. Individual differences in resource use, growth and emigration under the influence of a dominance hierarchy in fluvial red-spotted masu salmon in a natural habitat. J. Anim. Ecol. **64**: 75–84.

Nakano, S., Kachi, T., and Nagoshi, M. 1991. Individual growth variation of red-spotted masu salmon, *Oncorhynchus masou rhodurus*, in a mountain stream. Jpn. J. Ichthyol. **38**: 263–270.

© 2005 NRC Canada

Power, M.E. 1984. Depth distributions of armored catfish: predator-induced resource avoidance? Ecology, **65**: 523–528.

Quinn, T.P., and Peterson, N.P. 1996. The influence of habitat complexity and fish size on over-winter survival and growth of individually marked juvenile coho salmon (*Oncorhynchus kisutch*) in Big Beef Creek, Washington. Can. J. Fish. Aquat. Sci. **53**: 1555–1564.

Railsback, S.F., and Harvey, B.C. 2002. Analysis of habitat-selection rules using an individual-based model. Ecology, **83**: 1817–1830.

Reinhardt, U.G., Yamamoto, T., and Nakano, S. 2001. Effects of body size and predators on intracohort competition in wild and domesticated juvenile salmon in a stream. Ecol. Res. **16**: 327–334.

Rosenfeld, J.S., and Boss, S. 2001. Fitness consequences of habitat use for juvenile cutthroat trout: energetic costs and benefits in pools and riffles. Can. J. Fish. Aquat. Sci. **58**: 585–593.

Spalding, S., Peterson, N.P., and Quinn, T.P. 1995. Summer distribution, survival, and growth of juvenile coho salmon under varying experimental conditions of brushy instream cover. Trans. Am. Fish. Soc. **124**: 124–130.

Vøllestad, L.A., Olsen, E.M., and Forseth, T. 2002. Growth-rate variation in brown trout in small neighbouring streams: evidence for density-dependence? J. Fish Biol. **61**: 1513–1527.

Wilzbach, M.A., Cummins, K.W., and Hall, J.D. 1986. Influence of habitat manipulations on interactions between cutthroat trout and invertebrate drift. Ecology, **67**: 898–911.

© 2005 NRC Canada

Using geostatistics to quantify seasonal distribution and aggregation patterns of fishes: an example of Atlantic cod (*Gadus morhua*)

L.G.S. Mello and G.A. Rose

Abstract: Geostatistical methods were used to (*i*) quantify fish aggregation patterns over a range of scales (100 m to 67 km) using both simulated and acoustic density data of Atlantic cod (*Gadus morhua*) and (*ii*) examine how changes in aggregation patterns influenced the precision of geostatistical density indices. Variogram parameters (range, sill, and nugget) reflected changes in distribution patterns. Variograms of dispersed and low-density aggregations had large range and small sill and nugget values. In contrast, when fish were aggregated in a small portion of the study area, the range was low and the sill and nugget large. The precision of density indices (coefficient of variation) was below 20% in all cases but at a maximum during summer when cod were broadly distributed in small, moderate to dense aggregations. Geostatistical modeling allowed us to describe and quantify distribution patterns of fish density over different scales of observation, comparisons of spatiotemporal changes in density distribution, and estimations of the precision of density indices while accounting for the effects of heterogeneous distributions, outliers and the typically large number of zero and low-density observations. Geostatistical methods have particular applicability to fishes exhibiting gregarious behaviour and seasonally variable distributions, which include many temperate and high-latitude fish species.

Résumé : Nous avons utilisé des méthodes géostatistiques afin de (*i*) quantifier les patterns de répartition contagieuse des poissons à différentes échelles (100 m à 67 km) à l'aide de données de densité simulées et de données d'inventaires acoustiques chez la morue franche (*Gadus morhua*) et (*ii*) examiner comment les changements dans les patterns de contagion influencent la précision des indices géostatistiques de densité. Les paramètres des variogrammes (portée, palier et pépite) reflètent les changements dans les patterns de répartition. Les variogrammes des contagions dispersées et de faible densité ont une grande portée, mais des valeurs faible de palier et de pépite. En revanche, quand les poissons se rassemblent dans une petite portion de la zone d'étude, la portée est faible et le palier et la pépite sont élevés. La précision des indices de densité est inférieure à 20 % dans tous les cas, mais elle atteint un sommet en été quand les morues sont largement réparties dans de petites contagions de densité moyenne à grande. La modélisation géostatistique nous a permis de décrire et de quantifier les patterns de répartition de la densité des poissons à différentes échelles d'observation, les comparaisons des changements spatio-temporels de répartition de la densité, ainsi que les estimations de la précision des indices de densité, tout en tenant compte des distributions hétérogènes, des valeurs aberrantes et du nombre généralement élevé d'observations de densité faible ou nulle. Les méthodes géostatistiques s'appliquent particulièrement bien aux poissons qui possèdent un comportement grégaire et qui ont des répartitions variables au cours des saisons, ce qui inclut plusieurs espèces de poissons des régions tempérées et des zones de haute latitude.

[Traduit par la Rédaction]

Introduction

Temperate-water fishes typically exhibit changes in distribution and aggregation patterns at seasonal, annual, and decadal time scales (Rose et al. 2000; Vilhjálmsson 2002). Likewise, fish often exhibit contagious distribution in association with particular habitats (Imbrock et al. 1996; Fréon and Misund 1999) or behavioural changes, for example, during migrations, spawning and overwintering periods (Nøttestad et al. 1996; Rose 2003) and growth and feeding cycles (Stoner and Abookire 2002; Hovde et al. 2002). Survey designs and analytical methods normally used in fisheries may not always be appropriate for assessing such distribution patterns of fish (MacLennan and Simmonds 1992; Hanselman et al. 2001) and invertebrates (Vining et al. 2001) and have tended to rely on ad hoc measures to describe distributions and changes in spatially structured data (e.g., deYoung and Rose 1993; Hutchings 1996).

Geostatistical methods were developed for spatially structured mining data during the 1960s (Matheron 1963).

Received 10 November 2003. Accepted 29 September 2004. Published on the NRC Research Press Web site at http://cjfas.nrc.ca on 18 April 2005.
J17832

L.G.S. Mello[1] and G.A. Rose. Fisheries Conservation Chair, Memorial University of Newfoundland, Box 4920, St. John's, NL A1C 5R3, Canada.

[1]Corresponding author (e-mail: luiz.mello@mi.mun.ca).

 doi: 10.1139/F04-227 © 2005 NRC Canada

Fig. 1. (*a*) East coast of North America showing Placentia Bay (inside the square) on the south coast of Newfoundland and (*b*) detailed view of the bay showing the 100-m depth contour (fine lines) and geographic references (1) head of the bay, (2) outer bay banks, and (3) Cape St. Mary's. Squares represent the sampling unit area (one square = 120 km^2).

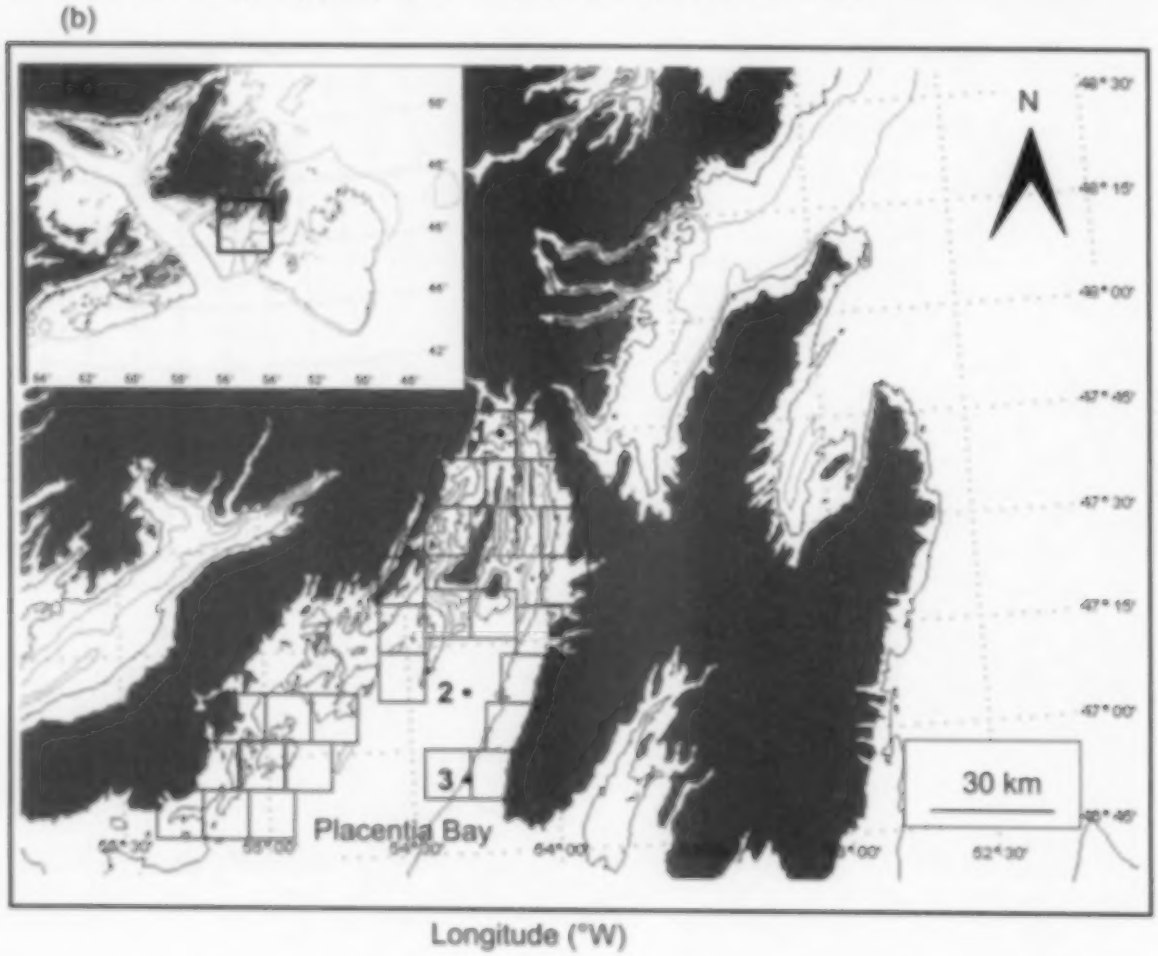

Geostatistical methods are particularly relevant to serially correlated acoustic survey data because they do not require sample independence and have been used with pelagic fish (Simard et al. 1993; Maravelias et al. 1996), demersal fish (Williamson and Traynor 1996; Rivoirard et al. 2000), shellfish (Simard et al. 1992; Maynou et al. 1998), and plankton (Simard and Lavoie 1999; Romsine et al. 2002). The use of randomly positioned stations may lead to sample independence, but such methods tend to limit spatial resolution (Langton et al. 1995). Geostatistical methods are commonly used for estimating patchiness in fish distribution (Fréon and Misund 1999). However, there is a limited understanding about how geostatistical methods may be used to describe and quantify fish aggregations and their effects on the precision of acoustic density indices.

Atlantic cod (*Gadus morhua*) exhibit marked (seasonal to decadal) changes in distribution and aggregation patterns (Rose 2003). Several methods have been used in attempts to quantify such patterns from trawl or acoustic survey data (e.g., Myers and Cadigan 1995; Rose et al. 2000). This study investigated the use of geostatistical methods to quantify seasonal distribution patterns over a broad range of scales from 100 m to approximately 70 km using both simulated and acoustic survey data. First, conceptual models were developed using simulated data distributions and used to demonstrate the interaction of various distribution patterns with variogram parameters. These concepts were then applied to variograms estimated from cod surveys conducted in Placentia Bay, Newfoundland, and results discussed in relation to season, habitat, and migration patterns. Effects of the distribution patterns on the precision of the acoustic density indices were also examined.

Materials and methods

Area of study

Placentia Bay is a large embayment (132 km × 100 km) on the south coast of Newfoundland (Fig. 1). Based on topo-

© 2005 NRC Canada

Table 1. Dates of acoustic surveys conducted in Placentia Bay in 1999.

Month	Start	End	No. of fish sampled	No. of blocks surveyed
April	7	22	417	9
May	3	11	136	21
July	15	27	281	26
October	22	30	215	19
November	2	10	279	24

Note: Surveys employed a BioSonics DT 4000 echosounder (120 kHz). The study area comprised 28 blocks of 120 km^2 each.

graphic and bathymetric features, the bay was divided in two components (inner and outer bay) or strata. The inner bay is divided by a series of islands into three deep channels that merge to form a deep basin (outer bay), which extends from the bay into the offshore. Placentia Bay remains ice free year-round, except for areas near strong freshwater inflows. Depths in the western channel reach 450 m, while the eastern and central channels have maximum depths of 375 m. The bottom topography is rugged and variable (Willey 1976), particularly in the inner bay, and the sediment types vary markedly over small distances (Stehman 1976).

Acoustic surveys

Five acoustic surveys were conducted in Placentia Bay between April and November 1999 (Table 1). Surveys were run over relative short periods of time (9–16 days) to minimize the effects of temporal (intraseasonal) variability caused by changes in fish distribution and movement. The surveys employed a BioSonics DT 4000 echosounder with a 120-kHz transducer mounted on a towed body. The system was calibrated in situ with a tungsten–carbide standard target (Foote et al. 1987).

Areas of the bay at depths between 10 and 120 m were stratified into 28 blocks (one block = 120 km^2) (Fig. 1). Earlier work had shown that cod are uncommon at depths greater than 100 m in Placentia Bay from spring to fall (Lawson and Rose 1999). Block size was chosen based on logistic considerations such as the survey area covered in a day including acoustic and biological sampling (two or three blocks per day) and the total number of days available for surveying. Contiguous blocks were allocated across the study area starting at the innermost region of the bay. For each block, transects were run during the daytime period only along lines of latitude with start position randomly selected. This coverage was then followed by a more intense acoustic sampling (approximately 0.5-km equally spaced parallel transects) in areas (both strata) where cod aggregations were found. Such aggregations were typically dense (0.1–1 fish·m^{-2}) and small (<1 km in length). The overall transect distance covered in each block was in most cases the same (11 km), but transect selection within blocks depended on the topographic and bathymetric features of the area surveyed, navigational obstacles (e.g., shoals and fishing gears), and fish distribution, resulting in many cases of a series of short transects. Most blocks were covered during each survey, except in April. However, when and where blocks were surveyed was dictated primarily by the weather conditions at the time.

Acoustic data (echograms) were edited manually and integrated using FASIT software (Lefeuvre et al. 2000) to determine an area backscattering coefficient for each 100 m. Fish density (fish per square metre) was estimated as

$$(1) \qquad \text{Fish density} = s_a \theta_{bs}^{-1} D^{-1}$$

where s_a is the area backscattering coefficient (square metres per square metre), θ_{bs} is the arithmetic mean acoustic backscattering cross section of one fish (e.g., $\theta_{bs} = 10^{TS/10}$), and D is detectability (Lawson and Rose 1999). Detectability was determined in independent experiments (Rose and Mello 2001). Target strength (TS) was estimated as (Rose and Lawson 1999; Rose 2003)

$$(2) \qquad \text{TS (dB)} = 20 \log(\text{length (cm)}) - 67.5$$

For each block, the raw acoustic densities were averaged over each minute of latitude and two minutes of longitude, which at latitude 47°N (study area) is roughly equivalent to an area of 3.5 km^2. This procedure standardized sampling effort while preserving the spatial structure of the data. Averaging data over regular distance intervals is a common procedure in fisheries acoustics (MacLennan and Simmonds 1992; Rivoirard et al. 2000; Rose 2003). One reason is because acoustic data are recorded continuously along the survey transects and integrated over short distance intervals (in this case, for each 100 m), generating a very high number of observations. There are no general rules about averaging data over distance or area, and for this study, it was based on (*i*) the spatial scales of the surveyed areas (block and stratum), (*ii*) sampling design, (*iii*) computational efficiency to perform analyses, and (*iv*) the authors' understanding of biological effects of cod aggregation in Placentia Bay (e.g., aggregation patterns and cod behaviour during spawning or feeding periods). The approach used reduced (i.e., smoothed) to some extent the variability of the data, but the scale used to average the data (3.5 km^2) is small enough to preserve the spatial structure of the data while considering the four points as listed above.

Next, fish density indices (mean fish density per stratum) and coefficient of variation (CV) for each survey and stratum were estimated using geostatistics. Biological samples were obtained in all surveys from cod aggregations identified acoustically. Fishing sets used four hand-lines with six equal-sized hooks (10.2 cm long by 2.6 cm wide) fished for 30 min. A total of 1328 fish were sampled for length (centimetres). Mean length per 4-cm class interval was calculated and used for estimating the acoustic target strengths (eq. 2), which were used to obtain fish density estimates.

Geostatistics

In geostatistical methods, the spatial variability of the data is modeled as autocorrelation and incorporated into the estimation procedure by weighting the sample values with the appropriate variogram model (Matheron 1963). The variogram is the main tool of geostatistics and measures the spatial correlation by describing how the data are related over distance and direction. In the case of gregarious fish, acoustic density data are typically characterized by many small

© 2005 NRC Canada

and a few large values (Rivoirard et al. 2000), which can significantly impact the variogram pattern and parameters (Krige and Magri 1982). Therefore, a robust estimator of the variogram (Cressie and Hawkins 1980) was used:

$$(3)\qquad \overline{\gamma}(h) = \frac{\left\{\frac{1}{2|N(h)|}\sum_{N(h)}|z_i - z_j|^{\frac{1}{2}}\right\}^4}{0.457 + 0.494/|N(h)|}$$

where $N(h)$ is the set of all pairwise distances $i - j = h$ in a two-dimensional plan, $|N(h)|$ is the number of distinct pairs in $N(h)$, z_i and z_j are data values at spatial locations i and j, respectively, and 0.457 and 0.494 are model coefficients.

The geostatistical analysis consisted of evaluating stationarity, estimation of empirical variograms, fitting a theoretical variogram model, and calculating predictions and standard errors of the unknown values using kriging (Matheron 1971) as an extrapolation method. The spatial stationarity assumption implies a process with a constant mean and with the variance defined only as a function of distance and not location (Cressie 1993). Directional variograms were used to check for the presence of trends in the data, anisotropy in the variograms, or some other form of nonstationarity. Multiple directional variograms were computed by specifying a vector of azimuths (0, 15,..., 135°). Variograms considered only distances h for which $|N(h)| > 30$ (Journel and Huijbregts 1978). When detected, trends were removed from the data by a linear transformation using the residuals of a local regression or Loess model (Cleveland and Devlin 1988). Directional variograms were computed and compared using Loess models to fit and remove trends from the data using latitudinal and longitudinal distances across the sampling area as predictors. The variograms were then estimated using these corrected locations. Details on this technique may be found in Journel and Huijbregts (1978).

Geometric anisotropy (i.e., variogram range varies with direction) was detected in some cases, and empirical variograms were calculated based on the appropriate correction, that is, incorporating the detected direction of anisotropy in the variogram model and generating an equivalent isotropic model. All geostatistical analyses were performed using S+ Spatial Stats software (Insightful Corporation). The resulting empirical variograms were then fitted with appropriate theoretical variogram models. The initial model fitting was done manually based on the shape of the empirical variogram. Spherical, exponential, Gaussian, and power models (Cressie 1993; Rivoirard et al. 2000) were fitted. Variogram parameters were modified and the results overlaid onto the empirical variogram until a satisfactory fit was obtained. The final model was chosen based on the measurement of model fit that minimizes the objective function $\sum_h \left[\gamma(h) - \gamma^*(h)\right]^2$, that is, the residual sum of squares between the theoretical and empirical variograms $\gamma(h)$ and $\gamma^*(h)$, respectively (Cressie 1993). In all cases, spherical models with or without a nugget term provided the best fit (i.e., minimizes the objective function). Nugget refers to the microscale variations of data that are not described by spatial scale. The model is

$$(4)\qquad \gamma(h) = c\left[\frac{3|h|}{2a} - \frac{|h|^3}{a^3}\right] \text{ for } |h| < a$$

$$(5)\qquad \gamma(h) = c \text{ for } |h| \geq a$$

where c is the sill of the variogram $\gamma(h)$ representing the maximum level of variability in data measurements, $|h|$ is the scalar distance between two measurements, and a is the range of the variogram $\gamma(h)$ and represents the distance at which data are no longer correlated. The nugget model used was

$$(6)\qquad \gamma(h) = 0 \text{ for } h = 0$$

$$(7)\qquad \gamma(h) = c \text{ for } |h| > 0$$

Ordinary kriging was used to interpolate unsampled locations based on the theoretical variogram weighted by a linear combination of available samples. Ordinary kriging allows incorporating a model of the covariance when estimating predictions. Kriging predictions were computed as

$$(8)\qquad Z(V) = \sum_{i=1}^{N} \lambda_i Z(x_i)$$

where $Z(V)$ is the estimate of density at an unsampled point, N is the number of samples, and λ_i is the weight attributed to sample x_i. The use of weights ensures that the average error model is zero and the error variance is minimized (Isaaks and Srivastava 1989). The kriging output included the location (latitude and longitude), predictions (fish per square metre), and standard error of the predictions. The precision of the estimates was obtained by calculating the CV.

Next, the use of the variogram parameters range, sill, and nugget as quantitative indicators of distribution and aggregation patterns of fish was investigated using both simulated and acoustic density data of cod. In the case of variogram models described by asymptotic functions such as the spherical or Gaussian models, the nugget is the y-intercept, while the range and sill are both determined by the upper inflexion point where the line becomes flat. The x-coordinate of this inflexion point is the range, while the y-coordinate is the sill. In practical terms, nugget represents the microscale variation of data and (or) possible measurement errors, that is, variability smaller than the sampling unit distance, so appearing as an effect not explained by spatial scale. The variogram range can be thought of as an indicator of the size of aggregations such as fish schools or cluster of schools (Petitgas 1993; Maravelias et al. 1996; Fréon and Misund 1999), and the sill corresponds to the extent of the variance related to spatial scale (Hanselman et al. 2001) and hence an indicator of the degree of variability in autocorrelated data such as acoustic density measurements.

Aggregation types

There are varying views about what comprises a fish school. Breder and Halpern (1946) defined schools as groups of fish equally oriented, regularly spaced, and with similar swimming speed and Radakov (1973) simply as a group of fish swimming together. Fréon and Misund (1999) considered a fish school as a functional unit and Petitgas et

© 2005 NRC Canada

Fig. 2. Spatial patterns of simulated data according to (*a* and *b*) random and (*c*–*i*) gregarious distributions.

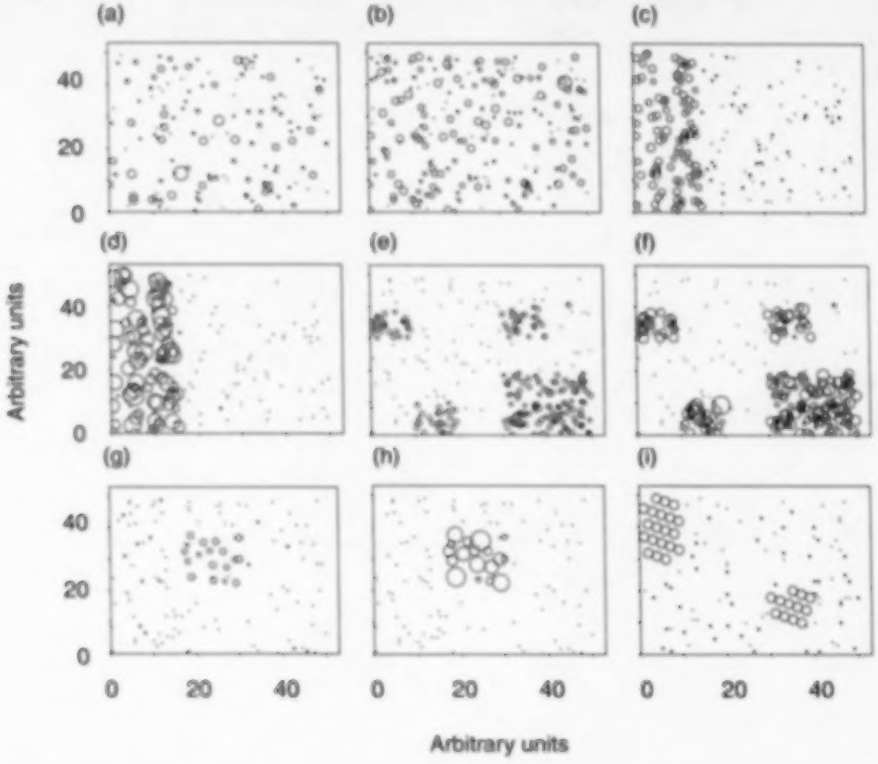

Fig. 3. Empirical (circles) and theoretical (line) variogram models computed from simulated data according to (*a* and *b*) random and (*c*–*i*) gregarious distribution patterns. The minimum number of pairs used to compute lag distances (*h*) was 30.

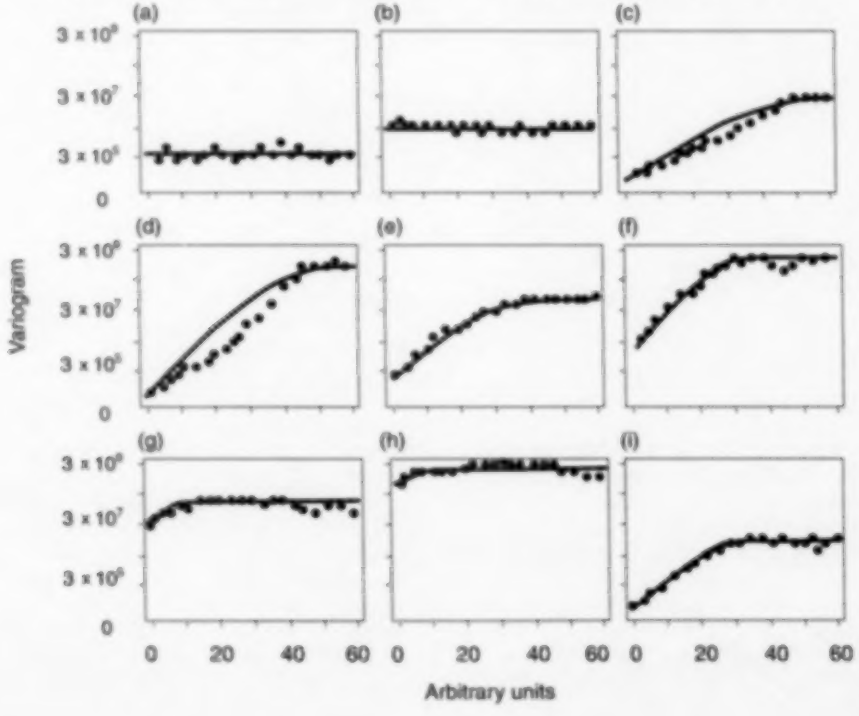

© 2005 NRC Canada

Fig. 4. Frequency distribution of acoustic density data for Placentia Bay Atlantic cod (*Gadus morhua*) in (*a*) April, (*b*) May, (*c*) July, (*d*) October, and (*e*) November 1999.

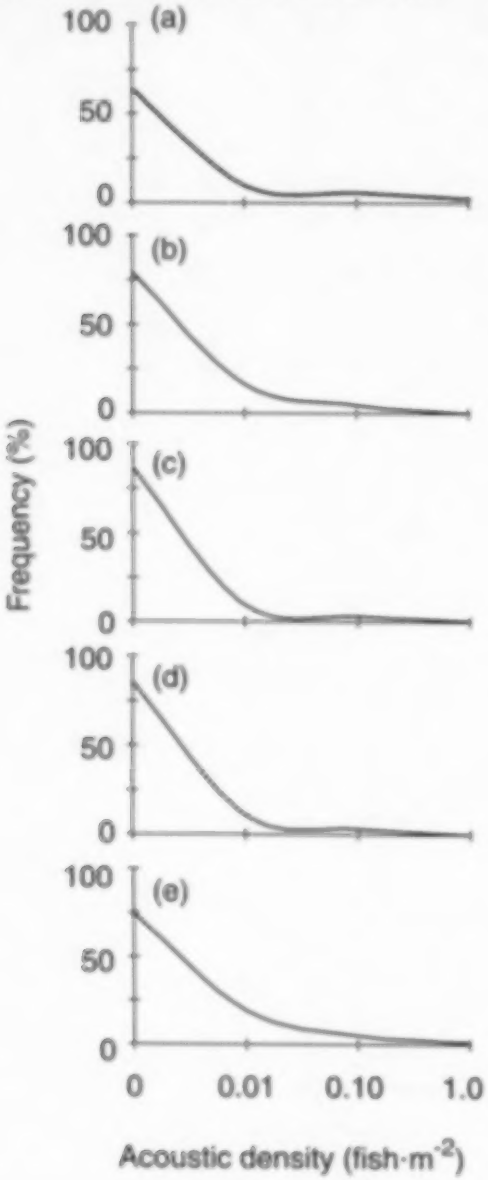

al. (2001) as discrete events in space. Also, the size of schools and clusters of schools vary greatly. Fréon et al. (1992) observed that a school of false pilchard (*Harengula clupeola*) varied between 145 and 522 m^2 in a 1-h period, and Maravelias et al. (1996) observed Atlantic herring (*Clupea harengus*) schools over distances of 12 km. Similarly, clusters of schools have been reported to reach lengths of 55 km for walleye pollock (*Theragra chalcogramma*) (Sullivan 1991) or larger for tunas (Fréon and Misund 1999). Reid et al. (2000) suggested that morphometric (e.g., length, area), energetic (e.g., acoustic backscattering), and positional parameters (e.g., latitude and longitude, depth) could be used to characterize fish schools and clusters of schools. In this study, the definitions of aggregation types were based on (*i*) morphological and energetic parameters, density estimates and size of aggregations based on acoustic data analysis and integration, and (*ii*) empirical approach based on the authors' knowledge of biological and behavioural effects of cod aggregation in Placentia Bay. Using these criteria, three types of aggregations were identified: (*i*) fish schools, single dense (0.1–1 fish·m^{-2}) and small (<2 km) groupings of fish, (*ii*) clusters of schools (≥ 2 km), and (*iii*) large (>25 km) and low-density (< 0.01 fish·m^{-2}) aggregations.

Conceptual models

Conceptual models for interpreting spatial structure through variogram parameters were developed using simulated data. The simulations produced measurements of aggregation size and spatial variability in data samples. The spatial patterns used in the simulations were arbitrarily chosen but believed to encompass spatial distributions observed for most fish populations. In general terms, the spatial distribution of a population can follow three basic types, random, regular, and contagious (Elliott 1977), and the simulated data incorporated such distribution patterns. Coordinated two-dimensional data (e.g., arbitrary unit (au) is the number of fish per surface unit) consisting of 2500 locations (1 au × 1 au grid) were generated using an ordinary spreadsheet package. For each scenario, sample values consisting of 95% zero and low values were randomly selected from a normal distribution ranging from 1 to 10 000 and the remaining values from 10 001 to 30 000. Scenarios containing aggregations were created with (*i*) relatively low variability in sample values within aggregations (values were randomly selected from a normal distribution ranging from 50 000 to 100 000), (*ii*) high variability in sample values (12 000 – 1 000 000), and (*iii*) an equally spaced and uniform value of 100 000. The locations and size of aggregations were arbitrarily selected with aggregation size varying from 100 to 750 au^2.

Results

Conceptual models

The simulations showed that when fish were randomly distributed (Figs. 2*a* and 2*b*), the variogram tended to be flat, indicating only a nugget effect. The size of the nugget was dependent on the amount of sample variability. The nugget was relatively smaller when variability in sample values was low (Fig. 3*a*) but increased as variability in samples increased (Fig. 3*b*).

Alternatively, in scenarios containing a contagious distribution, $\gamma(h)$ increased with distance and then leveled off where correlation with distance approached zero (range). The range, sill, and nugget values depended on the size, number, and proximity of aggregations and the degree of variability in sample values within aggregations. In the case of a large aggregation (15 au × 50 au) with low variability in sample values across the aggregation (Fig. 2*c*), the variogram exhibited relatively large range (50 au), small sill (3×10^7 au^2), and no nugget effect (Fig. 3*c*). When the variability

© 2005 NRC Canada

Fig. 5. Transect track and Atlantic cod (*Gadus morhua*) density distribution estimated from acoustic surveys in (*a*) April, (*b*) May, (*c*) July, (*d*) October, and (*e*) November 1999 in Placentia Bay. Fish densities: lines, < 0.01 fish·m^{-2}; ■, 0.01 and < 0.1 fish·m^{-2}; ○, 0.1 fish·m^{-2}. Squares represent the sampling unit area (120 km^2).

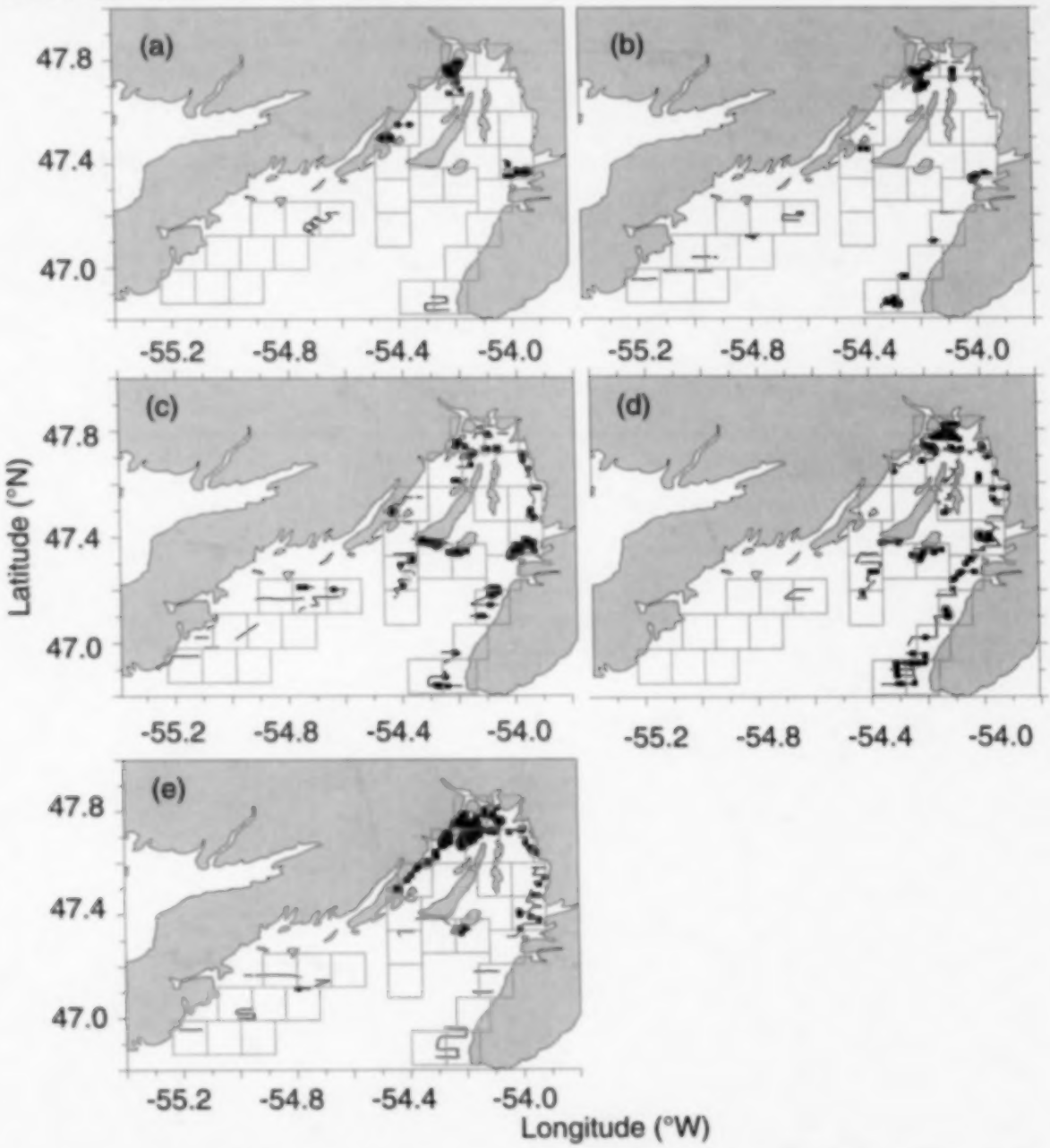

in sample values increased (Fig. 2*d*), a comparable increase in sill was observed (7×10^8 au^2) (Fig. 3*d*).

Smaller and denser neighbouring aggregations (Figs. 2*e* and 2*f*), each varying from approximately 10 au × 10 au to 20 au × 20 au, resulted in smaller range (42–44 au) and larger sill (2×10^9 au^2), and nugget effect varied from 2×10^5 au^2 to 2×10^6 au^2 (Figs. 3*e* and 3*f*). In these simulations, the variogram range and sill reflected cluster size and a larger spatial heterogeneity in sample values rather than the spatial properties of any single aggregation.

The scenarios where most large sample values were distributed within a small portion of the area (10 au × 18 au) (Figs. 2*g* and 2*h*) resulted in the smallest ranges (14 au) and the largest sill (3×10^9 au^2) and nugget values (3×10^8 au^2)

© 2005 NRC Canada

Fig. 6. Empirical (circles) and theoretical (line) variogram models computed for the inner bay (left panels) and outer bay (right panels) for each survey in (*a* and *b*) April, (*c* and *d*) May, (*e* and *f*) July, (*g* and *h*) October, and (*i* and *j*) November. The minimum number of pairs used to compute lag distances (*h*) was 30.

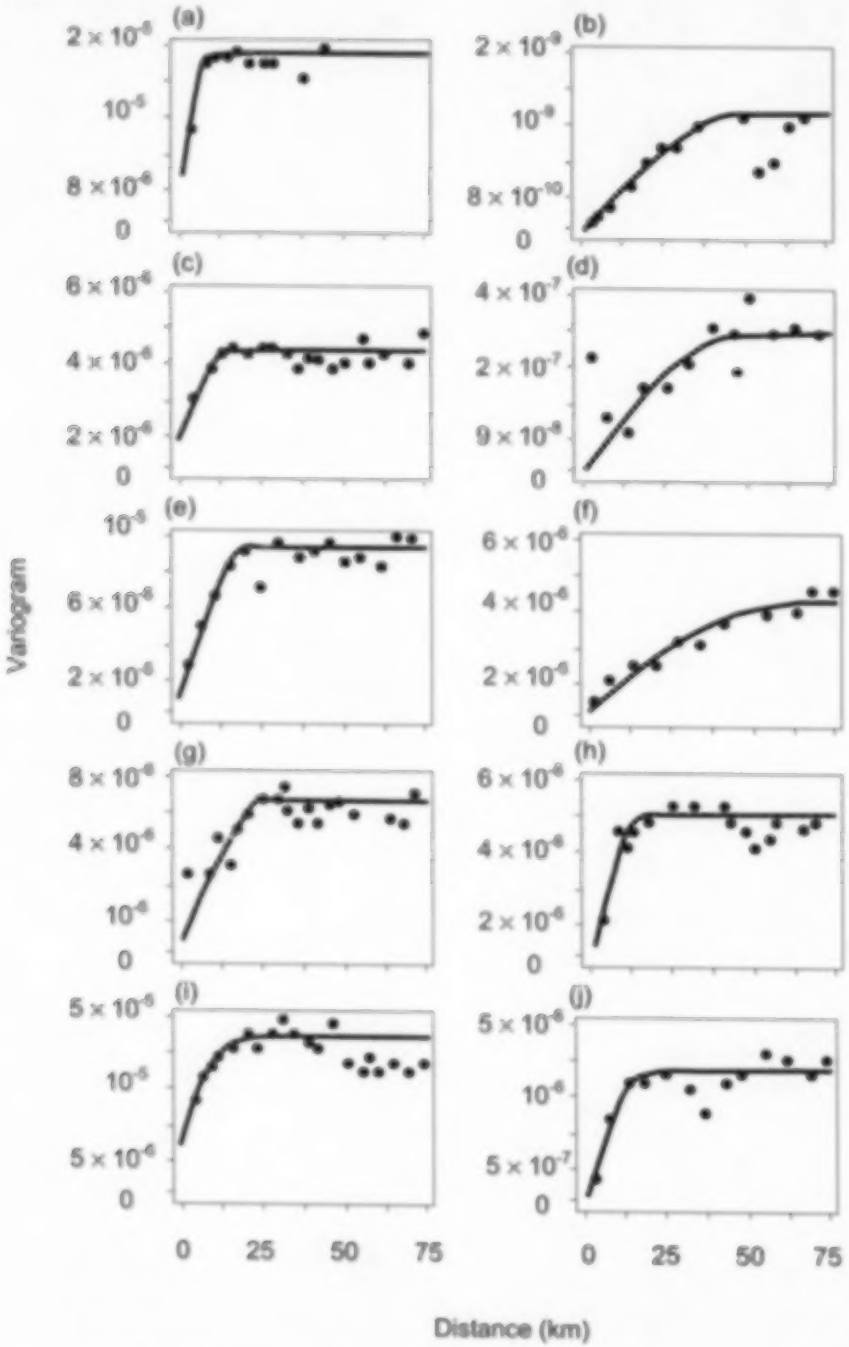

(Figs. 3*g* and 3*h*). In contrast, the smallest sill value (7×10^5 au^2) was observed for the scenario containing uniformly distributed samples within aggregations, reflecting low spatial variability in sample values (Figs. 2*i* and 3*i*).

Cod data

In all periods, fish densities were characterized by a large dispersion of values (three orders of magnitude) and skewed frequency distributions with many low and a few high values

© 2005 NRC Canada

Table 2. Geostatistical fish density indices and CV estimated for the inner bay and outer bay based on acoustic surveys conducted in Placentia Bay between April and November 1999.

Survey month	Stratum	Index (fish·m^{-2})	CV (%)
April	Inner bay	0.003	10
	Outer bay	0.001	13
May	Inner bay	0.008	17
	Outer bay	0.001	19
July	Inner bay	0.015	5
	Outer bay	0.003	8
October	Inner bay	0.001	19
	Outer bay	0.002	13
November	Inner bay	0.004	17
	Outer bay	0.001	14

(Fig. 4). In April and May, most cod were found in a few dense aggregations (≥0.1 fish·m^{-2}) in the inner bay and on the east side of the bay to Cape St. Mary's (May) (Figs. 5*a* and 5*b*). By July, cod were more dispersed in moderate to dense aggregations (≥0.01 fish·m^{-2}) (Fig. 5*c*). A similar distribution pattern predominated in October, although fewer cod were located over the outer bay banks (Fig. 5*d*). In November, dense aggregations again formed at the head of the bay, and low cod densities (< 0.01 fish·m^{-2}) were observed in the outer bay (Fig. 5*e*). Higher proportions of dense aggregations were found in July and November.

Variograms were determined for each survey and stratum to address interseasonal differences in fish distribution. All variograms showed evidence of spatial structure (Fig. 6), although nonrandom dispersion of points around the theoretical variogram was observed in some cases (November). The variogram range varied between 9 and 67 km and was higher in the outer bay than in the inner bay in all months except October. The variogram sill varied between 10^{-9} and 3×10^{-5} (fish·m^{-2})^2 and was lower in the outer bay than in the inner bay in all months. A nugget effect was observed in several variograms. A large nugget effect occurred in the inner bay in April, May, and November (20–27% of the sill). However, overall, the nugget effect was low (<8% of the sill).

Kriged cod density indices increased from 0.003 to 0.015 fish·m^{-2} from April to July in the inner bay and from 0.001 to 0.003 fish·m^{-2} in the outer bay (Table 2). Density indices decreased between July and October, particularly in the inner bay, to 0.001 fish·m^{-2} and then increased in November to 0.004 fish·m^{-2}. Overall, indices were higher in the inner bay in all periods except October. The CVs varied between 5% in July in the inner bay and 19% in May and October in the outer and inner bay, respectively.

Discussion

The simulations and analyses of fish density distribution show that variogram parameters provide an effective way of describing and quantifying fish aggregations at different scales of observation as well as examining the effect of changes in aggregation patterns to the precision of density indices. In the case of cod density distributions, the variogram range, sill, and nugget reflected changes in distribution patterns over the surveyed area, consistent with those observed in the simulated data. In both analyses, variograms of low-density and large aggregations were characterized by large range and small sill and nugget values. In the cod surveys, such a scenario occurred in the outer bay when cod were distributed over larger aggregations (range > 42 km) and densities ≤ 0.001 fish·m^{-2}, particularly in April and May. However, when most fish were located in relatively small portions of the study area (large spatial heterogeneity in sample values), range was small and sill and nugget values were large, as seen in variograms for the inner bay in April, May, and November when cod were found in denser (up to 0.008 fish·m^{-2}) and smaller aggregations (range < 22 km).

Marine habitats often contain directional gradients with which fish might be associated (Swartzman et al. 1999; Maravelias et al. 2000). In the case of Placentia Bay cod, the differences in distribution between the inner bay and outer bay may relate in part to the scale of habitat complexity. The inner bay is characterized by complex small-scale bathymetric features, with semienclosed embayments, deep channels, and shallow banks, whereas the outer bay bathymetry is simpler and characterized by a short shelf and a deep basin extending to the offshore.

The observed fish distribution patterns may also relate to spawning (April–May) and feeding cycles (July) and seasonal migrations (Davis et al. 1994; Lawson and Rose 2000; Robichaud and Rose 2001). Variograms for the inner bay tended to have smaller ranges throughout the year, suggesting that habitat may be a limiting factor in this case. Of note, sill and nugget values increased sharply in the preoverwintering period (November) as fish concentrated into a small area of the bay, behaviour similar to that observed in Smith Sound, Trinity Bay, on the northeast Newfoundland coast (Rose 2003). By contrast, in the outer bay, there is little variation in sill and nugget in July, October, and November, but variogram ranges differ. This may reflect a lack of preferred habitat coupled with a positive relationship between the percentage of habitat utilized and abundance.

The precision of the geostatistical density indices (CVs) was in every case below the maximum level of variability (25%) suggested by Pope (1982) as necessary to produce stock assessments and calculate a total allowable catch with acceptable confidence limits. However, changes in aggregation patterns had important effects in the precision of density indices. For example, CVs declined when fish were highly aggregated in November (14–17%), whereas the smallest CVs (5–8%) were observed in July when cod were more dispersed in small, moderate to dense aggregations throughout the study area.

Regarding the adequacy of the surveys and the precision of abundance estimations, the July indices may not represent accurately the local (spawning) stock abundance. Previous studies (Davis et al. 1994; Lawson and Rose 2000) indicated that cod from adjacent stocks move into the bay mostly between July and September and mix with local fish. The index was higher in the outer bay in October, suggesting that the stock was broadly dispersed throughout the bay during this period. The November survey indices likely reflected stock abundance more accurately, as most local cod are believed to be present in the bay at this time of the year preparing for overwintering (Mello and Rose 2005). Also, the differences in indices between October and November sug-

© 2005 NRC Canada

gest an important shift in distribution from the outer bay to the inner bay in a relatively short period of time (<21 days).

Surveying during periods when the stock is highly aggregated is more favourable than survey designs such as the one employed in this study because most stock biomass could be easily and cost effectively covered and suitable for replicated surveys and further improvement of estimates of variability in survey data (Romaine et al. 2002; Rose 2003). Some points of concern include surveying during the peak of the commercial fishery (Brattey et al. 2002) and also the possibility of rough fall weather, which may affect the quality of acoustic data.

Previous techniques used to analyse spatial distribution patterns of fish include Taylor's power law model (Gauthiez 1997), negative binomial distribution models (Welsh and Ishida 1993; Jarvela and Thorsteinson 1999), density composition and nested aggregation models (Hutchings 1996), cluster analysis (Magill and Sayer 2002), geostatistical aggregation curves (Petitgas 1998), and linear models applied to commercial catch rates (Vignaux 1996). These techniques are often (*i*) dependent on assumptions such as constant density, abundance, or area of population distribution (Langton et al. 1995; Petitgas 1998), (*ii*) limited by the size of the sampling unit or scale of observation (Elliott 1977), and (*iii*) dependent on the understanding of functional relationships of model parameters (Booth 2000). For example, indices of spatial pattern such as Taylor's power law b index and the negative binomial k index are based on the relationship between the variance and mean of the observations measured. Hence, these indices should only be used to compare distributions when the sample mean, total number of individuals in the sample, and number of sampling units are similar. In practice, these assumptions are often difficult to meet, and indices based on the variance to mean ratio may not represent a good measure of the degree of aggregation in a population (Elliott 1977).

Previous studies based on geostatistical analysis have related the variogram parameters to the scale and spatial variability of fish aggregations. Petitgas and Levenez (1996) related the variogram range and sill to the dimensions and number of clusters of pelagic schools per sampling unit area, respectively. Variogram range has been used as an indicator of cluster size for both demersal and pelagic fish schools (Sullivan 1991; Petitgas 1993). Maravelias et al. (1996) implicitly related the size of Atlantic herring aggregations to different range values by suggesting that mesoscale values (12 km) represented herring schools and larger range values (37 km) represented larger scale aggregations. Bez and Rivoirard (2001) used variogram parameters to describe the spatial structure and identify the different scales of Atlantic mackerel (*Scomber scombrus*) ichthyoplankton aggregations. Our results concur with the results of these studies but extend them by developing a conceptual framework to interpret the properties of variogram parameters.

In conclusion, geostatistical modeling allowed us to describe and quantify distribution patterns of fish density over different scales of observation, comparisons of the temporal and spatial changes in density distribution, and estimations of the precision of fish density indices while accounting for the effects of heterogeneous distributions, outliers, and the typically large number of zero and low-density observations. Geostatistical methods have particular applicability to fishes exhibiting gregarious behaviour and seasonally variable distributions, which include many temperate and high-latitude fish species such as Atlantic cod.

Acknowledgements

We thank W. Hiscock and the crew of the RV *Mares* for assistance at sea and F. Mowbray for making suggestions to improve the manuscript. Funding for this study came from the Natural Sciences and Engineering Research Council of Canada Industrial Chair in Fisheries Conservation (Memorial University) and from the Department of Fisheries and Oceans.

References

Bez, N., and Rivoirard, J. 2001. Transitive geostatistics to characterise spatial aggregations with diffuse limits, an application on mackerel ichthyoplankton. Fish. Res. **50**: 41–58.

Booth, A.J. 2000. Incorporating the spatial component of fisheries data into stock assessment models. ICES J. Mar. Sci. **57**: 858–865.

Brattey, J., Cadigan, N.G., Healey, B.P., Lilly, G.R., Murphy, E.F., Shelton, P.A., Stansbury, D.E., Morgan, M.J., and Mahé, J.-C. 2002. An assessment of the cod (*Gadus morhua*) stock in NAFO Subdivision 3Ps in October 2002. DFO Can. Stock Assess. Secretariat Res. Doc. 2002/96.

Breder, C.M., and Halpern, F. 1946. Innate and acquired behaviour affecting the aggregation of fishes. Physiol. Zool. **19**: 154–190.

Cleveland, W.S., and Devlin, S.J. 1988. Locally-weighted regression: an approach to regression analysis by local fitting. J. Am. Stat. Assoc. **83**: 596–610.

Cressie, N.A.C. 1993. Statistics for spatial data. John Wiley & Sons, Inc., New York.

Cressie, N., and Hawkins, D.M. 1980. Robust estimation of the variogram. Math. Geol. **12**: 115–125.

Davis, M.B., Lundrigan, P., and Ripley, R. 1994. A description of cod stock structure in Placentia Bay, NAFO Subdivision 3Ps. DFO Atl. Fish. Res. Doc. 94/32.

deYoung, B., and Rose, G.A. 1993. On recruitment and distribution of Atlantic cod (*Gadus morhua*) off Newfoundland. Can. J. Fish. Aquat. Sci. **50**: 2729–2741.

Elliott, J.M. 1977. Some methods for the statistical analysis of samples of benthic invertebrates. Freshw. Biol. Publ. No. 25.

Foote, K.G., Knudsen, H.P., and Vestnes, G. 1987. Calibration of acoustic instruments for fish density estimation: a practical guide. ICES Coop. Res. Rep. No. 144.

Fréon, P., and Misund, O.A. 1999. Dynamics of pelagic fish distribution and behaviour: effects on fisheries and stock assessment. Blackwell Scientific Publications, Inc., Cambridge, Mass.

Fréon, P., Gerlotto, F., and Soria, M. 1992. Changes in school structure according to external stimuli: description and influence on acoustic assessment. Fish. Res. **15**: 45–66.

Gauthiez, F. 1997. Structuration spatiale des populations de poissons marins démersaux. Thèse de Doctorat, Université Claude Bernard, Lyon I, France.

Hanselman, D.H., Quinn, T.J., Heifetz, J., Clausen, D., and Lunsford, C. 2001. Spatial inferences from adaptive cluster sampling of Gulf of Alaska rockfish. *In* Spatial processes and management of marine populations. *Edited by* G.H. Kruse, N. Bez, A. Booth, M.W. Dorn, S. Hills, R.N. Lipcius, D. Pelletier, C. Roy, S.J. Smith, and D. Witherells. Lowell Wakefield Fish. Symp. Ser. **17**: 303–325.

© 2005 NRC Canada

Hovde, S.C., Albert, O.T., and Nilssen, E.M. 2002. Spatial, seasonal and ontogenetic variation in diet of Northeast Arctic Greenland halibut (*Reinhardtius hippoglossoides*). ICES J. Mar. Sci. **59**: 421–437.

Hutchings, J.A. 1996. Spatial and temporal variation in the density of northern cod and review of hypotheses for the stock's collapse. Can. J. Fish. Aquat. Sci. **53**: 943–962.

Imbrock, F., Appenzeller, A., and Eckmann, R. 1996. Diel and seasonal distribution of perch in Lake Constance: a hydroacoustic study and in situ observations. ICES J. Mar. Sci. **49**: 1–13.

Isaaks, E.H., and Srivastava, R.M. 1989. Applied geostatistics. Oxford University Press, New York.

Jarvela, L.E., and Thorsteinson, L.K. 1999.The epipelagic fish community of Beaufort Sea coastal waters, Alaska. Arctic, **52**: 80–94.

Journel, A.G., and Huijbregts, C.J. 1978. Mining geostatistics. Academic Press, London, U.K.

Krige, D.G., and Magri, E.J. 1982. Studies on the effects of outliers and data transformation on variogram estimates for a base metal and a gold ore body. Math. Geol. **14**: 557–564.

Langton, R.W., Auster, P.J., and Schneider, D.C. 1995. A spatial and temporal perspective on research and management of groundfish in the northwest Atlantic. Rev. Fish. Sci. **3**: 201–229.

Lawson, G.L., and Rose, G.A. 1999. The importance of detectability to acoustic surveys of semi-demersal fish. ICES J. Mar. Sci. **56**: 370–380.

Lawson, G.L., and Rose, G.A. 2000. Seasonal distribution and movements of coastal cod (*Gadus morhua*) in Placentia Bay, Newfoundland. Fish. Res. **49**: 61–75.

Lefeuvre, P., Rose, G.A., Gosine, R., Hale, R., Pearson, W., and Khan, R. 2000. Acoustic species identification in the Northwest Atlantic using digital image processing. Fish. Res. **47**: 137–147.

MacLennan, D.N., and Simmonds, E.J. 1992. Fisheries acoustics. Chapman and Hall, London, U.K.

Magill, S.H., and Sayer, M.D.J. 2002. Seasonal and interannual variation in fish assemblages of northern temperate rocky subtidal habitats. J. Fish Biol. **61**: 1198–1216.

Maravelias, C.D., Reid, D.G., Simmonds, J., and Haralabous, J. 1996. Spatial analysis and mapping of acoustic survey data in the presence of high local variability: geostatistical application to North Sea herring (*Clupea harengus*). Can. J. Fish. Aquat. Sci. **53**: 1497–1505.

Maravelias, C.D., Reid, D.G., and Swartzman, G. 2000. Modelling spatio-temporal effects of environment on Atlantic herring, *Clupea harengus*. Environ. Biol. Fishes, **58**: 157–172.

Matheron, G. 1963. Principles of geostatistics. Econ. Geol. **58**: 1246–1266.

Matheron, G. 1971. The theory of regionalized variables and its applications. Cah. C Morphol. Math. **5**.

Maynou, F.X., Sarda, F., and Conan, G.Y. 1998. Assessment of the spatial structure and biomass evaluation of *Nephrops norvegicus* (L.) populations in the northwestern Mediterranean by geostatistics. ICES J. Mar. Sci. **55**: 102–120.

Mello, L.G.S., and Rose, G.A. 2005. Seasonal variation in abundance and stock composition of Atlantic cod (*Gadus morhua* L.) in Placentia Bay, Newfoundland, in relation to fisheries. Fish. Res. In press.

Myers, R.A., and Cadigan, N.G. 1995. Was an increase in natural mortality responsible for the collapse of northern cod? Can. J. Fish. Aquat. Sci. **52**: 1274–1285.

Nottestad, L., Aksland, M., Beltestad, A., Fernö, A., Johannessen, A., and Misund, O.A. 1996. Schooling dynamics of Norwegian spring spawning herring (*Clupea harengus* L.) in a coastal spawning area. Sarsia, **80**: 277–284.

Petitgas, P. 1993. Geostatistics for fish stock assessment: a review and acoustic application. ICES J. Mar. Sci. **50**: 285–298.

Petitgas, P. 1998. Biomass-dependent dynamics of fish spatial distributions characterized by geostatistical aggregations curves. ICES J. Mar. Sci. **55**: 443–453.

Petitgas, P., and Levenez, J.J. 1996. Spatial organization of pelagic fish: echogram structure, spatial-temporal condition, and biomass in Senegalese waters. ICES J. Mar. Sci. **55**: 147–153.

Petitgas, P., Reid, D., Carrera, M., Iglesias, J., Georgakarakos, S., Liorzou, B., and Massé, J. 2001. On the relation between schools, clusters of schools, and abundance in pelagic fish stocks. ICES J. Mar. Sci. **58**: 1150–1160.

Pope, J.G. 1982. Shortcut formulae for the estimation of coefficient of variation of status quo TAC's. ICES CM 1982/G:12.

Radakov, D.V. 1973. Schooling in the ecology of fish. John Wiley & Sons, New York.

Reid, D., Scalabrin, C., Petitgas, P., Massé, J., Aukland, R., Carrera, P., and Georgakarakos, S. 2000. Standard protocols for the analysis of school based data from echo sounder surveys. Fish. Res. **47**: 125–136.

Rivoirard, J., Simmonds, J., Foote, K.G., Fernandes, P., and Bez, N. 2000. Geostatistics for estimating fish abundance. Blackwell Science, Cornwall.

Robichaud, D., and Rose, G.A. 2001. Multiyear homing of Atlantic cod to a spawning ground. Can. J. Fish. Aquat. Sci. **58**: 2325–2329.

Romaine, S.J., Mackas, D.L., and Macaulay, M.C. 2002. Comparison of euphausiid population size estimates using replicated acoustic surveys of coastal inlets and block average vs. geostatistical spatial interpolation methods. Fish. Oceanogr. **11**: 102–115.

Rose, G.A. 2003. Monitoring coastal northern cod: towards an optimal survey of Smith Sound, Newfoundland. ICES J. Mar. Sci. **60**: 453–462.

Rose, G.A., and Lawson, G.L. 1999. Acoustic surveys in Placentia Bay and 3Ps, June 1996–1998. Can. Stock Assess. Secretariat Res. Doc. 99/41.

Rose, G.A., and Mello, L.G.S. 2001. Acoustic surveys of Placentia Bay in springtime, 1996–2001. Can. Stock Assess. Secretariat Working Pap. 2001/11.

Rose, G.A., deYoung, B., Kulka, D.W., Goddard, S.V., and Fletcher, G.L. 2000. Distribution shifts and overfishing the northern cod (*Gadus morhua*): a view from the ocean. Can. J. Fish. Aquat. Sci. **57**: 644–663.

Simard, Y., and Lavoie, D. 1999. The rich krill aggregation of the Saguenay – St. Lawrence Marine Park: hydroacoustic and geostatistical biomass estimates, structure, variability, and significance for whales. Can. J. Fish. Aquat. Sci. **56**: 1182–1197.

Simard, Y., Legendre, P., Lavoie, G., and Marcotte, D. 1992. Mapping, estimation biomass, and optimizing sampling programs for spatially auto-correlated data: case study of the northern shrimp (*Pandalus borealis*). Can. J. Fish. Aquat. Sci. **49**: 32–45.

Simard, Y., Marcotte, D., and Bourgault, G. 1993. Exploration of geostatistical methods for mapping and estimating acoustic biomass of pelagic fish in the Gulf of St. Lawrence: size of echo-integration unit and auxiliary environmental variables. Aquat. Living Resour. **6**: 185–199.

Stehman, C.F. 1976. Pleistocene and recent sediments of northern Placentia Bay, Newfoundland. Can. J. Earth Sci. **13**: 1386–1392.

Stoner, A.W., and Abookire, A.A. 2002. Sediment preferences and size-specific distribution of young-of-the-year Pacific halibut in an Alaska nursery. J. Fish Biol. **61**: 540–559.

Sullivan, P.J. 1991. Stock abundance estimation using depth-dependent trends and spatially correlated variation. Can. J. Fish. Aquat. Sci. **48**: 1691–1703.

© 2005 NRC Canada

Swartzman, G., Brodeur, R., Napp, J., Hunt, G., Demer, D., and Hewitt, R. 1999. Spatial proximity of age-0 walleye pollock (*Theragra chalcogramma*) to zooplankton near the Pribilof Islands, Bering Sea, Alaska. ICES J. Mar. Sci. **56**: 545–560.

Vignaux, M. 1996. Analysis of spatial structure in fish distribution using commercial catch and effort data from the New Zealand hoki fishery. Can. J. Fish. Aquat. Sci. **53**: 963–973.

Vilhjálmsson, H. 2002. Capelin (*Mallotus villosus*) in the Iceland – East Greenland – Jan Mayen ecosystem. ICES J. Mar. Sci. **59**: 870–883.

Vining, I., Blau, S.F., and Pengilly, D. 2001. Evaluating changes in spatial distribution of blue king crab near St. Matthew Island. *In* Spatial processes and management of marine populations. *Edited by* G.H. Kruse, N. Bez, A. Booth, M.W. Dorn, S. Hills, R.N. Lipcius, D. Pelletier, C. Roy, S.J. Smith, and D. Witherells. Lowell Wakefield Fish. Symp. Ser. **17**: 327–348.

Welsh, D.W., and Ishida, Y. 1993. On the statistical distribution of salmon in the sea: application of the negative binomial distribution, and the influence of sampling effort. Can. J. Fish. Aquat. Sci. **50**: 1029–1038.

Willey, J.D. 1976. Geochemistry and environmental implications of the superficial sediments in northern Placentia Bay, Newfoundland. Can. J. Earth Sci. **13**: 1393–1410.

Williamson, N.J., and Traynor, J.J. 1996. Application of a one-dimensional geostatistical procedure to fisheries acoustic surveys of Alaskan pollock. ICES J. Mar. Sci. **53**: 423–428.

© 2005 NRC Canada

Differential isotopic enrichment and half-life among tissues in Japanese temperate bass (*Lateolabrax japonicus*) juveniles: implications for analyzing migration

Keita W. Suzuki, Akihide Kasai, Kouji Nakayama, and Masaru Tanaka

Abstract: As a first step for field applications of stable isotope techniques to investigate the migration of Japanese temperate bass (*Lateolabrax japonicus*) (Perciformes) juveniles, we conducted a diet switch experiment and fitted an exponential model to changes in stable carbon ($\delta^{13}C$) and nitrogen ($\delta^{15}N$) isotope ratios for muscle, fin, and liver. The trophic enrichment values were ranked liver < muscle < fin for $\delta^{13}C$ (range –0.80‰ to +3.66‰) and liver < fin < muscle for $\delta^{15}N$ (+0.59‰ to +3.12‰). The half-life values were similar for muscle and fin for both $\delta^{13}C$ and $\delta^{15}N$ (19.3–25.7 days), while those for liver were 5.3 days for $\delta^{13}C$ and 14.4 days for $\delta^{15}N$. Both the $\delta^{13}C$ and $\delta^{15}N$ values of muscle reached the asymptotic value after a threefold body weight increase, reflecting the diet after the switch. These results suggest that fin is a useful substitute for muscle in field applications of stable isotope techniques and that liver, with a shorter half-life, has the potential to provide more recent information about migration.

Résumé : Comme première étape de l'application des techniques d'isotopes stables à l'étude sur le terrain de la migration des jeunes bars japonais (perciformes; *Lateolabrax japonicus*), nous avons fait une expérience de changement de régime alimentaire et ajusté un modèle exponentiel aux changements des rapports des isotopes stables de carbone ($\delta^{13}C$) et d'azote ($\delta^{15}N$) du muscle, de la nageoire et du foie. Les valeurs d'enrichissement trophique sont par ordre foie < muscle < nageoire pour $\delta^{13}C$ (étendue –0.80 ‰ à +3,66 ‰) et foie < nageoire < muscle pour $\delta^{15}N$ (+0,59 ‰ à +3,12 ‰). Les valeurs de demi-vie de $\delta^{13}C$ et $\delta^{15}N$ sont semblables dans le muscle et la nageoire (19,3–25,7 jours), alors que, dans le foie, elles sont de 5,3 jours pour $\delta^{13}C$ et de 14,4 jours pour $\delta^{15}N$. Les valeurs de $\delta^{13}C$ et de $\delta^{15}N$ du muscle atteignent toutes deux une valeur d'asymptote, après une augmentation de masse corporelle par un facteur de trois, reflétant ainsi le régime alimentaire après le changement. Ces résultats indiquent que la nageoire peut être utilisée comme substitut du muscle dans les études de terrain qui emploient les techniques d'isotopes stables et que le foie, à cause de sa demi-vie plus courte, peut fournir des renseignements plus récents sur la migration.

[Traduit par la Rédaction]

Introduction

Japanese temperate bass (*Lateolabrax japonicus*) (Perciformes) is a euryhaline marine fish of commercial importance that inhabits the coastal areas of Japan and Korea. In the Chikugo River Estuary on Kyusyu Island, Japan, some juveniles migrate upstream from the sea and grow in the river, while others reside in the estuary (Matsumiya et al. 1982, 1985) or the littoral zone (M. Hibino et al., hibino-m@sea.sannet.ne.jp, Aichi Fisheries Promotion Fund, Department of Sea-Farming, 1–3 Ichizenmatsu, Nakayama, Atsumi-tyou, Atsumi-gun, Aichi 441-3615 Japan, personal communication). In recent years, Ohta et al. (1997) and Secor et al. (1998) conducted otolith Sr and Ca analysis to elucidate this amphidromous-migratory ecology and succeeded in detecting the ingress into fresh water during the early life stages; the otolith Sr/Ca ratio falls significantly only in those individuals exposed to fresh water. However, these analyses were unable to distinguish between individuals that had inhibited in brackish water from those that had lived in seawater. Consequently, the ability to make this distinction has become a challenging research question.

Recently, tracking techniques using stable isotopes, especially C and N, have been widely used in studies on animal migration (reviewed in Hobson 1999). This approach has several advantages over traditional techniques in that it does reveal the links between animals and their food chains before and after migration using the intrinsic signatures associ-

Received 30 March 2004. Accepted 25 November 2004. Published on the NRC Research Press Web site at http://cjfas.nrc.ca on 14 April 2005.
J18055

K.W. Suzuki[1] and A. Kasai. Division of Applied Biosciences, Graduate School of Agriculture, Kyoto University, Kitashirakawa, Sakyo-ku, Kyoto 606-8502, Japan.
K. Nakayama and M. Tanaka. Division of Applied Biosciences, Graduate School of Agriculture, and Field Science Education and Research Center, Kyoto University, Kitashirakawa, Sakyo-ku, Kyoto 606-8502, Japan.

[1]Corresponding author (e-mail: keita@kais.kyoto-u.ac.jp).

 doi: 10.1139/F04-231 © 2005 NRC Canada

ated with animal tissues. Following migration, stable isotope ratios of animal tissue gradually change toward the value reflecting the new diet and converge on it, as is adequately described by negative exponential models for relative growth (Fry and Arnold 1982) or time (Tieszen et al. 1983). To maximize the utility of these models for analyzing temporal migration, it is essential to know two factors about the stable isotope ratios of each tissue through laboratory experiments. First, the diet tissue enrichment of stable isotope ratios is critical to predict stable isotope ratios of animal tissue from those of diets before and after migration and has been reported to vary among tissues (Tieszen et al. 1983; Roth and Hobson 2000) as well as among animal species and (or) diets (DeNiro and Epstein 1978; McCutchan et al. 2003). Second, the turnover rate of change in stable isotope ratios, usually expressed as a half-life value, is characteristic of each tissue; the more rapidly a tissue changes, the more recent the dietary information from the tissue becomes (Tieszen et al. 1983; Hobson and Clark 1992). As for fish species, there has been a shortage of information about both trophic enrichment and half-life for each tissue, except for muscle (but see Hesslein et al. 1993; Pinnegar and Polunin 1999). Among fish tissues, fin is a good substitute for muscle because it can be easily collected without killing the fish (Tyus et al. 1999), and liver has the potential to provide more recent dietary information than muscle owing to its shorter half-life (Tieszen et al. 1983; Hobson and Clark 1992).

As a first step toward field applications of stable isotope techniques for investigations into the migration of Japanese temperate bass juveniles, we conducted a diet switch experiment comparable with the field. Our objectives were (*i*) to determine the values of trophic enrichment and half-life of both stable C and N isotopes for muscle, fin, and liver through model fitting and (*ii*) to evaluate the utility of each tissue.

Materials and methods

Culture before the diet switch

Japanese temperate bass eggs were obtained from adults collected in Tokyo Bay, Japan, and artificially fertilized at the Chiba Prefectural Tokyo Bay Fish Farming Center. Larvae were hatched on 3 December 2002 and cultured at 17–18 °C. Following their development, larvae were fed rotifers, *Artemia* nauplii, frozen Copepoda, and two artificial diets (Ezukehru, Tyubu Shiryo Co., Japan; Minami, Higashimaru Co., Japan).

Juveniles were transported from the Center to the Maizuru Fisheries Research Station, Kyoto University, on 14 March 2003 (101 days after hatching). The juveniles were cultured in a 500-L tank with filtered seawater and fed another artificial diet (C-type, Kyowa Hakko Kogyo Co., Japan, hereafter called the control diet) three times per day for 65 days. Based on data from a preliminary experiment, the culturing period before the diet switch was set long enough for the stable isotope ratios of juveniles to converge on the value reflecting the control diet. Water temperature was maintained at 18 °C for the first 45 days and then gradually increased to 23 °C.

Diet switch experiment

On 19 May 2003 (167 days after hatching, hereafter called the initial day), 10 individuals were randomly captured prior to feeding and anesthetized in a 0.1‰ 2-phenoxyethanol bath. The standard length (SL) and wet body weight (BW) of the individuals were measured. These specimens were frozen at –30 °C to provide the initial stable isotope ratios before the diet switch. The remaining fish were randomly divided into a treatment group (58 individuals) and a control group (23 individuals) and transferred to the respective 500-L tanks.

From the following day, the diet of the treatment group was switched to another artificial diet (Hirame-S, Higashimaru Co., Japan, hereafter called the treatment diet), while that of the control group remained the control diet. Fish were fed to repletion, or as much as possible within 10 min, three times per day (every morning, noon, and evening) and the weight of the diet supplied to each group was recorded.

Filtered seawater (mesh size = 30 μm) (Nihon Rosuiki Kogyo Co., Japan) was aerated and controlled to flow through each tank at a rate of 1.0–1.5 L·min^{-1}. Water temperature was maintained at 23 °C to mimic the mean water-surface temperature that Japanese temperate bass juveniles would have encountered in the Chikugo River Estuary (K.W. Suzuki, personal observation). As soon as a dead fish was found, it was removed from the tank and its SL and BW were measured.

Five individuals from the treatment group were sampled 4, 9, 15, 22, 30, 40, 50, 65, and 80 days after the initial day, whereas from the control group, five individuals were sampled 30 and 65 days after the initial day. All remaining fish from both groups were sampled 100 days after the initial day (hereafter called the final day). Samples of the fish and diets were kept frozen at –30 °C until analyzed.

Stable isotope analysis

From every fish sample, lateral white muscle anterior to the dorsal fin was excised, and a small piece (about 1 cm^2) of caudal fin, which consisted of both ray and membrane, was clipped. Whole-liver tissue was excised from every individual that had been sampled within 65 days of the initial day. The fin was rinsed using distilled water and the liver was homogenized in a 1.5-mL vial with a pestle. All tissues and diet samples were dried at 60 °C for over 24 h and ground to a fine powder. The powdered samples (0.4–0.7 mg) were put directly into tin containers without removing lipid.

The C and N stable isotope ratios and the C:N ratios were determined from each single sample. These analyses were made using a stable isotope ratio mass spectrometer (Delta S, Finnigan MAT Co., Germany) in the continuous-flow mode equipped with an elemental analyzer (EA1108, Fisons Instrument Co., Italy) at the Center for Ecological Research, Kyoto University.

The stable isotope ratios are described by a per mil (‰) deviation from the respective international standards using the following equation:

$$(1) \qquad \delta X = [(R_{sample}/R_{standard}) - 1] \times 1000$$

where X represents ^{13}C or ^{15}N and R is the $^{13}C/^{12}C$ or $^{15}N/^{14}N$ ratio. Peedee Belemnite and atmospheric N_2 are the standards for C and N, respectively. DL-Alanine was used as a secondary standard to verify the accuracy of stable isotope analysis. The standard deviations for the secondary standard were less than 0.15‰ for $\delta^{13}C$ and 0.16‰ for $\delta^{15}N$.

© 2005 NRC Canada

Table 1. Composition and stable isotope ratios of the control and treatment diets used in the Japanese temperate bass (*Lateolabrax japonicus*) diet switch experiment.

	Control	Treatment
Crude protein (% dry mass)[a]	≥55	≥51
Crude fat (% dry mass)[a]	≥10	≥9
Crude fiber (% dry mass)[a]	≤4	≤2
Crude ash (% dry mass)[a]	≤17	≤15
$\delta^{13}C$ (‰)	−23.19±0.05 (N = 4)	−19.94±0.46 (N = 4)
$\delta^{15}N$ (‰)	7.41±0.55 (N = 4)	13.76±0.46 (N = 4)
C:N	4.73±0.08 (N = 4)	5.05±0.09 (N = 4)

[a]Values guaranteed by the manufacturers of each artificial diet.

Model fitting

An exponential model (Tieszen et al. 1983; Hesslein et al. 1993) was fitted to the stable isotope data of the treatment group:

$$\delta X_t = \delta X_a + (\delta X_i - \delta X_a)\exp(c \cdot t) \quad (2)$$

where δX_t is the stable isotope ratio of fish tissue t days after the initial day, c is the turnover rate for each stable isotope change, and δX_i and δX_a are the initial and asymptotic stable isotope ratios, respectively, of fish tissue. During the model fitting procedure, the value of δX_i was fixed to the mean stable isotope ratio of 10 individuals sampled on the initial day. The values of c and δX_a with approximate standard errors were estimated by the least-squares method in JMP version 5 (SAS Institute Inc., Cary, North Carolina).

The trophic enrichment of $\delta^{13}C$ and $\delta^{15}N$ was simply defined as described by Minagawa and Wada (1984):

$$\Delta\delta X_{tissue} = \delta X_{tissue} - \delta X_{diet} \quad (3)$$

where $\Delta\delta X_{tissue}$ represents the trophic enrichment of $\delta^{13}C$ or $\delta^{15}N$ for a specific tissue derived from individuals fed a specific diet. The values of δX_{tissue} and δX_{diet} are the mean stable isotope ratios of the tissue and diet, respectively. For the treatment group, the value of δX_a was substituted for the value of δX_{tissue} and theoretical values of $\Delta\delta X_{tissue}$ were calculated.

The half-life of $\delta^{13}C$ and $\delta^{15}N$ was calculated for each combination of tissue and diet:

$$HL_{tissue} = \ln(0.5)/c \quad (4)$$

where HL_{tissue} stands for the half-life of a specific tissue derived from individuals fed a specific diet.

The growth of each individual was expressed as the relative BW increase (BW_r). To validate the application of eq. 2 to stable isotope data of growing individuals, an exponential growth model was separately fitted to growth data from the control and treatment groups (Hesslein et al. 1993):

$$BW_r = BW_t/BW_i = \exp(k \cdot t) \quad (5)$$

where BW_t and BW_i represent the BW value of each individual sampled t days after the initial day and the mean BW value of 10 individuals sampled on the initial day, respectively, and k is the growth rate of the group (per day).

Results in the text were expressed as the mean ± SD with N (the number of samples analyzed).

Fig. 1. Relative body weight increase (BW_r) of Japanese temperate bass (*Lateolabrax japonicus*) juveniles during the diet switch experiment. Squares indicate the control fish and triangles indicate the treatment fish. Exponential growth curves represent the growth of the control (broken line) and treatment (dotted line) groups with best-fit equations and coefficients of determination (R^2). The mean BW was 9.87 ± 4.16 g (N = 10) on the initial day (167 days after hatching).

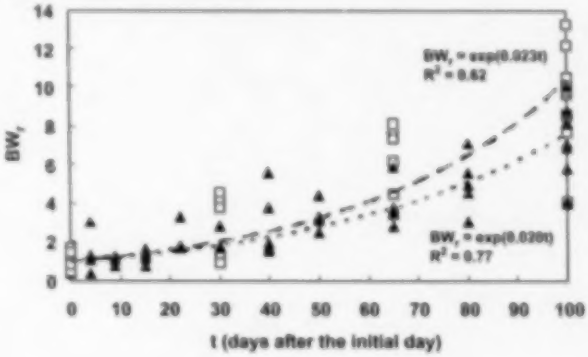

Results

Culture conditions

The water conditions and the amount of diet that was supplied were similar between the control and treatment groups (data not shown). The differences in the stable isotope ratios between the control and treatment diets were 3.25‰ for $\delta^{13}C$ and 6.35‰ for $\delta^{15}N$ (Table 1). Based on the guarantees by each artificial diet manufacturer, both diets had almost the same nutritional composition, except that the control diet had more crude protein and a lower C:N ratio (Table 1).

Fish growth

The fish were 84.0 ± 10.4 mm SL and 9.87 ± 4.16 g BW (N = 10) on the initial day and increased in mass over the course of the experiment (Fig. 1). On the final day, the fish were 178.0 ± 14.4 mm SL and 94.1 ± 22.7 g BW (N = 12) for the control group and 164.9 ± 13.2 mm SL and 72.7 ± 18.4 g BW (N = 8) for the treatment group. The exponential growth model well represented fish growth; the growth rate was slightly higher in the control group than in the treatment group (0.023 and 0.020, respectively).

In the control group, only one individual died during the experiment. Conversely, three of the smallest individuals in

© 2005 NRC Canada

Fig. 2. Values of (*a*) $\delta^{13}C$ and (*b*) $\delta^{15}N$ for muscle from Japanese temperate bass (*Lateolabrax japonicus*) juveniles during the diet switch experiment. Squares indicate the control fish and triangles indicate the treatment fish. Solid lines and equations represent the best-fit model with coefficients of determination (R^2). The mean $\delta^{13}C$ and $\delta^{15}N$ values for the control diet (long-dashed lines) and the treatment diet (short-dashed lines) are also shown.

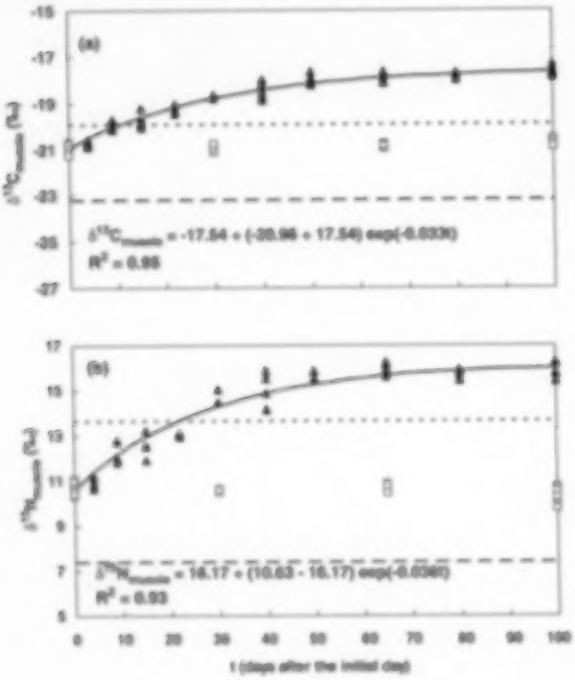
(a)
$\delta^{13}C_{muscle}$ = -17.54 + (-20.96 + 17.54) exp(-0.033t)
R^2 = 0.95
(b)
$\delta^{15}N_{muscle}$ = 16.17 + (10.53 - 16.17) exp(-0.034t)
R^2 = 0.93
t (days after the initial day)

Fig. 3. Values of (*a*) $\delta^{13}C$ and (*b*) $\delta^{15}N$ for fin from Japanese temperate bass (*Lateolabrax japonicus*) juveniles during the diet switch experiment. Squares indicate the control fish and triangles indicate the treatment fish. Solid lines and equations represent the best-fit model with coefficients of determination (R^2). The mean $\delta^{13}C$ and $\delta^{15}N$ values for the control diet (long-dashed lines) and the treatment diet (short-dashed lines) are also shown.

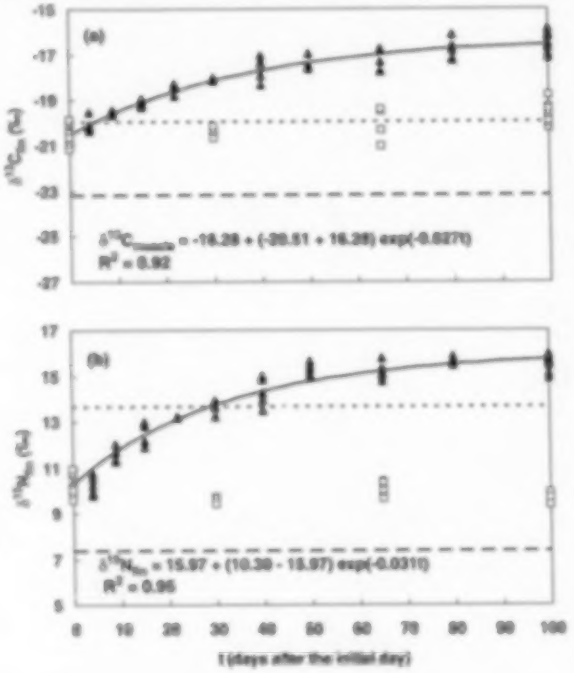

the treatment group became feeble and died 12, 19, and 40 days after the initial day, and two individuals jumped out of the tank and died. In addition, since seven individuals refused to eat the treatment diet and did not gain any weight, the data from these individuals were not included in further analyses.

Stable isotope ratios of the control group

In the control group, both $\delta^{13}C$ and $\delta^{15}N$ values differed among tissues on the initial day but were almost fixed during the experiment for each tissue (Figs. 2, 3, and 4). The mean values over the course of the experiment (N = 32) were $\delta^{13}C_{liver}$ (–23.99 ± 0.74‰) < $\delta^{13}C_{muscle}$ (–20.89 ± 0.15‰) < $\delta^{13}C_{fin}$ (–20.08 ± 0.57‰) and $\delta^{15}N_{liver}$ (8.95 ± 0.78‰) < $\delta^{15}N_{fin}$ (9.89 ± 0.43‰) < $\delta^{15}N_{muscle}$ (10.53 ± 0.25‰) (Table 2). Consequently, the values of trophic enrichment for each tissue were calculated as $\Delta\delta^{13}C_{liver}$ (–0.80‰) < $\Delta\delta^{13}C_{muscle}$ (+2.30‰) < $\Delta\delta^{13}C_{fin}$ (+3.11‰) and $\Delta\delta^{15}N_{liver}$ (+1.54‰) < $\Delta\delta^{15}N_{fin}$ (+2.48‰) < $\Delta\delta^{15}N_{muscle}$ (+3.12‰).

Changes in stable isotope ratios of the treatment group

Both the $\delta^{13}C$ and $\delta^{15}N$ values of each tissue from the treatment group changed toward the more enriched values and converged on the asymptotic values reflecting the treatment diet during the experiment (Figs. 2, 3, and 4). The exponential model provided a good fit for changes in both $\delta^{13}C$ and $\delta^{15}N$ of the three tissues, but $\delta^{13}C$ of liver had a large dispersion on each sampling day. The theoretical trophic enrichment for each tissue was calculated using the value of δX_∞: $\Delta\delta^{13}C_{liver}$ (+0.34‰) < $\Delta\delta^{13}C_{muscle}$ (+2.40‰) < $\Delta\delta^{13}C_{fin}$ (+3.66‰) and $\Delta\delta^{15}N_{liver}$ (+0.59‰) < $\Delta\delta^{15}N_{fin}$ (+2.21‰) < $\Delta\delta^{15}N_{muscle}$ (+2.41‰). The half-life values for the three tissues were calculated as HL_{liver} (5.29 days) < HL_{muscle} (21.00 days) < HL_{fin} (25.67 days) for $\delta^{13}C$ and HL_{liver} (14.44 days) < HL_{muscle} (19.25 days) < HL_{fin} (22.36 days) for $\delta^{15}N$. After a threefold BW increase, both the $\delta^{13}C$ and $\delta^{15}N$ values almost reached the asymptotic value in muscle (Fig. 5) and fin (data not shown). In liver, although isotopic values changed more rapidly, the precise point of the arrival at the asymptotic value was hard to determine owing to a larger dispersion.

Discussion

Fish growth and changes in stable isotope ratios

There was a tendency for the control group fish to gain more weight than the treatment group fish. Dietary conditions, culturing density, and sampling intervals could have influenced fish growth, since both groups were cultured under almost the same conditions except for these factors. In addition, some individuals were observed to refuse the treatment diet after the diet switch and became feeble and died. However, most individuals in the treatment group showed

© 2005 NRC Canada

Table 2. Values of trophic enrichment and half-life of $\delta^{13}C$ and $\delta^{15}N$ for muscle, fin, and liver from the Japanese temperate bass (*Lateolabrax japonicus*) control and treatment groups.

	Muscle		Fin		Liver	
	$\delta^{13}C$	$\delta^{15}N$	$\delta^{13}C$	$\delta^{15}N$	$\delta^{13}C$	$\delta^{15}N$
Control						
δX_{tissue} (‰)	−20.89±0.15	10.53±0.26	−20.08±0.57	9.89±0.43	23.99±0.74	8.95±0.78
$\Delta\delta X_{tissue}$ (‰)	+2.30	+3.12	+3.11	+2.48	−0.80	+1.54
Treatment						
δX_0 (‰)	−17.54±0.09	16.17±0.17	−16.28±0.18	15.97±0.20	−19.60±0.22	14.35±0.31
$\Delta\delta X_{tissue}$ (‰)	+2.40	+2.41	+3.66	+2.21	+0.34	+0.59
HL_{tissue} (days)	21.00±1.91	19.25±1.60	25.67±2.85	22.36±2.16	5.29±1.17	14.44±2.11

Note: δX_{tissue} denotes the mean ± SD for a specific tissue during the experiment (N = 32), $\Delta\delta X_{tissue}$ denotes the trophic enrichment for a specific tissue, δX_0 denotes the asymptotic value ± approximate SE estimated through model fitting, and HL_{tissue} denotes the half-life ± approximate SE estimated through model fitting for a specific tissue.

Fig. 4. Values of (*a*) $\delta^{13}C$ and (*b*) $\delta^{15}N$ for liver from Japanese temperate bass (*Lateolabrax japonicus*) juveniles during the diet switch experiment. Squares indicate the control fish and triangles indicate the treatment fish. Solid lines and equations represent the best-fit model with coefficients of determination (R^2). The mean $\delta^{13}C$ and $\delta^{15}N$ values for the control diet (long-dashed lines) and the treatment diet (short-dashed lines) are also shown.

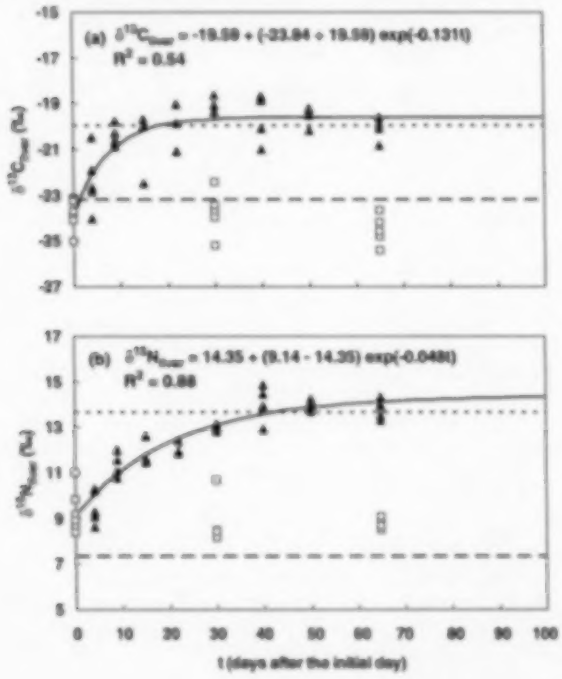
(a) δ13Cliver = -19.59 + (-23.84 + 19.59) exp(-0.1311t)
R2 = 0.54
δ13Cliver (‰)
(b) δ15Nliver = 14.35 + (9.14 - 14.35) exp(-0.048t)
R2 = 0.88
δ15Nliver (‰)
t (days after the initial day)

Fig. 5. Relative body weight increase (BW_r) and the values of (*a*) $\delta^{13}C$ and (*b*) $\delta^{15}N$ for muscle from Japanese temperate bass (*Lateolabrax japonicus*) juveniles during the diet switch experiment. Squares indicate the control fish and triangles indicate the treatment fish. The mean $\delta^{13}C$ and $\delta^{15}N$ values for the control diet (long-dashed lines) and the treatment diet (short-dashed lines) are also shown.

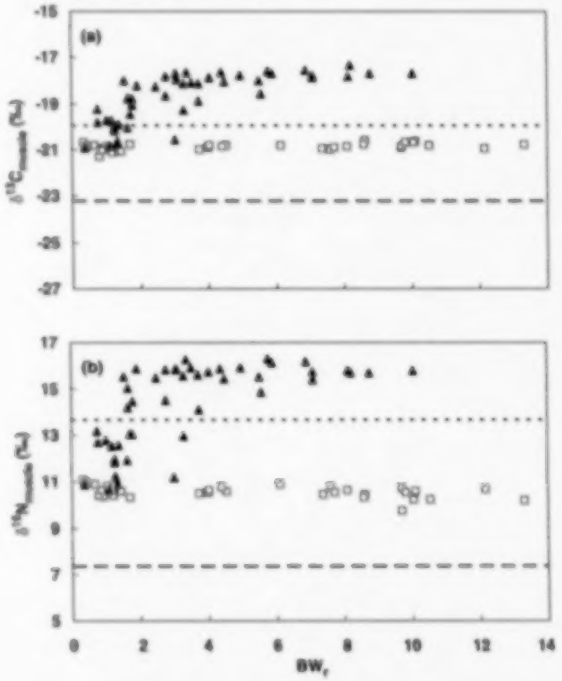

normal growth, with BW increasing sevenfold by the final day.

A new equilibrium with the $\delta^{13}C$ and $\delta^{15}N$ values of the treatment diet was reached at equal rates in muscle and fin tissue (after a threefold increase in BW) and more rapidly in liver. The isotopic changes in tissue that succeed a diet switch are brought about by addition of new mass made from the new diet (growth) and the replacement of old mass from the previous diet (metabolic turnover) (Fry and Arnold 1982; Hesslein et al. 1993). Without metabolic turnover, the dilution by growth alone would change stable isotope ratios of a tissue toward a new equilibrium with the new diet; a twofold growth would bring a 50% change and a threefold growth would bring a 67% change. It has been reported that the isotopic values of the whole body in fast-growing fish are changed almost entirely by growth, only reaching equilibrium after the body mass increased by many times, approximately sixfold for larval red drum (*Sciaenops*

© 2005 NRC Canada

ocellatus) (Herzka and Holt 2000) and more than 10-fold for juvenile winter flounder (*Pleuronectes americanus* (previously *Pseudopleuronectes americanus*)) (Bosley et al. 2002). In tissues of moderate- or slow-growing fish, our results suggest that both metabolic turnover and growth are likely to play a major role in isotopic changes, with a new equilibrium established after a severalfold increase in mass.

Trophic enrichment

Standard deviations for both $\delta^{13}C$ and $\delta^{15}N$ in the three tissue types showed that muscle had the smallest deviation, fin tissue had intermediate deviation, and liver had the largest deviation. In terms of analytical accuracy, therefore, we found muscle to be the most suitable tissue for stable isotope analysis, a finding that corroborates those of Pinnegar and Polunin (1999). Considering that many fin samples can be collected with ease and without killing the fish (Tyus et al. 1999), fin could be the most ideal tissue in some cases. As a center of metabolism (Ballantyne 2001), the liver is likely to be characterized by dynamic changes in biochemical composition, reflecting the condition of each individual. This would account for the relatively large dispersion of $\delta^{13}C$ and $\delta^{15}N$ values observed in liver.

Both the control and treatment groups had a consistent order with respect to $\delta^{13}C$ enrichment in each tissue: $\Delta\delta^{13}C_{liver} < \Delta\delta^{13}C_{muscle} < \Delta\delta^{13}C_{fin}$. A similar order was reported for mammalian tissues ($\Delta\delta^{13}C_{liver} < \Delta\delta^{13}C_{muscle} < \Delta\delta^{13}C_{hair}$), which has been attributed mainly to variations in the biochemical composition of tissues (Tieszen et al. 1983; Roth and Hobson 2000). Among the major biochemical fractions, lipid is the most depleted in ^{13}C. Consequently, tissue with a high lipid content has a lower $\delta^{13}C$ value than tissue with a low lipid content (DeNiro and Epstein 1977, 1978). We did not remove lipid from tissue but analyzed the whole tissue to minimize the dispersion of $\delta^{13}C$ and $\delta^{15}N$ (Pinnegar and Polunin 1999) and to get a shorter half-life of liver containing lipid (Tieszen et al. 1983). Consequently, $\delta^{13}C$ enrichment was the highest for fin, which consists of mainly collagen (Nagai and Suzuki 2000), and lowest for liver, which contains much lipid (Jørgensen et al. 1997; Pinnegar and Polunin 1999). As for muscle, the $\delta^{13}C$ enrichment obtained in this study was within the range of values for cultured fish muscle containing lipid (Pinnegar and Polunin 1999; McCutchan et al. 2003). Although the higher $\delta^{13}C$ enrichment in the treatment group than in the control group could be due to differences in the biochemical composition of diets (Pearson et al. 2003), substantial causes for diet-dependent differences in $\delta^{13}C$ enrichment remain to be studied.

In contrast with $\delta^{13}C$, the control fish showed slightly higher $\delta^{15}N$ enrichment values than the treatment fish for every tissue. In general, animals excrete ^{15}N-depleted N leaving ^{15}N-enriched N, which gives rise to a higher $\delta^{15}N$ in animal tissue than in their diet (Steele and Daniel 1978; Minagawa and Wada 1984). According to Peres and Oliva-Teles (2001), a high-protein diet caused no change in N intake but did increase N excretion when the diets were supplied to repletion for European sea bass (*Dicentrarchus labrax*) juveniles. In the present study, the control diet contained more protein than the treatment diet, and the control fish might therefore have excreted more ^{15}N-depleted N and showed higher $\delta^{15}N$ enrichment than the treatment fish. Adams and Sterner (2000) and McCutchan et al. (2003) reported that the $\delta^{15}N$ enrichment tends to be high when the dietary N level is above or much below the level required by animals. It is considered necessary, especially in fish, to note dietary protein levels in $\delta^{15}N$ enrichment studies because amino acids play a primary role in fish metabolism (Ballantyne 2001). Conversely, variations in the biochemical composition of tissues, mainly in the amino acid composition, possibly account for the differences in $\delta^{15}N$ enrichment among the tissues (Gaebler et al. 1966; Pinnegar and Polunin 1999).

Half-life

The half-life values of both $\delta^{13}C$ and $\delta^{15}N$ were almost identical between muscle and fin at approximately 20–25 days. While there were slight differences in trophic enrichment between muscle and fin tissue, our results promote the use of fin as a substitute for muscle in field applications of stable isotope techniques. It has been reported that the HL_{muscle} values of $\delta^{13}C$ were longer than 1 year for 2.5-year-old broad whitefish (*Coregonus nasus*) (Hesslein et al. 1993) and 5.0–17.3 days for juvenile Japanese flounder (*Paralichthys olivaceus*) (calculated from the original data of the turnover rate; Tominaga et al. 2003). As for the HL_{muscle} values of $\delta^{15}N$, although there are no data available from laboratory experiments, Maruyama et al. (2001) derived the value of 1.1–3.3 months for wild gobies (*Rhinogobius* sp.). Despite large variations in the half-life values among fish species and (or) life stages, the excellent fit of the model in the present study demonstrated that the value of 20–25 days is appropriate for muscle and fin from Japanese temperate bass juveniles.

The half-life values of liver were shorter than those of muscle and fin, indicating the potential to provide more recent information, as described by Tieszen et al. (1983). In liver, the $\delta^{15}N$ values, whose temporal changes have not been reported for any animal, converged on the asymptotic value less rapidly but more steadily than did the $\delta^{13}C$ values. This finding indicates a more regular metabolism in N than in C during the experiment. Its generality needs to be examined under other experimental conditions, since protein metabolism is subject to various factors (reviewed in Carter and Houlihan 2001).

Potential for field applications

The results of the present study encourage applications of stable isotope techniques for temporal analyses of fish migration between isotopically different food chains with scales of several days to several weeks. In field applications, the use of fin as a substitute for muscle will make it easier to collect and analyze a large number of samples. On the other hand, liver can be used to obtain more recent information than muscle and fin. Three influential factors must be considered when interpreting data from the field using a knowledge base from experiments. First, natural diets with a different biochemical composition from that of experimental diets possibly bring about different trophic enrichment values (e.g., dietary protein level for $\delta^{15}N$) (this study; McCutchan et al. 2003). Second, variations in the biochemical composition of a single tissue, according to the ontogeny

© 2005 NRC Canada

and (or) season (Jørgensen et al. 1997), will influence the stable isotope ratios (e.g., lipid fraction for $\delta^{13}C$; DeNiro and Epstein 1978). Third, different external conditions affect both growth and metabolic turnover, leading to different half-life values (e.g., temperature, Bosley et al. 2002; diet ration, Tominaga et al. 2003). Therefore, to investigate migration using stable isotope techniques, it is important to conduct laboratory experiments comparable with the field and to make proper use of tissues according to the intended purpose (Gannes et al. 1997). Furthermore, it is equally important to collect potential food items and survey environmental conditions before and after migration when collecting animals in the field. In addition to stable isotope techniques, other tracking techniques and gut content analysis would provide supplementary information and improve our understanding of migration.

Acknowledgements

We are grateful to Mr. N. Makino, Chiba Prefectural Tokyo Bay Fish Farming Center, for supplying Japanese temperate bass juveniles. Dr. A. Sugimoto of CER, Kyoto University, allowed us to use the IRMS and helped us to analyze stable isotopes. Dr. Y. Yamashita and Dr. R. Masuda of Maizuru Fisheries Research Station, Field Science Education and Research Center, Kyoto University, provided us with useful advice. Our study benefitted considerably from discussion with Dr. T. Ohta, Tottori Prefectural Fisheries Research Center. We thank Dr. J. Syoji, Mr. T. Iseki, and graduate students of Kyoto University for their helpful assistance and comments.

References

Adams, T.S., and Sterner, R.W. 2000. The effect of dietary nitrogen content on trophic level ^{15}N enrichment. Limnol. Oceanogr. **45**: 601–607.

Ballantyne, J.S. 2001. Amino acid metabolism. *In* Nitrogen excretion. *Edited by* P. Wright and P. Anderson. Academic Press, San Diego, Calif. pp. 77–107.

Bosley, K.L., Witting, D.A., Chambers, R.C., and Wainright, S.C. 2002. Estimating turnover rates of carbon and nitrogen in recently metamorphosed winter flounder *Pseudopleuronectes americanus* with stable isotopes. Mar. Ecol. Prog. Ser. **236**: 233–240.

Carter, C.G., and Houlihan, D.F. 2001. Protein synthesis. *In* Nitrogen excretion. *Edited by* P. Wright and P. Anderson. Academic Press, San Diego, Calif. pp. 31–75.

DeNiro, M.J., and Epstein, S. 1977. Mechanism of carbon isotope fractionation associated with lipid synthesis. Science (Wash., D.C.), **197**: 261–263.

DeNiro, M.J., and Epstein, S. 1978. Influence of diet on the distribution of carbon isotopes in animals. Geochim. Cosmochim. Acta, **42**: 495–506.

Fry, B., and Arnold, C. 1982. Rapid $^{13}C/^{12}C$ turnover during growth of brown shrimp (*Penaeus aztecus*). Oecologia, **54**: 200–204.

Gaebler, O.H., Vitti, T.G., and Vukmirovich, R. 1966. Isotope effects in metabolism of ^{14}N and ^{15}N from unlabeled dietary proteins. Can. J. Biochem. **44**: 1249–1257.

Gannes, L.Z., O'Brien, D.M., and Martínez del Río, C. 1997. Stable isotopes in animal ecology: assumptions, caveats, and a call for more laboratory experiments. Ecology, **78**: 1271–1276.

Herzka, S.Z., and Holt, G.J. 2000. Changes in isotopic composition of red drum (*Sciaenops ocellatus*) larvae in response to dietary shifts: potential applications to settlement studies. Can. J. Fish. Aquat. Sci. **57**: 137–147.

Hesslein, R.H., Hallard, K.A., and Ramal, P. 1993. Replacement of sulfur, carbon, and nitrogen in tissue of growing broad whitefish (*Coregonus nasus*) in response to a change in diet traced by $\delta^{34}S$, $\delta^{13}C$, and $\delta^{15}N$. Can. J. Fish. Aquat. Sci. **50**: 2071–2076.

Hobson, K.A. 1999. Tracing origins and migration of wildlife using stable isotopes: a review. Oecologia, **120**: 314–326.

Hobson, K.A., and Clark, R.G. 1992. Assessing avian diets using stable isotopes, I: Turnover of ^{13}C in tissues. Condor, **94**: 181–188.

Jørgensen, E.H., Johansen, S.J.S., and Jobling, M. 1997. Seasonal patterns of growth, lipid deposition and lipid depletion in anadromous Arctic charr. J. Fish Biol. **51**: 312–326.

Maruyama, A., Yamada, Y., Rusuwa, B., and Yuma, M. 2001. Change in stable nitrogen isotope ratio in the muscle tissue of a migratory goby, *Rhinogobius* sp., in a natural setting. Can. J. Fish. Aquat. Sci. **58**: 2125–2128.

Matsumiya, Y., Mitani, T., and Tanaka, M. 1982. Changes in distribution pattern and condition coefficient of the juvenile Japanese sea bass with the Chikugo River ascending. Nippon Suisan Gakkaishi, **48**: 129–138.

Matsumiya, Y., Masumoto, H., and Tanaka, M. 1985. Ecology of ascending larval and early juvenile Japanese sea bass in the Chikugo Estuary. Nippon Suisan Gakkaishi, **51**: 1955–1961.

McCutchan, J.H., Jr., Lewis, W.M., Jr., Kendall, C., and McGrath, C.C. 2003. Variation in trophic shift for stable isotope ratios of carbon, nitrogen, and sulfur. Oikos, **102**: 378–390.

Minagawa, M., and Wada, E. 1984. Stepwise enrichment of ^{15}N along food chains: further evidence and the relation between $\delta^{15}N$ and animal age. Geochim. Cosmochim. Acta, **48**: 1135–1140.

Nagai, T., and Suzuki, N. 2000. Isolation of collagen from fish waste material — skin, bone and fins. Food Chem. **68**: 277–281.

Ohta, T., Arai, N., and Tanaka, M. 1997. Otolith Sr concentration analyzed by PIXE in Ariake estuary-dependent sea bass juveniles. Int. J. PIXE, **17**: 147–151.

Pearson, S.F., Levey, D.J., Greenberg, C.H., and Martínez del Río, C. 2003. Effects of elemental composition on the incorporation of dietary nitrogen and carbon isotopic signatures in an omnivorous songbird. Oecologia, **135**: 516–523.

Peres, H., and Oliva-Teles, A. 2001. Effect of dietary protein and lipid level on metabolic utilization of diets by European sea bass (*Dicentrarchus labrax*) juveniles. Fish Physiol. Biochem. **25**: 269–275.

Pinnegar, J.K., and Polunin, N.V.C. 1999. Differential fractionation of $\delta^{13}C$ and $\delta^{15}N$ among fish tissues: implications for the study of trophic interactions. Funct. Ecol. **13**: 225–231.

Roth, J.D., and Hobson, K.A. 2000. Stable carbon and nitrogen isotopic fractionation between diet and tissue of captive red fox: implications for dietary reconstruction. Can. J. Zool. **78**: 848–852.

Secor, D.H., Ohta, T., Nakayama, K., and Tanaka, M. 1998. Use of otolith microanalysis to determine estuarine migrations of Japanese sea bass *Lateolabrax japonicus* distributed in Ariake Sea. Fish. Sci. **64**: 740–743.

Steele, K.W., and Daniel, R.M. 1978. Fractionation of nitrogen isotopes by animals: a further complication to the use of variations

© 2005 NRC Canada

in the natural abundance of ^{15}N for tracer studies. J. Agric. Sci. **90**: 7–9.

Tieszen, L.L., Boutton, T.W., Tesdahl, K.G., and Slade, N.A. 1983. Fractionation and turnover of stable carbon isotopes in animal tissues: implications for $\delta^{13}C$ analysis of diet. Oecologia, **57**: 32–37.

Tominaga, O., Uno, N., and Seikai, T. 2003. Influence of diet shift from formulated feed to live mysids on the carbon and nitrogen stable isotope ratio ($\delta^{13}C$ and $\delta^{15}N$) in dorsal muscles of juvenile Japanese flounders, *Paralichthys olivaceus*. Aquaculture, **218**: 265–276.

Tyus, H.M., Starnes, W.C., Karp, C.A., and Saunders, J.F. 1999. Effects of invasive tissue collection on rainbow trout, razorback sucker, and bonytail chub. N. Am. J. Fish. Manag. **19**: 848–855.

© 2005 NRC Canada

Multivariate life-history indices of exploited coral reef fish populations used to measure the performance of no-take zones in a marine protected area

Gavin A. Begg, Bruce D. Mapstone, Ashley J. Williams, Samantha Adams, Campbell R. Davies, and Dong C. Lou

Abstract: We investigate the use of multivariate life-history indices to assess the performance of no-take zones with respect to ameliorating the impacts of harvest on exploited coral reef fish populations in the Great Barrier Reef Marine Park. A range of life-history parameters were estimated for the two major target species of the Great Barrier Reef (GBR) line fishery, common coral trout (*Plectropomus leopardus*) and red throat emperor (*Lethrinus miniatus*), collected from five adjacent reefs (three of which were closed to all forms of fishing) in each of three geographically dispersed regions between 1995 and 1998. Life-history parameters were used to compare the status of populations on open and closed reefs over regions and years. Principal components (PC) analyses were used to effectively reduce the number of parameters to four significant PCs for each species, accounting for 84% and 94% of the total variation in the data for common coral trout and red throat emperor, respectively. We were able to clearly identify those populations that were sampled from reefs open or closed to fishing based on the multivariate descriptors of life-history parameters. The concurrent use of several life-history indices maximised our potential to differentiate changes related to no-take zones from background variation.

Résumé : Nous examinons l'utilisation des indices démographiques multidimensionnels pour évaluer la performance des zones de protection marines (MPA) établies pour atténuer l'impact de la récolte sur les populations de poissons des récifs coralliens dans le parc marin de la Grande Barrière de Corail. Nous avons estimé un nombre de variables démographiques pour les deux espèces qui sont le plus couramment ciblées par la pêche à la ligne sur la Grande Barrière de Corail (GBR), la loche saumonée (*Plectropomus leopardus*) et l'empereur gueule longue (*Lethrinus miniatus*), récoltées sur cinq récifs adjacents (dont trois où toute forme de pêche est interdite) dans chacune de trois régions séparées géographiquement de 1995 à 1998. Les variables démographiques ont servi à comparer l'état des populations dans les récifs protégés et non protégés au cours des années dans les différentes régions. Des analyses des composantes principales (PC) ont permis de réduire le nombre de variables à quatre PC significatives pour chaque espèce, expliquant ainsi respectivement 84 % et 94 % de la variation totale des données pour la loche saumonée et l'empereur gueule longue. Les descripteurs multidimensionnels des variables démographiques nous ont permis de distinguer clairement les populations échantillonnées sur les récifs protégés et sur les récifs non protégés. L'utilisation conjointe de plusieurs indices démographiques a maximisé notre capacité de reconnaître les changements dus à la présence des MPA de la variation sous-jacente.

[Traduit par la Rédaction]

Introduction

Increasing impacts on natural resources of marine ecosystems, coupled with ineffective fisheries management and the need to maintain biodiversity in perpetuity, have led to implementations of marine protected areas (MPAs) around the globe. One management strategy frequently promoted within MPAs is the concept of "no-take" zones where all extractive activities such as fishing and collecting are prohibited. Although the concept of no-take zones has been around for decades (Beverton and Holt 1957), their use as an alternate ecosystem-based management strategy is relatively new

Received 10 November 2003. Accepted 4 December 2004. Published on the NRC Research Press Web site at http://cjfas.nrc.ca on 14 April 2005.
J17830

G.A. Begg,[1] B.D. Mapstone,[2] A.J. Williams, S. Adams, C.R. Davies,[3] and D.C. Lou.[4] CRC Reef Research Centre, School of Tropical Environment Studies and Geography, James Cook University, Townsville, 4811 Queensland, Australia.

[1]Corresponding author (e-mail: gavin.begg@jcu.edu.au).
[2]Present address: Antarctic Climate and Ecosystems CRC, Private Bag 80, Hobart, 7001 Tasmania, Australia.
[3]Present address: CSIRO Marine Research, GPO Box 1538, Hobart, 7001 Tasmania, Australia.
[4]Present address: School of Marine Biology and Aquaculture, James Cook University, Townsville, 4811 Queensland, Australia.

 doi: 10.1139/F04-237 © 2005 NRC Canada

(Roberts and Polunin 1991; Agardy 1997; Russ 2002). In this study, we examine the utility of multivariate life-history indices, generated from a suite of life-history parameters of exploited coral reef fish populations, to assess the degree to which no-take zones ameliorated the impacts of fishing within the Great Barrier Reef Marine Park (GBRMP) and World Heritage Area (GBRWHA), Australia. No-take zones are a vital part of the multiple-use zoning approach applied in the GBRMP (Day 2002) and have recently been increased to comprise 33% of the entire Marine Park (GBRMPA 2004).

MPAs have increased in popularity as an alternate management strategy because of the poor state of global fisheries resources and the failure of traditional fisheries management to stem the flow of overcapitalised and overexploited fisheries (Roberts and Polunin 1991; Fogarty et al. 2000; Russ 2002). Traditional fisheries management typically has been based on single-species and stock-specific strategies that have failed to encompass the diversity of multispecies and metastock assemblages, leading to the depletion, extirpation, and collapse of fish stocks throughout the world. Management problems are exacerbated in coral reef fisheries, which tend to be data-limited, community-based, and inherently complex as the result of multispecies and multigear interactions (Crowder et al. 2000). MPAs, however, potentially provide an expedient and efficient ecosystem-based management strategy that embodies the directives of the precautionary approach, fulfilling the dual functionality of biodiversity conservation and, potentially, sustainable utilisation of selected resources (Agardy 1997; Bohnsack 2000).

Several authors have argued that no-take zones can provide an array of potential benefits to fisheries, both ecological and socio-economic, in the face of management uncertainty (e.g., Roberts and Polunin 1991; Murray et al. 1999; Fogarty et al. 2000). Postulated benefits of no-take zones include the following: provision of sanctuary for exploited species from anthropogenic impacts; maintenance of species, population, and habitat biodiversity; protection of ecosystem structure and function; and insurance against fisheries recruitment and management failure (Roberts and Polunin 1991; Bohnsack 1998; Agardy 2000). Recent studies have indicated that abundance, biomass, and (or) size of target species increase within the boundaries of no-take zones (e.g., Buxton 1993; Dugan and Davis 1993; Halpern and Warner 2002), potentially leading to spill-over and larval dispersal effects that might increase fishery yields and replenish unproductive or "sink" habitats in adjacent unprotected areas (Russ and Alcala 1996*a*; Roberts et al. 2001; Halpern 2003). Moreover, no-take zones are considered to be particularly effective in the preservation of coral reef fish species, which tend to be relatively sedentary as adults but widely dispersed as larvae, thereby providing a mechanism for the protection of refuges of spawning stock biomass from which harvested local populations elsewhere might be replenished (Bohnsack 2000).

Despite the widespread advocacy of MPAs and no-take zones, however, their performance has proved difficult to measure because most are established without any clearly defined objectives against which their success (or otherwise) can be evaluated (Agardy 2000). Reviews of MPAs, including no-take zones, and modelling studies evaluating their hypothetical performance abound in the scientific literature (e.g., Polacheck 1990; Allison et al. 1998; Russ 2002), but fewer well-designed and replicated empirical studies testing specific hypotheses exist (but see, for example, Buxton 1993; Russ and Alcala 1996*b*; Mapstone et al. 2004). Typically, once a MPA or a no-take zone is established, there is little follow-up to assess the performance or efficacy of the area, even though routine monitoring and assessment studies should be the default scenario to facilitate performance assessment and review. Those studies that do exist tend to be limited on a spatial and (or) temporal scale (Russ and Alcala 1996*b*; Mapstone et al. 1999), restricting the generalities that can be derived from such studies (Russ 2002; Adams 2002; Mapstone et al. 2004); however, meta-analysis approaches may provide some insight (Mosquera et al. 2000). Furthermore, performances of the respective no-take zones are often limited to gross measures of abundance, biomass, or size of individuals (see reviews of Russ 2002 and Halpern 2003).

Multiple-use MPAs have been established to protect and conserve complex coral reef ecosystems such as those in the GBRMP where precautionary principles of conservation are rated very highly. The Great Barrier Reef (GBR) is the largest coral reef ecosystem in the world, and the GBRMP was established in 1975 to facilitate conservation management of most of the GBR. In 1981, an area including the GBRMP was inscribed on the World Heritage list as the GBRWHA. The GBRMP contains a number of no-take zones, the best known and most widespread are the Marine National Park Zones (locally referred to as "green" zones). Until recently, no-take zones accounted for about 5% of the total area of the GBRMP and approximately 24% of the area of the mapped coral reef habitat in the Marine Park. A major rezoning program, called the Representative Areas Program, was undertaken by the Great Barrier Reef Marine Park Authority (GBRMPA) and resulted in a more comprehensive, adequate, and representative zoning network encompassing all habitats and increased the coverage of no-take zones to 33% of the entire GBRMP. The legislation for the GBRMP sets out the broad objectives of zoning, requiring both conservation and protection of biodiversity while allowing multiple uses, including fishing in some zones.

Fishing is the major extractive use on the GBR, with the various zones determining what activities can occur. The reef line fishery is one of a variety of commercial fisheries, with an annual economic value of about AU$60–100 million. Each year the commercial sector harvests between 3000 and 4000 tonnes (t) from the multispecies reef line fishery of the GBR, while significant quantities are also harvested by the recreational (~2000 t) and charter boat (~300 t) sectors. Common coral trout (*Plectropomus leopardus*) and red throat emperor (*Lethrinus miniatus*) are the two major target species of the reef line fishery for all sectors in most regions of the GBRWHA, comprising nearly 50% of the total catch (Higgs 1996; Mapstone et al. 1996, 2004). In addition to the use of no-take zones, current management strategies for the reef line fishery include seasonal spawning closures and size limits for all sectors, limited entry and an individual transferable catch quota system for the commer-

© 2005 NRC Canada

Table 1. Total number of common coral trout (*Plectropomus leopardus*) and red throat emperor (*Lethrinus miniatus*) sampled during the Effects of Line Fishing (ELF) Experiment, 1995–1998.

			Common coral trout				Red throat emperor			
Region	Reef	Zone	1995	1996	1997	1998	1995	1996	1997	1998
Townsville	Dip	Closed	185	54	154	183	90	23	33	39
	Glow	Closed	339	148	172	197	112	34	95	89
	Faraday	Closed	116	33	123	166	53	25	40	20
	Fork	Open	165	69	74	104	19	10	36	15
	Knife	Open	108	67	32	60	6	10	20	21
Mackay	20–137	Closed	333	193	87	165	97	57	40	43
	20–142	Closed	306	261	144	214	91	53	44	58
	Bax	Closed	317	243	107	264	98	51	52	47
	Boulton	Open	396	96	42	152	79	31	36	56
	Liff	Open	195	129	79	99	49	46	18	22
Storm Cay	21–131	Closed	321	248	242	289	74	31	51	50
	21–132	Closed	332	338	151	341	82	52	50	88
	21–133	Closed	270	154	109	113	69	48	24	46
	21–124	Open	219	116	164	171	20	16	16	13
	21–139	Open	238	167	94	116	51	23	39	39

cial sector, and hook and bag limits for the recreational sector.

Protection from significant fishing mortality via the establishment of no-take zones would be predicted to precipitate, over time, several contrasts between the closed areas and those that remained open to exploitation. Fish in the no-take zones would be expected on average to be more abundant and larger, have increased survivorship, and possibly different population level reproductive characteristics than those in the open areas. Both species considered in this study have been shown to be protogynous hermaphrodites (Ferreira 1995; Adams 2003; Bean et al. 2003), and common coral trout has been shown to be diandric (Adams 2003). Consequently, despite the presence of some small, young males, the larger, older groups of these species are generally male-dominated (Adams et al. 2000; Bean et al. 2003). Fishing has a tendency to disproportionately reduce the abundance of these larger, older males through either direct removal or increased mortality of younger fish (Vincent and Sadovy 1998), potentially leading to larger females changing sex earlier and so also reducing the average age and size of females in the population (Adams 2002). If sex change is insufficiently flexible, however, or fishing removes males at a rate faster than can be replaced by earlier sex change, a highly female-biased sex ratio is expected (Vincent and Sadovy 1998; Adams 2002). In the latter case, it would be expected that sex ratios on reefs open to fishing would be significantly more female-biased than those on reefs closed to fishing.

We assess the relative effects of no-take zones on life-history parameters of the two major target reef fish species over large spatial and temporal scales on the GBR based on a suite of multivariate indices. This multivariate approach reduces the dimensionality in the data while assimilating the influence of a range of individual life-history parameters. We discuss the utility of these indices in evaluating the performance of no-take zones and propose strategies for applying them to monitor the relative success of no-take zones for their potential contribution to the conservation and sustainability of exploited coral reef fish populations.

Materials and methods

Sample collection

Common coral trout and red throat emperor samples were collected between 1995 and 1998 from research line fishing catch surveys for the Effects of Line Fishing (ELF) Experiment (Davies et al. 1998; Mapstone et al. 2004) implemented by the Cooperative Research Centre for the Great Barrier Reef World Heritage Area (CRC Reef). Samples were collected from clusters of six adjacent reefs in four geographic regions. Four of the six reefs in each region had been no-take zones and closed to all forms of fishing for 10–12 years before 1995. The remaining two reefs in each cluster were historically open to fishing and provided the necessary "impact" treatment against which the performance of the no-take zones could be assessed. For the purposes of this study, we analysed multivariate life-history indices derived from a range of life-history parameters for common coral trout and red throat emperor from three of the closed reefs and the two open reefs in three of the four regions (Townsville, Mackay, and Storm Cay) (Table 1; Fig. 1). Typically, red throat emperor does not occur in the fourth region (around Lizard Island, 14°S) and so data from that region were not considered for this study. The fourth closed reef in each region was excluded because it was subjected to experimental fishing in 1997 as part of the CRC Reef ELF Experiment, effectively losing its MPA status, and therefore was not comparable to either the three closed reefs or the two open reefs.

All reefs were sampled each year in the austral spring (October–December) to coincide with the peak spawning period of the main target species, common coral trout. Each reef was divided into six approximately equal-sized, contiguous blocks and sampled on a single day on each sampling occasion. Standardised commercial reef line fishing effort

© 2005 NRC Canada

Fig. 1. Location of the Effects of Line Fishing (ELF) Experimental clusters of reefs (Townsville, Mackay, Storm Cay) from which samples of common coral trout (*Plectropomus leopardus*) and red throat emperor (*Lethrinus miniatus*) were analysed for this study. Asterisks (*) indicate reefs closed to fishing (no-take zone).

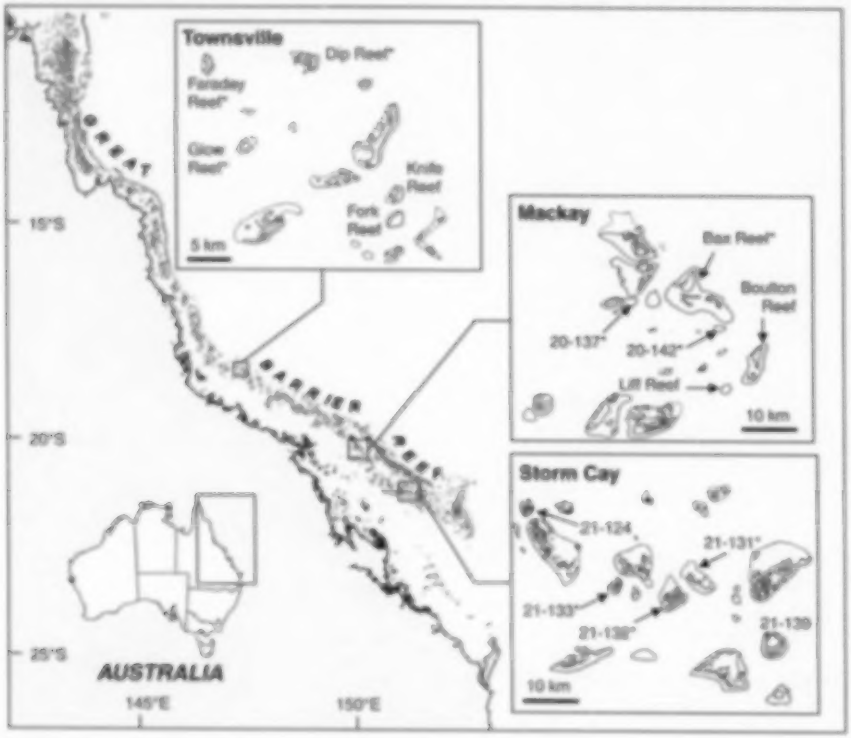

was distributed uniformly across two depth strata within each block. Consequently, diel variations in catch rates, if present, did not affect the outcomes of the study because of the standardised method of sampling where any differences would be relative and applicable across all reefs. All fish caught were measured, tagged for later identification, and kept for weighing and extraction of gonads and otoliths. For further sampling details of the ELF Experiment, see Davies et al. (1998) and Mapstone et al. (2004).

Samples of common coral trout and red throat emperor were aged using standardised methods developed by Ferreira and Russ (1994) and Williams et al. (2003), respectively. In addition, gonads from a random subsample of common coral trout were extracted for histological examination and form the basis of the reproductive parameters used in this study. Common coral trout were classified into functional reproductive categories following Adams et al. (2000).

Parameter estimation

A suite of life-history parameters was estimated from the samples collected for each species at each reef to test the relative performance of no-take zones in the GBRMP (Table 2). Age (Age) and length (Len) richness were used as proxies for age and size frequency distributions, respectively, and estimated for the harvested portion of the population as the number of age (years) and length (10 mm) groups above the minimum legal sizes for the fishery. Harvested populations of common coral trout and red throat emperor were

Table 2. Description of life-history parameters used in the analyses.

Life-history parameter	Description
Age	Number of age groups (years)
Len	Number of length groups (10 mm)
LAA	Mean length-at-age
WAA	Mean weight-at-age
A_{90}	90th percentile of age
L_{90}	90th percentile of length
W_{90}	90th percentile of weight
S	Survivorship estimated from instantaneous mortality rate (e^{-Z})
A_{90m}	90th percentile of age of mature females
L_{90m}	90th percentile of length of mature females
Sex	Operational sex ratio based on proportion of mature males to females
Abun	Relative CPUE index of abundance
Biom	Relative CPUE index of biomass

Note: Harvested population of common coral trout (*Plectropomus leopardus*) and red throat emperor (*Lethrinus miniatus*) were fish equal to or greater than 358-mm and 322-mm fork length (FL), respectively. These FLs correspond to the minimum legal total lengths for harvest of 380 mm and 350 mm, respectively. Mean length- and weight-at-age were estimated for common coral trout fully recruited to the fishery at age 4 years. CPUE, catch-per-unit-effort.

© 2005 NRC Canada

considered to be fish equal to or greater than the minimum legal sizes of 358- and 322-mm fork length (FL), respectively. Similarly, the 90th percentiles of age (A_{90}), fork length (L_{90}), and weight (W_{90}) were estimated for the harvested portion of the respective populations and used as relative indices of senescence, longevity, and growth potential. Catch-per-unit-effort (CPUE) of the total number of fish caught·min^{-1} (Abun) and total weight of fish caught·min^{-1} (Biom) were also estimated for the harvested portions of the populations of each species and used as relative indices of abundance and biomass, respectively.

Additional life-history parameters (LAA, WAA, S, A_{fem}, L_{fem}, Sex) (Table 2) were estimated for common coral trout because of their numerical abundance in the catch and importance as the major target species in the reef line fishery. Common coral trout were considered to be fully recruited to the fishery at 4 years of age, the age at which mean length-at-age (LAA) and weight-at-age (WAA) were estimated. Instantaneous rates of total mortality (Z) were estimated from age-based catch curves for fully recruited fish and used to calculate survivorship ($S = e^{-Z}$) (Beverton and Holt 1957). Age-based catch curves assume constant recruitment among the fully recruited age groups over time (Quinn and Deriso 1999). Although this assumption was untested for common coral trout, there was no clear evidence of significant recruitment events in the observed age frequency distributions. Catch curve regressions were fitted from the first fully selected age group (4 years) through to the oldest age group that was preceded by no more than two consecutive zero frequencies. As a result, the age range used to estimate S varied slightly among reefs. There were insufficient data to estimate S for one of the closed reefs in the Townsville region in 1996 and 1998 and for one of the open reefs off Townsville in 1997. Consequently, estimates of S for each of these reefs in the years with poor data were imputed as the mean value for that reef from the remaining years.

The 90th percentiles of age (A_{fem}) and fork length (L_{fem}) of mature females and the operational sex ratio (Sex) of mature males to mature females were also estimated for *P. leopardus* sampled at each reef (Table 2). There were insufficient data to estimate the sex ratio for one of the open reefs in the Townsville region in 1997 and so an estimate was imputed as the mean value across the remaining years for that reef.

Statistical analysis

Multivariate statistical analyses were used to examine the effects of year (1995–1998), region (Townsville, Mackay, Storm Cay), and reef zone (open, closed) on a suite of life-history parameters for each species. The numerous life-history parameters were used to construct multivariate life-history indices for the two species at each reef to test for discrimination between the closed (no-take) and open reefs. Principal components analysis (PCA) was used initially to reduce the dimensionality in the multivariate data. The original data were transformed to values standardised against their means by their standard deviation because of the different measurement scales of the various parameters and then transformed into principal components (PCs). Consequently, the PCs were weighted averages of the normalised estimates of life-history parameters and as such can be interpreted as multivariate life-history indices. Individual PCs that accounted for 5% or more of the total variation in the data were selected for further analysis. The PC loadings were used to provide a summary of the influence of the original parameters, and biplots were used to represent both the original parameters and transformed observations on pairs of PCs.

Repeated-measures analysis of variance was then used to test the within-group (repeated-measures) effect of year and the between-group effects of region and zone and their interactions for common coral trout and red throat emperor on each significant PC selected in the data-reduction step (SAS 1989). Sphericity tests were used to examine the assumption of type-H covariance structure for the within-group effects, and the Huynh–Feldt estimator was used to adjust tests of significance if this assumption was not satisfied (SAS 1989). Significance criteria were also adjusted for multiple testing of the individual PC multivariate life-history indices using the Bonferroni adjustment (Sokal and Rohlf 1995). Jackknifed cross-validation procedures were used to estimate unbiased classification rates of open and closed reefs based on the significant PC scores.

Results

The initial PCAs for common coral trout and red throat emperor were based on all data, incorporating the effects of year (1995–1998), region (Townsville, Mackay, Storm Cay), and zone (open, closed) on the full suite of life-history parameters. From the 13 parameters (Age, Len, LAA, WAA, A_{90}, L_{90}, W_{90}, S, A_{fem}, L_{fem}, Sex, Abun, Biom) for common coral trout and seven parameters (Age, Len, A_{90}, L_{90}, W_{90}, Abun, Biom) for red throat emperor (Table 1), the PCAs identified four significant principal components (PCs) for each species (Table 3). Additional PCs could be discarded with relatively little loss of explanatory information. The four PCs combined explained 84% and 94% of the total variation in the data for common coral trout and red throat emperor, respectively (Table 3).

Effects of zone

Significant and unconfounded main effects of zone were evident on PC I for both common coral trout and red throat emperor (Table 4; Fig. 2), indicating an effect of zone across the aggregate weighted average scores of all parameters (Table 3). Populations of common coral trout sampled on reefs closed to fishing tended to have broader age and length distributions, older, larger and heavier individuals, greater abundance and biomass, higher survivorship, more males, and larger and older females, all indicators of a healthy population (Fig. 3). Like common coral trout, populations of red throat emperor sampled on reefs closed to fishing tended to have broader age and length distributions and greater abundance and biomass (Fig. 3). In contrast, there was no consistent pattern in the morphometric life-history parameters (A_{90}, L_{90}, W_{90}) for red throat emperor sampled on reefs open and closed to fishing. The PC I loadings and relative magnitude of the influence of these parameters were typically lower than those observed for the other life-history parameters (Abun, Biom, Age, Len) (Table 3; Fig. 3).

© 2005 NRC Canada

Table 3. Significant (equal or greater than 5% of the total variation in the data) principal components (PCs) and PC loadings of life-history parameters for common coral trout (*Plectropomus leopardus*) and red throat emperor (*Lethrinus miniatus*) collected from open and closed reefs off Townsville, Mackay, and Storm Cay, 1995–1998.

Life-history parameter	PC I	PC II	PC III	PC IV
(*a*) Common coral trout				
Age	0.353	0.127		
Len	0.353	0.155	0.149	–0.177
LAA		–0.488	0.344	0.306
WAA		–0.468	0.376	0.321
A_{∞}	0.303		–0.447	
L_{∞}	0.366	–0.127		
W_{∞}	0.369	–0.123		
S	0.210	–0.220	–0.449	0.264
$A_{50\%}$	0.285	–0.142	–0.334	
$L_{50\%}$	0.242	–0.264		–0.487
Sex	0.119	0.381		0.669
Abun	0.289	0.327	0.315	
Biom	0.309	0.282	0.303	
Proportion of variance	0.45	0.20	0.13	0.06
Cumulative proportion	0.45	0.65	0.78	0.84
(*b*) Red throat emperor				
Age	0.421		0.629	–0.104
Len	0.365	0.326		–0.772
A_{∞}		–0.482	0.581	0.180
L_{∞}	0.244	–0.558	–0.237	–0.184
W_{∞}	0.227	–0.528	–0.396	–0.198
Abun	0.525	0.241	–0.119	0.350
Biom	0.547	0.104	–0.192	0.406
Proportion of variance	0.39	0.33	0.14	0.08
Cumulative proportion	0.39	0.72	0.86	0.94

Note: See Table 2 for explanation of abbreviations.

Zone effects were suggested also on PC III for common coral trout, but in interaction with year and region (Table 4). Bi-plots of the interaction on PC III indicated, however, that there were no consistent regional patterns for common coral trout sampled on open and closed reefs for each year (Fig. 4). In 1995, common coral trout on open and closed reefs off Townsville, Mackay, and Storm Cay appeared to be distinct, with no overlap in their PC III scores (Fig. 4). Similarly, in 1996 off Mackay and Storm Cay and in 1998 off Townsville and Mackay, there was no overlap in the PC III scores for common coral trout from open or closed reefs (Fig. 4). *S*, $A_{50\%}$, WAA, and LAA were the main parameters underlying the effect of PC III (Table 3). Zone effects were not clearly separated on either PC II or PC IV, either as main effects or in interaction with region or year for common coral trout or red throat emperor (Table 4).

Effects of region

Regional effects varied significantly with year on PC II for common coral trout and on PC I for red throat emperor (Fig. 5), varied with both year and zone on PC III for common coral trout (Fig. 4), and were evident as an unconfounded main effect for red throat emperor on PC II (Fig. 6) (Table 4). PC II reflected a difference between the standardised abundance and biomass and standardised age and length variables, indicating differential changes in population structures (Table 3). In 1995, 1996, and 1998, populations of common coral trout sampled off Mackay and Storm Cay differed from those off Townsville, with relatively little overlap in their PC II scores (Fig. 5). In 1996 and 1998, common coral trout sampled off Mackay and Townsville, respectively, also appeared to differ in their PC III scores from those off Storm Cay (Fig. 4). In contrast, populations of red throat emperor on reefs off Townsville and Mackay were more dissimilar, with limited overlap in their PC I scores in 1996 and 1997 (Fig. 5). Similarly, for red throat emperor, there was less overlap in the overall PC II scores from reefs off Townsville and Mackay than there was overlap between samples from Mackay and Storm Cay. This result was mainly influenced by the morphometric life-history parameters (L_{∞}, W_{∞}, $A_{50\%}$) (Table 4; Fig. 6).

Effects of year

Significant and unconfounded main effects of year were evident for common coral trout on PC I and PC IV and for red throat emperor on PCs II–IV (Table 4), although the separation among years was less dramatic than that among zones or regions for both species. Mean PC IV scores for common coral trout were significantly greater in 1996, 1997, and 1998 than those in 1995 (Fig. 7) and were mainly influenced by sex ratio (Sex) and length of mature females ($L_{50\%}$) (Table 3). In contrast, mean PC III scores for red throat emperor were significantly greater in 1997 and 1998 than those in 1995 and 1996, and PC IV scores were greater in 1995, 1996, and 1998 than those in 1997 (Fig. 7). Age and A_{∞} were the main life-history parameters influencing PC III, whereas Len was the main parameter underlying PC IV (Table 3).

Year × region interactions were also significant on PC II for common coral trout and PC I for red throat emperor (Fig. 5) and varied with both region and zone on PC III for common coral trout (Fig. 4). Plots of the interactions for PC II for common coral trout and PC I for red throat emperor indicated that populations on reefs in all three regions tended to cluster by year of sampling, albeit with some overlap in scores, particularly for Storm Cay (Fig. 5). Populations of common coral trout sampled off Townsville and Mackay demonstrated little overlap in their PC II scores in 1996 and 1998. Similarly, populations of common coral trout tended to cluster by zone, region, and year according to their PC III scores (Fig. 4). Red throat emperor sampled off Townsville in 1997 and 1998 and off Mackay in 1996 and 1997–1998 demonstrated little overlap in their PC I scores (Fig. 5).

Classification power of PC scores

Unbiased, jackknifed cross-validation tests on the significant PC (I–IV) scores for the combined data across years and regions indicated relatively high rates of classification success between open and closed reefs for both common coral trout and red throat emperor. Classification success (to zone) for common coral trout was 83% for open reefs and 89% for closed reefs, with a total error rate of 14%. The analogous rates for red throat emperor were 75% (open reefs) and 86% (closed reefs) with a total error rate of 19%.

© 2005 NRC Canada

Table 4. Results of repeated-measures analysis of variance of within-group (repeated-measures) effects of year and between-group effects of region and zone for multivariate life-history indices (PCs) for common coral trout (*Plectropomus leopardus*) and red throat emperor (*Lethrinus miniatus*) collected from open and closed reefs off Townsville, Mackay, and Storm Cay, 1995–1998.

Term	$P > F$			
	PC I	PC II	PC III	PC IV
(*a*) Common coral trout				
Within groups				
Year	**0.0023***	0.2295	**0.0001**	**0.0077**
Year × region	0.2199*	**0.0013**	**0.0044**	0.5446
Year × zone	0.5957*	0.5112	0.3111	0.5203
Year × region × zone	0.4913*	0.0535	**0.0001**	0.1978
Between groups				
Region	0.1543	**0.0003**	0.0719	0.2719
Zone	**<0.0001**	0.8978	0.6113	0.9029
Region × zone	0.6021	0.3482	0.0189**	0.5366
(*b*) Red throat emperor				
Within groups				
Year	**0.0005**	**0.0002**	**<0.0001**	**0.0022**
Year × region	**0.0002**	0.1828	0.4421	0.5285
Year × zone	0.4320	0.0650	0.3234	0.3373
Year × region × zone	0.2932	0.0384**	0.0227**	0.5092
Between groups				
Region	0.0787	**0.0074**	0.0198**	0.0375**
Zone	**0.0001**	0.0443**	0.0283**	0.3546
Region × zone	0.9183	0.1492	0.5029	0.5678

Note: Tabulated values are probabilities of the observed data under the null hypotheses of no effect of the indicate terms. Bold values were statistically significant; *, probability adjusted for unequal correlations of within-group effects using Huynh–Feldt estimator; **, probability not significant at adjusted Bonferroni level for multiple testing ($P > 0.0125$).

Discussion

We found clear evidence of accrued life-history benefits to fish populations in no-take zones compared with exploited populations outside such closed areas. Zone-related patterns in the multivariate life-history indices for both of the major target species of the reef line fishery on the GBR were consistent over large spatial and temporal scales. The nature of the overall differences in life-history indices between areas open and closed to fishing was consistent with a generally positive effect of no-take zones on the likely productivity and ecological sustainability of fish populations subject to exploitation in open areas. By analysing collectively a range of life-history parameters, we were able to clearly distinguish those populations that were sampled on reefs closed to fishing from those that were sampled from reefs historically open to fishing.

Populations of common coral trout and red throat emperor sampled within selected no-take zones of the GBRMP tended to have broader age and length distributions and greater abundance and biomass than populations in adjacent areas that had been subjected to fishing for many years. Life-history benefits of increased abundance, biomass, and size have been found for other exploited species within no-take zones elsewhere, or at least in areas that are not subjected to extractive activities such as fishing (Roberts and Polunin 1991; Russ and Alcala 1996*a*; Halpern and Warner 2002). We also found additional life-history benefits for common coral trout besides the typically measured parameters of abundance, biomass, and size, including increased survivorship, more males, and older and larger females, emphasizing further the apparent benefits of protecting populations of exploited fish in no-take zones. Such effects, including lower mortality rates and greater numbers of older and larger females, also have been found in other studies of common coral trout (Russ et al. 1998; Adams et al. 2000; Mapstone et al. 2004), though the effects were not consistently observed for all closed reefs examined (Mapstone et al. 1999, 2004).

Life-history characteristics accrued to populations of reef fish within no-take zones most likely lead to increased productivity (i.e., greater numbers of viable eggs and larvae). Populations with more diverse age and length distributions arising from enhanced survivorship, as we observed for common coral trout and red throat emperor on reefs closed to fishing, may have enhanced reproductive output and result in enhanced recruitment, both within and outside the no-take zones (Russ 2002). Marteinsdottir and Thorarinsson (1998) determined that age diversity within a spawning stock of cod (*Gadus morhua*) influenced recruitment, where increased diversity resulted in a more protracted spawning distribution, which maximised conditions for progeny survival. Similarly, Lambert (1990) found above average recruitment in herring (*Clupea harengus*) populations with more diverse age structures.

Adams et al. (2000) also found that female common coral trout above the size and age at recruitment to the fishery were significantly more abundant, larger, and older on reefs

© 2005 NRC Canada

Fig. 2. Bi-plots of total data for multivariate life-history indices, principal components (PCs) I and II, for (*a*) common coral trout (*Plectropomus leopardus*) and (*b*) red throat emperor (*Lethrinus miniatus*) collected from open (□) and closed (■) reefs off Townsville, Mackay, and Storm Cay, 1995–1998. These plots demonstrate the significant between-group effect of zone on PC I for both species. Total variation in the data explained by PCs I and II was 64% and 72% for common coral trout and red throat emperor, respectively. The bi-plots represent both the original life-history parameters and transformed observations on the first two PCs, where the relative strength and influence of the original parameters are reflected by the size and direction of the arrows. See Table 2 for an explanation of abbreviations.

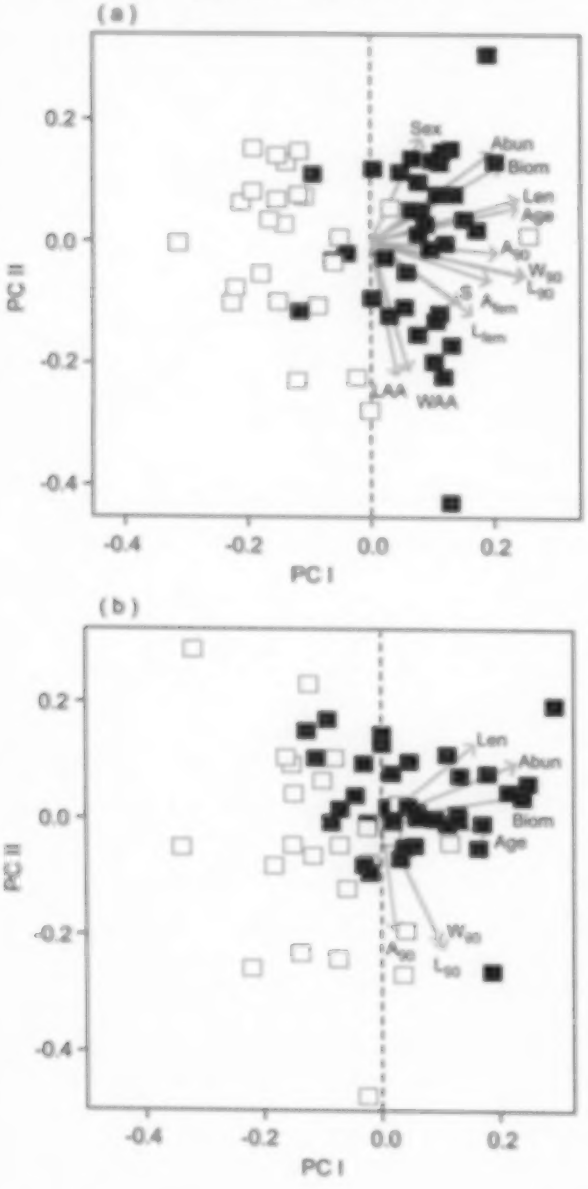

Fig. 3. Mean standardised plots of individual life-history parameters for total data of common coral trout (*Plectropomus leopardus*) and red throat emperor (*Lethrinus miniatus*) collected from open (open bars) and closed (solid bars) reefs off Townsville, Mackay, and Storm Cay, 1995–1998. See Table 2 for an explanation of abbreviations.

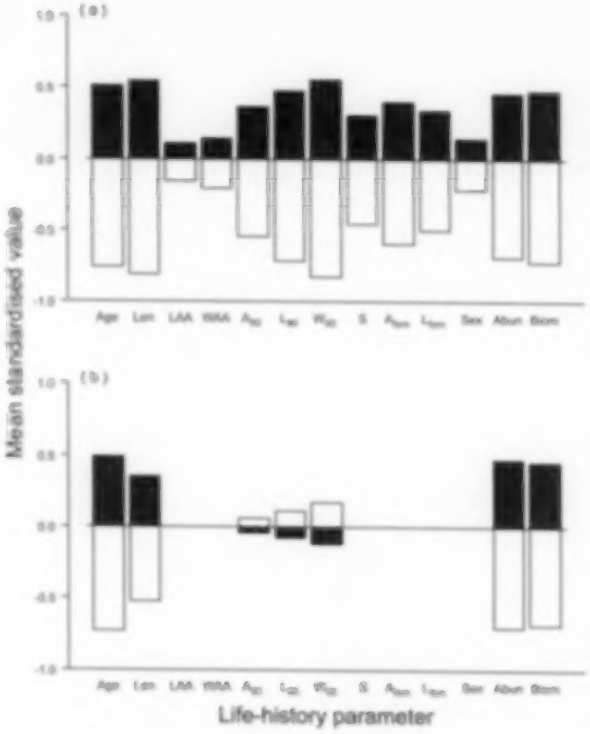

closed to fishing in the GBRWHA than those on reefs open to fishing and suggested that no-take zones were an effective insurance policy against fecundity limitation in protogynous hermaphrodites. Recent studies have also found that, as well as being more fecund, older, larger, and experienced ("repeat") spawning females also produce more viable progeny with traits that favour higher survivorship than those of younger, smaller, and first-time ("recruit") spawning females (e.g., Kjesbu et al. 1996; Marshall et al. 1998; Marteinsdottir and Steinarsson 1998). Older females also tend to have more protracted spawning seasons, thereby increasing the probability that their progeny will encounter favourable environmental conditions for growth and survival (Trippel 1998). In so far as these characteristics are likely to increase the prospects for survival and recruitment of offspring, selective removal or reduced abundance of larger and older individuals on grounds open to fishing may therefore have detrimental effects on the long-term sustainability of a population (Begg and Marteinsdottir 2002). There is a growing number of studies from temperate systems suggesting that the excessive removal of large, repeat spawners from a population, such as by fishing, may have greater impacts on recruitment success than simply removing absolute biomass (e.g., Marshall et al. 1998; Scott et al. 1999; Trippel 1999). In contrast, very lim-

© 2005 NRC Canada

Fig. 4. Principal components (PCs) I and III for common coral trout (*Plectropomus leopardus*) collected from open (open symbols) and closed (solid symbols) reefs off Townsville (squares), Mackay (circles), and Storm Cay (triangles) in (*a*) 1995, (*b*) 1996, (*c*) 1997, and (*d*) 1998. These plots demonstrate the significant interaction effect of zone, year, and region on PC III for common coral trout.

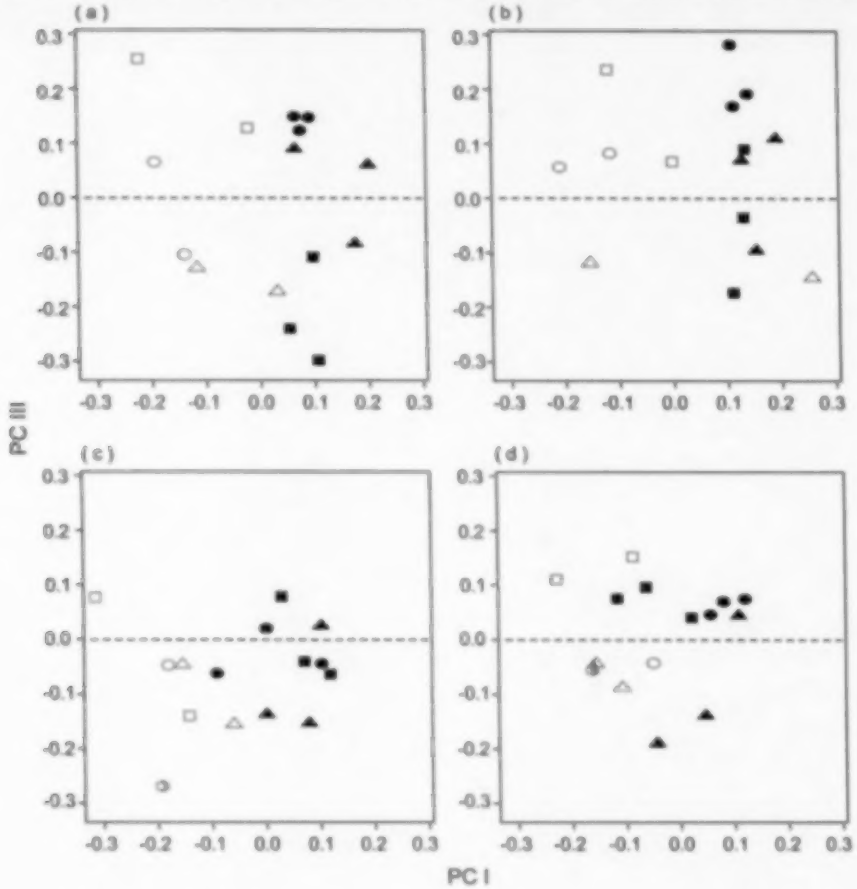

ited research on these impacts and associated maternal effects has been conducted on tropical reef fish species (Kerrigan 1997; McCormick 1998, 1999). The relevance of such effects in tropical systems needs to be investigated, particularly with respect to protogynous hermaphrodites (changing sex from female to male) such as common coral trout and red throat emperor, where the impacts of fishing may lead to reduction in abundances of mature, repeat spawning females through both direct removal by fishing and indirect removal via earlier sex change. Thus, populations with greater biomass and more abundant older and larger spawners, such as those in no-take zones, would be expected to lead to the production of greater numbers of more viable eggs and larvae and potentially result in fisheries benefits through spillover of adults or net export of larvae, or both, to surrounding areas where harvest occurs (e.g., Russ and Alcala 1996*a*; Roberts 1997; Russ 2002).

The benefits of net export of larvae from no-take zones might be expected to be greatest for populations of reef fish that are relatively sedentary, such as common coral trout (Davies 1995; Zeller and Russ 1998), because the zero or negligible flux of mature individuals across MPA boundaries means that there is no dilution of the effects of no-take zones through migration of mature fish to areas where they are vulnerable to fishing. In contrast, the benefits of spillover of adults from no-take zones would most likely be greatest in populations that are more mobile and reside outside the no-take zones for extended periods (Dahlgren and Sobel 2000). Red throat emperor may be such a species as tag–recapture data have indicated that these fish are capable of movements greater than 20 km across several reefs in a period of 6 months (Williams 2003; Bill Sawynok, Infofish Services, 142 Venables Street, North Rockhampton, Queensland 4701, Australia, unpublished data).

Although a clear separation was observed between populations of both common coral trout and red throat emperor sampled on reefs open and closed to fishing, the separation was more apparent (and subsequent classification total error rate lower) for populations of common coral trout than for populations of red throat emperor. The difference between the species might be due to the potentially more mobile life-history strategy of red throat emperor. Alternatively, the dif-

© 2005 NRC Canada

Fig. 5. Principal components (PCs) I and II for common coral trout (*Plectropomus leopardus*) and red throat emperor (*Lethrinus miniatus*) collected from reefs off Townsville (open squares), Mackay (shaded squares), and Storm Cay (solid squares), 1995–1998. These plots demonstrate the significant interaction effect of region and year on PC II for common coral trout and PC I for red throat emperor.

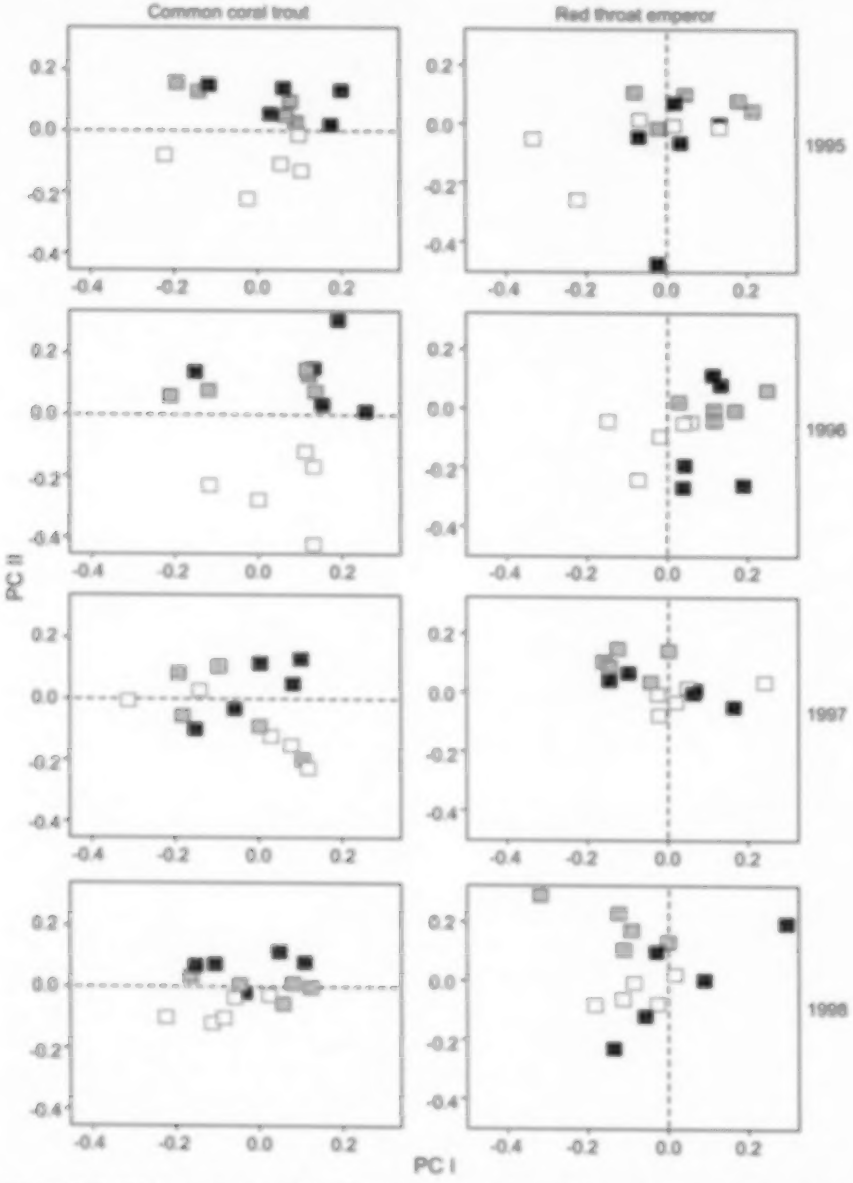

ferences might be an artefact of the greater number of common coral trout in our samples and the greater diversity of life-history parameters examined for this species. Similarly, the less consistent patterns observed for some of the morphometric life-history parameters (A_{50}, L_{50}, W_{50}) for red throat emperor may reflect the species' greater movement combined with morphological patterns that perhaps reflect environmentally induced phenotypic variation derived from movements among different habitats (Stearns 1989; Swain and Foote 1999). Accordingly, the benefits and protection derived from no-take zones would potentially be reduced more for red throat emperor than for the typically more site-attached common coral trout. The degree to which the benefits of no-take zones depend directly on rates of movement and home ranges of different species (Polacheck 1990; Bohnsack 2000; Cole et al. 2000) warrants more empirical examination, especially from a fishery perspective (Davies 1995; Crowder et al. 2000).

Most previous studies on the effects of no-take zones have included only a limited number of parameters, mainly abundance, biomass, and some measure of size (e.g., Buxton and Smale 1989; Roberts 1995; Russ and Alcala 1996*b*). We at-

© 2005 NRC Canada

Fig. 6. Bi-plot of total data for multivariate life-history indices, principal components (PCs) I and II, for red throat emperor (*Lethrinus miniatus*) collected from reefs off Townsville (open squares), Mackay (shaded squares), and Storm Cay (solid squares), 1995–1998. This plot demonstrates the significant between-group effect of region on PC II for red throat emperor. Total variation in the data explained by PCs I and II was 72%. The bi-plot represents both the original life-history parameters and transformed observations on the first two PCs, where the relative strength and influence of the original parameters are reflected by the size and direction of the arrows. See Table 2 for an explanation of abbreviations.

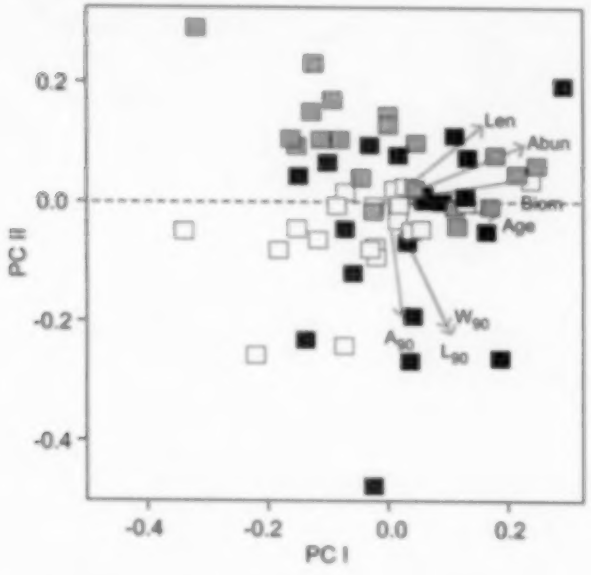

tempted to assimilate a diverse range of parameters that encapsulated more completely the life-history strategies of two species most likely to be impacted by fishing and, conversely, benefit from no-take zones on the GBR. Incorporating the information derived from these parameters into multivariate life-history indices provided a holistic view of differences between populations on open and closed reefs that were correlated with, and potentially brought about by, the implementation of no-take zones. Several of the parameters we used could be obtained only by killing the fish, emphasising that thorough assessments of performance of no-take zones will require some destructive sampling within these areas, as well as outside them. However, considering the relative harvests that have been removed from the respective reefs, we do not believe that the low level of destructive sampling used in this study impacted on the underlying population dynamics. In any given year and from any given reef, the maximum number of common coral trout and red throat emperor sampled were 396 fish and 454 kg and 112 fish and 166 kg, respectively. In comparison, the average annual commercial harvests of demersal reef fish species (including common coral trout and red throat emperor, which constitute 55–75% of the harvest) in a 1° latitude around each group of study reefs were about 600 t in Storm Cay, 450 t in Mackay, and 250 t in Townsville (Mapstone et al. 2004). Furthermore, when the experimental closed reefs in each region were open to fishing in 1999, about 3 t of common coral trout

Fig. 7. Bi-plots of total data for multivariate life-history indices principal components (PCs) I and IV for (*a*) common coral trout (*Plectropomus leopardus*) and PCs III and IV for (*b*) red throat emperor (*Lethrinus miniatus*) collected from reefs off Townsville, Mackay, and Storm Cay in 1995 (open squares), 1996 (lighter shaded squares), 1997 (darker shaded squares), and 1998 (solid squares). These plots demonstrate the significant within-group effect of year on PCs I and IV for common coral trout and PCs III and IV for red throat emperor. Total variation in the data explained by the PCs was 52% and 23% for common coral trout and red throat emperor, respectively. The bi-plots represent both the original life-history parameters and transformed observations on the respective PCs, where the relative strength and influence of the original parameters are reflected by the size and direction of the arrows. See Table 2 for an explanation of abbreviations.

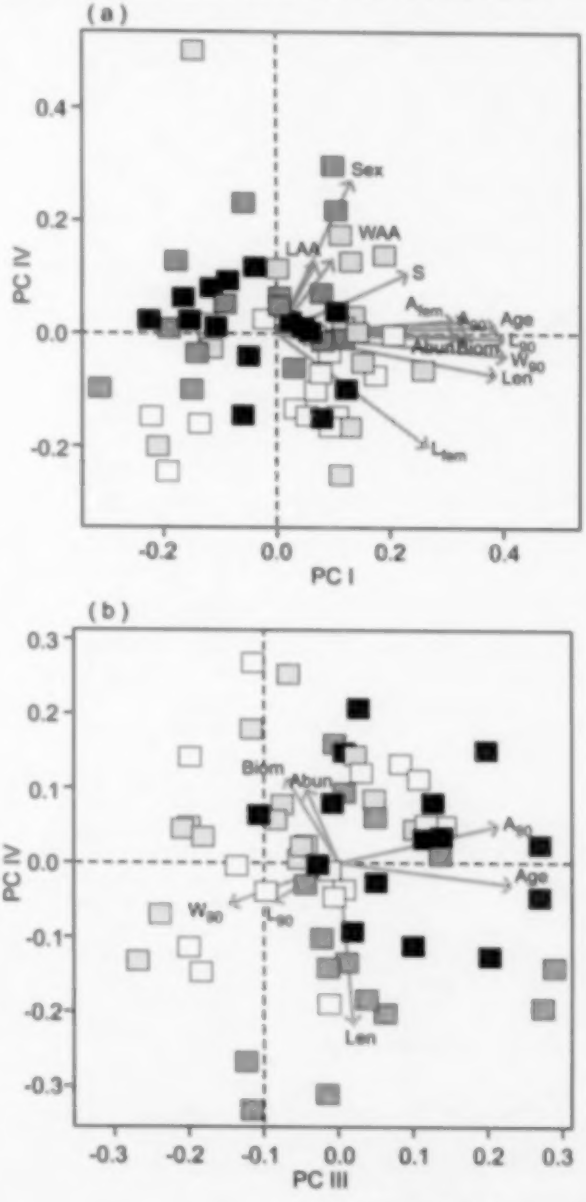

© 2005 NRC Canada

and 2 t of other species (including red throat emperor) was harvested in a 2-week period from these reefs. Consequently, it was assumed that the fish populations on each of our experimental reefs were not significantly impacted by our relatively low level of sampling, considering the harvests that have been observed on these and surrounding reefs.

Without such sampling and (or) monitoring designs as the CRC Reef ELF Experiment, it would not have been possible to obtain estimates of parameters used in this study to provide the holistic life-history perspective presented here. In addition, the temporal and spatial variability observed within and among populations of common coral trout and red throat emperor also demonstrated the need for routine and consistent monitoring programs over space and time to account for the inherent variability within life-history performance measures. Failure to account for such variation, for example, through sampling at only one time or in one area, has the potential to generate significantly misleading results about the merits or otherwise of MPA strategies such as no-take zones (Mapstone et al. 2004). Ultimately, though, the degree of assessment should depend on the objectives for establishing the MPA in the first place. Management agencies should recognise the importance of structured, regular research sampling and (or) monitoring programs if there is a genuine interest in determining the performance of MPAs, rather than accepting on faith that they achieve desired outcomes. Generally, however, once MPAs are established, there is very little monitoring to determine their performance and efficacy (Russ and Alcala 1996*b*; Agardy 1997), even though this should be the default scenario within an effective management framework.

No-take zones have been advocated as a management strategy that embodies the precautionary approach by providing an insurance against the uncertainty that pervades traditional fisheries management (Agardy 1997; Bohnsack 2000). Although no-take zones most likely provide an array of conservation benefits within their boundaries, we should be cautious in extrapolating these results to direct fisheries benefits. The extent to which fisheries benefits will be realised is as dependent on what happens outside the no-take zone (i.e., the nature of the fisheries management regime in the area open to fishing) as what happens inside (Beverton and Holt 1957; Polacheck 1990; Mapstone et al. 2004). Notably, when designing MPAs and particularly no-take zones, we need to incorporate a routine monitoring and assessment program to evaluate the performance of the areas to determine if they are indeed achieving the objectives for which they were established (Mapstone et al. 1999; Agardy 2000; Russ 2002). If an MPA is not fulfilling such objectives, then management needs to be able to adapt accordingly. If these objectives are related to sustaining fisheries production outside the no-take zones or MPAs, then examining a multivariate suite of life-history parameters as part of a routine monitoring program should provide a holistic performance indicator to measure the performance of MPAs in relation to exploited fish species.

Acknowledgements

We would like to thank the CRC Reef Fishing and Fisheries team for collecting and processing the data, Robin Stewart and Mary Petersen for tireless operational support in the field, and Jon Day for comments on the draft manuscript. Funding for this research was provided by the Cooperative Research Centre for the Great Barrier Reef Word Heritage Area, the Fisheries Research and Development Corporation, and the Great Barrier Reef Marine Park Authority. This manuscript is a contribution from the CRC Reef Effects of Line Fishing Project.

References

Adams, S. 2002. The reproductive biology of three species of *Plectropomus* (Serranidae) and responses to fishing. PhD. thesis, James Cook University, Townsville, Australia.

Adams, S. 2003. Morphological ontogeny of the gonad of three plectropomid species through sex differentiation and transition. J. Fish Biol. **63**: 22–36.

Adams, S., Mapstone, B.D., Russ, G.R., and Davies, C.R. 2000. Geographic variation in the sex ratio, sex-specific size, and age structure of *Plectropomus leopardus* (Serranidae) between reefs open and closed to fishing on the Great Barrier Reef. Can. J. Fish. Aquat. Sci. **57**: 1448–1458.

Agardy, T.S. 1997. Marine protected areas and ocean conservation. Academic Press, San Diego, Calif.

Agardy, T.S. 2000. Information needs for marine protected areas: scientific and societal. Bull. Mar. Sci. **66**: 875–888.

Allison, G.W., Lubchenco, J., and Carr, M.H. 1998. Marine reserves are necessary but not sufficient for marine conservation. Ecol. Appl. **8**(Suppl.): S79–S92.

Bean, K., Mapstone, B.D., Davies, C.R., Murchie, C.D., and Williams, A.J. 2003. Gonad development and evidence of protogyny in the red throat emperor (*Lethrinus miniatus*: Bloch and Schneider) on the Great Barrier Reef. J. Fish Biol. **62**: 299–310.

Begg, G.A., and Marteinsdottir, G. 2002. Environmental and stock effects on spatial distribution and abundance of mature cod *Gadus morhua*. Mar. Ecol. Prog. Ser. **229**: 245–262.

Beverton, R.J.H., and Holt, S.J. 1957. On the dynamics of exploited fish populations. Fisheries Investigations Series II, Vol. XIX, Ministry of Agriculture, Fisheries and Food, Lowestoft.

Bohnsack, J.A. 1998. Application of marine reserves to reef fisheries management. Aust. J. Ecol. **23**: 298–304.

Bohnsack, J.A. 2000. A comparison of the short-term impacts of no-take marine reserves and minimum size limits. Bull. Mar. Sci. **66**: 635–650.

Buxton, C.D. 1993. Life-history changes in exploited reef fishes on the east coast of South Africa. Environ. Biol. Fishes, **36**: 47–67.

Buxton, C.D., and Smale, M.J. 1989. Abundance and distribution patterns of three temperate marine reef fish (Teleostei: Sparidae) in exploited and unexploited areas off the southern cape coast. J. Appl. Ecol. **26**: 441–451.

Cole, R.G., Villouta, E., and Davidson, R.J. 2000. Direct evidence of limited dispersal of the reef fish *Parupercis colias* (Pinguipedidae) within a marine reserve and adjacent fished areas. Aquat. Conserv. Mar. Freshw. Ecosyst. **10**: 421–436.

Crowder, L.B., Lyman, S.J., Figueira, W.F., and Priddy, J. 2000. Source–sink population dynamics and the problem of siting marine reserves. Bull. Mar. Sci. **66**: 799–820.

Dahlgren, C.P., and Sobel, J. 2000. Designing Dry Tortugas Ecological Reserve: how big is big enough? ... to do what? Bull. Mar. Sci. **66**: 707–719.

Davies, C.R. 1995. Patterns of movement of three species of coral reef fish on the Great Barrier Reef. PhD. thesis, James Cook University, Townsville, Australia.

© 2005 NRC Canada

Davies, C.R., Mapstone, B.D., Ayling, A., Lou, D.C., Punt, A.E., Russ, G.R., Samoilys, M.A., Smith, A.D.M., Welch, D.J., and Williams, D.M. 1998. Effects of line fishing experiment 1995–1997: project structure and operations. A supplementary document to progress report. CRC Reef Research Centre, Townsville, Australia.

Day, J.C. 2002. Zoning — lessons from the Great Barrier Reef Marine Park. Ocean Coast. Manag. **45**: 139–156.

Dugan, J.E., and Davis, G.E. 1993. Applications of marine refugia to coastal fisheries management. Can. J. Fish. Aquat. Sci. **50**: 2029–2042.

Ferreira, B.P. 1995. Reproduction of the common coral trout *Plectropomus leopardus* (Serranidae: Epinephelinae) from the central and northern Great Barrier Reef, Australia. Bull. Mar. Sci. **56**: 653–669.

Ferreira, B.P., and Russ, G.R. 1994. Age validation and estimation of growth rate of the coral trout, *Plectropomus leopardus* (Lacépède 1802), from Lizard Island, northern Great Barrier Reef. Fish. Bull. **92**: 46–57.

Fogarty, M.J., Bohnsack, J.A., and Dayton, P.K. 2000. Marine reserves and resource management. *In* Seas at the millennium: an environmental evaluation. *Edited by* C.R.C. Sheppard. Pergamon, Oxford. pp. 375–392.

GBRMPA. 2004. New GBR zoning. Available at the Great Barrier Reef Marine Park Authority website: www.gbrmpa.gov.au/corp_site/management/zoning/index.html.

Halpern, B.S. 2003. The impact of marine reserves: do reserves work and does reserve size matter? Ecol. Appl. **13**(Suppl. 1): S117–S137.

Halpern, B.S., and Warner, R.R. 2002. Marine reserves have rapid and lasting effects. Ecol. Lett. **5**: 361–366.

Higgs, J.B. 1996. A review of published fisheries dependent and independent surveys of the recreational Great Barrier Reef line fisheries and demersal reef fish stocks. Report to the Queensland Fisheries Management Authority, CRC Reef Research Centre, Townsville.

Kerrigan, B.A. 1997. Variability in larval development of a tropical reef fish (Pomacentridae: *Pomacentrus amboinensis*): the parental legacy. Mar. Biol. **127**: 395–402.

Kjesbu, O.S., Solemdal, P., Bratland, P., and Fonn, M. 1996. Variation in annual egg production in individual captive Atlantic cod (*Gadus morhua*). Can. J. Fish. Aquat. Sci. **53**: 610–620.

Lambert, T.C. 1990. The effect of population structure on recruitment in herring. J. Cons. Int. Explor. Mer, **47**: 249–255.

Mapstone, B.D., McKinlay, J.P., and Davies, C.R. 1996. A description of the commercial reef line fishery logbook data held by the Queensland Fisheries Management Authority. Report to the Queensland Fisheries Management Authority, CRC Reef Research Centre, Townsville.

Mapstone, B.D., Ayling, A.M., and Choat, J.H. 1999. A visual survey of demersal biota in the Cairns section of the Great Barrier Reef Marine Park. Great Barrier Reef Marine Park Authority Res. Publ. Ser. **60**: 1–47.

Mapstone, B.D., Davies, C.R., Little, L.R., Punt, A.E., Smith, A.D.M., Pantus, F., Lou, D.C., Williams, A.J., Jones, A., Ayling, A.M., Russ, G.R., and MacDonald, A.D. 2004. The effects of line fishing on the Great Barrier Reef and evaluations of alternative potential management strategies. CRC Reef Research Centre Technical No. 52, CRC Reef Research Centre, Townsville, Australia.

Marshall, C.T., Kjesbu, O.S., Yaragina, N.A., Solemdal, P., and Ulltang, O. 1998. Is spawner biomass a sensitive measure of the reproductive and recruitment potential of Northeast Arctic cod? Can. J. Fish. Aquat. Sci. **55**: 1766–1783.

Marteinsdottir, G., and Steinarsson, A. 1998. Maternal influence on the size and viability of Iceland cod *Gadus morhua* eggs and larvae. J. Fish Biol. **52**: 1241–1258.

Marteinsdottir, G., and Thorarinsson, K. 1998. Improving the stock–recruitment relationship in Icelandic cod (*Gadus morhua*) by including age diversity of spawners. Can. J. Fish. Aquat. Sci. **55**: 1372–1377.

McCormick, M.I. 1998. Behaviourally induced maternal stress in a fish influences progeny quality by a hormonal mechanism. Ecology, **79**: 1873–1883.

McCormick, M.I. 1999. Experimental test of the effect of maternal hormones on larval quality of a coral reef fish. Oecologia, **118**: 412–422.

Mosquera, I., Côté, I.M., Jennings, S., and Reynolds, J.D. 2000. Conservation benefits of marine reserves for fish populations. Anim. Conserv. **4**: 321–332.

Murray, S.N., Ambrose, R.F., Bohnsack, J.A., Botsford, L.W., Carr, M.H., Davis, G.E., Dayton, P.K., Gotshall, D., Gunderson, D.R., Hixon, M.A., Lubchenco, J., Mangel, M., MacCall, A., McArdle, D.A., Ogden, J.C., Roughgarden, J., Starr, R.M., Tegner, M.J., and Yoklavich, M.M. 1999. No-take reserve networks: sustaining fishery populations and marine ecosystems. Fisheries, **24**: 11–25.

Polacheck, T. 1990. Year around closed areas as a management tool. Nat. Res. Model. **4**: 327–354.

Quinn, T.J., II, and Deriso, R.B. 1999. Quantitative fish dynamics. Oxford University Press, New York.

Roberts, C.M. 1995. Rapid build-up of fish biomass in a Caribbean marine reserve. Conserv. Biol. **9**: 815–826.

Roberts, C.M. 1997. Connectivity and management of Caribbean coral reefs. Science (Wash., D.C.), **278**: 1454–1457.

Roberts, C.M., and Polunin, N.V.C. 1991. Are marine reserves effective in management of reef fisheries? Rev. Fish Biol. Fish. **1**: 65–91.

Roberts, C.M., Bohnsack, J.A., Gell, F., Hawkins, J.P., and Goodridge, R. 2001. Effects of marine reserves on adjacent fisheries. Science (Wash., D.C.), **294**: 1920–1923.

Russ, G.R. 2002. Marine reserves as reef fisheries management tools: yet another review. *In* Coral reef fishes. *Edited by* P. Sale. Academic Press, Sydney, Australia. pp. 421–444.

Russ, G.R., and Alcala, A.C. 1996*a*. Do marine reserves export adult fish biomass? Evidence from Apo Island, central Philippines. Mar. Ecol. Prog. Ser. **132**: 1–9.

Russ, G.R., and Alcala, A.C. 1996*b*. Marine reserves: rates and patterns of recovery and decline of large predatory fish. Ecol. Appl. **6**: 947–961.

Russ, G.R., Lou, D.C., Higgs, J.B., and Ferreira, B.P. 1998. Mortality rate of a cohort of the coral trout, *Plectropomus leopardus*, in zones of the Great Barrier Reef Marine Park closed to fishing. Mar. Freshw. Res. **49**: 507–511.

SAS. 1989. SAS/STAT user's guide. Version 6. 4th ed. Vol. 2. SAS Institute Inc., Cary, N.C.

Scott, B., Marteinsdottir, G., and Wright, P. 1999. Potential effects of maternal factors on spawning stock–recruitment relationships under varying fishing pressure. Can. J. Fish. Aquat. Sci. **56**: 1882–1890.

Sokal, R.R., and Rohlf, F.J. 1995. Biometry. The principles and practice of statistics in biological research. W.H. Freeman and Company, New York.

Stearns, S.C. 1989. The evolutionary significance of phenotypic plasticity. Bioscience, **39**: 436–445.

Swain, D.P., and Foote, C.J. 1999. Stocks and chameleons: the use of phenotypic variation in stock identification. Fish. Res. **43**: 113–128.

© 2005 NRC Canada

Trippel, E.A. 1998. Egg size and viability and seasonal offspring production of young Atlantic cod. Trans. Am. Fish. Soc. **127**: 339–359.

Trippel, E.A. 1999. Estimation of stock reproductive potential: history and challenges for Canadian Atlantic gadoid stock assessments. J. Northw. Atl. Fish. Sci. **25**: 61–81.

Vincent, A.C.J., and Sadovy, Y.J. 1998. Reproductive ecology in the conservation and management of fishes. *In* Behavioural ecology and conservation biology. *Edited by* T.M. Caro. Oxford University Press, New York. pp. 209–245.

Williams, A.J. 2003. Spatial patterns in population biology of a large coral reef fish: what role can movement play? Ph.D. thesis, James Cook University, Townsville, Australia.

Williams, A.J., Davies, C.R., Mapstone, B.D., and Russ, G.R. 2003. Scales of spatial variation in demography of a large coral-reef fish — an exception to the typical model? Fish. Bull. **101**: 673–683.

Zeller, D.C., and Russ, G.R. 1998. Marine reserves: patterns of adult movement of the coral trout (*Plectropomus leopardus* (Serranidae)). Can. J. Fish. Aquat. Sci. **55**: 917–924.

© 2005 NRC Canada

Likelihood-based confidence intervals of relative fitness for a common experimental design

Steven T. Kalinowski and Mark L. Taper

Abstract: Statistical inferences concerning the relative fitness of different types of individuals in a population have not been well developed. We present a method for calculating confidence intervals for maximum likelihood estimates of relative fitness obtained from an experimental design that is common in the fisheries literature. Analysis and simulation show that these confidence limits are reliable. We also show that the bias of the estimates is low for realistic sample sizes.

Résumé : Les inférences statistiques sur la fitness relative des différents types d'individus dans une population sont encore peu élaborées. Nous présentons une méthode pour calculer les intervalles de confiance des estimations de vraisemblance maximale de la fitness relative obtenues d'un plan d'expériences couramment utilisé dans la littérature halieutique. L'analyse et la simulation montrent que ces intervalles de confiance sont fiables. Nous établissons aussi qae l'erreur des estimations est faible pour des tailles d'échantillons réalistes.

[Traduit par la Rédaction]

Introduction

Measuring fitness in the wild is essential for understanding evolution and often important for managing populations. It is also notoriously difficult to do in natural populations. Molecular markers, such as microsatellites, however, offer a relatively new tool for estimating reproductive success. The method is general but has been used most often in the fisheries literature to estimate the relative fitness of different strains of anadromous fishes (e.g., Garant et al. 2003; Hendry et al. 2003; McLean et al. 2004). In this literature, studies are often conducted as follows. Adult salmon are intercepted during their upstream migration and genotyped at multiple microsatellite loci. Once sampled, the fish are released to continue their upstream migration, after which they spawn in the wild. The offspring from these fish are then captured in subsequent years and genotyped. These genotypes identify the parents of each fish, and the fitness of the parents can be estimated. This allows the fitness of different types of fish (e.g., hatchery vs. wild) to be compared (McLean et al. 2004).

These studies have brought to light limitations in the statistical methods used for inference concerning fitness. In particular, there is no report of a reliable method to produce confidence limits for estimates of relative fitnesses (e.g., Haldane 1956; Manly 1985). Wald confidence intervals based on the t distribution have been constructed by estimating the sampling variance of relative fitnesses (e.g., Manly 1972, 1985). However, the sampling distribution of estimates of relative fitness is not normal and is even asymmetric, so confidence limits estimated this way are unlikely to perform well. Hinrichsen (2003), for example, derived an expression for the approximate sampling variance for estimates of relative fitness, but did not use this variance in his power analysis. Authors reporting the relative fitness of different stocks of fish have usually not included measures of uncertainty in their work (for examples see Hinrichsen 2003).

The purpose of this article is twofold: (1) to present a profile-likelihood method for constructing confidence limits around estimates of relative fitness, and (2) to evaluate the bias and sampling error of the maximum likelihood estimates themselves.

Estimating relative fitness

We begin by summarizing the conventional population genetic model for how natural selection affects the frequencies of different types of individuals in a population (for a more detailed presentation and examples of studies that estimate the fitness of specific genotypes see Hedrick 2000). Let k represent the number of different types of individuals in a population and p_i represent the frequency of the ith type of individual, i.e., $\sum_{i=1}^{k} p_i = 1.0$. By type of individual, we mean genotype, phenotype, stock, life history, morph, or any other feature that natural selection might act upon. For example, p_1 and p_2 might represent the frequency of hatchery- and wild-born salmon migrating up a river. To simplify our presentation, we use "stock" as shorthand for "type of individual".

Let p_i' represent the frequency of the ith stock after selection. This will be equal to

$$(1) \qquad p_i' = \frac{\omega_i p_i}{\bar{\omega}}$$

Received 11 June 2004. Accepted 30 November 2004. Published on the NRC Research Press Web site at http://cjfas.nrc.ca on 18 April 2005.
J18171

S.T. Kalinowski[1] and M.L. Taper. Department of Ecology, Montana State University, Bozeman, MT 59717, USA.

[1]Corresponding author (e-mail: skalinowski@montana.edu).

 doi: 10.1139/F04-239 © 2005 NRC Canada

where ω_i denotes the fitness of the ith stock and $\bar{\omega}$ is the average fitness in the population, $\bar{\omega} = \sum_i p_i \omega_i$. Equation 1 has two notable characteristics: it can model the effects of both differential viability and fecundity and it applies to both absolute measures of fitness as well as relative fitness measures.

In many study designs, estimating the actual fitness of each stock is not possible. This is because eq. 1 depends on ratios of fitnesses and not their magnitudes. Therefore, fitness is often measured relative to a standard stock. Let w_i represent the relative fitness of the ith stock:

$$(2) \qquad w_i = \frac{\omega_i}{\omega_0}$$

where ω_0 is the fitness of the stock that is being used as a standard of comparison. Substituting eq. 1 into eq. 2 gives the relationship between relative fitness and the frequencies of the stocks before and after selection:

$$(3) \qquad w_i = (p_i'/p_i)/(p_0'/p_0)$$

where p_0 and p_0' are the frequencies of the standard stock before and after selection.

Obtaining maximum likelihood estimates of relative fitness is straightforward. Let $\mathbf{w}$ represent a vector of the relative fitnesses for the stocks in a population, i.e., $[w_1, w_2, \ldots, w_k]$. If we assume that the frequencies of each stock before selection are known without error, the likelihood is multinomial with the probabilities for each stock given by eq. 1:

$$(4a) \qquad L(\mathbf{w}) = \left(\frac{N!}{\prod_i n_i!}\right) \prod_i \left(\frac{p_i w_i}{\bar{w}}\right)^{n_i}$$

where n_i is the number of individuals from the ith stock found in the sample after selection and N is the total sample size, $N = \sum_i n_i$. By definition, the values of $\mathbf{w}$ that maximize the right-hand half of eq. 4*a* are the maximum likelihood estimates of the relative fitnesses of the stocks. Expression 4*a* can be modified in two ways that do not alter the location of the maximum, but facilitate computation. First, the multinomial coefficient may be dropped, and second, the logarithm of each side of the equation can be taken. Therefore, maximizing the right-hand side of the following expression is sufficient to find maximum likelihood estimates of $\mathbf{w}$:

$$(4b) \qquad \operatorname{Ln} L(\mathbf{w}) \propto \sum_{i=1}^{k} n_i \ln\left(\frac{p_i w_i}{\bar{w}}\right)$$

This expression (eq. 4*b*) is maximized by

$$(5) \qquad \hat{w}_i = \frac{\hat{p}_i' p_0}{\hat{p}_0' p_i}$$

where $\hat{p}_i'$ is the proportion of stock i in the samples taken after selection, $\hat{p}_i' = n_i/N$ (e.g., Manly 1985).

In some studies, combining results from different experiments may be desired. This can be done by assuming that the relative fitness of each stock is constant. With this assumption, the log-likelihood is proportional to

$$(6) \qquad \operatorname{Ln} L(\mathbf{w}) \propto \sum_j \sum_{i=1}^{k} n_{i,j} \ln\left(\frac{p_{i,j} w_i}{\bar{w}_j}\right)$$

where j indexes experiments. This equation is equivalent to eq. 1 of Hinrichsen (2003). Our paper will concentrate on studies with data from one experiment because this study design has the lowest power and highest bias (Hinrichsen 2003).

Confidence limits for the estimates of relative fitness can be obtained by the hypothesis test inversion method (Casella and Berger 2001). This technique produces confidence limits by finding the set of all points in a univariate or multivariate parameter space where the likelihood ratio comparing the maximum likelihood estimates with a point in the set just equals the critical value for a test of the desired size. Let $\mathbf{w}_A$ be a point in the confidence set. The set is defined as all points satisfying the equality:

$$(7) \qquad 2[\operatorname{Ln} L(\mathbf{w}_{ML}) - \operatorname{Ln} L(\mathbf{w}_A)] = \chi^2_{1,\alpha}$$

where $\chi^2_{1,\alpha}$ is the χ^2 value with 1 degree of freedom, and $\operatorname{Ln} L(\mathbf{w}_{ML})$ is the log-likelihood (eq. 4*b*) evaluated at the maximum likelihood values of $\mathbf{w}$. A $1 - \alpha$ confidence interval for each of the stocks is given by the largest and smallest values of w_i in the confidence set (Pawitan 2000). Such intervals are known as profile-likelihood intervals and are generally considered superior to Wald confidence intervals constructed with parameter variance estimated on the basis of the inverse of the Fisher information matrix. The simplest approach to making joint confidence intervals that have a $1 - \alpha'$ probability of capturing all parameters (as opposed to each interval having a $1 - \alpha$ probability of capturing one parameter) is to use the Dunn–Šidák probability, $\alpha' = 1 - (1 - \alpha)^{1/k}$, in eq. 7 (Sokal and Rohlf 1995). Alternatively, a joint confidence region can be constructed using eq. 7 with $k - 1$ degrees of freedom (McCullagh and Nelder 1989; Meeker and Escobar 1995).

We illustrate the profile-likelihood method with a pair of examples, one with two stocks and one with three. In the first case, assume that there are two stocks in a river and that they both had a frequency of 0.5 before selection. A sample of 25 fish is taken after selection, and this sample contains 15 fish from stock 1 and 10 fish from stock 2 (Fig. 1 shows the likelihood profile of these data). The likelihood profile has a maximum at $\hat{w}_1 = 1.5$, which means that 1.5 is the maximum likelihood estimate of w_1. At this point, the log-likelihood is approximately –16.83. We search downwards from 1.5 for a value of w_1 satisfying eq. 7 that is our lower confidence limit. Searching upwards from 1.5 yields the upper confidence limit. The 95% confidence interval for $\hat{w}_1$ is approximately [0.68, 3.45]. Note the asymmetry in this interval.

The case of three stocks is a little more complicated, because two relative fitnesses must be estimated: w_1 and w_2. Consider an example in which each of three stocks had a frequency of 0.3333 before selection, and that a sample of 100 fish is collected from a river after selection that contains 51 fish from stock 1, 17 fish from stock 2, and 32 fish from

© 2005 NRC Canada

Fig. 1. The log-likelihood of w_1 for a sample of 25 individuals containing 15 individuals from stock 1 and 10 individuals from stock 2 (assuming that both stocks had a frequency of 0.5 before selection).

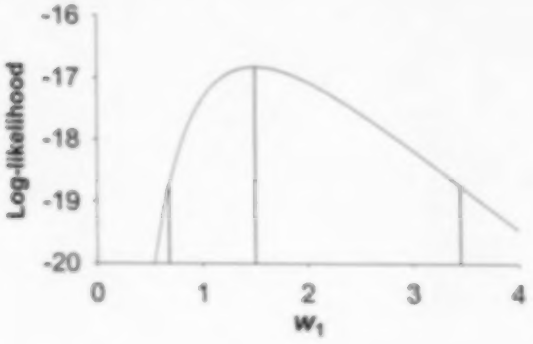

stock 3 (the stock with which relative fitnesses are compared). The confidence set is constructed as before, but is now a closed curve in a two-dimensional parameter space. Profile confidence intervals for w_1 and w_2 are obtained by finding the smallest and largest values of w_1 and w_2 within this region.

Methods

Now that we have shown how to estimate relative fitness and how to obtain confidence intervals for these estimates, we will evaluate (*i*) the bias of these estimates, (*ii*) the variability of the estimates, and (*iii*) the accuracy of the confidence intervals.

Statistical properties of estimates of relative fitness

To evaluate how effectively samples estimate relative fitness, we used several metrics: bias, geometric mean bias, confidence-interval coverage, and geometric mean error. We examined two types of studies, those with two stocks (the most common application in the fisheries literature) and those with four stocks (less common). For studies with two stocks, we calculated each of the four metrics analytically. An example illustrates how we did this and why we chose the statistics listed.

Consider two stocks that have equal frequency before selection. If the relative fitness of the first stock is twice that of the second, the frequencies of the stock after selection will be 0.6667 and 0.3333 (from eq. 1). Now assume that the relative fitness of stocks is estimated by sampling 25 fish from the system after selection. If, for example, this sample consists of 15 fish from the first stock and 10 fish from the second stock, the maximum likelihood estimate of relative fitness will be 1.5 (eq. 5). If, however, the sample consists of 16 fish from stock 1 and 9 fish from stock 2, then the maximum likelihood estimate of relative fitness for stock 1 is 1.78 (which is a little closer to the parametric value of 2.0). The probability for each of these samples (and every other possible sample) can be calculated from the binomial formula. The probability of observing k fish from stock 1 is

$$(8) \qquad P(n_1 = k) = \left(\frac{N!}{k!(N-k)!}\right)(0.6667)^k(0.3333)^{N-k}$$

where N is the total sample size (25 in our case). For example, there is approximately a 12.6% chance that 15 fish from stock 1 will be in observed in the sample (Table 1).

Table 1 provides all the information required to calculate the sampling statistics we used to evaluate the statistical properties of maximum likelihood estimates of relative fitness (Table 1). For example, statistical bias is the difference between the expected value of an estimate and the actual value of the parameter being estimated:

$$(9) \qquad \text{bias} = E(\hat{w}_i) - w_i$$

The expected value of $\hat{w}_i$ (directly from Table 1) is

$$(10) \qquad E(\hat{w}_i) = \sum P(\hat{w}_i)\hat{w}_i$$

where summation is taken over all possible samples. For the example shown (Table 1), the expected value of $\hat{w}_1$ is approximately 2.3, which is about 15% too high. The calculation is approximate because there is a small chance that $\hat{w}_1$ will equal infinity (this occurs if no individuals from stock 2 are observed in the sample). Strictly speaking, this means that estimates of relative fitness are infinitely biased. However, the expected value of $\hat{w}_1$ is relatively insensitive to this problem. For example, the expected value of $\hat{w}_1$ is approximately 2.31 if the problem sample is not included in the calculation and 2.32 if 99 is used as an estimate when no individuals from stock 2 are included in the sample.

The bias is caused by an asymmetric sampling distribution for $\hat{w}_1$ (Fig. 2). The sampling distribution has a mode of approximately 2.0 (the parametric value being estimated), but has a long tail to the right (large values). The expectation of $\hat{w}_1$ is the arithmetic average value of $\hat{w}_1$, so the tail on the right raises the expected value above 2.0. However, further examination of the example shows that the observed bias is not a problem — and is actually a by-product of a desirable property of maximum likelihood estimates of relative fitness. Consider two potential estimates of $\hat{w}_1$: 1 and 4. They are equally poor. The former is half of the actual value of 2.0, while the latter is twice as large. If these estimates were equally likely, the sampling distribution for $\hat{w}_1$ would look something like Fig. 2*a*, and the arithmetic mean estimate would be greater than 2. The geometric mean, however, would be equal to 2. The geometric mean is a more appropriate measure of central tendency because relative fitnesses are used multiplicatively (and not additively) in eq. 1. In the example shown (Table 1), the geometric mean of the estimates is 2.07 (see Fig. 2*b*), which is substantially closer to the parametric value than the arithmetic mean of 2.3.

Table 1 provides useful information regarding other statistical properties of estimates of relative fitness (Table 1). For example, there is a 96.8% chance that the nominal 95% confidence intervals for $\hat{w}_1$ contain the parametric value, which is quite close to the coverage they promise.

The variability of estimates of relative fitness is also of interest. The sampling variance or standard error is usually used for this purpose, but either statistic would be misleading for the same reasons that the arithmetic mean is not an appropriate measure of central tendency. Therefore, we cal-

© 2005 NRC Canada

Table 1. Sampling distribution of estimates of relative fitness for a sample of 25 individuals taken after two stocks underwent selection.

n_1[a]	n_2[b]	Probability[c]	$\hat{w}$[d]	$\hat{w}_{min}$[e]	$\hat{w}_{max}$[f]	CI successful?[g]	$\hat{w}_{min}$ > 1?[h]
0	25	1.18×10^{-12}	0.00	0.00	0.08		
1	24	5.90×10^{-11}	0.04	0.00	0.20		
2	23	1.42×10^{-9}	0.09	0.01	0.29		
3	22	2.17×10^{-8}	0.14	0.03	0.39		
4	21	2.39×10^{-7}	0.19	0.06	0.50		
5	20	2.01×10^{-6}	0.25	0.08	0.62		
6	19	1.34×10^{-5}	0.32	0.12	0.75		
7	18	7.26×10^{-5}	0.39	0.15	0.89		
8	17	3.27×10^{-4}	0.47	0.19	1.06		
9	16	0.0012	0.56	0.24	1.25		
10	15	0.0040	0.67	0.29	1.47		
11	14	0.0108	0.79	0.35	1.73		
12	13	0.0251	0.92	0.42	2.04	Yes	
13	12	0.0503	1.08	0.49	2.41	Yes	Yes
14	11	0.0862	1.27	0.58	2.87	Yes	Yes
15	10	0.1264	1.50	0.68	3.45	Yes	Yes
16	9	0.1580	1.78	0.80	4.20	Yes	Yes
17	8	0.1673	2.13	0.95	5.21	Yes	Yes
18	7	0.1487	2.57	1.12	6.61	Yes	Yes
19	6	0.1096	3.17	1.34	8.69	Yes	Yes
20	5	0.0658	4.00	1.62	12.0	Yes	Yes
21	4	0.0313	5.25	2.00	18.0	Yes	Yes
22	3	0.0114	7.33	2.54	30.9		Yes
23	2	0.0030	11.5	3.40	71.6		Yes
24	1	4.95×10^{-4}	24.0	5.08	99		Yes
25	0	3.96×10^{-5}	∞	—	—		Yes

Note: Both stocks had a frequency of 0.5 before selection. Stock 1 had a parametric relative fitness of 2.0.
[a]Number of individuals from stock 1 in the sample.
[b]Number of individuals from stock 2 in the sample.
[c]Probability for the sample.
[d]Estimate of relative fitness for the sample.
[e]Lower end of the 95% confidence interval for $\hat{w}$.
[f]Upper end of the 95% confidence interval for $\hat{w}$.
[g]Does the confidence interval (CI) for $\hat{w}$ contain the parametric value of 2.0?
[h]Is $\hat{w}$ significantly greater than 1.0?

culated the geometric mean multiplicative error (GMME) for each study design that we evaluated (see below). GMME is the average (geometric mean) factor by which estimates of relative fitness are in error. For example, a GMME of 1.25 indicates that the average estimate is in error by a factor of 1.25 (i.e., needs to be multiplied or divided by 1.25 to get the parametric fitness). GMME is defined as

$$(11) \quad \text{GMME} = \exp(E|\ln(\hat{w}_i/w_i)|)$$

where $\exp(\cdot)$ denotes the exponential function and $E(\cdot)$ denotes expectation.

The enumeration method for calculating bias and confidence-interval coverage described above can be extended to study designs with multiple stocks. However, the number of possible samples quickly becomes prohibitively large and the method becomes computationally impracticable. In such cases, computer simulation can be used to estimate bias, confidence-interval coverage, etc.

Evaluation of study designs

We examined two sets of study designs, those with two stocks, and those with five stocks. The set of study designs we examined that had two stocks are listed in Table 2. In brief, we varied sample size from 50 to 400, varied relative fitness from 0.1 to 10, and varied initial frequencies from 0.10 to 0.90. We used the analytic method described above to analyze study designs with two stocks. Computer simulation was used to evaluate a study design with five stocks that had relative fitnesses of {1.0, 0.8, 0.9, 1.1, 1.2} for samples sizes of 50, 100, 200, and 400.

For each study design we calculated the expected value of estimates of relative fitness, geometric means of estimates, the error rate for 95% confidence intervals, and GMME.

Software

A computer program, relative fitness analysis, is available to apply the statistical methods described above. The program estimates relative fitnesses (and their confidence limits) for empirical data sets and simulates data. Relative fitness analysis is available for download from www.montana.edu/kalinowski (Kalinowski 2004).

Results

Maximum likelihood estimates of relative fitness had low

© 2005 NRC Canada

Fig. 2. The sampling distribution of estimates of relative fitness for two stocks having parametric relative fitnesses of 2.0 and 1.0 when both stocks were equally abundant before selection and a sample size of 25 individuals is collected after selection. The scale is linear in *a* and logarithmic in *b*.

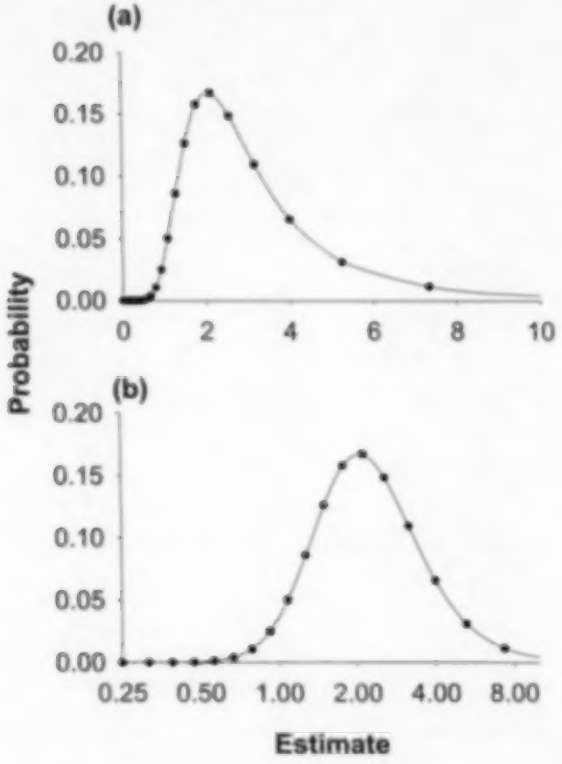

bias, accurate confidence intervals, and reasonable variability. The results for the study designs with two stocks are provided in Tables 3–6. Small sample sizes showed a modest amount of bias, which usually declined to a negligible amount when samples were expected to include at least 10 individuals in each of the stocks. Furthermore, the geometric mean estimate was almost always quite close to the parametric value being estimated. The 95% confidence intervals were very reliable across the entire range of sample sizes and relative fitnesses. GMME also appears acceptable. For a wide range of relative fitnesses, GMME was approximately 1.3 for a sample size of 50 — and lower for larger samples.

Estimates of relative fitness for the study designs with five stocks also had low bias, accurate confidence intervals, etc. (results not shown).

Discussion

This work shows that maximum likelihood estimates of relative fitness are relatively unbiased, have reasonable sampling error, and have nearly true sized confidence limits — even for sample sizes as low as 10 individuals for the least abundant stock. This is reassuring, for it indicates that small samples can be informative. However, this does not mean that small samples will be sufficient to precisely estimate relative fitnesses. Larger sample sizes give increased power and tighter confidence intervals.

Table 2. Expected numbers of stock 1 in the two-stock study designs examined in this study as a function of the initial frequencies of two stocks (p), the relative fitness of stock 1 (w_1), and the number of fish sampled after selection (N).

		N			
$p_1 : p_2$	w_1	50	100	200	400
0.5 : 0.5	0.10	5*	9*	18	36
	0.50	17	33	67	133
	0.80				
	1	25	50	100	200
	1.2	27	54	109	218
	2	33	67	133	267
	10	45	91	181	363
0.25 : 0.75	0.80	11	21	42	84
	1	13	25	50	100
	1.2	14	28	57	114
0.75 : 0.25	0.80	35	70	141	282
	1	38	75	150	300
	1.2	39	79	156	313
0.10 : 0.90	0.80	4*	8*	16	32
	1	5*	10*	20	40
	1.2	6*	12	23	47
0.90 : 0.10	0.80	44*	87	175	351
	1	45*	90	180	360
	1.2	46*	92*	183	366

*The expected number of individuals in the sample for one of the stocks is 10.0 or fewer.

The profile confidence intervals that we describe above are expected to perform better than the more traditional Wald intervals. Wald intervals are constructed by assuming that the likelihood is distributed normally with a variance/covariance matrix approximated by the inverse of the Fisher information matrix. Confidence intervals can then be constructed using t, z, or χ^2 distributions. At large sample sizes such intervals will be equivalent to profile-likelihood intervals, but at smaller sample sizes the estimated likelihood will generally not be normally distributed, and profile-likelihood intervals will be superior (Kalbfleisch and Sprott 1970; Venzon and Moolgavkar 1988; for reviews see Meeker and Escobar 1995; Pawitan 2000). Our investigations (result not reported) have shown this trend — the coverage properties of the Wald interval for relative fitness generally were poorer than the profile interval. Undesirable properties of Wald intervals included high error rates, bias, and intervals that extended below zero. In the past, Wald intervals have been reasonably justified on the basis of their greater ease of computation. With current computation power, this issue is much less relevant than before.

The model (eq. 1) for selection that we have examined is the most basic available for studying evolution (e.g., Hedrick 2000). Its advantage is simplicity and insight into how two groups compare. One disadvantage is that it usually will not indicate which genetic or physical traits contribute to fitness. If selection gradients are of interest they can be estimated by fitting a curve to a plot of fitness versus phenotype for the individuals sampled (e.g., Smouse et al. 1999; Morgan and Conner 2001; Hendry et al. 2003).

© 2005 NRC Canada

Table 3. Expected values of $\hat{w}_i$ as a function of the initial frequencies of two stocks (p), the relative fitness of stock 1 (w_1), and the number of fish sampled after selection (N).

		N			
$p_1 : p_2$	w_1	50	100	200	400
0.5 : 0.5	0.10	0.10*	0.10*	0.10	0.10
	0.50	0.52	0.51	0.50	0.50
	0.80	0.83	0.81	0.81	0.81
	1	1.04	1.02	1.01	1.00
	1.2	1.26	1.23	1.21	1.21
	2	2.13	2.06	2.03	2.02
	10	13.0	11.4	10.6	10.3
0.25 : 0.75	0.80	0.82	0.81	0.81	0.80
	1	1.02	1.01	1.01	1.00
	1.2	1.23	1.22	1.21	1.20
0.75 : 0.25	0.80	0.86	0.83	0.81	0.81
	1	1.09	1.04	1.02	1.01
	1.2	1.33	1.26	1.23	1.21
0.10 : 0.90	0.80	0.82*	0.81*	0.80	0.80
	1	1.02*	1.01*	1.00	1.00
	1.2	1.22*	1.21	1.21	1.20
0.90 : 0.10	0.80	0.99*	0.88	0.84	0.82
	1	1.28*	1.13	1.06	1.03
	1.2	1.57*	1.39*	1.28	1.24

*The expected number of individuals in the sample for one of the stocks is 10.0 or fewer.

Table 4. Geometric mean values of $\hat{w}_i$ as a function of the initial frequencies of two stocks (p), the relative fitness of stock 1 (w_1), and the number of fish sampled after selection (N).

		N			
$p_1 : p_2$	$w_1 : w_2$	50	100	200	400
0.5 : 0.5	0.10	0.09*	0.09*	0.10	0.10
	0.50	0.49	0.50	0.50	0.50
	0.80	0.80	0.80	0.80	0.80
	1	1.00	1.00	1.00	1.00
	1.2	1.20	1.20	1.20	1.20
	2	2.03	2.02	2.01	2.00
	10	10.8	10.6	10.3	10.1
0.25 : 0.75	0.80	0.77	0.79	0.79	0.80
	1	0.97	0.99	0.99	1.00
	1.2	1.17	1.19	1.19	1.19
0.75 : 0.25	0.80	0.82	0.81	0.80	0.80
	1	1.03	1.01	1.01	1.00
	1.2	1.24	1.22	1.21	1.21
0.10 : 0.90	0.80	0.72*	0.75*	0.78	0.79
	1	0.91*	0.95*	0.98	0.99
	1.2	1.10*	1.15	1.18	1.19
0.90 : 0.10	0.80	0.87*	0.83	0.81	0.80
	1	1.10*	1.05	1.02	1.01
	1.2	1.32*	1.27*	1.23	1.21

*The expected number of individuals in the sample for one of the stocks is 10.0 or fewer.

Table 5. Error rates of 95% confidence intervals for $\hat{w}_i$ as a function of the initial frequencies of two stocks (p), the relative fitness of stock 1 (w_1), and the number of fish sampled after selection (N).

		N			
$p_1 : p_2$	$w_1 : w_2$	50	100	200	400
0.5 : 0.5	0.10	0.06	0.06	0.05	0.05
	0.50	0.05	0.06	0.05	0.05
	0.80	0.05	0.04	0.05	0.05
	1	0.06	0.06	0.06	0.05
	1.2	0.05	0.04	0.05	0.05
	2	0.05	0.06	0.05	0.05
	10	0.05	0.06	0.05	0.05
0.25 : 0.75	0.80	0.06	0.05	0.05	0.05
	1	0.05	0.05	0.05	0.05
	1.2	0.06	0.06	0.05	0.05
0.75 : 0.25	0.80	0.04	0.05	0.05	0.05
	1	0.05	0.05	0.05	0.05
	1.2	0.05	0.05	0.05	0.05
0.10 : 0.90	0.80	0.02*	0.05*	0.05	0.05
	1	0.05*	0.04*	0.05	0.05
	1.2	0.05*	0.04	0.06	0.04
0.90 : 0.10	0.80	0.06*	0.05	0.05	0.05
	1	0.05*	0.04	0.05	0.05
	1.2	0.02*	0.05*	0.04	0.05

*The expected number of individuals in the sample for one of the stocks is 10.0 or fewer.

Table 6. Geometric mean multiplicative error (GMME) of estimates of $\hat{w}_i$ as a function of the initial frequencies of two stocks (p), the relative fitness of stock 1 (w_1), and the number of fish sampled after selection (N).

		N			
$p_1 : p_2$	$w_1 : w_2$	50	100	200	400
0.5 : 0.5	0.10	1.52	1.34	1.22	1.15
	0.50	1.27	1.19	1.13	1.08
	0.80	1.26	1.17	1.12	1.08
	1	1.26	1.17	1.12	1.08
	1.2	1.26	1.18	1.12	1.08
	2	1.27	1.18	1.13	1.09
	10	1.52	1.34	1.22	1.15
0.25 : 0.75	0.80	1.33	1.22	1.15	1.10
	1	1.31	1.20	1.14	1.10
	1.2	1.29	1.20	1.13	1.09
0.75 : 0.25	0.80	1.29	1.19	1.13	1.09
	1	1.31	1.20	1.13	1.10
	1.2	1.33	1.22	1.15	1.10
0.10 : 0.90	0.80	1.53*	1.36*	1.24	1.16
	1	1.49*	1.32*	1.21	1.14
	1.2	1.46*	1.29	1.19	1.13
0.90 : 0.10	0.80	1.44*	1.28	1.19	1.13
	1	1.49*	1.32	1.21	1.14
	1.2	1.54*	1.36*	1.23	1.16

*The expected number of individuals in the sample for one of the stocks is 10.0 or fewer.

© 2005 NRC Canada

The favorable results presented here support the development of maximum likelihood estimates of relative fitness (and confidence intervals for those estimates) for more complex or realistic study designs. For example, the study designs reviewed here assumed that the initial proportions of each stock were known at the beginning of the experiment. This may not always be the case. Manly (1972) has provided formulae for maximum likelihood estimates of relative fitness, along with estimates of the standard error of the estimates, but the confidence intervals are likely to be inaccurate. Alternatively, the method could be extended to account for uncertainty in stock identification.

Acknowledgements

We thank Mike Ford and an anonymous reviewer for suggestions that improved the manuscript. MLT was supported by NSF grant DEB-0415932.

References

Casella, G., and Berger, R.L. 2001. Statistical inference. 2nd ed. Brooks Cole, Pacific Grove, Calif.

Garant, D., Dodson, J.J., and Bernatchez, L. 2003. Differential reproductive success and heritability of alternative reproductive tactics in wild Atlantic salmon (*Salmo salar* L.). Evolution, **57**: 1133–1141.

Haldane, J.B.S. 1956. The estimation and significance of the logarithm of a ratio of frequencies. Ann. Hum. Genet. **20**: 309–311.

Hedrick, P.W. 2000. Genetics of populations. Jones and Bartlett, Boston.

Hendry, P.A., Letcher, B.H., and Gries, G. 2003. Estimating natural selection acting on stream dwelling Atlantic salmon: implications for the restoration of extirpated populations. Conserv. Biol. **17**: 795–805.

Hinrichsen, R.A. 2003. The power of experiments for estimating relative reproductive success of hatchery-born spawners. Can. J. Fish. Aquat. Sci. **60**: 864–872.

Kalbfleisch, J.D., and Sprott, D.A. 1970. Application of likelihood methods to models involving large numbers of parameters. J. R. Stat. Soc. Ser. B Stat. Methodol. **32**: 175–208.

Kalinowski, S.T. 2004. Relative fitness analysis (1.0). *Available at* www.montana.edu/kalinowski.

Manly, B.F.J. 1972. Estimating selective values from field data. Biometrics, **28**: 1115–1125.

Manly, B.F.J. 1985. The statistics of natural selection on animal populations. Chapman and Hall, New York.

McCullagh, P., and Nelder, J.A. 1989. Generalized linear models. 2nd ed. Chapman and Hall, New York.

McLean, J.E., Bentzen, P., and Quinn, T.P. 2004. Differential reproductive success of sympatric, naturally spawning hatchery and wild steelhead, *Oncorhynchus mykiss*. Environ. Biol. Fishes, **69**: 359–369.

Meeker, W.Q., and Escobar, L.A. 1995. Teaching about approximate confidence-regions based on maximum-likelihood estimation. Am. Stat. **49**: 48–53.

Morgan, M.T., and Conner, J.K. 2001. Using genetic markers to directly estimate male selection gradients. Evolution, **55**: 272–281.

Pawitan, Y. 2000. A reminder of the fallibility of the Wald statistic: likelihood explanation. Am. Stat. **54**: 54–56.

Smouse, P.E., Meagher, T.R., and Kobak, C.J. 1999. Parentage analysis in *Chamaelirium luteum* (L.) Gray (Liliaceae): why do some males have higher reproductive contributions? J. Evol. Biol. **12**: 1069–1077.

Sokal, R.R., and Rohlf, F.J. 1997. Biometry. 3rd ed. W.H. Freeman and Co., New York.

Venzon, D.J., and Moolgavkar, S.H. 1988. A method for computing profile-likelihood-based confidence-intervals. J. R. Stat. Soc. Ser. C Appl. Stat. **37**: 87–94.

© 2005 NRC Canada

Thermal histories, stress, and metabolic rates of chinook salmon (*Oncorhynchus tshawytscha*) in Lake Ontario: evidence from intra-otolith stable isotope analyses

C.M. Wurster, W.P. Patterson, D.J. Stewart, J.N. Bowlby, and T.J. Stewart

Abstract: We describe thermal histories for Lake Ontario chinook salmon (*Oncorhynchus tshawytscha*) as determined from otolith $\delta^{18}O$ thermometry using computer-controlled micromilling techniques to recover otolith aragonite at subseasonal resolution. We find that during the summer months chinook salmon inhabited epilimnetic waters with temperatures of ~19–20 °C as far back as the late 1980s. Chinook would approach but rarely exceed their reported upper incipient lethal limit of approximately 22 °C, which suggests that these fish were seeking water with temperatures as high as was tolerable while otolith growth occurred. These results contrast with expected midsummer temperatures for this cold-water salmonine. Bioenergetic simulations indicate significant stress imposed upon chinook salmon. We estimate consumption to be up to 20% more and gross conversion efficiency 18% less annually relative to nominal simulations where chinook salmon are modeled nearer their preferred temperature, reinforcing previous inferences that the chinook salmon population may be near the limits of sustainability. We also find a strong negative correlation between $\delta^{18}O$ and $\delta^{13}C$ values. Therefore, seasonal and ontogenetic variation in $\delta^{13}C$ values of chinook salmon otoliths appear to be related to metabolic rate during pelagic residence and may provide an indirect method for evaluating field activity and other aspects of fish life history.

Résumé : Nous décrivons l'histoire thermique des saumons quinnat (*Oncorhynchus tshawytscha*) du lac Ontario d'après la thermométrie $\delta^{18}O$ des otolithes à l'aide de techniques de moulinage sous contrôle d'ordinateur pour récupérer l'aragonite des otolithes à une échelle de résolution inférieure à une saison. Durant les mois d'été, les saumons quinnat habitent les eaux épilimnétiques de température ~19–20 °C depuis la fin des années 1980. Les saumons quinnat s'approchent du seuil de leur limite thermique létale supérieure connue qui est d'environ 22 °C, mais la dépassent rarement, ce qui laisse croire que les poissons recherchent des eaux de la plus haute température tolérable durant la période de croissance des otolithes. Ces résultats tranchent avec les températures attendues en mi-été pour ce salmoniné d'eau froide. Des simulations bioénergétiques indiquent qu'il se produit un important stress chez le saumon. Nous estimons que la consommation est de 20 % supérieure et que l'efficacité brute de conversion est de 18 % inférieure à l'échelle annuelle par rapport à des simulations nominales dans lesquelles les saumons quinnat sont traités plus près de leur température préférée; cela renforce les déductions antérieures voulant que la population de saumons quinnat soit près de ses limites de maintien. Il y a aussi une forte corrélation négative entre les valeurs de $\delta^{18}O$ et de $\delta^{13}C$. Ainsi, les variations saisonnières et ontogéniques des valeurs de $\delta^{13}C$ des otolithes des saumons quinnat semblent être reliées au taux de métabolisme durant leur temps de résidence pélagique et cela peut fournir une méthode indirecte d'évaluer l'activité en nature et d'autres aspects du cycle biologique des poissons.

[Traduit par la Rédaction]

Introduction

There is considerable concern that Lake Ontario's salmonine sport fishery is reaching the limits of sustainability (e.g., Rand et al. 1994; Rand and Stewart 1998*a*; Mills et al. 2003). Chinook salmon (*Oncorhynchus tshawytscha*; hereinafter referred to as chinook) were estimated to generate five times as much lake-wide production than either coho salmon (*Oncorhynchus kisutch*) or lake trout (*Salvelinus namaycush*) in Lake Ontario (Rand and Stewart 1998*b*) and, therefore,

Received 29 April 2004. Accepted 29 September 2004. Published on the NRC Research Press Web site at http://cjfas.nrc.ca on 15 April 2005.
J18096

C.M. Wurster[1] and W.P. Patterson. Department of Geological Sciences, University of Saskatchewan, 114 Science Place, Saskatoon, SK S7N 5E2, Canada.
D.J. Stewart. College of Environmental Science and Forestry, State University of New York, 1 Forestry Drive, Syracuse, NY 13210, USA.
J.N. Bowlby and T.J. Stewart. Ontario Ministry of Natural Resources, Glenora Fisheries Station, Picton, ON K0K 2T0, Canada.

[1]Corresponding author (e-mail: chris.wurster@usask.ca).

 doi: 10.1139/F04-241 © 2005 NRC Canada

chinook were the top predators, with the highest forage demand of all stocked salmonines (Jones et al. 1993). Because the diet of chinook in Lake Ontario during their pelagic residence is composed almost entirely of alewife (*Alosa pseudoharengus*) (Brandt 1986; Rand and Stewart 1998*b*; Lantry 2001), chinook energetics are key to understanding ecological stress in this system. Originally introduced in the 1970s to control a burgeoning population of non-native alewife, chinook have subsequently been found, in a number of studies, to rely predominantly on alewife, despite the latter's decreasing abundance and quality (e.g., Mason et al. 1995; Rand and Stewart 1998*b*; Lantry 2001). The presence of chinook subsequently allowed the development of an important recreational fishery that generates considerable economic activity for many coastal districts (Talhelm 1988; Mills et al. 2003). This substantial economic resource stimulated the growth of salmonine hatcheries around the lake (Hartig et al. 1991). However, prey fish production may be inhibited by significant reductions in total phosphorus concentrations and nutrient loading in Lake Ontario (Johengen et al. 1994), and subsequent zebra and quagga mussel invasions (e.g., Mills et al. 2003). In addition to the increase in predatory pressure (e.g., O'Gorman and Stewart 1999), these conditions in Lake Ontario may have contributed to the observed rapid reduction in prey availability and quality (e.g., Mills et al. 2003), and the concern that chinook cannot maintain current growth and survival rates (e.g., Rand and Stewart 1998*a*).

Bioenergetic simulations suggest that consumption by chinook is near the maximum rate for the current environment in Lake Ontario (e.g., Rand and Stewart 1998*b*), although consumption may be limited more by thermal stress than by production itself. Rand et al. (1994) originally predicted that chinook would have to triple their ingestion of prey fish to make up for decreases in prey size and condition, an inference that was subsequently supported (e.g., Rand and Stewart 1998*a*; Lantry 2001). Chinook in Lake Michigan, undergoing similar stress due to reduction in prey abundance and quality, have already been observed to undergo a reduction in growth and survival, coupled with an increase in disease (Stewart and Ibarra 1991; Rand and Stewart 1998*a*). Bioenergetic simulations were conducted with the assumption that chinook occupy water at 11 °C during midsummer. However, the highest alewife biomass density in Lake Ontario is in the epilimnion at temperatures of 21 °C (Mason et al. 1995), and there is some evidence that chinook may move to warmer water to obtain increasingly scarce food resources (e.g., Olson et al. 1988; Goyke and Brandt 1993). Higher temperatures require higher food intake to compensate for the increased energetic cost of respiration. We can now reconstruct individual thermal-history records preserved in sagittal otoliths of chinook to test the hypothesis that chinook in Lake Ontario are now found in warmer water than in the past.

Otoliths are aragonitic biominerals produced in the inner ear of teleost fish and used in hearing and balance (Campana 1999). This structure grows sequentially, without resorption, and often displays yearly and daily banding patterns that provide age and growth information for most fish species (e.g., Panella 1980). Therefore, high-resolution $\delta^{18}O$ and $\delta^{13}C$ subseasonal records can be acquired from these biominerals. Because $\delta^{18}O$ values of otoliths have been determined to form at or near equilibrium with the ambient water (e.g., Patterson et al. 1993; Thorrold et al. 1997; Høie et al. 2004*a*), the temperature experienced by the fish can be tracked throughout its life if the $\delta^{18}O$ value of the ambient water is known, and variations in this value are unlikely (in a large lake with relatively constant $\delta^{18}O$ values, for example). Conversely, widely disparate $\delta^{18}O_{(H_2O)}$ values can be used to track migration patterns (tributary-to-lake migrations, for example).

The $\delta^{13}C$ values of otoliths were originally thought to reflect the $\delta^{13}C$ values of dissolved inorganic carbon (DIC) only (Degens et al. 1969). However, otolith $\delta^{13}C$ values are considerably lower than those predicted assuming equilibrium with ambient water, suggesting that there is a metabolic contribution of respiratory carbon to the otolith (e.g., Kalish 1991). Recent studies clearly indicate a relationship between metabolic rate and incorporation of otolith carbon (Tohse and Mugiya 2002; Høie et al. 2003), and intra-otolith $\delta^{13}C$ values have been shown to record ontogenetic variations in metabolic rate (Schwarcz et al. 1998; Wurster and Patterson 2003; Høie et al. 2004*b*). Although more work is necessary to evaluate intra-otolith $\delta^{13}C$ values, given the confounding influences of environment, diet, and tissue turnover, $\delta^{13}C$ values may become a powerful proxy for fish physiology and (or) environment once relative controls are quantified. So $\delta^{13}C$ values may provide a unique proxy for individual energetic behavior, such as the cost of activity (Sherwood and Rose 2003; Wurster and Patterson 2003), especially in fishes whose diet is relatively stable and whose reproduction is reserved for the end of life, such as adult chinook. Therefore, intra-otolith $\delta^{18}O$ and $\delta^{13}C$ values may provide both an indirect record of the most fundamental variable, temperature (He and Stewart 1998), and, arguably the most difficult parameter to estimate, respiration of activity in free-ranging fishes (e.g., Rowan and Rasmussen 1996; Trudel et al. 2004).

The primary goal of this study is to track temperatures that chinook experience during their pelagic residence in Lake Ontario. Temperatures are estimated from an otolith-specific aragonite temperature–fractionation relationship for freshwater fish (Patterson et al. 1993), using intra-otolith $\delta^{18}O$ values and measured $\delta^{18}O$ values of Lake Ontario water. Intra-otolith $\delta^{18}O$ and $\delta^{13}C$ values are analyzed for a suite of otoliths collected in 1991 (archived group) and in 1997 (Salmon River group) to compare potential changes in temperature of waters occupied as prey fish abundance and quality declined after 1991. We coupled this new information with a chinook bioenergetic model (Stewart and Ibarra 1991) to evaluate the level of stress within the Lake Ontario pelagic food web using specific growth rate and gross conversion efficiency (GCE; gross production/prey consumption) as a measure of that stress. We examined rates of exploitation of prey fish and compared the results with earlier simulations that modeled chinook at preferred temperatures in midsummer (Rand et al. 1994; Rand and Stewart 1998*b*). A secondary goal of this study is to evaluate intra-otolith $\delta^{13}C$ values as a potential indicator of metabolic rate.

Methods

Field collection, micromilling, and analysis of $\delta^{18}O$ and $\delta^{13}C$ values

Archived otoliths were obtained from angler-caught chinook from Ontario waters of Lake Ontario in 1991 (Stewart

© 2005 NRC Canada

et al. 2003). Chinook were also taken during their spawning run into the Salmon River, New York, on 7 October 1997. Sex and total length were noted, and both otoliths were removed and stored in an envelope. Six archived otoliths collected in 1991 and a subset of nine otoliths collected in 1997 were chosen for application of micromilling techniques. Chinook otolith lengths were generally 9–10 mm for a sagittal section. The monthly trend in body condition was determined as the mean weight of a 600 mm long chinook after adjusting for differences in length and year using analysis of covariance. Fork length and wet weight of chinook were measured in angler surveys during 1988–1992 (Stewart et al. 2003). Fork lengths ranged from 300 to 780 mm. Body condition was not significantly different between ages 1 and 2, so these fish were combined for this analysis.

The detailed methodology for micromilling is described by Wurster et al. (1999). Specimens were polished to reveal growth annuli, attached to a stage beneath a fixed dental drill, and viewed on a computer monitor via a color digital video camera. Annuli were subsequently digitized in real time as a series of three-dimensional coordinates, while intermediate coordinates were interpolated using a cubic spline algorithm. An array of intermediate sampling paths was calculated between digitized curves. Sample path arrays guided three high-precision actuators, which positioned the sample stage relative to the fixed dental drill. Approximately 30 to 50 µg aliquots of sample carbonate were recovered for routine analysis.

Once extracted, samples were roasted in vacuo for 1 h at 200 °C to remove volatiles that may have interfered with $\delta^{18}O$ and $\delta^{13}C$ measurement. Samples were reacted in a Kiel III automated carbonate preparation device directly coupled to a Finnigan MAT 252 or a MAT 253 stable isotope ratio mass spectrometer. Carbon dioxide was generated by the reaction of carbonate with 3–4 drops of anhydrous phosphoric acid in individual reaction vessels at 70 °C. Individual samples were analyzed using a micro-inlet, which reduces sample "memory" and permits analysis of ~20 µg of carbonate. Carbonate samples were analyzed with a precision of ±0.08‰ (1σ), determined by analysis of international carbonate standards NBS-18 and NBS-19, and reported relative to Vienna Pee Dee Belemnite (VPDB).

Water samples were collected from the surface of the Salmon River and Lake Ontario in Nalgene™ containers, which were sealed until analyzed for $\delta^{18}O_{(H_2O)}$. Most samples were measured using a Finnigan HDO-II water-equilibration device directly coupled to a Finnigan MAT 252 gas ratio mass spectrometer. For measuring $\delta^{18}O_{(H_2O)}$, standard carbon dioxide gas was equilibrated with water samples for 6 h at 25 °C and then analyzed sequentially. Values are reported to ±0.1‰ for $\delta^{18}O_{(H_2O)}$ relative to Vienna Standard Mean Ocean Water (VSMOW). Replicate analyses of water samples were better than ±0.1‰. A few additional Lake Ontario $\delta^{18}O_{(H_2O)}$ values were analyzed on a Finnigan high temperature conversion/elemental analyzer via high-temperature pyrolysis. Samples analyzed for $\delta^{18}O_{(H_2O)}$ via both high-temperature pyrolysis and water-equilibrator methods agreed within ±0.1‰. Carbonate and water stable isotope analyses were performed at the isotope laboratories of Syracuse University, Syracuse, New York, and the University of Saskatchewan, Saskatoon.

Estimation of chinook temperatures

Temperature can be calculated from otolith aragonite with a precision and accuracy better than 1 °C (Thorrold et al. 1997; Høie et al. 2004*b*). Several otolith-specific aragonite temperature–fractionation relationships have been determined from well-constrained environments (e.g., Patterson et al. 1993; Thorrold et al. 1997; Høie et al. 2004*a*). These relationships have slopes that are statistically indistinguishable from each other and from Kim and O'Neil's (1997) theoretical temperature–fractionation relationship for inorganic aragonite, although the intercepts may differ significantly (Campana 1999; Thorrold and Hare 2002). Because of the similar slopes, we calculated chinook temperatures from the aragonite temperature–fractionation relationship of Patterson et al. (1993) (which included freshwater salmonid otoliths) using the measured otolith $\delta^{18}O$ value and the Lake Ontario $\delta^{18}O$ value. We used –6.8‰ VSMOW as the $\delta^{18}O$ value of Lake Ontario water (e.g., Hodell et al. 1998; Coplen and Kendall 2000; this study).

Because of differing growth rates and size of otoliths, not all the specimens were microsampled at the same resolution. To compare seasonal values, we assume limited otolith growth for winter months. We matched each calculated minimum temperature to the average Lake Ontario water temperature to estimate both the spring and the fall Julian day that the minimum temperature represents. We then assumed equal growth through the growing season to determine the day of the year each temperature estimate represents. Therefore, we are not accounting for seasonal growth changes within and among otoliths; nonetheless, this is a relatively unbiased way to transform data and compare individual years. Estimates of Lake Ontario water temperature are derived from Hodell et al. (1998) and from the National Oceanic and Atmospheric Administration's Great Lakes Environmental Research Laboratory (http://coastwatch.glerl.noaa.gov).

Chinook energetics

We used the chinook bioenergetics model of Stewart and Ibarra (1991), implemented with the "Fish Bioenergetics 3.0" computer application (Hanson et al. 1997), to evaluate production, predation, and stress for chinook in Lake Ontario. Detailed inputs to the model differ from those used by Rand and Stewart (1998*b*) in temperature only, therefore we do not include a detailed description of the energetics model or the inputs. Energy density of predator and prey, and diet proportions (including invertebrates and prey fish), can be found in other publications (Elrod and O'Gorman 1991; Stewart and Ibarra 1991; Rand et al. 1993).

Most chinook in Lake Ontario spawn in their third or fourth year, and discounting age 0+ and the year of spawning, most chinook have spent 1 or 2 "full" summers as offshore residents (e.g., Rand and Stewart 1998*b*). We therefore modeled the dominant life forms of chinook for an average fish from 1989 to 1991 and an average fish from 1995 to 1997 to compare with a nominal simulation by Rand and Stewart (1998*b*). From the bioenergetic model outputs we estimated specific growth rate, GCE, and prey consumption of an average individual chinook in Lake Ontario as a measure of stress. This modeling exercise was repeated using assumed preferred temperatures (nominal simulation) to

© 2005 NRC Canada

Table 1. Covariation between intra-otolith $\delta^{18}O$ and $\delta^{13}C$ values of individual Lake Ontario chinook salmon (*Oncorhynchus tshawytscha*).

Specimen	Equation	R^2
Salmon River group		
CHK1	$\delta^{13}C = 1.3 \cdot \delta^{18}O + 1.5$	0.73
CHK4	$\delta^{13}C = 1.3 \cdot \delta^{18}O + 1.7$	0.73
CHK7	$\delta^{13}C = 1.3 \cdot \delta^{18}O + 1.5$	0.73
CHK13	$\delta^{13}C = 1.8 \cdot \delta^{18}O + 4.6$	0.78
CHK14	$\delta^{13}C = 1.3 \cdot \delta^{18}O + 2.6$	0.84
CHK15	$\delta^{13}C = 1.4 \cdot \delta^{18}O + 2.8$	0.90
CHK23	$\delta^{13}C = 1.5 \cdot \delta^{18}O + 2.7$	0.81
Pooled	$\delta^{13}C = 1.2 \cdot \delta^{18}O + 1.5$	0.71
Archived group		
SAM12	$\delta^{13}C = 1.7 \cdot \delta^{18}O + 3.3$	0.87
SAM54	$\delta^{13}C = 1.9 \cdot \delta^{18}O + 4.9$	0.85
SAM84	$\delta^{13}C = 2.2 \cdot \delta^{18}O + 4.6$	0.87
SAM92	$\delta^{13}C = 1.6 \cdot \delta^{18}O + 4.0$	0.84
SAM93	$\delta^{13}C = 1.6 \cdot \delta^{18}O + 2.5$	0.87
SAM108	$\delta^{13}C = 1.6 \cdot \delta^{18}O + 3.4$	0.70
Pooled	$\delta^{13}C = 1.4 \cdot \delta^{18}O + 1.8$	0.57
All data pooled	$\delta^{13}C = 1.3 \cdot \delta^{18}O + 1.1$	0.55

compare bioenergetic outputs with chinook temperatures found via the otolith thermometry technique.

Results

Intra-otolith $\delta^{18}O$ and $\delta^{13}C$ values

Specimens from the archived group, collected in 1991 from Lake Ontario, display cyclic patterns in $\delta^{18}O$ values that range from –7.4 ± 0.3‰ to –5.3 ± 0.6‰ VPDB (±SD). The $\delta^{13}C$ values covary with $\delta^{18}O$ values (Table 1; Fig. 1). Specimens collected in 1997 from the Salmon River (Salmon River group) also display cyclicity; however, both $\delta^{18}O$ and $\delta^{13}C$ values in the first and last years are much more negative than the other values (Fig. 2). We assume that each cycle represents 1 year of otolith growth, and pelagic residence is assumed to include all cycles except the first, which corresponds to age 0+, and the last half-year of growth in the Salmon River group, which corresponds to the spawning run. Intra-otolith $\delta^{18}O$ and $\delta^{13}C$ values of specimen CHK20 (CHK is a sample code for chinook from the Salmon River group) are unique relative to the other 14 otoliths sampled (Fig. 2*g*). This specimen's $\delta^{18}O$ values are generally more negative and show a much greater seasonal range. Because no distinct pelagic-residence years could be interpreted from CHK20, we did not consider this data set in analyses requiring Lake Ontario residence, but it should be noted as an example of alternative behavior; perhaps this fish spent a year in a river before smolting.

Minimum $\delta^{18}O$ values for all pelagic-residence years were remarkably consistent for both the archived group and the Salmon River group (–7.4 ± 0.3‰ and –7.5 ± 0.1‰ VPDB, respectively), and mean values did not differ significantly between groups (*t* test, $p < 0.05$). However, maximum $\delta^{18}O$ values for individual pelagic-residence years did vary somewhat more among specimens, yet they had the same mean value, –5.3 ± 0.6‰ and –5.3 ± 0.5‰ VPDB for the archived group and Salmon River group, respectively. Mean maximum $\delta^{18}O$ values for pelagic-residence years also did not differ significantly between the groups (*t* test, $p < 0.05$).

In contrast to the remarkable consistency in seasonal minimum $\delta^{18}O$ values among individual chinook otoliths, seasonal minimum $\delta^{13}C$ values are inconsistent despite strong covariations between $\delta^{13}C$ and $\delta^{18}O$ values (Table 1; Figs. 1 and 2). Both groups have notable covariation between $\delta^{18}O$ and $\delta^{13}C$ values, with CHK15 having the highest correlation coefficient ($R^2 = 0.90$; Table 1). Least squared linear regressions are significantly different and cannot be considered to have the same relationship between $\delta^{13}C$ and $\delta^{18}O$ values for any of the populations — archived, Salmon River, or grouped. However, linear regressions for specimens in the archived group, except specimen SAM84 (SAM is a sample code for chinook from the archived group), are not significantly different, based on analysis of covariance ($\alpha = 0.05$, $F_{[4,375]} = 2.26$).

Chinook thermal histories and energetics

We measured $\delta^{18}O_{(H_2O)}$ values of –6.9 ± 0.05‰ VSMOW for Lake Ontario in 1998 and 2000 ($n = 4$) that are consistent with Hodell et al.'s (1998) $\delta^{18}O_{(H_2O)}$ values of –6.7 ± 0.13‰ VSMOW from Rochester basin surface waters and a depth transect during the years 1993–1995 ($n = 37$). Those authors concluded that Lake Ontario showed relatively little variation with depth, time, or space. Additionally, these values agree well with that of the Niagara River (–6.8‰ VSMOW; Gat et al. 1994; Coplen and Kendall 2000), which is considered characteristic of the eastern portion of the Great Lakes system (Gat et al. 1994). We used a value of –6.8‰ VSMOW to calculate chinook temperatures and consider this value stable through space, depth, and time for Lake Ontario's water.

Midsummer temperatures calculated using this $\delta^{18}O_{(H_2O)}$ value (–6.8‰ VSMOW) and Patterson et al.'s (1993) temperature–fractionation relationship are consistently near 20 °C (Fig. 3), and exceed 22 °C in two specimens (Figs. 1*b* and 1*f*). The lowest maximum temperature calculated was 18 °C from SAM93 in the archived group (Fig. 3*a*). Most specimens appear to reach and stay within a narrow temperature range in midsummer for 2 or 3 weeks (Fig. 3). Several pelagic-residence years show evidence of a two-step temperature change, where the chinook remain at one temperature for a period of time and then move into water that is 1–2 °C warmer or colder for the remainder of the midsummer period (for examples, see Figs. 1*a* and 2*g*). We do not know the extent to which deviation from this dominant pattern is merely a result of differences in seasonal growth in the otolith or in fish movement in Lake Ontario. We then averaged temperatures for the Salmon River group and archived group separately (Fig. 3). To weight each specimen equally we interpolated daily temperatures for each specimen using a cubic spline. Averages for both groups show a similar pattern, reaching relatively stable temperatures at about 19 °C in midsummer. Despite the similarity, mean temperatures of each group from day 210 to day 250 (midsummer) are significantly different (*t* test, $p < 0.05$), with the mean temperature of the Salmon River group +0.4 °C higher than that of the archived group. Additionally, we find that linear regres-

© 2005 NRC Canada

Fig. 1. Intra-otolith $\delta^{18}O$ values and calculated temperatures (●) and $\delta^{13}C$ values (○) relative to Vienna Pee Dee Belemnite (VPDB) for the archived group of chinook salmon (*Oncorhynchus tshawytscha*) in Lake Ontario. Archived specimens were collected in 1991 from offshore waters of Lake Ontario. Each subplot represents one otolith from an individual fish. The $\delta^{18}O$ and $\delta^{13}C$ values are plotted according to the number of the sample from the core of the otolith; note that $\delta^{18}O$ values are plotted with more negative values toward the top. The temperature scale (inset on *y* axis) is calculated using a Lake Ontario $\delta^{18}O$ value of –6.8‰ Vienna Standard Mean Ocean Water (VSMOW) and Patterson et al.'s (1993) temperature–fractionation relationship for otolith aragonite of freshwater fish.

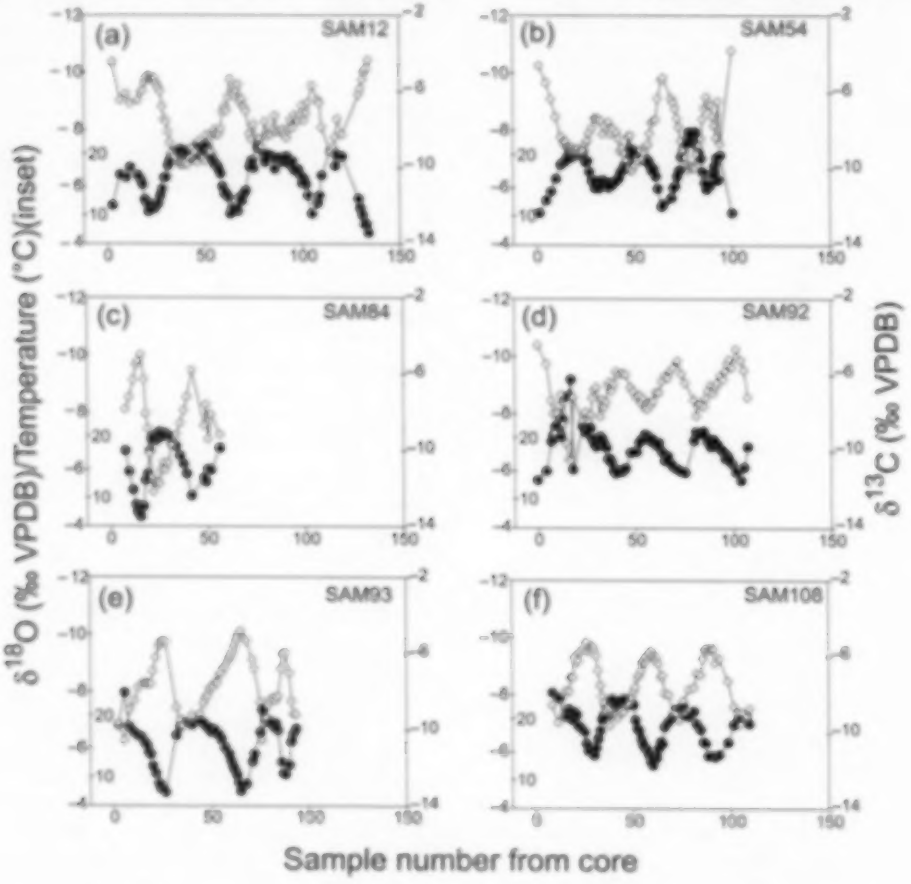

sions between estimated pelagic temperatures and $\delta^{13}C$ values are homogeneous for otoliths within the archived group (except SAM84), the Salmon River group, and between these two groups, which suggests that given the same Lake Ontario environment, the relationship between $\delta^{13}C$ and $\delta^{18}O$ values is the same. SAM84 displays unusually negative $\delta^{13}C$ values during pelagic residence (Fig. 1*c*), resulting in a much greater slope (Table 1).

Otolith thermometry of the archived and Salmon River groups suggests that chinook are reaching and staying for some time in ~19 °C water. We therefore re-ran the bioenergetic simulation of Rand and Stewart (1998*b*) assuming that chinook inhabited the warmest available water, up to but not exceeding 11 °C (nominal simulation) or 19 °C (otolith thermometry simulation). Energetic comparisons between the nominal and otolith thermometry simulations indicate significant stress imposed upon Lake Ontario chinook in midsummer (Fig. 4). The specific growth rate declines to near zero in midsummer for the otolith thermometry simulation and is nearly six times lower than for the comparative nominal simulation in midsummer (Fig. 4). However, the specific growth rate is higher for the otolith thermometry simulation relative to the nominal simulation just prior to and just after the growth depression in midsummer. GCE imitates this pattern, declining in midsummer to less than 0.1 (Fig. 4). To maintain observed growth, in the otolith-based simulation chinook are consuming prey fish near the maximum rate, and annually consume 18% more prey by weight relative to the nominal simulation (Table 2). Since chinook must eat more to attain the same growth at higher temperatures, annual GCE is estimated to be 18.2% lower than in the nominal simulation (Table 2).

Discussion

Derivation of temperature histories of adult chinook

Before further interpreting chinook temperature histories, we must first qualify uncertainties associated with the use of

© 2005 NRC Canada

Fig. 2. Intra-otolith $\delta^{18}O$ values and calculated temperatures (●) and $\delta^{13}C$ values (◇) relative to VPDB for chinook from the Salmon River group collected on 7 October 1997 during the annual Salmon River, New York, spawning run. Each subplot represents one otolith from an individual fish. The $\delta^{18}O$ and $\delta^{13}C$ values are plotted by the number of the sample from the core of the otolith; note that $\delta^{18}O$ values are plotted with lower values toward the top. The temperature scale (inset on *y* axis) is calculated using a Lake Ontario $\delta^{18}O$ value of –6.8‰ VSMOW and Patterson et al.'s (1993) temperature–fractionation relationship for otolith aragonite of freshwater fish.

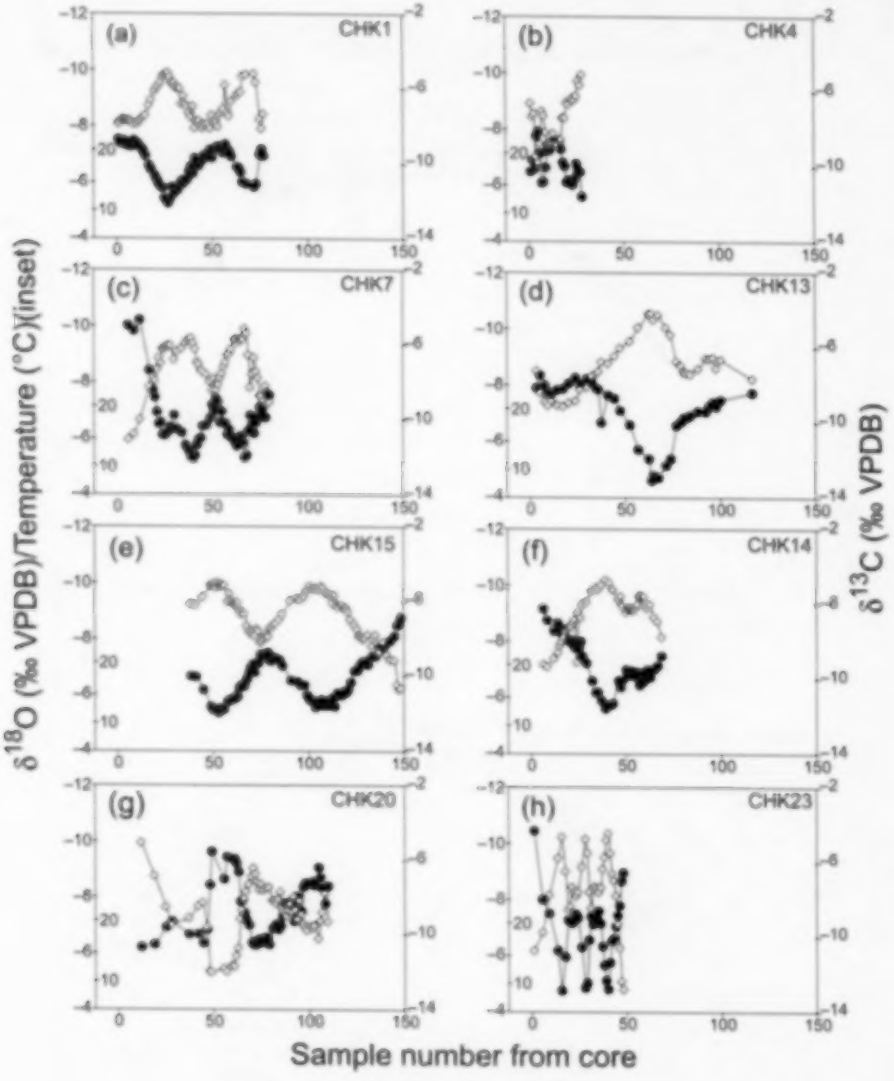

the otolith thermometry technique. This requires discussion of two key elements: (1) the temperature–fractionation relationship and (2) the appropriate $\delta^{18}O_{(H_2O)}$ value used in the selected temperature–fractionation relationship. We therefore begin our discussion by addressing these key issues.

Although it is well established that otoliths produce aragonite at least close to equilibrium with the ambient water (Campana 1999) with a temperature precision and accuracy better than 1 °C (Thorrold et al. 1997; Høie et al. 2004*b*), there may still be species-dependent temperature–fractionation relationships (Høie et al. 2004*a*). Therefore, we must choose the appropriate temperature–fractionation relationship if direct estimation of environmental temperatures is to be done accurately. We chose to calculate temperatures using Patterson et al.'s (1993) equation because it was specifically developed for freshwater fishes in natural systems and includes freshwater salmonids from the Great Lakes. We consider this equation representative of those calculated using the equations of Radtke et al. (1996), Høie et al. (2004*a*), and Kim and O'Neil (1997) because the temperatures calculated are all within 1 °C. Thorrold et al.'s (1997) equation, however, produces temperatures ~4 °C higher than the other

© 2005 NRC Canada

Fig. 3. Estimated seasonal temperatures during pelagic residence of chinook in (*a*) the archived group and (*b*) the Salmon River group in Lake Ontario calculated via otolith thermometry. Minimum calculated temperature was used to determine the Julian day for the first day of growth (spring) and the last day of growth (fall) for each yearly profile. Invariant growth rates were assumed within one growing season to reconstruct and compare chinook seasonal temperature variation. Average seasonal temperature profiles and confidence intervals were determined from cubic spline interpolations of each specimen's temperature profile to ensure equal representation of each year. Each symbol represents one pelagic-residence year.

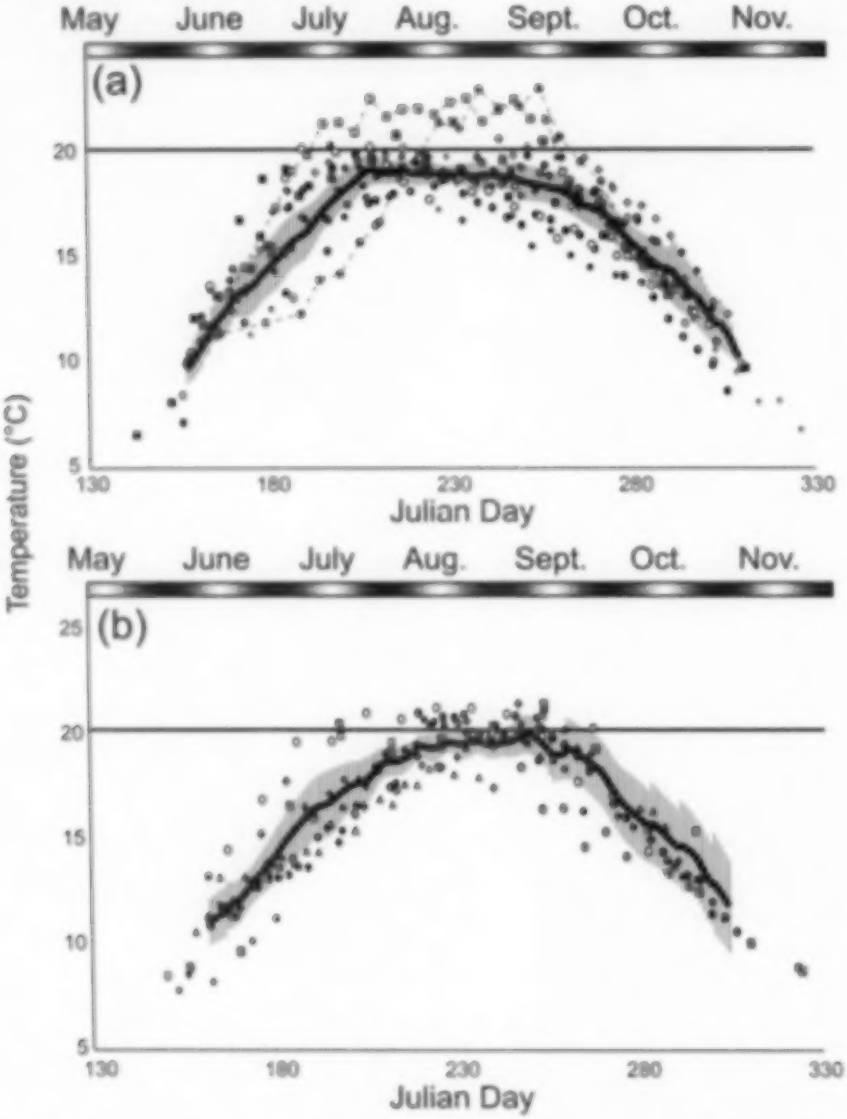

equations. Thorrold et al.'s (1997) equation therefore predicts temperatures beyond lethal limits for chinook and is thus not appropriate.

The slope of the temperature–fractionation relationship is such that an error in $\delta^{18}O_{(H_2O)}$ value of ~0.25‰ results in a temperature error of 1 °C, and it is therefore critical to have accurate $\delta^{18}O$ values of Lake Ontario water. In addition to Hodell et al.'s (1998) values, which are in close agreement with our own measured values for Lake Ontario, we plot seasonal values for Sodus Bay and Lake Ontario (this study), the Niagara River and St. Lawrence River (Gat et al. 1994; Yang et al. 1996; Coplen and Kendall 2000) at Lake Ontario's outflow to address variability in Lake Ontario $\delta^{18}O_{(H_2O)}$ values (Fig. 5). Also plotted are seasonal $\delta^{18}O$ values for the Salmon River (this study) and Genesee River (Coplen and Kendall 2000) as an example of potential river inputs to the Lake Ontario system. River waters have lower and more seasonally variable $\delta^{18}O$ values than Lake Ontario and the Niagara River and St. Lawrence River systems. Although there is distinct seasonality to the larger Niagara and St. Lawrence river systems, this is modified to a high degree from the original precipitation input, as they are dominantly

© 2005 NRC Canada

Fig. 4. Energetic output for pelagic residence of age 3+ chinook comparing nominal (shaded line) and otolith thermometry (solid line) bioenergetic simulations. Model parameters were kept constant, and only temperature and associated p value (i.e., the proportion of maximum consumption estimated by iterative fit to growth) differed between the two simulations. The nominal simulation assumes that chinook stay at 11 °C in midsummer, whereas in otolith-based simulations, temperatures indicate chinook swimming at up to 19 °C during midsummer.

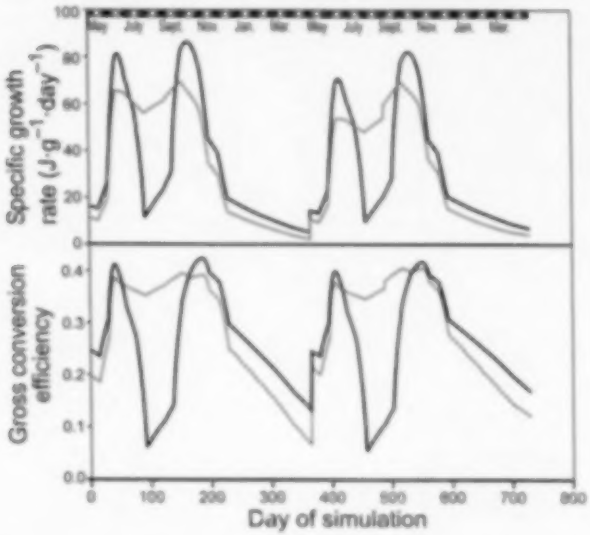

Table 2. Comparison of bioenergetic simulation (otolith thermometry and nominal) output of total consumption and gross conversion efficiency (GCE) of adult chinook during pelagic residence in Lake Ontario.

	Year 1	Year 2	Total	GCE
Consumption (g)				
Otolith, age 3+	5323	24 128	29 451	0.27
Nominal, age 3+	4742	19 400	24 142	0.33
Difference (%)	11	20	18	18
Consumption (g)				
Nominal, age 2+	7546	*	7 546	0.27
Otolith, age 2+	6656	*	6 656	0.33
Difference (%)	12	*	12	18

*No estimate.

outflow from stable sources (Lakes Erie and Ontario). These rivers show variations of –6.7 ± 0.14‰ and –6.9 ± 0.26‰ VSMOW, respectively. However, Lake Ontario proper shows no seasonal variation in isotope values. Ignoring the Genesee and Salmon rivers and focusing on Lake Ontario and the Niagara and St. Lawrence rivers, $\delta^{18}O$ values are more variable in the fall and early summer, but converge on –6.8 ± 0.19‰ VSMOW, the value used in our calculations, in July and August. We therefore consider this value appropriate to use in determining at least maximum temperatures in midsummer using our otolith thermometry technique; we estimate the precision to be approximately 1 °C. However, spring and early-summer $\delta^{18}O$ values may be more variable, possibly because of snowmelt, especially near river inputs (L.I.

Fig. 5. Seasonal $\delta^{18}O_{(H_2O)}$ values relative to VSMOW for Lake Ontario, Niagara River, and St. Lawrence River (at Lake Ontario outflow) and smaller tributaries. The $\delta^{18}O_{(H_2O)}$ values represented are from various years. Data sources are represented on the plot.

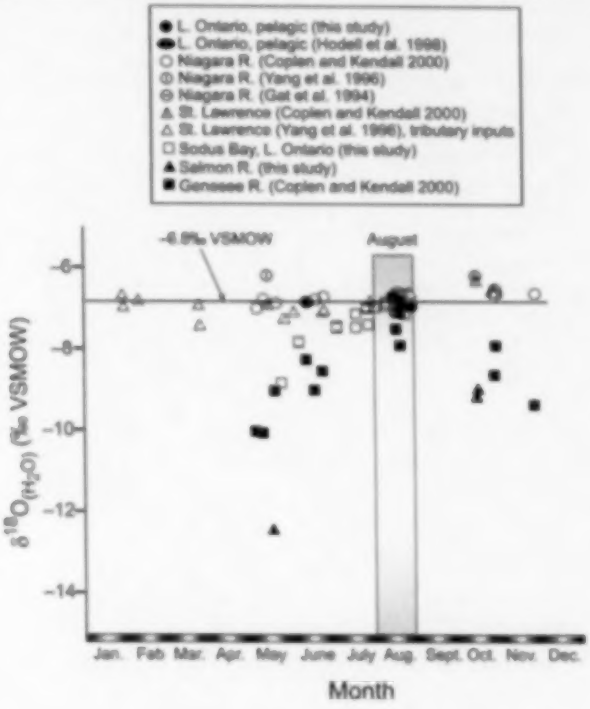
L. Ontario, pelagic (this study)
L. Ontario, pelagic (Hodell et al. 1998)
Niagara R. (Coplen and Kendall 2000)
Niagara R. (Yang et al. 1996)
Niagara R. (Gat et al. 1994)
St. Lawrence (Coplen and Kendall 2000)
St. Lawrence (Yang et al. 1996), tributary inputs
Sodus Bay, L. Ontario (this study)
Salmon R. (this study)
Genesee R. (Coplen and Kendall 2000)
–6.8‰ VSMOW
August
δ18O(H2O) (‰ VSMOW)
Jan. Feb Mar. Apr. May June July Aug. Sept. Oct. Nov. Dec.
Month

Wassenaar, National Hydrology Research Centre, Environment Canada, Saskatoon, SK S7N 3H5, Canada, personal communication). Additionally, we will overestimate temperatures for chinook that migrate toward a tributary. It is important to recognize that Lake Ontario's $\delta^{18}O_{(H_2O)}$ value does not vary spatially (including with depth) in August, and is not dependent on temperature changes in the lake.

Chinook pelagic residence: temperature histories and energetics

The interpretive character of chinook intra-otolith $\delta^{18}O$ and $\delta^{13}C$ values is illustrated using two exemplary figures, one specimen from each group, both micromilled from the core to the edge of the otolith (Fig. 6). SAM92 displays a cyclic (seasonal) pattern ranging from approximately –5.5‰ to about –7.3‰ VPDB after an initial decrease in $\delta^{18}O$ values to as low as –9‰ VPDB in the first year of growth (Fig. 6*a*). There are just over three seasonal patterns, which is consistent with an independent age count of 3+. Otolith growth is negligible during the winter, therefore maximum $\delta^{18}O$ values record a spring and (or) fall minimum temperature. This young of the year is interpreted as moving in or near a tributary (recorded as relatively low $\delta^{18}O$ values), permitting inference of juvenile migration to Lake Ontario (Fig. 6). For example, a temperature of 12 °C is calculated using a Salmon River tributary $\delta^{18}O_{(H_2O)}$ value of –10‰ VSMOW (Fig. 5). Age 1+, 2+, and 3+ represent pelagic residence in Lake Ontario. Converting $\delta^{18}O$ value to tempera-

© 2005 NRC Canada

Fig. 6. Example plots of intra-otolith $\delta^{18}O$ values and calculated temperatures (●) and $\delta^{13}C$ (○) values relative to VPDB from two chinook otoliths, one from specimen SAM92 from the archived group (*a*) and the other from specimen CHK23 from the Salmon River group (*b*). The temperature scale (inset on *y* axis) is calculated using a Lake Ontario $\delta^{18}O$ value of –6.8‰ VSMOW and Patterson et al.'s (1993) temperature–fractionation relationship for otolith aragonite of freshwater fish. Pelagic residence indicates the time the chinook spent in Lake Ontario proper. We modeled 2 full years of growth, indicated by the solid line. Chinook may also be Lake Ontario residents during the fall of their first year and just prior to spawning, indicated by the dotted lines. Otolith growth decreases or ceases in winter, so winter temperatures are not recorded. Only a minimum temperature just prior to cessation of otolith growth can be determined; this is noted on the plot. Assuming that otoliths grew during days above the minimum seasonal temperature calculated, the average resolution is 4 days per sample for specimen SAM92 and 14 days per sample for CHK23. The double horizontal lines mark 20 °C temperature.

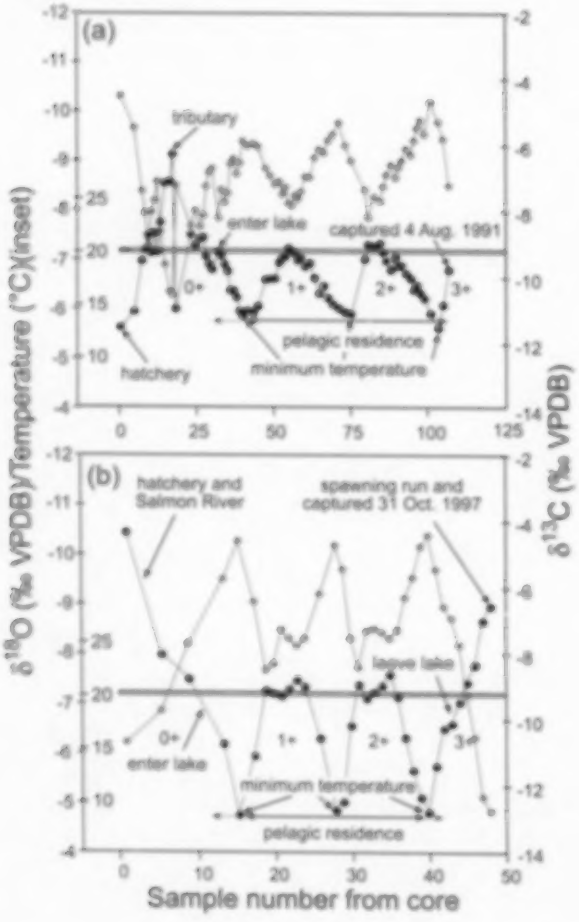

ture using the Lake Ontario $\delta^{18}O_{(H_2O)}$ value, we plot the thermal history of this fish from age 1+ to age 3+, when it was captured offshore on 18 August 1991 (Fig. 6*a*). Maximum seasonal temperatures are very near 20 °C, and remain stable just above 20 °C during year 2+, before decreasing. The temperature estimated nearest the time of capture was 18 °C, consistent with the season of capture. We estimate a resolution that averages less than 4 days per sample for this specimen, typical for specimens in this study.

CHK23 from the Salmon River group displays four seasonal cycles, indicating that this fish was also aged 3+ at the time of capture (Fig. 6*b*). Age 1+ and age 2+ display a similar pattern to the same age class for SAM92, and calculated midsummer temperatures appear to remain stable at 20 °C during this fish's pelagic residence. Lower $\delta^{18}O$ values in the first and last year of growth are representative of the lower $\delta^{18}O$ values of Salmon River water experienced in the hatchery and during the spawning migration, respectively (Fig. 5). We estimate a resolution of 14 days per sample, which is the lowest sample resolution in this study. Although intra-otolith $\delta^{18}O$ and $\delta^{13}C$ values agree with known life-history traits of chinook, this technique should be validated by using otoliths from fish fitted with archival tags that provide an independent measure of temperature.

Our otolith thermometry results indicate that adult chinook inhabit water with temperatures considerably higher than those they prefer (e.g., McCullough 1999). We estimate that chinook commonly occupied water at temperatures near 19 °C in midsummer. We also suggest that chinook are actively seeking water at this temperature through midsummer, as most pelagic-residence years for nearly all specimens with adequate resolution show evidence of a temperature plateau for at least 2 weeks. Because Lake Ontario stratifies in the summer and surface temperatures are often above 20 °C, chinook must occupy the epilimnion of Lake Ontario near to but not at the surface, even though the presumed optimal temperature for this species was always available near the thermocline. The highest mean alewife densities are found in the epilimnion (at temperatures above 17 °C), and the highest prey fish biomass is found near 20 °C (Mason et al. 1995). Therefore, it is likely that chinook must search epilimnetic water in Lake Ontario to find prey. It may be that as prey production has become limiting, chinook have had to search the warmer epilimnion more often for food, or it may be that chinook have always foraged here since they were first stocked. The absence of a strong alewife year class from 1992 to 1997, with year classes in 3 of these years amongst the smallest from 1977 to 1997, indicates that alewife numbers decreased after 1991 (e.g., Mills et al. 2003). However, we found no corresponding change in chinook thermal orientation over the same period of time.

We find very little difference between chinook maximum temperatures calculated for the archived group and Salmon River group, in contrast to our hypothesis that thermal orientation of the chinook would change with prey quality and quantity. Interestingly, Haynes and Keleher (1986) found one chinook in 19.7 °C water in the beginning of September as early as 1984. Although it was the only chinook (out of three) found at a temperature this high in the summer/fall, they were unable to closely track the other tagged fish during midsummer, owing to the methodology used (no fish were found in August). They assumed that this was due to chinook moving into deeper waters. However, they were only able to track fish near the shore, and the other chinook may have moved offshore. Our results appear to contradict other

© 2005 NRC Canada

reports of these fish being captured closer to the thermocline. Olson et al. (1988) found 82% of chinook above the thermocline and offshore, although they were vertically distributed widely and averaged 14.4 ± 2.9 °C at depths where they were captured using nets set overnight for 12–28 h. Using similar methods, Stewart and Robertson (1991) also found chinook at a similar median temperature, 13.2 °C, and did not capture chinook in 19 °C water. To calculate temperatures nearer to these observations, the Lake Ontario $\delta^{18}O_{(H_2O)}$ value must be 1.5‰ more negative than those we and others have measured.

A possible interpretation that would allow the results of these capture studies to be correlated with ours is that chinook migrate vertically to warmer water to catch prey, and then seek thermal refugia nearer the thermocline. To be consistent with this interpretation, otolith growth must be greatly reduced when chinook are not occupying warmer epilimnetic waters. Otolith growth has been highly correlated with metabolic rate (Wright 1991; Tohse and Mugiya 2002) and metabolic rate increases with temperature, indicating that there would be a bias toward higher temperature estimates. However, even with this bias, some carbonate accretion should occur while chinook inhabit water near the thermocline. Therefore, our temperature estimates suggest that chinook would experience near-lethal temperatures for limited periods if this vertical migration occurred.

Based on a literature review, McCullough (1999) concluded that 21–22 °C was the upper incipient lethal level for adult chinook. Although Bjorn and Reiser (1991) noted an upper incipient lethal level for adult chinook as high as 26.2 °C, they reported that environmental temperatures from 23 to 25 °C could be lethal and were actively avoided. Finally, Eaton et al. (1995) reported 23.7 °C as the upper habitat temperature limit for chinook. The remarkable consistency in minimum $\delta^{18}O$ values (maximum temperatures) for pelagic residence regardless of the group (where group members vary both with lake location and time), and the close agreement between maximum calculated temperatures and the chinook's upper incipient lethal limit, suggest that chinook in Lake Ontario are seeking alewife prey in water of temperatures as high as are tolerable. We found only 2 years out of a total of 22 where chinook were recorded at temperatures above 22 °C. Such exceedingly high temperature estimates may result if the fish entered waters with more negative $\delta^{18}O_{(H_2O)}$ values than those typical of the open lake, indicating that the true temperature experienced is less than that estimated. For example, the fish may have resided in a harbor or near a major tributary input to seek food. Forays into warm littoral habitats are likely to be uncommon because Lake Ontario has very little of such habitat outside the eastern basin and few small embayments (Mason et al. 1995). However, if chinook do migrate to littoral regions, they are still likely to encounter high water temperatures that are not optimal for growth.

Maximum seasonal $\delta^{18}O$ values (minimum temperatures) are considerably more variable. Interestingly, temperatures are often nearer the preferred temperature of chinook (McCullough 1999). It is tempting to speculate that chinook are moving to high-temperature waters in search of food for as long as can be tolerated, then moving into water at preferred temperatures, where body and otolith growth are reduced, so these are the minimum temperatures recorded via otolith thermometry. However, calculated temperatures may be elevated artificially by more negative and more variable $\delta^{18}O_{(H_2O)}$ values measured in the fall and spring (L.I. Wassenaar, National Hydrology Research Centre, Environment Canada, Saskatoon, SK S7N 3H5, Canada, personal communication). Finally, we note that mean midsummer temperatures for the archived and Salmon River groups are significantly different, although mean temperatures differed by just 0.4 °C. Although this "increased temperature" may be a reflection of ecological adaptation or environmental warming, the observed temperature difference might also be a result of slightly different mean $\delta^{18}O$ values for Lake Ontario. In fact, Hodell et al. (1998) reported a mean Lake Ontario $\delta^{18}O_{(H_2O)}$ value of –6.7‰ VSMOW for 1993–1995, while we measured a mean $\delta^{18}O_{(H_2O)}$ value of –6.9‰ VSMOW for 1998 and 2001. Mean calculated temperatures would be within 0.2 °C using Hodell et al.'s (1998) value for the archived group and our measured $\delta^{18}O_{(H_2O)}$ value for the Salmon River group. Regardless, such small differences are unlikely to be ecologically significant for chinook.

Adult chinook thermal histories determined from intra-otolith $\delta^{18}O$ values indicate that Lake Ontario's chinook population could be under energetic stress during midsummer. Bioenergetic modeling simulations predict severe growth reductions to near zero in midsummer, and slightly negative growth is predicted for chinook inhabiting water at 20 °C (unpublished data). GCE is also reduced during midsummer, providing further evidence of stress. Corresponding to reduced GCE, total annual consumption by chinook is estimated to be up to 20% higher in the otolith thermometry simulation relative to the nominal simulation. This growth stress is corroborated by an observed decrease in condition factor in chinook captured by anglers (Fig. 7*a*). Additionally, summer stress marks are often observed in chinook scales and otoliths. Summer stress marks on chinook scales from Lake Ontario preclude accurate aging, and otolith or fish length is used instead (J.N. Bowlby and T.J. Stewart, Ontario Ministry of Natural Resources, Glenora Fisheries Station, Picton, unpublished data). Many otoliths from Lake Ontario chinook show summer growth checks, opaque regions in the otolith that are less distinct than opaque regions associated with winter growth checks (Fig. 7*b*).

There is recent evidence that modeled respiration, a key component of the bioenergetic model, is in error (Trudel et al. 2004). Specifically, the model we used (Stewart and Ibarra 1991) underestimates respiration at lower ranges and overestimates it at higher ranges with a total mean-squared error of 0.18 (Trudel et al. 2004). However, this bioenergetic model can still be used to compare estimates on a relative basis and to contrast the outcome of various scenarios if the biases are consistent (Trudel et al. 2004). We compare two model outputs, changing the temperature input only, thus fulfilling this requirement. In addition, growth and consumption obtained from model-output and field studies of Lake Ontario chinook agree (Rand and Stewart 1998*a*), and midsummer stress predicted by our bioenergetic analysis is corroborated by observed condition factor and by otolith and scale stress marks (Fig. 7).

Rand and Stewart (1998*b*) suggested that the limit to salmonine production in this ecosystem is being approached. GCE has been trending downward in Lake Ontario, owing to

© 2005 NRC Canada

Fig. 7. (*a*) Monthly trend in body condition determined as the mean weight of a 600 mm long chinook after adjusting for differences in length and year using analysis of covariance at 95% confidence intervals. Fork length and wet weight of chinook were measured during angler surveys in 1988–1992 (n = 2468). (*b*) Image of a chinook otolith (specimen SAM12; this study) showing summer and winter check marks. Summer check marks, induced by stress, are opaque regions in the otolith that are less distinct than opaque regions associated with winter growth checks. It should be noted that this section is used for micromilling and not aging.

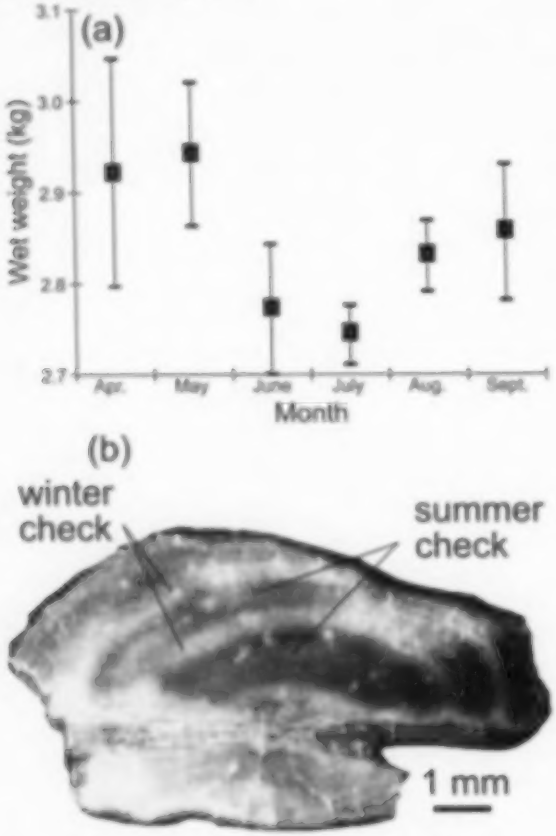

a reduction in prey quality. Rand et al. (1994) and Rand and Stewart (1998*b*) concluded that the chinook population might not have been sustainable at 1990 stocking rates because of declines in alewife population and quality. These conclusions were based on a bioenergetic analysis using assumptions about the thermal orientation of chinook that we determined to be inaccurate. We find adult chinook to be consuming more and growing less in midsummer than was previously modeled.

Intra-otolith $\delta^{13}C$ value and metabolic rate

Biological carbonates appear to derive carbon from two major sources: DIC from environmental water and blood carbon derived from the diet (e.g., McConnaughey et al. 1997). These two major pools of carbon are therefore reflected in the $\delta^{13}C$ value of the otolith (e.g., Høie et al. 2003). Tohse and Mugiya (2002) demonstrated, via radiocarbon labeling, both an ambient-water and a dietary carbon contribution in fish otoliths, the ratio of which was linked to metabolic activity. Although DIC is often the dominant source of otolith carbon (e.g., McConnaughey et al. 1997), intra-otolith variation in the $\delta^{13}C$ value might reflect changes in contributions between the two sources; this changing ratio is predominantly a result of a changing metabolic rate in the individual fish (Wurster and Patterson 2003; Høie et al. 2004*b*). This observation should hold true especially for fish, such as chinook, that do not change their diet greatly during pelagic residence (e.g., Brandt 1986; Rand and Stewart 1998*a*; Lantry 2001).

Chinook otolith $\delta^{13}C$ values display seasonal variability, with higher values during spring/fall and lower values in midsummer. This pattern is highlighted by a relatively strong covariation with $\delta^{18}O$ values, and is consistent with the metabolic-contribution hypothesis. Higher temperatures (lower $\delta^{18}O$ values) lead to a higher metabolic rate and a greater contribution of respiratory carbon to the otolith (and therefore lower $\delta^{13}C$ values relative to DIC). In contrast to intra-otolith $\delta^{18}O$ values, $\delta^{13}C$ values of individual otoliths are quite variable. The highest $\delta^{13}C$ values are approximately –4‰ to –5‰ VPDB, whereas lower values are approximately –8‰ to –10‰, with one specimen as low as –12‰. We estimate a summer metabolic contribution to otolith carbon as high as 50%–60% assuming a dietary $\delta^{13}C$ value of –25‰ VPDB (Kiriluk et al. 1995) and a $\delta^{13}C_{(DIC)}$ value of 0‰ VPDB (Hodell et al. 1998; Leggett et al. 1999; Hélie et al. 2002). Despite the individual variability in intra-otolith $\delta^{13}C$ values, we find least-squares regressions between seasonal pelagic-residence temperatures and $\delta^{13}C$ values not significantly different among archived (α = 0.05, $F_{[5,297]}$ = 1.59; ignoring SAM84) and Salmon River (α = 0.05, $F_{[5,184]}$ = 2.14) specimens and groups (α = 0.05, $F_{[1,529]}$ = 2.72). This suggests that although individual chinook may vary in activity, they respond similarly to temperature changes given a similar environment.

The environmental $\delta^{13}C_{(DIC)}$ value appears to have the largest modifying influence on intra-otolith $\delta^{13}C$ values because it represents the largest proportion of otolith carbon. Tributary $\delta^{13}C_{(DIC)}$ values are much lower than Lake Ontario values (e.g., Leggett et al. 1999; Hélie et al. 2002) and this is recorded by otolith $\delta^{13}C$ values, even during the spawning run, when dietary $\delta^{13}C$ values are derived from reserves stored during pelagic residence. In many cases, variation in intra-otolith $\delta^{13}C$ and $\delta^{18}O$ values can be used to infer when chinook migrate between Lake Ontario and tributaries (Fig. 6), although this should be corroborated using growth models. Therefore, seasonal changes in Lake Ontario $\delta^{13}C_{(DIC)}$ values and variation in habitat depth (e.g., Legget et al. 1999) may influence $\delta^{13}C$ values of chinook otoliths.

The diet of chinook in Lake Ontario varies little during pelagic residence (Brandt 1986; Rand and Stewart 1998*b*; Lantry 2001), and during the summer, $\delta^{13}C_{(DIC)}$ values in the epilimnion increase because of preferential incorporation of ^{12}C by phytoplankton, whereas values in the hypolimnion remain invariant (e.g., Leggett et al. 1999). However, $\delta^{13}C_{(otolith)}$ values decrease during the summer, suggesting an increasing influence of dietary carbon, with lower $\delta^{13}C$ values, over more positive $\delta^{13}C_{(DIC)}$ values. We therefore conclude that

© 2005 NRC Canada

Table 3. Estimates of metabolic contribution to otolith carbon made using a simple mass balance model.

	$\delta^{13}C$ (‰)		$\delta^{13}C_{(DIC)}$ (‰)		*M*	
	Otolith	Diet	Epilimnion	Hypolimnion	Epilimnion	Hypolimnion
Salmon River group						
Summer	–7.9	–25.2	–0.6	–2.5	0.41	0.36
Fall/spring	–5.3	–25.2	*	–2.5	*	0.24
Archived group						
Summer	–8.7	–25.2	–0.6	–2.5	0.44	0.39
Fall/spring	–6	–25.2	*	–2.5	*	0.27

Note: Metabolic contribution to otolith carbon is calculated using a model described by Wurster and Patterson (2003): $\delta^{13}C_{(otolith)} = M\delta^{13}C_{(diet)} + (1 - M)\delta^{13}C_{(DIC)} + 2.7$, where *M* is the proportional metabolic contribution. The $\delta^{13}C$ value of the dissolved inorganic carbon (DIC) is estimated for the epilimnion and hypolimnion and fall/spring (same as the hypolimnion) from Leggett et al. (1999). The $\delta^{13}C$ values for alewife (*Alosa pseudoharengus*) and rainbow smelt (*Osmerus mordax*) reported in Kiriluk et al. (1995) were used in conjunction with dietary estimates to determine average $\delta^{13}C$ values for the chinook (*Oncorhynchus tshawytscha*) diet (*, no estimate).

intra-otolith $\delta^{13}C$ values are primarily influenced by a changing metabolic rate, as further evidenced by a strong and similar covariation with estimated temperature and corroborated by a covariation with the modeled specific respiration rate. A direct temperature effect of biogenic carbonates on $\delta^{13}C$ values is equivocal (e.g., Thorrold et al. 1997; Schwarcz et al. 1998) and, if it exists, is small (approximately –1.3‰ VPDB for a temperature increase of 10 °C (Grossman and Ku 1986).

We estimated various metabolic contributions assuming different depth habitats or varying $\delta^{13}C_{(DIC)}$ values (Table 3). It is important to note that $\delta^{13}C$ values vary greatly among individuals; on average, however, summer $\delta^{13}C$ values for the archived group are almost 0.8‰ more negative than those for the Salmon River group. This corresponds to an additional 3% metabolic contribution to the otolith carbon of the archived group. An alternative explanation is that chinook inhabited the hypolimnion more often in the late 1980s and early 1990s than in the mid-1990s (Table 3). This, however, contrasts with our contention that chinook are feeding in the epilimnion, inferred from $\delta^{18}O$ values.

This study clearly demonstrates the need for detailed laboratory studies to determine the relationship between metabolic rate, diet, and intra-otolith $\delta^{13}C$ values. However, we hope that we have demonstrated that $\delta^{13}C$ can be used to determine metabolic rate "in the field", and perhaps can be used as an additional proxy with which to infer vertical distributions of fish within a water column. Alternatively, if metabolic rate can be accurately modeled and the environmental $\delta^{13}C_{(DIC)}$ value is known, it may be possible to estimate diet changes in longer lived fish.

Acknowledgments

We express our appreciation for comments, suggestions, and useful discussions from E. Dufour, J. Catterall, A. Zazzo, H. Foster, and two anonymous reviewers. We especially thank Ji He, P. Arnold, M. Cheatham, and T. Prokopiuk, who provided technical assistance. This research was funded by National Oceanic and Atmospheric Administration (NOAA) award NA86RG0056 to the Research Foundation of the State University of New York for New York Sea Grant and a Sea Grant Scholarship award. The US Government is authorized to produce and distribute reprints for government purposes notwithstanding any copyright notation that may appear hereon. The views expressed herein are those of the authors and do not necessarily reflect the views of NOAA or any of its subagencies.

References

Bjorn, T.C., and Reiser, D.W. 1991. Influences of forest and rangeland management on salmonid fishes and their habitats. Am. Fish. Soc. Spec. Publ. No. 19. pp. 83–138.

Brandt, S.B. 1986. Food of salmon and trout in Lake Ontario. J. Gt. Lakes Res. **12**: 200–205.

Campana, S.E. 1999. Chemistry and composition of fish otoliths: pathways, mechanisms and applications. Mar. Ecol. Prog. Ser. **188**: 263–297.

Coplen, T.B., and Kendall, C. 2000. Stable hydrogen and oxygen isotope ratios for selected sites of the U.S. Geological Survey's NASQAN and Benchmark Surface-water networks. US Geological Survey Open-File Rep. 00-160.

Degens, E.T., Deuser, W.G., and Haedrich, R.L. 1969. Molecular structure and composition of fish otoliths. Mar. Biol. (Berl.), **2**: 105–113.

Eaton, J.G., McCormick, J.H., Goodno, B.E., O'Brien, D.G., Stefan, H.G., Hondzo, M., and Scheller, R.M. 1995. A field information-based system for estimating fish temperature tolerances. Fisheries (Bethesda), **20**: 10–18.

Elrod, J.H., and O'Gorman, R. 1991. Diet of juvenile lake trout in southern Lake Ontario in relation to abundance and size of prey fishes, 1979–1987. Trans. Am. Fish. Soc. **120**: 290–302.

Gat, J.R., Bowser, C.J., and Kendall, C. 1994. The contribution of evaporation from the Great Lakes to the continental atmosphere: estimate based on stable isotope data. Geophys. Res. Lett. **21**: 557–560.

Goyke, A.P., and Brandt, S.B. 1993. Spatial models of salmonine growth rates in Lake Ontario. Trans. Am. Fish. Soc. **122**: 870–883.

Grossman, E.L., and Ku, T.L. 1986. Oxygen and carbon isotope fractionation in biogenic aragonite: temperature effects. Chem. Geol. **59**: 59–74.

Hanson, P.C., Johnson, T.B., Schindler, D.E., and Kitchell, J.F. 1997. Fish bioenergetics 3.0. University of Wisconsin, Sea Grant Institute, Madison. Tech. Rep. WISCU-T-97-001.

Hartig, J.H., Kitchell, J.F., Scavia, D., and Brandt, S.B. 1991. Rehabilitation of Lake Ontario: the role of nutrient reduction and food web dynamics. Can. J. Fish. Aquat. Sci. **48**: 1574–1580.

© 2005 NRC Canada

Haynes, J.M., and Kelcher, C.J. 1986. Movements of Pacific salmon in Lake Ontario in spring and summer: evidence for wide dispersal. J. Freshw. Ecol. **3**: 289–297.

He, J., and Stewart, D.J. 1998. Ontogeny of energetic relationships and potential effects of tissue turnover: a comparative modeling study on lake trout. Can. J. Fish. Aquat. Sci. **55**: 2518–2532.

Hélie, J.-F., Hillaire-Marcel, C., and Rondeau, B. 2002. Seasonal changes in the sources and fluxes of dissolved inorganic carbon through the St. Lawrence River — isotopic and chemical constraint. Chem. Geol. **186**: 117–138.

Hodell, D.A., Schelske, C.L., Fahnenstiel, G.L., and Robbins, L.L. 1998. Biologically induced calcite and its isotopic composition in Lake Ontario. Limnol. Oceanogr. **43**: 187–199.

Høie, H., Folkvord, A., and Otterlei, E. 2003. Effect of somatic and otolith growth rate on stable isotopic composition of early juvenile cod (*Gadus morhua* L.). otoliths. J. Exp. Mar. Biol. Ecol. **289**: 41–58.

Høie, H., Otterlei, E., and Folkvord, A. 2004*a*. Temperature-dependant fractionation of stable oxygen isotopes in otoliths of juvenile cod (*Gadus morhua* L.). ICES J. Mar. Sci. **61**: 243–251.

Høie, H., Andersson, C., Folkvord, A., and Karlsø, Ø. 2004*b*. Precision and accuracy of stable isotope signals in otoliths of pen-reared cod (*Gadus morhua*) when sampled with a high-resolution micromill. Mar. Biol. (Berl.), **144**: 1039–1049.

Johengen, T.H., Johannsson, O.E., Pernie, G.L., and Millard, E.S. 1994. Temporal and seasonal trends in nutrient dynamics and biomass measures in Lakes Michigan and Ontario in response to phosphorus control. Can. J. Fish. Aquat. Sci. **51**: 2570–2578.

Jones, M.L., Koonce, J.F., and O'Gorman, R. 1993. Sustainability of hatchery-dependent salmonine fisheries in Lake Ontario: the conflict between predator demand and prey supply. Trans. Am. Fish. Soc. **122**: 1002–1018.

Kalish, J.M. 1991. ^{13}C and ^{18}O isotopic disequilibria in fish otoliths: metabolic and kinetic effects. Mar. Ecol. Prog. Ser. **75**: 191–203.

Kim, S.T., and O'Neil, J.R. 1997. Equilibrium and nonequilibrium oxygen isotope effects in synthetic carbonates. Geochim. Cosmochim. Acta, **61**: 3461–3475.

Kiriluk, R.M., Servos, M.R., Whittle, D.M., Cabana, G., and Rasmussen, J.B. 1995. Using ratios of stable nitrogen and carbon isotopes to characterize the biomagnification of DDE, mirex, and PCB in a Lake Ontario pelagic food web. Can. J. Fish. Aquat. Sci. **52**: 2660–2674.

Lantry, J.R. 2001. Spatial and temporal dynamics of predation by Lake Ontario trout and salmon. M.S. thesis, College of Environmental Science and Forestry, State University of New York, Syracuse.

Leggett, M.F., Servos, M.R., Hesslein, R., Johannsson, O., Millard, E.S., and Dixon, D.G. 1999. Biogeochemical influences on the carbon isotope signatures of Lake Ontario biota. Can. J. Fish. Aquat. Sci. **56**: 2211–2218.

Mason, D.M., Goyke, A., and Brandt, S.B. 1995. A spatially explicit bioenergetics measure of habitat quality for adult salmonines: comparison between Lakes Michigan and Ontario. Can. J. Fish. Aquat. Sci. **52**: 1572–1583.

McConnaughey, T.A., Burdett, J., Whelan, J.F., and Paull, C.K. 1997. Carbon isotopes in biological carbonates: respiration and photosynthesis. Geochim. Cosmochim. Acta, **61**: 611–622.

McCullough, D.A. 1999. A review and synthesis of effects of alterations to the water temperature regime on freshwater life stages of salmonids, with special reference to chinook salmon. US Environmental Protection Agency, Seattle, Wash. USEPA Rep. 910-R-00-010.

Mills, E.L., Casselman, J.M., Dermott, R., Fitzsimons, J.D., Gal, G., Holeck, K.T., et al. 2003. Lake Ontario: food web dynamics in a changing ecosystem (1970–2000). Can. J. Fish. Aquat. Sci. **60**: 471–490.

O'Gorman, R., and Stewart, T.J. 1999. Ascent, dominance, and decline of the alewife in the Great Lakes: food web interactions and management strategies. *In* Great Lakes fisheries policy and management: a binational perspective. *Edited by* W.W. Taylor and C.P. Ferreri. Michigan State University Press, East Lansing. pp. 489–514.

Olson, R.A., Winter, J.D., Nettles, D.C., and Haynes, J.M. 1988. Resource partitioning in summer by salmonids in south-central Lake Ontario. Trans. Am. Fish. Soc. **117**: 552–559.

Panella, G. 1980. Growth patterns in fish sagittae. *In* Skeletal growth of aquatic organisms. *Edited by* D.C. Rhodes and R.A. Lutz. Plenum Press, New York. pp. 519–560.

Patterson, W.P., Smith, G.R., and Lohmann, K.C. 1993. Continental paleothermometry and seasonality using the isotopic composition of aragonitic otoliths of freshwater fishes. *In* Continental climate change from isotopic records. *Edited by* P.A. Swart, K.C. Lohmann, J. McKenzie, and S. Savin. Monogr. No. 78, American Geophysical Union, Washington, D.C. pp. 191–202.

Radtke, R.L., Showers, W., Moksness, E., and Lenz, P. 1996. Environmental information stored in otoliths: insights from stable isotopes. Mar. Biol. (Berl.), **127**: 161–170.

Rand, P.S., and Stewart, D.J. 1998*a*. Dynamics of salmonine diets and foraging in Lake Ontario, 1983–1993: a test of a bioenergetic model prediction. Can. J. Fish. Aquat. Sci. **55**: 307–317.

Rand, P.S., and Stewart, D.J. 1998*b*. Prey fish exploitation, salmonine production, and pelagic food web efficiency in Lake Ontario. Can. J. Fish. Aquat. Sci. **55**: 318–327.

Rand, P.S., Stewart, D.J., Seelbach, P.W., Jones, M.L., and Wedge, L.R. 1993. Modeling steelhead population energetics in Lakes Michigan and Ontario. Trans. Am. Fish. Soc. **122**: 977–1001.

Rand, P.S., Lantry, B.F., O'Gorman, R., Owens, R.W., and Stewart, D.J. 1994. Energy density and size of pelagic prey fishes in Lake Ontario: implications for salmonine energetics. Trans. Am. Fish. Soc. **123**: 519–534.

Rowan, D.J., and Rasmussen, J.B. 1996. Measuring the bioenergetic cost of fish activity in situ using a globally dispersed radiotracer (^{137}Cs). Can. J. Fish. Aquat. Sci. **54**: 734–745.

Schwarcz, H.P., Gao, Y., Campana, S., Browne, D., Knyf, M., and Brand, U. 1998. Stable carbon isotope variations in otoliths of Atlantic cod (*Gadus morhua*). Can. J. Fish. Aquat. Sci. **55**: 1798–1806.

Sherwood, G.D., and Rose, G.A. 2003. Influence of swimming form on otolith $\delta^{13}C$ in marine fish. Mar. Ecol. Prog. Ser. **258**: 283–289.

Stewart, D.J., and Ibarra, M. 1991. Predation and production by salmonine fishes in Lake Michigan, 1978–1988. Can. J. Fish. Aquat. Sci. **48**: 909–922.

Stewart, T.J., and Robertson, D.G. 1991. Lake Ontario temperature studies. 1990 annual report, LOA 91.1 20, Lake Ontario Fisheries Unit, Ontario Ministry of Natural Resources, Picton, Ontario. pp. 1–5.

Stewart, T.J., Bowlby, J.N., Rawson, M., and Eckert, T.H. 2003. The recreational boat fishery for salmonids in Lake Ontario 1985–1995. *In* State of Lake Ontario: past, present and future. *Edited by* M. Munawar. Aquatic Ecosystem Health and Management Society and Goodword Books Pvt. Ltd., New Delhi. pp. 517–537.

Talhelm, D.R. 1988. Economics of Great Lakes fisheries: a 1985 assessment. Gt. Lakes Fish. Comm. Tech. Rep. No. 54.

© 2005 NRC Canada

Thorrold, S.R., and Hare, J.A. 2002. Otolith applications in reef fish ecology. *In* Coral reef fishes: dynamics and diversity in a complex ecosystem. *Edited by* P.F. Sale. Academic Press, London. pp. 243–264.

Thorrold, S.R., Campana, S.E., Jones, C.M., and Swart, P.K. 1997. Factors determining ^{13}C and ^{18}O fractionation in aragonitic otoliths of marine fish. Geochim. Cosmochim. Acta, **61**: 2909–2919.

Tohse, H., and Mugiya, Y. 2002. Diel variations in carbonate incorporation into otoliths in goldfish. J. Fish Biol. **61**: 199–206.

Trudel, M., Geist, D.R., and Welch, D.W. 2004. Modeling the oxygen consumption rates in Pacific salmon and steelhead: an assessment of current models and practices. Trans. Am. Fish. Soc. **133**: 326–348.

Wright, P.J. 1991. The influence of metabolic rate on otolith increment width in Atlantic salmon parr, *Salmo salar* L. J. Fish Biol. **38**: 929–933.

Wurster, C.M., and Patterson, W.P. 2003. Metabolic rate of late Holocene freshwater fish: evidence from $\delta^{13}C$ values of otoliths. Paleobiology, **29**: 492–505.

Wurster, C.M., Patterson, W.P., and Cheatham, M.M. 1999. Advances in micromilling techniques: a new apparatus for acquiring high-resolution oxygen and carbon stable isotope values and major/minor elemental ratios from accretionary carbonate. Comput. Geosci. **25**: 1155–1162.

Yang, C., Telmer, K., and Viezer, J. 1996. Chemical dynamics of the St. Lawrence riverine system: $\delta^{18}D_{(H_2O)}$, $\delta^{18}O_{(H_2O)}$, $\delta^{13}C_{(DIC)}$, $\delta^{34}S_{(sulfate)}$, and dissolved $^{87}Sr/^{86}Sr$. Geochim. Cosmochim. Acta, **59**: 1107–1146.

© 2005 NRC Canada

Spatial and temporal gradients in artisanal fisheries of a large Neotropical reservoir, the Itaipu Reservoir, Brazil

Edson Kiyoshi Okada, Angelo Antonio Agostinho, and Luiz Carlos Gomes

Abstract: Physical, chemical, and biological gradients along reservoirs are clear and exhibit marked spatial and temporal variations. These variations are rarely quantified and may produce spatial gradients in fisheries. We analyzed trends in total yield and gradients and relationships between catch-per-unit-effort (CPUE) and some characteristics of the fishery in the large Neotropical Itaipu Reservoir in Brazil. Data on the artisanal fisheries were collected over an 11-year period (414 213 daily trips). Annual yield (especially after 1993) and CPUE (annual total and for each species) decreased over the studied period. A clear longitudinal pattern in the CPUE values for the main species was recognized, and this pattern presented a significant relationship with the type of gear and characteristics of the vessels used in the fisheries. The decline in yield and CPUE is apparently due to changes in trophic state, as well as to the construction of reservoirs upstream from the region and to overfishing. It is clear that the spatial zonation influenced fish species distribution along the reservoir and, therefore, the fishery. We conclude that for this large Neotropical reservoir, spatial gradient cannot be ignored in management plans, and this appears to be true for any reservoir that exhibits zonation.

Résumé : Il y a des gradients physiques, chimiques et biologiques bien marqués le long des réservoirs et ils présentent de nettes variations dans l'espace et dans le temps. Ces variations sont rarement mesurées quantitativement, bien qu'elles puissent produire des gradients spatiaux dans les pêches. Nous avons analysé les tendances du rendement total et des gradients, ainsi que les relations entre la capture par unité d'effort (CPUE) et quelques caractéristiques de la pêche dans le grand réservoir néotropical Itaipu (Brésil). Les statistiques sur les pêches artisanales ont été compilées sur une période de onze années (414 213 sorties journalières). Le rendement annuel (surtout après 1993) et la CPUE (totale annuelle et spécifique à chaque espèce) ont décliné au cours de la période d'étude. Il existe un net patron longitudinal de CPUE des espèces principales qui est en corrélation significative avec le type d'engin de pêche et les caractéristiques des bateaux utilisés pour la pêche. Le déclin du rendement et de CPUE est apparemment dû à des changements d'état trophique, mais aussi à la construction de réservoirs en amont et à la surpêche. Il est clair que la zonation spatiale influence la répartition des poissons le long du réservoir et, par conséquent, la pêche. En conclusion, on ne peut négliger le gradient spatial dans les plans d'aménagement de ce grand réservoir néotropical; la même contrainte s'impose à tout réservoir qui présente de la zonation.

[Traduit par la Rédaction]

Introduction

Reservoirs are intermediary systems between rivers and natural lakes, the processes in which can be considered more complex and variable. Temporal and spatial variations in water flow through reservoirs can alter, for example, the predominant direction of the axis around which the processes are organized, passing from the vertical (as in lakes) to the horizontal (as in rivers) and vice versa (Noble 1980). In addition to flow, basin morphometry, circulation pattern, hydraulic retention time, and dam design and operation have a notable influence on the nature, intensity, and duration of the physical and chemical gradients in reservoirs, affecting the structure and dynamics of their biotic communities (Tundisi 1993).

Thornton et al. (1981) described three main zones along a reservoir continuum: the fluvial (including the delta region), transition, and lacustrine zones. These zones can be identified by the sedimentation rate, and their extent is strongly related to the inflow of water and hydraulic retention time. Physical and chemical gradients such as sedimentation rates (Thornton 1990; Pagioro and Thomaz 2002), nutrient concentrations (Tundisi et al. 1988; Kennedy and Walker 1990; Thomaz et al. 1997), and factors related to primary production (Brylinsky and Mann 1973; Hoyer and Jones 1983; Kimmel et al. 1990) have been considered determinants of spatial- and temporal-variation patterns in fish communities (O'Brien 1990; Agostinho et al. 1999*a*) and other communi-

Received 2 December 2003. Accepted 21 October 2004. Published on the NRC Research Press Web site at http://cjfas.nrc.ca on 18 April 2005.
J17867

E.K. Okada,[1] A.A. Agostinho, and L.C. Gomes. Núcleo de Pesquisa em Limnologia, Ictiologia e Aquicultura (Nupélia), Universidade Estadual de Maringá, Avenida Colombo, 5790, 87020-900 Maringá, Paraná, Brazil.

[1]Corresponding author (e-mail: edsonko@nupelia.uem.br).

 doi: 10.1139/F05-015 © 2005 NRC Canada

ties (Marzolf 1990; Bini 1997; Nakamoto et al. 1997). Although biotic and abiotic gradients along reservoirs are clear and exhibit marked spatial and temporal variations (Thornton et al. 1990; Gido and Matthews 2000), they are rarely quantified and considered in fishery-management plans.

Spatial and temporal patterns of abiotic or biotic variables verified in reservoirs are expected to influence spatial gradients in fishing systems, including operational fishing strategies, yield, species composition, investments, and profitability. However, the role of spatial gradients has not been explored. Thus, recognition of these patterns and their variations (spatial and temporal) has the potential to support management of fishing resources.

In this study, artisanal-fishery landing data obtained along a large Neotropical reservoir (Itaipu Reservoir) during an 11-year period are analyzed for relationships between catches of the main species and the operational strategies of the fishery along the longitudinal axis of the reservoir. Specifically, the following questions were addressed. (*i*) How do species yields vary temporally (annually) and spatially (along the zones of the reservoir)? (*ii*) Does a relationship exist between yield and the type of gear and the characteristics of the vessels used in the fisheries along the reservoir?

Material and methods

Study area

Itaipu Reservoir, formed in October 1982, is located on the Brazil–Paraguay border, extending for approximately 170 km between 24°05′ and 25°33′S and 54°00′ and 54°37′W. It has a surface area of 1350 km^2 and a basin area of approximately 820 000 km^2. Its average depth is 22 m, reaching 170 m near the dam. Average hydraulic retention is 40 days; however, retention is only 29 days in the main channel. The reservoir was divided into 12 fishing areas (main landing points): (1) Guaíra, (2) Guaíra and vicinity, (3) Oliveira Castro, (4) Arroio Guaçu, (5) Porto Mendes, (6) Pato Bragado, (7) Entre Rios, (8) Santa Helena, (9) Missal, (10) Itaipulândia, (11) São Miguel do Iguaçu, and (12) Santa Terezinha de Itaipu (Fig. 1).

Data collection and analyses

Fishing in Itaipu Reservoir was prohibited for the first 28 months after its formation, and started officially in March 1985. Recording of landings began 2 years later, in January 1987, and continued through December 1998 (except in 1994 (grant interruption)). Reservoir landings (daily catches) from the artisanal fishery were monitored for each species and each fisher, providing a data set of 414 213 daily trips. The information was obtained by a collection network consisting of local people (with experience in the fishery) and organizations, such as fishing associations. Fishing effort was represented by the number of days (trips) fished, expressed at the specific level for each fishery area. Yield was presented as CPUE (kg·fisher^{-1}·day^{-1}).

Firstly, we characterized the fishery at Itaipu Reservoir in terms of changes in total yield (tons (t)) and CPUE along the years studied and of the species that contributed most to the landings (90% of the total). Secondly, we examined the adequacy of the zonation (fluvial, transition, and lacustrine zones) described by Pagioro and Thomaz (2002) for the fishery conducted at Itaipu Reservoir. To achieve this, we used a multivariate analysis technique to reduce data dimensionality, and then, using detrended correspondence analysis (DCA), summarized the longitudinal gradient of yield based on the CPUE values of only the species that contributed to 90% of the landings because rare species may have a disproportionate influence on DCA results (Palmer 1993). Axes with eigenvalues above 0.20 were retained for interpretation (ter Braak and Šmilauer 1998). Axis sample scores for each fishing area were retained for interpretation and plotted against the sedimentation rates found by Pagioro and Thomaz (2002) along the reservoir. A Spearman's rank correlation (r_S) was then used to test the adequacy of the zones, i.e., the association between the sedimentation rates and scores of the DCA axes retained for interpretation, which in turn synthesized the variations in yield of the main species.

To evaluate spatial and temporal variations in the CPUE values for the main species along the longitudinal axes of the reservoir, fishing areas were grouped into the previously identified zones (fluvial, transition, and lacustrine), and two-way analyses of variance (ANOVAs) were applied using zone and year as factors. As several ANOVAs were applied (most abundant species), we used the protected ANOVA protocol to minimize Type I error (Scheiner 1993). In accordance with this protocol, a two-way multivariate analysis of variance (MANOVA) was applied considering the main species before the ANOVAs. If the MANOVA is significant, then ANOVAs can be applied (for each species separately). CPUE values were log-transformed (log(CPUE + 1)) to meet assumptions of the tests.

During the sampling period, information related to type of gear (operational fishing strategy) and vessel used was collected. Information related to gear type consisted of the number of fishers that used gillnets, long lines, cast nets, and other gear (e.g., a hook and line attached to a float, set near macrophyte stands, like a jug line, locally named espera, used to catch mainly the traíra (*Hoplias malabaricus*), and similar gear, but with larger hooks, that drifts in the reservoirs, locally named cavalinho, which targets the barbado (*Pinirampus pirinampu*)). Vessel characteristics included paddle, stationary (center) engine (10–12.5 h.p. (1 h.p. = 746 W)), outboard engine, and "rabeta" engine (3.5–4.5 h.p.). These data, obtained for each fishery area, were log-transformed (log(x + 1)) and analyzed using principal components analysis (PCA) to reduce dimensionality. Axes that presented eigenvalues greater than those produced by the randomness hypothesis of the broken-stick model were retained for interpretation (Jackson 1993). Pearson's correlations (r) were determined between the DCA and PCA axes retained for interpretation to evaluate the relationship between main-species yields and the types of gear and vessel characteristics.

Results

Temporal variations in the fishery

Annual yield from 1987 to 1998 fluctuated between 1727 t (1989) and 1192 t (1998), remaining almost constant from 1987 to 1993. The average CPUE values, high in the initial years of exploitation (e.g., 21.7 kg·fisher^{-1}·day^{-1} in 1987), decreased over time, with values of 15.5 kg·fisher^{-1}·day^{-1}

© 2005 NRC Canada

Fig. 1. Map of Itaipu Reservoir (Brazil–Paraguay border) showing the longitudinal gradient (fluvial, transition, and lacustrine zones) and fishery areas.

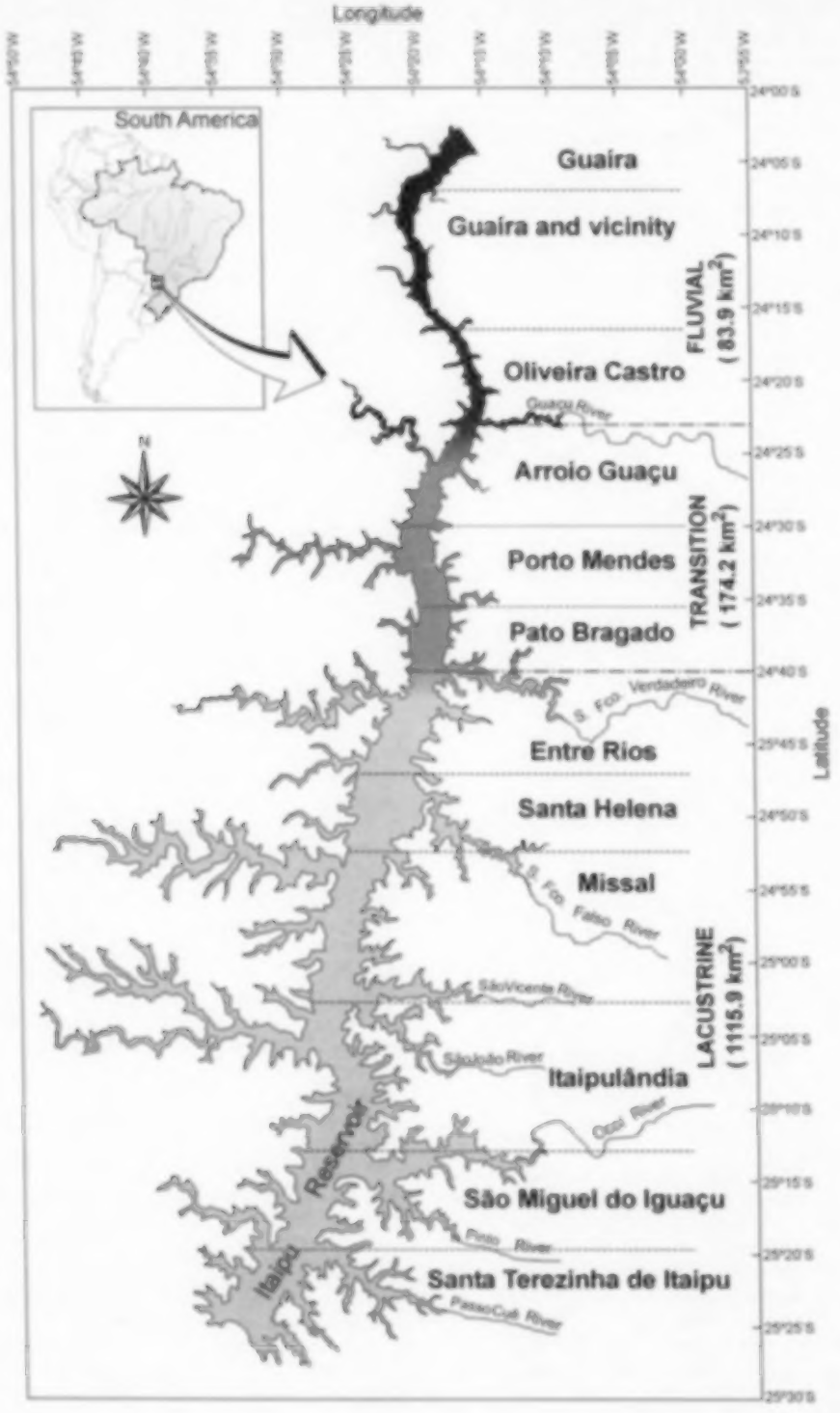

© 2005 NRC Canada

Fig. 2. Temporal variations in (*a*) catch-per-unit-effort (CPUE) in the artisanal fishery of Itaipu Reservoir (vertical lines represent standard error) and (*b*) total annual yield in tons (t).

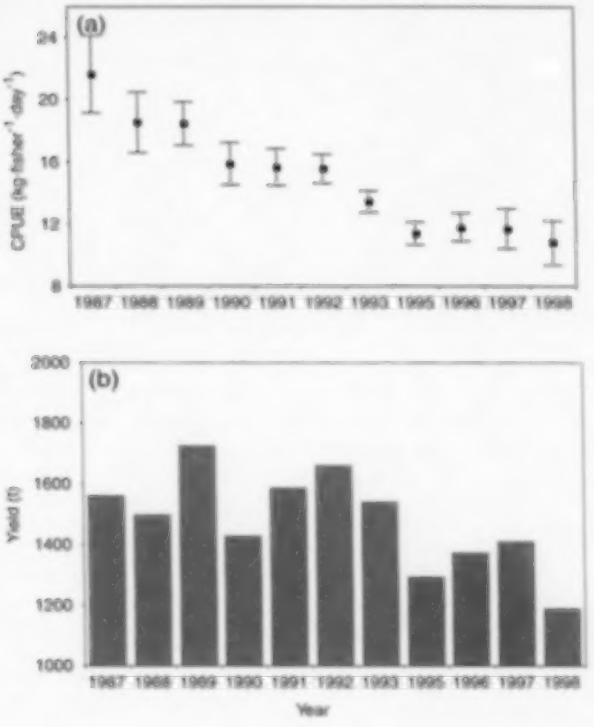

Fig. 3. Scatterplot of detrended correspondence analysis axis 1 (DCA1) scores applied to CPUE values for the 10 main species in the artisanal fishery landings and the sedimentation rates along Itaipu Reservoir (■, fluvial zone; +, transition zone; ●, lacustrine zone; ◇, sedimentation rate). Spearman's $r = 0.77$, $P = 0.0034$, $n = 12$. DW, dry weight.

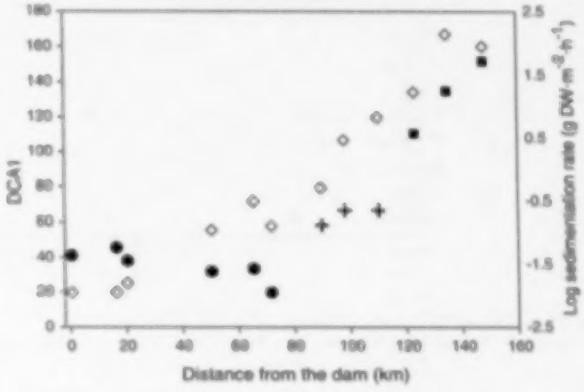

from 1990 to 1992 and about 11.5 kg·fisher^{-1}·day^{-1} from 1995 to 1998 (Fig. 2). The main species caught in the artisanal fishery during the period, in order of decreasing abundance, were perna-de-moça (*Hypophthalmus edentatus*), armado (*Pterodoras granulosus*), curvina (*Plagioscion squamosissimus*), curimba (*Prochilodus lineatus*), mandi (*Pimelodus maculatus*), mandi-prata (*Iheringichthys labrosus*), cascudo-preto (*Rhinelepis aspera*), *P. pirinampu*, *H. malabaricus*, and jaú (*Paulicea luetkeni*), which together composed approximately 90% of the landings.

Spatial gradients in CPUE

Application of DCA to the CPUE data revealed that the first axis presented eigenvalues greater than 0.20 ($\lambda = 0.27$) and therefore was retained for interpretation. The spatial distribution of the scores on axis 1 of the DCA (DCA1) is consistent with variations in sedimentation rates (Spearman's rank correlation, $r_S = 0.77$, $P = 0.0034$). Sedimentation rates were high in the fluvial zone, intermediate in the transition zone, and low in the lacustrine zone (Fig. 3; for details see Pagioro and Thomaz 2002). Therefore, the spatial distribution of the scores on axis 1 showed a clear longitudinal gradient, which allowed separation into the zones identified by Pagioro and Thomaz (2002) (Fig. 3). The fluvial zone includes the fishery areas of Guaíra, Guaíra and vicinity, and Oliveira Castro and is located in the first 25 km of the reservoir. The transition zone comprises the fishery areas of Arroio Guaçu, Porto Mendes, and Pato Bragado and extends approximately for 35 km. The lacustrine zone is in the interior and extends for 90 km, comprising the fishery areas of Entre Rios, Santa Helena, Missal, Itaipulândia, São Miguel do Iguaçu, and Santa Terezinha de Itaipu (see Fig. 1).

MANOVA applied to the yield of the main species, with zone and year as independent factors, showed significant differences (*R* of Rao (Linderman et al. 1980; Rao 1952; Tatsuoka 1971): $\text{zone}_{[6,722]} = 25.18$, $\text{year}_{[30,1060]} = 2.90$, zone × $\text{year}_{[60,1078]} = 1.80$, all with $P < 0.0001$), indicating the relevance of applying ANOVAs for each species. For the separate ANOVAs, interactions were significant ($F_{[20,363]} > 2.20$ and $P < 0.01$) for *P. squamosissimus* and *P. maculatus*, indicating that the yields of these species varied among the zones and years considered (Table 1; Fig. 4). Yields of *H. malabaricus* and *I. labrosus* varied only among years ($F_{[2,363]} > 2.60$ and $P < 0.01$), whereas *R. aspera* yields varied among zones ($F_{[10,363]} = 43.43$ and $P < 0.001$) (Table 1; Fig. 4). For the other species (*P. granulosus*, *H. edentatus*, *P. pirinampu*, *P. luetkeni*, and *P. lineatus*), patterns of yield were clearer because both factors were significant ($F > 2.10$ and $P < 0.03$; Table 1; Fig. 4).

The two main species comprised almost half of all fish landings during the years analyzed (*H. edentatus* 22.3% and *P. granulosus* 22.1%). They showed obvious longitudinal gradients in abundance (Table 1; Fig. 4). Catches of *H. edentatus*, a zooplanktivorous filter feeder, occurred essentially in the lacustrine and transition zones. Temporal variations, also significant, were especially evident in the lacustrine zone, where CPUE values for *H. edentatus* in the initial years of exploitation were approximately double those in the transition zone; after 1993, however, CPUE values in the lacustrine zone were below those in the transition zone (although CPUE in the transition zone was less variable over the period). *Pterodoras granulosus*, an omnivore more abundant in the fisheries of the fluvial zone, also exhibited marked annual variation in catches (Table 1; Fig. 4), with a peak in CPUE in the fluvial zone in 1989 and an increase in the transition zone starting in 1993. Among the most abun-

© 2005 NRC Canada

Table 1. Two-way analysis of variance (ANOVA) applied to the catch-per-unit-effort (CPUE; kg·fisher^{-1}·day^{-1}) data for the main species, with reservoir zone and year as factors.

	Zone		Year		Zone × year	
	$F_{[2]}$	P	$F_{[10]}$	P	$F_{[20]}$	P
Pterodoras granulosus	**257.35**	<0.001	**2.83**	0.004	1.54	0.084
Hypophthalmus edentatus	**86.39**	<0.001	**2.15**	0.027	1.33	0.176
Pinirampus pirinampu	**58.35**	<0.001	**2.88**	0.003	0.81	0.691
Rhinelepis aspera	**43.43**	<0.001	1.40	0.191	1.15	0.312
Pseudoplatystoma fasciatum	**23.73**	<0.001	**4.72**	<0.001	0.57	0.922
Prochilodus lineatus	**13.36**	<0.001	**6.09**	<0.001	0.93	0.548
Plagioscion squamosissimus	**6.32**	0.003	**6.42**	<0.001	**4.48**	<0.001
Pimelodus maculatus	**4.73**	0.011	1.02	0.429	**2.30**	0.004
Hoplias malabaricus	1.99	0.143	**2.64**	0.007	1.33	0.180
Iheringichthys labrosus	0.47	0.624	**2.88**	0.003	1.00	0.473

Note: Numbers in boldface type are significant at $P < 0.05$; F, Fisher's statistic; P, probability of finding a greater F value; zone × year, interaction of zone and year.

dant species, the piscivorous *P. squamosissimus* is the only one that is introduced (from the Amazon basin). During the period, it yielded more or less constant CPUE values in the fluvial and lacustrine zones. However, catches of this species in the fluvial zone, formerly superior to catches of the other species, decreased markedly over the years studied (8.2 kg·fisher^{-1}·day^{-1} in 1987, 0.9 kg·fisher^{-1}·day^{-1} in 1998), with conspicuous decreases in 1991 and 1995.

The other species with significant differences in longitudinal gradients were all large migratory species. Of these, *P. pirinampu*, *P. maculatus*, and *P. lineatus* were more abundant in the fluvial and transition zones, whereas *R. aspera* and *P. luetkeni* were caught essentially in the fluvial zone. The sedentary species *H. malabaricus* and *I. labrosus* showed no clear patterns of variation in CPUE along the longitudinal axis of the reservoir, with capture peaks alternating between the zones. The latter species, however, showed high CPUE values in 1993 and 1997 but with great variations in averages. Overall, reductions in total fishery yield were not uniform along the reservoir. They were more conspicuous in the lacustrine and fluvial zones, whereas mean yields in the transition zone fluctuated less during the period (Fig. 5).

Spatial gradients in the fisheries and relationship with gear type and vessel characteristics

Two PCA axes presented eigenvalues greater than the broken-stick eigenvalues, and they were retained for interpretation. These two components explained 71.6% of the variability in fishing strategies related to gear type and vessels used in the reservoir (Table 2). Variables that most contributed to the first PCA axis (PC1) were cast nets and stationary engine (positively) and rabeta engine, gillnets, and paddle (negatively). For PC2, long lines were the most negatively correlated variable. Significant correlations between DCA1 (which summarized the CPUE values for the most important species) and PC1 and PC2 (which summarized gear type and vessel characteristics) were observed (Table 2). These significant correlations demonstrate an association between DCA and PCA. Therefore, it can be inferred that negative scores on PC1 were associated with gear type and vessel used in the *H. edentatus* fishery (represented by the low DCA scores), i.e., the use of gillnets and boats driven by paddle and rabeta engines in the more interior regions of the reservoir. Positive scores on PC1 were associated with the use of cast nets and a stationary engine, mainly in the *R. aspera* fishery and, to a lesser degree, in the *P. granulosus* fishery in the upper stretches of the reservoir, especially Guaíra and vicinity (Fig. 6*a*). The association of the *P. granulosus* fishery and, to a lesser degree, the *P. luetkeni* fishery with the use of long lines and a stationary engine in the fluvial zone, especially in Guaíra and vicinity, is better visualized when the relationship between DCA1 and PC2 is analyzed (Fig. 6*b*).

Discussion

Daily monitoring of landings and effort of the artisanal fishery, carried out over 11 years, allowed the characterization of variations in the spatial and temporal dynamics of the exploited stocks in Itaipu Reservoir. The fishery declined markedly during the analyzed period. This decline can be attributed mainly to alterations in trophic state over the years (i.e., a trophic upsurge, a general occurrence in reservoirs; Kimmel and Groeger 1986; Petrere 1996; Williams et al. 1998).

In general, the release of nutrients immediately following reservoir closure leads to increases at all trophic levels (O'Brien 1990) and there is a high availability of food resources for fish in the new environment, although extensive anoxic areas may be formed, temporarily restricting colonization by the original communities. These conditions lead to processes that select species with high physiological tolerance and behavioral plasticity that, using the abundant resources, proliferate and reach high biomass levels (Lowe-McConnell 1987; Agostinho et al. 1999*a*). The heterotrophic phase, however, ends with mineralization of the flooded organic material, and resources become essentially autochthonous (Petrere 1996). This leads to population alterations and, consequently, modifications in stocks of exploited fish. However, the effects of these events in fish communities are difficult to predict inasmuch as reservoirs are managed environments and responses of communities to a given disturbance may be aborted before completion (Agostinho et al. 1999*a*). The result is a chaotic succession of reactions marked by a reduction in interdependence between species and low biotic

© 2005 NRC Canada

Fig. 4. Spatial and temporal variations in yields (CPUE) of the main species, (*a*) *Hypophthalmus edentatus*, (*b*) *Plagioscion squamosissimus*, (*c*) *Pimelodus maculatus*, (*d*) *Iheringichthys labrosus*, (*e*) *Hoplias malabaricus*, (*f*) *Pterodoras granulosus*, (*g*) *Prochilodus lineatus*, (*h*) *Rhinelepis aspera*, (*i*) *Pinirampus pirinampu*, and (*j*) *Paulicea luetkeni*, from the artisanal fisheries of Itaipu Reservoir (vertical lines represent standard error; ■, fluvial zone; +, transition zone; ●, lacustrine zone).

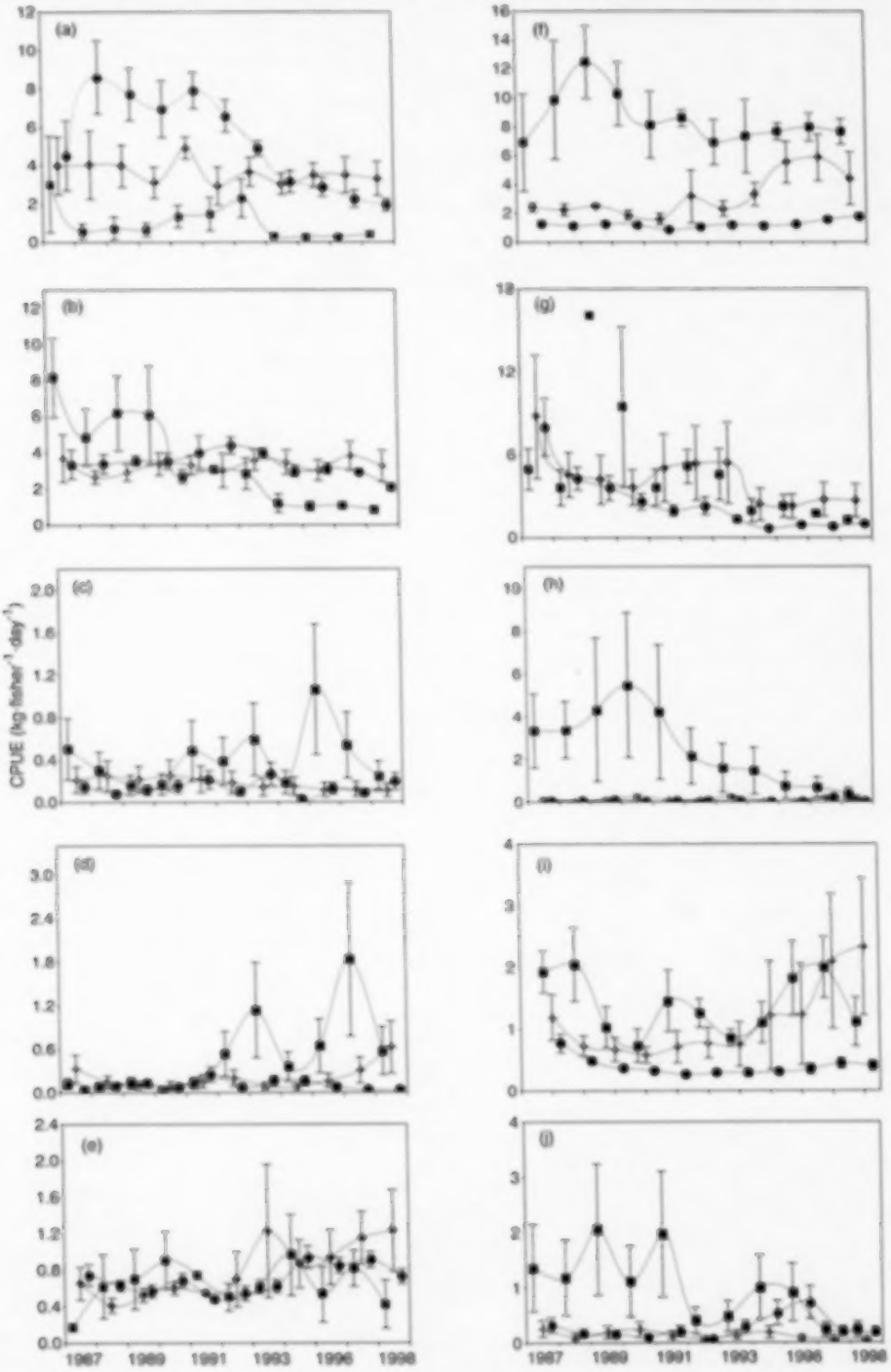

© 2005 NRC Canada

Fig. 5. Temporal variations in CPUE in the artisanal fishery of Itaipu Reservoir according to the longitudinal gradient (vertical lines represent standard error; ■, fluvial zone; +, transition zone; ●, lacustrine zone).

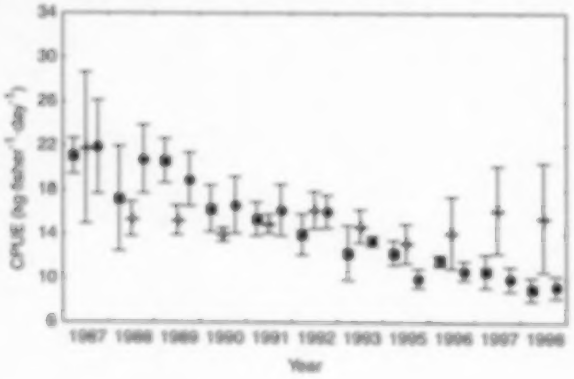

stability, altering the biota and the succession process (Wetzel 1990).

In addition to changes in trophic state, operation of the upstream reservoirs (in some years in association with low precipitation) greatly affects the flood regime of the Paraná River floodplain, with a direct influence on the fishery. Six out of the 10 species that sustain the Itaipu Reservoir fishery are large migratory species that use the free stretches of the basin above the reservoir (230 km) for spawning and the floodplain for their initial development (Agostinho et al. 2001). Gomes and Agostinho (1997) observed high correlations between the flood regime of the upper Paraná River floodplain and the yield of *P. lineatus* in the reservoir, fry of this species having stayed in floodplain lagoons for 2 years. Agostinho et al. (2004), monitoring marginal lagoons along the free stretch of the Paraná River, observed that the density of juveniles of the most migratory species that make up the reservoir fishery is related to the duration and period of floods. These authors give an account of the absolute absence of juveniles of migratory species in the years in which waters of the Paraná River did not reach the floodplain.

Processes of transport and deposition of sediments are important forces in determining spatial (longitudinal) gradients in reservoirs (Thornton 1990; Kimmel et al. 1990). Patterns of variation in sedimentation rate in Itaipu Reservoir were consistent with spatial variations in catches of the main species of the artisanal fishery (summarized by DCA1), allowing recognition of zonation. Spatial gradients were insignificant only for *H. malabaricus* and *L. labrosus*, two sedentary species that inhabit the littoral areas of the entire reservoir and complete their life cycles there. The first species is essentially piscivorous, builds littoral refuges, and provides parental care, whereas the second has a benthivorous diet, feeding on aquatic invertebrates in shallow areas (Hahn et al. 1998). Both have shown significant increases in abundance in recent years. This is attributed to the relative stability in the level of the reservoir.

The other two species restricted to the reservoir areas (*H. edentatus* and *P. squamosissimus*) exhibited significant spatial and temporal variations in abundance. *Hypophthalmus edentatus*, the main species in the fishery during the entire period, occupied mainly the interior pelagic areas of the reservoir, principally the lacustrine zone. Its stock in the reservoir is decreasing, however, as is demonstrated by the annual CPUE variations. Although alterations in the diet of this species have been slight over the last 10 years (Ambrosio et al. 2001), with substitution of bosminid for daphniid cladocerans as the dominant item in its diet, it is probable that the change in trophic state of the reservoir has affected food availability for the species. In this sense, flow regulation and nutrient retention by the new reservoirs upstream probably made an important contribution through the expected effects on productivity in Itaipu Reservoir, mainly in the more interior lacustrine areas (the abundance of *H. edentatus* in the transition zone remained constant during the study period).

Table 2. Eigenvectors of axes 1 and 2 of the principal components analysis (PCA) applied to the gear type and vessel characteristics data matrix, eigenvalues (for each axis and the broken-stick), percent explanation of the axes retained for interpretation, and Pearson's correlation values between PCA axes and axis 1 of the detrended correspondence analysis (DCA1).

Eigenvector	Axis 1	Axis 2
Gillnets	–0.4351	–0.2996
Long lines	0.0894	–0.5326
Cast nets	0.3612	–0.4022
Others	–0.0317	–0.4932
Paddle	–0.4322	–0.1384
Stationary engine	0.3342	–0.3934
Outboard motor	–0.3746	–0.1983
"Rabeta" motor	–0.4820	–0.0917
Eigenvalues (broken-stick)	3.459 (2.718)	2.272 (1.718)
Percent explanation	43.24	28.4
Pearson's correlation with DCA1	0.614 (<0.001)	–0.472 (<0.001)

Plagioscion squamosissimus, the adults of which prey intensively on the annual fry of *H. edentatus* (Hahn et al. 1997), is the main piscivore in the Itaipu Reservoir fish landings. Its abundance showed little variability in the transition and lacustrine zones; however, it presented a marked decline in the fluvial zone, where it had been concentrated in the first 4 years of the study period. The predator–prey interactions between these two species, allied with changes in trophic state, seem to be the most appropriate explanation for the decline of both.

Rhinelepis aspera, *P. luetkeni*, and *P. granulosus*, which preferentially inhabit the bottom (Freire and Agostinho 2001), were typical of the fluvial zone. *Prochilodus lineatus*, *P. pirinampu*, and *P. maculatus*, which have little association with the lower portions of the water column, were more abundant in the transition zone. These six species can be categorized into three distinct trophic groups (Hahn et al. 1997): detritivorous (*R. aspera* and *P. lineatus*), omnivorous (*P. granulosus* and *P. maculatus*), and piscivorous (*P. pirinampu* and *P. luetkeni*). They are able to use the transported allochthonous food resources that enter both zones and small prey that are abundant in the entire reservoir (Benedito-Cecílio and Agostinho 1999). The important sedentary species in the fishery (with and without spatial gradients in the

© 2005 NRC Canada

Fig. 6. Ordination of the data on type of gear and vessel characteristics in Itaipu Reservoir (significant axes of the principal components analysis axis 1 (PC1; *a*) and axis 2 (PC2; *b*) in relation to the variations in catch of the main species (DCA1). The number above each symbol indicates the fishing area (see "Study area") (■, fluvial zone; +, transition zone; ●, lacustrine zone).

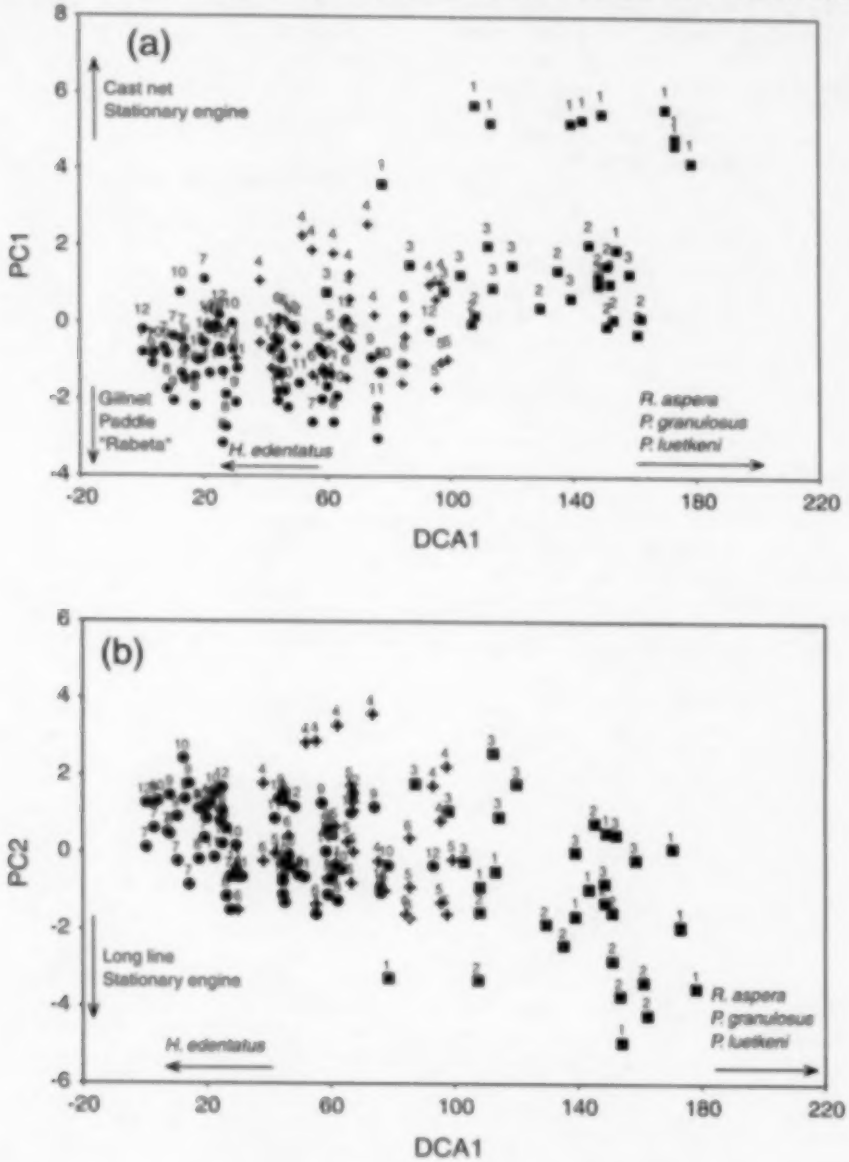

catches) fed essentially on autochthonous resources (plankton and aquatic invertebrates, in addition to fish).

Four of the six migratory species (*P. granulosus*, *R. aspera*, *P. lineatus*, and *P. luetkeni*) showed a decline in catches in the fluvial zone because of multiple factors, especially local overfishing (*R. aspera*; Okada et al. 1996) and flood regulation on the upper Paraná River floodplain. The tendency towards depletion in the artisanal fishery, involving all species, reflects spatial and temporal variations of the main species, particularly declines in catches of *H. edentatus* in the lacustrine zone and *P. granulosus* in the fluvial zone. CPUE values were constant in the transition zone but decreased in the others. The fact that the fluvial and lacustrine zones contained species with distinct environmental demands, and whose distributions overlapped in the transition zone, suggests that the decrease in total fishing yield over the period could be a result of distinct adverse factors.

Longitudinal gradients in the abundance and composition of the catches reflect the degree of dependence of the species on the lentic conditions in the reservoir (availability of autochthonous resources, water transparency) and the lotic condition in the river (availability of allochthonous re-

© 2005 NRC Canada

sources, turbidity, and water circulation), both mainly determined by the processes of transport and sediment deposition. Fishing strategies, on the other hand, are dependent on intrinsic components of local stocks (specific composition, feeding behavior, microhabitat) and the environment (water velocity and turbidity), in addition to cultural (fishing tradition and empirical knowledge) and socioeconomic (specific demand, cost, profitability, investment capacity) aspects. Understanding the dynamics of these factors, besides those of the resource itself, is fundamental to the delineation of management strategies (Hilborn and Walters 1992). However, the heterogeneity with which they are presented in a multispecific fishery such as that of Itaipu Reservoir makes analysis of this fishery-system component a complex task. The use of a multivariate approach seems, however, promising (Pelletier and Ferraris 2000). In this study, spatial variations in some of these variables were satisfactorily summarized. Spatial variations in the type of gear used and vessel characteristics, summarized on the first two PCA axes, were plotted against variations in catches of the main species, summarized on the first DCA axis. This analysis made it possible to identify patterns in the capture of at least three of the main species.

The *R. aspera* fishery is typical of the fluvial zone (Guaíra) and is carried out using cast nets. This species lives on irregular rocky bottoms in depths of up to 6 m at the entrance of the reservoir (Delariva and Agostinho 2001). Wooden boats propelled by a stationary engine strong enough to overcome the more rapid currents in the region are used (Okada et al. 1996). Fisheries of *P. granulosus* and *P. lutkeni*, species more abundant in the fluvial zone, also involve the use of a wooden boat propelled by a stationary engine and long lines. On the other hand, gillnets capture *H. edentatus* in the more interior zones, with the use of wooden boats propelled by paddle or a rabeta engine. These types of propulsion are suitable in these zones because of low water velocities and low operational costs of the boat (Okada et al. 1997).

Although it can be considered low-yield when compared with similar environments in other basins (Marshall 1984; Paiva et al. 1994; Gomes and Miranda 2001), the Itaipu Reservoir fishery plays an important social and economic role for a great number of fishers who, in general, would not have any alternative legal employment, inasmuch as most have been marginalized by other productive sectors of the economy. Carried out in a border area (Brazil–Paraguay) where illicit activities such as smuggling, drug trafficking, and transporting stolen vehicles across the border are common practices, the fishery in this reservoir needs increased government attention to address the tendency towards successive yield decreases that threaten to push these fishers to the brink of absolute marginality.

The decline in yield of Itaipu Reservoir appears to be mainly due to a change in trophic state, which is a common occurrence in reservoirs (Kimmel and Groeger 1986; Petrere 1996). However, in this reservoir, other factors may be worsening the situation, such as the construction of reservoirs upriver (Agostinho et al. 2004) and overfishing (Okada et al. 1996; Agostinho et al. 1999*b*; Miranda et al. 2000). It is also evident that the longitudinal gradients in the reservoir identified by Pagioro and Thomaz (2002) influence fish species distribution along the reservoir and, consequently, the fishery. Therefore, these longitudinal gradients should be considered in any management plan. Ignorance of the existence of these gradients led, for example, to the construction of infrastructures to support the fishery in the inner part of another reservoir (Sobradinho Reservoir, São Francisco River), which later became less productive (Agostinho 1998).

Acknowledgements

We thank Dr. Luiz Maurício Bini for helping in the statistical analysis of the data, Dr. Harumi Irene Suzuki for reviewing the text and making suggestions, University employees Vanderlei Pereira da Silva and Maria de Lourdes Batista Nunes and Dr. Angela Maria Ambrósio for helping in the field collection and laboratory analyses, and David Hocinghaus for his suggestions and English improvements. This study was carried out with the financial support of Itaipu Binacional and Nupélia, Universidade Estadual de Maringá.

References

Agostinho, A.A. 1998. A pesca no reservatório de Sobradinho : considerações sobre a pesca no reservatório de Sobradinho e ações recomendadas para sua otimização. Universidade Estadual de Maringá – Nupélia, Maringá, Brazil. Tech. Rep. 1998.

Agostinho, A.A., Miranda, L.E., Bini, L.M., Gomes, L.C., Thomaz, S.M., and Suzuki, H.I. 1999*a*. Patterns of colonization in neotropical reservoirs, and prognoses on aging. *In* Theoretical reservoir ecology and its applications. *Edited by* J.G. Tundisi and M. Straškraba. International Institute of Ecology, São Carlos, Brazil. pp. 227–265.

Agostinho, A.A., Okada, E.K., and Gregorio, J. 1999*b*. A pesca no reservatório de Itaipu : aspectos sócioeconômicos e impactos do represamento. *In* Ecologia de reservatórios: estrutura, função e aspectos sociais. *Edited by* R. Henry. Fundação de Amparo à Pesquisa do Estado de São Paulo / Fundação do Instituto de Biociências (FUNDIBIO/FAPESP), Botucatu, São Paulo, Brazil. pp. 279–320.

Agostinho, A.A., Gomes, L.C., and Zalewski, M. 2001. The importance of floodplains for the dynamics of fish communities of the upper river Paraná. Ecohydrol. Hydrobiol. **1**(1–2): 209–217.

Agostinho, A.A., Gomes, L.C., Veríssimo, S., and Okada, E.K. 2004. Flood regime, dam regulation and fish in the upper Paraná River: effects on assemblage attributes, reproduction and recruitment. Rev. Fish Biol. Fish. **14**(1): 11–19.

Ambrósio, A.M., Agostinho, A.A., Gomes, L.C., and Okada, E.K. 2001. The fishery and fishery yield of *Hypophthalmus edentatus* (Spix. 1829), (Siluriformes, Hypophthalmidae), in the Itaipu reservoir, Paraná state, Brazil. Acta Limnol. Bras. **13**(1): 93–105.

Benedito-Cecílio, E., and Agostinho, A.A. 1999. Determination of patterns of ichthyofauna co-occurrence in the Paraná river basin, area of influence of the Itaipu reservoir. Interciência, **24**(6): 360–365.

Bini, L.M. 1997. Spatial variation of some limnological parameters in Barra Bonita reservoir (São Paulo, Brazil): a geostatistical approach. Verh. Int. Ver. Theor. Angew. Limnol. **26**: 229–231.

Brylinsky, M., and Mann, K.H. 1973. An analysis of factors governing productivity in lakes and reservoirs. Limnol. Oceanogr. **18**(1): 1–14.

© 2005 NRC Canada

Delariva, R.L., and Agostinho, A.A. 2001. Relationship between morphology and diets of six neotropical loricariids. J. Fish Biol. **58**: 832–847.

Freire, A.G., and Agostinho, A.A. 2001. Ecomorfologia de oito espécies dominantes da ictiofauna do reservatório de Itaipu (Paraná/Brasil). Acta Limnol. Bras. **13**(1): 1–9.

Gido, K.B., and Matthews, W.J. 2000. Dynamics of the offshore fish assemblage in a southwestern reservoir (Lake Texoma, Oklahoma–Texas). Copeia, **4**: 917–930.

Gomes, L.C., and Agostinho, A.A. 1997. Influence of the flooding regime on the nutritional state and juvenile recruitment of the curimba, *Prochilodus scrofa*, Steindachner, in upper Paraná river, Brazil. Fish. Manag. Ecol. **4**(4): 263–274.

Gomes, L.C., and Miranda, L.E. 2001. Riverine characteristics dictate composition of fish assemblages and limit fisheries in reservoirs of the upper Paraná River Basin. Regul. Rivers Res. Manag. **17**: 67–76.

Hahn, N.S., Agostinho, A.A., and Goiten, R. 1997. Feeding ecology of curvina *Plagioscion squamosissimus* (Heckel, 1840) (Osteichthyes, Perciformes) in the Itaipu reservoir and Porto Rico floodplain. Acta Limnol. Bras. **9**: 11–22.

Hahn, N.S., Agostinho, A.A., Gomes, L.C., and Bini, L.M. 1998. Estrutura trófica da ictiofauna do reservatório de Itaipu (Paraná–Brasil) nos primeiros anos de sua formação. Interciência, **23**(5): 299–305.

Hilborn, R., and Walters, C.J. (*Editors*). 1992. Quantitative fisheries stock assessment: choice, dynamics and uncertainty. Chapman and Hall, New York.

Hoyer, M.V., and Jones, J.R. 1983. Factors affecting the relationship between phosphorus and chlorophyll *a* in Midwestern reservoirs. Can. J. Fish. Aquat. Sci. **40**: 192–199.

Jackson, D.A. 1993. Stopping rules in principal components analysis: a comparison of heuristical and statistical approaches. Ecology, **74**(8): 2204–2214.

Kennedy, R.H., and Walker, W.W. 1990. Reservoir nutrient dynamics. *In* Reservoir limnology: ecological perspectives. *Edited by* K.W. Thornton, B.L. Kimmel, and F.E. Payne. John Wiley & Sons, New York. pp. 109–131.

Kimmel, B.L., and Groeger, A.W. 1986. Limnological and ecological changes associated with reservoir aging. *In* Reservoir Fisheries Management: Strategies for the 80's: Proceedings of a National Symposium on Managing Reservoir Fishery Resources, June 1983, Lexington, Kentucky. *Edited by* G.E. Hall and M.J. Van Den Avyle. Reservoir Committee Southern Division, American Fisheries Society, Bethesda, Md. pp. 103–109.

Kimmel, B.L., Lind, O.T., and Paulson, L.J. 1990. Reservoir primary production. *In* Reservoir limnology: ecological perspectives. *Edited by* K.W. Thornton, B.L. Kimmel, and F.E. Payne. John Wiley & Sons, New York. pp. 133–193.

Linderman, R.H., Merenda, P.F., and Gold, R. 1980. Introduction to bivariate and multivariate analysis. Scott, Foresman and Co., New York.

Lowe-McConnell, R.H. 1987. Ecological studies in tropical fish communities. Cambridge University Press (Cambridge Tropical Biology Series), Cambridge.

Marshall, B.E. 1984. Predicting ecology and fish yields in African reservoirs from preimpoundment physico-chemical data. Committee for Inland Fisheries of Africa, Food and Agriculture Organization, Rome. Tech. Pap. No. 12.

Marzolf, G.R. 1990. Reservoirs as environments for zooplankton. *In* Reservoir limnology: ecological perspectives. *Edited by* K.W. Thornton, B.L. Kimmel, and F.E. Payne. John Wiley & Sons, New York. pp. 195–208.

Miranda, L.E., Agostinho, A.A., and Gomes, L.C. 2000. Appraisal of the selective properties of gill nets and implications for yield and value of the fisheries at the Itaipu Reservoir, Brazil–Paraguay. Fish. Res. (Amst.), **45**: 105–116.

Nakamoto, N., Tundisi, J.G., Marins, M.A., and Godinho, M.J.L. 1997. Longitudinal distribution of plankton in a shallow reservoir of Broa in Brazil. Verh. Int. Ver. Theor. Angew. Limnol. **26**(2): 553–557.

Noble, R.L. 1980. Management of lakes, reservoirs and ponds. *In* Fisheries management. *Edited by* R.T. Lackey and L.A. Nielsen. Blackwell Scientific Publications, Oxford and London. pp. 265–295.

O'Brien, W.J. 1990. Perspectives on fish in reservoir limnology. *In* Reservoir limnology: ecological perspectives. *Edited by* K.W. Thornton, B.L. Kimmel, and F.E. Payne. John Wiley & Sons, New York. pp. 209–225.

Okada, E.K., Agostinho, A.A., and Petrere Júnior, M. 1996. Catch and effort data and the management of the commercial fisheries of Itaipu reservoir in the upper Paraná River, Brazil. *In* Stock assessment in inland fisheries. *Edited by* I.G. Cowx. Fishing News Books, Oxford. pp. 154–161.

Okada, E.K., Gregoris, J., Agostinho, A.A., and Gomes, L.C. 1997. Diagnóstico da pesca profissional em dois reservatórios do rio Iguaçu. *In* Reservatório de Segredo : bases ecológicas para o manejo. *Edited by* A.A. Agostinho and L.C. Gomes. Editora da Universidade Estadual de Maringá, Maringá, Paraná, Brazil. pp. 293–318.

Pagioro, T.A., and Thomaz, S.M. 2002. Longitudinal patterns of sedimentation in a deep, monomictic subtropical reservoir (Itaipu, Brazil–Paraguay). Arch. Hydrobiol. **154**(3): 515–528.

Paiva, M.P., Petrere Junior, M., Petenate, A.J., Nepomuceno, F.H., and Vasconcelos, E.A. 1994. Relationship between the number of predatory fish species and fish yield in large northeastern Brazilian reservoirs. *In* Rehabilitation of freshwater fisheries. *Edited by* I.G. Cowx. Fishing News Books, Oxford. pp. 120–130.

Palmer, M.W. 1993. Putting things in even better order: the advantages of canonical correspondence analysis. Ecology, **74**: 2215–2230.

Pelletier, D., and Ferraris, J. 2000. A multivariate approach for defining fishing tactics from commercial catch and effort data. Can. J. Fish. Aquat. Sci. **57**: 51–65.

Petrere, M. 1996. Fisheries in large tropical reservoirs in South America. Lakes Reserv. Res. Manag. **2**: 111–133.

Rao, C.R. 1952. Advanced statistical methods in biometric research. Wiley, New York.

Scheiner, S.M. 1993. MANOVA: multiple response variables and multispecies interactions. *In* Design and analysis of ecological experiments. *Edited by* S.M. Scheiner and J. Gurevitch. Chapman & Hall, New York. pp. 94–112.

Tatsuoka, M.M. 1971. Multivariate analysis. Wiley, New York.

ter Braak, C.J.F., and Šmilauer, P. 1998. Reference manual and user's guide to CANOCO for Windows: software for canonical community ordination. Version 4 [computer program]. Microcomputer Power, Ithaca, N.Y.

Thomaz, S.M., Bini, L.M., and Alberti, S.M. 1997. Limnologia do reservatório de Segredo : padrões de variação espacial e temporal. *In* Reservatório de Segredo : bases ecológicas para o manejo. *Edited by* A.A. Agostinho and L.C. Gomes. Editora da Universidade Estadual de Maringá, Maringá, Paraná, Brazil. pp. 19–37.

Thornton, K.W. 1990. Sedimentary processes. *In* Reservoir limnology: ecological perspectives. *Edited by* K.W. Thornton, B.L. Kimmel, and F.E. Payne. John Wiley & Sons, New York. pp. 43–69.

© 2005 NRC Canada

Thornton, K.W., Kennedy, R.H., Carroll, J.H., Walker, W.W., Gunkel, R.C., and Ashby, S. 1981. Reservoir sedimentation and water quality — an heuristic model. *In* Proceedings of the Symposium on Surface Water Impoundments, June 1980, Minneapolis, Minnesota. *Edited by* H.G. Stefan. American Society of Civil Engineers, New York. pp. 654–661.

Thornton, K.W., Kimmel, B.L., and Payne, F.E. (*Editors*). 1990. Reservoir limnology: ecological perspectives. John Wiley & Sons, New York.

Tundisi, J.G. 1993. Represas do Paraná Superior : limnologia e bases científicas para o gerenciamento. *In* Proceedings of the Conferencias de Limnologia La Plata, Instituto de Limnologia "Dr. R.A. Ringuelet", November 1992, Buenos Aires, Argentina. *Edited by* A. Boltovskoy and H.L. López. pp. 41–52.

Tundisi, J.G., Matsumura-Tundisi, T., Henry, R., Rocha, O., and Hino, K. 1988. Comparação do estado trófico de 23 reservatórios do Estado de São Paulo: eutrofização e manejo. *In* Limnologia e manejo de represas. *Edited by* J.G. Tundisi. Série Monografias em Limnologia, Universidade de São Paulo, Escola de Engenharia de São Carlos, Cent. Recursos Hídricos Ecol. Aplicada, São Paulo, **1**: 165–204.

Wetzel, R.G. 1990. Reservoir ecosystems: conclusions and speculations. *In* Reservoir limnology: ecological perspectives. *Edited by* K.W. Thornton, B.L. Kimmel, and F.E. Payne. John Wiley & Sons, New York. pp. 227–246.

Williams, J.D., Winemiller, K.O., Taphorn, D.C., and Balbas, L. 1998. Ecology and status of piscivores in Guri, an oligotrophic tropical Reservoir. N. Am. J. Fish. Manag. **18**(2): 274–285.

© 2005 NRC Canada

Bret C. Harvey, Jason L. White, and Rodney J. Nakamoto	**650–658**	Habitat-specific biomass, survival, and growth of rainbow trout (*Oncorhynchus mykiss*) during summer in a small coastal stream
L.G.S. Mello and G.A. Rose	**659–670**	Using geostatistics to quantify seasonal distribution and aggregation patterns of fishes: an example of Atlantic cod (*Gadus morhua*)
Keita W. Suzuki, Akihide Kasai, Kouji Nakayama, and Masaru Tanaka	**671–678**	Differential isotopic enrichment and half-life among tissues in Japanese temperate bass (*Lateolabrax japonicus*) juveniles: implications for analyzing migration
Gavin A. Begg, Bruce D. Mapstone, Ashley J. Williams, Samantha Adams, Campbell R. Davies, and Dong C. Lou	**679–692**	Multivariate life-history indices of exploited coral reef fish populations used to measure the performance of no-take zones in a marine protected area
Steven T. Kalinowski and Mark L. Taper	**693–699**	Likelihood-based confidence intervals of relative fitness for a common experimental design
C.M. Wurster, W.P. Patterson, D.J. Stewart, J.N. Bowlby, and T.J. Stewart	**700–713**	Thermal histories, stress, and metabolic rates of chinook salmon (*Oncorhynchus tshawytscha*) in Lake Ontario: evidence from intra-otolith stable isotope analyses
Edson Kiyoshi Okada, Angelo Antonio Agostinho, and Luiz Carlos Gomes	**714–724**	Spatial and temporal gradients in artisanal fisheries of a large Neotropical reservoir, the Itaipu Reservoir, Brazil

National Research Council Canada
Ottawa, Canada K1A 0R6

Conseil national de recherches Canada
Ottawa, Canada K1A 0R6

Postage paid at Ottawa
Publications mail
Registration No. 40062581

Port payé à Ottawa
Poste-publication
Enregistrement n° 40062581

USPS periodical postage paid at Champlain, NY 12919, USA

Canadian Journal of Fisheries and Aquatic Sciences

Volume 62, Number 3, March 2005

Journal canadien des sciences halieutiques et aquatiques

Volume 62, numéro 3, mars 2005

	ARTICLES	ARTICLES
A.D. Persaud and N.D. Yan	483–491	Developmental differences and a test for reciprocity in the tolerance of *Chaoborus punctipennis* larvae to ultraviolet radiation
Erwin E. Van Nieuwenhuyse	492–504	Empirical model for predicting a catchment-scale metric of surface water transit time in streams
Melania E.A. Cristescu and Paul D.N. Hebert	505–517	The "Crustacean Seas" — an evolutionary perspective on the Ponto-Caspian peracarids
Akihiro Koyama, Kathleen Kavanagh, and Andrew Robinson	518–526	Marine nitrogen in central Idaho riparian forests: evidence from stable isotopes
Mark F. Baumgartner and Bruce R. Mate	527–543	Summer and fall habitat of North Atlantic right whales (*Eubalaena glacialis*) inferred from satellite telemetry
Jon Brodziak and Christopher M. Legault	544–562	Model averaging to estimate rebuilding targets for overfished stocks
Anik Giguère, Peter G.C. Campbell, Landis Hare, and Carole Cossu-Leguille	563–577	Metal bioaccumulation and oxidative stress in yellow perch (*Perca flavescens*) collected from eight lakes along a metal contamination gradient (Cd, Cu, Zn, Ni)
Gesche Winkler, Pascal Sirois, Ladd E. Johnson, and Julian J. Dodson	578–592	Invasion of an estuarine transition zone by *Dreissena polymorpha* veligers had no detectable effect on zooplankton community structure
John R. Zeldis, John Oldman, Sira L. Ballara, and Laura A. Richards	593–610	Physical fluxes, pelagic ecosystem structure, and larval fish survival in Hauraki Gulf, New Zealand
Roy Deng, Cathy Dichmont, David Milton, Mick Haywood, David Vance, Natasha Hall, and David Die	611–622	Can vessel monitoring system data also be used to study trawling intensity and population depletion? The example of Australia's northern prawn fishery
Paul A. Hamer, Gregory P. Jenkins, and Bronwyn M. Gillanders	623–630	Chemical tags in otoliths indicate the importance of local and distant settlement areas to populations of a temperate sparid, *Pagrus auratus*
Trevor A. Branch, Ray Hilborn, and Eugenia Bogazzi	631–642	Escaping the tyranny of the grid: a more realistic way of defining fishing opportunities
D. Álvarez and A.G. Nicieza	643–649	Is metabolic rate a reliable predictor of growth and survival of brown trout (*Salmo trutta*) in the wild?

Continued on inside back cover / Suite au verso

Printed in Canada by / Imprimé au Canada par
NRC Reprographic Services / Service de reprographie CNRC
Page production by / Mise en page par
NRC Research Press / Presses scientifiques du CNRC

0706-652X(200503)62:3;1-B